Steven A. Murawski · Cameron H. Ainsworth
Sherryl Gilbert · David J. Hollander
Claire B. Paris · Michael Schlüter
Dana L. Wetzel *Editors*

Scenarios and Responses to Future Deep Oil Spills

Fighting the Next War

EXTRAS ONLINE

Springer

Scenarios and Responses to Future Deep Oil Spills

Steven A. Murawski • Cameron H. Ainsworth
Sherryl Gilbert • David J. Hollander
Claire B. Paris • Michael Schlüter
Dana L. Wetzel
Editors

Scenarios and Responses to Future Deep Oil Spills

Fighting the Next War

Springer

Editors
Steven A. Murawski
College of Marine Science
University of South Florida
St. Petersburg, FL, USA

Sherryl Gilbert
College of Marine Science
University of South Florida
St. Petersburg, FL, USA

Claire B. Paris
Rosenstiel School of Marine
& Atmospheric Science
University of Miami
Miami, FL, USA

Dana L. Wetzel
Mote Marine Laboratory
Sarasota, FL, USA

Cameron H. Ainsworth
College of Marine Science
University of South Florida
St. Petersburg, FL, USA

David J. Hollander
College of Marine Science
University of South Florida
St. Petersburg, FL, USA

Michael Schlüter
Hamburg University of Technology
Hamburg, Germany

ISBN 978-3-030-12962-0 ISBN 978-3-030-12963-7 (eBook)
https://doi.org/10.1007/978-3-030-12963-7

This Springer imprint is published by the registered company Springer Nature Switzerland AG
The registered company address is: Gewerbestrasse 11, 6330 Cham, Switzerland

Foreword and Dedication

Global production of liquid fossil hydrocarbons was 34 billion barrels in 2017,[1] with production increasing an average 1.1% per year during the preceding decade (BP 2018). Maintaining and increasing production now involves expansion into "frontier" areas including nontraditional terrestrial and aquatic realms. Marine oil exploration and production has advanced steadily offshore since its inception in the Gulf of Mexico in the 1930s (Murawski et al. 2020). For the first time, in 2017, more crude oil was generated from ultra-deep (>1 mile deep) waters of the Gulf of Mexico than in shallower waters (Murawski et al. 2020). This trend to deeper production is occurring in all major marine oil provinces of the world.

The *Deepwater Horizon* (DWH) oil spill was the world's first ultra-deep well blowout, but likely not the last. Deep well fields in the Gulf of Mexico now extend to depths nearly twice that of DWH. Ultra-deep wells present unique technical and environmental challenges. Because of the immense depths and pressures, ultra-deep wells are more complex, risk-prone, and expensive to construct and maintain as compared to equivalent shallower facilities. Notwithstanding these issues, and depending on the price of oil, the volumes of oil produced at ultra-deep wells can be enormously profitable, yielding many times the production rates of those inshore (Murawski et al. 2020).

The purposes of this book are to synthesize relevant science related to potential oil spills in frontier marine domains and to project the fate and impacts of simulated ultra-deep blowouts. No two spills are alike, and the conditions of the next ultra-deep well blowout will be different from both the DWH and the shallower Ixtoc 1 experiences. Prior to DWH, response planning for marine oil spills primarily assumed a scenario similar to the last major marine oil spill in the United States – the *Exxon Valdez* tanker accident in Alaska. Thus, responders were generally unprepared for the scenario of a deep and unconstrained well blowout in terms of infrastructure and basic science to reasonably inform the use of novel response measures.

[1] One stock tank barrel = 42 gallons = 158 l; includes crude oil, shale oil, oil sands, and NGLs (natural gas liquids, the liquid content of natural gas where this is recovered separately)

Rather than concentrating on unresolved issues remaining post-DWH, we simulate spills in the Gulf of Mexico regions where oil and gas exploration and production may in the future occur (e.g., deep water in the eastern, western, and southern Gulf). Likewise, we consider spills in other frontier areas (e.g., off West Africa and in the Arctic). These location-specific simulations of oil fates and their relative impacts on ecological communities and economic activities (fishing) differ from the DWH scenario in fundamental and important ways. Under alternative conditions of oil type, gas/oil ratios, water depth, etc., oil fate and effects will vary still. The point of these simulations, and the importance of closing existing research gaps, is that conditions will be different and therefore response strategies must be nimble to effectively deal with the next ultra-deep oil well blowout, pipeline rupture, tanker-platform collision, industrial sabotage incident, or whatever the scenario may be. Assuming a replay of DWH will surely repeat the cycle of anticipating the next "war" by preparing for the last. Having a fuller repertoire of science applicable to a wide array of idiosyncratic conditions is the key to anticipating and effectively responding to the next spill of significance.

Despite the nearly $1 billion spent on relevant science since the DWH accident, there remain a number of critical science gaps that preclude consensus on best options to prevent or at least more efficiently respond to the next major spill. A short list of recommended science priorities and policy options is discussed. Nevertheless, there will always be uncertainty concerning the physics, chemistry, geology, and ecology associated with particular ultra-deep well blowouts. Perhaps as important to closing the science gaps that remain, identifying the attributes of locations that are too risk-prone or too ecologically or economically sensitive to permit oil exploration and production should be a priority. Should all frontier areas where oil and gas resources are technically feasible to recover be produced? This is the domain of policy, and informing the consequences of policy choices is the province of environmental science as characterized in the chapters that follow.

Much of the science synthesized in this volume was a result of support and funding from the Gulf of Mexico Research Initiative (GoMRI). The GoMRI enterprise was funded through a $500 million grant established in the wake of the DWH accident. Many of the authors and all of the coeditors of this book are members of the Center for Integrated Modeling and Analysis of Gulf Ecosystems (C-IMAGE), one of the several research centers supported by GoMRI. Authorship of this volume also includes contributions by members of other GoMRI-funded centers, as well as those from government, academic, and private research organizations. We are deeply grateful to the leadership, staff, and research board of GoMRI for supporting these efforts to better understand the science of deep oil spills and to synthesize that science into actionable alternatives to inform government and industry.

This volume is dedicated to the 11 men who lost their lives aboard the MODU (Mobile Offshore Drilling Unit) *Deepwater Horizon* on April 20, 2010:

Jason C. Anderson, age 35
Aaron Dale Burkeen, age 37
Donald Clark, age 49
Stephen Ray Curtis, age 39
Gordon L. Jones, age 28
Roy Wyatt Kemp, age 27
Karl D. Kleppinger, Jr., age 38
Keith Blair Manuel, age 56
Dewey A. Revette, age 48
Shane M. Roshto, age 22
Adam Weise, age 24

The work described herein has been undertaken with the goal of preventing such accidents from ever happening again and reducing risks to the environment and people should they reoccur. In this way, we honor those whose lives were lost that they helped stimulate national and international action to make marine oil and gas production safer. The families of those who lost their lives in the *Deepwater Horizon* accident expect and deserve nothing less.

St. Petersburg, FL, USA — Steven A. Murawski
St. Petersburg, FL, USA — Cameron H. Ainsworth
St. Petersburg, FL, USA — Sherryl Gilbert
St. Petersburg, FL, USA — David J. Hollander
Miami, FL, USA — Claire B. Paris
Hamburg, Germany — Michael Schlüter
Sarasota, FL, USA — Dana L. Wetzel

References

BP (2018) BP Statistical Review of World Energy. 67th edn 25 pp. https://www.bp.com/content/dam/bp/business-sites/en/global/corporate/pdfs/energy-economics/statistical-review/bp-stats-review-2018-full-report.pdf

Murawski SA, Hollander DJ, Gilbert S, Gracia A (2020) Deep-water oil and gas production in the Gulf of Mexico, and related global trends (Chap. 2). In: Murawski SA, Ainsworth C, Gilbert S, Hollander D, Paris CB, Schlüter M, Wetzel D (eds) Scenarios and responses to future Deep Oil Spills – fighting the next war. Springer, Cham

The C-IMAGE research consortium, January 2014, Mobile, Alabama

Contents

Part I
Overview

Photo Credit: C-IMAGE Consortium

Chapter 1
Introduction to the Volume

Steven A. Murawski, Cameron H. Ainsworth, Sherryl Gilbert, David J. Hollander, Claire B. Paris, Michael Schlüter, and Dana L. Wetzel

Abstract Ultra-deep water production of oil and gas – from depths greater than 1 mile (1500 m) – comprises an ever-increasing proportion of the world's supply of hydrocarbons. In the Gulf of Mexico, ultra-deep production now exceeds that from shallower waters. The ultra-deep domains of the world's oceans are home to unique and highly sensitive communities of animals, are characterized by extremes in environmental conditions (low temperatures, high pressures), and are exceedingly challenging regions in which to work safely. *Deepwater Horizon* (DWH) was the world's first and largest ultra-deep water well blowout and likely not the last. In the wake of that incident, scientific research and industrial development have been focused to better understand the ultra-deep domain, to lessen the likelihood of accidents there, and to better respond to future incidents. This volume summarizes trends in the development of ultra-deep drilling, synthesizes the state of knowledge relevant to ultra-deep oil spill prevention and response, and contrasts the effects of simulated ultra-deep spills in the frontier regions of the Gulf and elsewhere. Recommendations for additional research and public policy changes to lessen the likelihood and impacts of future spills and to improve oil spill response are provided.

S. A. Murawski (✉) · C. H. Ainsworth · S. Gilbert · D. J. Hollander
University of South Florida, College of Marine Science, St. Petersburg, FL, USA
e-mail: smurawski@usf.edu; ainsworth@usf.edu; sherryl@usf.edu; davidh@usf.edu

C. B. Paris
University of Miami, Department of Ocean Sciences, Rosenstiel School of Marine & Atmospheric Science, Miami, FL, USA
e-mail: cparis@rsmas.miami.edu

M. Schlüter
Hamburg University of Technology, Hamburg, Germany
e-mail: michael.schlueter@tuhh.de

D. L. Wetzel
Mote Marine Laboratory, Sarasota, FL, USA
e-mail: dana@mote.org

S. A. Murawski et al. (eds.), *Scenarios and Responses to Future Deep Oil Spills*,
https://doi.org/10.1007/978-3-030-12963-7_1

Keywords Marine oil spills · Ultra-deep · *Deepwater Horizon* · Ixtoc 1 · Frontier oil and gas

1.1 Introduction

Major industrial/environmental disasters – and responses to them – have elicited a wide variety of reactions, including, in some cases, paradigm shifts in oversight, industrial safety practices, legislation, and even political change (Wilson 1973; Jasanoff 1994; Sheail 2007; EVOS 2012; Fidler and Noble 2012; Revkin 2013); no more so than the compelling cases of marine oil spills. After the *Torrey Canyon* tanker grounding and spill off the Cornwall Coast of England in 1967, there were major changes in the international regulation of tanker traffic carrying crude oil. As well, "lessons learned" from that accident were applied during subsequent spills, including foregoing the use of large quantities of detergents, used in quantity during the *Torrey Canyon* spill, in the response to the *Amoco Cadiz* oil spill off Brittany, France, in 1978. Similarly, in the aftermath of the *Exxon Valdez* tanker spill in Prince William Sound, Alaska, in 1989, the US Clean Water Act of 1972 provisions regulating oil spill preparedness and response were updated and memorialized in the Oil Pollution Act of 1990 (OPA-90). While tanker-based accidents have plummeted since those high-profile accidents (Ramseur 2010), the offshore oil industry has become more reliant on ultra-deep sources, particularly for crude oil (Murawski et al. 2020a), and on pipeline transfers from offshore fields to refineries. After the catastrophic *Deepwater Horizon* (DWH) accident in the Gulf of Mexico (GoM), the oil industry has become more cognizant of the need for rapid response to uncontrolled blowouts in ultra-deep waters (≥1500 m), inventing and deploying new "capping stack" configurations (Wood Group Kenny 2016) and equipping blowout preventers with the capability to more efficiently treat uncontrolled blowouts with sub-surface dispersants injected (SSDI) directly into multiphase oil/gas/water flows exiting from blown-out wells. Additionally, and notwithstanding the open questions that persist regarding the efficacy and effects of SSDI (e.g., NASEM 2019; Murawski et al. 2020b), the common perception among regulators and the oil industry is that SSDI was effective in reducing the presence of volatile organic compounds in the vicinity of response workers (Gros et al. 2017) and that the environmental trade-offs of sequestering oil in the deep sea by the application of SSDI outweigh the costs of oil spill mitigation of surfacing oil (French-McCay et al. 2018). The experimental use of SSDI may be one of the enduring legacies of DWH given the few tools available at the time to respond to large, uncontrolled spills in such extreme environments. Clearly, the next deep oil spill response "war" will begin where the DWH spill scenario ended. Despite the ambiguous evidence of the utility of some of the novel approaches used in that response (Gros et al. 2017; Paris et al. 2018; NASEM 2019), government and industry are preparing to conduct large-scale SSDI to combat future uncontrolled deep blowouts.

The global oil industry is rapidly expanding exploration and production into "frontier" areas including the ultra-deep realm (Pinder 2001), regions of the world that are ill-equipped to muster both vigorous industry oversight and large-scale oil spill response (e.g., in the developing world), and some of the harshest environments on earth (e.g., the Arctic; Noble et al. 2013; Suprenand et al. 2020). Expansions into both the geographic and technological (Jin and Castais 2016) frontiers of oil and gas development beg the question regarding the state of preparedness of governments, industries, and the independent science community to anticipate likely oil spill scenarios, reduce or eliminate risk factors, and better prepare for and more efficiently respond to spills in the future.

Using the DWH disaster as a point of departure, this volume considers the questions of oil spill risk reduction, anticipation of the circumstances of future accidents, and oil spill response, from a variety of perspectives. The DWH oil spill occurred at a water depth of 1500 m in the relatively quiescent spring and summer of 2010. How would the scenario have changed had the spill occurred during a different season? Winters in the northern GoM have predominantly northern winds as illustrated by the drifter experiment conducted from the DWH site in January and February described in Haza et al. (2018), showing strong southerly forcing with many drifters moving toward the Yucatan shelf. Likewise, how would have the response and environmental effects of the spill changed if a strong and persistent hurricane had occurred or if the Loop Current system had not formed a strong eddy blocking normal transport to the Florida Straits? While the DWH blowout occurred at about 1500 m, the deepest oil lease in the northern Gulf is nearly twice as deep (2960 m; Murawski et al. 2020a). How would the behavior of released oil and gas and the response scenario have differed had the spill occurred at these extreme depths? Similarly, the oil type involved in the DWH spill (Louisiana Sweet Crude, or LCS) is one of many crude oil types both in the Gulf and elsewhere that are the objects of ultra-deep drilling. Had that accident occurred with a heavier, more viscous, more sulfur-rich ("sour") crude, how would these have altered the characteristics of the spill, its impacts, and the efficacy of response measures?

With respect to locations of future oil spills in the GoM, all three countries (USA, Mexico, Cuba) are now exploring in or developing ultra-deep fields (Murawski et al. 2020a). In the case of the USA and Mexico, spills close to their maritime boundaries (Fig. 1.1) doubtlessly will impact and require multinational responses only peripherally evident for DWH. Currently, a congressionally mandated moratorium in the US eastern GoM (Fig. 1.1) prohibits activities in the region where the highly dynamic Loop Current (Sturges and Lugo-Fernandez 2005; Weisberg and Liu 2017) flows eventually into the Florida Straits and up the Atlantic Seaboard as the Gulf Stream. If oil production occurred along the Florida Escarpment (Fig. 1.1), how would a spill there behave in relation to Loop Current dynamics? Are the risks to ecosystems and livelihoods of a catastrophic spill in the moratorium area (Fig. 1.1; e.g., Nelson and Grubesic 2018) greater than in the western and central GoM?

In the western GoM, both the USA and Mexico are aggressively pressing ocean drilling into the Perdido formation (BOEM 2017; Murawski et al. 2020a and Locker and Hine 2020). A major spill at the Perdido formation would doubtlessly impact

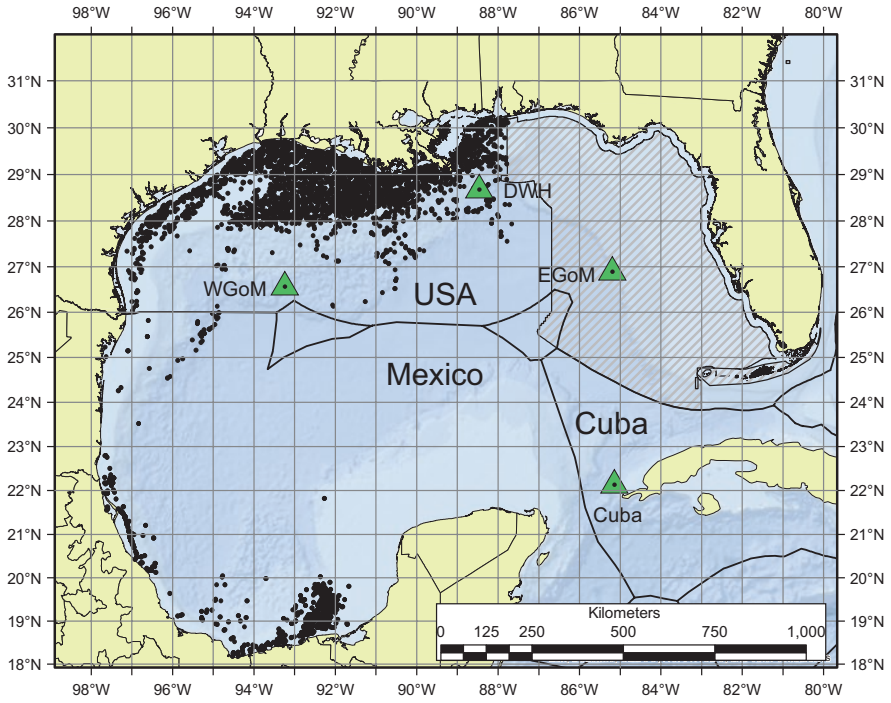

Fig. 1.1 Map of the Gulf of Mexico illustrating the exclusive economic zones (EEZs) of the USA, Mexico, and Cuba. Black dots are the current (2018) locations of oil and gas infrastructure. Triangles are the locations of simulated oil spills in the Gulf that are analyzed herein. Hatched area is the region of the congressionally mandated moratorium on oil and gas development, in place until 2022

US and Mexican ecosystems and a variety of particularly vulnerable species including the Kemp's ridley (*Lepidochelys kempii*) turtle population and their nesting areas at Rancho Nuevo, Mexico (Bevan et al. 2016), migrating sea- and land-based birds, fisheries, and other public uses of coastal areas. Again, how would the impacts and responses to such a spill differ from those of DWH? As the Ixtoc 1 spill demonstrated, oil spills in the SW GoM can have extended footprints and in the extreme advancing to the USA-Mexican border and beyond (Soto et al. 2014; Sun et al. 2015).

The Cuban government and its partners in the global oil and gas exploration and production industries continue to search for lucrative offshore quantities within the Cuban EEZ (Slav 2017; Fig. 1.1). While a number of exploration wells so far have not apparently discovered economically recoverable quantities of oil and gas, this effort continues. Because of the strategic location of Cuba at both the entrance and exit of the GoM (Fig. 1.1), there is a concern that spills at either location would result in broad-scale transport beyond Cuba's territory, and impacts on migratory species.

1.2 Focus of the Book

This volume has three main foci: (1) to summarize the state of knowledge of relevant physical, chemical, geological, and biological properties and processes in the environments where ultra-deep drilling and development are occurring, (2) to simulate and contrast likely scenarios and impacts of hypothetical spills occurring in frontier areas of the GoM and elsewhere, and (3) to evaluate the state of information and recommend additional high-priority science necessary for reducing the likelihood of catastrophic deepwater accidents and for mounting more effective responses to ultra-deep spills should they occur.

The volume overview (Murawski et al. 2020a) provides a narrative history of oil and gas development in the entirety of the GoM and illustrates the evolution from shallow-to-deep sourcing. Recent trends in the GoM mirror those globally (Pinder 2001), as facilitated by rapid advances in oil and gas drilling and production technologies. A petro-geological analysis of the GoM (Chap. 3) provides spatial context for the processes involved in oil and gas formation across geological epochs and provides strong evidence for likely targets of future oil and gas exploration and production in the next several decades (Locker and Hine 2020; BOEM 2017).

Because of the enormous investment in GoM research following the DWH spill, we now have measurements of oil-derived contaminants and associated indicators for broad spatial swaths of the GoM and, in some cases, time series of a variety of oil indicators in the regions of the DWH and Ixtoc 1 blowouts (Lubchenco et al. 2012; Soto et al. 2014). These indicators will be enormously important as broad-scale (but *not* facility-specific) baselines for analyzing the impacts of future spills. Some time series show declining trends in oil contamination levels and recovery of biota 9 years after DWH and nearly 40 years after the Ixtoc 1 spill, while the events remain recorded in continually sequestered, chronologized bottom sediments, in biota and, surprisingly, in GoM waters (Chanton et al. 2020).

Gulf of Mexico's sediments faithfully record not only climate proxies but evidence of volcanic eruptions, human interventions, and, importantly, a chronological history of the use of hydrocarbons over the past century or so (Santschi et al. 2001). Sediments also record large-scale oil spills and their impacts on benthic infauna (Brooks et al. 2020; Schwing et al. 2020; Montagna et al. 2020). The use of novel and advanced technological approaches revealed a persistent carbon isotopic signature of large-scale oil spills in the water column (long after the oil was dissolved, diluted, or transformed; Chanton et al. 2020) which aids in separating oil spill effects from naturally occurring hydrocarbon sources.

The application of "omics-based" "big data" approaches to microbial community analyses provides a quantitative framework for evaluating the resilience of such communities to large-scale contaminant exposure and reveals the opportunistic nature of methanotropic and oil-consuming bacteria when applied to significant spills (Kostka et al. 2020). During DWH there were many proposals to cultivate and release oil-consuming strains of bacteria into the environment to enhance the rate of degradation of oil and other hydrocarbons. However, naturally occurring strains of

the bacterial genome responded quickly to the available food source resulting in relatively rapid degradation. The issue of whether the presence of dispersants retarded or accelerated this process remains a significant uncertainty (Kleindienst et al. 2015; Prince et al. 2016; NASEM 2019).

Isotope analyses of fish and other tissues reveal natural tracers documenting fish migratory pathways and thus exposure potential to localized and broad-scale oil spills (Peebles and Hollander 2020). As well, isotope analyses document biogeochemical pathways that trace petro-carbon through trophic food webs once spilled (Patterson III et al. 2020). Toxicological baselines for GoM fishes now extend throughout the Gulf's continental shelves (Pulster et al. 2020) and into the mesopelagic realm (Romero et al. 2018). Interpreting the significance of contaminants in biota is facilitated by combining field-derived data with laboratory-based exposure trials (Mitchelmore et al. 2020; Raimondo et al. 2020) and aided by modeling studies (Paris et al. 2020a). Impact studies from previous spills, when combined with extensive collections during and after the DWH spill, provide a much more complete picture of both static and dynamic components of environmental baseline parameters, thus allowing much more precise evaluations of the relative exposures and impacts from future GoM spills.

The second focus of this volume is understanding mechanisms of oil spill dynamics under differing circumstances, including physical processes influencing sedimentation and transport of oil (Foekema et al. 2020; Daly et al. 2020). Formation of oiled marine snow ("MOSSFA") was a pathway for sedimentation of significant quantities of oil in both the cases of DWH and Ixtoc 1 (Brooks et al. 2020), resulting in negative effects on benthic habitats and biota (Schwing et al. 2020; Montagna et al. 2020). Both of those spills occurred seaward of riverine deltaic systems (Fig. 1.1). Although the antecedents of MOSSFA formation are not precisely known (Daly et al. 2016), they likely require high concentrations of phytoplankton, fine particle sediments, and oil. Indications are that oil and dispersants result in the production of extracellular polymeric substances (EPS) a glue-like substance enhancing oil/mineral aggregate formation. The oil and gas industries of the GoM and elsewhere are pushing much further offshore, into less productive waters with lower sediment loads. Under these circumstances would we expect as strong MOSSFA events to occur if a sub-surface blowout occurred there (MacDonald et al. 2020; Armenteros et al. 2020; Daly et al. 2020; Berenshtein et al. 2020a)? The specific location of oil spills as well as ancillary environmental conditions (depth, temperature, oil type, season, hydrodynamics, and other factors) is likewise critical in determining the outcomes with respect to spill impacts and severity. A series of oil spill simulations, using the CMS modeling package (Paris et al. 2013, 2020a, b; Berenshtein et al. 2020a, b; Murk et al. 2020, Sutton et al. 2020; Frasier 2020; Chancellor et al. 2020), are described for four GoM locations in frontier oil development areas (Fig. 1.1). These include additional simulations at the DWH site using different seasonal and flow condition sites, as well as eastern, western, and southern GoM locations (Paris et al. 2020a). These simulations are used to rank the relative impacts of the spills on several metrics including the degree of shoreline impact, including ecosystem implications (Berenshtein et al. 2020a). Importantly, one of the

stated reasons for using SSDI is to minimize the degree to which shorelines and coastal areas are oiled (French-McCay et al. 2018). However, spills in the deep central Gulf may result in relatively little weathered oil reaching shorelines (Berenshtein et al. 2020a).

The resilience potential of ecological resources; efficacy of response measures, including fishery closures; and the potential sensitivity of deepwater fish communities, sea turtle populations, and marine mammals are evaluated, with particular reference to resources potentially affected by ultra-deep blowouts (Sutton et al. 2020; Frasier 2020; Chancellor et al. 2020). Oil and gas facility siting and oil spill contingency planning historically have used environmental sensitivity indices (ESIs) to reserve particularly unique areas from siting consideration or to note where special precautions in spill response and mitigation should occur (Jensen et al. 1998). Chancellor et al. (2020) outline a quantitative approach to EISs specifically taking into account deepwater resources and economic dependencies. Unique environmental and human community sensitivities applicable to oil and gas development in frontier Arctic ecosystems are discussed in Suprenand et al. (2020).

The third focal area of this book considers oil spill risk reduction as well as preparations for, and responses to, future ultra-deep spills. Given the controversial use of dispersants as a response measure, applied at the sea surface, and as SSDI, the state of knowledge of the efficacy, mode of application, and environmental and human health effects are reviewed (NASEM 2019; Murawski et al. 2020b). Despite the hundreds of millions of dollars spent on research and oil spill preparedness and prevention in the wake of DWH, there remain important unresolved scientific questions related to the siting of deepwater facilities to reduce risks of catastrophic spills. Likewise, gaps in research exist in spill prevention, preparedness, response, injury assessment, and ecosystem restoration (ICCOPR 2015; Murawski 2020).

1.3 Final Thoughts

The advent of ultra-deep oil and gas production carries with it enormous potential benefits as well as significant – and asymmetric – risks. The use of novel drilling and production technologies, in largely unexplored frontier regions, and with significant unknown, unknowns regarding oil and gas behavior at extreme pressures and temperatures, contributes to the increased risks of ultra-deep water development. Understanding the behavior of oil and gas under these extreme conditions as well as the efficacy of response and mitigation measures can be partially informed by past experience, but:

> "It is often said that the military… are always preparing to fight the last war rather than the next one". – Erwin Canham, 12 January 1945, Christian Science Monitor

In this regard, the next deep oil blowout and ensuing spill, wherever it may happen, will likely occur under fundamentally different conditions than have the two previous sub-surface mega-blowouts (DWH and Ixtoc 1; Fig. 1.1). While the

previous 80+ years of experience in oil exploration and production from the GoM have included responses to literally hundreds of oil spills (Ramseur 2010), a 3000 m blowout will be unlike any previous. Furthermore, the physical oceanographic conditions, appropriateness of response technologies, and the specifics of the casualty will require nimble response approaches informed by rigorous pre-spill planning and anticipatory research. Likewise, the types of significant accidents occurring in other frontier regions of oil and gas development (the Arctic, off developing nations, and in relation to novel recovery strategies, e.g., Jin and Castais 2016) also remain in the realm of "unknown-unknowns." Preparations for such accidents must include scenario analyses and training exercises that are informed by sophisticated modeling tools, experimental and field-level data collected under realistic ambient conditions, and deep understanding of the inherent environmental and human risks of drilling such areas in the first place, as well as the response options available. As the industry extends into *ignotas aquas* of frontier marine oil and gas regions, so too practical scientific research must be forthcoming to support the policy and response decisions necessary to minimize to near zero the risks of such catastrophic events. Furthermore, additional research and active dialog between government regulators, industry, and independent scientists are urgently needed in order to deploy effective, efficient, and environmentally sound response approaches applicable to ever-evolving deepwater scenarios. It is to this task that this book is dedicated.

Acknowledgments This research was made possible by a grant from the Gulf of Mexico Research Initiative/C-IMAGE I, II, and III.

References

Armenteros M, Díaz-Asencio M, Martínez-Suárez A, Hollander DJ, Schwing PT, Larson RA, Gregg Brooks G (2020) Geochemical and faunal characterization in the sediments off the Cuban north and northwest coast (Chap. 9). In: Murawski SA, Ainsworth C, Gilbert S, Hollander D, Paris CB, Schlüter M, Wetzel D (eds) Scenarios and responses to future deep oil spills – fighting the next war. Springer, Cham

Berenshtein I, Perlin N, Ainsworth C, Ortega-Ortiz J, Vaz AC, Paris CB (2020a) Comparison of the spatial extent, impacts to shorelines and ecosystem, and 4-dimensional characteristics of simulated oil Spills (Chap. 20). In: Murawski SA, Ainsworth C, Gilbert S, Hollander D, Paris CB, Schlüter M, Wetzel D (eds) Scenarios and responses to future deep oil spills – fighting the next war. Springer, Cham

Berenshtein I, Perlin N, Murawski SA, Graber H, Samantha Joye S, Paris CB (2020b) Evaluating the effectiveness of fishery closures for deep oil spills using a 4-dimensional model (Chap. 23). In: Murawski SA, Ainsworth C, Gilbert S, Hollander D, Paris CB, Schlüter M, Wetzel D (eds) Scenarios and responses to future deep oil spills – fighting the next war. Springer, Cham

Bevan E, Wibbels T, Najera BMZ, Sarti L, Martinez FI, Cuevas JM, Gallaway BJ, Pena LJ, Burchfield PM (2016) Estimating the historic size and current status of the Kemp's ridley sea turtle (*Lepidochelys kempii*) population. Ecosphere 7:e01244. https://doi.org/10.1002/ecs2.1244

Brooks GR, Larson RA, Schwing PT, Diercks AR, Armenteros-Almanza M, Diaz-Asencio M, Martinez-Suarez A, Sánchez-Cabeza JA, Ruiz-Fernandez A, Herguera-García JC, Perez-Bernal

LH, Hollander DJ (2020) Gulf of Mexico (GoM) bottom sediments and depositional processes: A baseline for future oil spills (Chap. 5). In: Murawski SA, Ainsworth C, Gilbert S, Hollander D, Paris CB, Schlüter M, Wetzel D (eds) Scenarios and responses to future deep oil spills – fighting the next war. Springer, Cham

Chancellor E, Murawski SA, Paris CB, Perruso L, Perlin N (2020) Comparative environmental sensitivity of offshore Gulf of Mexico waters potentially impacted by ultra-deep oil well blowouts (Chap. 26). In: Murawski SA, Ainsworth C, Gilbert S, Hollander D, Paris CB, Schlüter M, Wetzel D (eds) Scenarios and responses to future deep oil spills – fighting the next war. Springer, Cham

Chanton JP, Jaggi A, Radović J, Rosenheim BE, Walker BD, Larter SR, Rogers K, Samantha Bosman S, Oldenburg TBP (2020) Mapping isotopic and dissolved organic matter baselines in waters and sediments of Gulf of Mexico (Chap. 10). In: Murawski SA, Ainsworth C, Gilbert S, Hollander D, Paris CB, Schlüter M, Wetzel D (eds) Scenarios and responses to future deep oil spills – fighting the next war. Springer, Cham

Daly KL, Passow U, Chanton J, Hollander D (2016) Assessing the impacts of oil-associated marine snow formation during and after the Deepwater Horizon oil spill. Anthropocene 13:18–33. https://doi,org/10.1016/j.antecene,2016.01.006

Daly K, Vaz AC, Paris CB (2020) Physical processes influencing the sedimentation and lateral transport of MOSSFA in the NE Gulf of Mexico (Chap. 18). In: Murawski SA, Ainsworth C, Gilbert S, Hollander D, Paris CB, Schlüter M, Wetzel D (eds) Scenarios and responses to future deep oil spills – fighting the next war. Springer, Cham

Exxon Valdez Oil Spill Trustees (EVOS) (2012) Regulations, politics, and oversight: a selected bibliography on the *Exxon Valdez* oil spill. http://www.evostc.state.ak.us/static/PDFs/biblio_regulations.pdf

Fidler C, Noble B (2012) Advancing strategic environmental assessment in the offshore oil and gas sector: lessons from Norway, Canada, and the United Kingdom. Environ Impact Assess Rev 34:12–21. https://doi.org/10.1016/j.eiar.2011.11.004

Foekema EM, van Eenennaam JS, Hollander DJ, Langenhoff AM, Oldenburg TBP, Radović J, Rohal M, Romero IC, Schwing PT, Murk AJ (2020) Testing the effect of MOSSFA (marine oil snow sedimentation and flocculent accumulation) events in benthic microcosms (Chap. 17). In: Murawski SA, Ainsworth C, Gilbert S, Hollander D, Paris CB, Schlüter M, Wetzel D (eds) Scenarios and responses to future deep oil spills – fighting the next war. Springer, Cham

Frasier K (2020) Evaluating impacts of deep oil spills on oceanic marine mammals (Chap. 25). In: Murawski SA, Ainsworth C, Gilbert S, Hollander D, Paris CB, Schlüter M, Wetzel D (eds) Scenarios and responses to future deep oil spills – fighting the next war. Springer, Cham

French-McCay D, Crowley D, Rowe JJ, Bock M, Robinson H, Wenning R, Hayward Walker A, Joeckel J, Nedwed TJ, Parkerton TF (2018) Comparative risk assessment of spill response options for a deepwater oil well blowout: Part 1. Oil spill modeling. Mar Pollut Bull 133:1001–1015

Gros J, Socolofsky SA, Dissanayake AL, Jun I, Zhao L, Boufadel MC, Reddy CM, Areya JS (2017) Petroleum dynamics in the sea and influence of subsea dispersant injection during *Deepwater Horizon*. Proc Natl Acad Sci USA 114:10065–10070

Haza C, D'Asaro E, Chang H, Chen S, Curcic M, Guigand C, Hultley HS, Jacobs G, Novelli G, Özgökmen TM, Poje AC, Ryan E, Shcherbina A (2018) Drogue-loss detection for surface drifters during the Lagrangian Submesoscale experiment (LASER). J Atmos Ocean Technol 35:705–725

Interagency Coordinating Committee on Oil Pollution Research (ICCOPR) (2015) Oil pollution research and technology plan: fiscal years 2015–2021, 270 pp. https://www.bsee.gov/sites/bsee_prod.opengov.ibmcloud.com/files/bsee-interim-document/statistics/2015-iccopr-research-and-technology-plan.pdf

Jasanoff S (ed) (1994) Learning from disaster: risk management after Bhopal. University of Pennsylvania Press, Philadelphia, 291 pp

Jensen JR, Halls JN, Michel J (1998) Systems approach to environmental sensitivity index (ESI) mapping for oil spill contingency planning and response. Photogramm Eng Remote Sens 64:1003–1013

Jin C, Castais G (2016) New frontiers in oil and gas exploration. Springer, Switzerland, 521 pp. https://doi.org/10.1007/978-3-319-40124-9

Kleindienst S, Seidel M, Ziervogel K, Grim S, Loftis K, Harrison S, Malkin SY, Perkins MJ, Field J, Sogin ML, Dittmar T, Passow U, Medeiros PM, Joye SB (2015) Chemical dispersants can suppress the activity of natural oil-degrading microorganisms. Proc Natl Acad Sci USA 112:14900–14905

Kostka JE, Overholt WA, Rodriguez-R LM, Huettel M, Konstantinidis K (2020) Toward a predictive understanding of the benthic microbial community response to oiling on the northern Gulf of Mexico coast (Chap. 11). In: Murawski SA, Ainsworth C, Gilbert S, Hollander D, Paris CB, Schlüter M, Wetzel D (eds) Scenarios and responses to future deep oil spills – fighting the next war. Springer, Cham

Locker S, Hine AC (2020) An overview of the geologic origins of hydrocarbons and production trends in the Gulf of Mexico (Chap. 4). In: Murawski SA, Ainsworth C, Gilbert S, Hollander D, Paris CB, Schlüter M, Wetzel D (eds) Scenarios and responses to future deep oil spills – fighting the next war. Springer, Cham

Lubchenco J, McNutt MK, Dreyfus G, Murawski SA, Kennedy DM, Anastas PT, Chu S, Hunter T (2012) Science in support of the Deepwater Horizon response. Proceedings of the National Academy of Sciences 109(50):20212–20221

MacDonald IR, Gaytan-Caballero A, Escobar-Briones E (2020) The asphalt ecosystem of the southern Gulf of Mexico: abyssal habitats across space and time (Chap. 8). In: Murawski SA, Ainsworth C, Gilbert S, Hollander D, Paris CB, Schlüter M, Wetzel D (eds) Scenarios and responses to future deep oil spills – fighting the next war. Springer, Cham

Mitchelmore CL, Griffitt RJ, Coelho GM, Wetzel DL (2020) Modernizing protocols for aquatic toxicity testing of oil and dispersant (Chap. 14). In: Murawski SA, Ainsworth C, Gilbert S, Hollander D, Paris CB, Schlüter M, Wetzel D (eds) Scenarios and responses to future deep oil spills – fighting the next war. Springer, Cham

Montagna PA, Baguley J, Rowe GT, Wade T (2020) Linking abiotic variables with macrofaunal and meiofaunal abundance and community structure patterns on the Gulf of Mexico continental slope (Chap. 7). In: Murawski SA, Ainsworth C, Gilbert S, Hollander D, Paris CB, Schlüter M, Wetzel D (eds) Scenarios and responses to future deep oil spills – fighting the next war. Springer, Cham

Murawski SA (2020) Perspectives on research, technology, policy and human resources for improved management of ultra-deep oil and gas resources and responses to oil spills (Chap. 29). In: Murawski SA, Ainsworth C, Gilbert S, Hollander D, Paris CB, Schlüter M, Wetzel D (eds) Scenarios and responses to future deep oil spills – fighting the next war. Springer, Cham

Murawski SA, Hollander DJ, Gilbert S, Gracia A (2020a) Deep-water oil and gas production in the Gulf of Mexico, and related global trends (Chap. 2). In: Murawski SA, Ainsworth C, Gilbert S, Hollander D, Paris CB, Schlüter M, Wetzel D (eds) Scenarios and responses to future deep oil spills – fighting the next war. Springer, Cham

Murawski SA, Schlüter M, Paris CB, Aman ZM (2020b) Summary of contemporary research on use of chemical dispersants for deep sea oil spills (Chap. 28). In: Murawski SA, Ainsworth C, Gilbert S, Hollander D, Paris CB, Schlüter M, Wetzel D (eds) Scenarios and responses to future deep oil spills – fighting the next war. Springer, Cham

Murk AJ, Hollander DJ, Chen S, Chuanmin H, Liu Y, Vonk SM, Schwing PT, Gilbert S, Foekema EM (2020) A predictive strategy for mapping locations where future MOSSFA events are expected (Chap. 21). In: Murawski SA, Ainsworth C, Gilbert S, Hollander D, Paris CB, Schlüter M, Wetzel D (eds) Scenarios and responses to future deep oil spills – fighting the next war. Springer, Cham

National Academies of Sciences, Engineering and Medicine (NASEM) (2019) Report of the committee on evaluation of the use of chemical dispersants in oil spill response. National Academies Press, Washington, DC

Nelson JR, Grubesic TH (2018) The implications of oil exploration off the Gulf coast of Florida. J Mar Sci Eng 6. https://doi.org/10.3390/jmse6020030

Noble B, Ketilson S, Aitken A, Poelzer G (2013) Strategic environmental assessment opportunities and risks for Arctic offshore energy planning and development. Mar Policy 39:296–302. https://doi.org/10.1016/j.marpol.2012.12.011

Paris CB, Helgers J, van Sebille E, Srinivasan A (2013) Connectivity modeling system: a probabilistic modeling tool for the multi-scale tracking of biotic and abiotic variability in the ocean. Environ Model Softw 42:47–54

Paris CB, Berenshtein I, Trillo ML, Faillettaz R, Olascoaga MJ, Aman ZM, Schlüter M, Joye SB (2018) BP gulf science data reveals ineffectual subsea dispersant injection for the Macondo blowout. Front Mar Sci 5:389. https://doi.org/10.3389/fmars.2018.00389

Paris CB, Vaz AC, Berenshtein I, Perlin N, Faillettaz R, Aman ZM, Murawski SA (2020a) Simulating deep oil spills beyond the Gulf of Mexico (Chap. 19). In: Murawski SA, Ainsworth C, Gilbert S, Hollander D, Paris CB, Schlüter M, Wetzel D (eds) Scenarios and responses to future deep oil spills – fighting the next war. Springer, Cham

Paris CB, Murawski SA, Olascoaga MJ, Vaz AC, Berenshtein I, Beron-Vera FJ, Miron P, Faillettaz R (2020b) Connectivity of Gulf of Mexico continental shelf fish populations and implications of simulated oil spills (Chap. 22). In: Murawski SA, Ainsworth C, Gilbert S, Hollander D, Paris CB, Schlüter M, Wetzel D (eds) Scenarios and responses to future deep oil spills – fighting the next war. Springer, Cham

Patterson WF III, Chanton JP, Barnett B, Tarnecki JH (2020) The utility of stable and radio isotopes in fish tissues as biogeochemical tracers of marine oil spill food web effects (Chap. 13). In: Murawski SA, Ainsworth C, Gilbert S, Hollander D, Paris CB, Schlüter M, Wetzel D (eds) Scenarios and responses to future deep oil spills – fighting the next war. Springer, Cham

Peebles EB, Hollander DJ (2020) Combining isoscapes with tissue-specific isotope records to recreate the geographic histories of fish (Chap. 12). In: Murawski SA, Ainsworth C, Gilbert S, Hollander D, Paris CB, Schlüter M, Wetzel D (eds) Scenarios and responses to future deep oil spills – fighting the next war. Springer, Cham

Pinder D (2001) Offshore oil and gas: global resource knowledge and technological change. Ocean Coast Manag 44:579–600. https://doi.org/10.1016/S0964-5691(01)00070-9

Prince RC, Coolbaugh TS, Parkerton TF (2016) Oil dispersants do facilitate biodegradation of spilled oil. Proc Natl Acad Sci USA 113:E1421. https://doi.org/10.1073/pnas.1525333113

Pulster EL, Gracia A, Snyder SM, Romero IC, Carr B, Toro-Farmer G, Murawski SA (2020) Polycyclic aromatic hydrocarbon baselines in Gulf of Mexico fishes (Chap. 15). In: Murawski SA, Ainsworth C, Gilbert S, Hollander D, Paris CB, Schlüter M, Wetzel D (eds) Scenarios and responses to future deep oil spills – fighting the next war. Springer, Cham

Raimondo S, Awkerman JA, Yee S, Barron MG (2020) Case Study: using a combined laboratory, field, and modeling approach to assess oil spill impacts (Chap. 16). In: Murawski SA, Ainsworth C, Gilbert S, Hollander D, Paris CB, Schlüter M, Wetzel D (eds) Scenarios and responses to future deep oil spills – fighting the next war. Springer, Cham

Ramseur JL (2010) Oil spills in U.S. coastal waters: background, governance, and issues for congress. Congressional research service 7-5700, RL33705, 34 pp

Revkin AC (2013) Love Canal and its mixed legacy. New York Times, November 25, 2013. https://www.nytimes.com/2013/11/25/booming/love-canal-and-its-mixed-legacy.html

Romero IC, Sutton T, Carr B, Quintana-Rizzo E, Ross SW, Hollander DJ, Torres JJ (2018) Decadal assessment of polycyclic aromatic hydrocarbons in mesopelagic fishes from the Gulf of Mexico reveals exposure to oil-derived sources. Environ Sci Technol (online). https://doi.org/10.1021/acs.est.8b02243

Santschi PH, Presley BJ, Wade TL, Garcia-Romero B, Baskaran M (2001) Historical contamination of PAHs, PCBs, DDTs, and heavy metals in Mississippi River Delta, Galveston Bay and Tampa Bay sediment cores. Mar Environ Res 52:51–79

Schwing PT, Montagna PA, Machain-Castillo ML, Escobar-Briones E, Rohal M (2020) Benthic faunal baselines in the Gulf of Mexico: a precursor to evaluate future impacts (Chap. 6). In: Murawski SA, Ainsworth C, Gilbert S, Hollander D, Paris CB, Schlüter M, Wetzel D (eds) Scenarios and responses to future deep oil spills – fighting the next war. Springer, Cham

Sheail J (2007) *Torrey Canyon*: the political dimension. J Contemp Hist 42:485–504

Slav I (2017) Cuba eager to develop offshore oil reserves. Oilprice.Com. Published online: https://oilprice.com/Latest-Energy-News/World-News/Cuba-Eager-to-Develop-Offshore-Oil-Reserves.html

Soto LA, Botello AV, Licea-Durán S, Lizárraga-Partida M, Yáñez-Arancibia A (2014) The environmental legacy of the Ixtoc 1 oil spill in Campeche sound, southwestern Gulf of Mexico. Front Mar Sci 1:1–9

Sturges W, Lugo-Fernandez A (eds) (2005) Circulation in the Gulf of Mexico: observations and models. American Geophysical Union, Geophysical Monograph 161, 347 pp

Sun S, Hu C, Tunnell JW Jr (2015) Surface oil footprint and trajectory of the Ixtoc-I oil spill determined from Landsat/MSS and CZCS observations. Mar Pollut Bull 101:632–641. https://doi.org/10.1016/j.marpolbul.2015.10.036

Suprenand PM, Hoover C, Ainsworth CH, Dornberger L, Johnson CJ (2020) Preparing for the inevitable: ecological and indigenous community impacts of oil spill-related mortality in the United States Arctic marine ecosystem (Chap. 27). In: Murawski SA, Ainsworth C, Gilbert S, Hollander D, Paris CB, Schlüter M, Wetzel D (eds) Scenarios and responses to future deep oil spills – fighting the next war. Springer, Cham

Sutton T, Frank T, Judkins H, Romero IC (2020) As Gulf oil extraction goes deeper, who is at risk? Community structure, distribution, and connectivity of the deep-pelagic fauna (Chap. 24). In: Murawski SA, Ainsworth C, Gilbert S, Hollander D, Paris CB, Schlüter M, Wetzel D (eds) Scenarios and responses to future deep oil spills – fighting the next war. Springer, Cham

U.S. Bureau of Ocean Energy Management (BOEM) (2017) Assessment of technically and economically recoverable hydrocarbon resources of the Gulf of Mexico Outer Continental Shelf as of January 1, 2014. OCS Report BOEM 2017-005, 44 pp. https://www.boem.gov/BOEM-2017-005/

Weisberg RH, Liu Y (2017) On the loop current penetration into the Gulf of Mexico. J Geophys Res Oceans 122:9679–9694. https://doi.org/10.1002/2017JC013330

Wilson CV (1973) The impact of the *Torrey Canyon* disaster on technology and national and international efforts to deal with supertanker generated oil pollution: an impetus for change? M.A. Thesis, University of Montana. Graduate student theses, dissertations, & professional papers 8988. https://scholarworks.umt.edu/etd/8988?utm_source=scholarworks.umt.edu%2Fetd%2F8988&utm_medium=PDF&utm_campaign=PDFCoverPages

Wood Group Kenny (2016) Subsea capping stack technology requirements. Final report prepared for the Bureau of Safety and Environmental Enforcement, 188 pp. https://www.bsee.gov/sites/bsee.gov/files/research-reports//756aa.pdf

Chapter 2
Deepwater Oil and Gas Production in the Gulf of Mexico and Related Global Trends

Steven A. Murawski, David J. Hollander, Sherryl Gilbert, and Adolfo Gracia

Abstract The marine oil industry in the Gulf of Mexico (GoM) began in 1938 with the construction of the first oil well platform built in 4 meters of water, a mile off the Louisiana coast. The Mexican marine oil industry began in the 1950s with exploration and low-level production off the city of Tampico in the state of Tamaulipas. The discovery of the massive Cantarell oil field off Campeche in 1976 led to rapid expansion of the Mexican industry, surpassing US production of GoM-derived oil. Total annual oil production from the GoM peaked in 2003 at 1.6 billion barrels, but has since declined to about 1.2 billion barrels. Production at the Cantarell field peaked in 2004 and has since declined by 90%. Both the US and Mexican oil industries have focused more recently on deepwater plays to support production. The US oil production by lease depth showed a steady offshore migration through the 1990s but a dramatic rise in ultra-deep (e.g., ≥1500 m water depth) production beginning in the 2000s. In 2017, 52% of US oil production was from ultra-deep wells. Beginning in 2013, Mexico liberalized its policies to allow international cooperative ventures for exploration and production, particularly focusing on deepwater sources. Several large discoveries off Mexico since 2015 portend higher offshore production in the 2020s when these fields come online. In the US GoM, marine-derived natural gas production has declined by 79% since 1997, to about 1 trillion ft^3 in 2017, reflecting rapid increases in land-based gas sources from hydraulic fracturing, which are less expensive to produce that marine-derived gas. Over the next decade, shallow-water sources of oil and gas in the US GoM will be phased out or reduced in importance as additional ultra-deep sources are developed. In the US GoM these include plays in depths to 3000 m and potentially deeper off Mexico. Ultra-deep sources occurring in the "Golden Triangle" between West Africa, Brazil, and the GoM will likely dominate global ultra-deepwater production, but other frontier

S. A. Murawski (✉) · D. J. Hollander · S. Gilbert
University of South Florida, College of Marine Science, St. Petersburg, FL, USA
e-mail: smurawski@usf.edu; davidh@usf.edu; sherryl@usf.edu

A. Gracia
Universidad Nacional Autónoma de México, Instituto de Ciencias del Mar y Limnología, México City, Mexico
e-mail: gracia@unam.mx

S. A. Murawski et al. (eds.), *Scenarios and Responses to Future Deep Oil Spills*,
https://doi.org/10.1007/978-3-030-12963-7_2

regions will doubtlessly be explored. The inherent risks of catastrophic well blowouts at extreme depths will increase as the productivity of oil facilities increases exponentially with water depth.

Keywords Ultra-deep oil · Congressional moratorium · Gulf of Mexico · Cantarell

2.1 Introduction

This book considers the potential impacts and responses to another large-scale, deepwater oil spill occurring in the Gulf of Mexico (GoM; Fig. 2.1) or elsewhere in the world. We synthesize many published research studies and especially focus on scientific investigations conducted during and after the *Deepwater Horizon* accident (Lubchenco et al. 2012). While the focus of the book is on factors controlling the fate, distribution, and ecological consequences of such spills, equally important

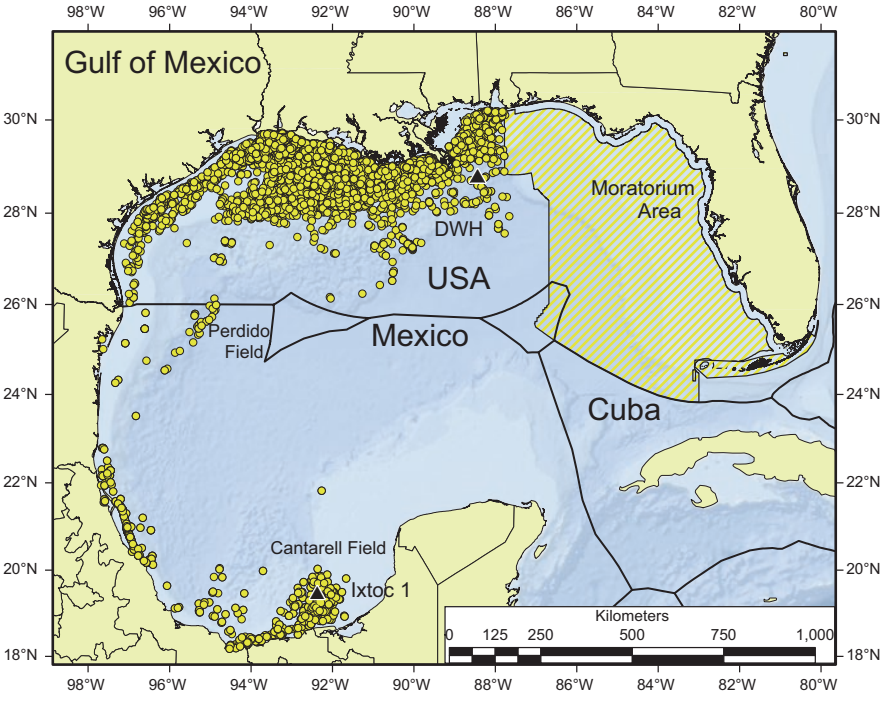

Fig. 2.1 Geographic distribution of offshore oil and gas infrastructure facilities (yellow circles) in the Gulf of Mexico (GoM), 2017. (Data are from BOEM and PEMEX). Also illustrated are the exclusive economic zone (EEZ) boundaries between the USA, Mexico, and Cuba, as well as the US Congressional moratorium boundary on new oil and gas drilling (applicable until 2022). The locations of the Ixtoc 1 and *Deepwater Horizon* (DWH) oil blowouts are plotted as black triangles

considerations are where and under what circumstances such a deepwater blowout might again occur. Using the eight-decade history of marine oil and gas exploration and production from the GoM, including documentation from the USA and Mexico, we review the history and trends in spatial distribution, production, utilization, and management of the Gulf's oil industries. We also provide global perspectives on deepwater oil development and thus where in the world deep spill responses are most likely to be necessary.

2.2 History of Oil Development and Production in the Gulf of Mexico

Marine oil and gas development in the GoM was initiated in 1938 with the construction of a 320 × 180 ft wooden deck from which a drilling derrick sank a well in 4 m (14 ft) of water. The initial Superior-Pure State No. 1 well was located about a mile offshore of Creole, Louisiana (AOGHS 2018; Duncan et al. 2018). It successfully produced oil but was destroyed by a hurricane in 1940, then subsequently rebuilt, and put back into production. In 1947 Kerr-McGee drilled the first marine oil well out of sight of land in 6 m of water 10 miles from shore. This well would eventually yield 1.4 million stock tank barrels (=42 gallons, defined at sea level pressure) and 307 million ft^3 of natural gas (AOGHS 2018). By the end of 1949, there were 11 oil and natural gas fields in the northern GoM (AOGHS 2018). A critical management issue resolved in the 1940s and early 1950s was the ownership of so-called tidelands (Austin et al. 2008), finally investing the authority to sell leases and regulate the offshore industry extensive of state territorial waters, in the federal government, through the Outer Continental Shelf (OCS) Lands Act of 1953. The OCSLA defines the OCS as all submerged lands lying seaward of state coastal waters which are now under the US jurisdiction (Austin et al. 2008). The OCSLA thus substantially predated the establishment of the 200 nm exclusive economic zone (EEZ) by the USA in 1980 (Fig. 2.1), which asserted control over a wider variety of natural resources.

Between the 1940s and the 1970s, the US oil industry in the GoM gradually evolved to mid-continental shelf depths (Table 2.1) as technology advanced and larger plays of higher producing oil and gas were discovered. Annual oil production increased between the 1940s and 1970s from about 7 million barrels per year (MBPY) in the 1950s to about 290 MBPY in the 1970s (Table 2.1; Fig. 2.2). Throughout this period, the technology for exploratory drilling evolved but was primarily based on derricks fixed to the ocean bottom or so-called "jack-up" rigs, consisting of a platform the legs of which could be systematically lowered to the sea bottom to support drilling operations, but subsequently jacked up and moved to other locations. These types of MODUs (Mobile Offshore Drilling Units) are appropriate for water depths to about 200 m. During the 1970s to the early 1990s, total oil production was stable, but the maximum depths of wells increased to about 700 m in the 1980s and 1300 m in the 1990s. This necessitated the development of drilling

Table 2.1 Total oil production by decade and water depths of extraction from US waters of the Gulf of Mexico, 1948–2018

Years	Total production (million barrels)	Mean depth (m)	Median depth (m)	Maximum depth (m)	Proportion from ultra-deep waters (>1500 m)
1947–1949	0.28	7	6	17	0.00
1950–1959	70.24	17	14	59	0.00
1960–1969	1324.06	26	19	159	0.00
1970–1979	2888.99	42	34	399	0.00
1980–1989	2727.25	81	56	728	0.00
1990–1999	2966.50	250	79	1337	0.00
2000–2009	4261.41	869	790	2432	0.15
2010–2018*	3984.04	1346	1355	2936	0.41
2017	587.15	1510	1670	2936	0.52

Depths are the maximum lease block depths as reported to BOEM/MMS. The data for 2018 (*) include only the months of January and February

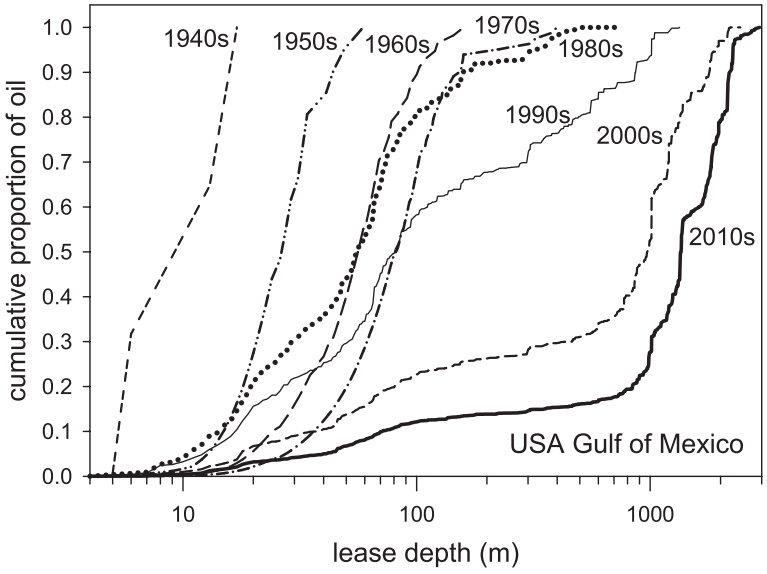

Fig. 2.2 Cumulative decadal oil production (Table 2.1) by maximum lease depth in US waters of the GoM, 1948–2017. (Data are derived from the Bureau of Ocean Energy Management (BOEM): https://www.data.boem.gov/)

apparatus not fixed to the sea bottom but rather tethered by anchoring systems or dynamically positioned with the platforms floating at the surface (see Nixon et al. 2016 for a timeline of technology developments in offshore exploration and production equipment). The discovery and later production from the deepwater *Cognac* field by Shell Exploration and Production Company in 1975 was the first platform to exceed 300 m water depth and ushered in a new era of engineering development for deep tethered drilling and production systems. These deepwater technologies have included:

Semi-submersible platforms Floating and semi-submersible platforms that can be moved, have buoyancy tanks, and are anchored to the seafloor. Their positions over well drilling or production operations are maintained through mooring systems or dynamic positioning (DP) technologies based on global positioning systems (GPS). The maximum depth of semi-submersibles is about 3000 m water depth.

Drill ships Vessels with drilling capabilities used primarily for exploration of new oil fields or specific wells. As with semisubmersible platforms, positions over the well are maintained with anchoring systems and DP. Maximum depths of drill ships can be ~3700 m.

Compliant towers These production platforms are modifications of shallow-water systems that consist instead of thinner, flexible towers and affixed to a traditional foundation. Compliant towers can withstand significant torsion, typical in ocean currents, and are used in water depths ranging up to 1000 m.

Floating production systems Floating production systems (FPSs) are used to support marine operations and do not, themselves, drill for or produce from existing wells; there are a number of types of FPSs including FPSOs (floating production, storage, and offloading systems), FSOs (floating storage and offloading systems), and FSUs (floating storage units).

Tension-leg platforms Are floating platforms tethered to the seabed in ways that eliminate most lateral movements. Tension-leg platforms can be deployed in water depths to 2000 m.

Spar platforms Spar platforms consist of a large cylindrical center tank with ballast weights and mooring tethers. They are highly stable platforms that can be deployed in depths in excess of 3000 m.

Using variants of the above deepwater technologies, offshore oil production dramatically increased in the US GoM since the 1990s (Figs. 2.2, 2.3, and 2.4). In the USA, oil production since the early 1990s has risen to a record of 653 million barrels in 2017 and was 634 million barrels in 2018. Over the past 25 years, the total oil production from the US GoM has cycled with economic conditions (demand), the degree of regulation, and other factors (Fig. 2.4). Notwithstanding the 2010 *Deepwater Horizon* accident and short-term impacts on the industry (National Commission on the BP Deepwater Horizon Oil Spill and Offshore Drilling 2011; Lubchenco et al. 2012), however, production increased steadily between 2013 and

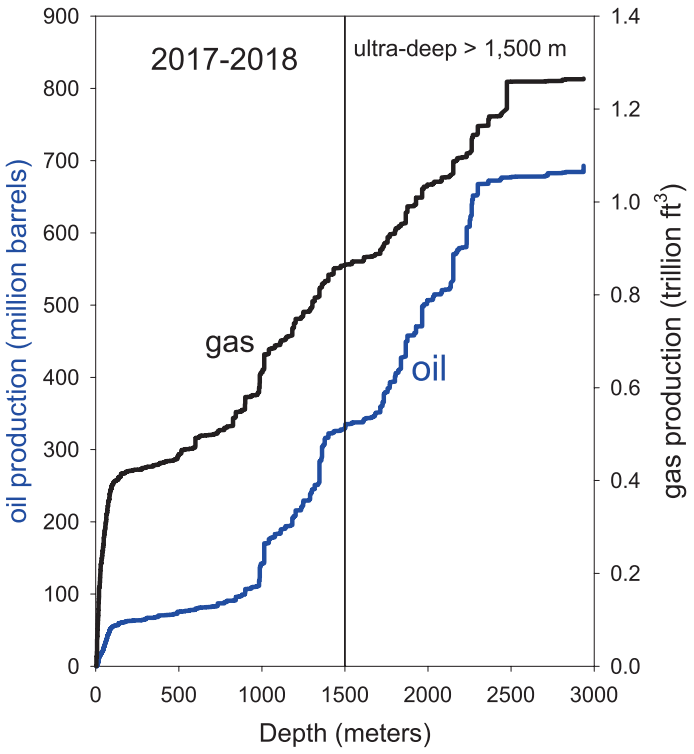

Fig. 2.3 Cumulative crude oil and natural gas production by maximum lease depth (m) in the US GoM, 2017–2018. The commonly accepted definition of "ultra-deep" production is ≥1500 m

2017 (Fig. 2.4). In 2010, GoM oil production accounted for nearly 30% of all domestic oil production in the USA including terrestrial and other ocean-derived sources. The proportion of total domestic production from the GoM has since declined to about 20% in 2017 as additional onshore supplies have been developed.

One of the most pronounced trends in US GoM production over the past two decades has been the rise in the contribution of ultra-deep oil sources to total oil removals (Figs. 2.2 and 2.3; Table 2.1). Since 2000, the fraction of total GoM production from ultra-deep wells has risen from about 15% (2000–2009) to, in 2017, 52% (Table 2.1; Figs. 2.2, 2.3, and 2.4). This trend has been fueled by additional discoveries of fields in 2–3000 m of water (Fig. 2.3). In recent years, the development of deep oil production facilities has allowed multiple well locations to be serviced on the same lease. Despite the extremely high costs to develop and deploy deepwater technologies, the average monthly lease production increases exponentially with lease depth (Fig. 2.5), and thus, depending on the break-even price for deepwater production, deepwater sources can be enormously profitable. For example, using 2017 data (Fig. 2.5), the average monthly production from a lease 200 m deep (on the continental shelf) is predicted to be about 20.9 thousand barrels

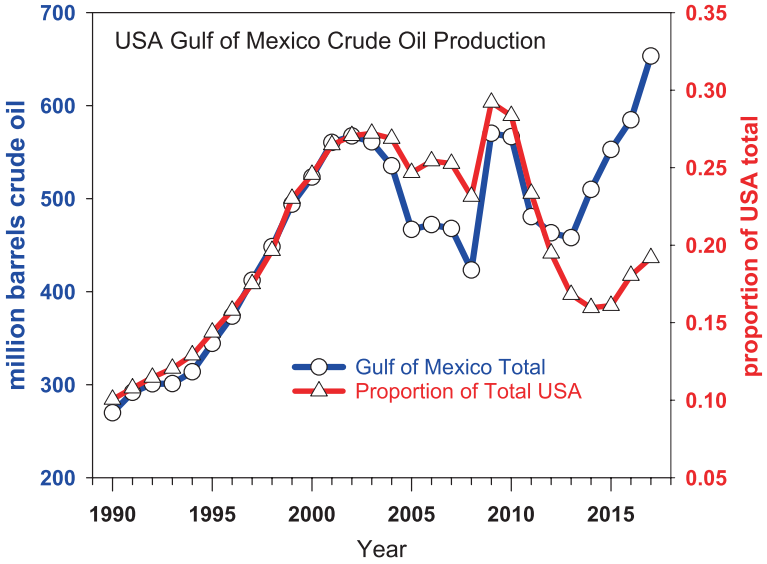

Fig. 2.4 Total US crude oil production from the GoM and proportion of all US oil production coming from marine waters of the Gulf, 1990–2017. Data may be slightly higher than Table 2.1 because of incomplete reporting by lease

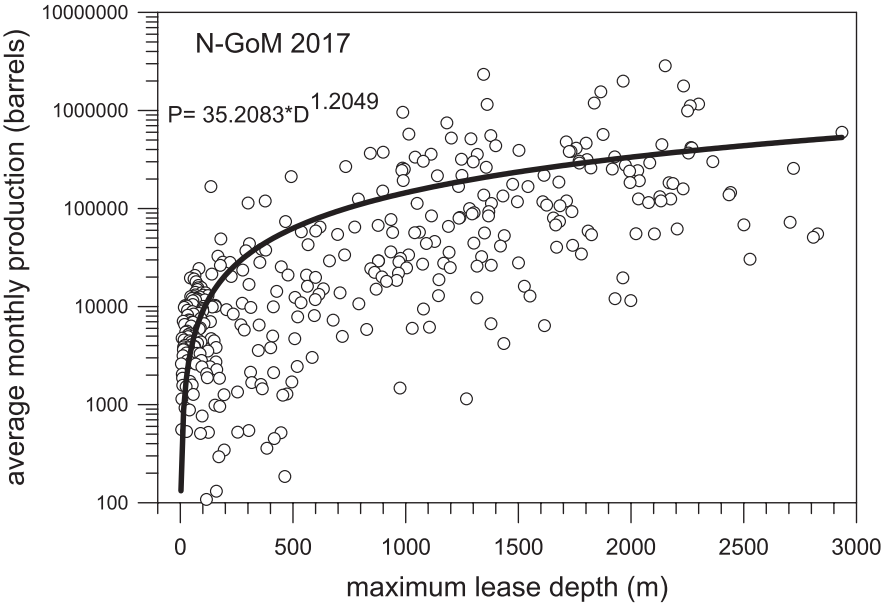

Fig. 2.5 Relationship between maximum lease depth (m) and monthly average crude oil production for each reporting lease block in the US Gulf of Mexico, 2017

per month, whereas an ultra-deep lease at 2200 m yields a predicted 374.9 thousand barrels per month – 18 times greater productivity. The highest producing lease in the US GoM in 2017 yielded 2.8 million barrels per month (Fig. 2.5). Of course, investment costs for deepwater operations are much higher than for shallower plays. Thus, depending on the cost-to-oil revenue ratio, offshore leases can be more profitable relative to traditional inshore sources. Higher productivity of the ultra-deep sources is due to the relatively large sizes of the underlying oil reservoirs and facilitated by the enormous reservoir pressures, which allow the oil to come to sea level without the aid of pumping equipment (N.B., overpressured wells also exist in shallower waters). This represents both a driver of the economics of deepwater production and a potential risk factor, as oil and gas mixtures are under enormous pressures and temperatures emanating from the source reservoirs.

Notwithstanding the increasing trend in oil production from the US portion of the GoM (Fig. 2.4), production of natural gas from the US GoM has plummeted since 1997 (Fig. 2.6). In the late 1990s, GoM gas comprised over 20% of all domestic gas production in the country. By 2017, the total quantity of gas produced from the GoM declined by 79% to just over 1 trillion ft^3 (Fig. 2.6). The proportion of total domestic gas production from the GoM declined from 22% to just 3% during this period (Fig. 2.6). This enormous decline in gas production from marine waters of the GoM can be attributed to the steep decline in gas prices and increased supplies

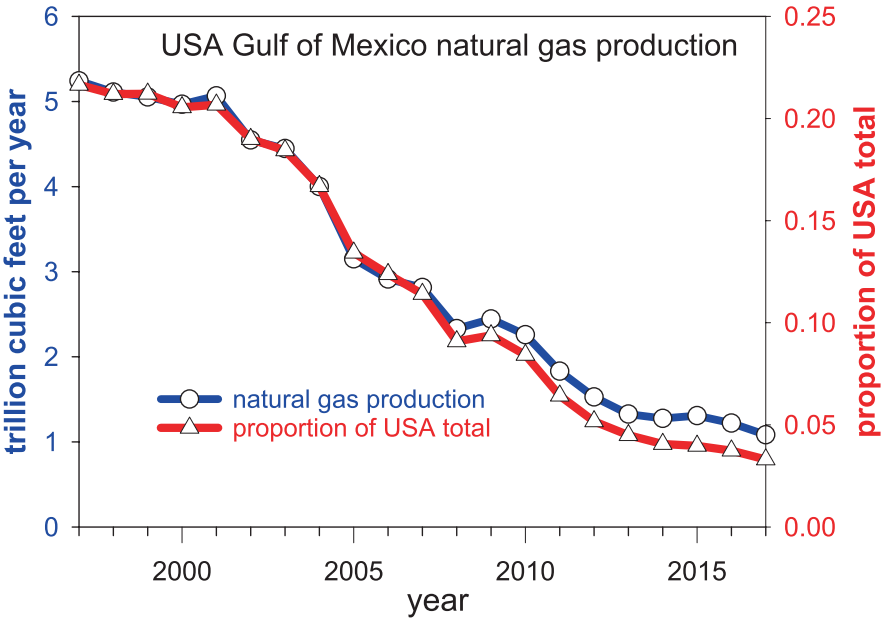

Fig. 2.6 Total natural gas production from US waters of the GoM and proportion of the US total gas production, 1990–2017. (Data are derived from BOEM: https://www.data.boem.gov/)

owing to the development of land-based hydraulic fracturing ("fracking"). Gas production in the Gulf is generally derived from shallower sources than for oil (e.g., Fig. 2.3); in 2017 and early 2018 30% of total gas production was from leases ≤100 m water depth, whereas only about 8% of oil came from ≤100 m (Fig. 2.3). Thus, many of the shallow-water, predominantly gas-producing, leases have been abandoned over the past decade, resulting in accelerated decommissioning of these plugged and abandoned structures, particularly in shallow waters off Texas and Louisiana (Fig. 2.1; GAO 2017). Since many of the deepwater structures have no permanent foundations or pillars, decommissioning will peak as the US industry continues its trend to ultra-deep oil production and reduced emphasis on shallow-water natural gas.

In 2006 the US Congress enacted and then President George W. Bush signed the Gulf of Mexico Energy Security Act of 2006. This law placed a large section of the federal government's Eastern Planning Area under a moratorium from oil and gas leasing, exploration, and development until 2022 (Fig. 2.1). The law was enacted ostensibly to limit offshore activities so as not to interfere with military training activities in the NE GoM and to address concerns about potential environmental harm to coastal tourism and fishing-centric economies off Florida.

Mexican Oil Industry With its beginnings at the turn of the twentieth century, the Mexican oil industry was landlocked until the 1950s. This included nationalization of Mexican petroleum industries in 1938 (Haber et al. 2003) and the subsequent formation of the state-run Petróleos Mexicanos (PEMEX), which had a monopoly on exploration, production, and distribution of oil, gas, and petrochemicals in Mexico. The development of the first offshore oil and gas wells off Mexico occurred in the 1950s off the city of Tampico in the northeastern state of Tamaulipas (adjacent to the USA). It was not until the 1970s, however, that significant offshore oil and gas resources off Mexico were identified and put into production. In 1972 fisherman Rudesindo Cantarell Jimenez noticed the presence of oil off the coast of Campeche, which eventually led in 1976 to the discovery of the massive Cantarell oil field complex (Guzmán 2013; Duncan et al. 2018; Fig. 2.1). The Cantarell field was for many years the primary production region for the Mexican industry (Fig. 2.7). Cantarell production increased steadily from its inception in 1976, to its peak of about 0.8 billion barrels 2004. The Cantarell field was the location of the Ixtoc 1 marine blowout in 1979–1980 (Soto et al. 2014), which resulted in, at that time, the largest marine blowout in history, leaking about 3.3 million barrels of crude oil over a 9-month period. The Ixtoc 1 blowout was in relatively shallow waters – 54 m water depth.

After the peak in crude oil production from the Cantarell field in 2004, crude oil production from the field has declined by 90% (Fig. 2.7). In the past decade, PEMEX has sought to sustain productivity of oil and gas at Cantarell by using a variety of techniques including nitrogen injection to increase yields from those aging fields. However, those strategies have not arrested declines. Resultantly, other shallow-

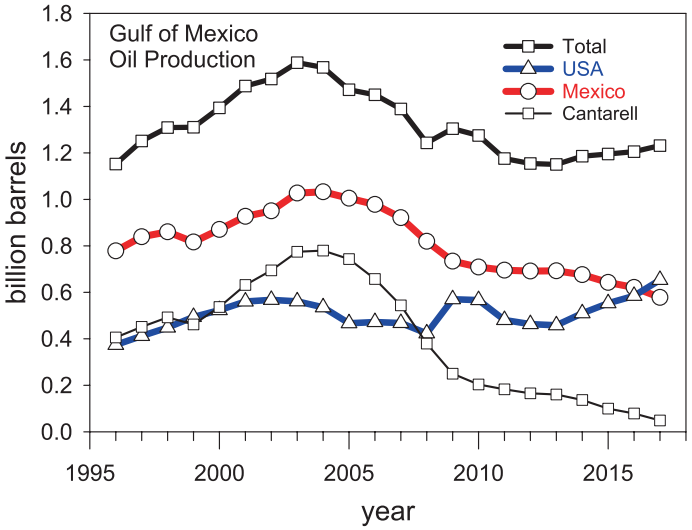

Fig. 2.7 Total GoM marine crude oil production, 1996–2017. Data are presented for the USA and Mexico individually and in total. Total crude oil production for the Cantarell oil field (Fig. 2.1), in the Campeche region off Mexico, is also presented. (Mexican data are from PEMEX (2007, 2016))

water fields are now producing the bulk of crude oil and gas from the Mexican GoM, but overall oil production still declined from about 1 billion barrels in 2004 to about 0.6 billion barrels in 2017. For the first time in several decades, US crude oil production from the GoM slightly exceeds that of Mexico (Fig. 2.7). Overall production (Mexico+USA) of crude oil from the GoM was about 1.2 billion barrels in 2017, about 25% below the maximum production of 1.6 billion barrels in 2003 (Fig. 2.7).

Recognizing the need to develop its deepwater assets, in 2013 the Mexican government liberalized its monopoly on oil and gas production to allow joint ventures with international partners. This has led to the discovery of extensive new deep and ultra-deep reservoirs in the Perdido region off Tamaulipas (Fig. 2.1) and off the state of Veracruz. Significant production from these fields, however, will not occur until the 2020s, and thus crude oil production off Mexico may decline further in the next few years as shallow-water fields exhaust.

Cuban Oil Industry Off Cuba the state-owned oil company Cuba Petrol Union (CUPET) produces about 4 million barrel equivalents per year with about 50,000 barrels per day mostly coming from the coastal reserve areas east of Havana (Slav 2017). These wells are in very shallow coastal areas or at the coastal margin (Fig. 2.8). Beginning in 2013, Cuba undertook several cooperative ventures with other international state-run oil companies to explore deepwater regions in the GoM. These exploration wells have not yet identified economically recoverable quantities of oil, but interest in deepwater sources off NW Cuba continues.

Fig. 2.8 Coastal oil production facility off the NW Cuban coast east of Havana. (Photograph credit: C-IMAGE)

2.3 The Future of Oil and Gas Development in the Gulf of Mexico

As noted above, the USA, Mexico, and Cuba are engaged in significant, ongoing efforts to identify, explore, and produce ultra-deepwater resources off their coasts. While only the USA now produces from ultra-deep wells, the share of total production from them has increased to more than half of all crude oil generated, and there is no indication of a reversal in trend. Much of the investment in exploration and expensive infrastructure for ultra-deep drilling in both the USA and Mexico occurred when crude oil prices were relatively low and profitability from ultra-deep was marginal. Given recent price increases (and recognizing the volatility in them), these facilities are now producing above break-even costs, and thus efforts directed to the ultra-deep GoM will likely intensify further.

Natural gas is produced both in wells specifically drilled into primarily gas-bearing formations and is a by-product of multiphase flow from predominantly oil fields. Over the next decade or two, investment in exclusive gas wells in the US GoM may be curtailed or phased out altogether, resulting in further declines in gas production for the USA and accelerated decommissioning of much of the shallow-water infrastructure along the Texas and Louisiana coasts (Fig. 2.9; GAO 2017). This scenario depends on market forces and developments in the terrestrial-based

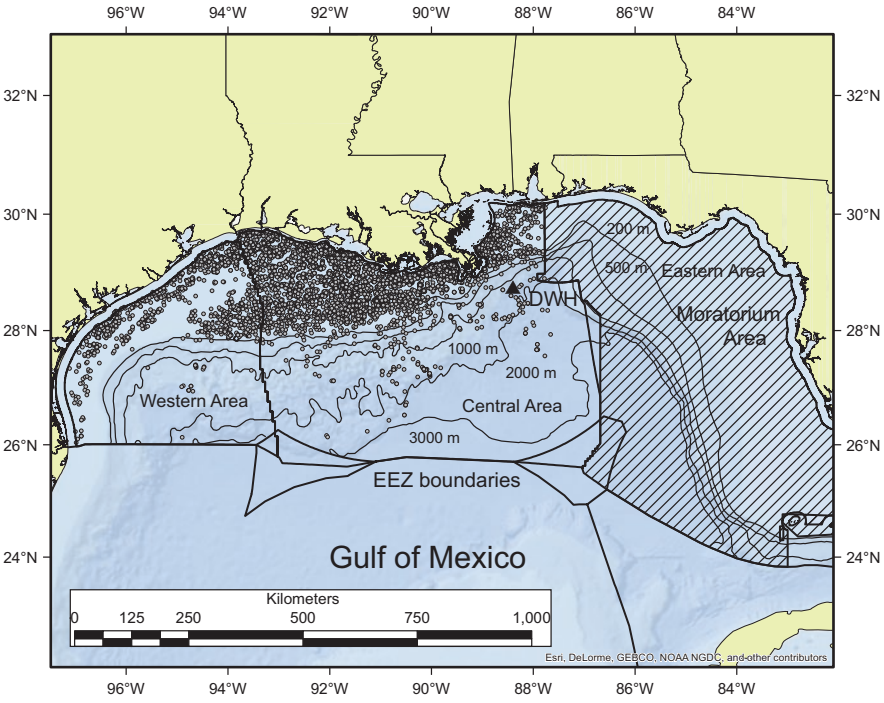

Fig. 2.9 The US GoM region with bathymetry (200, 500, 1000, 2000, and 3000 meter isobaths) and locations of existing oil and gas infrastructure, 2017. The boundaries of the Congressional moratorium as well as the Western, Central, and Eastern Planning areas of BOEM are also plotted

gas industries. Off Mexico, the situation is different since the country is a net importer of natural gas and fracking ashore is not yet prevalent in Mexico. Thus, predominantly shallow-water gas production will likely continue off Mexico for some time to come.

Deepwater fields in Mexico (e.g., Perdido; off Veracruz; Fig. 2.1) will come online in the 2020s. If the US example is pertinent, it is likely that the total Mexican crude oil production will thus increase as well. Given the large, relatively unexplored region in SW GoM >1,500 m deep (Fig. 2.1), it is likely that additional productive, ultra-deep plays will be discovered and produced there. Thus, concerns about the potential impacts of deepwater blowouts off Mexico will increase.

Off the USA, the directionalities of crude oil and gas production are clear. Extensive areas of BOEM's Western and Central Planning Districts exist in 2–3000 m water depths (Fig. 2.9), but development of ultra-deep fields there has been stagnant relative to those in the eastern portion of the Central Planning District (Fig. 2.9; Locker and Hine 2020). Some of the most extensive new finds are in the Central Planning area south and east of the DWH site (Fig. 2.9), including Shell's Appomattox field, and it is clear that the industry will press the western boundaries of the Congressional moratorium area (Fig. 2.9). What is unclear is the fate of the moratorium area post-2022. The moratorium area contains the majority of the

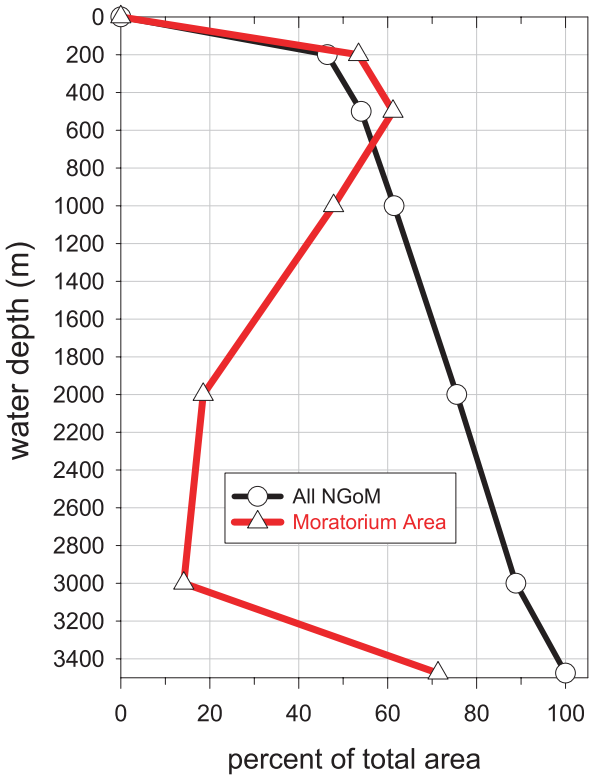

Fig. 2.10 Bathymetric profile (black line) of the northern GoM. The profile is a cumulative plot of the proportion of the US GoM existing at the shallower depths (e.g., 46% is 0–200 m, 89% is ≤3000 m). The red line is the proportion of the Gulf in each depth interval that occurs in the Congressional moratorium area (Fig. 2.9; e.g., 53% of the area ≤200 m is in the moratorium area, but only 14% of the region between 2000 and 3000 m is under moratorium)

Gulf's shallow water, including about 53% of the US GoM ≤200 m and over 60% of the area from 200 to 500 m (Figs. 2.9 and 2.10). On the other hand, the isobaths between 100 and 3000 m are very compact along the eastern shelf edge (known as the Florida Escarpment) with only 14% of the US GoM between 2 and 3000 m within the moratorium boundaries (Fig. 2.10). The majority of US areas >3000 m (71%) lie within the moratorium boundaries. However, the maximum lease depth as of 2017 was 2960 m. While not currently being explored, areas >3000 m are likely to be technically workable in the future.

Politics and the balance of sectoral economic issues (e.g., opposition from tourism, coastal real estate and fishing business, support from energy sectors) will determine the ultimate fate of the moratorium area post-2022. However, one important consideration regarding oil and gas production in the Florida Escarpment region is the presence of the Loop Current and its cyclonic and anticyclonic rings (Weisberg and Liu 2017). The current systems run northwestward from the Yucatan Channel, looping east and doubling back near the edge of the West Florida Shelf (Fig. 2.9). The current regularly flows at 0.8 ms^{-1} and can reach 1.7 ms^{-1}, which is be problematic for long pipe strings, particularly in ultra-deep waters. Thus, while the oil in this region may be technically recoverable, there are added risks associated with the much more dynamic oceanographic conditions in the moratorium area, and likewise,

should a deep blowout occur at a well below the Loop Current, some modeling scenarios show that oil impact Florida's east and west coasts, Cuba, and the Bahamas (Paris et al. 2020 and Berenshtein et al. 2020), depending on the strength and direction of the currents (Weisberg and Liu 2017) the well flow rate and duration of uncontrolled blowouts.

Recent developments in the land-based oil and gas industries have included various technological (well stimulation) approaches to increase productivity of marginal or abandoned fields by using various injection approaches. These have included fracking (fracturing shale formations with high-pressure fluids), nitrogen injection, and other approaches. While relatively rare in the marine environment (EPA 2017), some of these well stimulation approaches may be brought into greater use for under-producing GoM oil wells in the future. The ultra-deep sector will be dominated by large multinational companies with access to substantial capital resources necessary to explore and produce in that environment. What will the smaller, independent companies do then? While they may partner with larger companies, one strategy in the medium term may be to use these novel recovery techniques to put back into production fields abandoned as under-producing by the standards of ultra-deep wells (e.g., Fig. 2.6).

2.4 Global Deepwater Resource Development

The US Energy Information Administration currently estimates that about 30% of global oil production is derived from marine sources (EIA 2016). Five of the 50+ countries involved in offshore oil development – Saudi Arabia, Brazil, Mexico, Norway, and the USA – accounted for about 43% of marine oil production in 2015 (EIA 2016). Only three countries (Brazil, USA, and Angola) currently produce significant quantities from ultra-deep sources, with the USA and Brazil accounting for >90% of ultra-deep production, although this will change rapidly as the technical challenges of operating at extreme depths are resolved.

A number of oil companies and consultants have identified publically where they think viable ultra-deep resources will be produced either now or in the future (Fig. 2.11). Using maps by Reid (2014) and Guzman et al. (2013), we composited a map of these likely opportunities (Fig. 2.11). Consistently, the most favorable areas mentioned are within the so-called golden triangle between the Gulf of Mexico, Brazil, and West Africa. This is not surprising since these are proven oil fields with at least some current track record of ultra-deep plays and favorable administrative and regulatory environments. Whether ultra-deep oil and gas production is viable in regions such as East Africa, the Caspian Sea, off NW Europe, NW Australia, and in the South China Sea will depend on investment decisions for exploration, logistical considerations, and political issues.

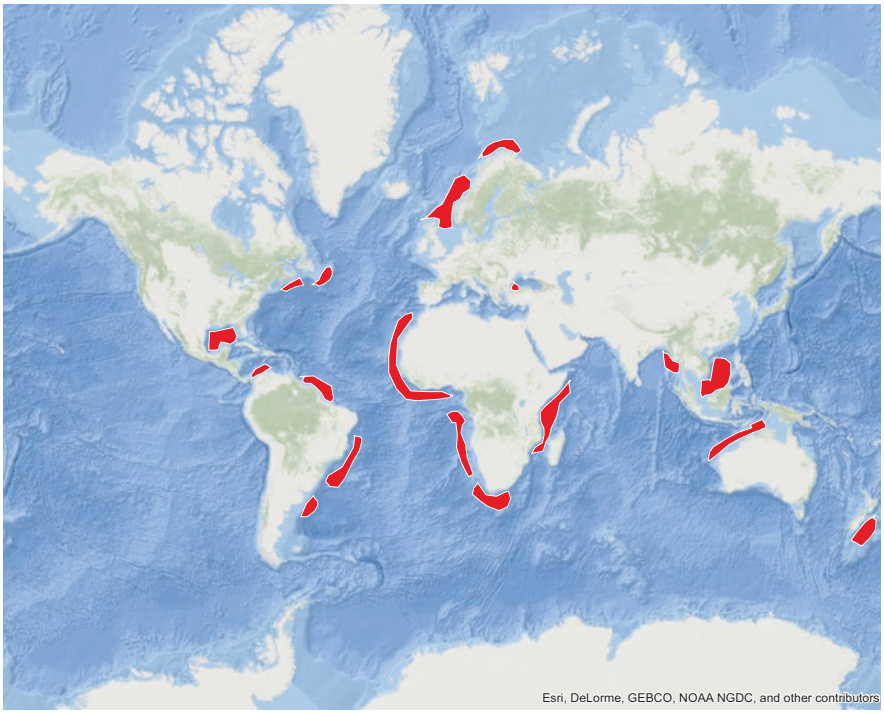

Fig. 2.11 Regions of the world's oceans where ultra-deep (≥1500 m) oil and gas production either exists today or are likely prospects for future exploration. (Data were compiled from various online sources including Reid (2014) and Guzman et al. (2013))

2.5 Summary

Continued exploration and production of ultra-deepwater fields will be a persistent trend for the marine oil and gas industries in the GoM and elsewhere for the foreseeable future. Increased scrutiny of the deepwater sector will occur with the objectives of that oversight being to reduce the likelihood of catastrophic blowouts and more effective mitigation and more timely attenuation of uncontrolled blowouts if they occur. Assisting in these efforts will be an increasingly sophisticated body of science synthesized herein.

Acknowledgments We very much appreciate the thorough manuscript review by Elmer (Bud) Danenberger and Ruth Perry, Shell Exploration and Production Company. This research was made possible by a grant from The Gulf of Mexico Research Initiative/C-IMAGE I, II, and III.

References

American Oil and Gas Historical Society (AOGHS) (2018) Offshore petroleum history. Published online: https://aoghs.org/offshore-history/offshore-oil-history/

Austin DE, Priest T, Penney L, Pratt J, Pulsipher AG, Abel J, Taylor J (2008) History of the offshore oil and gas industry in southern Louisiana. Volume I: Papers on the evolving offshore industry. U.S. Dept. of the Interior, Minerals Management Service, Gulf of Mexico OCS Region, New Orleans, LA. OCS Study MMS 2008-042, 264 pp

Berenshtein I, Perlin N, Ainsworth C, Ortega-Ortiz J, Vaz AC, Paris CB (2020) Comparison of the spatial extent, impacts to shorelines and ecosystem, and 4-dimensional characteristics of simulated oil Spills (Chap. 20). In: Murawski SA, Ainsworth C, Gilbert S, Hollander D, Paris CB, Schlüter M, Wetzel D (eds) Scenarios and responses to future deep oil spills – fighting the next war. Springer, Cham

Duncan T, Braathen BI, McCormack N, Stauble M, Campbell L, Cizek M, Rasmussen S, Khurana S, Wilson J (2018) One GoM: exploring cross-boundary synergies, challenges. Offshore (Published online): https://www.offshore-mag.com/articles/print/volume-78/issue-6/gulf-of-mexico/one-gom-exploring-cross-boundary-synergies-challenges.html

Guzmán AE (2013) The petroleum history of México: how it got to where it is today. Published online: http://www.searchanddiscovery.com/pdfz/documents/2013/10530guzman/ndx_guzman.pdf.html

Guzman R, Carvajal P, Thuriaux-Alemán B (2013) Opportunities and challenges for global deepwater players: an industry on the search for new growth areas. 2013. Published Online: http://www.adlittle.com/sites/default/files/prism/Global_deepwater.pdf

Haber S, Maurer N, Razo A (2003) When the law does not matter: the rise and decline of the Mexican oil industry. J Econ Hist 63:1–32

Locker S, Hine AC (2020) An overview of the geologic origins of hydrocarbons and production trends in the Gulf of Mexico (Chap. 4). In: Murawski SA, Ainsworth C, Gilbert S, Hollander D, Paris CB, Schlüter M, Wetzel D (eds) Scenarios and responses to future deep oil spills – fighting the next war. Springer, Cham

Lubchenco J, McNutt MK, Dreyfus G, Murawski SA, Kennedy DM, Anastas PT, Chu S, Hunter T (2012) Science in support of the *Deepwater Horizon* response. Proc Natl Acad Sci 109:20212–20221

National Commission on the BP *Deepwater Horizon* Oil Spill and Offshore Drilling (2011) Deep water: the gulf oil disaster and the future of offshore drilling. Report to the President, 398 pp. https://www.gpo.gov/fdsys/pkg/GPO-OILCOMMISSION/pdf/GPO-OILCOMMISSION.pdf

Nixon L, Kazanis E, Alonso S (2016) Deepwater gulf of Mexico, December 31, 2014. OCS Report BOEM 2016-057. Bureau of Ocean Energy Management, 89 pp

Paris CB, Vaz AC, Berenshtein I, Perlin N, Faillettaz R, Aman ZM (2020) Simulating deep oil spills beyond the Gulf of Mexico: key ingredients for successful oil transport prediction (Chap. 19). In: Murawski SA, Ainsworth C, Gilbert S, Hollander D, Paris CB, Schlüter M, Wetzel D (eds) Scenarios and responses to future deep oil spills – fighting the next war. Springer, Cham

PEMEX (2007) Statistical yearbook 2007. Published online: http://www.pemex.com/en/investors/publications/Paginas/statistical-yearbook.aspx

PEMEX (2016) Statistical yearbook 2016. Published online: http://www.pemex.com/en/investors/publications/Paginas/statistical-yearbook.aspx

Reid D (2014) Deepwater Gulf of Mexico emerging plays: the basin that continues to deliver. https://s3.amazonaws.com/images.hartenergy.com/Interactive+Article/Offshore+Optimism/docs/Shell%20Americas-Emerging%20Plays-Oct14.pdf

Slav I (2017) Cuba eager to develop offshore oil reserves. Published online: https://oilprice.com/Latest-Energy-News/World-News/Cuba-Eager-to-Develop-Offshore-Oil-Reserves.html

Soto LA, Botello AV, Licea-Durán S, Lizárraga-Partida M, Yáñez-Arancibia A (2014) The environmental legacy of the Ixtoc-1 oil spill in Campeche Sound, Southwestern Gulf of Mexico. Front Mar Sci 1:1–9

U.S. Energy Information Administration (EIA) (2016) Offshore production nearly 30% of global crude oil output in 2015. https://www.eia.gov/todayinenergy/index.php?tg=%20offshore

U.S. Environmental Protection Agency (EPA) (2017) Final National Pollutant Discharge Elimination System (NPDES) general permit No. GEG460000 for offshore oil and gas activities in the Eastern Gulf of Mexico. Region 4 permit

United States Government Accountability Office (GAO) (2017) Offshore oil and gas resources: information on infrastructure decommissioning and federal financial risk. Statement of Frank Rusco, Director, Natural Resources and Environment, Testimony Before the Subcommittee on Energy and Mineral Resources, Committee on Natural Resources, House of Representatives, Wednesday, May 17, 2017. GAO-17-642T, 23 pp

Weisberg RH, Liu Y (2017) On the Loop Current penetration into the Gulf of Mexico. J Geophys Res Oceans 122:9679–9694. https://doi.org/10.1002/2017JC013330

Chapter 3
Spilled Oil Composition and the Natural Carbon Cycle: The True Drivers of Environmental Fate and Effects of Oil Spills

Edward B. Overton, Dana L. Wetzel, Jeffrey K. Wickliffe, and Puspa L. Adhikari

Abstract Rachel Carson's 1962 landmark book, *Silent Spring*, describing the toxic effects of the persistent organic pesticide, DDT, was instrumental in bringing awareness to the notion of environmental pollution (Carson, Silent spring. Houghton Mifflin, Boston, 1962). This work was a catalyst that began the advancement of the global environmental pollution movement and the concern for persistent chemical pollutants (POP). By intentional design, POPs are chemically nonreactive and are resistant to degradation in aerobic environments. It is important to realize that oil pollution and toxicity derived from the polycyclic aromatic hydrocarbon (PAH) components in crude oil are fundamentally different from the chemistry of persistent organic pollutions and its bioaccumulation and magnification that were learned in the 1960s and 1970s. Petroleum hydrocarbons are not stable; they are, in fact, quite reactive in aerobic environments via microbial (Varjani, Bioresour Technol 223:277–286, 2017; Atlas and Hazen, Environ Sci Technol 45:6709–6715, 2011; Salminen et al., Biodegradation 15:29–39, 2004; Widdel and Rabus, Curr Opin Biotechnol 12:259–276, 2001) and photochemical (D'Auria et al., J Hazard Mater

E. B. Overton (✉)
Louisiana State University, Department of Environmental Sciences, Baton Rouge, LA, USA
e-mail: ebovert@lsu.edu

D. L. Wetzel
Mote Marine Laboratory, Environmental Laboratory for Forensics, Sarasota, FL, USA
e-mail: dana@mote.org

J. K. Wickliffe
Tulane University, School of Public Health and Tropical Medicine, New Orleans, LA, USA
e-mail: jwicklif@tulane.edu

P. L. Adhikari
Florida Gulf Coast University, Department of Marine and Ecological Sciences, Fort Myers, FL, USA
e-mail: padhikari@fgcu.edu

S. A. Murawski et al. (eds.), *Scenarios and Responses to Future Deep Oil Spills*,
https://doi.org/10.1007/978-3-030-12963-7_3

164:32–38, 2009; Plata et al., Environ Sci Technol 42:2432–2438, 2008; Garrett et al., Environ Sci Technol 32:3719–3723, 1998; Overton EB, Laseter JL, Mascarella SW, Raschke C, Nuiry I, Farrington JW (1980) Photochemical oxidation of IXTOC I oil, pp 341–383. In: Proceedings of symposium on preliminary results from the September 1979 Researcher/Pierce IXTOC I Cruise. Key Biscayne, Florida, June 9–10, 1980, NOAA Office of Marine Pollution Assessment, Boulder, CO) oxidations. To understand the implications of oil spills, we need to recognize that we are dealing with the reduced form of a pollutant that can readily react in most of the environments. The goal of this chapter is to present the dynamics of an oil spill from the molecular level with a description of the carbon cycle, the role of photosynthesis, diagenetic production of oil, its ultimate conversion back to carbon dioxide, and the fundamental carbon cycle processes in environmental chemistry. Only by understanding what happens chemically to spilled oil can we accurately predict and understand the biological consequences of these spills and the harm done by exposures to hydrocarbons from oil.

Keywords Carbon cycle · Diagenesis · Catagenesis · Live oil · Dead oil · Oxidation

3.1 Introduction

Rachel Carson's 1962 landmark book, *Silent Spring*, describing the toxic effects of the persistent organic pesticide, DDT, was instrumental in bringing awareness to the notion of environmental pollution (Carson 1962). This work was a catalyst that began the advancement of the global environmental pollution movement and the concern for persistent chemical pollutants. Listed by the International Stockholm Convention as chemicals targeted for elimination, persistent organic pollutants (POPs) were originally manufactured to be stable compounds (Stockholm Convention on Persistent Organic Pollutants 2005, http://www.pops.int/). By intentional design, POPs are chemically nonreactive (neither oxidizing nor reducing) and are resistant to degradation in an aerobic environment. It is important to realize that oil pollution and toxicity derived from the polycyclic aromatic hydrocarbon (PAH) components in crude oil are fundamentally different from the concepts of pollution that were learned in the 1960s and 1970s. Petroleum hydrocarbons are not stable; they are, in fact, quite reactive and readily react in an aerobic environment, e.g., microbial (Varjani 2017; Atlas and Hazen 2011; Salminen et al. 2004; Widdel and Rabus 2001) and photochemical (D'Auria et al. 2009; Plata et al. 2008; Garrett et al. 1998; Overton et al. 1980) degradation of petroleum hydrocarbons. To understand the implications of oil spills, we need to recognize that we are dealing with the reduced form of a pollutant that can readily react in most of the environments. The goal of this chapter is to present the dynamics of an oil spill from the molecular level with a description of the carbon cycle, the role of photosynthesis, diagenetic production of oil and its ultimate conversion back to carbon dioxide, and the fundamental carbon cycle processes in environmental chemistry. Only by understanding what

happens chemically to spilled oil can we accurately predict and understand the biological consequences of these spills and the harm done by exposures to hydrocarbons from oil.

3.2 Carbon Cycle

In order to fully appreciate the consequences of oil spills, we should have a general understanding of the environmental chemistry of oil's major component, carbon. Of all the elements in the periodic table, carbon is the primary element in all animals and living systems as well as dead and decaying matter. Further, carbon, in the form of molecules made up of a backbone carbon and hydrogen structures, together with lesser amounts of other atoms like oxygen, nitrogen, and sulfur, forms the major composition of living organisms and their nonliving residues. Thus, understanding the carbon cycle and the fates and effects of carbon-containing compounds in our environment is a first step toward understanding the chemistry, implications, and mitigative actions associated with oil spills.

3.3 Biologically Stored Energy

Basically, all organic matter on earth was derived from the most chemically stable form of carbon, carbon dioxide (CO_2). Through the process of photosynthesis, energy from sunlight, with the help of chlorophyll catalysts, breaks the carbon-oxygen bonds of CO_2 and the hydrogen-oxygen bonds of water (H_2O) and forms new molecules containing carbon, hydrogen, and oxygen with a general molecular ratio of $\{CH_2O\}$ (as in glucose). This is the approximated molecular ratio of the many organic components of living organic matter. The organic matter on earth is produced through photosynthesis. Life, in turn, requires the use of the energy stored in the carbon-hydrogen bonds of biomass, as food for metabolism and energy for motion. Hydrocarbons are produced with energy from the sun and have some of the sun's energy stored because of hydrocarbons' ability to react with oxygen, thus going back to the stable form of carbon, CO_2, while releasing stored energy. This reaction of hydrocarbon-type compounds with molecular oxygen releases the stored energy, through either metabolism or combustion, and can produce additional biomass. This reaction also clearly demonstrates that hydrocarbon-type compounds are chemically very reactive.

3.4 Environmental Redox Reactions

Chemists refer to reactions that reduce the oxygen content of molecules containing carbon as a "reduction reactions," while reactions that increase the oxygen content of molecules containing carbon as "oxidation reactions." Reduction reactions

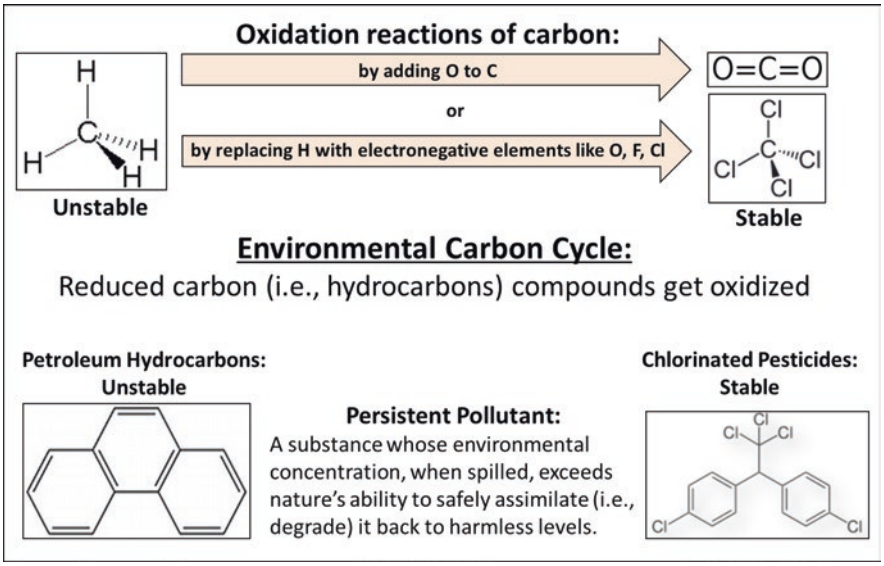

Fig. 3.1 Carbon cycle – oxidation of hydrocarbons to more stable compounds involves replacing hydrogen with more electronegative elements

require energy to cause the reaction to occur, while oxidation reactions release energy. Thus, photosynthesis is a reduction reaction, while metabolism and combustions are oxidation reactions (Fig. 3.1). Photosynthesis requires energy from the sun (or possibly some other source such as geothermal), while oxidations give off energy useful for life and movement. The bottom line is that reduced forms of carbon contain stored energy and are reactive, while the oxidized forms of carbon, like CO_2, are stable to further reactions. It is also important to realize that unstable forms of carbon (like hydrocarbons), while these compounds have the ability to react with oxygen, first require either the input of "activation energy" to start the reaction (such as a spark) or a catalyst to lower this activation energy, thus allowing the oxidation to proceed and evolve energy. Further, there must be an opportunity for oxidation reaction to occur, where the reactive hydrocarbons and oxygen are mixed. For example, if methane and air are mixed, but the methane levels are either below the LEL (lower explosion limit), or above the UEL (upper explosion limit), even with a spark, no oxidation will occur. Similar requirements exist for metabolism or combustion. Burning occurs in the air, and compounds with very low vapor pressures do not produce enough vapors to support combustion without being heated. Metabolism will not occur unless the hydrocarbons are soluble enough to be ingested by some mechanism, thus allowing enzymatically catalyzed oxidations. This is why asphalt roads do not degrade and why asphalt lakes exist around deep-sea oil seeps. Even though these lakes are made of a reduced form of carbon, they are so insoluble that they cannot be readily degraded by natural organisms.

Carbon- and hydrogen-containing compounds can go through a sequence of steps that lessens the stored energy content of these molecules. For example, each

addition of an oxygen atom to carbon-containing molecules lowers the stored energy content in that molecule, until all of the carbon has been converted to its most stable form, CO_2. Thus, as hydrogen atoms in hydrocarbon-type molecules are replaced with oxygen, the resulting molecule will give off less energy when either metabolized or combusted (ethanol gasoline produces less miles per gallon than normal gasoline). Chemists have formulated various descriptions to describe oxidation reaction that releases energy. The most common definition is that when an atom like carbon loses an electron, the carbon atom is oxidized. Another way of looking at this is that when a hydrogen atom in a hydrocarbon is replaced by an element like oxygen, which is more electronegative than hydrogen, this reaction is an oxidation. Thus, reducing the number of hydrogen atoms attached to a carbon atom in hydrocarbons or increasing the number of oxygen atoms in hydrocarbon molecules results in an oxidation reaction, and this reaction will release energy. This is the carbon cycle where CO_2 is converted into hydrocarbon-type molecules which have stored energy (Fig. 3.1). As these hydrocarbon-type molecules react with oxygen during metabolism or combustion, the stored energy is released in the conversion of carbon back to its most stable form, CO_2.

3.5 Understanding the Differences Between Persistent and Reactive Pollutants

To understand what happens when oil is spilled into our environment, we need to recognize the implications of the carbon cycle. All hydrocarbon-type molecules, which make up the complex mixture we call crude oil, are reactive and can be oxidized back to CO_2. The advent of the environmental movement in the 1960s and 1970s with the recognition of human activity putting hazardous chemicals into our environment was the impetus for the formation of the Environmental Protection Agency (EPA) and the passage of environmental laws like the Clean Air Act and the Clean Water Act, the Toxic Substance Control Act, and other important environmental legislations. This movement and these laws recognized that certain manufactured chemicals, such as the environmentally stable chlorinated chemicals (chlorinated pesticides, chlorofluorocarbons (CFCs), PCBs, etc.), were accumulating in our environment, implying that they were not being removed by the natural carbon cycle (Fig. 3.1). The resulting accumulation of these chemically stable compounds caused unanticipated harmful consequences on natural resources and human life. Why was this accumulation happening? In essence, during their manufacturing process, when the hydrogen atoms in the carbon-hydrogen bonds of these new man-made chemicals were replaced with atoms that are more electronegative than hydrogen (like chlorine or fluorine), an oxidation reaction occurred creating compounds that were much more environmentally stable than the hydrocarbons they replaced. For example, when methane (CH_4) is converted to a CFC like Freon (CCl_2F_2), an oxidized form of carbon is produced that is stable to further oxidation, meaning that the CFCs will not naturally react in our tropospheric environment. For many

applications, this inertness was a key characteristic. These CFC compounds were not toxic and would not explode and were very useful industrial chemicals in many important applications, from air conditioning to spray-can propellants. However, because these compounds were now an oxidized form of carbon, this means that they would not react, and they would also not degrade in our troposphere. The stability of these molecules, so important for use in a number of industrial applications, led to a buildup of CFC compounds in the tropospheric atmosphere. This buildup in the lower atmosphere ultimately caused severe environmental damage as these CFCs, stable in the troposphere, moved into the upper atmosphere (i.e., the stratosphere) encountering the extremely high solar energy UV radiation. This UV radiation caused CFCs to break apart, and then a chlorine atom reacted with upper-level ozone, removing ozone from the stratosphere. Removal of upper-level stratospheric ozone then allowed this extremely high solar energy UV radiation to penetrate into the zone of our atmosphere where all life occurs and where this high-energy radiation causes unwanted and very damaging reactions in living plants and animals (Solomon 1999). The same scenario, characterized by environmental persistence, initially thought useful in agricultural application, was encountered with chlorinated pesticides, such as the legacy pesticide DDT. Tragically, it was soon found that the buildup of DDT had significant, unanticipated, and harmful environmental effects associated with any number of hormonal reactions in fish and fowl, followed by insidious accumulation in the food chain consumed by humans (Pimentel 2005; Longnecker et al. 1997).

A vital step in assessing potential impacts of any chemicals introduced into our environment, including those from oil spills, is to recognize the difference in molecular reactivity between hydrocarbon (oil) pollution, the reduced form of carbon, and the oxidized form of carbon found in chlorocarbon pollutants. Hydrocarbons are extremely reactive compounds, and with the appropriate catalysts in place (microorganisms and/or tropospheric sunlight) and the opportunity to react, they can react quickly when entering the environment (Ward et al. 2018; Aeppli et al. 2014; Atlas and Hazen 2011; Garrett et al. 1998; Overton et al. 1980). This ability to react is the basis of concern for causing harm during an oil spill, as opposed to the inertness (persistence) of oxidized pollutant impacts found with environmental contaminants like the chlorocarbons. Oxidized environmental contaminants will build up in the environment and can be biomagnified to harmful levels, whereas reduced environmental contaminants readily react, and it is this reaction that can causes environmental harm. Thus, understanding the impacts and consequences of oil spills requires an understanding of the composition of crude oil.

3.6 Origin of Crude Oil

Crude oil is the common name for a very complex chemical mixture of many thousands of hydrocarbon-type compounds (and some small amounts of chelated heavy metals) that is extracted from deep below the earth's surface. This mixture has been

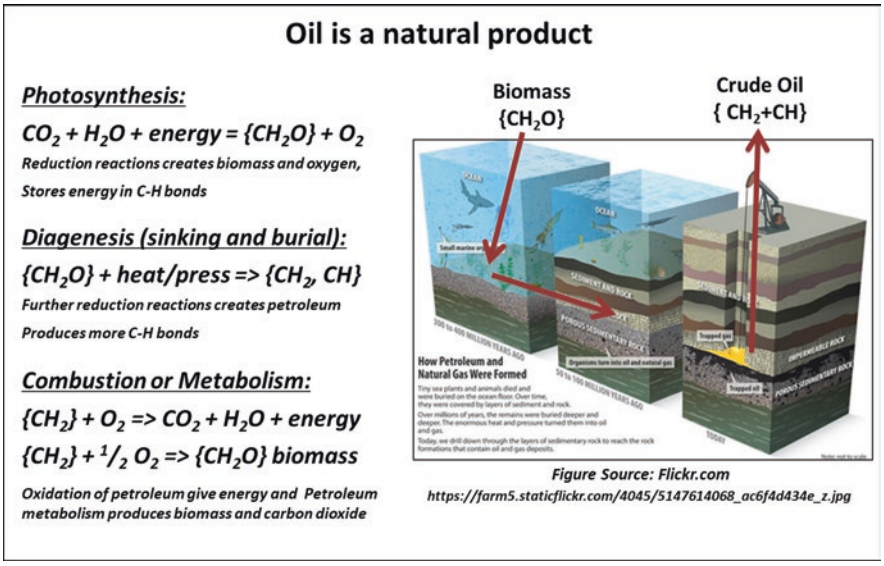

Fig. 3.2 The process of formation of oil in natural environments. (Image from: https://socratic.org/questions/how-does-the-formation-of-coal-differ-from-that-of-natural-gas-and-oil, http://creativecommons.org/licenses/by-nc-sa/4.0/)

produced from the long-ago deposition and degradation of mostly plant biological material. When organic biomass from plant residues were deposited deep within the earth's crust, the organic material was subjected to high temperatures and pressures (diagenesis), which over time transformed the plant residues into natural petroleum carbon resources (catagenesis) that can be extracted from the earth as crude oil and natural gas. So, oil and natural gas are derived from biological materials whose composition has been modified by diagenesis and catagenesis over many millions of years to produce the complex mixture of hydrocarbon and heteroatom hydrocarbon compounds that make up petroleum and the various fossil fuels (Overton et al. 2016). Typically, all crude oils, regardless of their source, are made up of the same types of molecular hydrocarbons. However, the quantities of specific hydrocarbon molecules in crude oil from a given reservoir will depend upon the reservoir's location, depth, and age. So, the same types of molecular structures are found in all oils, but their respective quantities will vary depending upon the source reservoir.

Figure 3.2 highlights the process leading to the formation of crude oil reservoirs deep beneath the earth's surface. Photosynthesis produces a reduced form of carbon with the general molecular formula $\{CH_2O\}$, which is the approximate carbon/hydrogen/oxygen ratios in all living matter and its residues. A portion of the plant residues from living matter were carried to the ocean floors and deposited deep within the earth's crust. Over the millennia, some of this organic material was further stripped of its remaining oxygen content, a reduction reaction, producing further reduced forms of organic compounds. The very complex chemical mixture, produced through a variety of subsurface processes, results from the conversion of

{CH_2O} biomass material into compounds containing mostly {CH_2} carbon-hydrogen ratios, with lesser amounts of {CH} carbon-hydrogen ratio compounds (i.e., aromatic compounds). Most of these newly reduced carbon compounds do not resemble their initial starting material found in the deposited biomass. However, there are some molecular structures in this complex mixture that are closely associated with their initial molecular compositions, with fused saturated rings similar to those structures found in steroid- and pigment-type biomass compounds. Also, some of the reduced material has incorporated sulfur and nitrogen atoms in their molecular structures. In general, diagenesis/catagenesis processes, acting on buried biomass, produce the complex mixture of carbon-containing molecules in deep earth reservoirs with from one to over a hundred carbon atoms in their molecular structures. The longer these organic-rich reservoirs are subjected to elevated temperatures and pressures, the more this buried material is converted to low molecular weight compounds such as methane and ethane (i.e., natural gas).

3.7 Composition of Crude Oils

Figure 3.3 outlines the various types of molecular structures found in crude oils. It is important to realize that, in addition to the many chemical structures that are in crude oil as reduced carbon, the molecular size or weight of these hydrocarbon compounds establishes the physical properties of the crude oil. Compounds with one to four carbons are gaseous at normal environmental temperatures and are called the natural gas components of the extracted reservoir fluids. Hydrocarbon-type compounds with ≈5–20 carbon atoms are nonviscous, are less dense than water, and exist as liquids at environmental conditions (volatiles and semi-volatiles). Further, hydrocarbon-type compounds with >20 carbons are viscous liquids to waxes and even solids, and these compound's densities are approaching and can exceed the density of water (non-volatiles). Therefore, the physical properties of this complex mixture of hydrocarbon-type compounds which comprise crude oil are dependent upon its relative composition of liquid compounds, viscous liquid compounds, and solid compounds. Light crude oils contain relatively large quantities of low molecular weight compounds that are volatile, nonviscous, less dense than water, and liquid and will solubilize readily when spilled in water. Heavier crude oils contain relatively larger proportions of the viscous liquid/solid hydrocarbon materials and are almost as dense as water (sometimes more dense) (Overton et al. 2016; Martínez-Palou et al. 2011). These heavy crudes tend to stick together or "glob" when spilled, strongly coat plants and animals, don't readily dissolve or evaporate, and are difficult to clean up. Thus, petroleum is made up of hydrocarbon-type compounds with molecular weights from 16 to 2000 or 3000 atomic mass units, and are generally classified as either saturates, aromatics, resins, or asphaltenes (SARA), and can be grouped into the following three hydrocarbon categories: Alaphatic Hydrocarbons, Aromatic Hydrocarbons, and Non-Hydrocarbons (Overton et al. 2016).

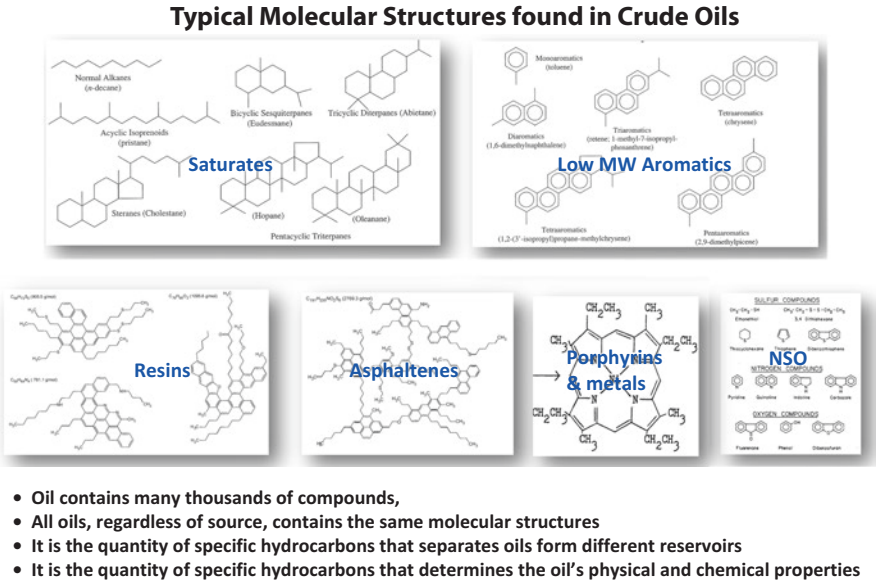

Fig. 3.3 Typical molecular composition and structure of crude oils. (Molecular structures from Overton et al. (2016, Fig. 1))

3.7.1 Aliphatic Hydrocarbons

An aliphatic is a hydrocarbon compound containing carbon and hydrogen joined together in straight chains, branched chains, or nonaromatic rings. While aliphatic hydrocarbons may be saturated (e.g., hexane and other alkanes) or unsaturated (e.g., hexene and other alkenes, as well as alkynes), only saturated aliphatics are produced during crude oil formations. Thus, crude oil contains mostly reduced aliphatic hydrocarbons and lesser amounts of aromatic compounds and (the so-called) non-hydrocarbon compounds (mostly aromatic compounds containing other atoms such as sulfur, nitrogen, or oxygen in addition to carbon and hydrogen) (Overton et al. 2016; Reddy et al. 2012). The saturated compounds can be as small as a one carbon compound (i.e., methane) to much larger molecules that contain many dozens of carbons atoms linked together. However, petroleum is mostly comprised of straight chain saturated hydrocarbon molecules, ranging from the simple one carbon methane compound up to molecules containing 40 or more carbons along with their associated branched and cyclic structures in this molecular size range (16 to almost 600). A small fraction of the saturated cyclic hydrocarbon structures in crude oils are ruminates of their initial molecular structures in the deposited biomass. These compounds are particularly resistant to natural biodegradation, and are known as petroleum biomarkers, useful for oil fingerprinting (Wang et al. 2006; Prince et al. 1994).

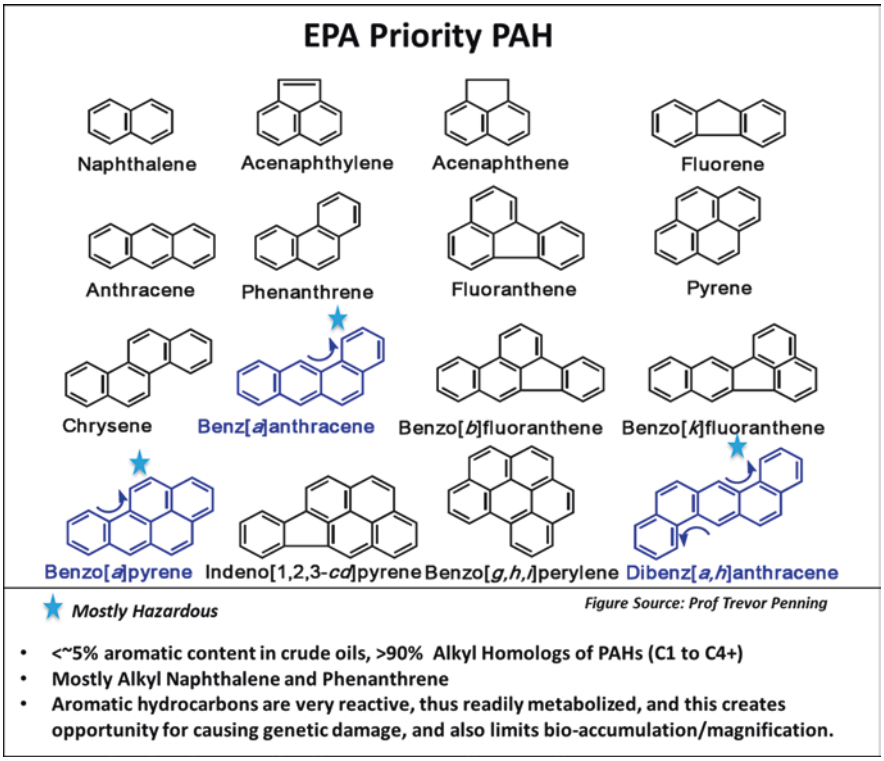

Fig. 3.4 Molecular structures of 16 PAHs listed as priority pollutants by the US EPA

3.7.2 Aromatic Hydrocarbons

One class of reduced hydrocarbon compounds produced from plant biomass by diagenesis/catagenesis processes is called the aromatics. Aromatic compounds are a slightly oxidized form of carbon, relative to the completely reduced saturate alkanes (the loss of some hydrogen atoms in these hydrocarbons is a partial oxidation, not complete oxidation to CO_2) (Fig. 3.4). Most of the aromatic hydrocarbons in oils have multiple rings in their molecular structures and are called polycyclic aromatic hydrocarbons (PAHs) (Overton et al. 2016; Neff 1979). This ring structure provides these aromatic compounds with unique shapes and reactivities when compared to saturated hydrocarbons (Fig. 3.4). First and foremost, these aromatic compounds can be readily metabolized by liver enzymes, and this enzymatic oxidation is the process designed to facilitate elimination of pollutants from the body (excretion). For example, this is why these oxidized metabolites are readily found in bile salts in fish as they are on their way out of the body. However, the enzymatic reactions can also produce unstable oxidized by-products that can react with cellular genetic material causing cell death, mutation, or permanent genetic change, potentially leading to future tolerance or lack thereof to these petroleum compounds (Yan et al.

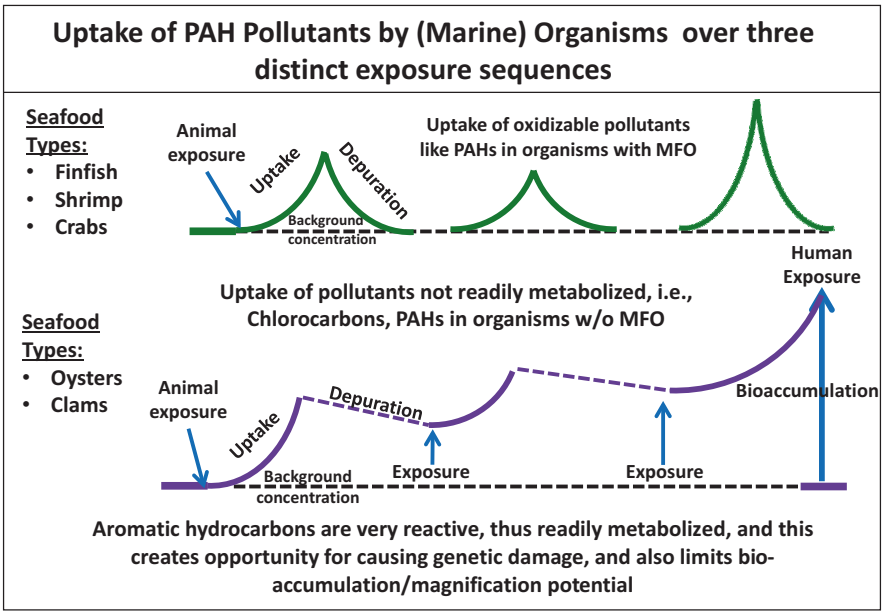

Fig. 3.5 Uptake of PAH pollutants by (marine) organisms over three distinct exposure sequences

2004; Albers 2003; Samanta et al. 2002). Further, these aromatics tend to be more water soluble than their equivalently sized completely saturated hydrocarbon counterparts and thus have readily available routes of exposure out of the oil phase into the water phase. This movement into the aqueous phase provides routes of exposure via ingestion, sorption, and/or inhalation for a number of organisms including humans (Tao et al. 2009; Albers 2003; Sverdrup et al. 2002). Of all of the components found in crude oil, it is because of their reactivity and solubility that aromatics have the greatest potential to cause harm. However, as outlined in Fig. 3.5, this reactivity and solubility also generally means that these aromatic compounds are not persistent pollutants, and they do not tend to bioaccumulate or magnify in living organisms that possess enzymes for xenobiotic metabolism. Thus, any bioaccumulation is followed by rapid depuration. PAH exposure in organisms without MFO metabolism results in slow depuration with corresponding accumulation in the organism's tissues.

The most common PAH compounds in crude oils typically have from two to five or six aromatic rings (Fig. 3.4). In general, PAHs can also have from one to four saturated carbon atoms attached to their basic ring structures (i.e., $-CH_3$ groups). These are called alkyl groups, and the various isomers resulting from the attachment of these alkyl groups are known as alkyl homologs of the parent PAHs. Some PAH homologs can have enhanced toxic properties when compared to their parent PAH compounds (Turcotte et al. 2011; Wang et al. 2007). In addition to their enzyme-mediated reactivity, one- to three-ringed PAHs and their alkyl homologs are fairly water soluble, especially when compared to the saturated hydrocarbons in crude oil

with a similar molecular size (Albers 2003; Neff 2002). It is this solubility that provides a route of exposure for animals and plants that live in or near the water column and the reason that most of the toxic consequences from crude oil exposure are associated with the one- to three-ringed PAH compounds. Larger, higher-numbered ring PAHs are much more potent carcinogens, but these compounds are also very insoluble in water, and this greatly limits their routes of exposure and potential for causing harm in most marine environments (Albers 2003; May et al. 1978; Mackay and Shiu 1977).

PAHs in the marine environment come from primary two sources, leaked and spilled petroleum (petrogenic) and incomplete combustion of the fossil carbon in various fuels and from the burning of terrestrial plants as in forest fires (pyrogenic). Additionally, very small number of PAH compounds can be produced anaerobically. These two primary petrogenic and pyrogenic sources of environmental PAH compounds can be readily identified by observing the composition of alkyl homolog isomers attached to the various PAH parent compounds (Fig. 3.6). Elevated concentrations in the parent PAH compounds compared to the concentrations of their respective alkyl homologs are a sure indication that these PAHs were produced from incomplete combustion (Fig. 3.6) and are called pyrogenic PAHs (Yunker et al. 2002). If the alkyl homolog compositions are higher than the corresponding parent PAH compounds, then they are petrogenic PAHs from sources such as crude oils (Bence et al. 2007; Yunker et al. 2002).

It is important to point out that PAH compounds are ubiquitous in the environment, and essentially all sediment and water samples collected from anywhere in the world contain very low yet detectable levels of PAH compounds. This is because, even though PAHs are a reduced form of carbon, and thus reactive, they can be sequestered and protected from oxidation by adsorption onto particles such as carbon black/soot or in total organic carbon (TOC) content of soils and sediments (Flores-Cervantes et al. 2009; Lima et al. 2005; Lohmann et al. 2005). This sorption/sequestration process possibility limits the reactive carbon's access to oxygen and/or the catalyst that facilitates oxidation (OH), thus preventing reaction and preserving the original PAH molecular structures at very low concentrations in environmental samples.

3.7.3 Non-hydrocarbons

Crude oils also contain compounds, called non-hydrocarbons, with mostly aromatic molecular structures that have atoms such as sulfur and nitrogen (and some oxygen) in addition to their aromatic hydrocarbon structures. Most of these non-hydrocarbon aromatic structures are also comprised of one to four or more alkyl groups attached to the parent ring structure. Crude oils also generally have small quantities of very large molecular structures, with some chelated heavy metals such as iron, nickel, copper, and vanadium. These very large crude oil components, known as resins and asphaltenes, are not very useful as a common source of fuels except for some cargo

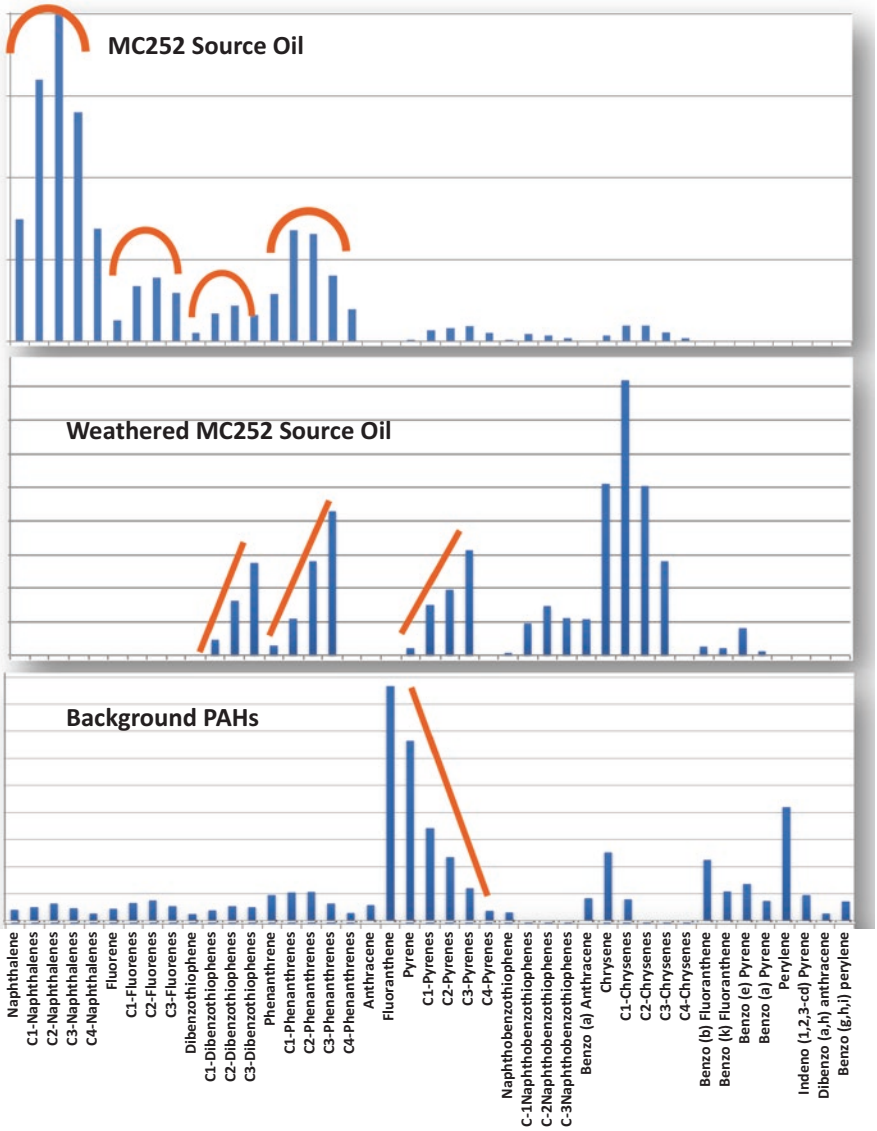

Fig. 3.6 Distribution of PAH compounds in MC252 source oil, weathered MC252 oil residues, and a coastal sediments with no oil residue contamination (no hopane biomarkers) – differentiation between petrogenic and pyrogenic sources of PAHs by alkyl homologs abundance. The red lines represent a typical distribution of parent and their alkylated homologs in petroleum vs pyrogenic sources

ships and fixed location power plant fuels and are practically resistant to microbial degradation. Refinery residues containing these types of very large insoluble compounds are commonly used as roofing tar and road asphalt. Crude oils produced from tar sands do contain mostly these large molecular weight asphaltene and resin-type compounds and can be encountered in spills of dilbit (diluted bitumen)- and synbit (synthetic bitumen)-type fossil fuels and the so-called Group 5-type fuels. Refinery residues containing these types of very large insoluble compounds are commonly used as roofing tar and road asphalt. While asphaltenes and resins are not easily reactive and bioavailable, and practically resistant to microbial degradation (Aeppli et al. 2014), their by-products of long-term photochemical leaching from roofing and paving structures can potentially have environmental effects.

3.7.4 Live Oil Versus Dead Oil

Crude oils that come out of deep reservoirs are generally a mixture of oil and natural gas (and can contain some produced water in depleted reservoirs) and are called "live oil" due to dissolved gas in solution with the oil. When this oil is processed at a surface facility (floating platform or ship) for transport to refineries, the gaseous components are separated from the liquid crude, and the crude is transported as a liquid product that typically has a vapor pressure of less than 10 psi. Once the gas is liberated, this liquid product is now called "dead oil." This vapor pressure is much reduced from the vapor pressure of the source oil. Consequently, oil spills from tanker accidents or pipeline ruptures (dead oil) are much less volatile than oils entering the environment from well blowouts such as the *Deepwater Horizon* (DWH) incident. Most of the experience gained from past oil spills has been from tanker accidents or pipeline ruptures.

High gas content crude oils behave differently when entering the marine environment. As the pressure of gassy oil is rapidly reduced upon entering the aquatic environment, the gas effervesces from the oil causing much of the liquid oil to be broken down into tiny droplets. These droplets have a variety of sizes, some very small, and this affects how the oil moves away from the source. Larger-sized droplets tend to rise to the surface fairly rapidly, while smaller droplets take longer. Extremely small droplets experience significant flow resistance from the water column and, in effect, become neutrally buoyant. These naturally dispersed extremely tiny droplets are carried away from the source, diluted with seawater, and biodegraded with natural microorganisms without ever rising to the surface. Much of the more water-soluble aliphatic and aromatic hydrocarbons in these tiny droplets can be dissolved into the water column and are carried away from the source by deep ocean currents. Again, these are reduced forms of carbon; they are highly reactive and have high water solubility that provides routes of exposure to marine organisms in deep-sea environments (Fig. 3.5). Their reactivity is both a removal mechanism and an opportunity for causing harm from both their toxicity and oxygen depletion potential.

Small droplets that have buoyancy rise to the surface but are continually being extracted as the droplets pass through the water column. This continuous liquid-liquid extraction process removes many of the small aliphatic hydrocarbons in the oil droplets, as well as the more soluble aromatic compounds with one and two aromatic rings. As the composition of the droplets change, so do the droplet's physical properties, including density and ability to form emulsions by mixing with seawater. The net effect is that oil released from blowouts can be significantly modified by its rapid decompression as well as the interactions with and in the water column. Surface oil slicks, produced from oil released in deep water, have undergone significant change from the original composition in their reservoir, and this change impacts the oil's surface behavior and reactivity. Generally, surface oil from deep releases is a mixture of oil and water called emulsions, which are generally thick and fairly viscous compared to the released oil. Many of the low molecular weight, solvent-type molecules in the released oil will have been extracted by water column contact, thus changing the floating oil's viscosity, stickiness, and ability to be removed by mechanical skimming, burning, or dispersing.

3.8 Oil Weathering

It is important to emphasize that spilled oil can cause environmental damage through several primary mechanisms. These include (a) the toxic and irritative effect caused when aromatic and possibly aliphatic components are ingested, inhaled, or adsorbed, (b) the smothering or coating effect from oil, (c) the oxygen-depleting effect as oil components are degraded by natural bacteria, and (d) carbon enrichment into the normal marine food web from bacterial degradation of spilled oil. The weathering process changes all of the fundamental implications associated with these mechanisms for causing environmental damage (toxicity, routes of exposure, bioavailability, carbon enrichment) and, in general, lessens the acute opportunity for environmental damage from oil hydrocarbons retained in the floating or stranded oil residues.

Weathering includes physical processes such as evaporation, dissolution, emulsification, sedimentation, as well as chemical oxidations caused by microbe metabolism and absorption of energy from the sun (photooxidation) (Meyer et al. 2018; Overton et al. 2016; Tarr et al. 2016; Aeppli et al. 2014; Atlas and Hazen 2011). Weathering, by changing the composition of the original spilled oil, changes the oil's physical and toxic properties. Fresh oil is more volatile, contains more water-soluble components, floats, is not very viscous, and easily spreads out from the source. All of these characteristics mean that fresh oil is the most environmentally dangerous type of spilled oil. Fresh oil hydrocarbons are readily available for ingestion, adsorption, and inhalation as well as for coating and oxidizing. As oil weathers, it first loses volatile components, which are the most water soluble; the oil then becomes more viscous and more likely to glob together in stringers as opposed to spreading out in a thin film (Tarr et al. 2016; Aeppli et al. 2014). Over time, these

weathering changes continue to alter the composition of the oil until it has been severely degraded in the environment, leaving behind only small quantities of insoluble, solid-like residues known as tarballs or surface residue mats. Even though weathered oil residues contain higher concentrations of the larger more toxic four to six ringed PAHs (Fig. 3.6), the routes of exposure for these more hazardous compounds is severely limited, and thus their capability for causing harm is limited (Tarr et al. 2016). Typically, during the weathering process, much of the oil (especially heavier oil) mixes with water and emulsifies, forming a viscous mixture that is fairly resistant to rapid weathering changes. Consequently, emulsification greatly slows down the weathering processes (Tarr et al. 2016; Belore et al. 2011; Garo et al. 2004). Further, emulsified oil is also somewhat more difficult to remove by skimming, dispersing, or burning. Fortunately, emulsified oil is generally less environmentally dangerous, becoming a mostly nuisance material that causes damage through covering or smothering as opposed to damage through toxic interactions. However, if emulsified oil is ingested through, for example, the preening of feathers, it can have significant toxic effects on internal organs. Heavily emulsified oil is slower to degrade and will stay in the environment longer than non-emulsified oil (Tarr et al. 2016; Belore et al. 2011).

It is important to point out that oil spills, particularly spills of live oil from deep-sea releases such as the DWH incident, introduce extremely large quantities of highly reactive saturate and aromatic hydrocarbons into the oceans in both an oil phase and a dissolved phase (Reddy et al. 2012; Diercks et al. 2010). In the dissolved aqueous phase, hydrocarbon molecules are readily available for uptake and metabolism, can cause irritations, and can be photooxidized in the upper water column. Dissolved hydrocarbons are readily available for reaction which, coupled with the exposure to a biocatalyst and a source of oxygen, provides an opportunity for causing harm not only through a variety of toxic and irritation reactions in animals but by removal of dissolved oxygen from the water column. Hydrocarbons in the oil phase, on the other hand, are less immediately available for reaction, but the oil phase can cause harm through coating and smothering, in addition to being ingested and adsorbed by cleaning processes such as preening.

3.8.1 Floating or Subsurface Oil

Fresh oil has a density that is less than water, so fresh oil floats or has a tendency to rise to the surface. As oil weathers, its density increases and can approach the density of water, making it less buoyant. In rare occasions, some heavy oils (like dilbit, synbits, Group 5 oils), when weathered, become more dense than water and sink. Some emulsified weathered oil, with near-neutral buoyancy, can pick up sediments and near-shore detritus and sink to the bottom in intertidal areas. Sunken oil poses potential exposure risk to intertidal organisms and bivalves such as oysters and clams. Some sunken oil residues can be buried in intertidal areas off sandy beaches. These tar-mats degrade very, very slowly, and normal coastal erosion processes can

dislodge these buried tar-mats during storm and weather fronts. Typically, this dislodged tar-mat material breaks apart and will wash up on beaches following storm events. This process of dislodging buried oil can last for several years following an oil spill and cause episodic recontamination of recreational beaches with tarballs.

Offshore floating oil can be dispersed by the action of winds and waves, as well as the application of chemical dispersants. Dispersion is the process of breaking oil residues into very tiny droplets and allowing these tiny droplets to move away from the oil slick (i.e., get dispersed) by currents and possibly by wind actions. These tiny droplets, because of their small size, act as though they were neutrally buoyant when mixed into the upper water column. Currents then move the droplets away from their source, and this movement causes a spreading out of the droplets in three dimensions of the upper water column. This is dispersion, and it results in diluting the quantity of oil residue floating in the oil slick down into the water column, allowing it to be further diluted by distributing it within the water column. However, the low molecular weight hydrocarbon compounds in the dispersed oil droplets can now be more readily dissolved into the water column, and this represents an enhanced route of exposure for animals residing in these regions of the upper water column near dispersed oil. This same analogy can be found with regard to subsurface injection of dispersants directly into a damaged and leaking seafloor oil well. Dispersion causes dilution of the oil phase but also enhances dissolution from the oil phase into the water column. Hydrocarbons in the tiny droplet oil phase, as well as in the dissolved aqueous phase, are available for biodegradation (metabolic oxidation) and any number of harmful and irritating interactions with living marine resources. The rationale for using oil dispersion is that diluted oil is less potentially damaging than concentrated oil, so dispersion should always be carried out in marine environments that allow ample dilution (i.e., in deep water and with strong currents).

3.8.2 Oil Impacts in Coastal Marshes

Oil floating on the surface can cause damage to organisms that live near or on the surface. Offshore, this damage is confined to near-surface environments unless the oil is dispersed into the water column with chemicals. As surface oil interacts with shoreline marshy coastal environments, it can cause damage through smothering and coating, or by the dissolving of toxic oil components in shallow water environments, and in and around the root structures of coastal plants (Meyer et al. 2018; Overton et al. 2016). Smothering can cause significant damage to coastal grasses and habitat dwellers, as does the dissolution of the toxic components into shallow water environments. Weathered oil has a significantly less soluble toxic component composition, and thus the potential damage comes mainly from its smothering/coating effect and ability to use up available dissolved oxygen. Some of the oxidized components from the microbial and photo-induced weathering of oil in these shallow coastal environments that are not well mixed can also cause harm.

3.8.3 Subsurface Oil at Released Depth

The oil from the DWH well blowout entered the environment 1500 meters below the Gulf's surface (Reddy et al. 2012; Diercks et al. 2010). As such, it contained very high quantities of natural gas which caused natural dispersion of much of the oil in the deep Gulf. The oil exiting the wellhead was also mixed for a while with chemical dispersant causing further dispersion at depth. The net effect of both natural and chemical dispersion is that much of the oil was broken into very tiny droplets with diameters less than 100 microns. Droplets of this size or smaller face significant flow resistance from the water column in their effort to rise to the surface, and essentially are trapped in the deep Gulf environment until degraded by natural bacteria. As this dispersed at-depth oil moves away from the wellhead, it becomes diluted with Gulf water; some components readily dissolve into the water column and were available for fairly rapid biodegradation (Baelum et al. 2012). The residual is dispersed and degraded by natural bacteria in the depths of the Gulf. Some heavily weathered oil residues were retained in deep-water sediments and deposited biomass from oil biodegradation. Because the concentration of the dispersed oil is well below the concentration of oxygen in the deep Gulf, no significant oxygen depletion has been observed from the degradation of the oil in the deep Gulf waters.

3.8.4 Subsurface Oil's Slow Transit to the Surface

Oil droplets larger than 100 microns in diameter will have a tendency to rise to the surface. Larger drop will rise faster than smaller drops. In this progression to the surface, small drops are extracted of their more water-soluble components by movement through the water column, and this caused some of the oil reaching the surface to be already weathered by dissolution and microbial degradation. Remember that water solubility is closely associated with volatility, particularly with the aromatic components in oil, so continuous water extraction on the 1500 m journey to the surface significantly alter the composition of oil in these small droplets. The net effect of this process of rising to the surface meant that surface oil was a mixture of weathered and fresh oil that took on a variety of appearances. Further, since this spill continued for 87 days, in essence a new spill occurred each of these days, oil at the surface was always a complex mixture of relatively fresh oil, oil weathered by movement to the surface, and oil weathered by processes at the surface (mostly evaporation and photooxidation). Further, since the spill occurred far offshore 50–100 miles from coastal impacts, and without strong Gulf currents or wind conditions moving it ashore, significant weathering of the oil occurred before coastal landfall. Most coastal oiling was from weathered oil, which posed primarily a smothering/coating hazard and, to a lesser extent, an oxygen-depriving hazard in near-coastal environments and a toxic hazard from dissolution and oxidation of its aromatic components. Oil residues in coastal marshes are subjected to continuous washing by wave action with muddy water, and the mineral organic-rich suspended sediments in these Mississippi River-laden waters can and do interact with coastal

oil residues to form oil mineral aggregates (OMA) (Daly et al. 2016; Passow 2016). Organic carbon particles in soil and sediments (TOC or POC) including combustion-derived soot/BC-type particles in these riverine muds as well as atmospheric particles preferentially sorb to hydrophobic hydrocarbons in oil residues (Adhikari et al. 2015; Flores-Cervantes et al. 2009). This interaction with suspended minerals represents an important mechanism for the gradual removal from, as well as for redistribution of, oil residues and soluble hydrocarbons in coastal marsh environments not initially impacted by the spill. It also provides a re-partitioning and low-level route of exposure to soluble hydrocarbons and insoluble oil residues for filter feeding coastal organisms such as oysters and clams.

3.9 What About the Next Big Spill?

3.9.1 Critical Review of DWH Incident

First and foremost, in preparation for the next big oil spill, scientists should now re-examine the basic assumptions associated with our understanding of not only the DWH incident but all we have learned regarding spill oil. These assumptions should be evaluated and then re-evaluated by looking back at what actually happens during the spill, not by what was thought to be happening during the spill. Massive amounts of data and results were generated by both government and BP and Natural Resource Damage Assessment (NRDA) efforts, as well as through the research funded by GoMRI and others. These results should be evaluated in terms of their scientifically verified, and not litigated, environmental impacts. For example, did the assumption that no petrogenic PAHs from this spill bioaccumulated into the marine web hold true? It is one thing for carbon from the spill to be incorporated into the food web, but quite another to say that specific and toxic PAH compounds were bioaccumulated at levels dangerous for human and environmental consumption. What do the data show? Another important investigation might be evaluating whether laboratory-observed toxic impacts were detected, and if so, did they persist in the GOM environment? Were species alterations and subsequent changes in distributions observed as a result of the spill? Is there evidence of modification of environmental genetics as the result of the spill? Did dispersing of the oil help or hurt recovery? We assumed that natural bacteria were available to degrade spilled oil, but did this recovery system get modified and permanently changed by the massive amount of this spill?

We certainly learned a lot about how natural microbial communities responded to oiling, is there anything we can do next time to enhance these useful processes and not do those that may have inhibited mother nature's natural processes (such as dispersing)? What did we learn about deep-water releases of oil and natural gas? It's interesting to find new marine species in the deep, but what did we learn about oil getting degraded in dark and cold environments and its mechanism for deposition and causing harm? Were there documented incidences of human health damages from oil exposures? The bottom line is that it's important and essential during a massive spill to look for and detect damages, but it's also equally important to

observe and substantiate recovery and to understand what worked and what didn't. The litigative NRDA process is designed as a preventative measure, to make sure that the financial pain of an oil spill is sufficient incentive to do everything reasonable for prevention. Human response efforts should work in harmony with the environment's natural adaptive and recovery processes. Science should be used for pre-spill monitoring, to support future spill contingency and planning efforts and to observe, verify, and where possible improve natural processes of recovery. The next big spill will occur, and it's now time to fully understand what happened during and after the DWH event.

3.9.2 Importance of Multidisciplinary Studies and Their Implications

A number of the following broad scientific disciplines are needed to not only help understand the environmental and human health consequences of an oil spill but to contribute to the human interventions used for mitigating or minimizing these consequences. These disciplines include nearly all subdisciplines of chemistry (analytical, physical, organic, inorganic, biochemistry); physics; multiple subdisciplines of biology and microbiology; oceanography; toxicology, human health, epidemiology, and geology (land loss issues in marshes); marine fisheries; environmental and circulation modeling; sociology and psychology; and economics. The implications of applying all of these broad disciplines toward understanding oil spill impacts and its consequences are profound. We quickly get into an issue of understanding of the big picture versus getting absorbed by understanding intricate disciplinary scientific details. Further, most disciplinary science has its own terminology, and frequently words have different means in different disciplines. A tiny oil droplet can be a particle to modelers, but there are important differences between droplets and particles in oceanography. Commonly used disciplinary terminology can cause misunderstanding in interpretation of results and confusion concerning impacts. The bottom line is multidisciplinary investigations are important, but we must keep in focus the challenges associated with integrating other science disciplines that are outside of our respective areas of competence.

3.9.3 Multidisciplinary Scientific Publications

Oil spill science must be multidisciplinary but must also be subjected to the same rigors of peer review as is found with conventional scientific discovery. This implies discipline in publications with results presented to support hard scientifically established understandings of the spill. Oil spill science should allow and encourage thinking and study outside of the box, but we should never forget the foundations of understanding that were used to build the box. For example, many

papers describing scientific studies or findings from the DWH spill have upward of 10 or more authors representing many different scientific disciplines. The normal peer review process, the foundation of our method of ensuring the integrity and validity of scientific results in the archival literature, usually involves three anonymous, discipline-specific scientific reviews of the submitted paper. With several broad scientific disciplines present in many multi-author published papers, one has to question the veracity of these three peer review processes. While it is incredibly important toward understanding oil spills for scientists to pull together the big picture results, perhaps these multidisciplinary publications need a different type of peer review process. We should try and present our results to disciplinary-focused journals. This means that not all aspects may have been peered reviewed in a given published article. The peer review process is way too sacred to not be fully used during review of oil spill science publications and its presentation to the wider scientific community. Perhaps broad multidisciplinary scientific papers should get reviewed by multidisciplinary panels prior to publication.

3.9.4 Explaining What Happened to Broad Audiences

Oil spills are events that generate intense interest not just from the scientific disciplines dealing with and studying marine pollution but communities that live in or make their living from and around coastal environments. Understanding and disseminating the implications associated with oil spills are not just a scientific imperative, it is our responsibility to be able to explain these findings to communities that are most affected by these devastating events. Clearly, hyped hyperbole associated with the anger over massive oil spills can cause a great deal of anxiety with communities affected by oil spills. Comments given publically must be made responsibly and must take into consideration the impacted audience. These are real people and this is their world. There is a very big difference between postulating a possible outcome and a probable outcome, and these differences should always be elucidated in both public presentations and scientific publication. Exaggerated improbable outcomes cause unnecessary and unneeded public apprehension and can cause further complications for the communities dealing with such traumatic events. Scientists studying oil spills and their impacts are regarded for their knowledge and wisdom and should stick to credible and proven/known facts when discussing their findings with society.

3.10 Conclusions

Our natural world is a wonderful and very complex system involving living and nonliving resources. Into this serene environment, humans have added many potentially useful (to them) activities, but they have also introduced chemicals that add stress to the natural environment. Oil spills are one of these stresses, and this stress

affects both our natural environment and humans living in this environment. Society has recognized the buildup of persistent man-made chemicals in our environment as harmful additions, and oil spills are commonly thought of as contributing additional burdens of persistent pollutants. However, as much as we decry the tragedy of an oil spill, the dangerous compounds in oils do react quickly, are readily oxidized and degrade, and do not persist. Thus, understanding the potential effects of oil spills on our natural environment and its inhabitants begins with a need for a fundamental understanding of the implications associated with molecular formational and reactive processes of carbon in our environment.

This understanding requires detailed knowledge from many scientific disciplines being applied to these infrequent but high-profile events with impacts ranging from deep ocean to the dinner table. With these diverse multidisciplinary types of research investigation comes incredible opportunity to factually document the comprehensive impacts of oil spill. At the same time, the broad aspects of these studies present challenges of working outside of our individual areas of expertise. Good science is only as good as its weakest link in the chain of discovery. It is important for all oil spill-related scientific research to be conducted within the objective framework, recognizing the constraints imposed by studies covering diverse scientific areas of expertise. Imagine and investigate possible outcomes, but be sure to understand and explain what's probable.

Acknowledgments This research was made possible by a grant from the Gulf of Mexico Research Initiative through its consortia C-IMAGE and CWC.

References

Adhikari PL, Maiti K, Overton EB (2015) Vertical fluxes of polycyclic aromatic hydrocarbons in the northern Gulf of Mexico. Mar Chem 168:60–68. https://doi.org/10.1016/j.marchem.2014.11.001

Aeppli C, Nelson RK, Radovic JR, Carmichael CA, Valentine DL, Reddy CM (2014) Recalcitrance and degradation of petroleum biomarkers upon abiotic and biotic natural weathering of Deepwater Horizon oil. Environ Sci Technol 48(12):6726–6734

Albers PH (2003) Petroleum and individual polycyclic aromatic hydrocarbons. In: Hoffman DJ, Rattner BA, Burton AG, Cairns J (eds) Handbook of ecotoxicology, 2nd edn. CRC Press LLC, Boca Raton, pp 342–360

Atlas RM, Hazen TC (2011) Oil biodegradation and bioremediation: a tale of the two worst spills in US history. Environ Sci Technol 45(16):6709–6715

Baelum J, Borglin S, Chakraborty R, Fortney JL, Lamendella R, Mason OU, Auer M, Zemla M, Bill M, Conrad ME, Malfatti SA (2012) Deep-sea bacteria enriched by oil and dispersant from the Deepwater Horizon spill. Environ Microbiol 14(9):2405–2416. https://doi.org/10.1111/j.1462-2920.2012.02780.x

Belore R, Trudel K, Morrison J (2011) Weathering, emulsification, and chemical dispersibility of Mississippi Canyon 252 crude oil: field and laboratory studies. In: International oil spill conference proceedings (IOSC), Vol. 2011, No. 1, p abs247. American Petroleum Institute. https://doi.org/10.7901/2169-3358-2011-1-247

Bence AE, Page DS, Boehm PD (2007) Advances in forensic techniques for petroleum hydrocarbons: the Exxon Valdez experience. In: Wang Z, Stout SA (eds) Oil spill environmental forensics, fingerprinting and source identification. Elsevier, Amsterdam, pp 449–487

Carson R (1962) Silent spring. Houghton Mifflin, Boston
D'Auria M, Emanuele L, Racioppi R, Velluzzi V (2009) Photochemical degradation of crude oil: comparison between direct irradiation, photocatalysis, and photocatalysis on zeolite. J Hazard Mater 164(1):32–38. https://doi.org/10.1016/j.jhazmat.2008.07.111
Daly KL, Passow U, Chanton J, Hollander D (2016) Assessing the impacts of oil-associated marine snow formation and sedimentation during and after the Deepwater Horizon oil spill. Anthropocene 13:18–33. https://doi.org/10.1016/j.ancene.2016.01.006
Diercks AR, Highsmith RC, Asper VL, Joung D, Zhou Z, Guo L, Shiller AM, Joye SB, Teske AP, Guinasso N, Wade TL (2010) Characterization of subsurface polycyclic aromatic hydrocarbons at the Deepwater Horizon site. Geophys Res Lett 37(20). https://doi.org/10.1029/2010GL045046
Flores-Cervantes DX, Plata DL, MacFarlane JK, Reddy CM, Gschwend PM (2009) Black carbon in marine particulate organic carbon: inputs and cycling of highly recalcitrant organic carbon in the Gulf of Maine. Mar Chem 113:172–181. https://doi.org/10.1016/j.marchem.2009.01.012
Garo JP, Vantelon JP, Souil JM, Breillat C (2004) Burning of weathering and emulsified oil spills. Exp Thermal Fluid Sci 28(7):753–761. https://doi.org/10.1016/j.expthermflusci.2003.12.013
Garrett RM, Pickering IJ, Haith CE, Prince RC (1998) Photooxidation of crude oils. Environ Sci Technol 32(23):3719–3723. https://doi.org/10.1021/es980201r
Lima AL, Farrington JW, Reddy CM (2005) Combustion-derived polycyclic aromatic hydrocarbons in the environment – a review. Environ Forensic 6:109–131. https://doi.org/10.1080/15275920590952739
Lohmann R, MacFarlane JK, Gschwend PM (2005) Importance of black carbon to sorption of native PAHs, PCBs, and PCDDs in Boston and New York harbor sediments. Environ Sci Technol 39:141–148. https://doi.org/10.1021/es049424+
Longnecker MP, Rogan WJ, Lucier G (1997) The human health effects of DDT (dichlorodiphenyltrichloroethane) and PCBS (polychlorinated biphenyls) and an overview of organochlorines in public health. Annu Rev Public Health 18(1):211–244. https://doi.org/10.1146/annurev.publhealth.18.1.211
Mackay D, Shiu WY (1977) Aqueous solubility of polynuclear aromatic hydrocarbons. J Chem Eng Data 22(4):399–402. https://doi.org/10.1021/je60075a012
Martínez-Palou R, de Lourdes Mosqueira M, Zapata-Rendón B, Mar-Juárez E, Bernal-Huicochea C, de la Cruz Clavel-López J, Aburto J (2011) Transportation of heavy and extra-heavy crude oil by pipeline: a review. J Pet Sci Eng 75(3–4):274–282. https://doi.org/10.1016/j.petrol.2010.11.020
May WE, Wasik SP, Freeman HF (1978) Determination of the solubility behavior of some polycyclic aromatic hydrocarbons in water. Anal Chem 50:997–1000. https://doi.org/10.1021/ac50029a042
Meyer BM, Adhikari PL, Olson GM, Overton EB, Miles MS (2018) Louisiana coastal marsh environments and MC252 oil biomarker chemistry. In: Oil spill environmental forensics case studies. Butterworth-Heinemann, Oxford, pp 737–756. https://doi.org/10.1016/B978-0-12-804434-6.00032-X
Neff JM (1979) Polycyclic aromatic hydrocarbons in the aquatic environment: sources, fates and biological effects. In: Polycyclic aromatic hydrocarbons in the aquatic environment: sources, fates and biological effects. Applied Science Publishers, London, 262 pp
Neff JM (2002) Bioaccumulation in marine organisms: effect of contaminants from oil well produced water. Elsevier, Amsterdam, 468 pp
Overton EB, Laseter JL, Mascarella SW, Raschke C, Nuiry I, Farrington JW (1980) Photochemical oxidation of IXTOC I oil, pp 341–383. In: Proceedings of symposium on preliminary results from the September 1979 Researcher/Pierce IXTOC I Cruise. Key Biscayne, Florida, June 9–10, 1980, NOAA Office of Marine Pollution Assessment, Boulder, CO
Overton EB, Wade TL, Radović JR, Meyer BM, Miles MS, Larter SR (2016) Chemical composition of Macondo and other crude oils and compositional alterations during oil spills. Oceanography 29(3):50–63. https://doi.org/10.5670/oceanog.2016.62
Passow U (2016) Formation of rapidly-sinking, oil-associated marine snow. Deep-Sea Res II Top Stud Oceanogr 129:232–240. https://doi.org/10.1016/j.dsr2.2014.10.001

Pimentel D (2005) Environmental and economic costs of the application of pesticides primarily in the United States. Environ Dev Sustain 7(2):229–252

Plata DL, Sharpless CM, Reddy CM (2008) Photochemical degradation of polycyclic aromatic hydrocarbons in oil films. Environ Sci Technol 42(7):2432–2438. https://doi.org/10.1021/es702384f

Prince RC, Elmendorf DL, Lute JR, Hsu CS, Haith CE, Senius JD, Dechert GJ, Douglas GS, Butler EL (1994) 17-α(H)-21-β(H)-Hopane as a conserved internal marker for estimating the biodegradation of crude oil. Environ Sci Technol 28(1):142–145. https://doi.org/10.1021/es00050a019

Reddy CM, Arey JS, Seewald JS, Sylva SP, Lemkau KL, Nelson RK, Carmichael CA, McIntyre CP, Fenwick J, Ventura GT, Van Mooy BA (2012) Composition and fate of gas and oil released to the water column during the Deepwater Horizon oil spill. Proc Natl Acad Sci 109(50):20229–20234. https://doi.org/10.1073/pnas.1101242108

Salminen JM, Tuomi PM, Suortti AM, Jørgensen KS (2004) Potential for aerobic and anaerobic biodegradation of petroleum hydrocarbons in boreal subsurface. Biodegradation 15(1):29–39. https://doi.org/10.1023/B:BIOD.0000009954.21526.e8

Samanta SK, Singh OV, Jain RK (2002) Polycyclic aromatic hydrocarbons: environmental pollution and bioremediation. Trends Biotechnol 20:243–248. https://doi.org/10.1016/S0167-7799(02)01943-1

Solomon S (1999) Stratospheric ozone depletion: A review of concepts and history. Rev Geophys 37(3):275–316. https://doi.org/10.1029/1999RG900008

Stockholm Convention on Persistent Organic Pollutants (2005) Stockholm Convention on Persistent Organic Pollutants. http://www.pops.int/

Sverdrup LE, Nielsen T, Krogh PH (2002) Soil ecotoxicity of polycyclic aromatic hydrocarbons in relation to soil sorption, lipophilicity, and water solubility. Environ Sci Technol 36:2429–2435. https://doi.org/10.1021/es010180s

Tao Y, Zhang S, Zhu YG, Christie P (2009) Uptake and acropetal translocation of polycyclic aromatic hydrocarbons by wheat (*Triticum aestivum* L.). Environ Sci Technol 43:3556–3560. https://doi.org/10.1021/es803368y

Tarr MA, Zito P, Overton EB, Olson GM, Adhikari PL, Reddy CM (2016) Weathering of oil spilled in the marine environment. Oceanography 29(3):126–135. https://doi.org/10.5670/oceanog.2016.77

Turcotte D, Headley JV, Abudulai NL, Hodson PV, Brown RS (2011) Identification of phase II in vivo metabolites of alkyl-anthracenes in rainbow trout (*Oncorhynchus mykiss*). Chemosphere 85(10):1585–1591

Varjani SJ (2017) Microbial degradation of petroleum hydrocarbons. Bioresour Technol 223:277–286. https://doi.org/10.4061/2011/941810

Wang Z, Yang C, Fingas M, Hollebone B, Yim UH, Oh JR (2006) Petroleum biomarker fingerprinting for oil spill characterization and source identification. In: Wang Z, Stout SA (eds) Oil spill environmental forensics – fingerprinting and source identification. Academic Press, Burlington/London, pp 73–146

Wang Z, Li K, Lambert P, Yang C (2007) Identification, characterization and quantitation of pyrogenic polycyclic aromatic hydrocarbons and other organic compounds in tire fire products. J Chromatogr A 1139(1):1426. https://doi.org/10.1016/j.chroma.2006.10.085

Ward CP, Sharpless CM, Valentine DL, French-McCay DP, Aeppli C, White HK, Rodgers RP, Gosselin KM, Nelson RK, Reddy CM (2018) Partial photochemical oxidation was a dominant fate of Deepwater Horizon surface oil. Environ Sci Technol 52(4):1797–1805. https://doi.org/10.1021/acs.est.7b05948

Widdel F, Rabus R (2001) Anaerobic biodegradation of saturated and aromatic hydrocarbons. Curr Opin Biotechnol 12(3):259–276. https://doi.org/10.1016/S0958-1669(00)00209-3

Yan J, Wang L, Fu PP, Yu H (2004) Photomutagenicity of 16 polycyclic aromatic hydrocarbons from the U.S. EPA priority list. Mutat Res 557(1):99–108. https://doi.org/10.1016/j.mrgentox.2003.10.004

Yunker MB, Macdonald RW, Vingarzan R, Mitchell H, Goyette D, Sylvestre S (2002) PAHs in the Fraser River basin: a critical appraisal of PAH ratios as indicators of PAH source and composition. Org Geochem 33:489–515. https://doi.org/10.1016/S0146-6380(02)00002-5

Part II
Geological, Chemical, Ecological and Physical Oceanographic Settings and Baselines for Deep Oil Spills in the Gulf of Mexico

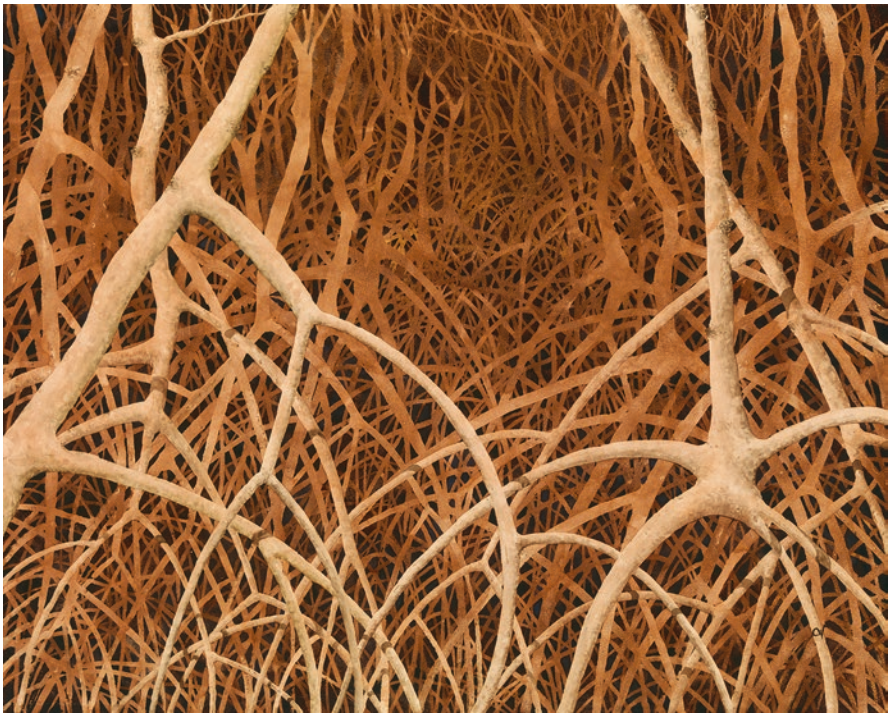

Curtis Whitwam
Ecotone
Watercolor on Aquaboard
20” × 16”

Chapter 4
An Overview of the Geologic Origins of Hydrocarbons and Production Trends in the Gulf of Mexico

Stanley D. Locker and Albert C. Hine

Abstract The Gulf of Mexico (GoM) region is one of the most important hydrocarbon-producing sedimentary basins in the world. Triassic rifting leads to formation of this small ocean basin characterized by the accumulation of thick salt deposits followed by a thick succession of continental- and marine-derived deposits that combined to generate and trap abundant hydrocarbons. This chapter presents a very brief overview of factors related to hydrocarbon accumulation and production trends in US waters. The offshore GoM has been producing from shelf to deep water for the past ~70 years. Ultra-deep-water drilling was reached in the late 1980s and progressed to depths near 3000 m by the 2000s. Although the extraction of the GoM's oil and natural gas is in its mature phase, studies indicate that oil and gas reserves are significant and that the GoM will be producing for many decades into the future.

Keywords Gulf of Mexico · Geologic history · Hydrocarbons · Production trends

4.1 Introduction

The Gulf of Mexico (GoM) is one of the most important hydrocarbon-producing sedimentary basins in the world—both *onshore* and *offshore*. Oil and gas primarily accumulate in sedimentary rocks that have been deposited when continents have been covered with seawater along the margins of continents or in small ocean basins such as the GoM. There are no economically viable oil and gas accumulations out in the middle of the Earth's large oceans where deep-sea sediments cover the oceanic crust. So, a first-order requirement for significant oil and gas accumulations is that a thick stratigraphic succession of sediments, eventually lithifying into sedimentary rocks, is deposited in some structurally defined basin. The GoM sedimentary basin has been defined by structural features in the Earth's crust, mostly faults, such that the basin's margins extend on land into Georgia, Alabama, Mississippi,

S. D. Locker (✉) · A. C. Hine
University of South Florida, College of Marine Science, St. Petersburg, FL, USA
e-mail: stan@mail.usf.edu; hine@usf.edu

S. A. Murawski et al. (eds.), *Scenarios and Responses to Future Deep Oil Spills*,
https://doi.org/10.1007/978-3-030-12963-7_4

Louisiana, Arkansas (almost into Oklahoma), Texas, and much of eastern Mexico including the Yucatan/Campeche carbonate platform and all of the Florida Platform. Some key sedimentary basins have been completely filled with evaporites, muds, siliciclastic sands, and carbonate/biogenic deposits to the point where oil and gas can be extracted from beneath dry land and from beneath the seafloor offshore.

Source rocks for oil and gas, reservoir rocks with porosity for storage, and structure or seals to trap the hydrocarbons all are abundant in the GoM.

The *onshore* portion of the GoM basin has produced and continues to produce an enormous amount of oil and natural gas. For the purpose of this paper, we consider only the *offshore* component, which is the seaward extension of geologic formations and structures that are contiguous beneath the coastline out beneath the continental shelf and deep water of the slope and basin floor. Offshore oil drilling is divided into three components by depth: (1) *shelf* out to 125 m depth, (2) *deep water* from 225 to 1500 m depth, and (3) *ultra- deep water* >1,500 m depth. The deepest part of the modern Gulf of Mexico, the Sigsbee Plain (Sigsbee Deep 2018), is estimated to be ~3750–4384 m deep and is underlain by oceanic crust (Fig. 4.1). The offshore GoM

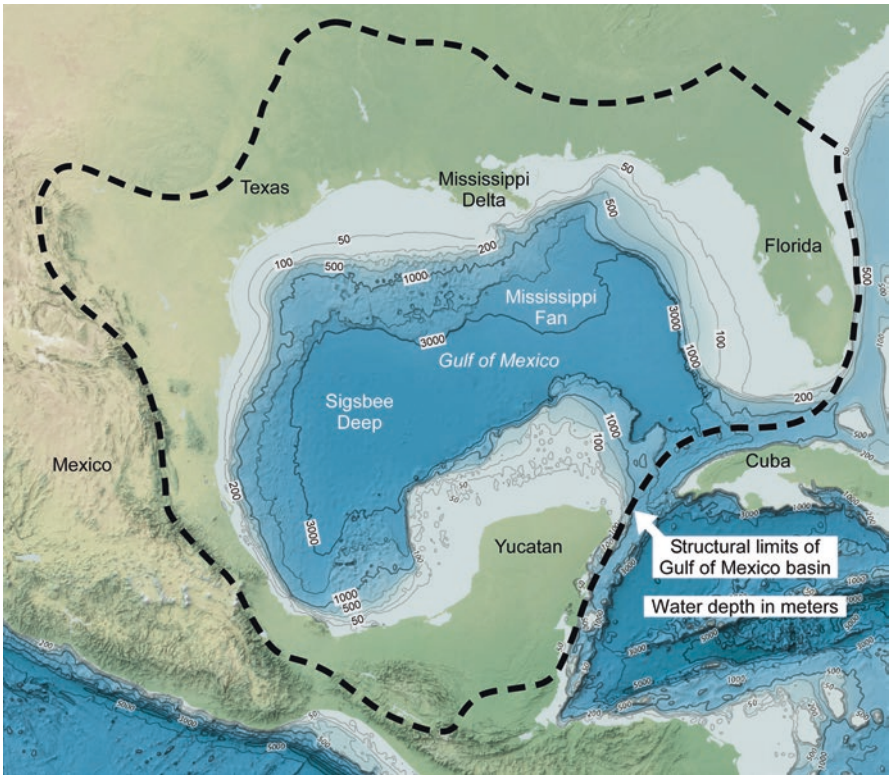

Fig. 4.1 Bathymetry of the Gulf of Mexico reveals the irregular seafloor caused by salt structures in the north and south and the wide flat carbonate platforms in the east and southeastern Gulf. Approximate structural limits of the Gulf of Mexico basin from Salvador (1991a). Background imagery from https://noaa.maps.arcgis.com/home/webmap/viewer.html is a combination of GEBCO_2014 30 arc-second global bathymetry with Natural Earth 2 landscape

has been producing from shelf to deep water for the past ~73 years, with drilling in ultra-deep-water depths since the late 1980s (BOEM 2017).

The deepest water well site is presently in a little over 3000 m water depth. The US offshore seabed subject to US federal jurisdiction portion of the GoM is referred to by the industry and the federal government (Bureau of Ocean Energy Management—BOEM) as the Outer Continental Shelf (OCS). From a geological perspective, this is a misleading term as most of the GoM hydrocarbon exploration and extraction is not on the continental shelf but on the slope and out into the deep basin. However, it is all considered to be federal OCS. In this chapter we will present a brief review of the geologic history and depositional architecture of one of the most geologically complex, and hydrocarbon-rich, sedimentary basins in the world.

4.2 Evolution of Gulf of Mexico

The GoM began to form in the Late Triassic about 225–200 million years ago (mya) by rifting and breaking up of the Pangaean megacontinent (cojoined North America, South America, and Africa) (Fig. 4.2). Phases of rifting and crustal thinning led to significant extension of continental basement crust forming numerous fault-defined arches and basins. The accompanying regional subsidence created the broader structural dimensions of the entire GoM sedimentary basin as North America (Laurasia) pulled apart from South America/Africa (Gondwana). The overall boundaries of the GoM basin extended far inland beyond the present-day coastline.

Early basin deposition included continental red beds and nonmarine sediments (rivers, lakes, eolian sand dunes) which were followed by evaporites in Middle to Late Jurassic time. As extension and subsidence continued, the GoM basin began

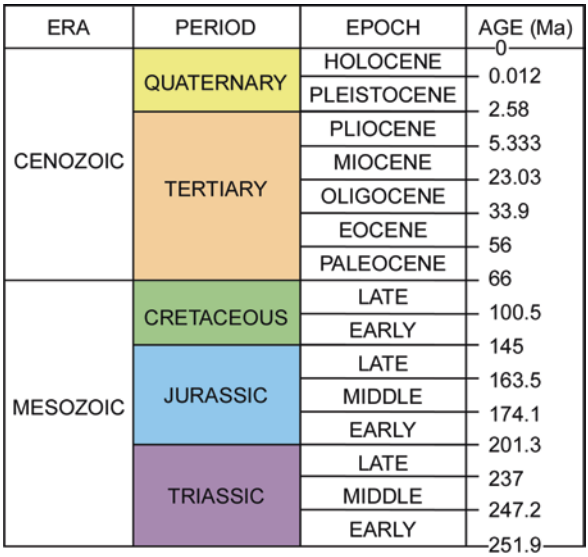

Fig. 4.2 Geologic time scale for events discussed in this paper. Epoch boundary ages after Walker et al. (2018)

flooding with seawater entering through gaps connecting it to the global ocean, specifically the Pacific. Due to multiple sea-level changes, restricted connections to the open ocean, and tectonic motions, the seawater became trapped and ensuing evaporation created brines which precipitated evaporite minerals, primarily halite or salt (NaCl). Evaporite deposits covered much of the basement topography, with an estimated 4 km of original salt thickness accumulating in the Texas to Louisiana slope area in a relatively short time period from ~167–165 mya (Salvador 1991b; Weimer et al. 2017).

Eventually, probably by 160 mya, normal salinity marine waters entered through permanent and fully opened connections to the global ocean thus shutting down evaporite deposition. Continued rifting and seafloor spreading extending to the end of Jurassic time led to seafloor spreading producing oceanic crust. This led to the separation of the salt deposits forming two primary hydrocarbon provinces in the GoM – the Louann Salt in the northern GoM and Campeche Salt in the southern GoM off Mexico (Fig. 4.3). The remobilization of these early salt deposits has played a key role in the structural development and entrapment of hydrocarbons in the GoM. However, possibly due to the combined and simultaneous effects of

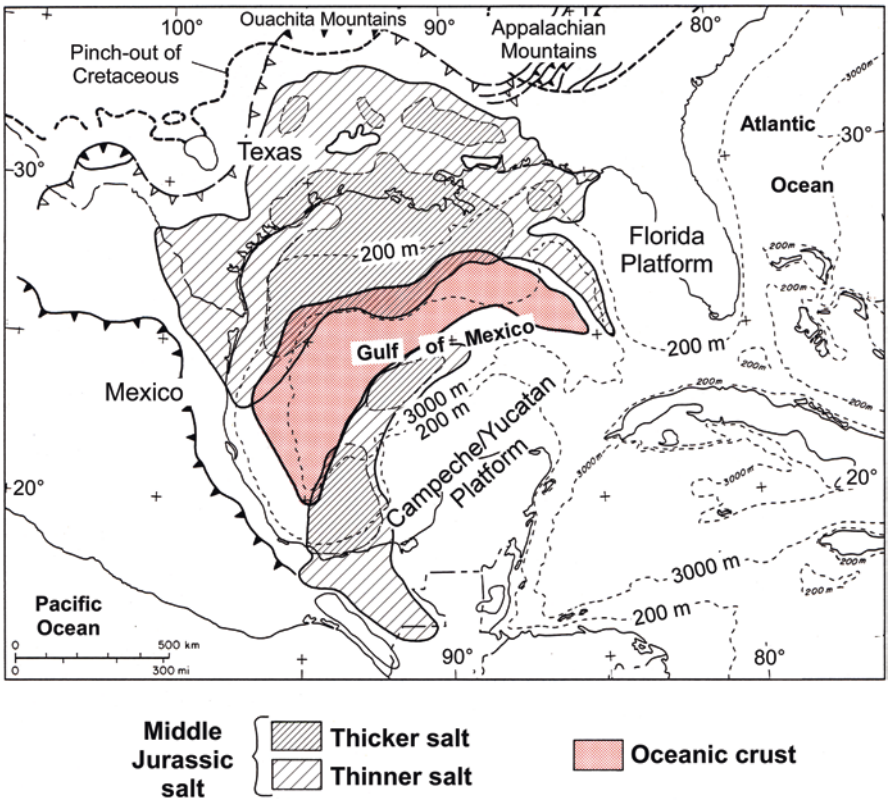

Fig. 4.3 Distribution of salt provinces and oceanic crust. (From Salvador 1991c)

restricted, physical circulation within the GoM and global oceanic anoxic events (OAE), significant amount of organic matter was deposited within the muds that were now being shed off the surrounding land mass. These organic-rich muds were deposited from ~160 to 145 mya from the Late Jurassic into the very Early Cretaceous when global OAEs were becoming prominent, global temperatures were increasing, sea level was rising, and the Earth was entering its greenhouse phase. Along with extensive Late Jurassic tidal flat deposits that produced lipid-rich algal organics, these early deposits contributed much of the primary source rocks that ultimately provided the hydrocarbons in the GoM.

The Late Jurassic transition to more open marine conditions also saw formation of two large carbonate platforms that framed the southern and eastern margins of the GoM. Significant growth of these shallow-water carbonate platforms in the Early Cretaceous formed the thick foundations of the Yucatan/Campeche Platform and the Peninsular Florida Platform—neither of which have become significant hydrocarbon-producing areas. Meanwhile, siliciclastic sediment (non-carbonate sand and mud) was delivered to the Gulf basin largely progressing from north to south and west to east. Following the Laramide orogeny (Laramide Orogeny 2018) in the Late Cretaceous (beginning ~70–80 ma), a massive influx and progradation of clastic sediment entered the northern GoM extending through the Cenozoic. Up to 20 km of sediments eventually accumulated on top of the Louann Salt and the organic-rich source beds which progressively loaded and remobilized the early salt deposits, creating complex subsurface structures that play a major role in trapping hydrocarbon accumulations targeted by oil and gas exploration. Throughout time, sea-level fluctuations have also acted to influence sedimentary facies distribution and stacking patterns of source rocks, reservoirs (e.g., sandstones), and seals (e.g., shales), including drowning of the GoM Early Cretaceous carbonate platforms.

The massive sedimentary influx had six major effects. First, it introduced sands into deep water as submarine fans, which became key reservoir rocks into which hydrocarbons would eventually flow and accumulate. Second, as the weight (lithostatic load) of the sedimentary overburden on top of the Louann increased, the salt started to flow plastically both vertically and laterally. These allochthonous salt systems continually evolve, imparting a multitude of diapiric structures and tectonic processes that reshaped the internal three-dimensional structure and geometries of the sedimentary section (Rowan 2017). This deformation of the 4 km of salt formed a huge number of enormously complex structures that resulted in trapping migrating oil and gas (Fig. 4.4). Third, the high sedimentation rate caused differential compaction creating extensive faulting (listric or growth faults) that also created an enormous number of traps. Fourth, as the sedimentary cover thickened, the lithostatic loading caused increased subsidence in the basin thus subjecting the source rocks to increased temperature and pressure. Thermal maturation resulted in the transformation from organic matter to crude oil and natural gas. Fifth, units of impermeable fine-grained sedimentary units formed seals completing the trapping ability of various structures. Sixth, the rapid sedimentation rate and compaction created widespread overpressurization common to many of the oil and gas accumulations in

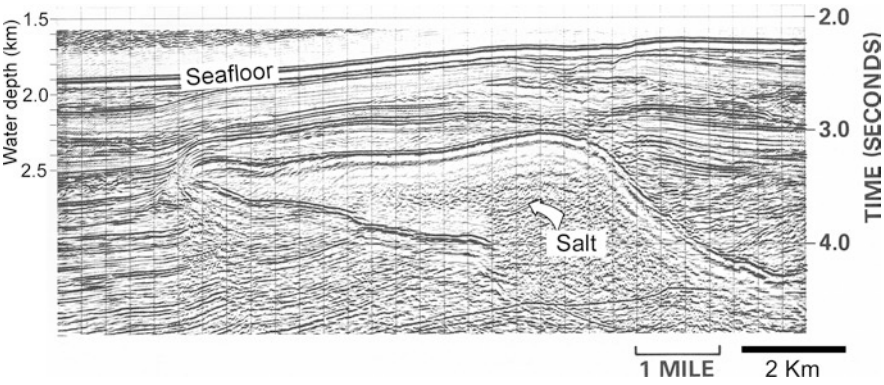

Fig. 4.4 Seismic section showing example of a salt sheet that intruded shallower sediment. Salt can migrate vertically and horizontally, trapping hydrocarbons in underlying and adjacent strata. (Source: Nelson (1991))

the northern GoM. Overpressurization of oil and natural gas accumulations poses a huge hazard during drilling and extraction operations.

Notable features of the present-day GoM include the wide carbonate platform ramps of the Florida and Yucatan shelf margins, Campeche-Sigsbee Knolls in the south, the Mexican Ridges along the western margin, a wide Texas-Louisiana continental shelf and slope across the northern Gulf which is flanked by the Sigsbee Escarpment (formed by horizontal subsurface salt extrusion), and the Mississippi Fan system (Buffler 1991) (Fig. 4.5). Some Early Cretaceous carbonate buildups that extend around the western and northern Gulf margins have been buried by the clastic influx from the west and north and are mostly far inland (USA) or beneath the present coastline (Mexico) (Nehring 1991). The shallow-water Florida and Campeche carbonate banks were drowned in the mid-Cretaceous, transitioning to deep-water environments of carbonate and Tertiary siliciclastic sediment accumulation (Worzel and Bryant 1973; Mitchum 1978).

4.3 Basic Ingredients Required to Generate Oil/Gas Accumulations

Simply stated, there are five primary ingredients that must be present in any sedimentary basin to form a hydrocarbon megaprovince. They are (1) a rich and abundant source of organic matter, commonly called *source rocks*; (2) *thermal maturity* (heat) to transform the organic matter into crude oil and natural gas; (3) *migration* through porous and permeable rocks—*reservoir rocks*; (4) multiple features such as folds, faults, or salt structures (diapirs and pillows) or an up-dip decrease in reservoir rock permeability to *trap* the migrating hydrocarbons; and (5) overlying or surrounding impermeable rocks forming part of the trap called *seals* such that the hydrocarbons cannot escape.

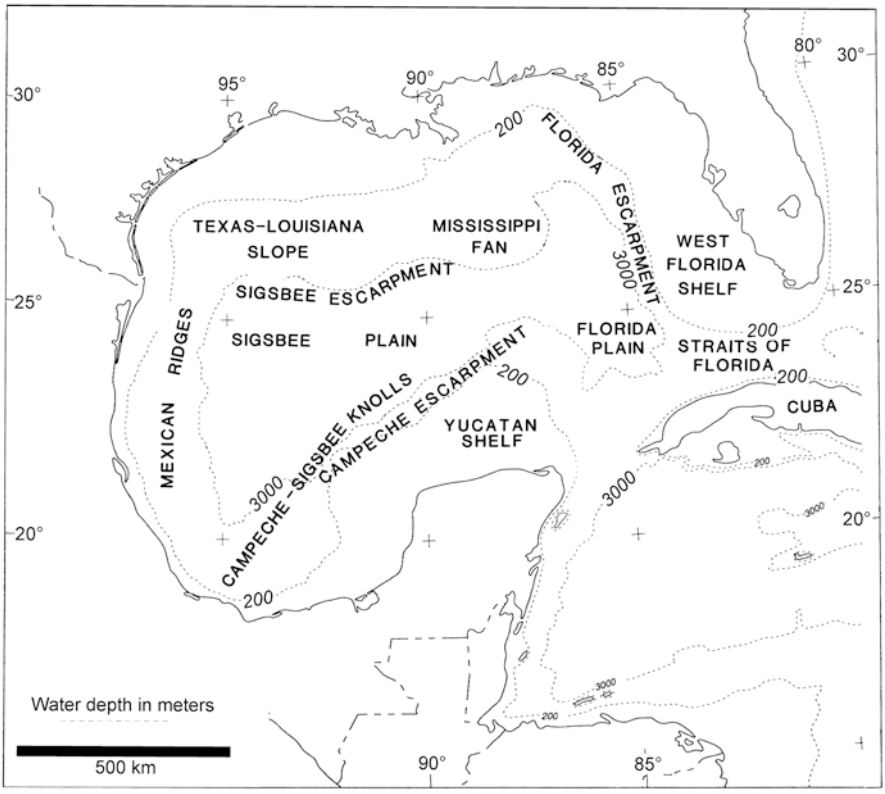

Fig. 4.5 Geographic features in the GoM. (Source: Buffler (1991))

A *source rock* is capable of generating great quantities of hydrocarbons of economic significance (Brooks et al. 1987). Since most hydrocarbon accumulations are associated with marine sedimentary rocks, the source of the organic matter comes from the primary productivity of the Earth's past oceans and marginal marine environments. Some source rocks do form in lacustrine or nonmarine deltaic environments. The total organic carbon (TOC) is the primary measurement and the quality of the organic matter indicated by the presence of key organic molecules.

In the marine environment, remains of planktonic organisms and bacteria, preserved under anoxic conditions, constitute the organic matter to be converted later to crude oil and gas through thermal maturation. Upwelling environments, whereby nutrients from deeper water are brought to the surface where light can drive photosynthesis, are primary organic matter production sites. Ultimately, sufficient organic matter has to sink, escape the biologic pump (recycling of sinking organic matter back to the surface), reach the seafloor along with inorganic muds, and become buried and lithified with time thus forming an organic-rich shale source rock. Overall, source rocks in general average 1.8–2.2% TOC. An average shale has 0.8% TOC. In stark comparison, source rocks in the GoM range reach up to 15%

TOC (Jacques and Clegg 2002). So, organic enrichment of the initially deposited marine muds is one of the primary reasons the GoM is one of the world's hydrocarbon megaprovinces.

Thermal maturation, also called thermal cracking, is the temperature and time required to convert buried organic matter to crude oil (kerogen, a commonly mentioned term, is a very early phase of crude oil). Crude oil is an unrefined liquid hydrocarbon composed of many hundreds of organic compounds. With burial, the TOC-rich shales experience increased heat as part of the evolving geothermal gradient, the rate at which temperature increases with respect to increasing depth in the Earth's interior. Obviously, the geothermal gradient can vary enormously depending upon geologic setting. But, away from plate tectonic boundaries, heat increases at depth at ~25–30 °C/km worldwide (Geothermal Gradient n.d.).

There are temperature ranges or windows where crude oil and gas will form, for oil, 60–120 °C, and for natural gas, 100–200 °C. For crude oil, if the ambient temperature is raised above 130 °C for even a short period of time, natural gas will begin to form (Hyne 2001). The transformation from organic matter to crude oil and natural gas takes place on multi-million-year time scales. In general, oil is most commonly found at subseafloor depths ~3 km. At subseafloor depths >5 km, mostly natural gas is found as the ambient temperature is too high for oil to remain stable.

Migration through *reservoir rocks* occurs as newly formed oil, and gas are created during thermal maturation along with burial and compaction. Faults and fractures within the relatively impermeable source rocks allow the hydrocarbons to seep upward into overlying more permeable sedimentary rocks (sandstones or limestones). These overlying sedimentary units were deposited later under different conditions than were the source rocks. These more porous and permeable units, also called *carrier beds*, provide the conduit for the hydrocarbons eventually to be trapped on the upward journey or to reach the seafloor forming seeps. The Mississippi River system includes both source and reservoir rocks extending from deltas to deep-water submarine fan. Oil and gas are less dense than the seawater that was trapped interstitially as sediments were deposited. This upward flow of the oil and gas is a fundamental process in the hydrocarbon development of a sedimentary basin (Hyne 2001).

Traps and *seals* prevent oil and gas from migrating further upward in a reservoir rock. As a result the hydrocarbons begin to accumulate commonly resulting in an economically viable extraction site. Traps may be anticlinal folds whose closure captures upwardly migrating fluids. Traps may be faults whereby hydrocarbon migration is blocked by the immediate juxtaposition of much lower permeable rocks immediately on the other side of the fault. Upwardly migrating fluids in reservoir rocks will be stopped by completely impermeable evaporites (mostly salt, NaCl, in the GoM) in vertical, diapiric structures or by laterally decreasing permeability in the reservoir rock (pinch out) ultimately becoming impermeable, forming a stratigraphic trap. Where impermeable, non-fractured, or non-faulted strata overlie reservoir rocks, a seal is created preventing further possible upward fluid migration. In the northern Gulf, traps and seals are constantly evolving in response to ongoing sediment loading and salt movement, reflected by hundreds of hydrocarbon seeps across the continental slope.

Finally, the natural gas may become overpressurized posing serious problems during extraction. In areas of high sedimentation rates and rapid burial, the pore pressure of the trapped gas increases (oil, being a liquid, cannot be compressed). If the gas cannot escape due to the efficiency of the trap, its pressure increases more dramatically than surrounding areas where pore fluids can escape at a rate that is in equilibrium with the sedimentation rate. If an overpressurized trap is penetrated by drilling, a blowout could occur—hence the universal need for blowout preventers on the seafloor surrounding each drill string, particularly in the GoM (Mello and Karner 1996).

4.4 Exploration and Production Trends

About 40 years after oil was discovered in east Texas in the early 1900s (famous discovery named Spindletop near Beaumont in 1901), the first offshore drilling rigs ventured into a few meters of water just off the coast. By 1947, a consortium led by Kerr-McGee successfully completed the first well off Louisiana out of sight of land via a drilling ship. Since then, more than 7000 drilling platforms have been constructed (and about 5000 have been removed) in the northern GoM making this offshore portion of the basin to be one of the largest hydrocarbon megaprovinces in the world (BOEM 2018). By 1987, the offshore GoM had produced 222.5 billion of barrels of oil equivalent (BOE; unit of energy released burning 1 barrel oil or 5620 ft^3 natural gas), which amounted to 9% of the world's oil and 11% of the world's natural gas. A hydrocarbon megaprovince at that time was defined as a basin that had produced >100 billion BOE. Only the Arabian/Iranian province had produced more (Nehring 1991). Today, the GoM in US-controlled waters has "technically recoverable resources of over 48 billion barrels of oil and 141 trillion ft^3 of gas" (Lease Sale 250 2018). This amounts to approximately 68 billion BOE. Seemingly, the GoM has produced much more BOE in the past than is known technically recoverable in the future. More recently (2015/2016), the offshore GoM generated ~18% of the total US crude oil (GoM, 1.6 million barrels/day; total US, 8.9 million barrels/day—late 2017/early 2018 data) and 5% of the total US natural gas. Additionally, 45% of the entire US oil and 51% of the US natural gas production is refined and processed along the northern GoM coastline.

The offshore GoM has been producing from shelf to deep water for the past ~70 years. Ultra-deep-water drilling was reached in the late 1980s and progressed to depths near 3000 m by the 2000s (Fig. 4.6). Maximum water depths have hovered around 3000 m for the past 15 years. Since 2005, activity on the shelf and upper slope has declined, while deep water activity has remained strong except for a drilling moratorium in 2010 following the *Deepwater Horizon* oil spill. A drop off in drilling activity in water depths shallower than ~800 m could indicate a depletion of remaining resources in the more accessible mid-water depths and mostly located off Texas (Fig. 4.7). However, deep water GoM oil and gas production as a percentage of total US OCS production shows continuing growth (Fig. 4.8). This record for

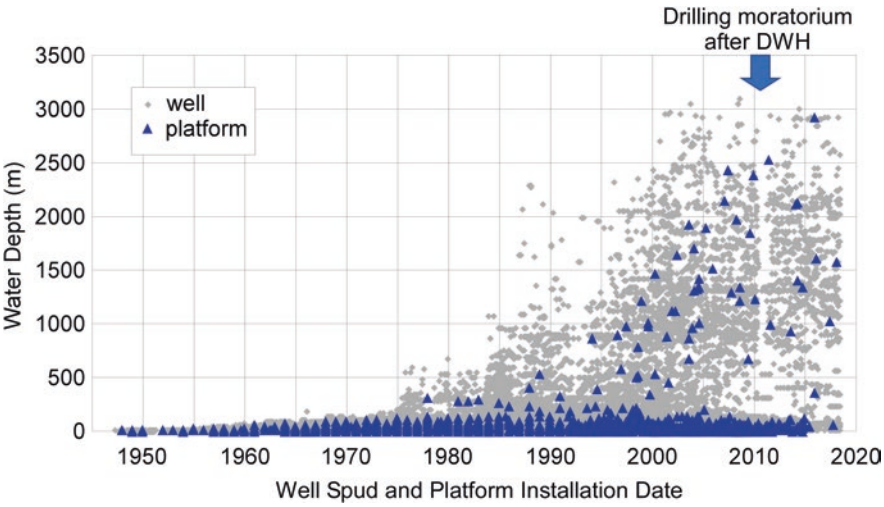

Fig. 4.6 Plot of well spud dates and platform installations versus water depth for US GoM from 1947 to 2018. Data from the BSEE web site in August 2018. Total number of wells is 53,238. Total number of platforms is 1964. Note the persistent trend into deep water. The deepest platform to date was installed January 2016 in 2914 meters water depth. Note the hiatus in drilling activity due to a drilling moratorium following the Deepwater Horizon oil spill in 2010. (Source: BSEE, Deepwater Natural Gas and Oil Qualified Fields. https://www.data.bsee.gov/Leasing/OffshoreStatsbyWD/Default.aspx)

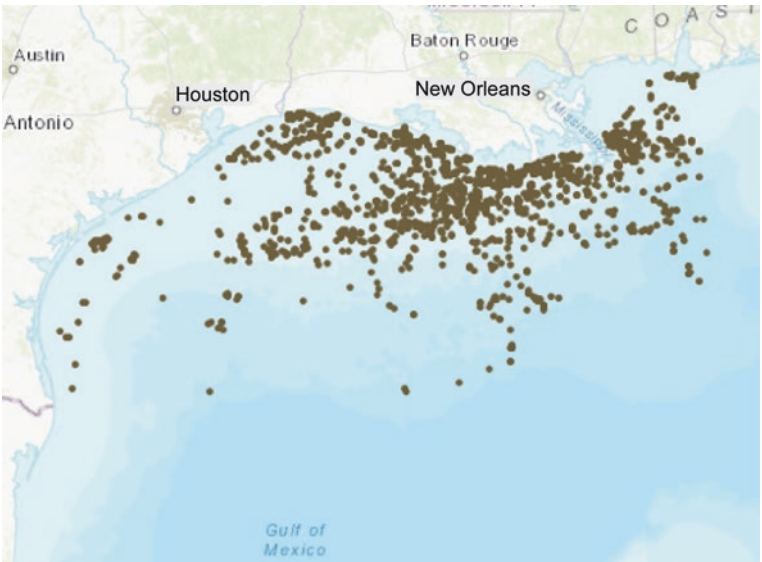

Fig. 4.7 Active oil and gas platforms in federal waters in November 2018. (Source: https://www.eia.gov/special/gulf_of_mexico/index.php)

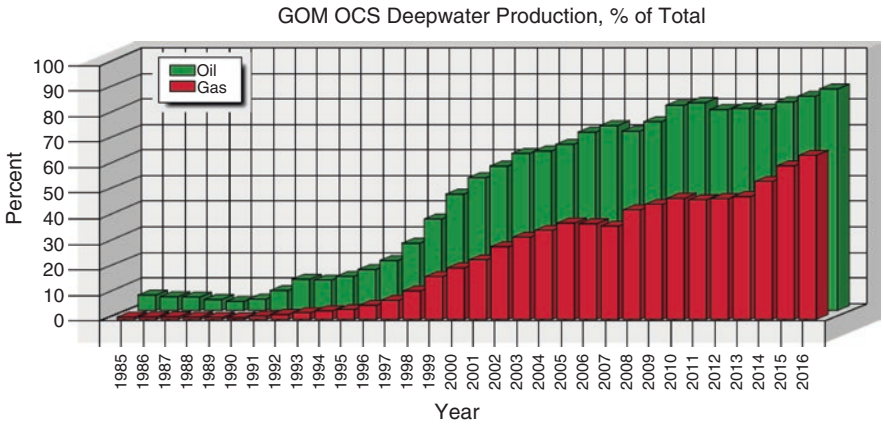

Fig. 4.8 Plot showing deep-water production as a % of all GoM OCS production. The share of production from deep water continues to increase. (Source: https://www.data.bsee.gov/Production/ProductionData/Summary.aspx)

well spudding is one measure of future trends, with production of discovered reserves following many years into the future (Fig. 4.6). Additionally, there is the remote possibility of hydrocarbon extraction east of the Florida moratorium line at some point in the future. And, of course, our neighbors, Mexico and Cuba, have conducted hydrocarbon exploration. PEMEX, the Mexican national oil company, has produced significant oil and gas in their own offshore exclusive economic zone (Pemex.com 2018). The Cubans have yet to do so, although oil and gas are produced in that country onshore along the northern coast (Hemlock 2017).

4.5 Where Is the Industry Headed Next and Why?

A review characterizing play areas based on geologic setting is provided in a recent BOEM report (BOEM 2017). This report lists some 12 assessment areas for Cenozoic strata and 13 Mesozoic play areas. Significant areas of potential that are the least explored are in the deep Gulf or within the eastern planning region that includes much of the west Florida offshore area currently under a drilling moratorium until 2022. Salt-influenced traps will continue to be important throughout the northern GoM slope region where extensive clastic deposition within slope basins and the Mississippi Fan created a thick section for reservoir accumulations (Fig. 4.9). Cenozoic strata will continue to be important targets that have trapped hydrocarbons migrating from deeper source rocks in association with faulting and salt deformation. In ultra-deepwater, some untapped areas of interest could include the Buried Hill play area (Fig. 4.10), an undrilled area that has characteristics similar to productive plays elsewhere in the world that include Jurassic to Cretaceous siliciclastics and carbonates intermixed with early rift blocks forming structural traps.

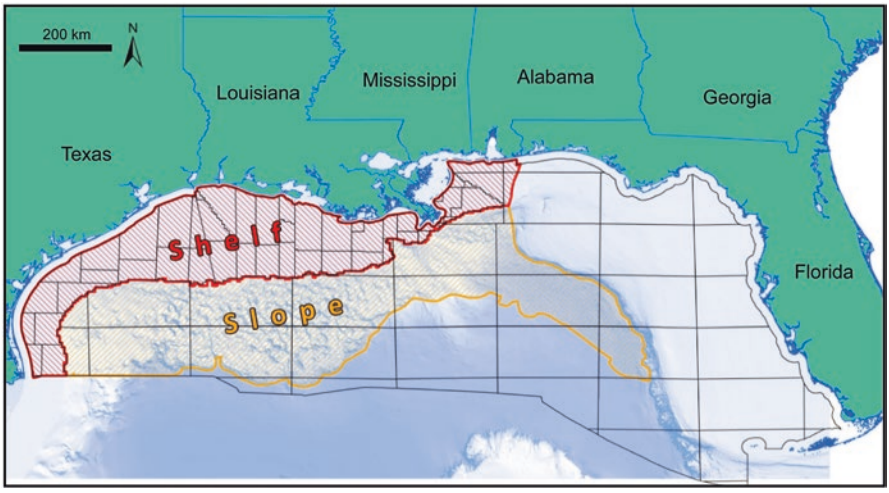

Fig. 4.9 Thick Cenozoic shelf and slope deposits extend into deep water. (From BOEM (2017))

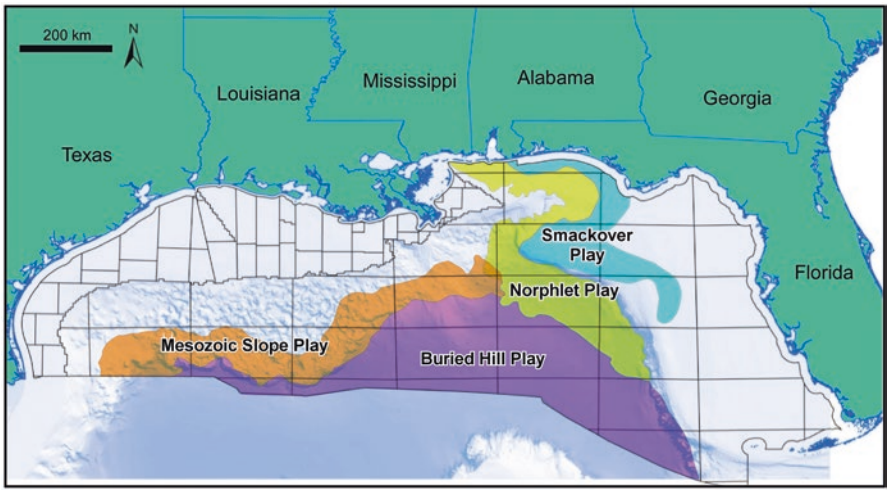

Fig. 4.10 Selected deepwater plays illustrating potential future exploration targets. (Modified from BOEM (2017))

In addition, the Jurassic Norphlet play area hosting important sandstone reservoirs and overlying Smackover known for source rocks as well as reservoirs is also promising. A recent Norphlet discovery in the northeastern GoM announced by Shell in early 2018 is an indicator of this future potential (OGJ editor 2018). The other unknown potential lies in the eastern planning region off west Florida which is currently under a drilling moratorium until 2022.

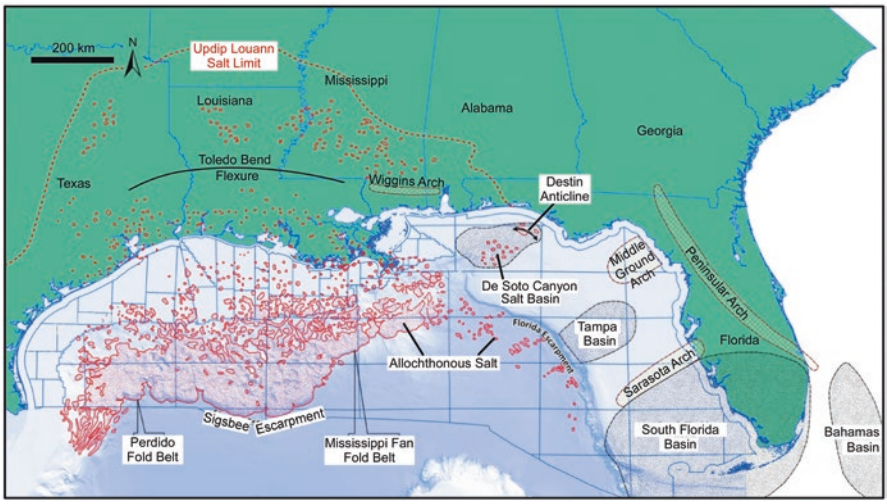

Fig. 4.11 Distribution of salt structures in northern GoM and potential basins of interest for hydrocarbons on the west Florida shelf. (From BOEM (2017))

Three important basins beneath the west Florida shelf and slope include the De Soto Canyon/Destin Dome area off the panhandle with known gas reserves, the Tampa Basin holding substantial Mesozoic to Cenozoic deposits, and the South Florida Basin that has been producing onshore for decades (Fig. 4.11). As always, salt structures along the base of the Florida Escarpment in deep water indicate potential structures for reserves. Exploration activity in Mexican waters is substantially less than the US waters, but similar factors are important.

4.6 Online Resources for Up-to-Date Information

Many statistics presented in this chapter are time sensitive and subject to change. Several online resources are easily accessible to provide up-to-date information on US oil and gas exploration activity.

1. Bureau of Ocean Energy Management (BOEM) – "manages development of US Outer Continental Shelf energy and mineral resources." Among other things, BOEM supports environmental assessment studies and manages lease sales (https://www.boem.gov).
2. Bureau of Safety and Environmental Enforcement (BSEE) – provides regulatory oversight and enforcement (https://www.bsee.gov). A particularly useful page for up-to-date data is at https://www.data.bsee.gov/Main/Default.aspx.
3. US Energy Information Administration (EIA) – provides data for statistics and analysis for all US energy resources (https://www.eia.gov).

4.7 Conclusions

Globally, offshore oil production amounts to ~30% of all the oil extracted. As such the GoM offshore produces ~6% of all the world's oil. The only other offshore basins that are about as productive as the GoM are off Norway, Angola, and Brazil. The rest of the global offshore production comes from many, much smaller basins. This very brief and simplified summary of the geologic history of the GoM reveals that the ingredients needed to produce a hydrocarbon megaprovince were all created in abundance within the past 200 my. The industry continues to explore ultra-deepwater sites as well as to continue to examine more challenging sites heretofore unexplored in shallower water. Additionally, there is the remote possibility of hydrocarbon extraction east of the Florida Moratorium line at some point in the future. Although the extraction of the GoM's oil and natural gas is in its mature phase, studies indicate that oil and gas reserves are significant (28–137 billion BOE in the northern GoM, Weimer et al. 2017) and that the GoM will be producing for many decades into the future.

Acknowledgments We thank Eugene Shinn for discussions and tips on current events, and Harry Roberts for helpful review comments.

References

BOEM (2018) https://www.data.boem.gov/Platform/PlatformStructures/Default.aspx

Brooks J, Cornford C, Archer R (1987) The role of hydrocarbon source rocks in petroleum exploration. In: Brooks J, Fleet AJ (eds) Marine petroleum source rocks, Geological Society Special Publication No. 26. Geological Society, London, pp 17–46

Buffler RT (1991) Seismic stratigraphy of the deep Gulf of Mexico basin and adjacent margins. In: Salvador A (ed) The geology of North America, vol J, The Gulf of Mexico Basin. The Geological Society of America, Boulder, pp 353–387

Bureau of Ocean Energy Management (2017) Assessment of technically and economically recoverable hydrocarbon resources of the Gulf of Mexico outer continental shelf as of January 1, 2014. Outer continental shelf report BOEM 2017-005, 44 p

Geothermal Gradient (n.d.) In Schlumberger Oilfield Glossary online. Retrieved from https://www.glossary.oilfield.slb.com/Terms/g/geothermal_gradient.aspx

Hemlock D (2017) Inside Cuba's plan to boost domestic oil production. CUBATRADE digital magazine. http://www.cubatrademagazine.com/inside-cuban-plan-boost-domestic-oil-production/. Accessed Oct 2018

Hyne NJ (2001) Nontechnical guide to petroleum geology, exploration, drilling, and production, 2nd edn. PenWell Corporation, Tulsa, 598 p

Jacques J, Clegg H (2002) Gulf of Mexico Late Jurassic source rock prediction. Offshore Mag 62(10). https://www.offshore-mag.com/articles/print/volume-62/issue-10/news/gulf-of-mexico-late-jurassic-source-rock-prediction.html. Accessed Oct 2018

Laramide Orogeny (2018) Wikipedia https://en.wikipedia.org/wiki/Laramide_orogeny. Accessed Oct 2018

Lease Sale 250 (2018) Bureau of Ocean Energy Management. www.boem.gov/sale-250. Accessed Oct 2018

Mello UT, Karner GD (1996) Development of sediment overpressure and its effect on thermal maturation: application to the Gulf of Mexico basin. AAPG Bull 80(9):1367–1396

Mitchum RM (1978) Seismic stratigraphic investigation of West Florida slope. In: Bouma AH Moore GT and M. Coleman M (eds) Framework, facies, and oil-trapping characteristics of the upper continental margin: AAPG Studies in Geology No. 7, pp 193–223

Nehring R (1991) Oil and gas resources. In: Salvador A (ed) The geology of North America, vol J, The Gulf of Mexico Basin. The Geological Society of America, Boulder, pp 445–494

Nelson TH (1991) Salt tectonics and listric-normal faulting. In: Salvador A (ed) The geology of North America, vol J, The Gulf of Mexico Basin. The Geological Society of America, Boulder, pp 73–89

OGJ editors (2018) Shell makes sixth discovery in Norphlet deepwater play. Oil Gas J. https://www.ogj.com/articles/2018/05/shell-makes-sixth-discovery-in-norphlet-deepwater-play.html. Accessed Aug 2018

Pemex.com (2018) Petróleos Mexicanos http://www.pemex.com/en/investors/publications/Paginas/default.aspx. Accessed Oct 2018

Rowan MG (2017) An overview of allochthonous salt tectonics. In: Permo-Triassic Salt Provinces of Europe, North Africa and the Atlantic Margins. Elsevier Inc. https://doi.org/10.1016/B978-0-12-809417-4.00005-7. Accessed Sept 2018

Salvador A (1991a) Introduction. In: Salvador A (ed) The Geology of North America, vol. J, The Gulf of Mexico Basin. The Geological Society of America, Boulder, Colorado, pp 1–12

Salvador A (1991b) Triassic-Jurassic. In: Salvador A (ed) The geology of North America, vol J, The Gulf of Mexico Basin. The Geological Society of America, Boulder, pp 131–180

Salvador A (1991c) Origin and development of the Gulf of Mexico basin. In: Salvador A (ed) The geology of North America, vol J, The Gulf of Mexico Basin. Boulder, The Geological Society of America, pp 389–444

Sigsbee Deep (2018) Wikipedia. https://en.wikipedia.org/wiki/Sigsbee_Deep. Accessed Oct 2018

Walker JD, Geissman JW, Bowring SA, Babcock LE (2018) Geologic Time Scale v. 5.0: Geological Society of America. https://doi.org/10.1130/2018.CTS005R3C. https://www.geosociety.org/documents/gsa/timescale. Accessed Sept 2018

Weimer P, Bouroullec R, Adson J, Cossey SPJ (2017) An overview of the petroleum systems of the northern deep-water Gulf of Mexico. Am Assoc Pet Geo Bull 101(7):941–993

Worzel JL, Bryant WR (1973) Regional aspects of deep sea drilling in the Gulf of Mexico leg 10. In: Worzel B et al (eds) Initial reports of the deep sea drilling project, v.10. U.S. Government Printing Office, Washington, DC, pp 737–748. https://doi.org/10.2973/dsdp.proc.10.129.1973. Accessed Oct 2018

Chapter 5
Gulf of Mexico (GoM) Bottom Sediments and Depositional Processes: A Baseline for Future Oil Spills

Gregg R. Brooks, Rebekka A. Larson, Patrick T. Schwing, Arne R. Diercks, Maickel Armenteros, Misael Diaz-Asencio, Adrian Martínez-Suárez, Joan-Albert Sanchez-Cabeza, Ana C. Ruiz-Fernandez, Juan Carlos Herguera, Libia H. Pérez-Bernal, and David J. Hollander

Abstract The deposition/accumulation of oil on the seafloor is heavily influenced by sediment/texture/composition and sedimentary processes/accumulation rates. The objective of this chapter is to provide a baseline of Gulf of Mexico sediment types and transport/depositional processes to help guide managers where oiled sediments may be expected to be deposited and potentially accumulate on the seafloor in the event of a future oil spill. Based solely on sediments/processes/accumulation rates, regions most vulnerable to oil deposition/accumulation include the deep eastern basin, followed by the western/southwestern basin, and north and west continental margins. The least vulnerable regions include the northwest Cuban shelf and the carbonate-dominated west Florida shelf and Campeche Bank. This is intended to be used as a general, "first cut" tool and does not consider local variations in sediments/processes.

Keywords Sediments · Geochronology · Sedimentary processes

G. R. Brooks (✉)
Eckerd College, Department of Marine Science, St. Petersburg, FL, USA
e-mail: brooksgr@eckerd.edu

R. A. Larson
Eckerd College, Department of Marine Science, St. Petersburg, FL, USA

University of South Florida, College of Marine Science, St. Petersburg, FL, USA
e-mail: larsonra@eckerd.edu; ralarso2@mail.usf.edu

P. T. Schwing · D. J. Hollander
University of South Florida, College of Marine Science, St. Petersburg, FL, USA
e-mail: pschwing@mail.usf.edu; davidh@usf.edu

A. R. Diercks
University of Southern Mississippi, School of Ocean Science and Engineering, Kiln, MS, USA
e-mail: Arne.Diercks@usm.edu

S. A. Murawski et al. (eds.), *Scenarios and Responses to Future Deep Oil Spills*,
https://doi.org/10.1007/978-3-030-12963-7_5

5.1 Introduction

Sediment properties and transport/depositional processes can have major influences on how, when, where, and to what extent contamination from oil spills may be distributed and incorporated into oceanic bottom sediments. Grain size is a dominant control as clay-sized particles can adsorb two to three times more oil than sands, due primarily to their larger surface area (Sorensen et al. 2014). Mineralogy plays a lesser role as both carbonates and siliciclastics have been found to adsorb the same amount of oil for a given grain size (Sorensen et al. 2014). Sedimentation rate can also be a key factor governing how much oil is deposited on the seafloor over a specific time period, but higher sedimentation rates may also lead to more rapid burial, thereby sequestering potentially contaminated sediments. Furthermore, sediment mixing by bioturbation under well-oxygenated conditions controls the degradation of organic matter and hydrocarbons in sediments. Though difficult to quantify in deep-sea sediments, it contributes to the accumulation of hydrocarbons. Recent studies have shown several relationships among geochemical variables, the benthic macrofauna and meiofauna, the bioturbation rates, and burial of organic carbon (Morse and Beazley 2008; Yeager et al. 2004). Processes that transport/deposit oil laden sediments to seafloor centers of deposition (i.e., depocenters) vary according to oceanographic and geologic settings and include pelagic settling, surface and subsurface currents, resuspension/re-sedimentation of previously deposited sediments, cascading, and near-inertial currents.

This chapter is not meant to be an exhaustive review of marine sediment types, transport, or depositional mechanisms but rather a synthesis to help guide managers to where oil-contaminated sediments may be distributed on the seafloor in the Gulf of Mexico (GoM) basin and surrounding continental margins in the event of a future oil spill (Fig. 5.1). It is divided first by oceanographic/tectonic setting (i.e., deep GoM basin vs continental margins) and then by dominant sediment type (i.e., carbonate vs siliciclastic). Each division is then discussed in terms of sedimentology (grain size and composition), transport/depositional processes, sedimentation rates, and susceptibility for oiled sediment deposition (Figs. 5.1, 5.2, 5.3, and 5.4).

M. Armenteros · A. Martínez-Suárez
Universidad de La Habana, Centro de Investigaciones Marinas, Havana, Cuba
e-mail: adrian@cim.uh.cu

M. Diaz-Asencio · J. C. Herguera
Center for Research and Higher Education at Ensenada, CICESE, Ensenada, BC, Mexico
e-mail: herguera@cicese.mx

J.-A. Sanchez-Cabeza
Universidad Nacional Autónoma de México, Unidad Académica Procesos Oceánicos y Costeros, Instituto de Ciencias del Mar y Limnología, Mexico City, Mexico
e-mail: jasanchez@cmarl.unam.mx

A. C. Ruiz-Fernandez · L. H. Pérez-Bernal
Universidad Nacional Autónoma de México, Unidad Académica Mazatlán, Instituto de Ciencias del Mar y Limnología, Mazatlán, Mexico
e-mail: caro@ola.icmyl.unam.mx; lbernal@ola.icmyl.unam.mx

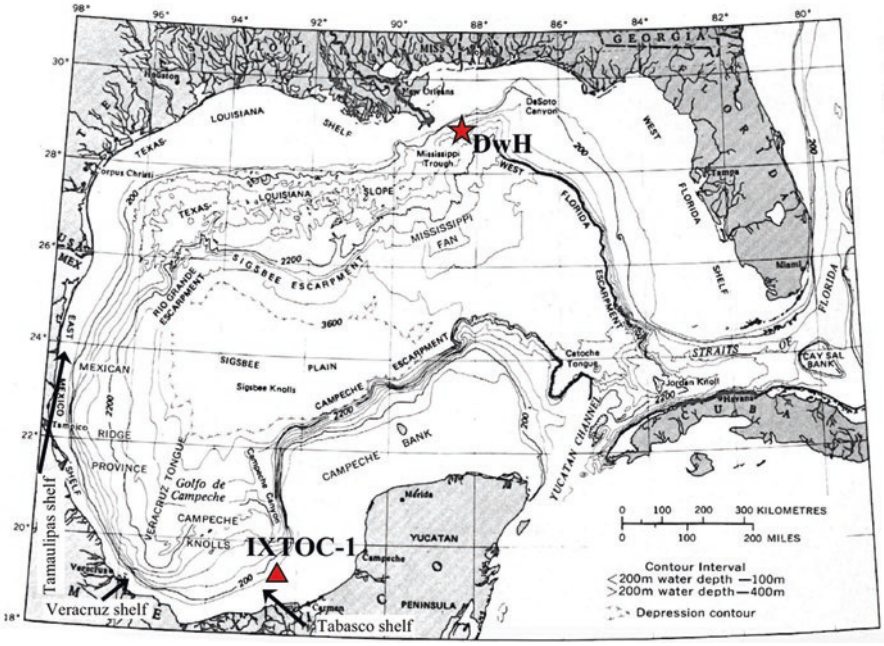

Fig. 5.1 Map of GoM. (Modified from Garrison and Martin (1973). Credit: US Geological Survey)

It is important to note that sedimentation rates may represent a variety of different time scales, and as such they may not be comparable. Recent sedimentation rates (i.e., last ~100 years) on the annual-decadal scale are determined using short-lived radioisotopes (SLR) (^{210}Pb, ^{137}Cs, ^{7}Be, ^{234}Th) and are not directly comparable to centennial-millennial scale rates determined using ^{14}C due to significant differences in time frames (Sadler 1981). Although rates determined for centennial- millennial time scales are included here for reference, they are not as relevant for the purpose of this paper, as rates determined for annual-decadal time scales. In addition, surficial activities of SLR are discussed here even if accumulation rates are not available, because they reflect the recent flux of material to the sea floor. It is important to note that the potential for oiled deposition is discussed here as a function of sedimentary processes only. We fully acknowledge the possibility of other processes that may convey oil to the seafloor.

5.2 Gulf of Mexico Basin

The Gulf of Mexico basin covers ~1.6 million km^2 and has a maximum water depth of >3600 m (Holmes 1976). It is almost completely surrounded by landmasses, and the major input of siliciclastic material is via the Mississippi River to the north, the rivers draining Sierra Madre Oriental to the west, and the Mexican Highlands to the

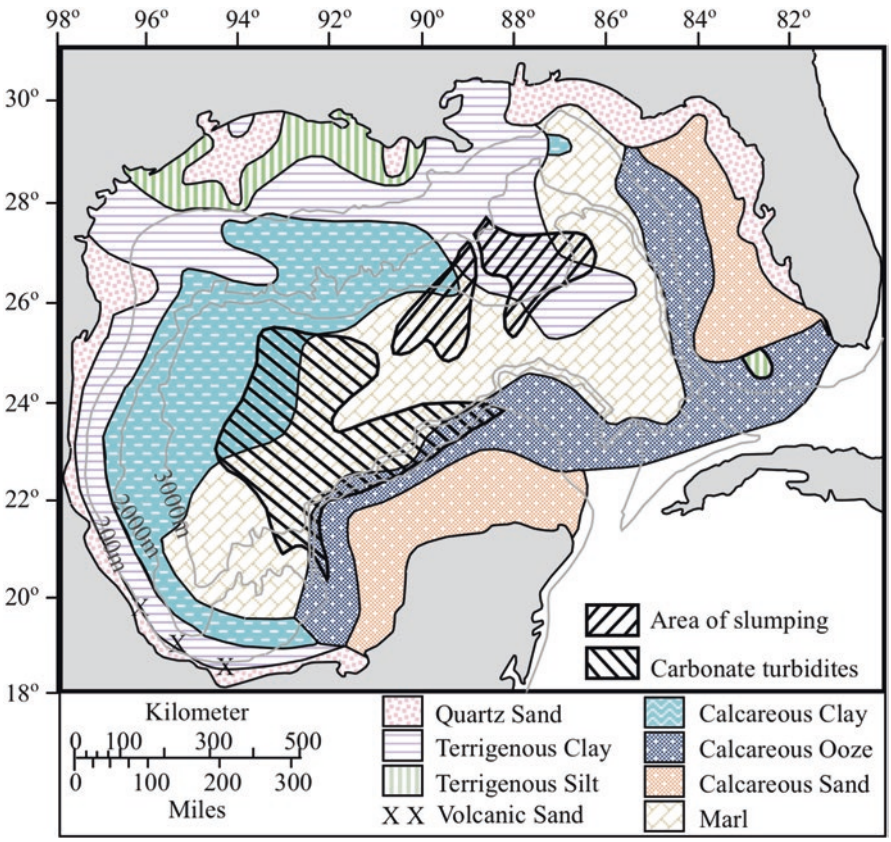

Fig. 5.2 Map showing GoM sediment distribution. (Modified from Holmes (1976). Credit: US Geological Survey; Balsam and Beeson (2003))

south by the Grijalva-Usumacinta river complex. Siliciclastic sediments cover the entire eastern portion of the basin and comprise the Mississippi Fan, which is the most prominent physiographic feature in the eastern GoM. Siliciclastic sediment from other river systems bordering the northern GoM is mostly deposited on the broad continental shelves. On the western and southern slopes, terrigenous sediments dominate, exhibiting a decreasing trend downslope to the abyssal plain. These patterns result from the transport by rivers that drain the Sierra Madre Oriental to the west and the lithogenic materials transported from the southern Mexico highlands to the southern slopes (Diaz-Asencio et al. 2019). The Florida and Campeche shelves are wide and dominated by carbonate sediments and therefore contribute essentially no siliciclastic sediment to the basin (Holmes 1976).

Bottom sediments throughout the GoM basin are generally fine grained (Fig. 5.2) (Balsam and Beeson 2003; Ellwood et al. 2006; Morse and Beazley 2008; Diaz-Asencio et al. 2019), with an average clay content of 71% (Holmes 1976). Sand-sized grains are locally present, especially in the eastern GoM, and consist

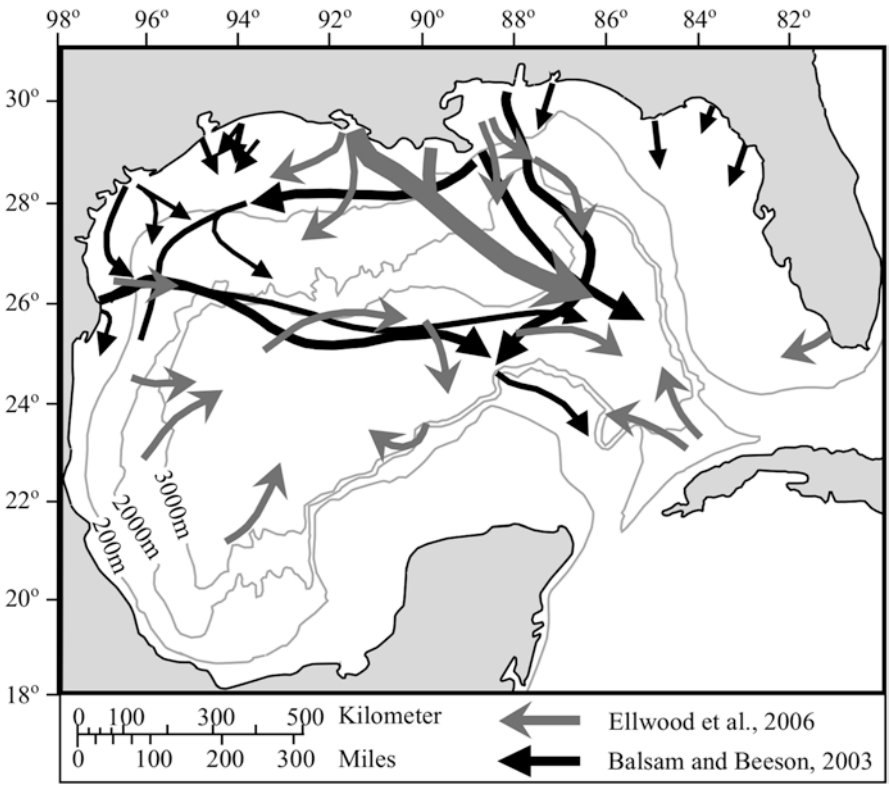

Fig. 5.3 Map showing GoM detrital sediment dispersal paths based on %$CaCO_3$, smear-slide, and diffuse reflectance spectrophotometry (Balsam and Beeson 2003) and magnetic susceptibility (Ellwood et al. 2006) data. (From Balsam and Beeson (2003); minimally altered from Ellwood et al. (2006), Copyright 2018 with permission from Elsevier)

dominantly of planktonic foraminifera (Holmes 1976). Western GoM sediments contain layers of carbonate detritus derived from the Campeche Bank (transported by gravity flow processes), volcanic ash from Mexico, and planktonic foraminifera (Holmes 1976). Short-lived radioisotopes in GoM basin sediments include ^{210}Pb and ^{234}Th, as ^{137}Cs and ^{7}Be are input only from the atmosphere and therefore are absent or undetectable in deep GoM sediments.

5.2.1 Eastern GoM Basin-Mississippi Fan

The Mississippi Fan dominates almost the entire eastern half of the GoM basin (Fig. 5.1). The dominantly clay-sized sediments consist of the clay minerals smectite (30–50%), with subordinate kaolinite (10–20%), chlorite (10–20%), and illite (5–15%) (Ishizuka et al. 1986; Pickering and Stow 1986; Thayer et al. 1986).

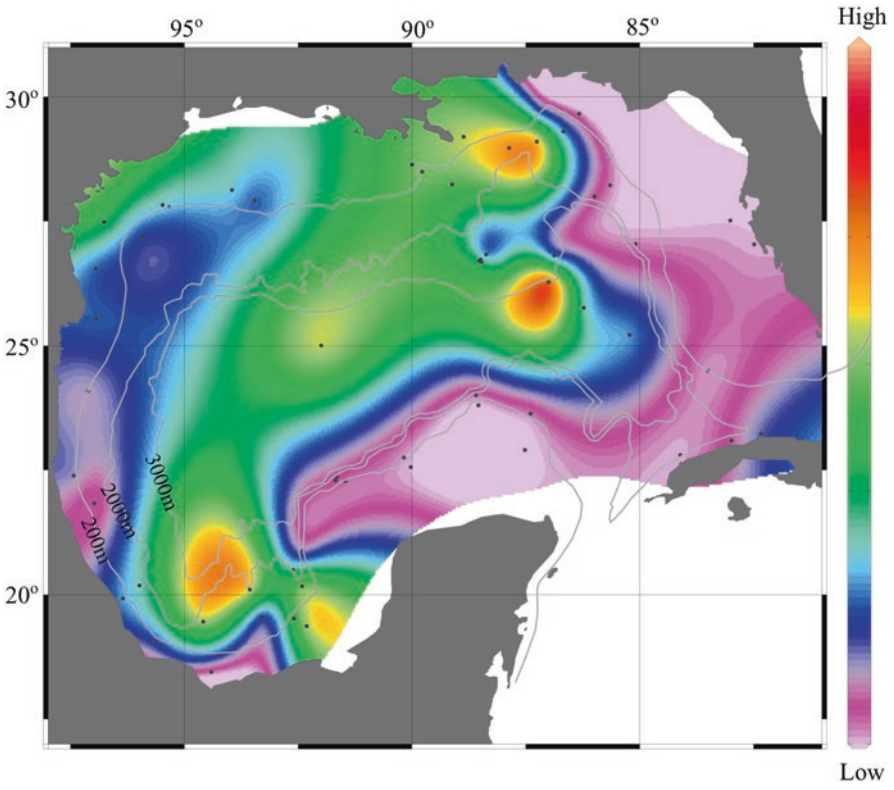

Fig. 5.4 Generalized DIVA gridded contour map showing the potential (blues to reds = low to high) for oiled sediment deposition/accumulation on the GoM seafloor based on sediment grain size, composition, and MAR weighted equally

The clay mineralogy is similar to that of the modern Mississippi River, which is consistent with the Mississippi River being the source for virtually all siliciclastic sediments in the eastern GoM basin (Fig. 5.3) (Thayer et al. 1986).

Stow et al. (1986) recognized eight lithologic facies in Mississippi Fan sediments. Most facies are dominantly fine grained and have a terrigenous origin, and are the result of deposition by re-sedimentation processes, as evidenced by abnormally high accumulation rates, the absence of bioturbation and biogenic components, and the abundance of primary sedimentary structures indicative of mass transport.

The dominant transport/depositional processes for Mississippi Fan sediments are gravity flows, primarily low-density, fine-grained turbidity currents, with subordinate slumps, slides, and debris flows (Coleman et al. 1986; Cremer and Stow 1986; Walker and Massingill 1970). Thin (mm-scale) planktonic foraminifera layers separating the turbidites are deposited by pelagic settling from the sea surface, and although they make up a very small portion of the sediments, they likely represent the greatest amount of time. Although the sediment composition, especially clay mineralogy, indicates the majority of gravity flows originate near the Mississippi

River delta to the north, it has been suggested that input from other surrounding continental margins by gravity flow processes may be common. Brooks et al. (1986) documented a 25-m-thick carbonate unit intercalated in the lower Mississippi Fan, interpreted to be input by a debris flow and/or high-density turbidity current originating from the upper west Florida carbonate slope to the east. Although the bulk of mass transport likely occurred when sea level was much lower (Wetzel and Kohl 1986), Twichell (2011) contends that they can occur during all stages of the sea-level cycle and suggests that modern Mississippi Fan sediments may also be redistributed by strong bottom currents.

Resuspension of material from the seafloor at different depths allows for redistribution of fine-grained suspended particulate material (SPM) within the benthic nepheloid layer (BNL), a zone of increased SPM concentrations and ubiquitous to the world oceans (Gardner et al. 2018). Resuspension events have been documented on different temporal and spatial scales, ranging from small-scale events driven by near-inertial currents to episodic large-scale events, such as the passage of tropical cyclones (Diercks et al. 2018). Fine-grained SPM resuspended in the BNL can travel significant distances before settling out through aggregation and differential settling. A process strongly affected by currents and seafloor morphology, resulting in uneven sedimentation patterns (Turnewitsch et al. 2004, 2013).

Yeager et al. (2004) reported one surface excess ^{210}Pb ($^{210}Pb_{xs}$) activity for the eastern basin of the Gulf of Mexico (20.8 ± 0.1 dpm g^{-1}; 346.7 ± 1.7 Bq kg^{-1}). Sediment mass accumulation rates (MAR) on the Mississippi Fan are highly variable and are a function of the depositional mechanism. In areas where pelagic settling is the dominant mechanism, rates are generally low, on the order of 0.001–0.01 g cm^{-2} yr^{-1}, which is consistent with similar oceanic environments where pelagic settling is the dominant depositional mechanism (Wetzel and Kohl 1986). However, where gravity flows (e.g., mostly turbidity currents in this case) are common, MAR increase dramatically, reaching up to 1.5 g cm^{-2} yr^{-1}. Therefore, MAR on the Mississippi Fan are highly dependent upon gravity flow frequency (Wetzel and Kohl 1986).

$^{234}Th_{xs}$ profiles in sediments generally reflect bioturbation depth, due to both the short half-life of $^{234}Th_{xs}$ (~24 days) and the normally slow accumulation rates of deep-sea sediments. $^{234}Th_{xs}$ can be used as a dating tool to calculate MAR, however in the absence of bioturbation and where sediments accumulate rapidly enough to detect $^{234}Th_{xs}$ downcore (Brooks et al. 2015), which has been shown to be the case for the majority of Mississippi Fan sediments (Coleman et al. 1986).

5.2.2 Western GoM Basin

Western GoM basin (Fig. 5.2) sediments are more pelagic as compared with Mississippi Fan sediments, as they are dominated by marl, which is a mixture of pelagic carbonates (mostly planktonic foraminifera and coccoliths), in combination with terrigenous clays (Fig. 5.2) (Balsam and Beeson 2003; Ellwood et al. 2006).

Pelagic carbonates are less common in the westward-most sections of the basin, as terrigenous clay input from western GoM rivers becomes more abundant. Hence, carbonate content is primarily controlled by dilution associated with fluvial clay influx. Mississippi River clay input is considerable in southwestern sections of the basin, suggesting the Mississippi Fan may be more extensive than previously described (Balsam and Beeson 2003).

The dominant depositional process in the western basin is pelagic settling, but gravity flow deposits entering via western GoM submarine canyons have been identified as well (Balsam and Beeson 2003). Input of shelf margin carbonates from the Campeche Bank via gravity flow processes has also been documented (Davies 1968). It is interesting to note that the pelagic input of carbonate has been little modified by dissolution and that sediments even in the deepest parts of the GoM basin do not appear strongly affected by dissolution (Balsam and Beeson 2003).

Surface $^{210}Pb_{xs}$ activities in the western basin range from 21.5 to 130.5 (± 1.2) dpm g^{-1} (358.4–2175.4 ± 20.0) Bq kg^{-1}) in water depths ranging from 2130 to 3737 m, which are consistent with a previous measurement in this area (29.22 ± 1.38 dpm g^{-1}; 487.1 ± 23.0 Bq kg^{-1}) by Yeager et al. (2004). Overall, $^{210}Pb_{xs}$ MAR for the western basin are spatially homogeneous and generally lower than those in the eastern basin. $^{210}Pb_{xs}$ MAR for one site previously collected at 3521 m water depth was 0.02 (± 0.1) g cm^{-2} yr^{-1} (Yeager et al. 2004), which is consistent with the $^{210}Pb_{xs}$ MAR from recent collections ranging from 0.01 to 0.04 (± 0.1) g cm^{-2} yr^{-1}.

Surface $^{210}Pb_{xs}$ activities in the southern GoM basin range from 18.4 ± 1.5 to 77.6 ± 5.1 dpm g^{-1} (307.0 ± 24.6–1293.2 ± 84.8 Bq kg^{-1}) in water depths of 583–1603 m and between 2.6 ± 0.3 and 7.1 ± 0.6 dpm g^{-1} (43.7 ± 5.2 to 118.7 ± 9.5 Bq kg^{-1}) in shallower areas (16–60 m) (Ruiz-Fernández et al. 2019). The $^{210}Pb_{xs}$ activities in the shallower cores were comparable with those observed in the Coatzacoalcos River (Tabasco shelf) discharge 2.4 ± 0.1 dpm g^{-1} (39.8 ± 1.8 Bq kg^{-1} at 25 m depth; Ruiz-Fernández et al. 2012) and at the discharge areas of Jamapa River discharge ~2.4 to ~4.8 dpm g^{-1} (~40–~80 Bq kg-1, at 21.3–25.5 m depth) and of La Antigua River ~8.4 dpm g^{-1} (~140 Bq kg-1, at 43–50 m depth; Celis-Hernández et al. 2017), as well as with the values reported for sediment cores collected in the Tamaulipas shelf (5.8–13.7 dpm g^{-1} (97 and 228 Bq kg^{-1}) at depth ranging from 38 m to 70 m (Celis-Hernández et al. 2018).

The interval of $^{210}Pb_{xs}$-derived MAR in the southern GoM range between 0.003 and 0.98 g cm^{-2} yr^{-1}, and the MAR values previously reported for the Coatzacoalcos River discharge (between 0.69 ± 0.16 and 0.80 ± 0.08 g cm^{-2} yr^{-1}; Ruiz-Fernández et al. 2012) fit within the higher values of this interval.

Sediments near the Campeche Escarpment show lower sediment accumulation rates (5–10 cm/kyr) and anomalous smaller mixed layers. The persistent deep flow in this region (Pérez-Brunius et al. 2018), as a consequence of the cyclonic boundary current over the Coatzacoalcos Canyon and along the continental slope of the southwestern GoM, controls the transport of finer sediments that are resuspended

by bioturbation and physical processes (e.g., winnowing) in the sediment mixed layers upstream (Diaz-Asencio et al. 2019).

The large region extending from the Sigsbee Abyssal Plain to the north, bounded by the Yucatan shelf and Campeche Escarpment to the northeast and east, by the Tamaulipas and Veracruz continental slopes to the west, by the Campeche Saline Complex to the south, and flanked by the Coatzacoalcos Canyon to the southwest and the Campeche Canyon to the southeast, is characterized by overall lower sediment accumulation rates (mean 4.6 cm/kyr,), deeper sediment mixing, and a balance between terrigenous and carbonate input (Diaz-Asencio et al. 2019).

5.2.3 Implications for Oiled Sediment Deposition/ Accumulation

The dominant mechanism for the initial deposition of oiled sediment in the GoM basin is pelagic settling, which can occur rapidly (days to a few months) (Passow 2016; Brooks et al. 2015) as documented in the northeast GoM as a depositional pulse of MOSSFA (marine oil snow sedimentation and flocculent accumulation) following the 2010 *Deepwater Horizon* (DWH) event. This MOSSFA event resulted in the deposition of a 1–2-cm-thick blanket of oiled sediment beneath the surface slick and subsurface plumes in the DeSoto Canyon region of the northeast GoM within 5 months of sinking from the sea surface (Brooks et al. 2015). Consequently, throughout the GoM basin, deposition may be expected immediately beneath surface slicks and subsurface plumes produced by a future spill. In the eastern GoM basin, dominated by the Mississippi Fan, redistribution of oiled bottom sediments by gravity flows may be expected. Transport would most likely be downgradient to the south-southeast of the Mississippi River delta and proximal fan (Fig. 5.3). The redistribution of oiled sediment originating on surrounding continental margins to the GoM basin may be expected to occur locally, especially off the west Florida shelf and slope, Campeche Bank, and the western GoM margins. Additionally, transport of SPM within the BNL is expected downgradient and will be strongly affected by bottom morphology and near seafloor currents.

Although deposition by MOSSFA may be relatively fast, oiled sediments are more likely to remain exposed on the seafloor (unless redistributed), especially in areas where redistribution processes (e.g., gravity flows) are less common, such as the western GoM basin. In areas where redistribution processes are more common, oiled sediments may be deposited more rapidly, but they would also likely be buried rapidly as well. In the GoM basin, this would be expected in the Mississippi Fan, as well as the basin margins, where gravity flows from the adjacent shelf/slope are more common, such as west Florida, Campeche Bank, and the western GoM margin (Figs. 5.3 and 5.4).

5.3 Carbonate-Dominated Margins: West Florida and Campeche Bank

The carbonate-dominated continental margins of peninsular west Florida and the Campeche Bank (Mexico) (Fig. 5.2) share a similar geologic evolution, morphology, and sediments/sedimentary processes. Bounded by the DeSoto Canyon in the northeast GoM and the Campeche Canyon in the southwest GoM, both consist of wide (up to 250 km), flat continental shelves and steep continental slopes, containing a thin, mostly relict, sediment cover (Antoine et al. 1974).

5.3.1 West Florida

Sediments residing on the west Florida shelf have been well studied (Gould and Stewart 1956; Ginsburg and James 1974; Doyle and Sparks 1980; Hine et al. 2003) and are distributed in shore-parallel facies belts. Inner shelf (within ~40 km of the coast) sediments consist of a mixture of quartz and biogenic carbonate (mostly molluscan skeletal material) sands (Doyle and Sparks 1980; Brooks et al. 2003). Seaward of ~40 km sediments become almost entirely carbonate, consisting of a thin, patchy molluscan sand/gravel, overlying a karstic limestone that is periodically exposed on the seafloor. At the shelf-slope break, sediments consist dominantly of ooids and calcareous algae deposited when sea level was much lower (Hine et al. 2003). Therefore, this part of the margin has experienced extremely low recent sediment deposition.

As sediments consist dominantly of biogenic carbonates and relict, reworked quartz sands, it can be concluded that there has been essentially no recent deposition of terrigenous sediments. Thus, deposition is dominated by in situ carbonate production. Bottom sediments can be remobilized, however, by a variety of processes including Gulf Loop Current intrusion onto the outer shelf along the southern margin (Weisberg and He 2003), strong extratropical storms that may produce large waves and currents, and tropical cyclones. The latter two reportedly impact the northern shelf more than the southern shelf (Hine and Locker 2011).

SLR data and recent shelf sedimentation rates are lacking, but amino acid and ^{14}C dates of surface sediments on the mid-shelf range from ~3.5 to ~7 ky (Back 1972; Brooks and Doyle 1991), which is consistent with extremely slow rates of sediment accumulation.

West Florida slope sediments consist dominantly of pelagic carbonates, specifically planktonic foraminifera and coccoliths, especially in water depths >600 m (Doyle and Holmes 1985; Mullins et al. 1988). The upper slope (<600 m depth) is characterized by a series of hardgrounds immediately below the shelf-slope break, with winnowed sands residing below. Both are reportedly a reflection of the strong southward flowing Gulf Loop Current (Mullins et al. 1988).

The dominant depositional mechanism on the slope is pelagic settling as the Gulf Loop Current provides a dynamic barrier to off-shelf transport of shallow-water

material. The pelagic input is amplified by the Gulf Loop Current, which induces upwelling and therefore increased biological productivity in overlying surface waters (Mullins et al. 1988). Redistribution of slope sediments by gravity flow processes, primarily turbidity currents, slumps, and slides, is common (Holmes 1981; Walker 1984; Doyle and Holmes 1985; Holmes 1985; Brooks et al. 1986), but sediments are likely ultimately deposited in the deep GoM basin (see previous section).

The east-west trending southwest Florida slope bordering the Florida Straits (Fig. 5.1), contains a thick sequence of muds input by off-shelf transport from the shelf to the north. Sediments are further modified by the Florida Current into an eastward prograding sediment drift. Off-shelf transport occurs by the cascading of dense, sediment-laden water from the north. Numerous gullies on the mid-lower slope reflect the periodic downslope movement by gravity flows (Brooks and Holmes 1989, 1990).

Average accumulation rates for slope sediments determined by ^{14}C methods are relatively low at ~2 mm yr^{-1} (Doyle and Holmes 1985). $^{210}Pb_{xs}$ MAR decrease with water depth with rates of 0.03–0.20 ± 0.05 g cm^{-2} yr^{-1} reported on the upper slope and 0.03–0.08 ± 0.04 g cm^{-2} yr^{-1} on the lower slope. Yeager et al. (2004) reported one surface $^{210}Pb_{xs}$ activity (23.2 ± 0.1 dpm g^{-1}; 386.7 ± 1.7 Bq kg^{-1}) on the slope at ~767 m water depth. Surface $^{210}Pb_{xs}$ activity values from Brooks et al. (2015) and more recent collections (this chapter) show a general and uniform increase with depth. Surface $^{210}Pb_{xs}$ activities range from 5.4 to 39.3 (± 1.3) dpm g^{-1} (90.0–655.1 ± 21.7 Bq kg^{-1}) in water depths of 108–406 m, whereas they range from 24.3 to 60.6 (± 1.7) dpm g^{-1} (405.1–1010.2 ± 28.3 Bq kg^{-1}) in water depths of 502–1200 m.

5.3.2 Campeche Bank

The Campeche Bank shelf exhibits shore-parallel facies similar in many ways to that of west Florida. It is almost pure carbonate, containing >70% $CaCO_3$ in the northern section (Diaz-Asencio et al. 2019). The inner shelf (<60 m depth) ranges from 130 to 190 km in width and is dominated by molluscan sands. The outer shelf, a few km to ~30 km in width, consists of ooids, peloids, and lithoclasts from the underlying limestone. Seaward, these sediments become progressively diluted with planktonic foraminifera. Shelf sediments are thin (<1 m thick), and relict (Logan et al. 1969), reflecting the lack of significant modern sediment input/deposition. Deposition is likely dominated by in situ carbonate production, and bottom sediments can be expected to be periodically remobilized by strong storms that may produce large waves and currents (Logan et al. 1969; Ginsburg and James 1974).

^{14}C dates for shelf sediments range from 3–5 ky for inner shelf sediments to 11–14 ky for outer shelf sediments. Therefore, like west Florida, sediment accumulation rates are extremely low. This is supported by surface $^{210}Pb_{xs}$ activities of 0.5–3.7 ± 0.1 dpm g^{-1} (8.3–61.7 ± 1.7 Bq kg^{-1}), which are among the lowest in the Gulf of Mexico.

The poorly studied continental slope bordering the Campeche Bank is steep and currently accumulating little sediment (Antoine et al. 1974; Davis 2017). The sediment cover is thin, and mostly relict, deposited when sea levels were much lower. Modern sediments, although scarce, consist of pelagic carbonates such as planktonic foraminifera and coccoliths (Logan et al. 1969; Ginsburg and James 1974; Davis 2017). Slope sediments can be expected to be periodically remobilized by gravity flow processes, where they will likely be eventually deposited in the deep GoM basin, as evidenced by Pleistocene-Holocene turbidites that reached as far north as the northern edge of the GoM abyssal plain (Davies 1968). Surface $^{210}Pb_{xs}$ activities of slope sediments (36.6 ± 1.4 dpm g^{-1}; 610.1 ± 23.3 Bq kg^{-1}), which are similar to the west Florida slope, support exceptionally slow accumulation.

5.3.3 Implications for Oiled Sediment Deposition/ Accumulation

The carbonate-dominated continental shelves of West Florida and Campeche Bank consist of in situ production/deposition of biogenic carbonate sands and gravels that accumulate very slowly. Consequently, there is very little fine-grained sediment input and essentially no accumulation from pelagic settling. Therefore, it is unlikely that oiled sediments from the sea surface would be deposited by the processes described here, and even if initially deposited, significant accumulation would be highly unlikely (Fig. 5.4). This is evidenced by the 2010 DWH event, as there was no indication of oiled sediment deposition/accumulation on the Florida carbonate shelf east of DeSoto Canyon, even though the original sea-surface oil slick was identified in overlying surface waters (Brooks et al. 2015).

Slope sediments can contain a large amount of fine-grained sediments deposited by pelagic settling. Therefore, in regions of the slope that are accumulating these sediments, oiled sediments from a future spill maybe expected to accumulate (Fig. 5.4). This has been documented by the rapid settling and accumulation (at least in the short term) of oiled sediments to the continental slope in the northeastern GoM following the 2010 DWH event (Daly et al. 2016; Passow and Hetland 2016; Ziervogel et al. 2016). In those portions of the slope where the gradient is steep, which applies to much of the west Florida and Campeche Bank slopes, sediments do not have a tendency to accumulate. Although initial deposition of oiled sediments may take place, gravity flows may periodically transfer these sediments to deeper depocenters in the GoM basin (Fig. 5.3).

5.4 Siliciclastic Margins: Northwest Florida to Mexico

Gulf of Mexico continental margins dominated by siliciclastic sediments extend westward from the DeSoto Canyon region of the Northwest Florida to central Texas, then southward into Mexico, and finally eastward to the Campeche Canyon area,

where sediments once again transition to carbonates (Fig. 5.2). Siliciclastic sediment input is dominated by rivers, the majority of which comes from the Mississippi River, followed by rivers entering the Texas and Tamaulipas to Veracruz shelves to the west, and the Tabasco and Campeche shelves to the south, and finally rivers entering the NE GoM (Fig. 5.3) (Davis 2017).

5.4.1 Northern GoM Continental Margin: Northwest Florida to Central Texas

The continental shelf stretching westward from DeSoto Canyon to the Mississippi River Delta complex borders the Northwest Florida, Alabama, and Mississippi and is dominated by quartz sand, with minor amounts of shell, termed the MAFLA sand sheet (Doyle and Sparks 1980). The primary input of sediments east of the Mississippi River Delta is from the Apalachicola River on the Northwest Florida. Shelf sediments tend to become finer grained westerly, toward the delta, with mud-sized sediments increasing off Mississippi and Alabama. The dominant clay mineral is kaolinite, also from the Apalachicola River, which is generally sequestered on the inner shelf (Balsam and Beeson 2003). The outer shelf is dominated by carbonate sediments of reefal origin mixed with terrigenous sand/silt/clay and lime muds that tend to increase toward the west. Carbonate hardgrounds and bioherms are common at the shelf edge (McBride et al. 2004; Flocks et al. 2011). Balsam and Beeson (2003) contend that most of the sediments on the MAFLA margin are relict, and hence accumulation rates are extremely slow.

The continental slope of the MAFLA region east of the Mississippi River delta coincides partially with the precipitous north wall of the DeSoto Canyon. Although the sediments correspond to what Balsam and Beeson (2003) refer to as marl (Fig. 5.2), sediment texture and composition are likely variable as sediment redistribution by gravity flow processes is common. The DeSoto Canyon has received very little modern sediment input/accumulation (Davis 2017).

West of the MAFLA region, the Mississippi River has a major impact on continental margin sediments of the entire northern GoM (Fig. 5.3). The modern delta extends across the entire shelf, with the river discharging sediments directly onto the continental slope. Except for the most proximal portions of the active delta, the sediment is dominantly clay sized (Balsam and Beeson 2003), and accumulation rates are the highest in the GoM at ~1 m/year. Consequently, slope failure is common as evidenced by slump structures and gullies (Fig. 5.3, Davis 2017).

To the west, the shelf is covered by a mud blanket <8 m thick, occasionally interrupted by sand shoals produced by the reworking of abandoned delta lobes. The grain size locally becomes coarser close to shore, especially off rivers, and near the shelf break (Balsam and Beeson 2003; Davis 2017).

Continuing westward to the approximate position of the Colorado/Brazos River systems of central Texas, Mississippi River muds continue to dominate on the shelf, but relict sands become more abundant (Davis 2017). As most of the modern

sediments entering the GoM in this area are trapped in the estuaries, accumulation rates are considered to be very slow (Balsam and Beeson 2003).

The continental slope in the northern GoM west of the Mississippi River Delta consists dominantly of a very thin (<1 m) layer of bioturbated hemipelagic muds, occasionally interrupted by localized thick slope sediment fans consisting of coarser grained material (Davis 2017). Reported accumulation rates range from 4.6 cm ky^{-1} (Bryant and Liu 2000) to 20 cm ky^{-1} (Davis 2017).

Overall, the dominant sedimentation processes on the shelf include fluvial input from the Mississippi River, bottom sediment reworking, and periodic sediment resuspension from waves and currents (Balsam and Beeson 2003). Hemipelagic slope muds were deposited primarily by pelagic settling, and although the modern sediment layer is generally considered to be quite thin (<1 m), thicker layers appear locally due to sediment ponding in depressions bounded by salt diapirs (Davis 2017). Remobilization of slope sediments by gravity flow processes is common, especially on the slope bordering east Texas (Holmes 2011). While some of this material is re-sedimented on lower portions of the slope, most is transported to the base of the slope and redeposited in the deep GoM basin (Fig. 5.3, Davis 2017).

Surface $^{210}Pb_{xs}$ activities on the northern GoM shelf and slope generally increase with depth, as expected. Surface $^{210}Pb_{xs}$ activity distribution also follows bathymetric features. A good example of this is the bilobate distribution with higher surface $^{210}Pb_{xs}$ activities near the DeSoto Canyon and Mississippi Canyon (aka Mississippi Valley). Surface $^{210}Pb_{xs}$ activities on the northern shelf range from 8.1 to 30.7 (± 0.8) dpm g^{-1} (135.0–511.8 ± 13.3 Bq kg^{-1}). Surface $^{210}Pb_{xs}$ activities on the northern slope range from 27.1 to 65.5 (± 2.0) dpm g^{-1} (451.8–1091.9 ± 33.3 Bq kg^{-1}).

5.4.2 Western GoM Margin: Texas to Mexico

Southward from the approximate position of the modern Colorado/Brazos Rivers, the western GoM continental shelf is generally mud dominated, with sand dominating the inner shelf to a depth of ~15 m (Fig. 5.2) (Balsam and Beeson 2003). Muds consist primarily of clay-sized material, input from the Mississippi River, Colorado/Brazos River system, and the Rio Grande (Fig. 5.3) (Balsam and Beeson 2003; Davis 2017). Consequently, the Mississippi River provides clay-sized sediment as far south as the Texas shelf (Balsam and Beeson 2003). Although the mud blanket is generally considered to be quite thin (m-scale) for most of the shelf, the central shelf between the Colorado and Rio Grande is the site of the second largest sediment depocenter (next to the Mississippi delta) of the GoM. Muds up to 40 m thick have accumulated within the past ~3 ky, originating from the Colorado/Brazos and Mississippi Rivers (Holmes 2011). Locally, the outer shelf contains a significant amount of carbonate sands derived from reworking of relict reefs and banks that thrived during lower sea levels (Holmes 2011).

Like the northern GoM shelf, the dominant sediment transport/depositional process is river input from the west Texas Gulf coast and Mississippi River (Fig. 5.3).

These rivers are responsible for the only modern sediment input, consisting of muds, the largest part of which are clays. The sand-sized sediments on the shelf are mostly relict (Holmes 2011).

Continental slope sediments are dominated by a bluish-brownish fossiliferous mud, believed to represent the reworked product of fluvial-deltaic sediments deposited during sea-level lowstands. Essentially no sediment is being input to this region at present (Davis 2017). Gravity flows are thought to be a common sediment redistribution process on the slope as an extensive set of submarine canyons dissect the continental slope and rise. The sediment source is likely the terrigenous mud deposits residing between the Colorado River and Rio Grande (Balsam and Beeson 2003).

5.4.3 Southwestern GoM Margin: Mexico

The continental shelf from the US-Mexico border to Campeche Canyon narrows considerably, reaching <10 km in width off Veracruz, before widening again toward the Yucatan Peninsula (Davis 2017). Terrigenous sand and mud from river input dominates the northern portion of the shelf. Where the shelf narrows near Veracruz, volcanic glass is an important component in some areas (Fig. 5.2) (Carranza-Edwards 2011). In general, the carbonate content of shelf sediments progressively increases from the Rio Grande to Campeche Canyon (Balsam and Beeson 2003).

The continental slope in this region has been described as rough and irregular and sometimes very steep. Salt diapirs are common, especially to the east approaching Campeche Bank, and create bathymetric depressions that act as sediment depocenters, very similar to the northwest GoM slope (Davis 2017). The Tamaulipas continental slope is dominated by terrigenous sediments (>70%), which decrease downslope. Accumulation rates range from 7 to 13 cm/kyr (Diaz-Asencio et al. 2019). The southern continental slope from Veracruz to Campeche Canyon is also dominated by siliciclastic sediments (>70%), which decrease downslope. Accumulation rates range from 6 to 25 cm/kyr (Diaz-Asencio et al. 2019), with the higher values in the Campeche Canyon.

The dominant sedimentary processes show some similarities to those described for Texas. Shelf sediments are input primarily by rivers entering from the Sierra Madre Oriental to the west and from the Mexican Highlands to the south. Slope sediments are hemipelagic, initially deposited by a combination of pelagic settling of coccoliths and planktonic foraminifera, and silt and clays exported from the shelf regions, and periodically redistributed downslope by gravity flow processes (Fig. 5.3, Diaz-Asencio et al. 2019).

Surface $^{210}Pb_{xs}$ activities on the southern GoM slope increase with depth and follow bathymetric features. One example of a bathymetric control is at a site located in a small (100's of meters in diameter) basin that acts as a depocenter for Campeche Canyon material, where surface $^{210}Pb_{xs}$ activities reach 105.6 ± 0.1 dpm g^{-1} (1760.4 ± 1.7 Bq kg^{-1}). Large river systems also act as a control, supported by high activities (reaching 117.7 ± 0.2 dpm g^{-1}; 1962.1 ± 3.3 Bq kg^{-1}) located just offshore

from the Coatzacoalcos River. The confounding factor is that this increase is not apparent in larger river systems in the northern GoM (e.g., Mississippi River). This disparity could potentially be caused by the type of clay minerals present in each watershed. Overall, surface $^{210}Pb_{xs}$ activities on the southern GoM slope range from 27.6 to 117.7 ± 1.4 dpm g^{-1} and 460.1 to 1962.1 ± 23.3 Bq kg^{-1}.

$^{210}Pb_{xs}$ MAR on the southern slope do not vary uniformly with water depth. Instead, the highest $^{210}Pb_{xs}$ MAR measured are primarily associated with bathymetric features and river inputs. The highest $^{210}Pb_{xs}$ MAR measured (0.27 ± 0.01 g cm^{-2} yr^{-1}) was in a small basin at the base of the Campeche Canyon. There are also subtle increases in $^{210}Pb_{xs}$ MAR associated with the Coatzacoalcos and Grijalva river systems in the south-central Bay of Campeche. $^{210}Pb_{xs}$ MAR on the southern GoM slope range from 0.02 to 0.27 (± 0.05) g cm^{-2} yr^{-1}.

5.4.4 Implications for Oiled Sediment Deposition/ Accumulation

The vast majority of siliciclastic sediment delivery to GoM continental margins is by river input. Although most modern sediments are trapped in estuaries, fine-grained sediments, especially clays, escape these coastal sediment traps and are transported to the shelf and slope. They accumulate very slowly, however, as most modern margins are considered to be sediment starved (Davis 2017). As it has been shown that fine-grained sediments have an affinity for oil, it can be expected that oil contamination from future spills may be delivered to the seafloor along with the fine-grained sediments (Figs. 5.2 and 5.4). Although this potential exists for essentially the entire northern, western, and southern GoM margins, the potential is especially high for the fine-grained depocenters of the Mississippi River Delta and the central Texas shelf (as discussed previously). The exceptionally narrow shelf in the Veracruz area in the southwestern GoM would likely have the least potential, as sediments consist dominantly of sands with a significant volcanic component (Fig. 5.4).

On the continental slopes, the pelagic settling of fine-grained sediments, inputted primarily by rivers, provides a potential conduit for oiled sediments to the seafloor throughout essentially the entire region. Transport of oiled sediments to the GoM basin by gravity flows may also be expected throughout, but especially from Louisiana to west Texas and from south Texas into Mexico (Fig. 5.3).

5.5 Cuba

The portion of the Cuba continental margin bordering the GoM extends from Guanahacabibes Peninsula (on the western tip) eastward to Havana Bay. It fundamentally differs from any other GoM margin due to the tectonic processes associated

with the active margin setting. This is reflected in the margin configuration and sediments. The margin is exceptionally narrow and steep, reaching only a few kilometers in width off Havana. Little scientific information is publicly available, and so much of what is discussed here is the result of a Gulf of Mexico Research Initiative (GoMRI) research cruise through the Florida Institute of Oceanography (FIO) in May 2017.

The narrow continental shelf is essentially devoid of sediments, consisting dominantly of coarse, carbonate rubble (Fig. 5.2). This is likely due to the strong (up to 6 kt) easterly flowing Florida Current that impinges across the entire shelf. Continental slope sediments consist dominantly of pelagic carbonate muds. The only terrigenous sediments identified on the slope are off Havana where the shelf is the narrowest. The carbonate content progressively increases to the west (Fig. 5.2).

The dominant sedimentary process on the shelf is in situ biogenic carbonate production, most of which are exported eastward by the strong outflow current from the GoM through the Florida straits. Pelagic settling is the dominant process on the slope, and downslope transport by gravity flows is likely.

Surface $^{210}Pb_{xs}$ activities range from 6.3 to 70.4 (± 1.2) dpm g^{-1} (105.0–1173.6 ± 1.2 Bq kg^{-1}) in water depths ranging from 316 to 1680 m. There are no bathymetric or spatial patterns apparent in the surface $^{210}Pb_{xs}$ activities, which is likely due to the heterogeneous nature of the bathymetric and physical oceanographic setting.

$^{210}Pb_{xs}$ MAR range from 0.01 to 0.40 (± 0.1) g cm^{-2} yr^{-1} with an apparent decrease from east (Havana) to west (San Antonio Bank). The decrease in $^{210}Pb_{xs}$ MAR from east to west may be due to the amount of anthropogenic development present near the eastern sites and the lack of development to the west. Alternatively, the eastern portion of the Cuban shelf (Punta Gobernadora to Havana) has four semi-enclosed bays connected to rivers. The western portion (Guanahacabibes Peninsula to P. Gobernadora) has no bays, but instead a relatively broad lagoon (Gulf of Guanahacabibes) with soft bottom and seagrass meadows bordered by coral reef tracts that trap sediments within the lagoon. This may also play a role in explaining the west-east patterns in MAR.

5.5.1 Implications for Oiled Sediment Deposition/ Accumulation

Significant deposition/accumulation of oiled sediments on the Cuba continental shelf bordering the GoM is highly unlikely due to the strong eastward-flowing current (Figs. 5.2 and 5.4). This is especially true for the eastern segment near Havana. Deposition of oiled sediments on the continental slope has a higher probability, as fine-grained sediments are being deposited by pelagic settling. The downslope movement of oiled sediments by gravity flows can be expected as well.

5.6 Conclusions

This chapter utilizes sediment texture/composition, transport/depositional processes and pathways, and input/accumulation rates to help predict where and to what extent oil may be incorporated into GoM bottom sediments in the event of a future spill. This document is designed to be used as a general guideline and is based solely upon the sediment characteristics listed above. We fully acknowledge that there may be parameters, other than sediments/processes that dictate the fate of oil on the seafloor, so this should be viewed as simply one tool. Figure 5.4 is a map showing the potential distribution of oiled sediments on the GoM seafloor based on these sediment characteristics. Regions most vulnerable to oil deposition/accumulation include the eastern basin, characterized by the Mississippi Fan, followed by the western/southwestern basin, and north and west continental margins. The least vulnerable regions include the northwest Cuban shelf and the carbonate-dominated west Florida and Campeche Bank. It is important to note this is very general and regional in nature, and numerous local exceptions can be expected.

Funding Information This research was made possible by grants from the Gulf of Mexico Research Initiative through its consortia: the Center for the Integrated Modeling and Analysis of the Gulf Ecosystem (C-IMAGE) and Deep Sea to Coast Connectivity in the Eastern Gulf of Mexico (Deep-C). Data are publicly available through the Gulf of Mexico Research Initiative Information & Data Cooperative (GRIIDC) at https://data.gulfresearchinitiative.org (doi: [10.7266/N7FJ2F94, 10.7266/N7FJ2F94, 10.7266/N7610XTJ, 10.7266/n7-4pg2-4755, 10.7266/n7-58a1-b761, 10.7266/n7-78ae-7m58, 10.7266/n7-3vmj-nk86, 10.7266/n7-7bcg-yk08].

References

Antoine JW, Martin RG, Pyle TG, Bryant WR (1974) Continental margins of the Gulf of Mexico. In: Burk CA, Drake CL (eds) The geology of continental margins. Springer, Berlin, Heidelberg

Back R (1972) Recent depositional history of the Florida middle ground. Thesis, Florida State University

Balsam WL, Beeson JP (2003) Sea-floor sediment distribution in the Gulf of Mexico. Deep-Sea Res I Oceanogr Res Pap 50(12):1421–1444

Brooks GR, Doyle LJ (1991) Geologic development and depositional history of the Florida Middle Ground: a mid-shelf, temperate-zone reef system in the northeastern Gulf of Mexico. In: Osborne RH (ed) From Shoreline to Abyss – Shepard Commemorative Volume Society of Economic Paleontologists and Mineralogists Special Publication 46, pp 189–203

Brooks GR, Holmes CW (1989) Recent carbonate slope sediments and sedimentary processes bordering a non-rimmed platform, southwest Florida continental margin. In: Crevello JF, Sarg JF, Wilson JL (eds) Controls on carbonate platform and basin development, Society of Economic Paleontologists and Mineralogists Special Publication 44, Tulsa, pp 259–272

Brooks GR, Holmes CW (1990) Modern configuration of the southwest Florida carbonate slope: development of shelf margin progradation. Mar Geol 94:301–315

Brooks GR, Doyle LJ, McNeillie JI (1986) A massive carbonate gravity flow deposit intercalated in the lower Misissippi Fan. Initial Reports of the Deep Sea Drilling Project. XCVI, pp 541–546

Brooks GR, Doyle LJ, Davis RA, De Witt NT, Suthard BC (2003) Patterns and controls of surface sediment distribution: west-central Florida inner shelf. In: Brooks GR (ed) A linked coastal/inner shelf depositional system, west-central Florida. Marine Geology Special Publication. Elsevier, Amsterdam, pp 307–24

Brooks GR, Larson RA, Schwing PT, Romero I, Morre C, Reichart GJ, Jilbert R, Chanton JP, Hastings DW, Overholt WA, Marks KP, Kostka JE, Holmes CW, Hollander D (2015) Sediment pulse in the NE Gulf of Mexico following the 2010 DWH blowout. PLoS One 10(7):e0132341. https://doi.org/10.1371/journal.pone.0132341

Bryant WR, Liu JY (2000) Deepwater Gulf of Mexico environmental and socioeconomic data search and literature synthesis, vol I, Narrative report. OCS study MMS 2000-048. U.S. Department of the Interior, Minerals Management Service, Washington, DC, pp 37–42

Carranza-Edwards E (2011) Mexican littoral of the Gulf of Mexico. In: Buster NA, Holmes CW (eds) Gulf of Mexico: origin, waters and biota, vol 3, geology. Texas A&M University Press, College Station, pp 293–296

Celis-Hernandez O, Rosales-Hoz L, Cundy AB, Carranza-Edwards A (2017) Sedimentary heavy metal (loid) contamination in the Veracruz shelf, Gulf of Mexico: a baseline survey from a rapidly developing tropical coast. Mar Pollut Bull 119:204–213

Celis-Hernandez O, Rosales-Hoz L, Cundy AB, Carranza-Edwards A, Croudace IW, Hernandez-Hernandea H (2018) Historical trace element accumulation in marine sediments from the Tamaulipas shelf, Gulf of Mexico: an assessment of natural vs anthropogenic inputs. Sci Total Environ 622–623:325–336

Coleman JM, Bouma AH, Roberts HH, Thayer P (1986) Stratification in Mississippi Fan cores revealed by X-ray radiography. Initial Reports of the Deep Sea Drilling Project. XCVI, pp 505–518

Cremer M, Stow DAV (1986) Sedimentary structures of fine-grained sediments from the Mississippi Fan: thin section analysis. Initial Reports of the Deep Sea Drilling Project. XCVI, pp 519–532

Daly KL, Passow U, Chanton J, Hollander D (2016) Assessing the impacts of oil-associated marine snow formation and sedimentation during and after the Deepwater Horizon oil spill. Anthropocene 13:18–33. https://doi.org/10.1016/j.ancene.2016.01.006

Davies BE (1968) Anomalous levels of trace elements in Welsh soils. Welsh Soils Discuss Group Rep 9:72–87

Davis RA (2017) Sediments of the Gulf of Mexico. In: Ward C (ed) Habitats and biota of the Gulf of Mexico: before the Deepwater Horizon oil spill. Springer, New York

Díaz-Asencio M, Bartrina VF, Herguera JC (2019) Sediment accumulation and composition in deep-water sites of the southern Gulf of Mexico. Deep Sea Research Part I, https://doi.org/10.1016/j.dsr.2019.01.003

Diercks AR, Dike C, Asper VL, DiMarco SF, Chanton JP, Passow U (2018) Scales of seafloor sediment resuspension in the northern Gulf of Mexico. Elem Sci Anth 6:32. https://doi.org/10.1525/elementa.285

Doyle LJ, Holmes CW (1985) Shallow structure, stratigraphy and carbonate sedimentary processes of the west Florida upper continental slope. Am Assoc Pet Geol Bull 69:1133–1144

Doyle LJ, Sparks TN (1980) Sediments of the Mississippi, Alabama, and Florida (MAFLA) continental shelf. J Sediment Petrol 50:905–916

Ellwood BB, Balsam WL, Roberts HH (2006) Gulf of Mexico sediment sources and sediment transport trends from magnetic susceptibility measurements of surface samples. Mar Geol 230(3–4):237–248

Flocks J, Ferina N, Kindinger J (2011) Recent geologic framework and geomorphology of the Mississippi–Alabama shelf, northern Gulf of Mexico. In: Buster N, Holmes CW (eds) Gulf of Mexico, waters and biota, vol 3, geology. Texas A&M Press, College Station, pp 157–174

Gardner WD, Mishonov AV, Richardson MJ (2018) Decadal comparisons of particulate matter in repeat transects in the Atlantic, Pacific, and Indian Ocean Basins. Geophys Res Lett 45:277–286. https://doi.org/10.1002/2017GL076571

Garrison LE, Martin RG (1973) Geologic structure in the Gulf of Mexico basin. Geological Survey Professional Paper 773. US Government Printing Office, Washington, DC

Ginsburg RN, James NP (1974) Holocene carbonate sediments of continental margins. In: Burke CA, Drake CL (eds) The geology of continental margins. Springer, New York, pp 137–155

Gould HR, Stewart RH (1956) Continental shelf sediments off the west coast of Florida. J Sediment Res 23(2):125

Hine AC, Locker SD (2011) The Florida Gulf of Mexico continental shelf—great contrasts and significant transitions. In: Buster NA, Holmes CE (eds) Gulf of Mexico: vol 3, geology, Harte Research Institute for Gulf of Mexico Studies. Texas A&M University Press, College Station, pp 101–127

Hine AC, Brooks GR, Davis RA, Duncan DS, Locker SD, Twichell DC, Gelfenbaum G (2003) The west -central Florida inner shelf and coastal system: a geologic conceptual overview and introduction to the special issue: Marine Geology Special Publication 200, pp 1–17

Holmes CW (1976) Distribution, regional variation, and geochemical coherence of selected elements in the sediments of the central Gulf of Mexico. Geological Survey Professional Paper 928. US Government Printing Office, Washington, DC

Holmes CW (1981) ^{210}Pb method for estimating the rate of carbonate and sedimentation. Geo-Mar Lett 1:237–241

Holmes CW (1985) Accretion on the south Florida platform, late Quaternary development. Am Assoc Pet Geol Bull 69:149–160

Holmes CW (2011) Development of the northwestern Gulf of Mexico continental shelf and coastal zone as a result of the Late Pleistocene-Holocene sea-level rise. In: Buster NA, Holmes CW (eds) Gulf of Mexico: origin, waters, and biota, vol 3, geology. Texas A&M University Press, College Station, pp 195–208

Ishizuka T, Kawahata H, Aoki S (1986) Interstitial water geochemistry and clay mineralogy of the Mississippi Fan and Orca and Pigmy Basins, Initial Reports of the Deep Sea Drilling Project. XCVI, pp 711–728

Logan BW, Harding JL, Ahr WM, Williams JD, Snead RG (1969) Late Quaternary carbonate sediments of Yucatan shelf Mexico. In: Logan BW, Bass MN, Cebulski, DE, McBirney AR (eds) Carbonate sediments and reefs, Yucatan shelf, Mexico. American Association of Petroleum Geologists Memoirs 11, Tulsa, pp 129–198

McBride RA, Moslow TE, Roberts HH, Diecchio RJ (2004) Late Quaternary geology of the northeastern Gulf of Mexico shelf: sedimentology, depositional history and ancient analogs of a modern sand shelf sheet of the transgressive systems tract. In: Anderson JB, Fillon RH (eds) Late Quaternary stratigraphic evolution of the northern Gulf of Mexico margin. Society of Economic Paleontologists and Mineralogists Special Publication 79, pp 53–83

Morse JW, Beazley MJ (2008) Organic matter in deep water sediments of the northern Gulf of Mexico and its relationship to the distribution of benthic organisms. Deep-Sea Res II Top Stud Oceanogr 55:2563–2571. https://doi.org/10.1016/j.dsr2.2008.07.004

Mullins HT, Gardulski AF, Hinchey EJ (1988) The modern carbonate ramp slope of central west Florida. J Sediment Petrol 58:273–290

Passow U (2016) Formation of rapidly-sinking, oil-associated marine snow. Deep-Sea Res II Top Stud Oceanogr (The Gulf of Mexico Ecosystem – before, during and after the Macondo Blowout) 129:232–240. https://doi.org/10.1016/j.dsr2.2014.10.001

Passow U, Hetland R (2016) What happened to all of the oil? Oceanography 29:88–95. https://doi.org/10.5670/oceanog.2016.73

Pérez-Brunius P, Furey H, Bower A, Hamilton P, Candela J, Garcia-Carrillo P, Leben R (2018) Dominant circulation patterns of the deep Gulf of Mexico. J Phys Oceanogr 48:511–529. https://doi.org/10.1175/JPO-D-17-0140.1

Pickering KT, Stow DAV (1986) Inorganic major, minor, and trace element geochemistry and clay mineralogy of sediments from the Deep Sea Drilling Project Leg 96, Gulf of Mexico. Initial Reports of the Deep Sea Drilling Project. XCVI, pp 733–746

Ruiz-Fernández AC, Sanchez-Cabeza JA, Alonso-Hernández C, Martinez-Herrera VM, Pérez-Bernal LH, Preda M, Hillaire-Marcel C, Gastaud J, Quejido Cabezas AJ (2012) Effects of land use change and sediment mobilization on coastal contamination (Coatzacoalcos River, Mexico). Cont Shelf Res 37:57–65

Ruiz-Fernández AC, Sanchez-Cabeza JA, Pérez-Bernal LH, Gracia A (2019) Spatial and temporal distribution of heavy metal concentrations and enrichment in the southern Gulf of Mexico. Sci Total Environ 651:3174–3186

Sadler P (1981) Sedimentation rates and the completeness of stratigraphic sections. J Geol 89:569–584

Sorensen L, Melbye AG, Booth AM (2014) Oil droplet interaction with suspended sediment in the seawater column: influence of physical parameters and chemical dispersants. Mar Pollut Bull 78((1–2)):146–152

Stow DAV, Cremer M, Droz L, Meyer AW, Normark WR, O'Connell S, Pickering KT, Stelting CE, Angell SA, Chaplin C (1986) Facies, composition, and texture of Mississippi Fan sediments, Deep Sea Drilling Project Leg 96, Gulf of Mexico. Initial Reports of the Deep Sea Drilling Project. XCVI, pp 475–488

Thayer P, Roberts HH, Bouma AH, Coleman JM (1986) Sedimentology and petrology of Mississippi Fan depositional environments, Deep Sea Drilling Project Leg 96. Initial Reports of the Deep Sea Drilling Project. XCVI, pp 489–504

Turnewitsch R, Reyss JL, Chapman DC, Thomson J, Lampitt RS (2004) Evidence for a sedimentary fingerprint of an asymmetric flow field surrounding a short seamount. Earth Planet Sci Lett 222:1023–1036. https://doi.org/10.1016/j.epsl.2004.03.042

Turnewitsch R, Falahat S, Nycander J, Dale A, Scott RB, Furnival D (2013) Deep-sea fluid and sediment dynamics—influence of hill- to seamount-scale seafloor topography. Earth Sci Rev 127:203–241. https://doi.org/10.1016/j.earscirev.2013.10.005

Twichell DC (2011) A review of recent depositional processes on the Mississippi Fan, eastern Gulf of Mexico. In: Buster NA, Holmes CW (eds) Gulf of Mexico: origin, waters, and biota, vol 3, geology. Texas A&M University Press, College Station, pp 141–154

Walker ST (1984) Sedimentary structures of the west Florida slope and eastern Mississippi cone: distribution and geological implications. Thesis, University of South Florida, St. Petersburg

Walker JR, Massingill JV (1970) Slump features in the Mississippi Fan, northeastern Gulf of Mexico. Geol Soc Am Bull 81:3101–3108

Weisberg RH, He R (2003) Local and deep-ocean forcing contributions to anomalous water properties on the west Florida shelf. J Geophys Res 108(C6):3184. https://doi.org/10.1029/2002JC001407

Wetzel A, Kohl B (1986) Accumulation rates of Mississippi Fan sediments cored during Deep Sea Drilling Project Leg 96. Initial Reports of the Deep Sea Drilling Project. XCVI, pp 595–600

Yeager KM, Santschi PH, Rowe GT (2004) Sediment accumulation and radionuclide inventories (^{239,240}Pu, ^{210}Pb and ^{234}Th) in the northern Gulf of Mexico, as influenced by organic matter and macro-faunal density. Mar Chem 91:1–14

Ziervogel K, Dike C, Asper V, Montoya J, Battles J, D'souza N, Passow U, Diercks A, Esch M, Joye S, Dewald C, Arnosti C (2016) Enhanced particle fluxes and heterotrophic bacterial activities in Gulf of Mexico bottom waters following storm-induced sediment resuspension. Deep-Sea Res II Top Stud Oceanogr (The Gulf of Mexico Ecosystem – before, during and after the Macondo Blowout) 129:77–88. https://doi.org/10.1016/j.dsr2.2015.06.017

Chapter 6
Benthic Faunal Baselines in the Gulf of Mexico: A Precursor to Evaluate Future Impacts

Patrick T. Schwing, Paul A. Montagna, Maria Luisa Machain-Castillo, Elva Escobar-Briones, and Melissa Rohal

Abstract This chapter provides a comparison between recently developed, post-oil spill baseline measurements throughout the Gulf of Mexico (GoM) and previous, pre-oil spill baselines for benthic foraminifera, meiofauna, and macrofauna for areas impacted by the *Deepwater Horizon* (2010) and Ixtoc 1 (1979–1980) oil spills. This comparison will provide two primary outcomes: (1) assessment of any lasting changes in benthic faunal assemblages caused by the *Deepwater Horizon* and Ixtoc 1 oil spills in the Gulf of Mexico and (2) augmentation of pre-oil spill baselines or establishment of "new normal" post-oil spill baseline measurements that can be utilized to quantitatively assess impact, response, and recovery of benthic fauna in the event of a future oil spill.

Keywords Benthic · Foraminifera · Macrofauna · Meiofauna · Oil spill · MOSSFA · Deepwater Horizon · Ixtoc 1 · Baseline

P. T. Schwing (✉)
University of South Florida, College of Marine Science, St. Petersburg, FL, USA
e-mail: pschwing@mail.usf.edu

P. A. Montagna · M. Rohal
Texas A&M University-Corpus Christi, Harte Research Institute for Gulf of Mexico Studies, Corpus Christi, TX, USA
e-mail: Paul.Montagna@tamucc.edu

M. L. Machain-Castillo · E. Escobar-Briones
Universidad Nacional Autónoma de México, Instituto de Ciencias del Mar y Limnología, Mexico City, Mexico
e-mail: machain@cmarl.unam.mx

S. A. Murawski et al. (eds.), *Scenarios and Responses to Future Deep Oil Spills*,
https://doi.org/10.1007/978-3-030-12963-7_6

6.1 Background

Comprehensive benthic baselines allow for the quantitative characterization and assessment of impact and recovery following both episodic natural (e.g., hurricanes) and anthropogenic perturbations (e.g., oil spills). Benthic baselines are also the first stage in the development of longer-term monitoring efforts related to persistent anthropogenic stressors such as heavy metal concentration and hypoxia related to nutrient loading.

The cumulative sea surface oil coverage during the *Deepwater Horizon* (DWH) event was 112,115 km^2 (NRDA 2015). Estimates of the extent of marine oil snow sedimentation and flocculent accumulation (MOSSFA) on the seafloor ranged from 8400 to 35,648 km^2 (Chanton et al. 2015; Romero et al. 2017; Schwing et al. 2017a). Benthic macrofaunal diversity was moderately impacted in an area of 148 km^2 (Montagna et al. 2013), and meiofaunal diversity was moderately impacted throughout an area of 406 km^2 (Baguley et al. 2015) surrounding the DWH wellhead. Meiofauna and macrofauna diversity did not recover in 2011 in these areas (Washburn et al. 2017), and it may take 50–100 years to bury the DWH layer below bioturbation depth, achieving full recovery (Montagna et al. 2017a). Benthic foraminifera diversity and density were impacted at sites ranging from 140 km southwest and 180 km northeast of the DWH wellhead (Schwing et al. 2015, 2017b). Benthic foraminifera density and diversity reached a steady state between 3 and 5 years following the DWH event, but may not have fully recovered to pre-DWH assemblages during that period (Schwing et al. 2018a). Benthic foraminifera shell (test) stable carbon isotope composition was also depleted by MOSSFA processes (Schwing et al. 2018b).

The cumulative sea surface oil coverage during the Ixtoc 1 oil spill was estimated to be approximately 70,000 km^2 (Sun et al. 2015), and approximately 120,000 metric tons of oil were deposited on the seafloor in the months following the spill (Jernelov and Linden 1981). Benthic faunal surveys were not performed at the time of the Ixtoc 1 spill. However, using fossil benthic foraminifera assemblages, impacts associated with the Ixtoc 1 spill have been assessed at sites up to 240 km west of the Ixtoc 1 wellhead (Machain-Castillo et al. unpublished).

Considering the scope and spatial extent of the impacts to benthic fauna related to these oil spills, it is necessary to develop post-oil spill baselines to augment existing (pre-spill) baselines or establish new baselines for the impacted areas. These baselines will also provide information necessary to disentangle impacts of future oil spills versus other stressors and variability such as anthropogenic watershed development, natural climate variability (precipitation, etc.), heavy metals, and hypoxia.

6.2 Developing a New Normal

6.2.1 Benthic Foraminifera

Many surveys and reviews of benthic foraminifera have been conducted throughout the Gulf of Mexico (GoM) (Phleger and Parker 1951; Parker 1954; Culver and Buzas 1983; Poag 1984, 2015; Denne and Sen Gupta 1991; Sen Gupta and Aharon 1994; Buzas et al. 2007; Lobegeier and Sen Gupta 2008; Bernhard et al. 2008). Poag (2015) have provided, to date, the most comprehensive review including the identification of 45 facies based on the predominance of genera and 5 additional geographically isolated biofacies distinguished by characteristic genera. In general, benthic foraminifera diversity is driven by environmental stability (physicochemical) especially in continental shelf settings, while flux rates (e.g., organic carbon) are particularly important in continental slope and abyssal settings (Poag 2015 and references therein).

Post-oil spill benthic foraminifera baseline measurements in the northern GoM (nGoM) are comprised of the following: (1) 35 sites in the nGoM, 7 of which have been sampled annually from 2010 to 2017, (2) 57 sites in the southern GoM (sGoM) collected from 2015 to 2016, and (3) 11 sites along the northern continental shelf and slope of Cuba collected in 2017 (Fig. 6.1).

To provide an assessment of any lasting changes caused by the DWH or Ixtoc 1 spills to the benthic foraminifera assemblages, this section compares the pre-oil spill predominance facies presented by Poag (2015) to the assemblages in the surface increments of sediment cores representing post-spill baselines from areas impacted by each spill.

In the northern GoM, the assemblages characterized by Schwing et al. (2018a) collected from seven time-series sites from 2012 to 2015 were used for this purpose. Note for all comparisons, Poag (2015) included calcareous taxa and not agglutinated taxa in the predominance facies. At the wellhead (DWH01), there was an increase in *Bolivina* spp. predominance from what was reported by Poag (2015). West of the wellhead (MV02 and SW01), the only additional predominant taxon was *Textularia* spp., which is an agglutinated taxon and was not included in the original characterization by Poag (2015). East of the wellhead (DSH10, DSH08, PCB06, MC04), there was a greater predominance of *Uvigerina* spp. than reported in Poag (2015). Considering the opportunistic nature of *Uvigerina* spp. under higher organic carbon flux (Altenbach et al. 1999), this could be a lasting change due to the DWH event or a longer-term (decadal) shift to higher organic carbon flux.

In the southern GoM, 14 sediment cores ranging from 1 to 1647 m water depth were collected in 2015–2016 and characterized by Machain-Castillo et al. (unpublished). These characterizations were used to assess any lasting changes in predominance after the Ixtoc 1 oil spill and augment existing baseline measurements. At sites ranging from 500 to 1500 m water depth, ranging spatially between the Campeche Canyon (east) and a transect offshore of Tampico, Mexico (west), the predominant taxa were *Bolivina* spp. (primarily *B. lowmani*). At depths between

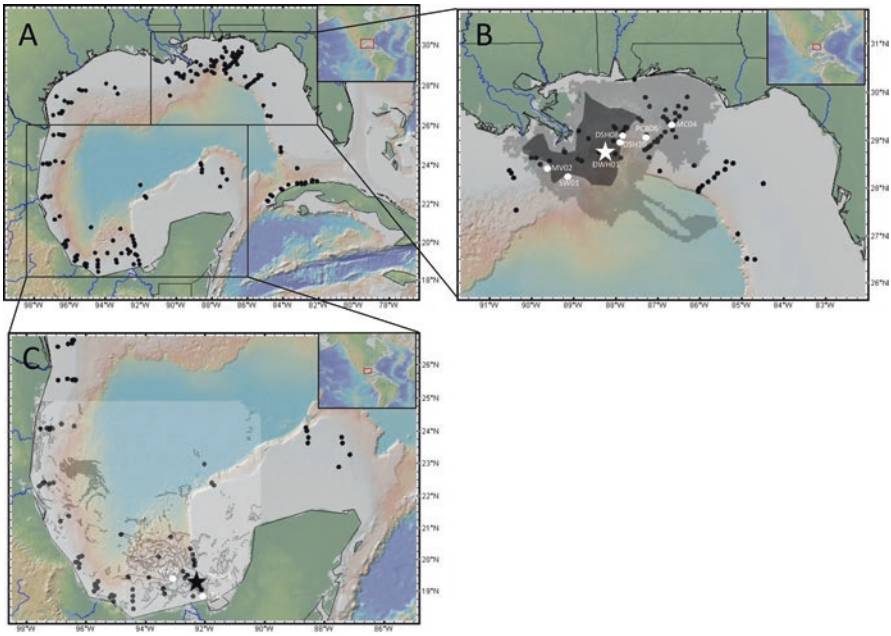

Fig. 6.1 Map of (**a**) all coring and surface sediment sampling locations (black circles) collected throughout the Gulf of Mexico from 2010 to 2017 as part of the C-IMAGE research effort including enlarged portions of the (**b**) northern Gulf of Mexico and the (**c**) southern Gulf of Mexico. In the enlarged northern Gulf of Mexico map (**b**), the dark gray shading is the surface extent of dispersant application (Environmental Response Management application, ERMA n.d.), the light gray shading is the surface oil extent (ERMA), the white star is the location of the Deepwater Horizon wellhead (site DWH01), and the white circles and corresponding labels represent the time-series sites. In the enlarged southern Gulf of Mexico map (**c**), the light gray-shaded areas are the surface oil extent (Sun et al. 2015), the black star is the location of the Ixtoc 1 wellhead (site Ixtoc 1), and the white circles and corresponding labels represent sites discussed in this chapter

200 and 2000 m water depths in these areas, Poag (2015) reported a *Bolivina-Uvigerina* predominance facies at shallower depths and a *Bulimina* predominance facies at deeper depths. The *Bolivina-Uvigerina* predominance facies should be revised to simply a *Bolivina* predominance facies, and this facies should be extended down to at least 1500 m water depth for this area in the sGoM. The IXW-250 site is also located in the area in central Bay of Campeche designated by Poag (2015) as a *Cibicidoides* predominance facies. This site (as of the 2015 collections) should also be included in the *Bolivina* predominance facies. At the 1500 m sites in the south-central and southwestern extent of the study area, agglutinated *Hyperamina* spp. were also predominant. The Ixtoc 1 site was predominantly *Fursenkoina* spp., which was located between the *Bolivina-Uvigerina* and miliolid predominance facies according to Poag (2015). At a site near Laguna de Términos (LT1), the 2015 records agreed with Poag (2015) that *Ammonia* spp. were predominant. Finally, coastal cores were also predominantly *Ammonia* spp., which suggests that the

Ammonia spp. predominance facies in Poag (2015) should be extended along the Campeche coastline to the north.

Predominance facies were not reported by Poag (2015) for the areas along the northern Cuban continental shelf and slope. Four sediment cores were collected in 2017 on the northwestern Cuban shelf and slope to provide baseline characterizations of benthic foraminifera. Along the outer shelf (~300 m water depth), *Cassidulina* spp. is predominant. At sites ranging from 970 to1590 m water depth, *Bolivina* spp. is predominant.

Surface samples from sites in addition to those reported above for the predominance comparison were measured to expand surface spatial coverage for additional benthic foraminifera data products including density, diversity (Shannon index, Fisher's Alpha index), and stable isotopes ($\delta^{13}C$, $\delta^{18}O$) (Fig. 6.2).

Benthic foraminiferal density tends to decrease Gulf-wide with depth, and the highest densities are located near large freshwater inputs in the nGoM (Mississippi River, Mobile Bay) and the sGoM (Laguna de Términos). The Shannon and Fisher's Alpha indices co-vary Gulf-wide. Both indices tend to increase with water depth in the southern GoM and reach minima on the Campeche bank. In the northern GoM, both indices are lowest near the outflow of the Mississippi River, likely due to opportunistic taxa dominating in area of high organic carbon deposition. Both indices are low along the west Florida shelf and slope and increase from east to west (away from Havana) along the Cuban shelf and slope. *Cibicidoides* spp. $\delta^{13}C$ tends to enrich with distance from fluvial sources (terrigenous carbon sources) as expected. The most depleted values near the outflow of the Mississippi River are the primary

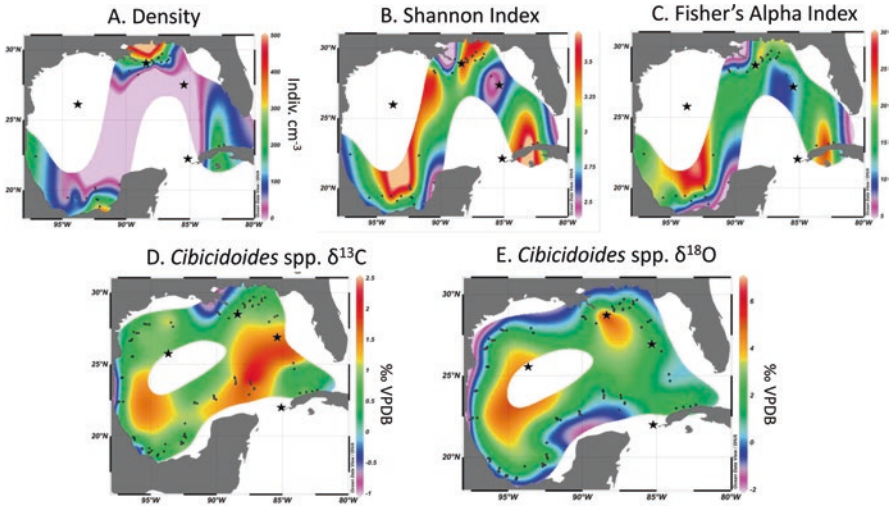

Fig. 6.2 DIVA-gridded baseline maps of benthic foraminifera parameters from surface sediments including (**a**) density (indiv. cm^{-3}), (**b**) Shannon index, (**c**) Fisher's Alpha index, (**d**) stable carbon isotope composition ($\delta^{13}C$) of *Cibicidoides* spp. (*pachyderma*, *wuellerstorfi*), and (**e**) stable oxygen isotope composition ($\delta^{18}O$) of *Cibicidoides* spp. (*pachyderma*, *wuellerstorfi*). Black stars are locations of modeled subsurface petroleum release (Parts III and IV, this volume)

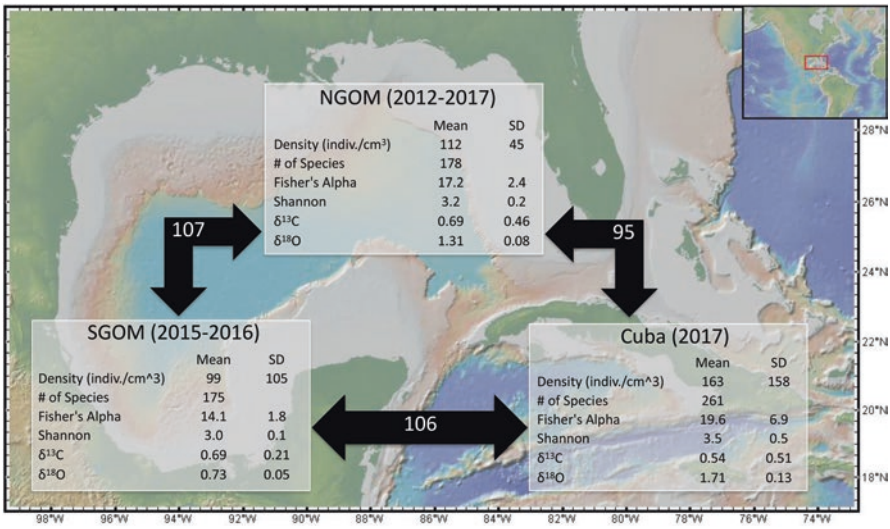

Fig. 6.3 Inter-regional comparison of the northern GoM (NGOM), southern GoM (SGOM), and Cuba including the mean density (indiv. cm^{-3}), number of species, Fisher's Alpha index, Shannon index, stable carbon isotope composition ($\delta^{13}C$) of *Cibicidoides* spp. (*pachyderma*, *wuellerstorfi*), and stable oxygen isotope composition ($\delta^{18}O$) of *Cibicidoides* spp. (*pachyderma*, *wuellerstorfi*). Uncertainties are presented as one standard deviation. Arrows and corresponding numbers between subregions represent the number of species shared between each subregion

feature. *Cibicidoides* spp. $\delta^{18}O$ is primarily a function of the $\delta^{18}O$ of seawater (salinity) and becomes enriched with water depth as expected.

Inter-regional comparisons between the several benthic foraminifera assemblage metrics were also performed between the northern GoM, southern GoM, and Cuban subregions of the GoM (Fig. 6.3). Overall, Cuba has the highest density, diversity, number of species, and diversity indices followed by the nGoM and sGoM. The mean $\delta^{13}C$ between each subregion was remarkably consistent, while the mean Cuban $\delta^{18}O$ was enriched compared to the nGoM, which was in turn enriched compared to the sGoM. These trends in $\delta^{18}O$ are likely caused by the proportion of predominant water masses (e.g., Antarctic Intermediate Water, Caribbean Midwater, and North Atlantic Deepwater) associated with each margin (Denne and Sen Gupta 1991; Machain-Castillo et al. 2010).

6.2.2 Meiofauna

It is possible to determine how the benthic meiofauna have changed as a result of the DWH oil spill using samples collected during the Deep Gulf of Mexico Benthos (DGoMB, Rowe and Kennicutt 2008) project. A total of 13 stations were sampled before and after the DWH event. During the DGoMB project, 51 stations were

sampled from 2000 to 2002 in the northern Gulf of Mexico along the continental slope and the abyssal plane (Baguley et al. 2006, 2008). The sediment was collected with a box corer and then subsampled with a small core tube mounted within the box. This work provides a snapshot in time to which we can compare the meiofauna community following the DWH accident. Meiofauna were subsampled from either a boxcore, grab, or larger core tube in all studies, so the results are comparable among the studies (Montagna et al. 2017b). Post-DWH oil spill data were collected as part of the Natural Resource Damage Assessment (NRDA) in 2010, 2011, and 2014 (Montagna et al. 2013; Reuscher et al. 2017). A total of 133 stations were sampled for meiofauna around the site of the oil spill, of which 56 were sampled during two cruises and 32 were sampled during all three cruises.

A comparison of the pre-DWH and post-DWH samples found that abundance significantly differed ($P \leq 0.0001$) and stations were different (P-value ≤ 0.0001) (Fig. 6.4). There were higher abundances after the DWH event, reaching 1.11E6 n/m^2 as opposed to pre-spill abundances assessed at 0.3511E6 n/m^2. Shannon's diversity significantly differed after the spill ($P \leq 0.0001$) with higher values (H′ 0.9) prior to the DWH event than after the event (H′ 0.5). The nematode-copepod (NC) ratio significantly differed after the DWH spill ($P \leq 0.0001$) and among stations ($P \leq 0.0001$) with higher ratios (NC 7.3) after the DWH oil spill than before (NC

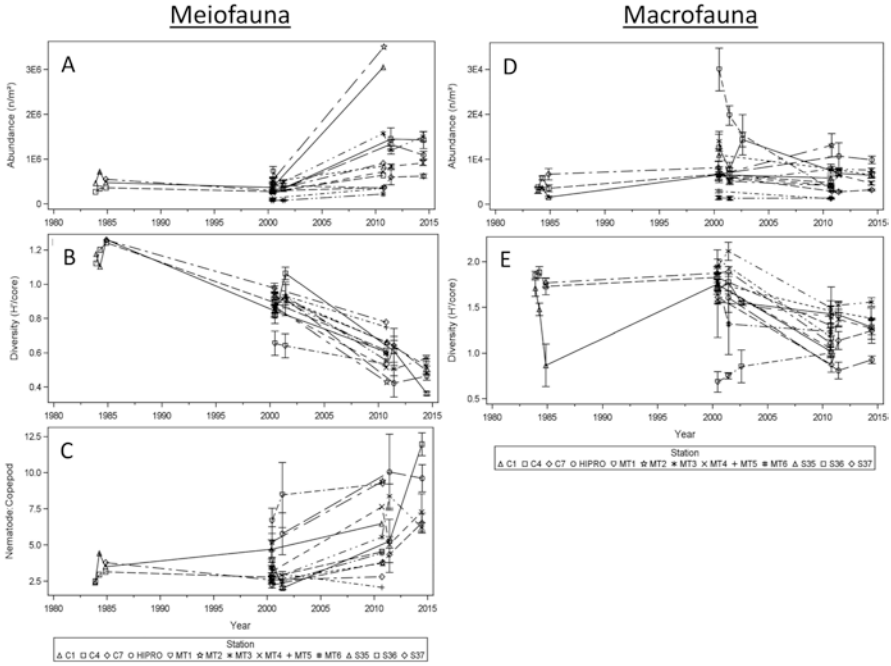

Fig. 6.4 Time series for meiofauna metrics at stations in the northern Gulf of Mexico for (**a**) abundance, (**b**) Shannon's diversity, (**c**) nematode-copepod ratio and for macrofauna (**d**) abundance and (**e**) Shannon's diversity

3.6). The increase in abundance and NC coupled with a decrease in diversity indicates there was a shift to a more disturbed environment in the GoM after the year 2010.

To provide information regarding the current state of the benthic community in the GoM, data were compiled from six different sampling efforts. For all surveys, the meiofauna were subsampled making the results comparable (Montagna et al. 2017b). All of the sampling sites were located in the northern GoM except for the Rohal et al. (unpublished) study which was in the southern GoM. The earliest large-scale survey was the northern Gulf of Mexico Continental Slope Study (NGOMCSS; Pequegnat et al. 1990), followed by the DGoMB Program. Both were performed to support environmental assessments required for leasing offshore areas for hydrocarbon exploration and production. The Gulf of Mexico Offshore Operations Monitoring Experiment (GOOMEX, Kennicutt II et al. 1996) was performed to determine the long-term effects of hydrocarbon production. One concern about the GOOMEX findings was that the contaminant effects might be confounded with the artificial reef effects of the platforms, as was the conclusion of the RIGS/REEFS study (Montagna et al. 2002). All of the studies used subcores to sample the sediment from larger cores or boxcores. The core sizes were not sufficiently different to be concerned about inter-comparability (Montagna et al. 2017b). The data sets differed in the level of taxonomic identification. Therefore, to compare diversity, the data were aggregated into 24 comparable taxonomic groups: Amphipoda, Anthozoa, Aplacophora, Acari, Bivalvia, Copepoda, Echinodermata, Gastropoda, Gastrotricha, Isopoda, Kinorhyncha, Loricifera, Nematoda, Nemertea, Mollusca, Oligochaeta, Ostracoda, Polychaeta, Rotifera, Scaphopoda, Sipuncula, Tanaidacea, Tardigrada, and Tunicata. To create gulf-wide coverage maps, all sample points were included in the kriging procedure (type, ordinary; output type, prediction; variable, semivariogram; lags, 12; and the model optimization feature was used) (Fig. 6.5).

There is higher abundance near the Louisiana coast, higher meiofauna diversity off the Texas-Louisiana coast, and higher NC off the Texas-Louisiana coasts (Fig. 6.5a, b). However, it is important to note that the number of samples collected in the nGoM (1409) is exponentially higher than in the sGoM (19). In addition, the samples from the southern Gulf were collected in an active oil field where meiofauna abundance tends to be higher and diversity tends to be lower. Therefore, more samples need to be analyzed in the southern Gulf to generate a more accurate representation in this region.

6.2.3 Macrofauna

Unlike the meiofauna, the methods for sampling macrofauna were quite different among the studies compared here (NGOMCSS-Gallaway 1988; GOOMEX-Montagna and Harper 1996; DGoMB-Haedrich et al. 2008; Rowe and Kennicutt 2008; DWH-Montagna et al. 2013; Seeps-Washburn et al. 2018; Ixtoc 1 – This chapter). For example, a 2209 cm^2 boxcore was used during the DGoMB study,

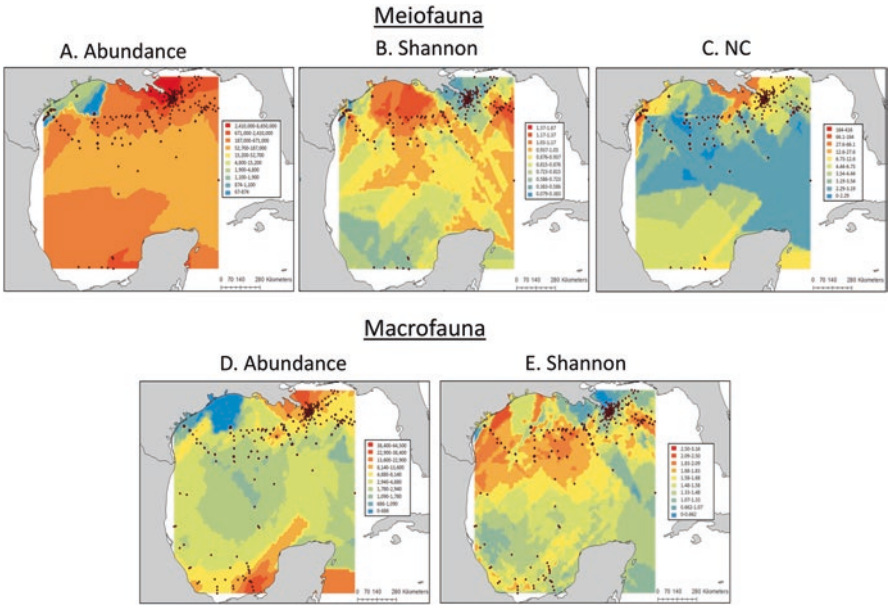

Fig. 6.5 Kriging map of meiofauna (**a**) abundance, (**b**) Shannon's diversity, (**c**) nematode-copepod ratio and macrofauna (**d**) abundance and (**e**) Shannon's diversity in the Gulf of Mexico. Circles represent sampling sites. The shaded contours are the predicted values. Red-shaded contour = high values. Blue-shaded contour = low values

although the actual sampled area was 1902 m^2 because of the subcores that were removed (Montagna et al. 2017b). In contrast, a 79 cm^2 core was used to sample macrofauna during the DWH NRDA studies (Montagna et al. 2013), which is 24 times smaller or only 4% of the area of the boxcore. In a direct comparison experiment, it was found that the boxcore underestimated abundance by 2.9 times relative to the multicore sampler (Montagna et al. 2017b). Also, even though the larger box core samples 24 times more area and captures more species, the diversity estimates are actually relatively lower than in cores. Another problem is that the level of taxonomic detail is different in all the studies. The NGOMCSS was the only one to identify everything to the lowest taxonomic level possible. The DGoMB study identified only Polychaeta, Bivalvia, Aplacophora, and mostly Crustacea species. The DWH NRDA study identified everything to the family level. The Ixtoc 1 study identified everything to a higher taxa level, mostly the class or order level. Therefore, to compare diversity, all taxa were aggregated to the higher taxa level so the northern and southern Gulf could be compared. Meiofauna and macrofauna data exist for 13 stations included in both the DGoMB and DWH projects. However, comparative diversity values could not be calculated for the 2000–2002 samples. There was a small decrease in the total abundance of macrofauna over time (Fig. 6.4). The abundance prior to the spill was 7192 n/m^2 and 6107 n/m^2 after the spill ($P = 0.0127$). Diversity decreased after the spill from 1.6 H′ to 1.2 H′ after the spill ($P = \leq 0.0001$).

The decrease in abundance and diversity indicates a more disturbed environment in the Gulf of Mexico in the post-spill era.

The highest macrofauna abundance was found at locations close to the coast, east of Louisiana in the nGoM, and north of Mexico in the Bay of Campeche specifically off of Laguna de Términos (Fig. 6.5d). However, it is important to note that the number of samples collected in the nGoM (1791) is exponentially higher than in the sGoM (103), so interpolations to the south are less certain. The lowest abundance was in the deepest part of the central GoM. There was a low abundance off the Texas coast, particularly off Galveston Bay; however these results are based on only one station, so it is likely that this is a statistical anomaly. The high values near the mouth of the Mississippi River and low values in the central Gulf are consistent with the idea that productivity in the GoM is related to runoff from land (Blomberg and Montagna 2014). The highest macrofauna diversity was in the northwestern, north central, and northeastern Gulf (Fig. 6.5e). In the northwestern part of the Gulf, samples close to land exhibited higher diversities; however in the central and northeastern part of the Gulf, the higher diversity was in deeper water between 500 and 1500 m. This is in contrast to the abundance, which was lowest off the Texas coast. The lowest diversity is found in stations near the mouth of the Mississippi River and in the middle of the Gulf of Mexico. Thus diversity increases to a certain depth and subsequently decreases. The southern Gulf has generally lower diversity than the nGoM.

6.3 Conclusions

Benthic environmental baselines have multiple applications. In the context of oil spills, comprehensive benthic baselines allow for the quantitative characterization and assessment of impact and recovery. Broad-scale benthic baselines also provide information about areas that are affected by other stressors such as anthropogenic development (oil and gas infrastructure, nutrient loading, heavy metal concentration, etc.). Baseline measurements that include multiple trophic levels provide the initial setting on which to develop monitoring programs that can establish longer-term trends in both natural and anthropogenic stressors and their controls. These measurements are also an effective measure of habitat suitability for benthic dependent and demersal fishes. Considering the gradients over which these baselines have been established (e.g., temperature, salinity, depth, latitude), they can also be used to refine or construct paleoceanographic proxies, particularly benthic foraminifera stable isotope baselines and assemblages (transfer function analysis). Through these analyses of benthic assemblages, we have gained a basic understanding of the characteristics of the benthic community and the connectivity, both spatially (within and between regions) and between trophic levels. Benthic environmental baselines have proven to be a critical metric following accidental submarine petroleum releases and should be established in every area in which there is petroleum and gas extraction in the marine setting. There are still spatial and knowledge gaps that need to be

filled in the Gulf of Mexico such as the Texas shelf, southwest Florida shelf, and below 2000 m water depth throughout the Gulf of Mexico with regard to petroleum impact on benthic fauna. The lack of highly spatially resolved records along the southwest Florida shelf is of particular concern considering the potential end of the moratorium on marine energy development in 2020. Benthic baselines for the Gulf of Mexico presented in this chapter can also be enhanced in the future. One example would be the development of a marine biotic index (e.g., foraminifera- and/or macrofauna-based AMBI) for the entire Gulf of Mexico that would provide an easy to interpret benthic habitat suitability and ecological health status tool that can be operationalized by living resource managers.

Acknowledgments This research was made possible in part by a grant from the Gulf of Mexico Research Initiative, C-IMAGE and DEEP-C, and in part by the British Petroleum/Florida Institute of Oceanography (BP/FIO)-Gulf Oil Spill Prevention, Response, and Recovery Grants Program. The authors also thank Bryan O'Malley for his assistance with laboratory analyses. Data are publicly available through the Gulf of Mexico Research Initiative Information and Data Cooperative (GRIIDC) at http://data.gulfresearchinitiative.org, UDI: R6.x805.000:0061, R6.x805.000:0062, DOI: 10.7266/n7-q3gc-ax92, DOI: 10.7266/n7-e90r-1v29, DOI: 10.7266/n7-repn-q515.

References

Altenbach AV, Pflaumann U, Schniebel R, Thies A, Timm S, Trauth MH (1999) Scaling percentages and distributional patterns of benthic foraminifera with flux rates of organic carbon. J Foraminifer Res 29(3):173–185

Baguley JG, Montagna PA, Hyde LJ, Kalke RD, Rowe GT (2006) Metazoan meiofauna abundance in relation to environmental variables in the northern Gulf of Mexico deep sea. Deep-Sea Res 1 53:1344–1362

Baguley JG, Montagna PA, Rowe GT, Hyde LJ (2008) Metazoan meiofauna biomass, grazing, and weight dependent respiration in the northern Gulf of Mexico deep sea. Deep Sea Res II 55:2607–2616

Baguley J, Montagna P, Cooksey C, Hyland JL, Bang HW, Kamikawa A, Bennets P, Morison C, Saiyo G, Parsons E, Herdener M, Ricci M (2015) Community response of deep-sea soft-sediment metazoan meiofauna to the Deepwater Horizon blowout and oil spill. Mar Ecol Prog Ser 528:127–140. https://doi.org/10.3354/meps11290

Bernhard JM, Sen Gupta BK, Baguley JG (2008) Benthic foraminifera living in Gulf of Mexico bathyal and abyssal sediments: community analysis and comparison to metazoan meiofaunal biomass and density. Deep-Sea Res II 55:2617–2626

Blomberg BN, Montagna PA (2014) Meta-analysis of Ecopath models reveals secondary productivity patterns across the Gulf of Mexico. Ocean Coast Manag 100:32–40. https://doi.org/10.1016/j.ocecoaman.2014.07.014

Buzas MA, Hayek LC, Culver SJ (2007) Community structure of benthic foraminifera in the Gulf of Mexico. Mar Micropaleontol 65:43–53

Chanton J, Zhao T, Rosenheim BE, Joye S, Bosman S, Brunner C, Yeager KM, Diercks AR, Hollander D (2015) Using natural abundance radiocarbon to trace the flux of petrocarbon to the seafloor following the Deepwater Horizon oil spill. Environ Sci Technol 49(2):847–854. https://doi.org/10.1021/es5046524

Culver SJ, Buzas MA (1983) Recent benthic foraminiferal provinces in the Gulf of Mexico. J Foraminifer Res 13:21–31

Denne RA, Sen Gupta BK (1991) Association of bathyal foraminifera with water masses in the northwestern Gulf of Mexico. Mar Micropaleontol 17:173–193

Draft Programmatic Environmental Impact Statement; Natural Resource Damage Assessment, National Ocean Service, National Oceanic and Atmospheric Administration (2015) http://www.Gulfspillrestoration.noaa.gov/wp-content/uploads/Chapter-4_Injury-to-Natural-Resources.pdf

ERMA (Environmental Response Management Application) (n.d.) ERMA deepwater Gulf response web application. http://gomex.erma.noaa.gov/

Gallaway BJ (ed) (1988) Northern Gulf of Mexico continental slope study, final report: year 4. Volume II: synthesis report. Final report submitted to the Minerals Management Service, New Orleans, LA. Contract No. 14-12-0001-30212. OCS Study/MMS 88-0053. 318

Haedrich RL, Devine JA, Kendall VJ (2008) Predictors of species richness in the deep-benthic fauna of the northern Gulf of Mexico. Deep-Sea Res II 55:2650–2656

Jernelöv A, Lindén O (1981) Ixtoc I: a case study of the world's largest oil spill. Ambio 10:299–306

Kennicutt MC II, Green RH, Montagna P, Roscigno PF (1996) Gulf of Mexico Offshore Operations Experiment (GOOMEX) Phase I: sublethal responses to contaminant exposure – introduction and overview. Can J Fish Aquat Sci 53:2540–2553

Lobegeier MK, Sen Gupta BK (2008) Foraminifera of hydrocarbon seep, Gulf of Mexico. J Foraminifer Res 38(2):93–116

Machain-Castillo ML, Gío-Argáez FR, Cuesta-Castillo LB, Alcala-Herera JA, Sen Gupta BK (2010) Last glacial maximum deep water masses in southwestern Gulf of Mexico: clues from benthic foraminífera. No. Esp. "Paleoclimas del Cuaternario en ambientes tropicales y subtropicales". Boletín de la Sociedad Geológica Mexicana 62(3):453–467. https://doi.org/10.18268/BSGM2010v62n3a9

Montagna PA, Harper DE Jr (1996) Benthic infaunal long-term response to offshore production platforms. Can J Fish Aquat Sci 53:2567–2588

Montagna PA, Jarvis SC, Kennicutt MC II (2002) Distinguishing between contaminant and reef effects on meiofauna near offshore hydrocarbon platforms in the Gulf of Mexico. Can J Fish Aquat Sci 59:1584–1592

Montagna PA, Baguley JG, Cooksey C, Hartwell I, Hyde LJ, Hyland JL, Kalke RD, Kracker LM, Reuscher M, Rhodes ACE (2013) Deep-sea benthic footprint of the Deepwater Horizon blow-out. PLoS One 8(8):e70540. https://doi.org/10.1371/journal.pone.0070540

Montagna PA, Baguley JG, Hyland JL, Cooksey C, Hollander D (2017a) Persistent impacts to the deep soft bottom benthos and potential for recovery after the Deepwater Horizon event. Gulf of Mexico oil spill and ecosystem science conference. New Orleans, 8 February 2017

Montagna PA, Baguley JG, Hsiang CY, Reuscher M (2017b) Comparison of sampling methods for deep-sea infauna. Limnol Oceanogr Methods 15:166–183

Parker FL (1954) Distribution of foraminifera in the northeastern Gulf of Mexico. Bull Mus Comp Zool 111:453–588

Pequegnat WE, Gallaway BJ, Pequegnat LH (1990) Aspects of the ecology of the deep-water fauna of the Gulf of Mexico. Am Zool 30:45–64

Phleger FB, Parker FL (1951) Gulf of Mexico foraminifera, Part 1 and 2. Geol Soc Am Mem 46:1–64

Poag WC (1984) Distribution and ecology of deep-water benthic foraminifera in the Gulf of Mexico. Palaeogeogr Palaeoclimatol Palaeoecol 48:25–37

Poag WC (2015) Benthic foraminifera of the Gulf of Mexico: distribution, ecology, paleoecology. Texas A&M University Press, College Station

Reuscher MG, Baguley JG, Conrad N, Cooksey C, Hyland JL, Lewis C, Montagna PA, Ricker RW, Rohal M, Washburn M (2017) Temporal patterns of the Deepwater Horizon impacts on the benthic infauna of the northern Gulf of Mexico continental slope. PLoS One 12(6):e0179923. https://doi.org/10.1371/journal.pone.0179923

Romero IC, Toro-Farmer G, Diercks AR, Schwing PT, Muller-Karger F, Murawski S, Hollander DJ (2017) Large scale deposition of weathered oil in the Gulf of Mexico following a deepwater oil spill. Environ Pollut 228:179–189. https://doi.org/10.1016/j.envpol.2017.05.019

Rowe GT, Kennicutt MC (2008) Introduction to the deep Gulf of Mexico Benthos program. Deep Sea Res II 55:2536–2540

Schwing PT, Romero IC, Brooks GR, Hastings DW, Larson RA, Hollander DJ (2015) A decline in deep-sea benthic foraminifera following the Deepwater Horizon event in the northeastern Gulf of Mexico. PLoS One 10(3):e0120565. https://doi.org/10.1371/journal.pone.0120565

Schwing PT, Brooks GR, Larson RA, Holmes CW, O'Malley BJ, Hollander DJ (2017a) Constraining the spatial extent of the Marine Oil Snow Sedimentation and Accumulation (MOSSFA) following the DWH event using a $^{210}Pb_{xs}$ inventory approach. Environ Sci Technol 51:5962–5968. https://doi.org/10.1021/acs.est.7b00450

Schwing PT, O'Malley BJ, Romero IC, Martinez-Colon M, Hastings DW, Glabach MA, Hladky EM, Greco A, Hollander DJ (2017b) Characterizing the variability of benthic foraminifera in the northeastern Gulf of Mexico following the Deepwater Horizon event (2010–2012). Environ Sci Pollut Res 24:2754. https://doi.org/10.1007/s11356-016-7996-z

Schwing PT, O'Malley BJ, Hollander DJ (2018a) Resilience of benthic foraminifera in the northern Gulf of Mexico following the Deepwater Horizon event (2011–2015). Ecol Indic 84:753–764. https://doi.org/10.1016/j.ecolind.2017.09.044

Schwing PT, Chanton JP, Romero IC, Hollander DJ, Goddard EA, Brooks GR, Larson RA (2018b) Tracing the incorporation of petroleum carbon into benthic foraminiferal calcite following the Deepwater Horizon event. Environ Pollut 237:424–429. https://doi.org/10.1016/j.envpol.2018.02.066

Sen Gupta BK, Aharon P (1994) Benthic foraminifera of bathyal hydrocarbon vents of the Gulf of Mexico: initial report on communities and stable isotopes. Geo-Mar Lett 14:88–96

Sun S, Hu C, Tunnell JW (2015) Surface oil footprint and trajectory of the Ixtoc-I oil spill determined from Landsat/MSS and CZCS observations. Mar Pollut Bull 101(2):632–641. https://doi.org/10.1016/j.marpolbul.2015.10.036

Washburn TW, Reuscher MG, Montagna PA, Cooksey C, Hyland JL (2017) Macrobenthic community structure in the deep Gulf of Mexico one year after the Deepwater Horizon blowout. Deep Sea Res Part 1 Oceanogr Res Pap 127:21–30. https://doi.org/10.1016/j.dsr.2017.06.001

Washburn TW, Demopoulous AWJ, Montagna PA (2018) Macrobenthic infaunal communities associated with deep-sea hydrocarbon seeps in the northern Gulf of Mexico. Mar Ecol 2018:e12508

Chapter 7
Linking Abiotic Variables with Macrofaunal and Meiofaunal Abundance and Community Structure Patterns on the Gulf of Mexico Continental Slope

Paul A. Montagna, Jeffrey G. Baguley, Michael G. Reuscher, Gilbert T. Rowe, and Terry L. Wade

Abstract The Deep Gulf of Mexico Benthos (DGoMB) program was designed to determine patterns of abundance and diversity of meiofauna and macrofauna in the northern Gulf of Mexico continental slope between 300 m and 3700 m depth. Abundance of all taxa was significantly influenced by the particulate organic carbon (POC) flux. The abundance of meiofauna, macrofauna, crustaceans, and mollusks increased with increasing clay content, but clay had no significant effect on harpacticoid or polychaete abundance. Polychaete diversity was significantly correlated to POC flux, but mollusk diversity was correlated to sediment properties. Polychaetes had the highest average abundance and species richness. Harpacticoids were the least abundant of the four taxa, but had the highest values of Hill's diversity index and Pielou's evenness index. Harpacticoids and Crustaceans had high species turnover rates, resulting in low similarities of the respective faunas between sampling stations, whereas mollusks and polychaetes were more similar between different

The original version of this chapter was revised. The correction to this chapter is available at https://doi.org/10.1007/978-3-030-12963-7_30

P. A. Montagna (✉) · M. G. Reuscher
Texas A&M University-Corpus Christi, Harte Research Institute, Corpus Christi, TX, USA
e-mail: Paul.Montagna@tamucc.edu

J. G. Baguley
University of Nevada-Reno, Department of Biology, Reno, NV, USA
e-mail: baguley@unr.edu

G. T. Rowe
Texas A&M University-Galveston, Department of Marine Biology, Galveston, TX, USA
e-mail: roweg@tamug.edu

T. L. Wade
Texas A&M University, Geochemical and Environmental Research Group,
College Station, TX, USA
e-mail: terry@gerg.tamu.edu

S. A. Murawski et al. (eds.), *Scenarios and Responses to Future Deep Oil Spills*,
https://doi.org/10.1007/978-3-030-12963-7_7

sampling stations. Overall, there were interannual differences in abundance patterns of meiofauna and macrofauna, similar community structure patterns among the taxa, and unique distributions of diversity with respect to depth and longitude.

Keywords Deep-sea benthos · DGoMB · Diversity · Infauna · Macrofauna · Meiofauna · Sediment characteristics · Sediment chemistry

7.1 Introduction

The Deep Gulf of Mexico Benthos (DGoMB) program was an interdisciplinary research project to explore structure and function of the deep-sea benthos in the Gulf of Mexico (Rowe and Kennicutt 2008). Its main goals were to determine the composition and structure of benthic biological communities of the Gulf of Mexico (GoM) continental slope, to infer relationships between biological patterns and major controlling processes, and to characterize the area as to its environmental "health" and in anticipation of the increasing offshore hydrocarbon exploration and production (Rowe and Kennicutt II 2009). The DGoMB program design was based on historical knowledge of deep-sea communities in the GoM (e.g., Pequegnat 1983; Gallaway 1988). The DGoMB results provide a predictive capability for areas not directly sampled or observed by extrapolation. This predictive capability is a framework for ascertaining the potential for, and the most likely impact from, fossil fuel exploration and exploitation in the deep-sea (Rowe and Kennicutt II 2009). Thus, the DGoMB samples provide a valuable baseline for the northern GoM continental slope benthos, preceding the devastating effects of the *Deepwater Horizon* (DWH) disaster in 2010 (Montagna et al. 2013).

Many (i.e., 21) of the individual, disciplinary, DGoMB studies have been published, primarily in a special issue of "Deep Sea Research Part II: Topical Studies in Oceanography," volume 55, issues 24–26 (2008). However, except for one modeling paper (Rowe et al. 2008), the papers were discipline-focused, and there has not been a focus on synthesizing results across disciplines. Considering the broad scope of studies performed during DGoMB (Rowe and Kennicutt 2008), a synthesis of cross-cutting results could provide many new insights into factors that control the deep benthic community of the GoM. The soft-bottom benthic invertebrate community of the continental slope and deep sea are composed of smaller meiofauna and larger macrofauna. While there are different taxa in the two groups, most studies define these groups operationally by extracting the groups on different sieve sizes (Thiel 1975). For deeper water, meiofauna are defined as those collected using <300 mm and >0.042 mm (sometimes as low as 0.020 mm), and macrofauna are collected on sieves >300 mm (Giere 2009; Danovaro 2010). Because the size range is so different, meiofauna and macrofauna represent different trophic levels as indicated by modeling (Rowe et al. 2008) and stable isotope (Iken et al. 2001) studies.

In the current study, we fused together interdisciplinary abiotic and biotic data sets and performed multivariate statistical analyses to synthesize the benthic data with a focus on soft sediment communities. The purpose of these analyses was to explain how different physical and chemical properties of the sediment and overlaying water column shape the structure of meiofauna and macrofauna communities.

7.2 Methods

The DGoMB samples were collected during three major oceanographic cruises in May–June 2000, June 2001, and June 2002, respectively. The interdisciplinary nature of the scientific objectives was incorporated into the study design that balanced the benthic survey aspects of the program with experimental (or "process")-oriented studies needed to understand the deep-sea community's structure and function (Rowe and Kennicutt 2008). While there were 53 stations sampled, only 43 contained data for all physical and biotic variables, so only these are included in this study. For maps and descriptions of the station locations, see Rowe and Kennicutt (2008, 2009). Five replicate box cores were taken at each station. All data used in the present analyses are available at http://marinecadastre.gov/espis/#/search/study/157.

Seven stations (C7, MT1, MT3, MT6, S36, S41, S42) were sampled twice (in 2000 and 2001), thus providing data for analysis of temporal change (for maps see Rowe and Kennicutt 2008, 2009). This is a simple two-way analysis of variance (ANOVA) with cruises and stations as the main effects. The ANOVA was performed on both meiofauna and macrofauna data that is log-transformed.

7.2.1 Abiotic Variables

Abiotic environmental variables included chlorophyll-a (Chl-a) in the overlying water column as measured from SeaWiFS satellite images as described by Biggs et al. (2008). Chl-a was adjusted for remineralization with increasing water depth by application of the exponential model proposed by Betzer et al. (1984) and updated by Berger et al. (1988). The amount of surface Chl-a reaching the sea floor is described by the equation:

$$J_{(z)} = \frac{0.409\mathrm{PP}^{1.41}}{Z^{0.628}} \tag{7.1}$$

where $J_{(z)}$ is the flux of Chl-a transported downward through some depth Z and PP is the overlying water column Chl-a concentration.

The sediment contaminant chemistry was collected from the top 2 cm from sediment cores collected from box core samples and included total polycyclic aromatic hydrocarbons (PAH) excluding perylenes and the trace metals calcium (Ca), chromium (Cr), tin (Sn), and strontium (Sr); and methods and data are described in Wade et al. (2008).

The remaining abiotic variables were all from sediment box core samples and included grain size (sand, silt, and clay content), total organic nitrogen (OrgN), and total organic carbon (OrgC) data, and methods are described by Morse and Beazley (2008). In addition porewater measurements for particulate organic carbon (POC), dissolved organic carbon (DOC), ammonium (NH_4^+), nitrate (NO_3^-), and urea were also made.

7.2.2 Biotic Variables

Taxa used were representative of meiofauna and macrofauna: Harpacticoida, Polychaeta, Crustacea Peracarida (Amphipoda, Isopoda, and Cumacea) (henceforth referred to as Crustacea), and Mollusca (Bivalvia and Aplacophora). The meiofauna data and methods are described by Baguley et al. (2006, 2008). The two dependent variables used to link abiotic factors were total abundance and diversity. The macrofauna community data have not been described before by Haedrich et al. (2008), and details of the Isopoda species are described in Wilson (2008). Bacterial counts were also collected from sediment cores, and the methods and data are described in Deming and Carpenter (2008).

7.2.3 Diversity and Evenness

Diversity of Harpacticoida, Crustacea, Mollusca, and Polychaeta was calculated using Hill's diversity number one (N1) (Hill 1973). N1 is an indicator of the number of abundant species in a sample and is a measure of the effective number of species (Ludwig and Reynolds 1988). The effective number of species is a measure of the degree to which proportional abundances are distributed among species (Hill 1973). It is calculated as the exponentiated form of the Shannon diversity index: $N1 = e^{H'}$. As diversity decreases, N1 will tend toward 1. The Shannon index (H') is the average uncertainty per species in an infinite community made up of species with known proportional abundances. Hill's N1 is used because the unit, numbers of species, is easier to interpret than most other diversity indices.

Evenness expresses the degree to which all species in a sample are equally abundant. Evenness is a component of diversity. Pielou's (1975) evenness index, J', was calculated for the same four taxa. It expresses H' relative to the maximum value of H'. J' is sensitive to S, which is the number of species in a sample.

7.2.4 Principal Component Analysis

Principal component analysis (PCA) was used to reduce the large set of intercorrelated variables into a smaller set of orthogonal (completely uncorrelated) variables. Each new variable (principal component) accounts for a percentage of the total variance in the original data set. The new variables are extracted in decreasing order of variance, such that the first few principal components (PC) explain most of the variation in the data set. The contribution of each environmental variable to the new PC is called a load. Typically, the new PC loads can be interpreted to indicate structure in the data set. Each observation contributing to the PC is called a score. Thus, the main advantage of PCA is the generation of station scores, which are

interpretable, and can subsequently be used in other analyses (i.e., correlation with abundance and diversity data). Also, it is more robust to run one correlation analysis on a data set, rather than to run a correlation on every environmental parameter.

The PCA was performed using the SAS FACTOR procedure on the covariance matrix and using the VARIMAX rotation option (SAS 1990). Details of implementations of the SAS program used are provided by Long et al. (2003). The PCA station scores were used to correlate the environmental setting with the biological variables (i.e., abundance and diversity) with Pearson product-moment correlation coefficients (r) using the SAS procedure CORR. Prior to analysis all data were transformed to conform with assumptions of parametric tests, and to weight the contribution of high or low measurements, and then averaged by station. The angular transformation (x = arcsin sqrt[y]) was used for the sediment grain size data (which is in percent), and a natural logarithm transformation (x = logn [y + 1]) was used on all other abiotic and biotic data.

One common problem with environmental data is that many variables measuring the same effects can skew the result. Thus pre-analysis was performed to determine if certain variables within classes of chemicals could be dropped from the analysis. Only the total amount of PAHs was used. Perylene was dropped from the total because there are natural sources in the environment, and the goal was to include only those originating from human activities. A total of 29 metals were measured and had to be reduced for the final analysis using an initial PCA of all trace metals only. The first metals PC1 accounted for 70.1% of the variance in the metals data set and was the only PC with an eigenvalue greater than one. Thus, four metals, the two with highest positive and two with the most negative loadings, were chosen for the final PCA analysis including all environmental variables. These four metals (Ca, Cr, Sn, and Sr) represent a proxy for the general trace metal pattern seen at all stations.

7.2.5 Nonmetric Multidimensional Scaling

Benthic community structure of macrofauna species was analyzed by nonparametric multivariate methods. The average abundance of each species at each station was calculated and transformed using the natural logarithm transformation ($x = \ln(y + 1)$). Ordination of samples was performed using the nonmetric multidimensional scaling (MDS) procedure described by Clarke and Warwick (2001) and implemented in Primer software (Clarke and Gorley 2001). The software creates a Bray-Curtis similarity matrix among all samples and then an MDS plot of the spatial relationship among the samples. The data set contains one main effect: sampling stations; thus MDS patterns were plotted using the station name. Cluster analysis on the similarity matrices was performed to determine the degree of relatedness of stations, and it was overlain on the MDS plot. Community structure station patterns for harpacticoids, polychaetes, crustaceans, and mollusks were compared using the RELATE procedure in Primer, which tests for matching among the station patterns.

7.3 Results

7.3.1 Environmental Analyses

In the PC analysis, 4 out of 15 PCs were significant with eigenvalues greater than one. They accounted for 71.8% of the total variance in the data set. The sign of variable loads (negative or positive) indicates gradients in concentrations. Variables that load negatively will have highest concentrations for negative PC loads with decreasing concentrations moving in the positive direction and vice versa. PC1 accounted for 33.5% of the total variance and had high positive loadings by clay, total PAHs, tin, and chromium and high negative loadings by sand, strontium, and calcium (Fig. 7.1a). PC2 accounted for 16.7% of the total variance and highly positive loadings by Chl-a and POC, weak positive loadings by OrgN and NH_4^+, and weak negative loadings by NO_3^- and urea (Fig. 7.1a). PC3 accounted for 11.3% of the total variance and had highly positive loadings by DOC and highly negative loadings by urea (Fig. 7.1b). PC4 accounted for 10.2% of the total variance and had moderate positive loadings by silt, NH_4^+, NO_3^-, and PAH.

The new PC1 axis is interpreted as being driven by differences in sediment properties, and the new PC2 axis is being driven by differences in particulate flux to the bottom (Fig. 7.1a). The higher mud (i.e., and silt plus clay) content is associated with stations in the Mississippi Trough (MT-x) which is a depositional environment (Fig. 7.2). The stations with higher particulate flux to the bottom are in shallower depths and close to the mouth of the Mississippi River (Fig. 7.2).

7.3.2 Benthic Abundance and Community Analyses

There are many correlations and autocorrelations among biotic components (Table 7.1). Many of these correlations are obvious, e.g., a strong correlation between total macrofauna abundance and abundance of polychaetes (the most abundant macrofauna taxon). Other correlations, however, are less trivial. For example, meiofauna abundance is strongly correlated with every metazoan taxon parameter except mollusk diversity. Yet, mollusk diversity is positively correlated to harpacticoid and crustacean diversity, but negatively to crustacean abundance. Bacterial abundance was not correlated with meiofauna abundance but showed a positive correlation with the abundance of the meiofaunal taxon Harpacticoida. Macrofauna abundance was positively correlated with bacterial abundance. However, among the macrofaunal taxa, only Mollusca was correlated to bacterial abundance, while Polychaeta and Crustacea were not. The only significant negative correlation that we found was between bacterial abundance and mollusk diversity. Some correlations are surprisingly weak, such as the harpacticoid and crustacean diversity correlation.

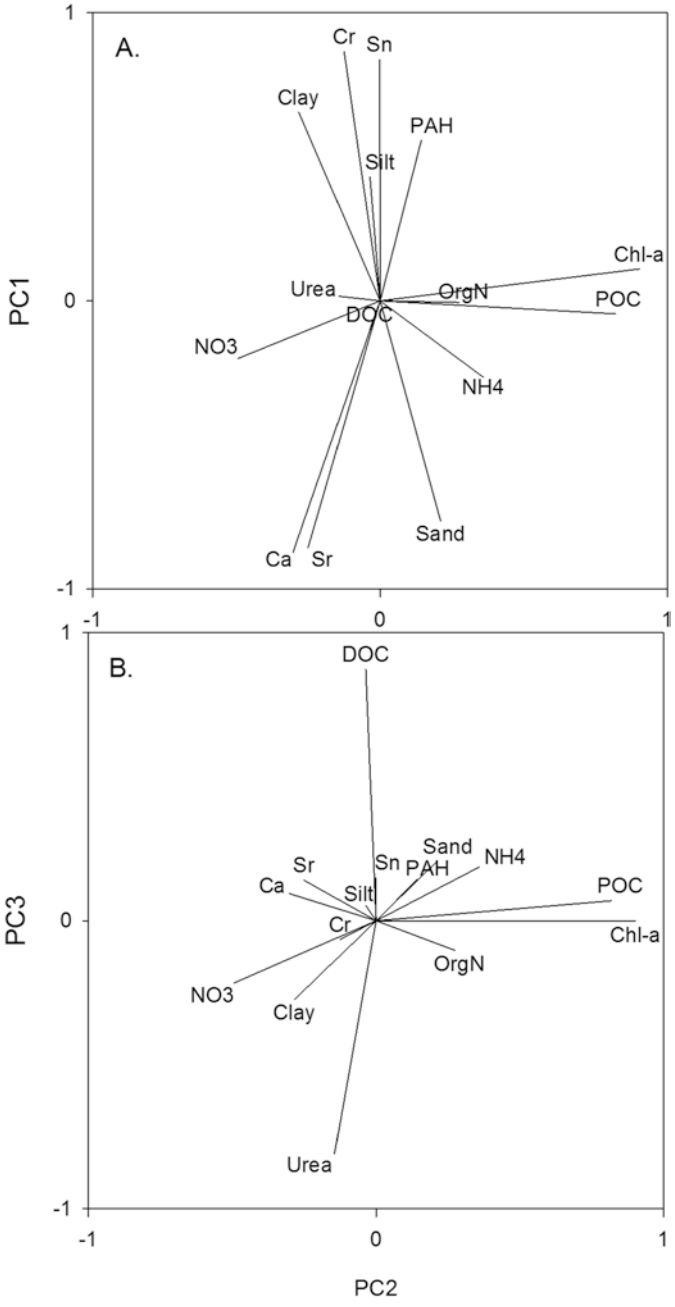

Fig. 7.1 Variable loads for the principal component (PC) analysis for abiotic variables. (**a**) PC1 and PC2. (**b**) PC2 and PC3

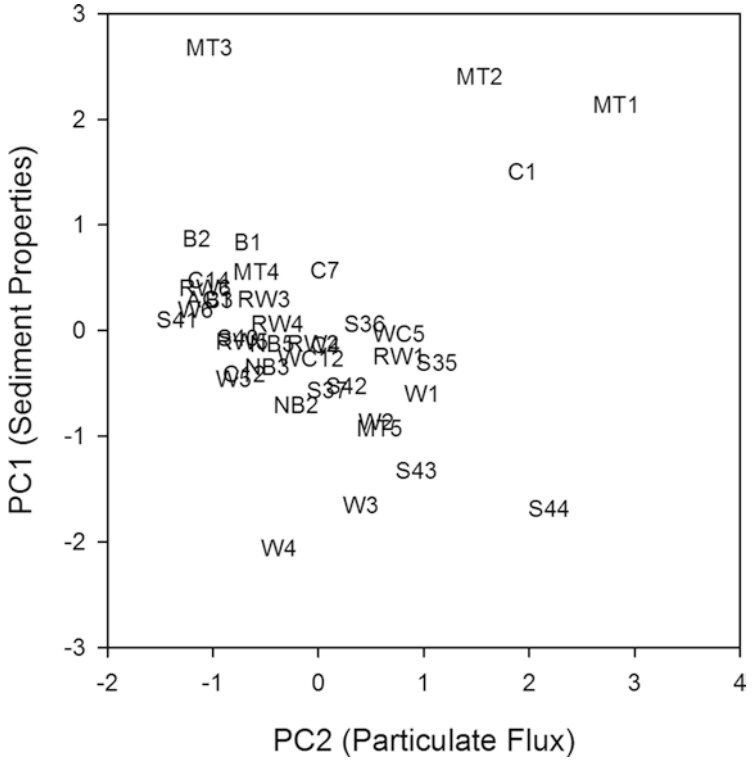

Fig. 7.2 Station scores for the principal component (PC) analysis for abiotic variables. PC1 is a continuum of sediment properties, and PC2 is a continuum of particle flux rates (see Fig. 7.1)

Another way to examine correlations and relationships among biotic variables is within the context of a PCA (Fig. 7.3). In the PCA, the first three principal components were significant with eigenvalues greater than one. They accounted for 79.7% of the total variance in the data set. PC1 accounted for 48.1% of the total variance and had high positive loadings by harpacticoid diversity and abundance and polychaete abundance. PC2 accounted for 31.6% and had high loadings for crustacean abundance. Thus, factors affecting crustacean abundance are orthogonal to factors affecting harpacticoid diversity and abundance and polychaete abundance.

Community structure of harpacticoids, crustaceans, mollusks, and polychaetes was examined for spatial patterns among stations using MDS. The analysis was limited to the 43 stations where all species were analyzed so that the analyses would be balanced with no data gaps. Polychaetes were the most abundant taxon with an average specimen count of 871.0 per sampling station, followed by Crustacea (482.4), Mollusca (147.2), and Harpacticoida (90.5) (Table 7.2). The high standard deviation of all four taxa indicates the large differences in the abundance between different sampling stations, particularly for Crustacea. The number of total species found in the different taxa was 696 for Harpacticoida, 369 for Crustacea (118

Table 7.1 Correlation between biotic components abundance (-ab) and Hill's number of dominant species (-N1)

	Macr-ab	Bact-ab	Harp-ab	Harp-N1	Poly-ab	Poly-N1	Crus-ab	Crus-N1	Moll-ab	Moll-N1
Meio-ab	****0.84	0.23	****0.76	*0.31	****0.78	****0.64	****0.54	**0.37	****0.76	−0.02
	<0.0001	0.1061	<0.0001	0.0453	<0.0001	<0.0001	<0.0001	0.0079	<0.0001	0.9119
	50	52	43	43	51	51	51	51	48	48
Macr-ab		*0.30	****0.74	0.20	****0.72	****0.54	****0.65	*0.33	****0.74	−0.07
		0.0329	<0.0001	0.2071	<0.0001	<0.0001	<0.0001	0.0189	<0.0001	0.6380
		50	42	42	50	50	50	50	47	47
Bact-ab			0.41	−0.06	0.13	0.08	0.16	−0.18	*0.34	***−0.45
			**0.0063	0.7109	0.3503	0.5624	0.2754	0.2055	0.0188	0.0014
			43	43	50	51	51	51	48	48
Harp-ab				****0.59	****0.84	**0.45	0.30	*0.38	****0.71	−0.07
				<0.0001	<0.0001	0.0025	0.0518	0.0115	<0.0001	0.6676
				43	43	43	43	43	43	43
Harp-N1					****0.60	0.16	−0.21	*0.38	0.16	*0.31
					<0.0001	0.3060	0.1765	0.0111	0.3107	0.0445
					43	43	43	43	43	43
Poly-ab						**0.43	**0.38	*0.29	****0.74	0.02
						0.0015	0.0066	0.0381	<0.0001	0.8810
						51	51	51	48	48
Poly-N1							0.14	****0.70	***0.49	0.25
							0.3127	<0.0001	0.0003	0.0820
							51	51	48	48
Crus-ab								−0.18	**0.41	*−0.29
								0.2057	0.0035	0.0475
								51	48	48

(continued)

Table 7.1 (continued)

	Macr-ab	Bact-ab	Harp-ab	Harp-N1	Poly-ab	Poly-N1	Crus-ab	Crus-N1	Moll-ab	Moll-N1
Crus-N1									0.25	****0.61
									0.0840	<0.0001
									48	48
Moll-ab										−0.07
										0.6571
										48

Pearson correlation coefficients (r) on top, probability that $r = 0$ (p) in the middle, and number of observations (n) at the bottom
Abbreviations: *Meio* Meiofauna, *Macr* Macrofauna, *Bact* Bacteria, *Harp* Harpacticoida, *Poly* Polychaeta, *Crus* Crustacea, *Moll* Mollusca
Significance levels: 0.05 < * < 0.01, 0.01 < ** <0.001, 0.001 < *** < 0.0001, and <0.0001 ****

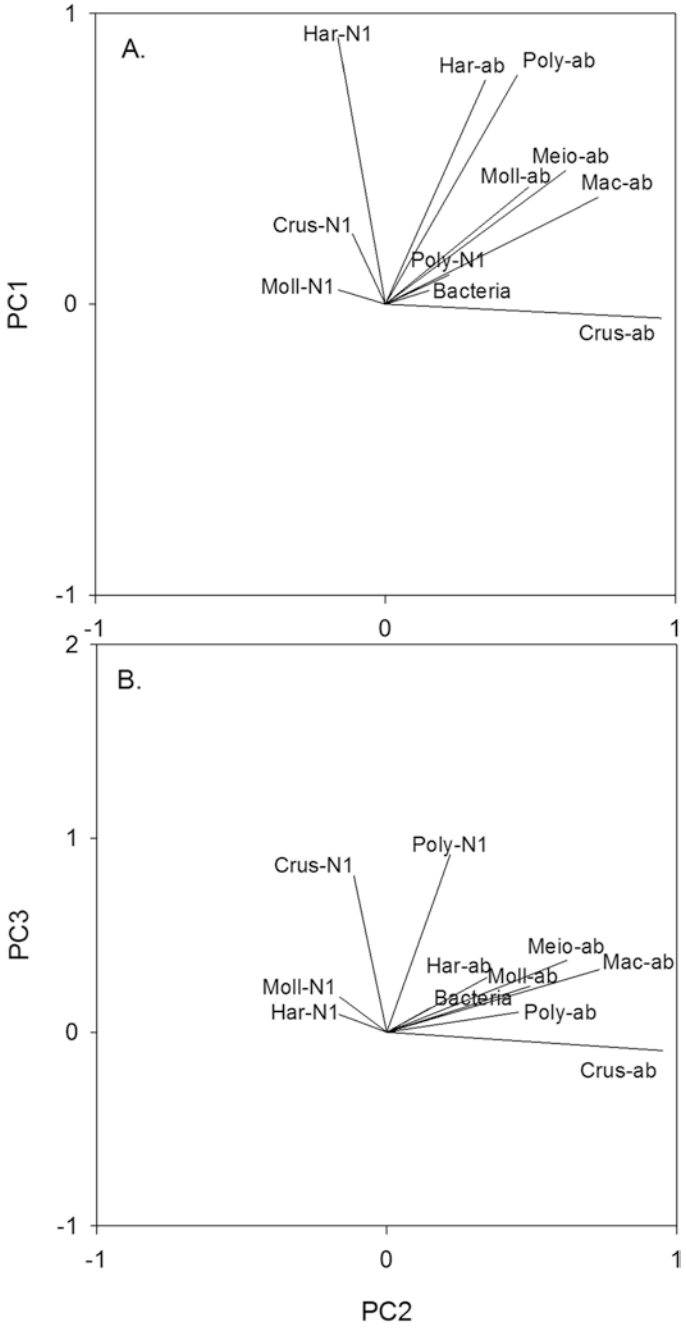

Fig. 7.3 Variable loads for the principal component (PC) analysis of biotic variables. (**a**) PC1 and PC2. (**b**) PC2 and PC3

Table 7.2 Mean and standard deviation of diversity measures for the major taxa

	Harpacticoida		Crustacea		Mollusca		Polychaeta	
Richness	51.7	(19.0)	31.9	(18.8)	21.2	(7.0)	59.7	(38.6)
Abundance	90.5	(50.6)	482.4	(2114.1)	147.2	(112.3)	871.0	(763.5)
J′	0.95	(0.03)	0.87	(0.11)	0.84	(0.12)	0.86	(0.07)
N1	42.6	(14.4)	20.4	(10.6)	13.5	(5.0)	30.2	(14.5)

Richness is number of species, abundance per sampling station, J′ is Pielou's evenness index, and N1 is Hill's number of abundant species diversity index

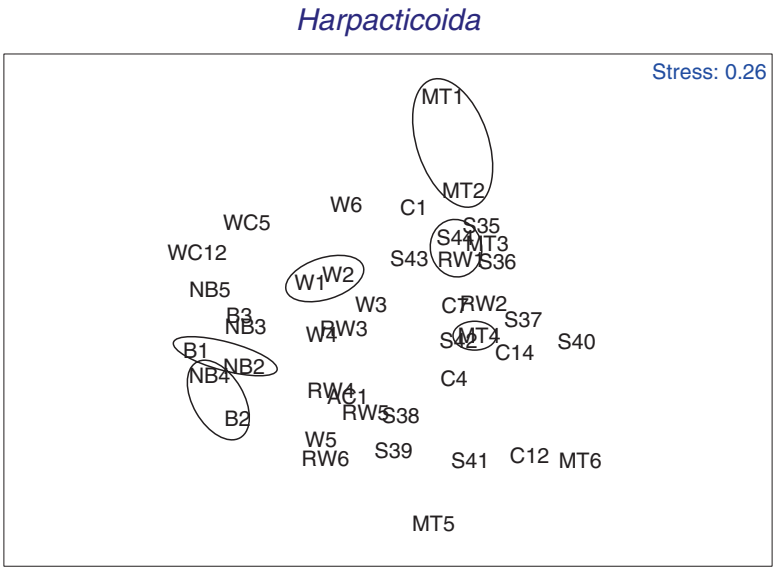

Fig. 7.4 MDS plot of Harpacticoida species similarity at stations. Circles share 35% similarity as indicated by cluster analysis

Amphipoda +119 Cumacea +132 Isopoda), 118 for Mollusca (94 Bivalvia +24 Aplacophora), and 498 for Polychaeta (Rowe and Kennicutt II 2009). Average species richness per sampling station was highest for polychaetes (59.7), followed by Harpacticoida (51.7), Crustacea (31.9), and Mollusca (21.2) (Table 7.2). The evenness index score for Harpacticoida was very high (J′ = 0.95). For the macrofauna taxa values were similar and somewhat lower, ranging from 0.84 to 0.87 (Table 7.2). A comparison of average diversity index measures indicates that harpacticoids are the most diverse, followed by polychaetes, crustaceans, and mollusks.

The cluster and MDS ordination plots indicate different trends between the different taxa (Figs. 7.4, 7.5, 7.6, and 7.7). There was more similarity among stations for polychaetes and mollusks than for crustaceans and harpacticoids. Choosing 35%, an arbitrary level of similarity, harpacticoids had the most number of stations (33) that did not share at least 35% of the species with another station (Fig. 7.4). Crustaceans had the second most number of stations (24) that did not share at least 35% of the species with another station (Fig. 7.5). Polychaetes had only nine stations

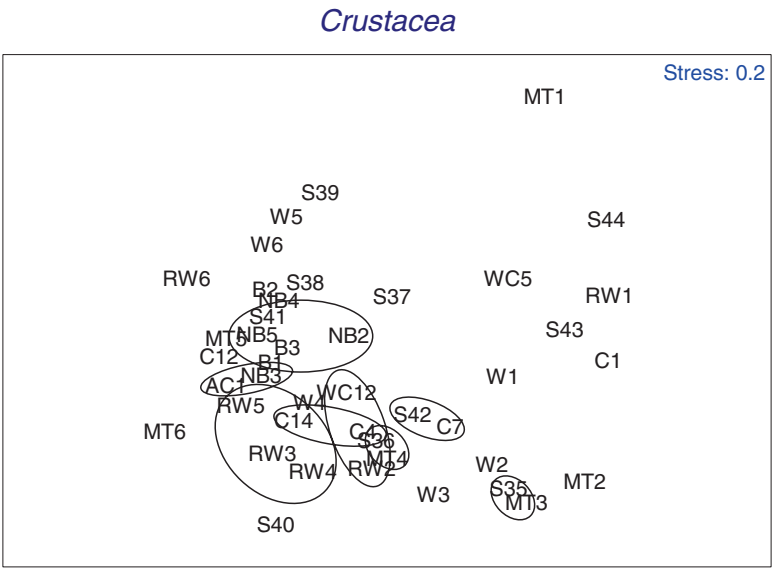

Fig. 7.5 MDS plot of Crustacea, Amphipoda, Cumacea, and Isopoda species only. Stations circled share 35% similarity as indicated by the cluster analysis

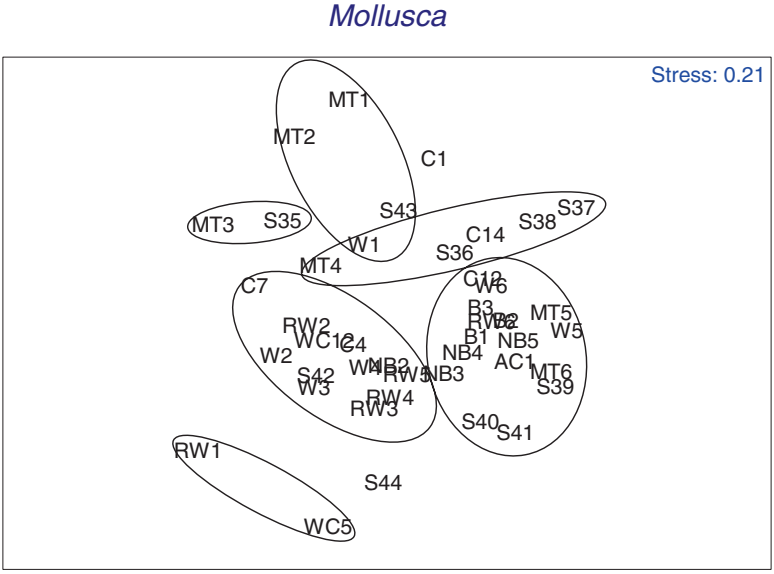

Fig. 7.6 MDS plot of Mollusca, Bivalvia and Aplacophora species only. Stations circled share 35% similarity as indicated by the cluster analysis

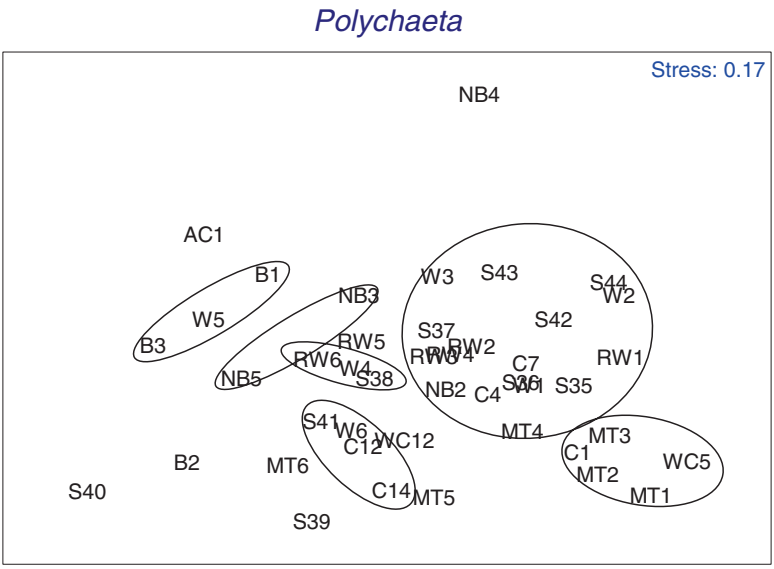

Fig. 7.7 MDS plot of Polychaeta species. Stations circled share 35% similarity as indicated by the cluster analysis

Table 7.3 Relatedness of the community structure patterns of different taxa Rho (ρ)

Taxa	Statistic	Crustacea	Mollusca	Polychaeta
Harpacticoida	ρ	0.214	0.172	0.349
	p	0.002	0.003	0.001
Crustacea	ρ		0.608	0.425
	p		0.001	0.001
Mollusca	ρ			0.318
	p			0.001

Sample statistics on top indicates the similarity of the compared taxa; the probability (p) values at the bottom indicate the significance level of the compared structure patterns

that did not share at least 35% of the species with another station (Fig. 7.6), and mollusks had only two stations that did not share at least 35% of the species with another station (Fig. 7.7). Another interesting characteristic is that more stations are contained within clusters for polychaetes and mollusks than for crustaceans and harpacticoids. In fact, nearly all the clusters for crustaceans and harpacticoids contain only two stations (Fig. 7.6). In nearly all instances, the clustering stations are adjacent to each other. While the community structure patterns of all four taxa were significantly correlated with each other, their similarity was mostly low (Table 7.3). The similarity between the distribution patterns of Harpacticoida and any macrofauna group was below Rho = 0.35, with Mollusca being least similar at Rho = 0.172.

Table 7.4 Relationship between biological components abundance and environmental principal components (Fig. 7.1a)

	PC1 (Sediment type)				PC2 (Particulate flux)			
Taxa		*r*	*p*	*n*		*r*	*p*	*n*
Meiofauna ab	**	0.48	0.0021	39	***	0.56	0.0002	39
Macrofauna ab	*	0.33	0.0415	38	****	0.70	<0.0001	38
Bacteria ab	*	0.39	0.0136	39	**	0.47	0.0028	39
Harpacticoida ab		0.25	0.1282	39	***	0.55	0.0003	39
Harpacticoida N1		−0.17	0.3048	39		0.25	0.1190	39
Polychaeta ab		0.27	0.0924	39	****	0.73	<0.0001	39
Polychaeta N1		0.20	0.2131	39	*	0.38	0.0185	39
Crustacea ab	*	0.39	0.0130	39	**	0.49	0.0017	39
Crustacea N1		−0.17	0.2962	39		0.07	0.6746	39
Mollusca ab	***	0.53	0.0005	39	***	0.52	0.0007	39
Mollusca N1	*	−0.32	0.0463	39		−0.18	0.2825	39

Pearson correlation coefficients (*r*), probability that $r = 0$ (*p*), and number of observations (*n*). Significance levels indicated by asterisks as in Table 7.1

Taxa abbreviations: *ab* abundance, *N1* Hill's number of dominant species diversity index Significance levels: 0.05 < * < 0.01, 0.01 < ** <0.001, 0.001 < *** < 0.0001, and <0.0001 ****

Most similar in this respect were crustaceans and mollusks at Rho = 0.608, followed by crustaceans and polychaetes at Rho = 0.425.

7.3.3 Linking Environment and Benthos

The PC1 and PC2 station scores for environmental variables were significantly correlated with bacterial, meiofaunal, and macrofaunal total abundance (Table 7.4). However, the association with PC2 was much stronger than with PC1. Thus, total abundance of the three main groupings generally increases with increasing fine sediment structure, and particulate organic matter flux, but the relationship with flux may be stronger. The abundance of specific taxa (i.e., harpacticoids, polychaetes, crustaceans, and mollusks) was correlated with PC2, whereas PC1 was only correlated to crustacean and mollusk abundance. Diversity had few correlations with the abiotic PC loads, except for a weak positive correlation with polychaete diversity and PC2 and a weak negative correlation with mollusk diversity and PC1. The strongest overall associations were with PC2 and meiofaunal abundance and polychaete abundance. Meiofauna abundance is dominated by nematode abundance. Thus, the trends indicate that nematode and polychaete abundance increases with increasing flux.

Table 7.5 ANOVA table for differences between cruises (2000 and 2001) and stations (C7, MT1, MT3, MT6, S36, S41, S42)

A. Macrofauna (log-transformed)					
Source	DF	Type III SS	Mean square	*F* value	Pr > *F*
Cruise	1	18.52	18.52	7.45	0.0085
Station	6	157.86	26.31	10.58	<0.0001
Cruise Station	6	18.66	3.11	1.25	0.2949
Corrected Total	69	334.26			

B. Meiofauna (log-transformed)					
Source	DF	Type III SS	Mean square	*F* value	Pr > *F*
Cruise	1	25.57	25.57	9.38	0.0034
Station	6	110.10	18.35	6.73	<0.0001
Cruise Station	6	17.90	2.98	1.09	0.3770
Corrected Total	69	306.19			

7.3.4 Temporal Change

There was a significant difference for both meiofauna and macrofauna between the 2 years (Table 7.5). There is no significant "cruise-station" interaction, meaning that change across the area happened in similar ways at all stations. The average abundance decreased 36% for macrofauna and 30% for meiofauna from 2000 to 2001. The average back-transformed abundance for macrofauna in 2000 was 3265 n/m^2 (range 971–10,957), and in 2001 it was 1167 n/m^2 (range 69–19,135). The average back-transformed abundance for meiofauna in 2000 was 1396 n/10 cm^2 (range 338–5729), and in 2001 it was 416 n/10 cm^2 (range 32–5091). This indicates that year-to-year variability exists in the deep GoM.

7.3.5 Diversity Spatial Change

There were differences in diversity with respect to depth, which is roughly along lines of latitude (Fig. 7.8) and across the Gulf with respect to longitude (Fig. 7.9). However the trends were not the same for all taxa. Harpacticoida diversity appeared to decrease somewhat linearly with depth. In contrast, Polychaeta, Crustacea, and Mollusca increased to about 1000 m and then decreased with depth. The mollusk diversity may increase between about 2600 and 3200 m. Harpacticoids, crustaceans, and mollusks have the highest diversity in the western Gulf and decrease moving eastward (Fig. 7.9). Polychaetes appear to have a bimodal diversity distribution, decreasing from west to east, but peaking in the center of the Gulf around 89 °W longitude due south of the Mississippi River.

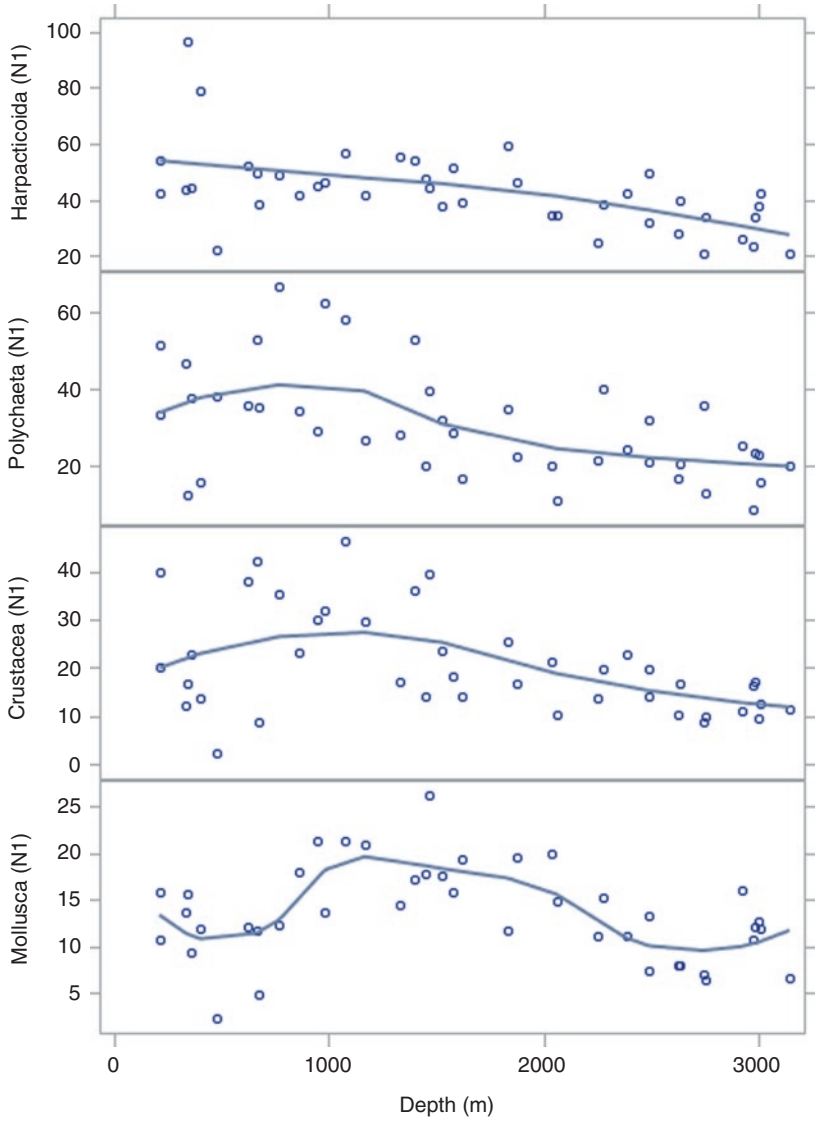

Fig. 7.8 Diversity of taxa with respect to depth. Line is a polynomial curve fit

7.4 Discussion

7.4.1 Environmental Analyses

In the environmental variable analysis (Figs. 7.1 and 7.2), PC1 is interpreted as the sediment properties with high silt, clay, organic (PAH), and metal (Cr and Sn) contaminants near the Mississippi River and higher sand and natural background metals

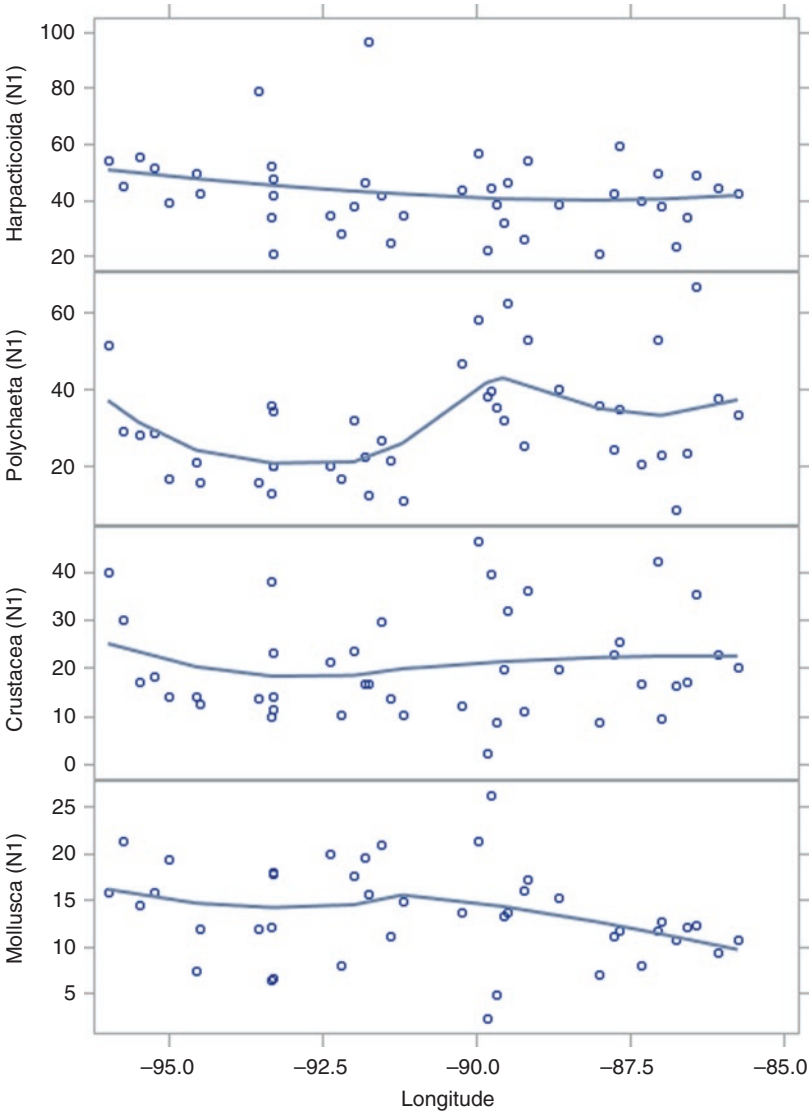

Fig. 7.9 Diversity of taxa with respect to longitude. Line is a polynomial curve fit

(Ca and Sr) with increasing distance from the Mississippi River. PC2 is interpreted as particulate organic matter (POM) flux. PC3 and PC4 did not present obvious interpretations.

7.4.2 Benthic Abundance and Community Analyses

On average, polychaetes were the most abundant and most speciose taxon examined (Table 7.2). Harpacticoida were the least abundant among the four taxa, but had the second highest average count of species per station. The relatively large number of species per individuals counted indicates the high values for evenness and overall diversity of Harpacticoida. The standard deviation of abundance measurements was quite high for all taxa, but particularly for crustaceans. This was caused by the extremely high counts of *Ampelisca mississippiana* (Soliman and Wicksten 2007) in the head of the Mississippi Canyon (Soliman and Rowe 2008).

The separate analyses of Harpacticoida, Polychaeta, Mollusca, and Crustacea in respect of their distribution patterns reveal that they have different turnover rates among sampling stations (Figs. 7.4, 7.5, 7.6, and 7.7). Harpacticoida have a particularly high turnover rate (Fig. 7.4), i.e., the similarity of the harpacticoid fauna at different stations was very low. Baguley et al. (2006) hypothesized that the endemism of harpacticoids in the deep sea may be caused by their high speciation potential. In contrast, polychaetes (Fig. 7.7) and mollusks (Fig. 7.6) had a relatively low species turnover rate between sampling stations. Many polychaete species have long-distance dispersal capabilities through their pelagic larvae, leading to wide distribution (Day 1967). Additionally, many polychaete species are opportunistic generalists (Reuscher and Shirley 2014) that have the ability to adapt to different environmental settings. It is very common to find several of these opportunistic species with overlapping ecological niches in large number in the same sample (Flint and Rabalais 1980), defying the classical checkerboard distribution pattern concept (Diamond 1973). Aplacophorans are in many ways the mollusk analogs of polychaetes, including their opportunistic adaptability and their wide species distributions (Scheltema 1979).

The lack of a correlation between N1 values of polychaetes and harpacticoids or mollusks with the physical PC axes (Table 7.4) indicates that there is no general pattern or suite of abiotic variables that can explain the diversity of each group. This corroborates the findings of Haedrich et al. (2008), whose generalized linear model showed that factors related to food, habitat, location, or pollution affected various taxa in different ways.

Many past studies in the global ocean have found that diversity of macrofauna taxa increases from the shelf to the deep sea to the abyssal plain (reviewed in Rex 1981). This pattern is not repeated in the GoM where diversity appears to peak on the continental slope between 800 and 1200 m (Fig. 7.8). Only Mollusca diversity appears to increase from the deep sea to the plain. The GoM is an enclosed sea and highly influenced by surrounding watersheds of North America. The two biggest

physical influences on the Gulf are the presence of the Mississippi River (which drains two-thirds of the continent) and the circulation pattern that is dominated by the loop current that brings water from the Caribbean Sea into the GoM. So, the unique combination of being an enclosed sea that is influenced by a large river outflow to the north, and a large current from the south, likely shapes the physical environment that is reflected in the observed diversity patterns.

7.4.3 Linking Environment and Benthos

The strong positive correlation of PC2 with abundance of bacteria, meiofauna, macrofauna, and the four specific taxa (Table 7.4) indicates that the influx of POM to the deep-sea benthos is a crucial food source for the organisms. Areas with an increased POM influx can be expected to have higher numbers in bacteria and metazoans. Polychaetes seem to benefit most from high POM fluxes, as their correlation with PC2 was strongest.

The abundance of all of the main groups – bacteria, meiofauna, and macrofauna – was also correlated with PC1 (Table 7.4), which indicates an increase with the clay content of the sediment. However, a closer look reveals that only some of the taxa were affected by the sediment properties. Mollusk abundance showed the strongest correlation among the examined taxa. Crustaceans were also significantly affected by the clay content, while polychaetes were not. The nonsignificant correlation between PC1 and harpacticoid abundance indicates that nematodes, the numerically dominant meiofauna taxon, must significantly increase when the clay content increases.

The only significant relationships between the environmental principal components and diversity were the negative correlation of mollusk diversity with PC1 (Table 7.4), which means that they are more diverse in sediment with higher sand content and lower clay content, and the positive correlation between polychaete diversity and PC2, which means they are more diverse in areas with increased POC flux. Both of these observations corroborate the species richness predictors by Haedrich et al. (2008).

The finding that there were differences in abundance for macrofauna and meiofauna between 2000 and 2001 was surprising. It was thought that the deep sea is relatively invariant over time, but this is clearly not the case. The average abundance decreased 2000–2001, which correlates to an increase in the size of the hypoxic zone from 4400 km^2 in 2000 to >19,840 km^2 in 2001 (Scavia et al. 2003; Rabalais 2016). Although the hypoxia zone is in shallow, shelf water, it is possible that the same factors that influence interannual variability in the hypoxia area also influence variability in the deep-sea GoM.

7.5 Conclusion

The Gulf of Mexico is an enclosed sea that acts as an integrated large marine ecosystem (Kumpf et al. 1999). The Mississippi River has a larger influence on benthic infaunal community structure and diversity in the Northern Gulf of Mexico spatially, and likely temporally. The Deep Gulf of Mexico Benthos (DGoMB) program was designed to determine patterns of abundance and diversity of meiofauna and macrofauna in the northern Gulf of Mexico continental slope between 300 m and 3700 m deep. Principal component analysis was used to link abiotic variables to the species distributions. The first two principal components of the abiotic variables were interpreted as sediment properties (high clay content and trace metals of anthropogenic sources vs. high sand content and natural trace metals) and particulate organic carbon (POC) flux. Abundance of all taxa was significantly influenced by the POC flux. High clay content significantly increased the abundance of meiofauna, macrofauna, crustaceans, and mollusks, but had no significant effect on harpacticoid or polychaete abundance. Polychaete diversity was significantly affected by POC flux and mollusk diversity by the sediment properties. Polychaetes had the highest average abundance and species richness. However, Harpacticoida despite being least abundant of the four taxa compared had the highest values for the Pielou evenness index and Hill's diversity index measurements. Harpacticoids and Crustaceans had high species turnover rates, resulting in low similarities of the respective faunas between sampling stations, whereas mollusk fauna and polychaete fauna were more similar between different sampling stations. Overall, there were similarities in community structure patterns, interannual differences in abundance patterns, and unique distributions of diversity with respect to depth and longitude.

Acknowledgments Most of this research was supported by the Minerals Management Service, US Department of the Interior (contract 30991). The writing and publication of the research was made possible in part by grants to P. Montagna from The Gulf of Mexico Research Initiative/C-IMAGE III (award SA 18-16), and the National Oceanic and Atmospheric Administration (award NA11SEC4810001). All data used are available at http://marinecadastre.gov/espis/#/search/study/157.

References

Baguley JG, Montagna PA, Lee W, Hyde LJ, Rowe GT (2006) Spatial and bathymetric trends in Harpacticoida (Copepoda) community structure in the northern Gulf of Mexico deep-sea. J Exp Mar Biol Ecol 330:327–341. https://doi.org/10.1016/j.jembe.2005.12.037

Baguley JG, Montagna PA, Hyde LJ, Rowe GT (2008) Metazoan meiofauna biomass, grazing, and weight-dependent respiration in the northern Gulf of Mexico deep sea. Deep-Sea Res II 55:2607–2616

Berger WH, Fischer K, Lai C, Wu G (1988) Ocean carbon flux: maps of primary production and export production. In: Agegian CR (ed) Biogeochemical cycling and fluxes between the deep euphotic zone and other oceanic realms. NOAA, Washington D.C., pp 131–176

Betzer PR, Showers WJ, Laws EA, Winn CD, DiTullio GR, Kroopnick PM (1984) Primary productivity and particle fluxes on a transect of the equator at 153 °W in the Pacific Ocean. Deep-Sea Res Part A 31:1–11

Biggs DC, Hu C, Müller-Karger FE (2008) Remotely sensed sea-surface chlorophyll and POC flux at Deep Gulf of Mexico benthos sampling stations. Deep-Sea Res II 55:2555–2562

Clarke KR, Gorley RN (2001) PRIMER v5: user manual/tutorial. Primer-E, Plymouth

Clarke KR, Warwick RM (2001) Change in marine communities: an approach to statistical analysis and interpretation, 2nd edn. Primer-E, Plymouth

Danovaro R (2010) Methods for the study of deep-sea sediments, their functioning and biodiversity. CRC Press/Taylor and Francis Group, Boca Raton

Day JH (1967) A monograph on the Polychaeta of the southern Africa, 2 volumes, 656 and 878 pp. British Museum (Natural History), London

Deming JW, Carpenter SD (2008) Factors influencing benthic bacterial abundance, biomass, and activity on the northern continental margin and deep basin of the Gulf of Mexico. Deep-Sea Res II 55:2597–2606

Diamond JM (1973) Distributional ecology of New Guinea Birds. Science 179(4075):759–769

Flint RW, Rabalais NN (1980) Polychaete ecology and niche patterns: Texas continental shelf. Mar Ecol Prog Ser 3:193–202

Gallaway BJ (ed) (1988) Northern Gulf of Mexico continental slope study, Final report: year 4. Volume II: synthesis report. Final report submitted to the Minerals Management Service, New Orleans, LA. Contract No. 14-12-0001-30212. OCS Study/MMS 88-0053, 378 pp

Giere O (2009) Meiobenthology, 2nd edn. Springer, Berlin

Haedrich RL, Devine JA, Kendall VJ (2008) Predictors of species richness in the deep-benthic fauna of the northern Gulf of Mexico. Deep-Sea Research II 55:24–26

Hill MO (1973) Diversity and evenness: a unifying notation and its consequences. Ecology 54:427–432

Iken K, Brey T, Wand U, Voight J, Junghans P (2001) Food web structure of the benthic community at the Porcupine Abyssal Plain (NE Atlantic): a stable isotope analysis. Prog Oceanogr 50:383–405

Kumpf H, Steidinger K, Sherman K (1999) The gulf of Mexico large marine ecosystem: assessment, sustainability, and management. Blackwell Science, Inc, Malden

Long ER, Carr RS, Montagna PA (2003) Porewater toxicity tests: value as a component of sediment quality triad assessments. In: Carr RS, Nipper M (eds) Porewater toxicity testing: biological, chemical, and ecological considerations. Society of Environmental Toxicology and Chemistry (SETAC) Press, Pensacola, pp 163–200

Ludwig JA, Reynolds JF (1988) Statistical ecology. Wiley, New York

Montagna PA, Baguley JG, Cooksey C, Hartwell I, Hyde LJ, Hyland JL, Kalke RD, Kracker LM, Reuscher M, Rhodes ACE (2013) Deep-Sea benthic footprint of the Deepwater Horizon blowout. PLoS One 8(8):e70540. https://doi.org/10.1371/journal.pone.0070540

Morse JW, Beazley MJ (2008) Organic matter in deep water sediments of the northern Gulf of Mexico and its relationship to the distribution of benthic organisms. Deep-Sea Res II 55:2563–2571

Pequegnat W (1983) The ecological communities of the continental slope and adjacent regimes of the northern Gulf of Mexico. Prepared by Tereco Corporation, US Dept of the Interior, Minerals Management Service, Gulf of Mexico OCS Region, New Orleans, LA Contract No AA851-CT-1-12, 398 pp

Pielou EC (1975) Ecological diversity. Wiley, New York

Rabalais NN (2016) Hypoxia in the northern Gulf of Mexico. http://www.gulfhypoxia.net/Research/Shelfwide%20Cruises/. Accessed 10 June 2016

Reuscher MG, Shirley TC (2014) Diversity, distribution, and zoogeography of benthic polychaetes in the Gulf of Mexico. Mar Biodivers 44:519–532

Rex MA (1981) Community structure in the deep-sea benthos. Annu Rev Ecol Syst 12:331–353

Rowe GT, Kennicutt MC (2008) Introduction to the deep Gulf of Mexico Benthos program. Deep-Sea Res II 55:2536–2540

Rowe GT, Kennicutt II MC (eds) (2009) Northern Gulf of Mexico continental slope habitats and benthic ecology study: final report. US Dept. of the Interior, Minerals Management Service, Gulf of Mexico OCS Region, New Orleans, OCS Study MMS 2009-039, 456 pp, https://www.boem.gov/ESPIS/4/4842.pdf accessed 28 July 2017

Rowe GT, Wei C, Nunnally C, Haedrich R, Montagna P, Baguley JG, Bernhard JM, Wicksten M, Ammons A, Escobar Briones E, Soliman Y, Deming JW (2008) Comparative biomass structure and estimated carbon flow in food webs in the deep Gulf of Mexico. Deep-Sea Res II 55:2699–2711

SAS Institute Inc (1990) SAS User's guide, version 6, vol 1, 4th edn. SAS Institute Inc, Cary, 943 p

Scavia D, Rabalais NN, Turner RE, Justić D, Wiseman WJ Jr (2003) Predicting the response of Gulf of Mexico hypoxia to variations in Mississippi River nitrogen load. Limnol Oceanogr 48:951–956

Scheltema AH (1979) Aplacophoran molluscs: deep-sea analogs to polychaetes. Bull Mar Sci 60:575–583

Soliman YS, Rowe GT (2008) Secondary production of *Ampelisca mississippiana* Soliman and Wicksten 2007 (Amphipoda, Crustacea) in the head of the Mississippi Canyon, northern Gulf of Mexico. Deep-Sea Res II 55:2692–2698

Soliman Y, Wicksten M (2007) *Ampelisca mississippiana*: a new species (Crustacea: Amphipoda: Gammaridea) from the Mississippi Canyon (northern Gulf of Mexico). Zootaxa 1389:45–54

Thiel H (1975) The size structure of the deep-sea benthos. Int Rev Gesamten Hydrobiol 60:575–606

Wade TL, Soliman Y, Sweet ST, Wollf GA, Presley BJ (2008) Trace elements and polycyclic aromatic hydrocarbons (PAHs) concentrations in deep Gulf of Mexico sediments. Deep-Sea Res II 55:2585–2593

Wilson GDF (2008) Local and regional species diversity of benthic Isopoda (Crustacea) in the deep Gulf of Mexico. Deep-Sea Res II 55:2634–2649

Chapter 8
The Asphalt Ecosystem of the Southern Gulf of Mexico: Abyssal Habitats Across Space and Time

Ian R. MacDonald, Adriana Gaytan-Caballero, and Elva Escobar-Briones

Abstract Recent findings cap more than a decade of research on habitats for chemoautotrophic fauna that are generated by hydrocarbon seepage at abyssal depths in the southern Gulf of Mexico. Extensive pavements (3300 m^2) of asphalt, created by repeated, slow discharges, are sparsely colonized by tubeworms that tap reduced sulfur compounds through cracks and fissures in the solidified material. At depths greater than 3000 m, gas hydrate forms instantaneously, generating frozen mounds 10 m or greater in diameter. These deposits are apparently stable for decades or longer, because they are colonized by massive arrays of tubeworms. The asphalt ecosystem of the southern Gulf poses special challenges for expanding deep-water oil production and many potential chemosynthetic habitats remain unexplored.

Keywords Chemosynthetic community · Cold seep · Gas hydrate · Asphalt volcanism · Deep sea

8.1 Introduction

Expansion of oil production onto the continental slope of the Northern Gulf of Mexico during the 1980s led to discoveries that have informed science, technology, and regulatory policy ever since. The Gulf is one of the most important sources of oil and gas in the world (Kaiser 2011). However, the hydrocarbon system that the industry seeks to exploit is imperfectly sealed due to diapiric activity of Jurassic

I. R. MacDonald (✉)
Florida State University, Earth, Ocean and Atmospheric Sciences, Tallahassee, FL, USA
e-mail: imacdonald@fsu.edu

A. Gaytan-Caballero · E. Escobar-Briones
Universidad Nacional Autónoma de México, El Instituto de Ciencias del Mar y Limnología, Mexico City, Mexico
e-mail: adriana.gaytan@ciencias.unam.mx; escobri@cmarl.unam.mx

S. A. Murawski et al. (eds.), *Scenarios and Responses to Future Deep Oil Spills*,
https://doi.org/10.1007/978-3-030-12963-7_8

Age salt deposits (Abrams 2005). In water depths of 500 m or more, oil and gas continuously seep into the benthos and the water column at hundreds of currently active sites (MacDonald et al. 2015) and thousands more inactive sites that are preserved in the geologic record (Frye 2008). Industrial production of hydrocarbons proceeds within a background of slow and widespread natural seepage. The flux of organic carbon supports lush ecosystems based on microbial chemoautotrophy and specially adapted tube worms, mussels, and clams, which host chemoautotrophic bacteria as endosymbionts (Fisher et al. 1989). Under the pressure and temperatures of extreme ocean depths, and the geologic instability caused by diapiric activity, oil and gas seepage generate novel features including mud volcanism (Milkov 2000), gas hydrates (Macdonald et al. 1994), and massive accretion of authigenic carbonate (Roberts et al. 2010).

The goal of this chapter is to highlight recent discoveries on three diapiric knolls in the deepest regions of the Gulf, part of the exclusive economic zone (EEZ) of Mexico. In these settings, hydrocarbon seepage is manifest in extensive flows of solidified asphalt and massive gas hydrate mounds that are colonized by chemosynthetic fauna (Sahling et al. 2016). Asphalt ecosystems include many of the fauna and processes known from previous research, but differences in the regional geology and effects of deep-sea pressure, temperature, and trophic isolation generate habitats and assemblages that push the envelope of benthic ecology. These unprecedented findings inspire appreciation of diversity and dynamics in the deep ocean and the profound impact of hydrocarbons across geologic time and into the present. The same oil and gas that energy companies extract for human consumption support thriving ecosystems that had until recently been far outside the reach of human activity. This dynamic underscores how much remains unknown in the deep sea and the realm's capacity to present investigators with the unexpected. Results from investigating living and nonliving processes that support these remarkable ecosystems can be applied to protect them from impact and potentially to safeguard industrial mishaps. Notably, the initial discovery of chemosynthetic communities supported by hydrocarbon seepage on the continental slope was almost immediately followed by issuance of regulations designed to protect "lush chemosynthetic communities" from harm (MMS 1988). This chapter should serve the interests of science and sensible policy by documenting the unique habitats within the asphalt ecosystem and the processes that maintain them.

8.2 Seep Habitats in the Northern Gulf of Mexico

Seeps and seep communities were first discovered in the Northern Gulf based on geochemical results that indicated significant contamination of seafloor sediments in areas that were prospective for oil and gas production (Brooks et al. 1987). Exploration of these areas was undertaken after trawling, photo-platform, and coring operations indicated presence of anomalously dense aggregations of tube

worms, clams, and mussels associated with thermogenic hydrocarbons (Kennicutt et al. 1985). The original findings in the Gulf followed shortly after discoveries of hydrothermal vent communities in the eastern Pacific Ocean; they contributed significantly to the emerging paradigm of chemoautotrophic life in the deep ocean. Physiological investigations of the dominant tube worm (*Lamellibrachia luymesi*, *Seepiophila jonesi*) (Gardiner et al. 2001) and bivalve (*Bathymodiolus childressi*, *B. fisheri*) (Gustafson et al. 1998) populations at the newly discovered seeps confirmed adaptations to the geochemical characteristics of seep environments: e.g., ability of tube worms to extract reduced sulfur compounds from sediments instead of hydrothermal fluids (Freytag et al. 1999) and bivalve endosymbionts able to use methane as a source of chemical energy and nutrient carbon during chemosynthesis (Childress et al. 1986). Observation and sampling from human-occupied submersibles confirmed the high biomass chemosynthetic animals and epifaunal diversity of seeps at depths of 500–2000 m (Bergquist et al. 2003; Cordes et al. 2009). Stable isotope studies of heterotroph fauna distinguished "resident" organisms (squat lobster, *Munidopsis* sp.; shrimp, *Alvinocaris stactophila)*, which showed $\delta^{13}C$ values indicative of a diet mostly derived from chemosynthetic biomass, and "vagrant" fauna (isopods, *Bathynomus gigas*; spider crabs, *Rochinia crassa*; fish, *Synaphbranchus* sp.), which showed oceanic food sources with lesser proportions of chemosynthetic carbon (MacAvoy et al. 2002). Regulatory agencies (Minerals Management Service, National Oceanic and Atmospheric Administration) supported research and exploration that illuminated the extent of chemosynthetic habitats across the Gulf and informed policies designed to protect them from impact due to hydrocarbon production (Roberts and Boland 2010).

An important breakthrough for discovery was the recognition that hydrocarbon seepage can be detected by satellite remote sensing (MacDonald et al. 1993) and multichannel seismic techniques (Reilly et al. 1996). Seeps produce distinctive oil slicks on the ocean surface above the seafloor source where oil and gas were released. Such slicks could be detected from satellites using optical or synthetic aperture radar sensors (Bern et al. 1993). Although false targets do occur, observing persistent slicks in that same ocean area provided a way to localize the probable location of a seep that could subsequently be explored with a submersible, remotely operated vehicle (ROV), or photosled (De Beukelaer et al. 2003). Geophysicists learned better to interpret gas blanking and faults as indicators of seepage in seismic and bathymetric data (Wood and Ruppel 2000). Consequently, the distribution of known sites steady expanded to cover the central and western regions of the US EEZ in the Gulf out to the limits of the Sigsbee Escarpment—approximately 2500 m depth (Roberts and Feng 2013).

Despite many gaps in exploration, many typical abiotic features of hydrocarbon seeps came to be recognized; prominent examples of such features included the following: Seafloor sediments were saturated with oil and gas that bubbled into the water column from localized vents; mud volcanoes discharged mudflows that formed high-relief knolls; brine pools filled craters with hypersaline, methane-rich fluids; outcropping gas hydrates appeared as mounds breached the sediments and subsequently dissolved (Roberts and Carney 1997). A conceptual model of habitat genera-

tion by hydrocarbon seep processes emerged from more than a decade of observation and sampling: Where liquid oil saturated the seabed, tube worms formed "bushes" or larger clusters several meters across, in which hundreds of individuals extended their ~1 cm tubes, 1 to 2 m into the oxygenated water, while much thinner sections of their tubes were deeply rooted in anoxic, sulfide-rich mud (Freytag et al. 1999). Seep mussels required more active methane flux and tended around localized vents with transient mounds of gas hydrate (Carney et al. 2006). Much larger beds of mussels also formed on the "shoreline" of pools of methane-saturated brine (MacDonald et al. 1990). Discrete aggregations of chemosynthetic fauna tended to be surrounded by larger areas characterized by bacteria mats and carbonate pavements (Roberts and Carney 1997). These concepts would shift dramatically after discoveries in the southern Gulf of Mexico.

8.3 A Novel Seep Process in the Southern Gulf of Mexico

In 2003, the German research group MARUM led a joint German, Mexican, US expedition to the Gulf of Mexico. A 9-day effort was undertaken with the research ship F/S Sonne to provide the first scientific investigation of possible seeps in the southern Gulf (Bohrmann and Schenck 2004). Following a nested exploration plan, investigators first identified probable seep areas based on satellite detection of surface oil slicks. This showed a region of persistent slicks in the Campeche Knolls area, located in near abyssal depths beyond the Mexican continental slope. Swath-mapping survey on this region identified numerous knolls and ridges, which were robustly correlated with individual clusters of surface slicks (Fig. 8.1). A prominent knoll, 200 m high and about 1.5 km in diameter, was chosen for detailed exploration. Acoustic returns from the water column indicated that plumes of bubbles were rising from near the top of the mound, and a photosled was launched to explore the benthos.

Investigators anticipating features familiar from the Northern Gulf, such as tube worm bushes surrounded by bacteria mats and carbonate, were astonished to encounter massive layers of solidified asphalt with tube worms growing through cracks and from under the edges of the pavement. Sampling with cores and grabs confirmed the chemistry of substrata comprising asphaltenes and short-chained hydrocarbons while also finding traces of "fresh" oil and methane. The site was dubbed "Chapopote" from the Aztec word for tar, and the process was designated "asphalt volcanism" to denote the growth of knolls and the generation of new, hard substrata (MacDonald et al. 2004). Photographic exploration indicated the affinity of chemosynthetic taxa, i.e., tube worms and mussels, with examples from the Northern Gulf and showed presence of familiar seep epifauna including squat lobster (*Munidopsis* sp.) and sea cucumber (*Chiridota heheva*). However, the limited time for exploration left unanswered questions regarding the timing and mode by which asphalt came to cover the Chapopote site, the extent of similar sites in the region, and the ways in which this newly discovered region would shape the chemosynthetic habitat.

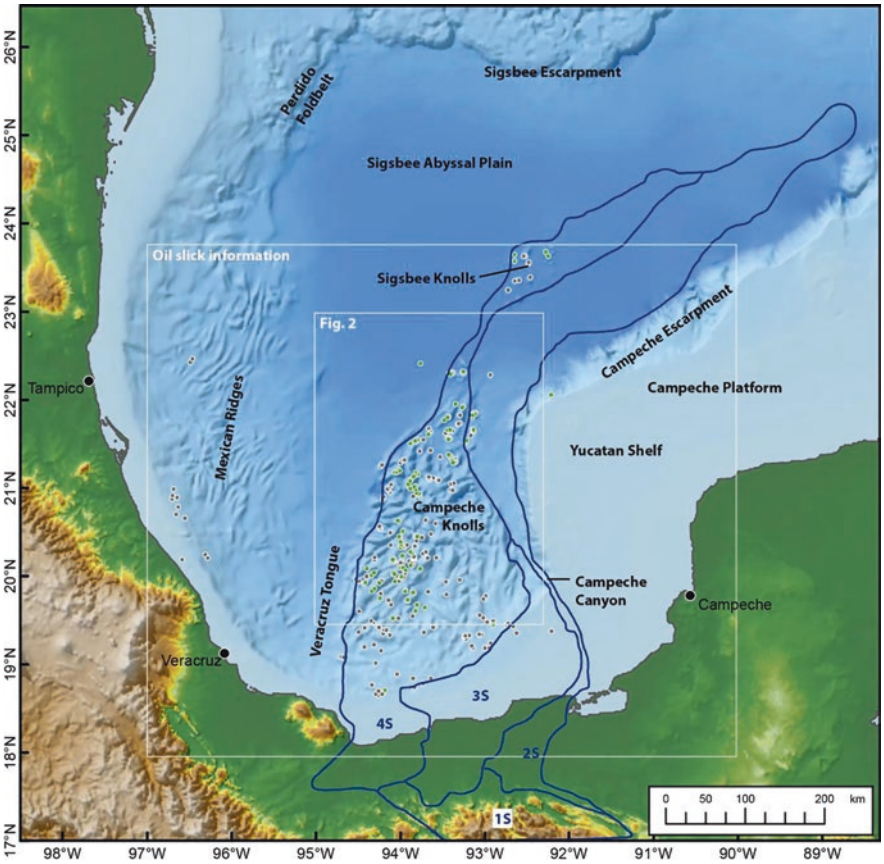

Fig. 8.1 Regional map of the southern Gulf of Mexico from Sahling et al. (2016). Locations of persistent oil slicks correspond with seafloor ridges and knolls. Potential area of seepage covers a large portion of the Campeche Bight

Subsequent research at the Chapopote site, including a second expedition in 2005, suggested that the asphalts covering Chapopote originated from relatively shallow reservoirs that were pressurized by salt diapiric activity (Ding et al. 2008). Detailed mapping of the site from AUV and ROV surveys quantified an asphalt flow occupying over 2000 m^2 of the bottom including relatively fresh and highly weathered material as well as extensive tube worm colonies (Bruening et al. 2010). Most recently, a 30-day research expedition greatly expanded swath-mapping, AUV, and ROV exploration in the region (Sahling et al. 2016). These findings confirmed that the region hosts numerous chemosynthetic communities and active seep sites (Fig. 8.2). The habitats described below exemplify the ways in which the seepage styles of asphalt, oil, and gas releases and gas hydrate formation combine to produce biological habitats similar to those known from shallower sites in the Northern Gulf of Mexico, but display characteristics thus far unique to the southern

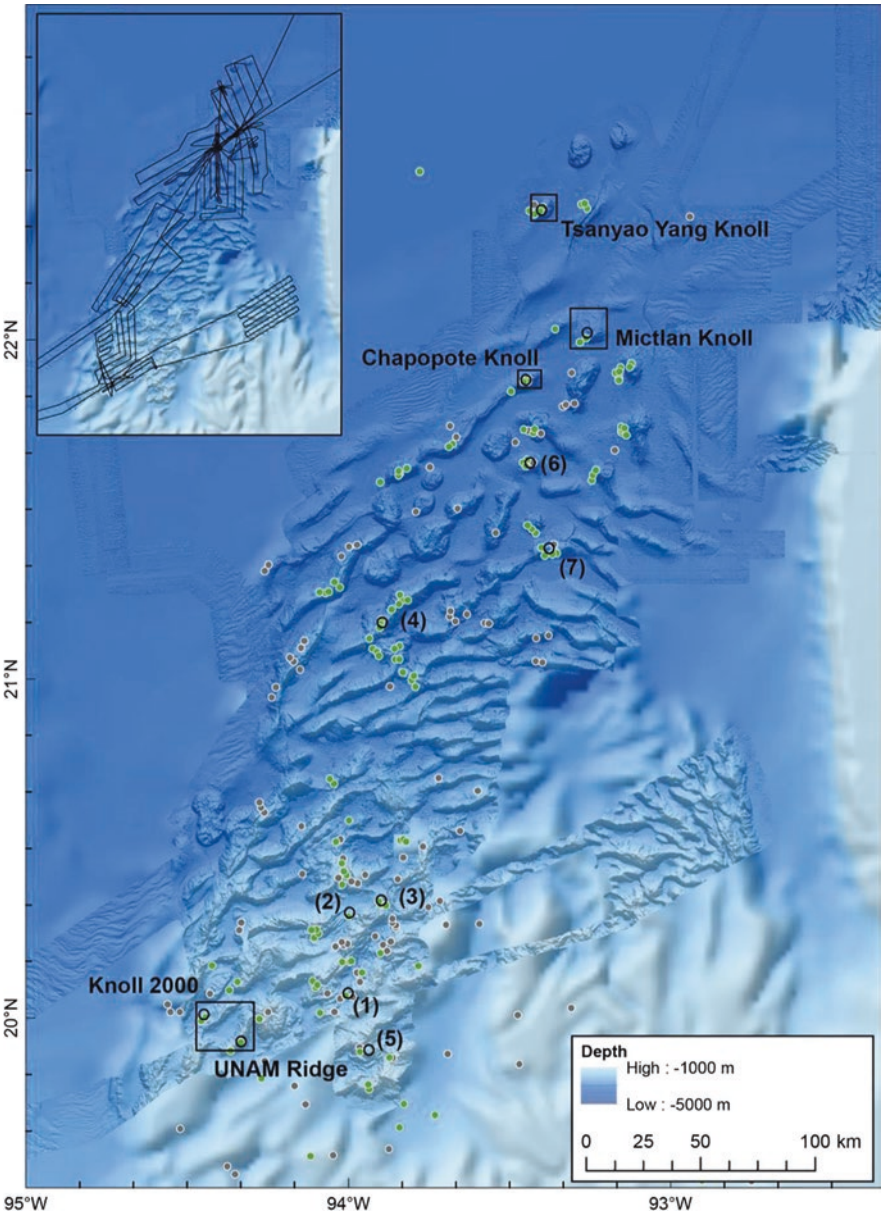

Fig. 8.2 Details of Campeche Knolls region showing locations of principal study sites described in text (Sahling et al. 2016)

Gulf of Mexico. The sites include the original site, Chapopote, and two newly explored sites dubbed Mictlan and Tsanyao Yang Knoll (TYK); their locations are shown in Fig. 8.2.

8.4 The Asphalt Flow at Chapopote

The discovery of Chapopote demonstrated that heavily weathered oil—asphalt—could support chemosynthetic tube worms on substrata apparently quite distinct from the oil-saturated sediments familiar from numerous examples in the Northern Gulf. Because sulfides needed to nourish tube worm endosymbionts are generated by anaerobic oxidation of hydrocarbons and reduction of seawater sulfate (Boetius et al. 2000), there was uncertainty as to how these microbial processes could yield a similar sulfide supply from largely refractory asphalt. Careful mapping and observation of the large, central asphalt flow at Chapopote provide important clues to the development of asphalt flows and their colonization by tube worms and other fauna (Marcon et al. 2018). A mosaic of 999 images covering over 3300 m^2 was constructed with the use of the large-area photomosaicking (LAPM) tool (Marcon et al. 2013). Figure 8.3 shows a greatly reduced version of the 15-billion-pixel mosaic and a diagram of the different features contained within the asphalt-covered seafloor.

The source of the material is a central region where smooth, bacterial-coated asphalt has discharged within an area about 10 m across. Comparison to earlier mapping efforts (Bruening et al. 2010) revealed that the detailed features of this region, including bacterial coatings and the morphology of the asphalt, were essentially unaltered between 2005 and 2015 when the large mosaic was compiled. However, details of the mosaic show clear evidence that the entire feature has issued from this source region and, moreover, that the present formation represents at least three different discharges. Uncertain is whether these discharges proceed at

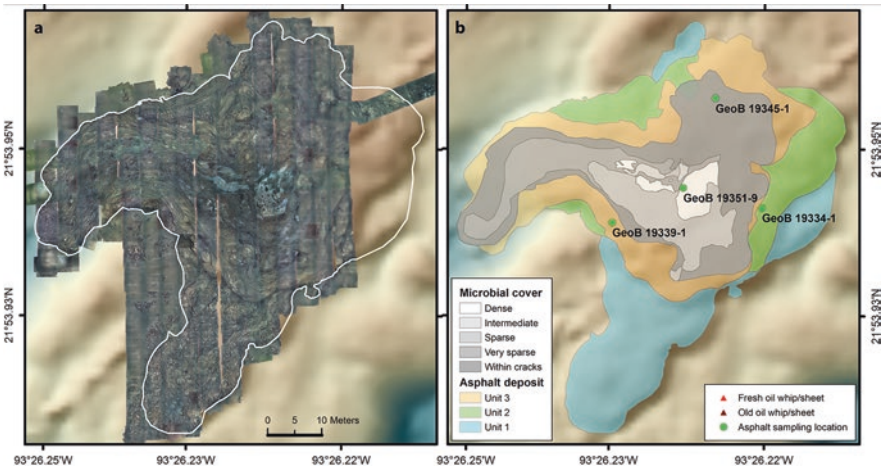

Fig. 8.3 Photomosaic and flow units of the Chapopote main asphalt field. Photomosaic overlain on area bathymetry. Extent of asphalts shown in white outline (left). The eastern limit of the field was inferred from the bathymetry and remotely operated vehicle (ROV) footage. Extent of the main asphalt units and microbial mats (right). Colors indicate three proposed flow units—in some areas inferred by abrupt elevation changes. Gravity core locations show where targeted asphalt collections were made. (From Marcon et al. 2018, Fig. 4)

a steady rate or pulses of more active flow followed by years of relative inactivity. Further sampling and development of dating methods will be required to constrain these possibilities, but the colonization of the asphalt by tube worms may offer some clues.

Resemblance of folded and braided asphalt flows to pahoehoe lava known from basalt volcanism has been noted since the first discoveries. Lava rheology has been described from examples on Hawaii (Harris and Rowland 2015) and is very briefly summarized in Fig. 8.4. Key to the process is continued supply of fresh, mobile material and the cooling of outer layers. As the outer layers stiffen with cooling, it folds and rolls in the characteristic pahoehoe form, even as new material is added from within. Eventually cracks and fissures open in the stiffened outer crust, which may allow extrusion of molten lava.

One can speculate that similar physical process occurs in asphalt flows, albeit at a vastly slower pace, as the volatile components of the material dissolve into seawater leaving behind a progressively brittle and indurated surface. Certain features are unique to the asphalt, however, because where it breaks through the brittle outer layer, the fresh asphalt is buoyant and can float upward in so-called whips (Fig. 8.4). Young tube worm recruit directly into these fissures and presence of bacteria and detritus feeders such as the holothuroid *Chiridota heheva*, which also localize in breaks in the outer crust, provide further evidence for presence of labile carbon under the weathered crust. Seep tube worms grow very slowly (~1 cm/y) at oil seeps in the Northern Gulf (Fisher et al. 1997). Therefore, clusters of large individuals at the outer edges of the Chapopote main asphalt field may indicate that these components are no longer expanding. One robust conclusion is that the movement of asphalt can extend the chemosynthetic habitat far beyond the flow source. This is distinct from the ecology of seeps in the Northern Gulf, where tube worms are confined to substrata that have been directly affected by active discharge.

8.5 Fresh Oil and Asphalt at Mictlan

The Mictlan Knoll features asphalt volcanism similar to Chapopote, but with a basal diameter of about 10 km and a crater-like summit over 250 m above the surrounding seabed, it is significantly larger. The asphalt flows remain largely unmapped but cover a very substantial area, including flows that descend from the summit onto the flanks of the feature. In many areas, the asphalt appears much fresher, and liquid oil seeps were observed in numerous locations. Figure 8.5 illustrates how an extrusion of fresh asphalt forms a typical dome of ductile material. Volatile hydrocarbon in the material is a food source for bacteria, which coat the surface. This production supports browsing organisms including *Alvinocaris stactophila* and an undescribed amphipod. Where oil is still fresher, it gives rise to an unusual feature that was dubbed “candles” (Fig. 8.5). These are 50- to 100-cm-tall columns of semiliquid oil coated with white material. Collections demonstrated that the oil within the coatings

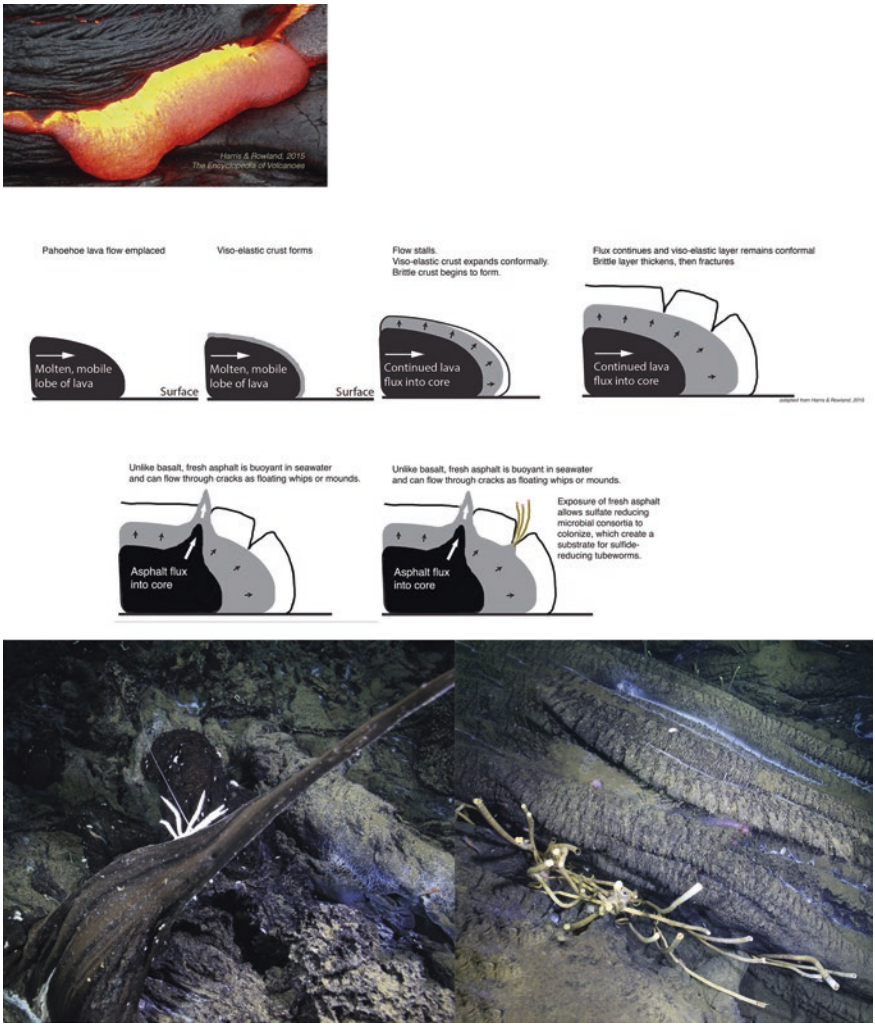

Fig. 8.4 Correspondence of asphalt to basalt lava. Glowing lava extruding from pahoehoe lava flow from Harris and Rowland (2015) (upper). Diagram of pahoehoe lava formation from Harris and Rowland (2015) (second row). Unique features of "pahoehoe asphalt" (third row). Asphalt whip (bottom left). Tube worms, bacteria, and detritus feeders in asphalt fissures (bottom right)

remained liquid, drops of oil were sometimes seen rising from the ends of the "candles," and the water column around the features swarmed with amphipods and other swimmers. Tube worms were thickly colonized with octocoral epibionts. Little else is known about the candle habitat, but its existence demonstrated the variety of ecological outcomes in the Campeche Knolls seep zone.

A second notable feature at the Mictlan site was Hydrate Hill. The impressive feature, described by Sahling et al. (2016), was a mound, with massive gas hydrate

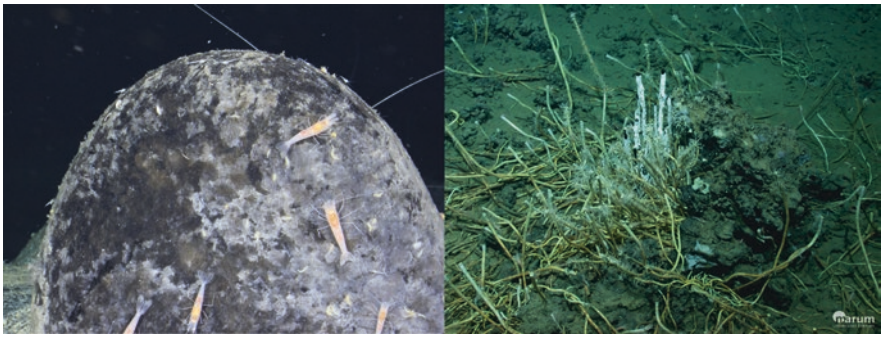

Fig. 8.5 Dome of fresh asphalt with *Alvinocaris* grazing bacteria from surface (left). "Candle" features of bacteria-coated oil. Image on right courtesy of MARUM

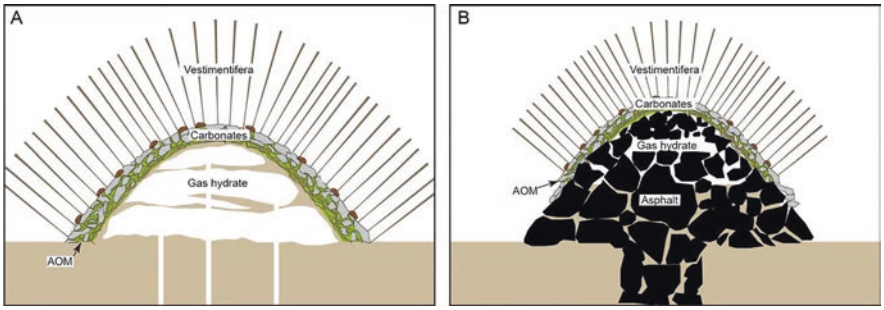

Fig. 8.6 Diagrammatic representation of tube worms colonizing a gas hydrate mound at TYK (**a**) and very large tube worm colony on Hydrate Hill at Mictlan Knoll (**b**) (Sahling et al. 2016)

ledges at its base that rose steeply for 30 m in a subcircular feature about 3 m across entirely covered with 2-m-long tube worms, almost certainly the largest single aggregation of tube worms yet discovered in the Gulf of Mexico. Those authors attributed its formation to the interaction of gas hydrate and carbonate precipitation (Fig. 8.6).

8.6 Gas Seeps and Hydrate at Tsanyao Yang Knoll

With over 400 m of relief above a surrounding seafloor at 3500 m, TYK was the deepest site explored among the Campeche Knolls. Gas seeps were quite active, however, and the extreme depth promoted nearly instantaneous formation of gas hydrate. Seep mussels, cosmopolitan across the Gulf and at seeps worldwide, clustered around actively bubbling sites (Fig. 8.7). However, the rapid formation of

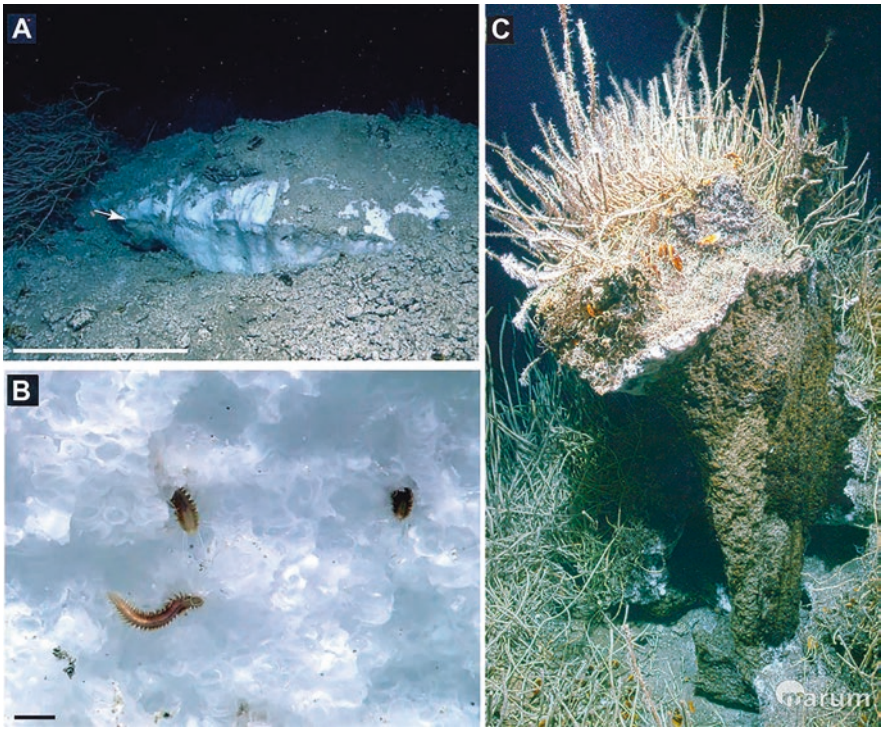

Fig. 8.7 Gas hydrate features at TYK. (**a**) Gas hydrate pingo indicates rapid formation and exhumation. (**b**) Ice worms and burrows on pingo. (**c**) Gas hydrate and oil mixture colonized by seep mussels and tube worms (Sahling et al. 2016)

hydrate and the presence of liquid oil produced remarkable hybrid structures. Gas hydrate ledges formed wherever gas was released. Bubbles would solidify into gas hydrate as they rose in the water, transforming into flakes within seconds. Exposed ledges of gas hydrate preserved a pellet-like fabric and broke through the seafloor like pingos in permafrost (Fig. 8.7a). The ice worm (*Hesiocaeca methanicola*) was commonly observed crawling across the exposed hydrate and entering small burrows that penetrated solid surfaces (Fig. 8.7b). The ice worm was discovered in the Northern Gulf at sites 550 m deep. To find it at TYK demonstrated a remarkable depth range and geographic distribution.

One of the remarkable discoveries at TYK was a ~3-m-high, 10-m-wide mound covered with a dense aggregation of tube worms. One side of the mound had collapsed to reveal the underlying structure (Fig. 8.7c). Gas hydrates displayed a bubble-like fabric seen elsewhere, but at this site the hydrate had mixed with oil or oil had been present in the bubbles when they solidified as gas hydrate. A 1.5-m-high opening led into the interior of the mound, revealing a cave-like section composed almost entirely of gas hydrate. Seep mussels were loosely clustered at the base and among tube worms on the top of the mound. Unlike any tube worm aggregation

previously described, the tube worms were rooted in a loose substratum of fine carbonates and extending into the gas hydrate. Masses of juvenile worms attached in an under layer demonstrated that this was a highly productive setting. No other description of tube worms directly colonizing a gas hydrate surface has been reported. In shallower depths, gas hydrate outcrops tend to be transient structures (Macdonald et al. 1994), unsuitable for slow-growing siboglinid tube worms. At abyssal depths in the southern Gulf, however, gas hydrate remains stable long enough for massive aggregations to recruit, colonize, and thrive. One can speculate that the worms may in fact promote stable preservation of gas hydrate by shielding the surface from dissolution.

8.7 Epifauna from the Campeche Knolls Chemosynthetic Communities

Collections of chemosynthetic and heterotrophic organisms were collected with the ROV arms during Leg M114. Traps and core samples were also used for collections. Many mobile fauna eluded capture and may be provisionally identified from video of photographic evidence. Video and other visual data were instrumental in determining associations of the species with habitat types. A provisional list of associated fauna is given in Table 8.1.

Based on this incomplete sampling, it appears the epifauna of the asphalt and gas hydrate/carbonate habitats are predominately opportunistic grazers, variously feeding on detritus tube worms and mussels, as well as bacterial cells. There is no evidence that the asphalt ecosystem supports a complex food chain with higher predators. Many of the species were cosmopolitan within the habitats—especially the *Munidopsis*, shrimp, fish, and cucumber. Gas seepage produced the most diverse and specialized fauna—mussels, gastropods, ice worms, and ophiuroids. Although visually dramatic, the asphalt ecosystem is a food-limited realm, and the epifauna are limited to direct association with chemosynthetic hosts. This lack of diversity may pose special issues for conservation.

8.8 Research Questions and Resource Protection

The impacts and risks inherent in economic production of oil and gas provide an essential context for exploration and research in the deep-sea Gulf of Mexico. Some 3800 structures are now emplaced across the Northern Gulf, connected with each other and shore-based facilities by over 37,000 km of pipelines. In the southern Gulf, the Cantarell Field is a sprawling complex of platforms, wells, and pipelines located relatively near to shore. However, Mexico plans to expand drilling and production into much deeper regions. Both regions have experienced catastrophic oil spills resulting from loss of well control during exploratory drilling. In the southern

Table 8.1 Fauna collected from Chapopote, Mictlan, and Tsanyao Yang Knolls. Association with substrata is indicated

			Asphalt type			
Common name	Taxon	Fresh-ductile	Whips	Rough	Gas hydrate	Carbonate
Bacteria	Filament bacteria (*Beggiatoa* spp.)	X				
Sponge	–				X	
Soft coral	c.f. Ellisellidae				X	
Tube worms	*Escarpia* sp.	X	X	X	X	X
Ice worm	*Hesiocaeca methanicola*				X	
Mussels	*Bathymodiolus heckere*				X	
Mussels	*Bathymodiolus brooksi*				X	X
Clam	*Abyssogena southwardae*					X
Clam	Lucinidae					X
Snail	Provannidae cf. *Bartia sp*				X	X
Snail	Neritidae				X	X
Snail	Gasteropoda_1					X
Snail	Gasteropoda_2				X	X
Sea cucumber	*Chiridota heheva*	X	X		X	X
Brittle star	*Ophioctenella acies*				X	
Brittle star	*Ophioctenella* sp.				X	
Isopod	Asellota: Janiroidea	X	X		X	
Amphipod	Gammaridae	X	X		X	X
Mysid	Mysidacea	X	X			
Crab	*Munidopsi*s spp.	X	X	X	X	X
Shrimp	*Alvinocaris muricola*	X			X	
Shrimp	*Alvinocaris* cf. *muricola*		X			
Fish	Zoarcidae *Pachycara* sp.	X			X	

Gulf, the Ixtoc 1 spill discharged oil from a site 50 m deep at rates from 10,000 to 30,000 bbl per day for 282 days in 1979 and 1980. Over 87 days in 2010, the *Deepwater Horizon* (DWH) spill discharged approximately 4,000,000 barrels from a site 1500 m deep in the northeastern Gulf. The much greater water depth in which contemporary and planned production transpire underscores the increased challenges of pursuing hydrocarbon production at the outer limits of technology. The Mexican government anticipates deep-sea energy production in association with international energy companies. The asphalt system poses challenges for environmental protection and for exploratory drilling. Consider, for example, the consequences of drilling into one of the very large hydrate mounds. More cryptic challenge might arise if a drill bit encountered a subbottom layer of asphalt—a material almost impossible to drill through with conventional techniques because it binds to the drill bit and closes in when the bit is withdrawn. Lessons from the asphalt ecosystem could serve expansion in the southern Gulf of Mexico by demonstrating its potential hazards as well as its certain beauty.

Acknowledgments We gratefully acknowledge contributions of the German research vessel METEOR, its crew, our colleagues in the MARUM group, University of Bremen, Germany, and especially the late Heiko Sahling, chief scientist. IRM also acknowledges support from the Gulf of Mexico Research Initiative/ECOGIG-2.

References

Abrams MA (2005) Significance of hydrocarbon seepage relative to petroleum generation and entrapment. Mar Pet Geol 22:457–477

Bergquist DC, Ward T, Cordes EE, McNelis T, Howlett S, Kosoff R, Hourdez S, Carney R, Fisher CR (2003) Community structure of vestimentiferan-generated habitat islands from Gulf of Mexico cold seeps. J Exp Mar Biol Ecol 289:197–222

Bern TI, Wahl T, Anderssen T, Olsen R (1993) Oil-spill detection using satellite based SAR – experience from a field experiment. Photogramm Eng Remote Sens 59:423–428

Boetius A, Ravenschlag K, Schubert CJ, Rickert D, Widdel F, Gieseke A, Amann R, Jorgensen BB, Witte U, Pfannkuche O (2000) A marine microbial consortium apparently mediating anaerobic oxidation of methane. Nature 407:623–626

Bohrmann G, Schenck S (2004) GEOMAR cruise report SO 174, OTEGA II, RV 'SONNE', GEOMAR report, Kiel

Brooks JM, Kennicutt MC II, Fisher CR, Macko SA, Cole K, Childress JJ, Bidigare RR, Vetter RD (1987) Deep-sea hydrocarbon seep communities: evidence for energy and nutritional carbon sources. Science 238:1138–1142

Bruening M, Sahling H, MacDonald IR, Ding F, Bohrmann G (2010) Origin, distribution, and alteration of asphalts at Chapopote Knoll, Southern Gulf of Mexico. Mar Pet Geol 27:1093–1106

Carney SL, Formica MI, Divatia H, Nelson K, Fisher CR, Schaeffer SW (2006) Population structure of the mussel "Bathymodiolus" childressi from Gulf of Mexico hydrocarbon seeps. Deep-Sea Res I Oceanogr Res Pap 53:1061–1072

Childress JJ, Fisher CR, Brooks JM, Kennicutt MC II, Bidigare R, Anderson A (1986) A methanotrophic marine mulluscan (Bivalvia, Mytilidae) symbiosis: mussels fueled by gas. Science 233:1306–1308

Cordes EE, Bergquist DC, Fisher CR (2009) Macro-ecology of Gulf of Mexico cold seeps. Annu Rev Mar Sci 1:143–168

De Beukelaer SM, MacDonald IR, Guinnasso NL, Murray JA (2003) Distinct side-scan sonar, RADARSAT SAR, and acoustic profiler signatures of gas and oil seeps on the Gulf of Mexico slope. Geo-Mar Lett 23:177–186

Ding F, Spiess V, Bruening M, Fekete N, Keil H, Bohrmann G (2008) A conceptual model for hydrocarbon accumulation and seepage processes around Chapopote asphalt site, southern Gulf of Mexico: from high resolution seismic point of view. J Geophys Res-Solid Earth 113:B08404

Fisher C, Childress J, Minnich E (1989) Autotrophic carbon fixation by the chemoautotorphic symbionts of Riftia pachyptila. Biol Bull 177:372–385

Fisher CR, Urcuyo I, Simpkins MA, Nix E (1997) Life in the slow lane: growth and longevity of cold-seep vestimentiferans. Mar Ecol 18:83–94

Freytag JK, Girguis PR, Andras JP, Bergquist DC, Fisher CR (1999) Sulfide uptake by buried portions of cold seep vestimentiferans can sustain autotrophic carbon fixation. Eos 80:OS5

Frye M (2008) Preliminary evaluation of in-place gas hydrate resources: Gulf of Mexico outer continental shelf. U.S. Dept. Interior, Minerals Management Service, Resource Evaluation Division OCS report MMS 2008-004, 192 p, appendices

Gardiner SL, McMullin E, Fisher CR (2001) Seepiophila jonesi, a new genus and species of vestimentiferan tube worm (Annelida : Pogonophora) from hydrocarbon seep communities in the Gulf of Mexico. Proc Biol Soc Wash 114:694–707

Gustafson RG, Turner RD, Lutz RA, Vrijenhoek RC (1998) A new genus and five new species of mussels (Bivalvia, Mytilidae) from deep-sea sulfide/hydrocarbon seeps in the Gulf of Mexico. Malacologia 40:63–112

Harris AJL, Rowland SK (2015) Chapter 17 – Lava flows and rheology. In: Sigurdsson H (ed) The encyclopedia of volcanoes, 2nd edn. Academic Press, Amsterdam, pp 321–342

Kaiser MJ (2011) Economic limit of outer continental shelf Gulf of Mexico structure production. Appl Energy 88:2490–2508

Kennicutt MC, Brooks JM, Bidigare RR, Fay RR, Wade TL, McDonald TT (1985) Vent-type taxa in a hydrocarbon seep region on the Louisiana Slope. Nature 317:351–353

MacAvoy SE, Carney RS, Fisher CR, Macko SA (2002) Use of chemosynthetic biomass by large, mobile, benthic predators in the Gulf of Mexico. Mar Ecol Prog Ser 225:65–78

MacDonald IR, Reilly JF II, Guinasso JRNL, Brooks JM, Carney RS, Bryant WA, Bright TJ (1990) Chemosynthetic mussels at a brine-filled pockmark in the northern Gulf of Mexico. Science 248:1096–1099

MacDonald I, Guinasso N, Ackleson S, Amos J, Duckworth R, Sassen R, Brooks J (1993) Natural oil-slicks in the Gulf of Mexico visible from space. J Geophys Res Oceans 98:16351–16364

Macdonald IR, Guinasso NL, Sassen R, Brooks JM, Lee L, Scott KT (1994) Gas hydrate that breaches the sea-floor on the continental-slope of the Gulf-of-Mexico. Geology 22:699–702

MacDonald IR, Bohrmann G, Escobar E, Abegg F, Blanchon P, Blinova V, Brückmann W, Drews M, Eisenhauer A, Han X, Heeschen K, Meier F, Mortera C, Naehr T, Orcutt B, Bernard B, Brooks J, de Faragó M (2004) Asphalt volcanism and chemosynthetic life, Campeche Knolls, Gulf of Mexico. Science 304:999–1002

MacDonald IR, Garcia-Pineda O, Beet A, Daneshgar Asl S, Feng L, Graettinger G, French-McCay D, Holmes J, Hu C, Huffer F (2015) Natural and unnatural oil slicks in the Gulf of Mexico. J Geophys Res Oceans 120:8364–8380

Marcon Y, Sahling H, Bohrmann G (2013) LAPM: a tool for underwater large-area photo-mosaicking. Geosci Instrum Methods Data Syst 2:189–198

Marcon Y, Sahling H, MacDonald IR, Wintersteller P, dos Santos Ferreira C, Bohrmann G (2018) Slow volcanoes: the intriguing similarities between marine asphalt and basalt lavas. Oceanography 31. https://doi.org/10.5670/oceanog.2018.202

Milkov AV (2000) Worldwide distribution of submarine mud volcanoes and associated gas hydrates. Mar Geol 167:29–42

Minerals Management Service (MMS) (1988) Implementation of measures to detect and protect deep water chemosynthetic communities. MMS Gulf of Mexico Regional OCS Office. Gulf of Mexico Regional OCS Office

Reilly JF, MacDonald IR, Biegert EK, Brooks JM (1996) Geologic controls on the distribution of chemosynthetic communities in the Gulf of Mexico. In: Schumacher D, Abrams MA (eds) Hydrocarbon migration and its near-surface expression. American Association of Petroleum Geologists, Tulsa, pp 38–61

Roberts H, Boland G (2010) Gulf of Mexico cold seeps: preface. Deep-Sea Res II Top Stud Oceanogr 57:1835–1837

Roberts HH, Carney RS (1997) Evidence of episodic fluid, gas, and sediment venting on the northern Gulf of Mexico continental slope. Econ Geol Bull Soc Econ Geol 92:863–879

Roberts HH, Feng D (2013) Carbonate precipitation at Gulf of Mexico hydrocarbon seeps: an overview. In: Abrams M, Aminzadeh F, Berge T, Connolly D, O'Brien G (eds) Hydrocarbon seepage: from source to surface. Society of Exploration Geophysicists and American Assocation of Petroleum Geologists

Roberts HH, Feng D, Joye SB (2010) Cold-seep carbonates of the middle and lower continental slope, northern Gulf of Mexico. Deep-Sea Res II Top Stud Oceanogr 57:2040–2054

Sahling H, Borowski C, Escobar-Briones E, Gaytan-Caballero A, Hsu CW, Loher M, MacDonald I, Marcon Y, Pape T, Romer M, Rubin-Blum M, Schubotz F, Smrzka D, Wegener G, Bohrmann G (2016) Massive asphalt deposits, oil seepage, and gas venting support abundant chemosynthetic communities at the Campeche Knolls, southern Gulf of Mexico. Biogeosciences 13:4491–4512

Wood W, Ruppel C (2000) Seismic and thermal investigations of hydrate bearing sediments on the Blake Ridge Crest: a synthesis of ODP Leg 164 results. Proc Ocean Drill Program Sci Results 164:253–264

Chapter 9
Geochemical and Faunal Characterization in the Sediments off the Cuban North and Northwest Coast

Maickel Armenteros, Patrick T. Schwing, Rebekka A. Larson, Misael Díaz-Asencio, Adrian Martínez-Suárez, Raúl Fernández-Garcés, David J. Hollander, and Gregg R. Brooks

Abstract This chapter provides a summary of the scientific knowledge about sediments and fauna in the margin of northwest Cuban shelf. Little scientific information is publicly available, and so much of what is discussed here is the result of the scientific expedition to the region in May 2017 on board the *R/V Weatherbird II* as part of the GoMRI consortium, C-IMAGE (see Foreword, this book). The goal was to set broad environmental baselines against which to evaluate the impacts of any potential future oil spill or other disturbance in the Gulf of Mexico (GoM). The chapter is organized in three parts: (1) overview of the geographical setting of Cuban margin of GoM; (2) sediment characterization including texture, composition, and geochronology of sediment cores; and (3) characterization of key bioindicators of oil impact: mollusks, meiofauna, and foraminifera.

M. Armenteros (✉) · A. Martínez-Suárez · R. Fernández-Garcés
Universidad de La Habana, Centro de Investigaciones Marinas, Havana, Cuba
e-mail: maickel.armenteros@gmail.com; adrian@cim.uh.cu

P. T. Schwing
University of South Florida, College of Marine Science, St. Petersburg, FL, USA

Eckerd College, St. Petersburg, FL, USA
e-mail: pschwing@mail.usf.edu

R. A. Larson · G. R. Brooks
Eckerd College, St. Petersburg, FL, USA
e-mail: larsonra@eckerd.edu; brooksgr@eckerd.edu

M. Díaz-Asencio
Centro de Investigación Científica y de Educación Superior de Ensenada, Ensenada, Baja California, Mexico

Centro de Estudios Ambientales de Cienfuegos, Cienfuegos, Cuba

D. J. Hollander
University of South Florida, College of Marine Science, St. Petersburg, FL, USA
e-mail: davidh@usf.edu

S. A. Murawski et al. (eds.), *Scenarios and Responses to Future Deep Oil Spills*,
https://doi.org/10.1007/978-3-030-12963-7_9

Keywords Baseline · Sediments · Geochemistry · Mollusk · Meiofauna · Foraminifera · Cuba

9.1 Introduction

This chapter provides a summary of the scientific knowledge about sediments and fauna in the margin of northwest Cuban shelf. Little scientific information is publicly available, and so much of what is discussed here is the result of the scientific expedition to the region in May 2017 on board the *R/V Weatherbird II* as part of the GoMRI consortium, C-IMAGE (see Foreword, this book). The goal was to set broad environmental baselines against which to evaluate the impacts of any potential future oil spill or other disturbance in the Gulf of Mexico (GoM). The chapter is organized in three parts: (1) overview of the geographical setting of Cuban margin of GoM; (2) sediment characterization including texture, composition, and geochronology of sediment cores; and (3) characterization of key bioindicators of oil impact: mollusks, meiofauna, and foraminifera.

9.2 Geographical Setting and Sampling

Cuba constitutes the southeast limit of the Gulf of Mexico (GoM) and determines the connection of this large marine ecosystem with the Caribbean Sea through the Yucatan Straits and with the North Atlantic Ocean through the Florida Straits. The northwestern region of Cuban island is the terrestrial border of the Cuban GoM and is characterized by a relatively narrow shelf. The Cuban margin is essentially different from the other borders of the south GoM which are bordered by the extensive shallow banks of Campeche to the west and Florida shelf to the north (Locker and Hine 2020). As result of the *R/V Weatherbird II* expedition to northwest Cuba, thirteen sites were sampled along eight transects (SL37 to SL44) using a multicorer between 316 and 1670 m depth (Table 9.1 and Fig. 9.1). Transects included sites at several nominal depths (300, 500, 1000, and 1500 m), but the steep slope of the margin and the scant amount of deposited sediments limited our successful retrieval of cores to only those at the deeper sites (usually 1000 and 1500 m).

9.3 Sediment Characterization

Sediment cores analyzed for sediment texture, composition, and short-lived radioisotope chronologies reflected the spatial and temporal variability in sedimentation patterns offshore of northwest Cuba (Table 9.1 and Fig. 9.1). Sediment texture, represented as % gravel, % sand, % silt, and % clay, generally reflects energy related

Table 9.1 The sampling sites off NW coast of Cuba sampled during the expedition of R/V Weatherbird II

Site code[a]	Location	Latitude (N)	Longitude (W)	Depth (m)	Cores retrieved (analyzed)
SL 37-250	San Antonio Cape	22 09.068	84 49.579	530	
SL 37-500	San Antonio Cape	22 11.094	84 52.245	1209	7(3)
SL 38-750	Gulf of Guanahacabibes	22 28.735	84 41.568	1670	11(5)
SL 39-750	Jutía Key	22 48.324	84 06.538	1296	14(6)
SL 40-750	Levisa Key	23 00.151	83 40.771	1580	16(6)
SL 41-750	Honda Bay	23 05.135	83 11.824	1513	15(6)
SL 41-500	Honda Bay	23 02.263	83 11.240	974	3(3)
SL 42-500	Cabañas Bay	23 03.703	82 58.732	1156	9(5)
SL 42-750	Cabañas Bay	23 05.849	82 59.035	1420	14(6)
SL 43-750	Mariel Bay	23 07.735	82 43.916	1535	15(6)
SL 44-150	Havana Bay	23 09.388	82 22.132	316	8(4)
SL 44-500	Havana Bay	23 11.799	82 21.067	970	8(4)
SL 44-750	Havana Bay	23 14.373	82 20.357	1430	15(6)

[a]Codes from Weatherbird II expedition. SL labels were removed from the text for simplicity

to sediment deposition (Folk 1965). Sediment composition, represented as % carbonate, % total organic matter (TOM), and % other (non-carbonate, nonorganic), indicates sediment source(s) with carbonate sediments reflecting marine source, organic matter reflecting biological productivity and/or terrestrial runoff, and the remaining fraction (% other) reflecting a terrigenous source (Milliman 1974). Short-lived radioisotope chronologies using excess ^{210}Pb ($^{210}Pb_{xs}$) provide age control and mass accumulation rates (MAR) to determine the timing of changes in deposition over the past ~100 years (Binford 1990; Swarzenski 2014). Cores were subsampled at 0.2 cm resolution (Schwing et al. 2016) and analyzed to determine baseline sedimentation patterns for northwest Cuba. This allows to compare with studies which describe the sedimentary impacts of the *Deepwater Horizon* (DWH) oil spill in the northern Gulf of Mexico (Brooks et al. 2015; Schwing et al. 2017a).

In the western portion of the study area (sites 37-250 and 38-750), sediments were dominantly carbonate (95–98%) and silts (82–95%) and have been consistently accumulating, with little to no variability over the past ~100 years (Fig. 9.2). The $^{210}Pb_{xs}$ chronology for site 37-250 dated 1900 at 14 cm downcore with an average MAR of 0.125 g cm^{-2} yr^{-1}. The $^{210}Pb_{xs}$ chronology for site 38-750 dated 1900 at 3.5 cm downcore with an average MAR of 0.027 g cm^{-2} yr^{-1}. This stable sedimentation pattern reflected the low-disturbed nature of the coastal region adjacent to these sites. The higher MAR at site 37-250 was likely due to exportation of sediments from the nearby Gulf of Guanahacabibes.

In the central portion of northwest Cuba, from Jutía Key (site 39-750) to Mariel Bay (site 43-750), sediments were still dominantly carbonate (78–92%) and silts (44–89%) but exhibited more variability over the past ~100 years (Fig. 9.3). There was an increase in accumulation of terrigenous sediments offshore of this region,

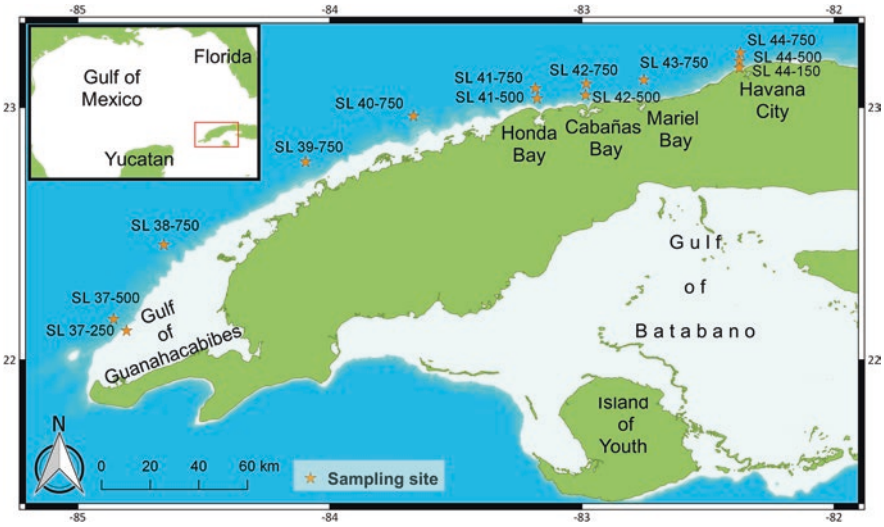

Fig. 9.1 Map of the NW region. The 13 sites sampled during Weatherbird II expedition in the shelf margin are indicated with starts

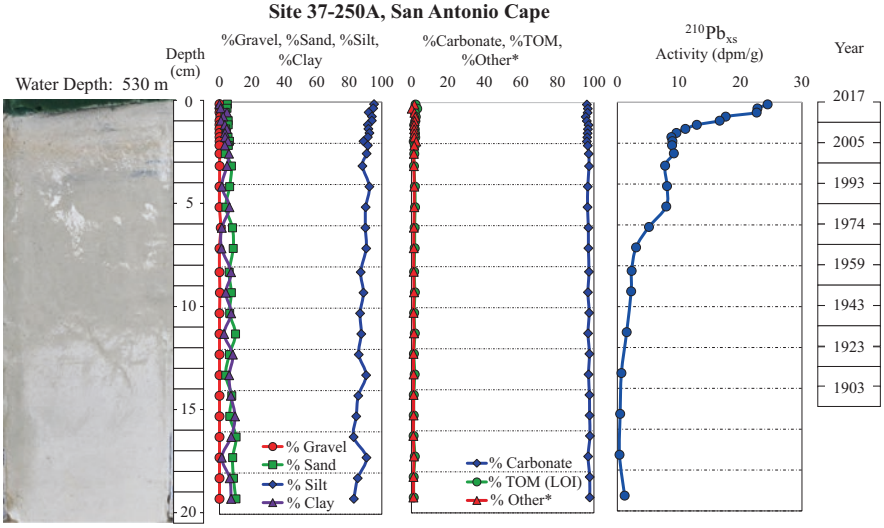

Fig. 9.2 Sediment core log for site 37-250 in the western portion of the study area, showing core photograph, sediment texture, sediment composition, 210Pbxs profile, and 210Pbxs chronology. Note the stable consistent sedimentation of carbonate silt over the past ~100 years

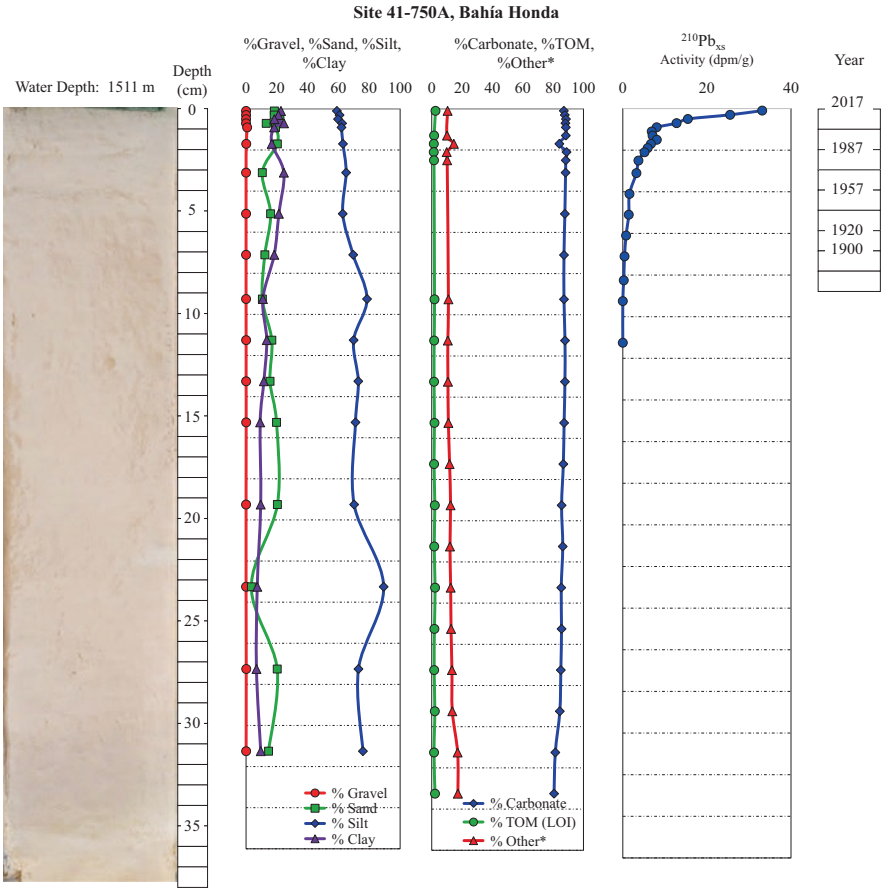

Fig. 9.3 Sediment core log for site 41-750 in the central portion of the study area, showing core photograph, sediment texture, sediment composition, 210Pbxs profile, and 210Pbxs chronology. Note the decrease in % silt upcore with no changes in composition over the past ~100 years

potentially associated with coastal anthropogenic activities and/or export from the adjacent bays (Honda, Cabañas, and Mariel). With the exception of site 39-750 (offshore Jutía Key), $^{210}Pb_{xs}$ chronologies were comparable to sites to the west, with dating the year 1900 for site 40-750 at 6 cm, site 41-750 at 6.5 cm, site 42-500 at 6 cm, site 42-750 at 4.5 cm, and site 43-750 at 5.5 cm depth downcore. MARs for these sites were also similar with site 40-750 at 0.034 g cm^{-2} yr^{-1}, site 41-750 at 0.045 g cm^{-2} yr^{-1}, site 42-500 at 0.052 g cm^{-2} yr^{-1}, site 42-750 at 0.032 g cm^{-2} yr^{-1}, and site 43-750 at 0.049 g cm^{-2} yr^{-1}. Site 39-750 had the deepest $^{210}Pb_{xs}$ profile (12.5 cm) and highest MAR of 0.112 g cm^{-2} yr^{-1} for this portion of northwest Cuba. Site 39-750 also showed a shift in sedimentation patterns over the top 0–1 cm with an increase in sand content from ~10% to 50%, concurrent with a decrease in silt

content from 80% to 45%. This recent shift in sedimentation pattern was present in all other cores in this portion of the study area, although magnitudes were generally lower. There were no detectable changes in sediment composition (% carbonate, % TOM, % other) indicating no significant changes in sediment source(s).

The eastern portion of the northwest Cuba resided offshore Havana Bay with sites 44-150, 44-500, and 44-750. Sediments were the most variable in this region with % carbonate for site 44-150 ranging from 50% to 75%, site 44-500 ranging from 28% to 50%, and site 44-750 ranging from 39% to 86% (Fig. 9.4). Sediment

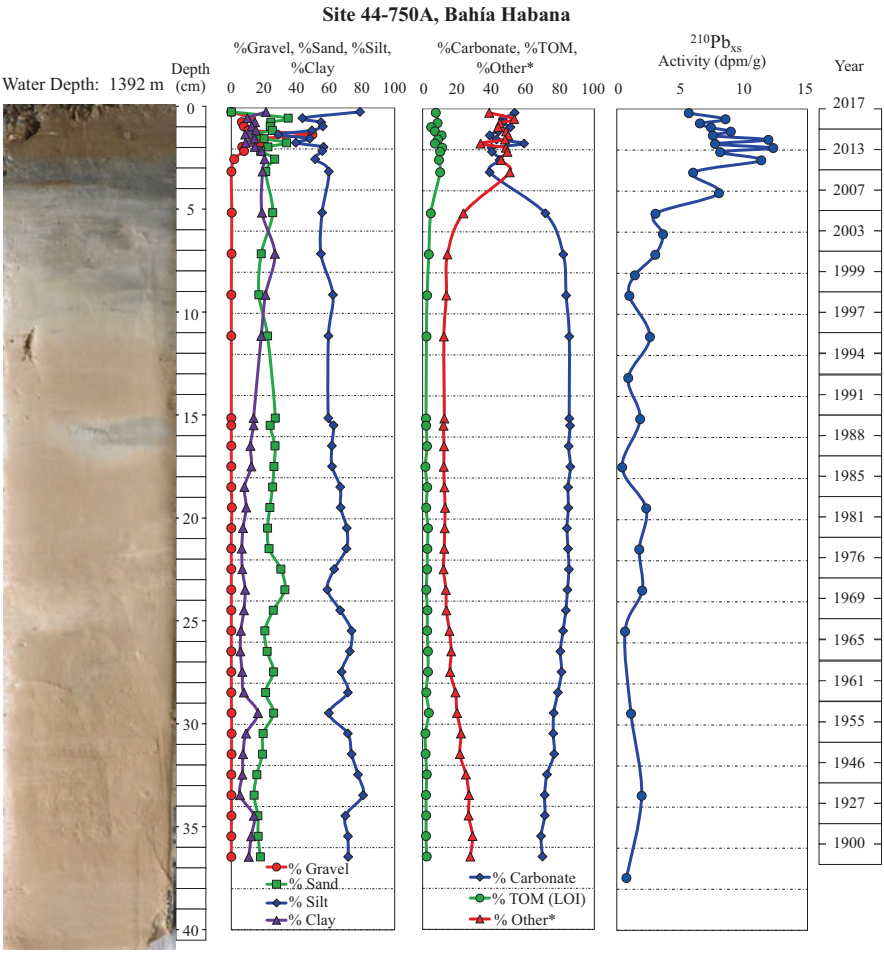

Fig. 9.4 Sediment core log for site 44-750 in the eastern portion of the study area, showing core photograph, sediment texture, sediment composition, 210Pbxs profile, and 210Pbxs chronology. Note the shifts in both sediment texture and composition in the recent portion of the sediment record

texture was also variable and coarser than the regions to the west, particularly with increased % gravel (0–50%), % sand (0–51%), and % silt (29–81%). This region also had the most variability in composition over the past ~100 years, with the highest % terrigenous (12–63%) and TOM (2–11%) indicating changes in sedimentation patterns and sources. $^{210}Pb_{xs}$ chronologies were also distinctly different from the western and central regions of northwest Cuba, with site 44-150 dating 1900 at 19.0 cm, site 44-500 at 11.5 cm, and site 44-750 at 35.5 cm depth downcore. MARs for these sites were also higher, with site 44-150 at 0.229 g cm^{-2} yr^{-1}, site 44-500 at 0.111 g cm^{-2} yr^{-1}, and site 44-750 at 0.405 g cm^{-2} yr^{-1}. These MARs were coherent with those estimated inside Havana Bay (0.04-0.38 g cm^{-2} yr^{-1}) before 1900 (Diaz-Asencio et al. 2011). The higher sedimentation rates and increased variability in sedimentation patterns over the past ~100 years may be attributed to the close proximity to terrigenous sediment sources (narrow shelf), as well as potential changes in anthropogenic activities and influences on sediment input and distribution (Diaz-Asencio et al. 2011).

9.4 Fauna Communities

9.4.1 Mollusks

The decline in species richness is one of the most powerful indicators of environmental impact (Armenteros et al. 2016). The northwest Cuban margin harbors a diverse mollusk assemblage constituted by 129 species. Eleven species of pteropods (families Cavolinidae and Peraclididae) occurred in all the sites and in most of the samples in high dominance: *Cavolinia inflexa*, *Creseis acicula*, *Creseis virgule*, *Diacavolinia deblainvillei*, *D. deshayesi*, *Limacina bulimoides*, *L. inflata*, *L. lesueurii*, *L. trochiformis*, *Peracle reticulata*, and *Styliola subula.* Four species of heteropods (family Atlantidae) were also broadly distributed across northwest Cuban margin: *Atlanta inclinata*, *A. peroni*, *Oxygyrus keraudrenii*, and *Protatlanta souleyeti* (Fig. 9.5). These pelagic species were likely broadly dispersed by currents and deposited on the seabed at death. Thus, they have limited importance as a proxy for sediment quality although they may indicate potential impacts in the water column. *Benthonella gaza* was the only benthic species broadly distributed (Fig. 9.5). Fifty-seven other species were rare, occurring in one sample (43 species) or two samples (14 species). The decline of the bulk of rare species is another indicator of potential impact and can be used to assess environmental health.

Species richness varied significantly among sites from 40 species at 42-750 (off Cabañas Bay) to 80 species at 40-750 (off Levisa Key) (Fig. 9.6a). Coastal mollusk species were well-represented in Mantua, Bahía Honda, and Mariel suggesting considerable transport of sediment offshore due to coastal circulation. Another anthro-

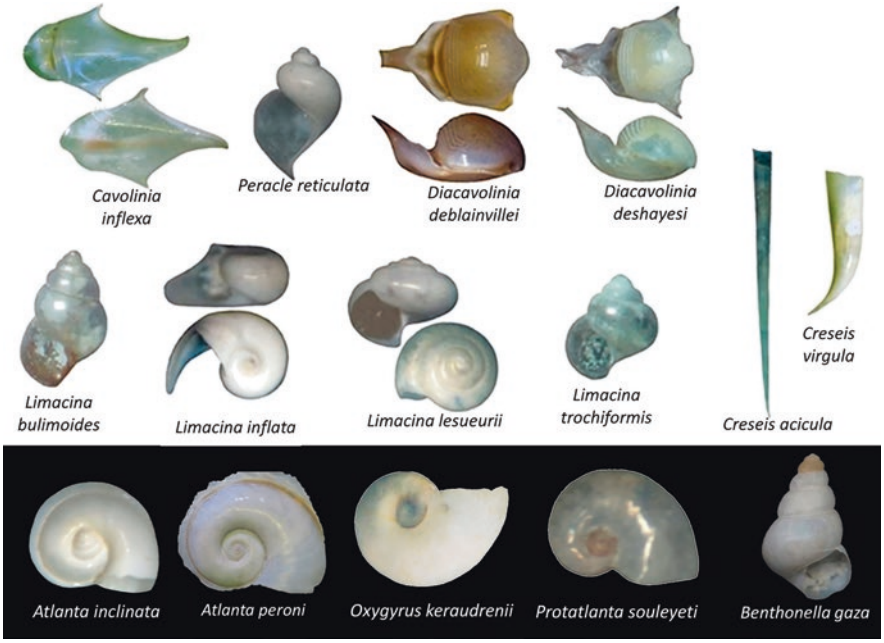

Fig. 9.5 The most broadly distributed species of mollusks from nine sites of the Cuban margin of GoM. Pelagic pteropods (families Cavolinidae and Peraclididae) in white background and pelagic heteropods (family Atlantidae) in black background. Note also to the single broad-distributed benthic species *Benthonella gaza* at bottom right corner

pogenic activity that may be responsible for the occurrence of coastal species in the deep-sea margin is the dumping of dredging material from nearby ports such as Santa Lucia (near to Jutía key) and Mariel (Fig. 9.6b).

9.4.2 Meiofauna

Meiofauna constitute one of the most used biological proxies for anthropogenic impact due to (i) relatively low dispersal capacity allowing the assessment of local impacts, (ii) high diversity represented by many species with different life histories (e.g., differential sensitivity to specific impacts), and (iii) tight association with sediment condition. Nematoda and Copepoda were the dominant groups of the meiofauna contributing to 66% and 12%, respectively, of the total abundance in the Cuban GoM; Halacaroidea and Foraminifera were also important (Fig. 9.7a). The meiofauna median density in the Cuban margin was 3.6 individuals/10 cm^{-2} (range 0–7 ind./10 cm^{-2}). This is one of the lowest values of meiofauna density ever reported for deep-sea environments in GoM (e.g., Baguley et al. 2006). Average estimates of meiofauna abundance in coastal habitats from northwest Cuban region

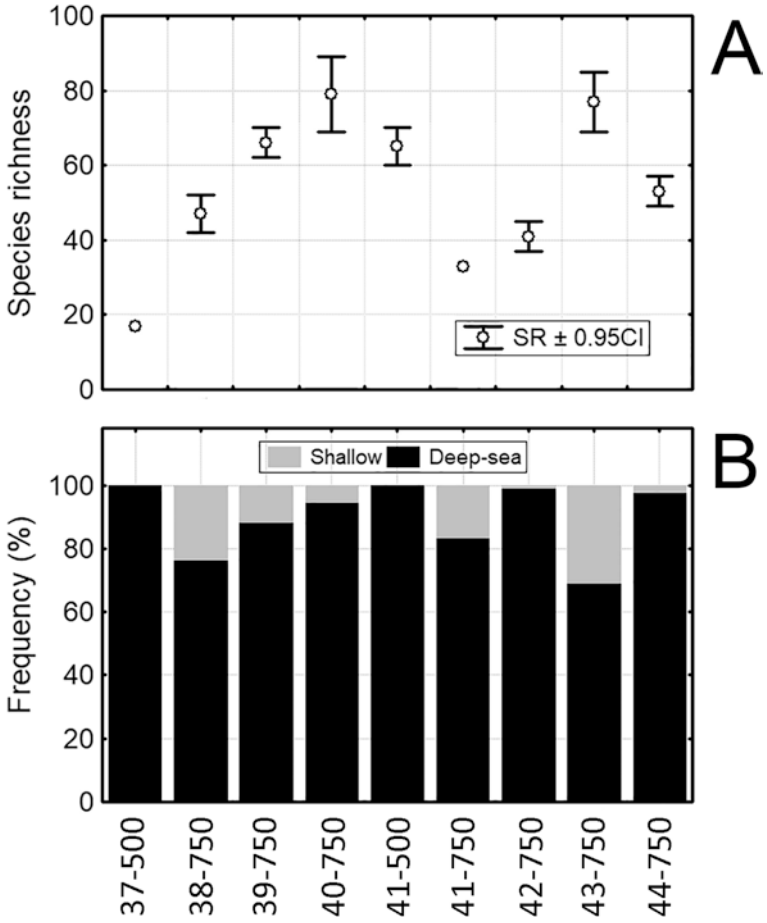

Fig. 9.6 Mollusks from nine sites of the Cuban margin of GoM. (**a**) The species richness with associated 0.95 confidence intervals (CI). (**b**) The frequency of shallow versus deepwater mollusk species

have been considerably higher (Armenteros et al. 2007, 2009): 24 ± 11 ind./10 cm^{-2} in mangroves, 148 ± 41 ind./10 cm^{-2} in seagrass meadows, and 243 ± 47 ind./10 cm^{-2} in spur and groove formations within coral reefs. The low abundance in deeper waters from the northwest Cuban margin is most likely caused by a combination of oligotrophic conditions in sediments and physical disturbance by water flows. The apparently natural low density considerably limits the use of meiofauna for environmental analysis since depletion in abundance is one of the main indicators of disturbance. Species composition of free-living nematodes, the most abundant taxon of meiofauna, could offer a potential baseline, but the analysis is still in progress.

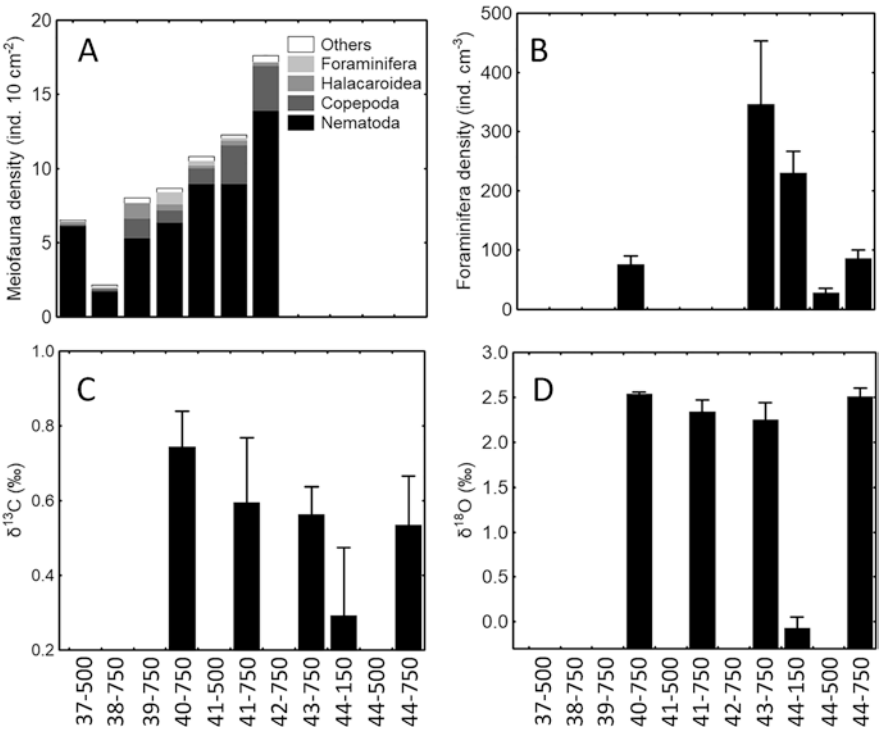

Fig. 9.7 Meiofauna in sampling sites of the Cuban margin of GoM. (**a**) Meiofauna (higher taxa). (**b**) Mean benthic foraminifera density (individuals/cm^{-3}). (**c**) Stable carbon (δ13C) isotope composition of benthic foraminiferal calcite. (**d**) Oxygen (δ18O) isotope composition of benthic foraminiferal calcite. Uncertainties are reported as standard deviation

9.4.3 Foraminifera

Benthic foraminifera density, diversity, and stable isotope composition have proven to be useful tools for assessment of impact, response, and recovery of the benthos in the event of an oil spill (Morvan et al. 2004; Lei et al. 2015; Schwing et al. 2015, 2017b; Schwing et al. 2018a, b). Cores collected at sites 44-150 (Havana Bay), 44-500, 44-750, 43-750 (Mariel Bay), 41-750 (Honda Bay), and 40-750 (Levisa Key) were analyzed for these variables to provide baseline measurements in advance of future perturbations.

The number of foraminifera species in the northwest Cuban margin was 261. Along the outer shelf (~300 m water depth), *Cassidulina* spp. was the predominant taxa. At sites ranging from 970 to 1590 m water depth, *Bolivina* spp. was predominant. *Bolivin*a spp. are widely abundant throughout the GoM continental slope

(Denne and Sen Gupta 1991). The total benthic foraminiferal density was highly variable and generally high relative to other regions within the GoM (Schwing et al. 2020) with a mean density of 163 ± 158 individuals/cm^{-3} (range 76–346 ind./cm^{-3}) (Fig. 9.7b).

The stable carbon isotope composition ($\delta^{13}C$) of benthic foraminiferal calcite was also highly variable between sites (mean 0.54‰ ± 0.51‰) and generally increased from near Havana Bay (44-150, 0.29‰; 44-750, 0.53‰) to the west (40-750, 0.7‰) (Fig. 9.7c). $\delta^{13}C$ was within natural variability throughout the northern and southern Gulf of Mexico continental shelf and slope (0.69‰ ± 0.46‰) (Schwing et al. 2020). However, the east-to-west enrichment is consistent with a decreasing terrigenous carbon source with distance from population centers such as Havana.

The mean stable oxygen isotope composition $\delta^{18}O$ (‰) of benthic foraminiferal calcite was 1.71‰ ± 0.13‰. $\delta^{18}O$ in the Cuban margin was generally higher than the northern (1.31‰ ± 0.08‰) and southern (0.73‰ ± 0.05‰) Gulf of Mexico. $\delta^{18}O$ varied primarily with water depth, which was likely due to changes in salinity (water mass) and proximity to sources of freshwater runoff. For example, a site near Havana Bay was depleted (44-150, −0.1‰) in contrast to sites farther offshore, which ranged from 0.22‰ to 0.25‰ (Fig. 9.7d).

9.5 Conclusions

In conclusion, offshore the northwest Cuban coast, there was a west-to-east sedimentation pattern as reflected by sediment texture, composition, MAR, and $\delta^{13}C$ of benthic foraminiferal calcite. This sedimentation pattern was likely caused by the combined increase of natural terrigenous influence and anthropogenic activities, which changed from west (almost pristine) to east (semi-enclosed bays with human development). Mollusk assemblages were dominated by relatively few pelagic species that distributed broadly along northwest margin suggesting strong connectivity due to oceanographic regime. Pelagic and coastal shells conformed large part of mollusk assemblages indicating deposition from both the water column and coastal sites.

Funding Information This research was made possible by grants from The Gulf of Mexico Research Initiative through its consortia: The Center for the Integrated Modeling and Analysis of the Gulf Ecosystem (C-IMAGE). Data are publicly available through the Gulf of Mexico Research Initiative Information and Data Cooperative (GRIIDC) at https://data.gulfresearchinitiative.org. Digital Object Identification (DOIs) for the databases presented in this chapter: core photographs (10.7266/n7-3vmj-nk86), bulk density/porewater (10.7266/n7-4pg2-4755), sediment texture and composition (10.7266/n7-58a1-b761), short-lived radioisotope analyses (10.7266/n7-78ae-7m58), mollusks and meiofauna (10.7266/n7-88ne-3229), foraminifera (10.7266/n7-e90r-1v29), and stable isotopes (10.7266/n7-repn-q515).

References

Armenteros M, Williams JP, Hidalgo G, González-Sansón G (2007) Community structure of meio- and macrofauna in seagrass meadows and mangroves from NW shelf of Cuba (Gulf of Mexico). Revista de Investigaciones Marinas. Universidad de La Habana 28:139–150

Armenteros M, Creagh B, González-Sansón G (2009) Distribution patterns of the meiofauna in coral reefs from the NW shelf of Cuba. Revista de Investigaciones Marinas. Universidad de La Habana 30:37–43

Armenteros M, Díaz-Asencio M, Fernández-Garcés R, Alonso-Hernández C, Helguera-Pedraza Y, Bolaños-Alvarez Y, Agraz-Hernández C, Sanchez-Cabeza JA (2016) One-century decline of mollusk diversity as consequence of accumulative anthropogenic disturbance in a tropical estuary (Cuban Archipelago). Mar Pollut Bull 113:224–231

Baguley JG, Montagna PA, Hyde LJ, Kalke RD, Rowe GT (2006) Metazoan meiofauna abundance in relation to environmental variables in the northern Gulf of Mexico deep sea. Deep-Sea Res I 53:1344–1362

Binford MW (1990) Calculation and uncertainty analysis of ^{210}Pb Dates for PIRLA Project Lake sediment cores. J Paleolimnol 3:253–267

Brooks GR, Larson RA, Schwing PT, Romero I, Moore C, Reichart GJ, Jilbert T, Chanton JP, Hastings DW, Overholt WA, Marks KP, Kostka JE, Holmes CW, Hollander D (2015) Sediment pulse in the NE Gulf of Mexico following the 2010 DWH blowout. PLoS One 10:e0132341

Denne RA, Sen Gupta BK (1991) Association of bathyal foraminifera with water masses in the northwestern Gulf of Mexico. Mar Micropaleontol 17:173–193

Díaz-Asencio M, Alvarado JAC, Alonso-Hernández C, Quejido-Cabezas A, Ruiz-Fernández AC, Sanchez-Sanchez M, Gómez-Mancebo MB, Froidevaux P, Sanchez-Cabeza JA (2011) Reconstruction of metal pollution and recent sedimentation processes in Havana Bay (Cuba): a tool for coastal ecosystem management. J Hazard Mater 196:402–411

Folk RL (1965) Petrology of sedimentary rocks. Hemphillis, Austin

Lei YL, Li TG, Bi H, Cui WL, Song WP, Li CC (2015) Responses of benthic foraminifera to the 2011 oil spill in the Bohai Sea, PR China. Mar Pollut Bull 96:245–260

Locker S, Hine AC (2020) An overview of the geologic origins of hydrocarbons and production trends in the Gulf of Mexico (Chap. 4). In: Murawski SA, Ainsworth C, Gilbert S, Hollander D, Paris CB, Schlüter M, Wetzel D (eds) Scenarios and responses to future deep oil spills – fighting the next war. Springer, Cham

Milliman JD (1974) Marine carbonates. Springer, New York

Morvan J, Le Cadre V, Jorissen FJ, Debenay J (2004) Foraminifera as potential bio-indicators of the "Erika" oil spill in the Bay of Bourgneuf: field and experimental studies. Aquat Living Resour 17:317–322

Schwing PT, Romero IC, Brooks GR, Hastings DW, Larson RA, Hollander DJ (2015) A decline in deep-sea benthic foraminifera following the Deepwater Horizon event in the northeastern Gulf of Mexico. PLoS One 10:e0120565

Schwing PT, Romero IC, Larson RA, O'Malley BJ, Fridrik EE, Goddard EA, Brooks GR, Hastings DW, Rosenheim BE, Hollander DJ, Grant G, Mulhollan J (2016) Sediment core extrusion method at millimeter resolution using a calibrated threaded-rod. J Vis Exp 114:e54363

Schwing PT, Brooks GR, Larson RA, Holmes CE, O'Malley BJ, Hollander DJ (2017a) Constraining the spatial extent of the marine oil snow sedimentation and accumulation (MOSSFA) following the DWH event using a $^{210}Pb_{xs}$ inventory approach. Environ Sci Technol 51:5962–5968

Schwing PT, O'Malley BJ, Romero IC, Martinez-Colon M, Hastings DW, Glabach MA, Hladky E, Greco A, Hollander DJ (2017b) Characterizing the variability of benthic foraminifera in the northeastern Gulf of Mexico following the Deepwater Horizon event (2010–2012). Environ Sci Pollut Res 24:2754–2769

Schwing PT, O'Malley BJ, Hollander DJ (2018a) Resilience of benthic foraminifera in the northern Gulf of Mexico following the Deepwater Horizon event (2011–2015). Ecol Indic 84:753–764

Schwing PT, Chanton JP, Hollander DJ, Goddard EA, Brooks GR, Larson RA (2018b) Tracing the incorporation of petroleum carbon into benthic foraminiferal calcite following the Deepwater Horizon event. Environ Pollut 237:424–429

Schwing PT, Montagna PA, Machain-Castillo ML, Escobar-Briones E, Rohal M (2020) Benthic faunal baselines in the Gulf of Mexico: a precursor to evaluate future impacts (Chap. 6). In: Murawski SA, Ainsworth C, Gilbert S, Hollander D, Paris CB, Schlüter M, Wetzel D (eds) Scenarios and responses to future deep oil spills – fighting the next war. Springer, Cham

Swarzenski PW (2014) ^{210}Pb dating. In: Encyclopedia of scientific dating methods. Springer, Dordrecht

Chapter 10
Mapping Isotopic and Dissolved Organic Matter Baselines in Waters and Sediments of the Gulf of Mexico

Jeffrey P. Chanton, Aprami Jaggi, Jagoš R. Radović, Brad E. Rosenheim, Brett D. Walker, Stephen R. Larter, Kelsey Rogers, Samantha Bosman, and Thomas B. P. Oldenburg

Abstract The *Deepwater Horizon* oil spill released petroleum hydrocarbons that were depleted in $\delta^{13}C$ and $\Delta^{14}C$ at depth into the Gulf of Mexico. Stable-carbon and radiocarbon isotopic values and high-resolution mass spectrometry were used to follow the distributions of this petroleum and to track its transformation into petrocarbon, a term used to describe crude oil or transformed crude oil following biodegradation, weathering, oxygenation, or loss of lighter components. The term petrocarbon includes oil- or methane-derived carbon assimilated or incorporated into microbial biomass or into the food web as well as degraded and undegraded petroleum constituents. Here we report (1) the increase in the relative abundance of oxygen-containing carbon compounds making up the dissolved organic matter (DOM) with increasing depth through the water column, indicating the biodegradation of DOM as it was transported to depth in the water column, (2) the finding of ^{14}C depletion in DOM indicating petrocarbon inputs, and (3) the decrease and subsequent increase of ^{14}C in the isotopic composition of sinking particles indicating the capture of petrocarbon in sediment traps. In addition, we discuss the ^{14}C depletion of

J. P. Chanton (✉) · K. Rogers · S. Bosman
Florida State University, Department of Earth, Ocean and Atmospheric Science, Tallahassee, FL, USA
e-mail: jchanton@fsu.edu; klrogers@fsu.edu; sbosman@fsu.edu

A. Jaggi · J. R. Radović · S. R. Larter · T. B. P. Oldenburg
University of Calgary, PRG, Department of Geoscience, Calgary, AB, Canada
e-mail: aprami.jaggi@ucalgary.ca; jagos.radovic@ucalgary.ca; slarter@ucalgary.ca; toldenbu@ucalgary.ca

B. E. Rosenheim
University of South Florida, College of Marine Science, St. Petersburg, FL, USA
e-mail: brosenheim@usf.edu

B. D. Walker
University of California, Irvine -Department of Earth System Science, Irvine, CA, USA

Now at: University of Ottawa, Department of Earth and Environmental Sciences, Ottawa, ON, Canada
e-mail: brett.walker@uci.edu; brett.walker@uottawa.ca

S. A. Murawski et al. (eds.), *Scenarios and Responses to Future Deep Oil Spills*,
https://doi.org/10.1007/978-3-030-12963-7_10

this material once it is sedimented to the seafloor and the implications for oil spill budgets of seafloor petrocarbon deposition.

Keywords Organic carbon · Sediment organic matter · Radiocarbon · Dissolved organic matter · Gulf baselines · FTICR-MS · High-resolution mass spectrometry · Ramped pyrolysis

10.1 Introduction

Establishing baseline ecosystem components and monitoring them relative to these baselines can reveal the recovery of the Gulf of Mexico marine ecosystem and the effects and relative importance of future insults to the Gulf. As Pulitzer Prize winner Jack E. Davis wrote, the *Deepwater Horizon* "milestone spill is not the greatest assault to befall Gulf nature – not even close. Every day in the Gulf is an environmental disaster, originating from sources near and far that eclipses the spill…. No place is the sum of a single tragedy or continuing ones." Davis (2017). Investigation of various carbon pools has revealed quantities and pathways of hydrocarbons released during the 2010 *Deepwater Horizon* (DWH) oil spill, as discussed in previous chapters. Here we will describe downstream effects and follow petrocarbon as it moved through the ecosystem and into three major pools of oceanic carbon in the northern Gulf of Mexico: dissolved organic matter (DOM), sinking particulate organic matter (POM_{sink}), and sedimentary organic matter (SOM). Knowledge and monitoring of the isotopic composition of these organic components relative to their baseline values provide invaluable information regarding the Gulf's health and the potency of the anthropogenic stressors affecting it.

These three pools of organic matter play key roles in the biogeochemical cycling of carbon and other nutrients such as phosphorus, nitrogen, and sulfur. They record varying time scales of the carbon inputs to the Gulf which are responsible for secondary production, and they influence the solubility, transport, and toxicity of organic and inorganic pollutants (Kujawinski et al. 2002; Kim et al. 2004; Nebbioso and Piccolo 2013). DOM is operationally defined as the fraction that can pass through a nominal size filter (usually between 0.2 and 0.7 μm), (POM_{sink}) is the material collected in a sediment trap (Passow et al. 2012; Yan et al. 2016), and SOM accumulates on the seafloor (Brooks et al. 2015; Schwing et al. 2017). The residence time of DOM in the ocean is on the order of thousands of years (Williams and Druffel 1987; Bauer et al. 1992, 2002; Druffel et al. 1992 1996). With a sinking velocity that varies from 68 to 553 m d^{-1} (Diercks and Asper 1997; Passow et al. 2012), $POM_{sink,}$ reflects at time scales of short duration. In a 2000 m water column, these sinking velocities would result in a residence time of 4–30 days for POM in the water column. However, longer residence times may occur at the sea surface prior to the initiation of sinking as the exopolymeric substances that bind particles are initially somewhat buoyant (Azetsu-Scott and Passow 2004). Sedimentary organic matter, by contrast, provides a sequence of time horizons of varying duration, depending upon the sedimentation rate, and provides a record on the decadal to millennial time scale in the northern Gulf of Mexico.

Globally, the DOM pool accounts for ~662 Pg of carbon (Hansell et al. 2009), making it one of the Earth's largest active carbon pools, comparable in magnitude to atmospheric carbon dioxide load (~750 PgC; Hedges 1992). Sinking POM accounts for about 11.1 Pg of carbon exported to the ocean interior annually (Hansell 2013; Libes 2011). The part of this sinking flux which escapes complete remineralization is preserved in the sediments (~2.60 PgC yr^{-1}; Burdige and Komada 2015) and, although small in comparison, represents an important transfer between active carbon pools (fast-cycling) and geological carbon pools (cycling on millennial or greater time scales). The burial of the organic matter in the marine sediments represents an important link between the "active" biological carbon cycle in the oceans and the "inactive" carbon pool in the marine sediments, which cycle over much longer geologic time scales. In this chapter we will review some of the latest findings related to the molecular and carbon isotope (stable and radiocarbon) composition of these three pools of marine OM in the Gulf of Mexico system.

10.2 Analytical Approaches

Two approaches to define background and excursions from background will be described in this chapter. The first approach is the application of ultra-high-resolution Fourier-transform ion cyclotron resonance mass spectrometry (FTICR-MS) to explore changes in molecular-level composition of organic compounds partitioning to aqueous phase. FTICR-MS provides a combination of high resolving power and high accuracy of mass detection, facilitating the assignment of molecular formulas to individual water-soluble components extracted from DOM and SOM via solid-phase extraction without the need for prior separation by chromatographic or other methods. The second approach is the tracing of petroleum- and methane-derived carbon (petrocarbon) through the pools described above, using natural abundance stable carbon and radiocarbon isotopes ($\delta^{13}C$ and $\Delta^{14}C$, Fig. 10.1) (Stuiver and Pollach 1977; Bosman et al. 2017) and for $POM_{sink,}$ $\delta^{34}S$.

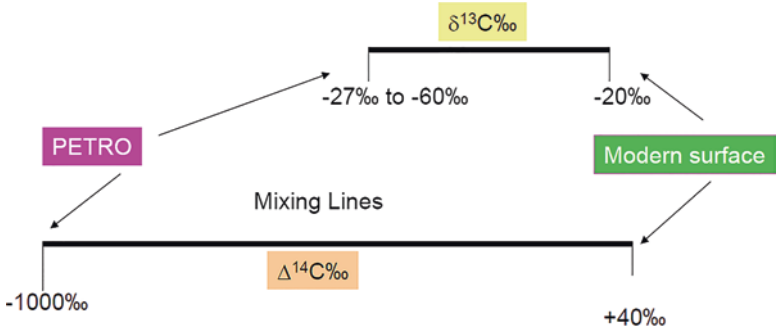

Fig. 10.1 Schematic drawing of the stable and radiocarbon two end-member mixing lines. Positions located closer to the left indicate samples containing petrocarbon, while positions located closer to the right indicate samples containing modern surface carbon in the Gulf of Mexico. (Bosman et al. 2017)

10.2.1 High-Resolution Mass Spectrometry: FTICR-MS

The pools of DOM in the water column and that extracted from the sediments by aqueous extraction (WEOM, water-extractable organic matter) encompass a cocktail of compounds with distinct molecular formulas, each of which constitutes a multitude of structural isomers, making the molecular assembly of the DOM one of the most complex and diverse organic mixtures on the planet (Dittmar and Stubbins 2013). The previously applied approaches for the characterization of this complex mixture, both dissolved in the water column and adsorbed on the sediment surface, have been constrained to the investigation of the bulk composition, with limited molecular characterization efforts (e.g., Benner et al. 1992; Ogawa et al. 2001). The application of ultra-high-resolution Fourier-transform ion cyclotron resonance mass spectrometry (FTICR-MS) provides a combination of high resolving power and high accuracy of mass detection, facilitating the assignment of molecular formulas to individual components, thereby making it sensitive to experimental processes that affect molecular-level composition (Stubbins et al. 2010). Its capability of analyzing high-molecular-weight, polyfunctional, and polar compounds makes it ideal for the characterization of dissolved organic matter in water and sediments.

FTICR-MS measures the mass to charge ratio (*m/z*) of an ion by measuring its cyclotron motion frequency in the influence of a magnetic field. The magnetic field, *B*, induces a cyclotron motion of the ions, because of the Lorentz force exerted on the ions, with mass *m* and a charge of *q*. For a given magnetic field strength, the cyclotron frequency of the ions in the ion cyclotron resonance (ICR) cell depends solely on the *m/z* ratio. The Bruker 12T SolariX FTICR-MS used in this study yields mass resolution of 2,000,000 at *m/z* 400, with maximum typical error as low as 150 ppb. The high resolving power and mass accuracy offered by the FTICR-MS can determine the mass of a molecule within 0.10 mDa, even lower than the mass of an electron (0.55 mDa).

The water DOM and sediment WEOM samples were analyzed using ultra-high-resolution mass spectrometry with electrospray ionization in negative (ESI-N) ion mode. The water samples were collected using a CTD-Niskin rosette sampler at various sites in the Gulf of Mexico in the summer of 2015 onboard the RV *Weatherbird II* and RV *Justo Sierra*. The DOM from the waters was extracted using the solid-phase extraction (SPE) protocol described by Dittmar et al. (2008). The extracts were then analyzed using FTICR-MS. The sediment samples were collected using an MC-800 multicoring system (Ocean Instruments, San Diego, CA, USA) from the Gulf of Mexico in the summer of 2015 onboard the RV *Weatherbird II* and RV *Justo Sierra*. Each sediment core was refrigerated at ~4 °C until subsampled by layer extrusion at 2 mm depth intervals, using a calibrated threaded-rod extrusion device (Verschuren 1993). The 2 mm extruded sediment samples were combined evenly for the top 15 cm of the sediment depth, to make a final dry weight of 23 g for each sampled site. The samples were then transferred into pre-combusted glass fiber thimbles (30 × 100 mm, Whatman) and Soxhlet extracted with 250 mL of deionized water for 48 h at 97 °C (Calgary altitude ~1100 m).

10.2.1.1 Stable Isotope Analysis

For both POM pools and SOM, a flash combustion elemental analyzer was used to convert organic molecules to CO_2 in a stream of He. This stream of He was continuously monitored for stable isotope ratios using a Finnigan Delta XP isotope ratio mass spectrometer. For purposes of interlaboratory comparison, laboratory reference materials of isotopic composition known relative to international standards are treated in the same way as the samples. All values are reported relative to the Vienna Pee Dee Belemnite (VPDB) standard with analytical precision of generally 0.2‰.

Methods for the determination of dissolved organic carbon (DOC) concentrations and isotopic composition are described in detail in Walker et al. (2017) and Beaupré et al. (2007). Briefly, UV photochemical oxidation (UVox) was used to convert dissolved organic molecules to aqueous CO_2. Prior to UV oxidation, it is necessary to remove existing dissolved inorganic carbon (DIC) from samples. Thus, samples were acidified with 1 mL of H_3PO_4 and sparged with He to carry out gaseous CO_2. Once samples were free of naturally occurring DIC, UV oxidation was employed, and the samples were sparged with He to remove the resultant CO_2. The CO_2 resulting from oxidation of the DOM was split 200–400 μg C aliquots for radiocarbon and 12–30 μg C aliquots for stable isotope analysis.

For DOC, equilibrated splits of sample CO_2 gas purified from DOC treated with UV oxidation were cryogenically isolated into 3 mm Pyrex tubes and sealed on a vacuum line. These 3 mm glass ampules were then placed in UHP He-flushed 12 mL Exetainer® vials and cracked in the He atmosphere. The resultant mixture of CO_2 and He was then introduced to a Finnigan Delta Plus isotope ratio mass spectrometer via a continuous flow Gas Bench II sample preparation system.

10.2.1.2 Radiocarbon Analysis

For all DOM, POM, and SOM samples, cryogenically purified CO_2 gas from sample UV oxidation or closed-tube combustion was cryogenically purified on a vacuum line and manometrically quantified. Equilibrated sample CO_2 gas splits were then catalytically reduced to graphite on a Fe catalyst either by the H_2 reduction method (Vogel et al. 1987) or the sealed-tube Zn method (Xu et al. 2007; Walker and Xu 2019). Graphite was then packed into ion source targets and sputtered with Cs^{+2} to form a negatively charged carbon ion beam for the detection of ^{14}C in an accelerator mass spectrometer (AMS). Radiocarbon analysis reported in this chapter was carried out in several AMS labs. POM and SOM $\Delta^{14}C$ measurements were made at the National Ocean Sciences Accelerator Mass Spectrometer (NOSAMS), the Center for Applied Isotopic Studies at the University of Georgia, or Lawrence Livermore National Lab. Total DOM $\Delta^{14}C$ measurements were performed at the University of California, Irvine Keck Carbon Cycle AMS Lab.

10.3 FTICR-MS

10.3.1 Geochemical Characterization of the FTICR-MS Composition of the Baseline Water Column Profile (at Multiple Depths) from Northern Gulf of Mexico

The identified peaks in the ESI-N FTICR-MS mass spectra of the analyzed water DOM extracts extended on average from *m/z* 200 to 750 with the spectra being dominated by four compound types: NO_x, N_2O_x, N_3O_x, and O_x, where x denotes variable number of oxygen (from 5 to 16). The DOM spectra show a Gaussian distribution was observed for the relative abundance of the individual heteroatom-dominated compound classes with increasing heteroatom number. The homogeneity in the compound class distribution of DOM and the uniform Gaussian distribution is expected, considering the constant diagenetic transformations ongoing in the marine ecosystems due to microbial degradation and photooxidation and longer residence time of dissolved fraction of organic matter pool (Opsahl et al. 1999; Spencer et al. 2009; Stubbins et al. 2010; Tarr et al. 2016).

The DOM spectra were enriched in multi-oxygenated species, with the classes $O_{2–18}$ having the highest contribution to the relative intensity of all compound classes present in the DOM, as also observed in previous studies analyzing DOM from natural systems (Fig. 10.2a) (Koch et al. 2007; Sleighter and Hatcher 2008). Across different sampling depths, these multi-oxygenated species exhibited a trend of the increasing intensity and number of oxygen atoms in the O_x compound class from surface to bottom of the water column (Fig. 10.2a). This trend suggests that the overall concentration of the DOM extracted using SPE is higher in the bottom waters compared to the surface. The published literature on DOM across marine ecosystems around the world (e.g., Koch et al. 2005; Mentges et al. 2017; Stubbins and Dittmar 2015) have also reported seeing a similar abundance gradient with depth.

The double bond equivalent (DBE) distribution of the O_x classes for the analyzed DOM spectra in ESI-N mode, when normalized to its relative intensity, shows a unit shift trend of the DBE with maximum relative intensity for each plotted class, similar to the pattern observed by Bae et al. (2011) for water column DOM. This increase of the intensity and inferred abundance of the O_x class group with an increase in sampling depth, combined with the pattern increase of DBE and carbon number by 1 unit, per addition of 2 oxygen atoms, suggests that the increase is due to transformation, resulting in the addition of -COOH groups. Previous characterization of deep marine DOM using NMR has also attributed the increased abundance of oxygen-containing species to the carboxylic functionality (Helms 2012; Stubbins and Dittmar 2015). Some of these compounds have been identified as microbially derived carboxylic-rich alicyclic molecules (CRAM) having a cyclic backbone with high carboxylation levels (Hertkorn et al. 2006). Hertkorn et al. (2006) also proposed that the deep-ocean refractory DOM was comprised of CRAM, which accounts for nearly 8% of the DOM pool.

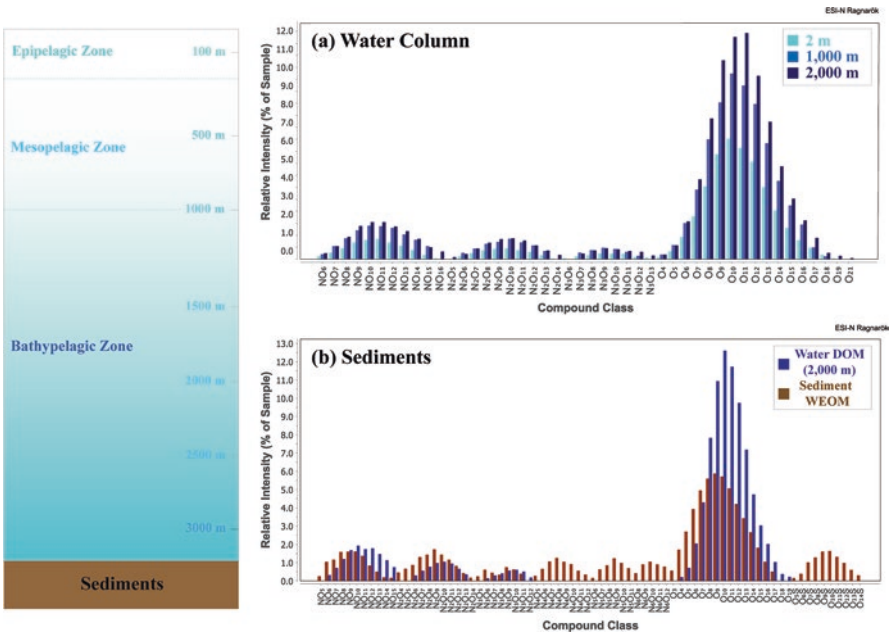

Fig. 10.2 FTICR-MS ESI-N compound class distribution of (**a**) water DOM along the water column at 2 m, 1000 m, and 2000 m, and (**b**) comparison of the water DOM (at 2000 m) and sediment WEOM for northern Gulf of Mexico data is publicly available through the Gulf of Mexico Research Initiative Information and Data Cooperative (GRIIDC) at https://data.gulfresearchinitiative.org R4.x267.179:0003

The increase in the relative abundance of the carboxyl group making up the DOM with increasing depth through the water column, indicates that biodegradation is occurring as DOM is transported to depth in the water column. Dittmar and Stubbins (2013) suggested that the increase in the species containing -COOH group with depth could be attributed to the corresponding depletion of labile DOM within the bathypelagic ocean, resulting in the production of an oxidized pool. The slow settling of this oxidized pool of DOM over thousands of years toward the bottom of the ocean would explain the increased relative intensity of multi-oxygenated species (Dittmar and Stubbins 2013).

10.3.2 Geochemical Characterization of the FTICR-MS Composition of the Baseline Sediment WEOM from Northern Gulf of Mexico

Bulk SOM and sediment DOM can itself be categorized into three operationally defined phases: pore water organic matter, water-extractable organic matter (WEOM) from the solid phase, and organic solvent-extractable organic matter from

the solid phase (Chen and Hur 2015). The aqueous Soxhlet extraction of sediment provides a more diverse pool of organics with fresher and less degraded constituents than the pore water organics extracted with conventional methods (Schmidt et al. 2014). The analysis of sedimentary organic matter using WEOM therefore offers a more comprehensive picture and a better alternative for sedimentary DOM characterization, especially when FTICR-MS analysis of pore water is limited by the sample volume availability.

The identified peaks in the ESI-N FTICR-MS mass spectra of the analyzed water extracts extended on average from *m/z* 150 to 650 with the spectra being dominated by eight compound types: NO_x, N_2O_x, N_3O_x, N_4O_x, N_5O_x, N_6O_x, O_x, and SO_x. The sediment WEOM spectra are enriched with nitrogen-containing compounds, containing up to six nitrogen heteroatoms with a wider compositional range compared to the water DOM extracts (Fig. 10.2b). The elevated nitrogen-containing species in the sediment WEOM suggests a release of molecules during water extraction, most likely from the protein-rich microbial cell walls present in the sediment. Schmidt et al. (2014), however, established this phenomenon to be minor for extraction of WEOM from sediments using Soxhlet, and insufficient to explain the increase in peptide-like compounds, thereby likely suggesting that these compounds are likely being produced in situ in the sediments. These nitrogen-rich moieties in the sediment WEOM could be related to melanoidins, which are formed by the condensation reaction between the sugars and amino acids via the Maillard or "browning" reaction (Hedges 1978). The high nitrogen-containing melanoidins produced in the marine waters have high affinities for clay material surfaces and bind to the suspended clay particulates forming aggregates, which sink through the water column adding to the sediment WEOM pool (Hedges 1978). This sinking of melanoidin-clay aggregates along the water column could explain absence of the melanoidin signature in the water DOM.

In addition to the nitrogen-containing moieties, the sediment WEOM contain a higher concentration of sulfur-containing compounds, which are likely formed by natural vulcanization reactions during sediment diagenesis, incorporating inorganic sulfur (from seawater sulfate reduction in the anaerobic zone) into lipids and carbohydrates (Wakeham et al. 1995; Aycard et al. 2003).

10.3.3 Continuum Between Water Column and Sediments

The water DOM extracts showed high relative intensities of oxygen-containing moieties, double bond equivalents, and carbon number values, compared to the sediment WEOM extracts, which showed a high relative intensity of nitrogen-containing compound classes. The lower carbon number and DBE values of the sediment WEOM in contrast to the aquatic DOM (Jaggi 2018) likely represent the low-molecular-weight intermediates from the series of hydrolytic, fermentative, and eventually respiratory processes taking place in the sediments (Henrichs 1992;

Arnosti et al. 1994; Burdige and Gardner 1998). The differences in the residence time of the DOM were also observed in the spectra between aquatic DOM and sediment WEOM. Whereas the aquatic DOM creates homogenous spectra owing to the slower transformations, dilutions, and longer residence times, the sediment WEOM show a higher variability in the composition between different locations, owing to the relatively faster deposition.

The biological processes are more robust in the water column resulting in the smoothing of the organic signature, while the anoxic conditions in the sediments restrict degradation, contributing to the preservation of more information regarding diagenetic changes and contaminations seen by a region (Emerson and Hedges 1988; Hedges and Keil 1995). For instance, an increased organic load in a natural setting, like an oil spill, would increase the aggregation of DOM in the water column with the suspended particles and diverse community of bacteria, phytoplankton, and protozoans, creating a sinking flux of organic matter (Turley and Stutt 2000). Such phenomenon of the sinking of the formed organic aggregates generates an action of "cleaning the water column" by moving the organics to the ocean floor. The characterization of organics in the sediments better preserves the signatures of different input sources.

10.4 Stable and Radiocarbon Isotopic Composition of Gulf of Mexico Organic Matter Pools

10.4.1 Dissolved Organic Carbon

A recent study by Walker and co-authors (2017) produced the first total dissolved organic carbon (DOC) $\Delta^{14}C$ and $\delta^{13}C$ water column profiles in the Gulf of Mexico. These data provide us with both baseline DOC concentrations and carbon isotopic data but also insight into the cycling of DOM in this key ocean region. DOC concentrations from most station depths in the Gulf of Mexico water column closely matched previous analysis of DO^{14}C from the open Atlantic Ocean adjacent to the Lesser Antilles (Druffel et al. 2016; Walker et al. 2017) (Fig. 10.3). Surface DOC isotopic data suggest primary production ($\delta^{13}C = -20.7‰$) is the predominant source of modern DOC in the surface Gulf. In the deep Gulf basin (Station P4), DOC $\delta^{13}C$ signatures range between -21.3 and $-21.8‰$. DOC $\Delta^{14}C$ values are slightly higher than expected from deepwater recharge sources (i.e., Caribbean and NADW). An ~11‰ offset from deep water at A20 and P4 suggests an apparent DOC ventilation time in the GOM of ~150 ^{14}C years. However, recent physical advection estimates of Gulf of Mexico basin suggest a ventilation of ~250 years (Rivas et al. 2005). This may indicate some modern deep DOC contributions from sinking particles. It is interesting to note that very low DOC $\Delta^{14}C$ values are not observed in the abyssal GOM. This is somewhat surprising given recent work

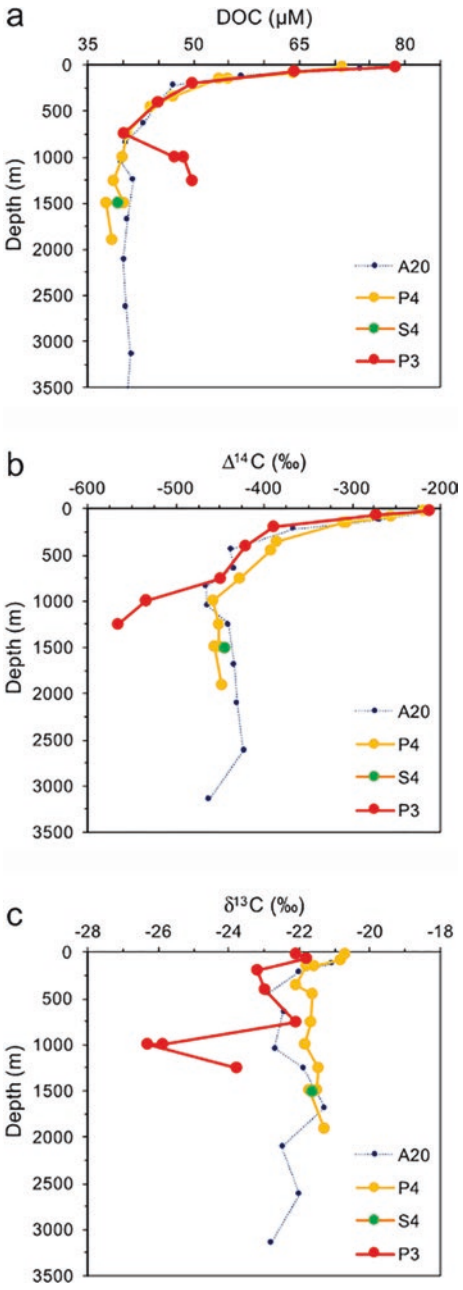

Fig. 10.3 Northern Gulf of Mexico dissolved organic carbon (DOC) concentrations (**a**) together with stable carbon ($\delta^{13}C$) (**b**) and radiocarbon ($\Delta^{14}C$) (**c**) isotopic values clearly indicate the presence of excess petrocarbon DOC at the Macondo wellhead site (P3; 28.65°N, −88.56°W) relative to offshore Gulf sites (S4; 28.04°N, −88.75°W and P4; 27.53°N, −88.75°W) and those in the Caribbean Sea (A20, Station 27, April 2012; 12.75°N, −52.33°W). For all plots, measurement uncertainties are smaller than the symbols. All Gulf samples were collected in July 2014 (R/V Pelican, PE15-01). (Data are publicly available through the Gulf of Mexico Research Initiative Information and Data Cooperative (GRIIDC) at https://data.gulfresearchinitiative.org (https://doi.org/10.7266/N7BZ63Z7))

suggesting deep hydrocarbon seeps are major deep-ocean DOC sources and the prevalence of hydrocarbon seeps in deep Gulf of Mexico (MacDonald et al. 2015; Pohlman et al. 2009, 2010). These data instead suggest that while seep DOC fluxes with very negative $\Delta^{14}C$ values may be locally significant, this seep DOC does not appear to accumulate at substantial levels in the deep Gulf of Mexico basin.

An exception to these otherwise "normal" ocean DOC isotopic profiles is observed at several deep sites (>750 m) nearest the Macondo wellhead (Station P3). Here, concentrations of DOC abruptly increase by 8–9 μM (~20–25%). At the same depths, both the $\delta^{13}C$ and $\Delta^{14}C$ compositions decrease significantly (Fig. 10.3). Using isotopic mass balance of a binary mixing model, the added DOC required $\delta^{13}C$ values to be −44.6‰ and −30.8‰ at 1000 m and 1250 m, respectively. Radiocarbon content (as $\Delta^{14}C$) of the added DOC was determined to be −965‰ and −1000‰ at 1000 m and 1250 m depth. The $\Delta^{14}C$ values of the added DOC indicate a petrocarbon source; the stable isotopic compositions at each depth represent a 42%:58% mixture of petroleum and methane at 1000 m and an 89%:11% mixture of petroleum and methane at 1250 m.

The presence of a persistent DOC petrocarbon plume, detected some 4 years after DWH near the Macondo wellhead site, is remarkable. The isotope signature of this DOC petrocarbon, however, is unmistakable. At the time of sampling, there was no measurable methane in the water column (Walker et al. 2017, supplemental information), and the presence of petroleum in the water samples in filtered vs. unfiltered replicates was not visually or isotopically perceptible. In addition, the methods used in the Walker study do not isolate methane carbon (only nonvolatile DOC). Thus, Walker and co-workers suggested that immediately following DWH, pre-aged "new" DOC was added following an intense microbial transformation of mesopelagic DWH oil and methane into a natural population of recalcitrant DOC molecules. It is likely this DOC petrocarbon signature will continue to persist until advection eventually "mixes out" this material with background DOC. Until that time, the DOC petrocarbon isotopic anomaly represents a novel geochemical tracer for ultimately further understanding the persistence and biogeochemistry of DOC in the Gulf of Mexico.

10.4.2 Sinking Particulate Organic Carbon

Marine snow is an aggregation of organic and inorganic debris including bacteria, phytoplankton feces, feeding webs, detrital material, biominerals, and lithogenic particles (Passow et al. 2012; Giering et al. 2018). These components are often bound together by ~~a~~ sticky substances called transparent exopolymer particles (TEP), which are produced by phytoplankton, frequently at the final stage of diatom blooms (Passow 2004). The presence of TEP can increase the flocculation of diatom cells by tenfold, and the process accumulates dissolved substances from the water column (Passow 2004). Initially upon formation, TEP is buoyant but, following

some degree of decomposition, will begin to sink (Azetsu-Scott and Passow 2004; Giering et al. 2018). Aggregations of foraminifera and radiolarians can also be mucus-rich and sticky (Geiring et al. 2018) binding components. In addition to incorporating dissolved organic matter into marine snow via TEP formation, these particulate accumulations can accumulate hydrophobic materials such as contaminants, including oil residues and PAHs (Giering et al. 2018; Yan et al. 2016; Broman et al. 1987; Lipiotou et al. 1993). When this material sediments out, and reaches the seafloor, it is referred to as marine oil snow sedimentation and flocculent accumulation (MOSSFA), a term coined at a GoMRI (Gulf of Mexico Research Initiative)-sponsored meeting.

Thus, in a direct manner, as it cleanses the water column of contaminants, marine snow also samples the water column for contaminants. Sediment traps serve as monitors of water column contamination and changes therein. Yan et al. (2016) offer direct evidence of the "scrubbing effect" of rapidly sinking diatom aggregations scavenging suspended substances and particles from the spill. Over a 3-month period, the barium contribution to the particulate flux decreased from some 1000 mg/kg of dry weight during the sedimentation event associated with the bloom to 400 mg/kg but then rebounded to 1200 mg/kg afterward. This temporary cleansing action was also reflected in the $\Delta^{14}C$ of the particulates which went from positive values in the bloom to the most negative values observed as Ba increased, reflecting the renewed input in the fossil carbon and oil-derived materials to the particulate flux. It was hypothesized that following the cleansing event, lateral advection renewed contamination of the water column above the sediment trap, causing the increase in deposition of contaminants. At the sinking rates of marine snow, it can be transported laterally to a great distance before it falls; thus the placement of material on the seafloor or in a sediment trap does not correspond with its surface formation site (Diercks et al. 2018).

Chanton et al. (2018) and Geiring et al. (2018) reported the flux and isotopic composition of sinking particles at three sites in the northern Gulf of Mexico following the oil spill and characterized the return of the POM_{sink} flux toward baseline values. The sediment trap at the DWH site (28°40′N, 88°21.6′W; at 1660 m depth) was about 5 km from the DWH site and was impacted by the oil discharge. Sample collection is reported from August 2010 to March 2015 (see also Yan et al. 2016). The reference site (AT357; see Fisher et al. 2014) was at 27°31.5 N (89°42.6 W; at 1160 m depth) and collected from April 2012 through August 2014. The third study site was a seep site, GC-600 (27°22.5′N, 90°30.7′W; at 1380 m depth). The seep frequently exhibits extensive oil slicks on the sea surface above it (MacDonald et al. 1993, 2015; Garcia-Pineda et al. 2013). Sample collection is reported from April 2012 to March 2016. Neither of the latter sites were visibly impacted by hydrocarbons from the DWH spill (Fisher et al. 2014).

Time-series isotope results for POM_{sink} at the DWH; reference and seep sites are depicted in Fig. 10.4 (Chanton et al. 2018). Here, $\Delta^{14}C$ varied from −180‰ to 93‰ at the DWH site, −52‰ to 66‰ at the reference site, and −200‰ to 62‰ at the seep site. In general, following an initial plankton bloom in August 2010, both $\Delta^{14}C$ and $\delta^{34}S$ at the DWH site were isotopically depleted, due to the influence of petro-

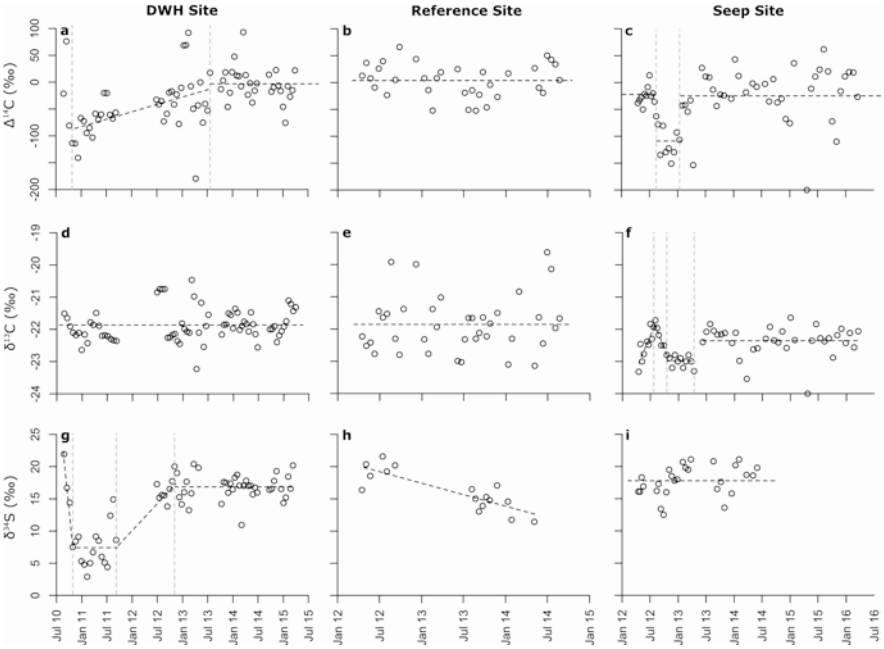

Fig. 10.4 Isotopic results on POM_{sink} for the three sites collected in sediment traps moored above the seafloor (Chanton et al. 2018; Giering et al. 2018). Trends in the time-series data for $\delta^{13}C$, $\Delta^{14}C$, and $\delta\,^{34}S$ at the three sites were assessed with the *envcpt* function of the R package *EnvCpt* (Killick et al. 2016). This analysis fits a best model fit to the data across time and identifies any change points if they are present. When change points were located, a piecewise simple linear regression was performed between them (Chanton et al. 2018). (Data are publicly available through the Gulf of Mexico Research Initiative Information and Data Cooperative (GRIIDC) at https://data.gulfresearchinitiative.org, https://doi.org/10.7266/N737775J. Reproduced from Elementa (Chanton et al. 2018))

carbon from the wellhead and possibly due to increased terrestrial organic matter input to the site. The most depleted DWH site values observed are given in Table 10.1. The $\Delta^{14}C$ values increased until July 2013, at which time they became relatively constant suggesting background or ambient values had been reached. The $\delta^{34}S$ values followed a similar pattern, leveling off toward presumed background in late 2012, at which time they became similar to the reference site values. Baseline isotopic values are indicated for these two sites, $\Delta^{14}C‰$ –3.2 ± 31.0 and 3.8 ± 31.1, while $\delta^{34}S$ values were 16.9 ± 2.0 and 16.2 ± 3.1 for the DWH and reference site respectively. Carbon-13 values for the two sites did not show any trends and were −21.9‰ ± 0.5 and −21.9‰ ± 0.9, respectively. Relative to these two sites, DWH post July 2013 and reference, seep site values were somewhat depleted for ^{14}C and ^{13}C, especially during a "trough" period when the sediment trap appeared to sample petrocarbon-rich particles from a natural oiled-sedimentation event (Fig. 10.4 and Giering et al. 2018; Chanton et al. 2018). However ^{34}S values did not reflect petrocarbon input at the seep site suggesting that the petrocarbon had been assimilated

Table 10.1 Isotopic values of POM_{susp} over collection intervals at different sites and times

Site, condition	Isotope values		
	$\Delta^{14}C‰$	$\delta^{13}C‰$	$\delta^{34}S‰$
DWH site, depleted values 8 December 2010	−141.0	−22.1	9.1
DWH site, after July 2013	−3.2 ± 31.0	−21.9 ± 0.5	16.9 ± 2.0
Reference site, average	3.8 ± 31.1	−21.9 ± 0.9	16.2 ± 3.1
Seep site, non-trough	−21.7 ± 45.7	−22.3 ± 0.5	18.4 ± 2.1
Seep site, trough	−109.0 ± 29.1	−23.0 ± 0.2	16.6 ± 2.3

For the DWH site, the 2010 values indicate effects from the oil spill, while a return to background is indicated after July 2013. The reference site is similar to the post 2013 DWH site values, confirming this hypothesis. At the seep site, "trough" conditions indicate the capture of a possible natural MOSSFA event in the sediment trap, while non-trough values are more background-like but still somewhat depleted possibly due to seep site influence
Chanton et al. (2018)

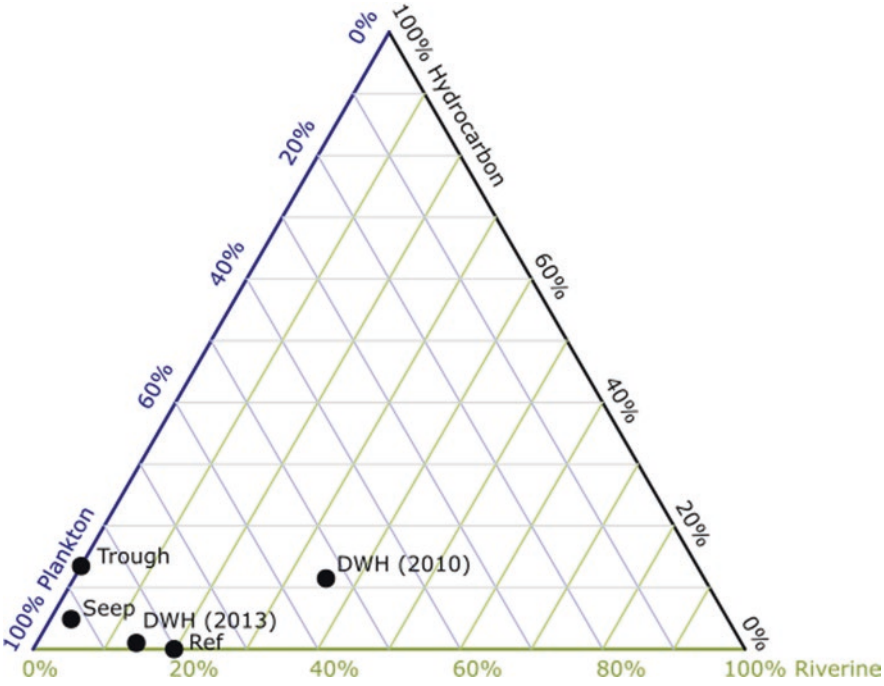

Fig. 10.5 The relative importance of differing carbon sources to sinking particulates in the northern Gulf of Mexico determined from a three end-member model. (Data from Chanton et al. 2018). The importance of marine photosynthetic production is clearly indicated relative to seep and riverine (terrestrial) inputs

by microbes and had entered the food web and subsequently incorporated into marine oil snow (Daly et al. 2016; Passow and Hetland 2016; Passow and Ziervogel 2016). Using a mixing model, Chanton et al. (2018) determined the relative importance of differing carbon sources to the POM_{sink} of the northern Gulf (Fig. 10.5). The model clearly indicated the importance of marine in situ production in all cases.

10.4.3 Sedimentary Organic Carbon

Marine oil snow (MOS) accumulated on the seafloor as far as 120–180 km from the wellhead and was observed to the SW and NE of the wellhead (Romero et al. 2015, 2017; Chanton et al. 2015; Valentine et al. 2014; Stout et al. 2017). As described above, the petrocarbon-affected sediment is referred to as the marine oil snow sedimentation and flocculent accumulation (MOSSFA). The sedimented oil could have been derived from oil that floated on the surface of the Gulf (MacDonald et al. 2015; Daly et al. 2016) or it could have been derived from the deep-sea plume that was focused to the southwest of the wellhead (Valentine et al. 2014; Daly et al. 2016, Mason et al. 2014). Consensus is that the MOSSFA layer was roughly a cm in thickness (Valentine et al. 2014; Brooks et al. 2015; Chanton et al. 2015; Romero et al. 2015).

Radiocarbon ($\Delta^{14}C$) measurements on the surface layers of sediments surrounding the oil spill site collected from 2010 to 2012 indicated the deposition of petrocarbon on the seafloor in a region of 2.4×10^{10} m^2 (Fig. 10.6, Chanton et al.

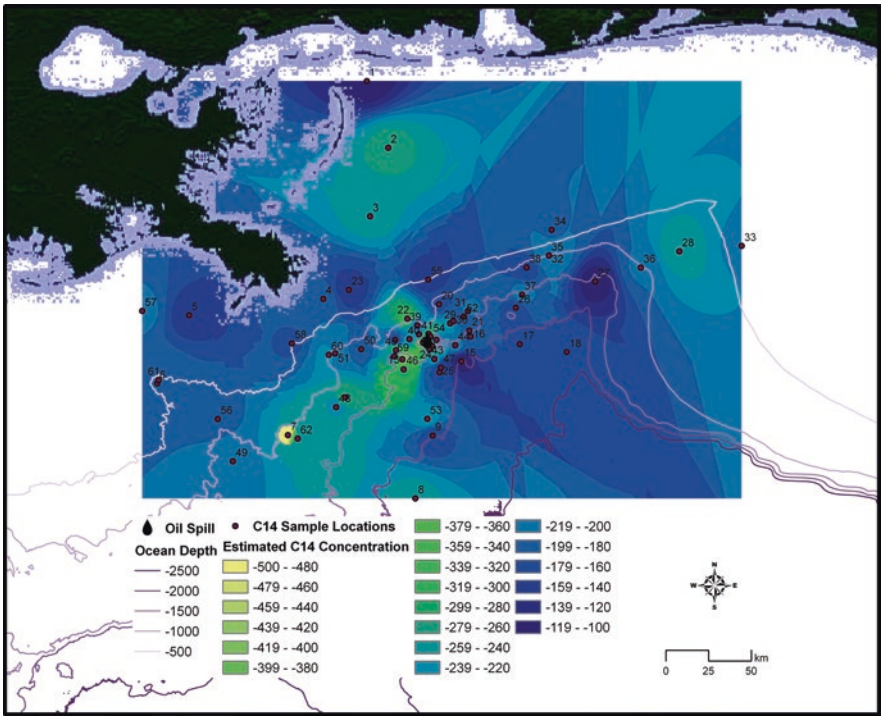

Fig. 10.6 Seafloor radiocarbon map. Points represent the 0–1 cm interval of surface sediments. Data were contoured with the inverse distance weighting (IDW) method and, within the black polygon, the surface area of each 20‰ interval calculated for the seafloor. (Reproduced from Chanton et al. 2015. Data are publicly available through the Gulf of Mexico Research Initiative Information and Data Cooperative (GRIIDC) at https://data.gulfresearchinitiative.org, UDI, R1.x138.078:0024. Reprinted with permission from Chanton et al. 2015. Copyright 2015 American Chemical Society)

2015). The amount of petrocarbon was estimated to be between 0.5% and 9.1% of the quantity of fossil carbon released with a best estimate of 3.0–4.9%. Surface values varied from −500‰ to −107‰ across the area. Background surface values were determined to be −200 ± 29‰ based on values underlying the contaminated sediments. The mean value for surface sedimentary organic matter was determined to be −21.5 ± 0.8‰, indistinguishable from compiled pre-spill surface sediment values for the Gulf of Mexico reported by Rosenheim et al. (2016) of −21.4 ± 1.9‰.

10.4.4 Ramped Pyrolysis-Oxidation of Sedimentary Organic Matter

Ramped pyrolysis-oxidation (Ramped PyrOx or RPO) analysis of the bulk organic matter followed by isotopic analysis of pyrolysates is helpful to gain further insight into how the oil pollution qualitatively changes in terms of thermochemical stability after release into the environment. Early work showed that samples with high polycyclic aromatic hydrocarbon (PAH, a type of compound released by petroleum in the environment and by burning of organic material) concentrations also had lower temperatures of pyrolysis in samples taken soon after the DWH spill from Barataria Bay, Louisiana (Pendergraft et al. 2013). As oil persisted in different forms in beach and marsh environments, compounds containing high amounts of petrocarbon gradually became more stable (Pendergraft and Rosenheim 2014), as indicated by higher temperature intervals registering depleted $\Delta^{14}C$ signatures through time. The shift from volatile (low pyrolysis temperatures) to stable (high pyrolysis temperatures) likely represents a suite of different chemical reactions; the chemical information in RPO analysis is simplified to pyrolysis temperature by nature of rapid combustion of the pyrolysates in preparation for isotopic analysis. Rogers et al. (2019) have recently reported on RPO analysis of deep Gulf sediments in a time series analysis.

In the open ocean, SOM petrocarbon transformations were captured by decreasing concentrations of PAH through time and space (Adhikari et al. 2016). Analysis of a suite of SOM samples in the Gulf of Mexico yielded little evidence for preservation of petrocarbon signatures far from the wellhead site. In fact, weathering stabilization of the petrocarbon is evidenced in deep-sea samples where the petrocarbon signal is still viable (Adhikari et al. 2016) because the strongest $\Delta^{14}C$ depletions are observed at the highest pyrolysis temperatures. However, at sites with low PAH concentrations, there is little evidence of radiocarbon depletion anywhere in the thermochemical reactivity spectrum. This can either be interpreted as full weathering of any petrocarbon signal through complete remineralization or absence of a petrocarbon pulse due to patchiness of the spill's projection in seafloor sediments at distances beyond a few km. Alternatively, the petrocarbon could have been resuspended and advected downslope (Diercks et al. 2018).

10.5 Conclusions and Baselines

An interesting and, perhaps, overlooked aspect of the work summarized in this chapter is the persistence of a water column isotopic signature of the DWH oil spill. For several years, during which there is evidence for degradation of the petrocarbon signature in SOM (Adhikari et al. 2016), water column DOM retained a petrocarbon signature. Whereas much effort has continued to model and measure surface mesoscale transportation processes (Olascoaga and Haller 2012; Poje et al. 2014; Olascoaga et al. 2013; Beron-Verra et al. 2015), comparatively little research has aimed to ascertain midlevel mesopelagic transport processes. In addition to the question of *who* (what microbial populations) were responsible for the transformation of petroleum and methane to DOC, the question of *how* this signature persisted for at least 4 years after the spill is withstanding and potentially illustrative of mid-ocean transport processes near the continental margin. The FTICR-MS data indicate that the DOM became increasingly oxygenated (via photooxidation and biodegradable processes) over time, and this may have led to this persistence.

From trajectories of isotopic values over time, and from spatial variations in isotopic compositions, the research discussed in this chapter has provided estimates of background isotopic values of organic matter pools prior to the oil spill. Baseline DOC isotopic composition in the deep Gulf (P4; >1000 m) appears to vary between −459 and −449‰ for $\Delta^{14}C$ and −21.3 to −21.8‰ for $\delta^{13}C$. For POM_{sink}, background $\Delta^{14}C$ values vary between −30 and +30‰, whereas $\delta^{13}C$ values vary between −21 and −23‰, and $\delta^{34}S$ varies from 13‰ to 20‰. Background values for sedimentary organic matter were −200 ± 29‰ for $\Delta^{14}C$ and 21.4 ± 1.9‰ for $\delta^{13}C$.

Funding Information This research was made possible by grants from the Gulf of Mexico Research Initiative through its consortia: the Center for the Integrated Modeling and Analysis of the Gulf Ecosystem (C-IMAGE), Ecosystem Impacts of Oil and Gas Inputs to the Gulf (ECOGIG), Deep Sea to Coast Connectivity in the Eastern Gulf of Mexico (Deep-C), and the Consortium for Advanced Research of Transport of Hydrocarbon in the Environment (CARTHE). We also acknowledge funding from an American Chemical Society (ACS) Petroleum Research Fund (PRF) New Directions (ND) grant (to B.D.W).

References

Adhikari PL, Maiti K, Overton EB, Rosenheim BE, Marx BD (2016) Distributions and accumulation rates of polycyclic aromatic hydrocarbons in the northern Gulf of Mexico sediments. Environ Pollut 212:413–423. https://doi.org/10.1016/j.envpol.2016.01.064

Arnosti C, Repeta DJ, Blough NV (1994) Rapid bacterial degradation of polysaccharides in anoxic marine systems. Geochim Cosmochim Acta 58:2639–2652. https://doi.org/10.1016/0016-7037(94)90134-1

Aycard M, Derenne S, Largeau C, Mongenot T, Tribovillard N, Baudin F (2003) Formation pathways of proto-kerogens in Holocene sediments of the upwelling influenced Cariaco Trench, Venezuela. Org Geochem 34:701–718. https://doi.org/10.1016/S0146-6380(03)00058-5

Azetsu-Scott K, Passow U (2004) Ascending marine particles: significance of transparent exopolymer particles (TEP) in the upper ocean. Limnol Oceanogr 49(3):741–748. https://doi.org/10.4319/lo.2004.49.3.0741

Bae E, Yeo IJ, Jeong B, Shin Y, Shin KH, Kim S (2011) Study of double bond equivalents and the numbers of carbon and oxygen atom distribution of dissolved organic matter with negative-mode FT-ICR MS. Anal Chem 83:4193–4199. https://doi.org/10.1021/ac200464q

Bauer JE, Williams PM, Druffel ER (1992) 14C activity of dissolved organic carbon fractions in the north-central Pacific and Sargasso Sea. Nature, 357(6380), 667

Bauer JE, Druffel ERM, Wolgast DM, Griffin S (2002) Temporal and regional variability in sources and cycling of DOC and POC in the northwest Atlantic continental shelf and slope. Deep Sea Res II 49:4387–4419

Beaupre SR, Druffel ERM, Griffin G (2007) A low-blank photochemical extraction system for concentration and isotopic analyses of marine dissolved organic carbon. Limnol Oceanogr Methods 5(6):174–184

Benner R, Pakulski JD, Mccarthy M, Hedges JI, Hatcher PG (1992) Bulk chemical characteristics of dissolved organic matter in the ocean. Science 255:1561–1564. https://doi.org/10.1126/science.255.5051.1561

Beron-Vera FJ, Olascoaga MJ, Haller G, Farazmand J, Wang TY (2015) Dissipative inertial transport patterns near coherent Lagrangian eddies in the ocean. Interdiscip J Nonlinear Sci 25:8

Bosman SH, Chanton JP, Rogers KL (2017) Using stable and radiocarbon analyses as a forensic tool to find evidence of oil in the particulates of the water column and on the seafloor following the 2010 Gulf of Mexico Oil Spill. In: Stout S, Wang Z (eds) Oil spill environmental forensics case studies. Butterworth and Heinemann, Cambridge, MA, pp 639–650

Broman D, Colmsjö A, Ganning B, Näf C, Zebühr Y, Östman C (1987) "Fingerprinting" petroleum hydrocarbons in bottom sediment, plankton, and sediment trap collected seston. Mar Pollut Bull 18(7):380–388. https://doi.org/10.1016/0025-326X(87)90317-1

Brooks GR, Larson RA, Schwing PT, Romero I, Moore C, Reichart GJ, Jilbert T, Chanton JP, Hastings DW, Overholt WA, Marks KP, Kostka JE, Homes CW, Hollander D (2015) Sedimentation pulse in the NE Gulf of Mexico following the 2010 DWH blowout. PLoS One 10(7):e0132341. https://doi.org/10.1371/journal.pone.0132341

Burdige DJ, Gardner KG (1998) Molecular weight distribution of dissolved organic carbon in marine sediment pore waters. Mar Chem 62:45–64. https://doi.org/10.1016/S0304-4203(98)00035-8

Burdige DJ, Komada T (2015) Sediment pore waters. In: Hansell DA, Carlson CA (eds) Biogeochemistry of marine dissolved organic matter, 2nd edn. Academic Press, New York. pp 535–577

Chanton J, Zhao T, Rosenheim BE, Joye S, Bosman S, Brunner C, Yeager KM, Diercks AR, Hollander D (2015) Using natural abundance radiocarbon to trace the flux of petrocarbon to the seafloor following the Deepwater Horizon oil spill. Environ Sci Technol 49(2):847–854

Chanton JP, Giering SL, Bosman SH, Rogers KL, Sweet J, Asper VL, Diercks AR, Passow U (2018) Isotopic composition of sinking particles: oil effects, recovery and baselines in the Gulf of Mexico, 2010–2015. Elementa Sci Anthropocene 6(43):1–19

Chen M, Hur J (2015) Pre-treatments, characteristics, and biogeochemical dynamics of dissolved organic matter in sediments: a review. Water Res 79:10–25. https://doi.org/10.1016/j.watres.2015.04.018

Daly KL, Passow U, Chanton J, Hollander D (2016) Assessing the impacts of oil-associated marine snow formation and sedimentation during and after the Deepwater Horizon oil spill. Anthropocene 13:18–33. https://doi.org/10.1016/j.ancene.2016.01.006

Davis JE (2017) The Gulf: the making of an American Sea. Liveright Publishing, New York

Diercks AR, Asper VL (1997) In situ settling speeds of marine snow aggregates below the mixed layer: Black Sea and Gulf of Mexico. Deep Sea Res Part I 44(3):385–398. https://doi.org/10.1016/S0967-0637(96)00104-5

Diercks AR, Dike C, Asper V, DiMarco SF, Chanton J, Passow U (2018) Scales of seafloor sediment resuspension in the northern Gulf of Mexico. Elementa: Science of the Anthropocene, 6(32) http://doi.org/10.1525/elementa.285

Dittmar T, Stubbins A (2013) Dissolved organic matter in aquatic systems, 2nd edn. Elsevier Ltd., New York

Dittmar T, Koch B, Hertkorn N, Kattner G (2008) A simple and efficient method for the solid-phase extraction of dissolved organic matter (SPE-DOM) from seawater. Limnol Oceanogr Methods 6:230–235. https://doi.org/10.4319/lom.2008.6.230

Druffel ERM, Williams PM, Bauer JE, Ertel JR (1992) Cycling of dissolved and particulate organic matter in the open ocean. J Geophys Res 97(C10):15639–15659. https://doi.org/10.1029/92JC01511

Druffel ERM, Bauer JE, Williams PM, Griffin S, Wolgast D (1996) Seasonal variability of particulate organic radiocarbon in the northeast Pacific Ocean. J Geophys Res 101(C9):20543–20552. http://dx.doi.org/10.1029/96JC01850

Druffel ERM, Griffin S, Coppola AI, Walker BD (2016) Radiocarbon in dissolved organic carbon of the Atlantic Ocean. Geophys Res Lett 43(10):5279–5286

Emerson S, Hedges JI (1988) Processes controlling the organic carbon content of open ocean sediments. Paleogeogr Paleoclimatol Paleoecol 3:621–634. https://doi.org/10.1029/PA003i005p00621

Fisher CR, Hsing P-Y, Kaiser CL, Yoerger DR, Roberts HH, Shedd WW, Cordes EE, Shank TM, Verlet SP, Saunders MG, Larcom EA, Brooks JM (2014) Footprint of Deepwater Horizon blowout impact to deep-water coral communities. Proc Natl Acad Sci U S A 111(32):11744–11749. https://doi.org/10.1073/pnas.1403492111

Garcia-Pineda O, MacDonald I, Hu C, Svejkovsky J, Hess M, Dukhovskoy D, Morey SL (2013) Detection of floating oil anomalies from the Deepwater Horizon oil spill with synthetic aperture radar. Oceanography 26:124–137. https://doi.org/10.5670/oceanog.2013.38

Giering SLC, Yan B, Sweet J, Asper V, Diercks A, Chanton J, Passow U (2018) The ecosystem baseline for particle flux in the Northern Gulf of Mexico. Elementa Sci Anthropocene 6(1):6. https://doi.org/10.1525/elementa.264

Hansell DA (2013) Recalcitrant dissolved organic carbon fractions. Annu Rev Mar Sci 5:421–445. https://doi.org/10.1146/annurev-marine-120710-100757

Hansell DA, Carlson CA, Repeta DJ, Schlitzer R (2009) Dissolved organic matter in the ocean—A controversy stimulates new insights. Oceanography 22(4):202–211

Hedges JI (1978) The formation and clay mineral reactions of melanoidins. Geochim Cosmochim Acta 42:69–76. https://doi.org/10.1016/0016-7037(78)90218-1

Hedges JI (1992) Global biogeochemical cycles: progress and problems. Mar Chem 39:67–93. https://doi.org/10.1016/0304-4203(92)90096-S

Hedges JI, Keil RG (1995) Sedimentary organic matter preservation: an assessment and speculative synthesis. Mar Chem 49:137–139. https://doi.org/10.1016/0304-4203(95)00013-H

Helms JR (2012) Spectroscopic characterization of dissolved organic matter: insights into composition photochemical transformation and carbon cycling. Dissertation, Old Dominion University

Henrichs SM (1992) Early diagenesis of organic matter in marine sediments: progress and perplexity. Mar Chem 39:119–149. https://doi.org/10.1016/0304-4203(92)90098-U

Hertkorn N, Benner R, Frommberger M, Schmitt-Kopplin P, Witt M, Kaiser K, Kettrup A, Hedges JI (2006) Characterization of a major refractory component of marine dissolved organic matter. Geochim Cosmochim Acta 70:2990–3010. https://doi.org/10.1016/j.gca.2006.03.021

Jaggi A (2018) Dissolved organic matter in marine environments: a study of the origin lability and molecular composition. Dissertation, University of Calgary

Kim S, Kaplan LA, Benner R, Hatcher PG (2004) Hydrogen-deficient molecules in natural riverine water samples - evidence for the existence of black carbon in DOM. Mar Chem 92:225–234. https://doi.org/10.1016/j.marchem.2004.06.042

Killick R, Beaulieu C, Taylor S. 2016. EnvCpt: Detection of Structural Changes in Climate and Environment Time Series. R package version 0.1.1. https://CRAN.Rproject.org/package=EnvCpt

Koch BP, Witt M, Engbrodt R, Dittmar T, Kattner G (2005) Molecular formulae of marine and terrigenous dissolved organic matter detected by electrospray ionization Fourier transform ion

cyclotron resonance mass spectrometry. Geochim Cosmochim Acta 69:3299–3308. https://doi.org/10.1016/j.gca.2005.02.027

Koch BP, Dittmar T, Witt M, Kattner G (2007) Fundamentals of molecular formula assignment to ultrahigh resolution mass data of natural organic matter. Anal Chem 79:1758–1763. https://doi.org/10.1021/ac061949s

Kujawinski EB, Hatcher PG, Freitas MA (2002) High-resolution fourier transform ion cyclotron resonance mass spectrometry of humic and fulvic acids: improvements and comparisons. Anal Chem 74:413–419. https://doi.org/10.1021/ac0108313

Libes S (2011) Introduction to marine biogeochemistry. Academic Press, New York

Lipiatou E, Marty J-C, Saliot A (1993) Sediment trap fluxes of polycyclic aromatic hydrocarbons in the Mediterranean Sea. Mar Chem 44(1):43–54. https://doi.org/10.1016/0304-4203(93)90005-9

MacDonald IR, Guinasso NL Jr, Acchleson SG, Amos JF, Duckworth R, Sassen R, Brooks JM (1993) Natural oil slicks in the Gulf of Mexico visible from space. J Geophys Res 98:16351–16364

MacDonald IR, Garcia-Pineda O, Beet A, Daneshgar Asl S, Feng L, Graettinger G, French-McCay D, Holmes J, Hu C, Huffer F, Leifer I, Muller-Karger F, Solow A, Silva M, Swayze G (2015) Natural and unnatural oil slicks in the Gulf of Mexico. J Geophys Res Oceans 120:8364–8380. https://doi.org/10.1002/2015JC011062

Mason OU, Scott NM, Gonzalez A, Robbins-Pianka A, Bælum J, Kimbrel J, Bouskill NJ, Prestat E, Borglin S, Joyner DC, Fortney JL, Jurelevicius D, Stringfellow WT, Alvarez-Cohen L, Hazen TC, Knight R, Gilbert JA, Jansson JK (2014) Metagenomics reveals sediment microbial community response to Deepwater Horizon oil spill. Int Soc Microb Ecol J 8(7):464–1475

Mentges A, Feenders C, Seibt M, Blasius B, Dittmar T (2017) Functional molecular diversity of marine dissolved organic matter is reduced during degradation. Front Mar Sci 4:1–10. https://doi.org/10.3389/fmars.2017.00194

Nebbioso A, Piccolo A (2013) Molecular characterization of dissolved organic matter (DOM): a critical review. Anal Bioanal Chem 405:109–124. https://doi.org/10.1007/s00216-012-6363-2

Ogawa H, Amagai Y, Koike I, Kaiser K, Benner R (2001) Production of refractory dissolved organic matter by bacteria. Science 292:917–920. https://doi.org/10.1126/science.1057627

Olascoaga MJ, Haller G (2012) Forecasting sudden changes in environmental pollution patterns. Proc Natl Acad Sci U S A 109(13):4738–4743

Olascoaga MJ, Beron-Vera FJ, Haller G, Triñanes J, Iskandarani M, Coelho EF, Haus BK, Huntley HS, Jacobs G, Kirwan AD Jr, Lipphardt BL Jr, Özgökmen TM, Reniers AJHM, Valle-Levinson A (2013) Drifter motion in the Gulf of Mexico constrained by altimetric Lagrangian coherent structures. Geophys Res Lett 40(23):6171–6175

Opsahl S, Benner R, Amon RMW (1999) Major flux of terrigenous dissolved organic matter through the Arctic Ocean. Limnol Oceanogr 44:2017–2023. https://doi.org/10.4319/lo.1999.44.8.2017

Passow U (2004) Switching perspectives: do mineral fluxes determine particulate organic carbon fluxes or vice versa? Geochem Geophys Geosyst 5(4):Q04002. https://doi.org/10.1029/2003GC000670

Passow U, Hetland RD (2016) What happened to all of the oil? Oceanography 29(3):88–95. https://doi.org/10.5670/oceanog.2016.73

Passow U, Ziervogel K (2016) Marine snow sedimented oil released during the Deepwater Horizon spill. Oceanography 29(3):118–125. https://doi.org/10.5670/oceanog.2016.76

Passow U, Ziervogel K, Asper V, Diercks A (2012) Marine snow formation in the aftermath of the Deepwater Horizon oil spill in the Gulf of Mexico. Environ Res Lett 7(3):1–11. https://doi.org/10.1088/1748-9326/7/3/035301

Pendergraft MA, Rosenheim BE (2014) Varying relative degradation rates of oil in different forms and environments revealed by ramped pyrolysis. Environ Sci Technol 48(18):10966–10974. https://doi.org/10.1021/es501354c

Pendergraft MA, Dincer Z, Sericano JL, Wade TL, Kolasinski J, Rosenheim BE (2013) Linking ramped pyrolysis isotope data to oil content through PAH analysis. Environ Res Lett 8:1–10. https://doi.org/10.1088/1748-9326/8/4/044038

Pohlman JW, Bauer JE, Canuel EA, Grabowski KS, Knies DL, Mitchell CS, Whiticar MJ, Coffin RB (2009) Methane sources in gas hydrate-bearing cold seeps: evidence from radiocarbon and stable isotopes. Mar Chem 115:102–109. https://doi.org/10.1016/j.marchem.2009.07.001

Pohlman JW, Bauer JE, Waite WF, Osburn CL, Chapman NR (2010) Methane hydrate-bearing seeps as a source of aged dissolved organic carbon to the oceans. Nat Geosci 4:37–41. https://doi.org/10.1038/ngeo1016

Poje AC, Özgökmen TM, Lipphart BL, Haus BK, Ryan EH, Haza AC, Jacobs GA, Reniers AJHM, Olascoaga MJ, Novelli G, Griffa A, Beron-Vera FJ, Chen SS, Coelho E, Hogan PJ, Kirwan AD Jr, Huntley HS, Mariano AJ (2014) Submesoscale dispersion in the vicinity of the Deepwater Horizon spill. Proc Natl Acad Sci U S A 111(35):12693–12698

Rivas D, Badan A, Ochoa J (2005) The ventilation of the deep Gulf of Mexico. J Phys Oceanogr 35:1763–1781

Rogers KL, Bosman SH, Lardie-Gaylord M, McNichol A, Rosenheim BE, Montoya JP, Chanton JP (2019) Petrocarbon evolution: Ramped pyrolysis/oxidation and isotopic studies of contaminated oil sediments from the Deepwater Horizon oil spill in the Gulf of Mexico. PloS one 14(2): e0212433

Romero IC, Schwing PT, Brooks GR, Larson RA, Hastings DW, Ellis G, Goddard EA, Hollander DJ (2015) Hydrocarbons in deep-sea sediments following the 2010 Deepwater Horizon blowout in the northeast Gulf of Mexico. PLoS One 10(5):e0128371

Romero IC, Toro-Farmer G, Diercks A-R, Schwing P, Muller-Karger F, Murawski S, Hollander DJ (2017) Large-scale deposition of weathered oil in the Gulf of Mexico following a deep-water oil spill. Environ Pollut 228:179–189. https://doi.org/10.1016/j.envpol.2017.05.019

Rosenheim BE, Pendergraft MA, Flowers GC, Carney R, Sericano J, Amer RM, Chanton J, Dincer A, Wade TL (2016) Employing extant stable carbon isotope data in Gulf of Mexico sedimentary organic matter for oil spill studies. Deep Sea Res II 129:249–258

Schmidt F, Koch BP, Witt M, Hinrichs K-UU (2014) Extending the analytical window for water-soluble organic matter in sediments by aqueous Soxhlet extraction. Geochim Cosmochim Acta 141:83–96. https://doi.org/10.1016/j.gca.2014.06.009

Schwing PT, Brooks GR, Larson RA, Holmes CW, O'Malley BJ, Hollander DJ (2017) Constraining the spatial extent of marine oil snow sedimentation and flocculent accumulation (MOSSFA) following the Deepwater Horizon event using an excess 210Pb flux approach. Environ Sci Technol 51(11):5962–5968. https://doi.org/10.1021/acs.est.7b00450

Sleighter RL, Hatcher PG (2008) Molecular characterization of dissolved organic matter (DOM) along a river to ocean transect of the lower Chesapeake Bay by ultrahigh resolution electrospray ionization Fourier transform ion cyclotron resonance mass spectrometry. Mar Chem 110:140–152. https://doi.org/10.1016/j.marchem.2008.04.008

Spencer RGM, Aiken GR, Butler KD, Dornblaser MM, Streigl RG (2009) Utilizing chromophoric dissolved organic matter measurements to derive export and reactivity of dissolved organic carbon exported to the Arctic Ocean: a case study of the Yukon River. Alaska Geophys Res Lett 36:1–6. https://doi.org/10.1029/2008GL036831

Stout SA, Rouhani S, Liu B, Oehrig J, Ricker RW, Baker G, Lewis C (2017) Assessing the footprint and volume of oil deposited in deep-sea sediments following the Deepwater Horizon oil spill. Mar Pollut Bull 114(1):327–342. https://doi.org/10.1016/j.marpolbul.2016.09.046

Stubbins A, Dittmar T (2015) Illuminating the deep: molecular signatures of photochemical alteration of dissolved organic matter from North Atlantic Deep Water. Mar Chem 177:318–324. https://doi.org/10.1016/j.marchem.2015.06.020

Stubbins A, Spencer RGM, Chen H, Hatcher PG, Mopper K, Hernes PJ, Mwamba VL, Mangangu AM, Wabakanghanzi JN, Six J (2010) Illuminated darkness: molecular signatures of Congo River dissolved organic matter and its photochemical alteration as revealed by ultrahigh precision mass spectrometry. Limnol Oceanogr 55:1467–1477. https://doi.org/10.4319/lo.2010.55.4.1467

Stuiver M, Polach HA (1977) Reporting Of 14C data. Radiocarbon 19:355–263

Tarr M, Zito P, Overton E, Olson GM, Adhikari AP, Reddy CM (2016) Weathering of oil spilled in the marine environment. Oceanography 29:126–135. https://doi.org/10.5670/oceanog.2016.77

Turley CM, Stutt ED (2000) Depth-related cell-specific bacterial leucine incorporation rates on particles and its biogeochemical significance in the Northwest Mediterranean. Limnol Oceanogr 45:419–425. https://doi.org/10.4319/lo.2000.45.2.0419

Valentine DL, Fisher GB, Bagby SC, Nelson RK, Reddy CM, Sylva SP, Woo MA (2014) Fallout plume of submerged oil from Deepwater Horizon. Proc Natl Acad Sci U S A 111(45):15906–15911. https://doi.org/10.1073/pnas.1414873111

Verschuren D (1993) A lightweight extruder for accurate sectioning of soft-bottom lake sediment cores in the field. Limnol Oceanogr 38:1796–1802. https://doi.org/10.4319/lo.1993.38.8.1796

Vogel JS, Southon JR, Nelson DE (1987) Catalyst and binder effects in the use of filamentous graphite for AMS. Nucl Instrum Methods Phys Res, Sect B 29(1–2):50–56

Wakeham SG, Sinninghe Damsté JS, Kohnen MEL, De Leeuw JW (1995) Organic sulfur compounds formed during early diagenesis in Black Sea sediments. Geochim Cosmochim Acta 59:521–533. https://doi.org/10.1016/0016-7037(94)00361-O

Walker BD, Xu X (2019) An improved method for the sealed-tube zinc graphitization of microgram carbon samples for and 14C AMS measurement. Nucl Instrum Methods Phys Res Sect B 438:58–65. https://doi.org/10.1016/j.nimb.2018.08.004

Walker BD, Druffel ERM, Kolasinski J, Roberts BJ, Xu X, Rosenheim BE (2017) Stable and radiocarbon isotopic composition of dissolved organic matter in the Gulf of Mexico. Geophys Res Lett 44:8424–8434. https://doi.org/10.1002/2017GL074155

Williams PM, Druffel ERM (1987) Radiocarbon in dissolved organic-matter in the Central North Pacific-Ocean. Nature 330(6145):246–248

Xu X, Trumbore SE, Zheng S, Southon JR, McDuffee KE, Luttgen M, Liu JC (2007) Modifying a sealed tube zinc reduction method for preparation of AMS graphite targets: reducing background and attaining high precision. Nucl Instrum Methods Phys Res Sect B 259:320–329. https://doi.org/10.1016/j.nimb.2007.01.175

Yan B, Passow U, Chanton JP, Nöthig E-M, Asper V, Sweet J, Pitiranggon M, Diercks A, De P (2016) Sustained deposition of contaminants from the Deepwater Horizon spill. Proc Natl Acad Sci U S A 113(24):E3332–E3340. https://doi.org/10.1073/pnas.1513156113

Chapter 11
Toward a Predictive Understanding of the Benthic Microbial Community Response to Oiling on the Northern Gulf of Mexico Coast

Joel E. Kostka, Will A. Overholt, Luis M. Rodriguez-R, Markus Huettel, and Kostas Konstantinidis

Abstract Benthic ecosystems often act as a repository for oil contamination that washes ashore or is deposited onto sediments following a major oil spill. Sedimentary microorganisms mediate central ecosystem services on the coast, such as carbon and nutrient cycling, and these services may be adversely impacted by oil perturbation. Thus, during the response to the *Deepwater Horizon* (DWH) oil discharge in the Gulf of Mexico, considerable effort went into characterizing the response of benthic microbial communities to oil deposition on shorelines of the Northern Gulf where oil came ashore. Oil perturbation elicited a pronounced microbial response in coastal ecosystems, altering the abundance, diversity, and community composition of sedimentary microorganisms. Next-generation gene sequencing and metagenomic approaches, which were not available during previous large oil spills, have revolutionized the field of microbiology, providing new insights into the microbial response after the DWH discharge. This review centers on a case study of the fate of oil contamination in Pensacola Beach sands, which sheds light on the mechanisms

J. E. Kostka (✉)
Georgia Institute of Technology, Schools of Biological and Earth and Atmospheric Sciences, Atlanta, GA, USA
e-mail: joel.kostka@biology.gatech.edu

W. A. Overholt
Georgia Institute of Technology, Schools of Biological and Earth and Atmospheric Sciences, Atlanta, GA, USA

Friedrich Schiller University, Institute of Biodiversity, Jena, Germany

L. M. Rodriguez-R · K. Konstantinidis
Georgia Institute of Technology, School of Civil and Environmental Engineering, Atlanta, GA, USA
e-mail: kostas.konstantinidis@gatech.edu

M. Huettel
Florida State University, Department of Earth, Ocean and Atmospheric Science, Tallahassee, FL, USA
e-mail: mhuettel@fsu.edu

S. A. Murawski et al. (eds.), *Scenarios and Responses to Future Deep Oil Spills*,
https://doi.org/10.1007/978-3-030-12963-7_11

of microbially mediated hydrocarbon degradation and the impacts of oiling to ecosystem functions. Analysis of field and laboratory results is discussed along with the technological advances that made these observations possible. Metagenomics enabled the application of ecological theory, thereby building a stronger foundation for the effective prediction of baseline microbial community structure/function and response to oiling. Oil perturbation was shown to resemble a press ecosystem disturbance according to the disturbance-specialization hypothesis. Benthic microbial communities were shown to be resilient, maintained ecosystem functions, and recovered quickly after oil disturbance.

Keywords Sediment · Nearshore · Gulf of Mexico · Microorganisms · Petroleum hydrocarbons · Bacteria · Benthic · Deepwater Horizon

11.1 Introduction

The scale and impacts of the *Deepwater Horizon* (DWH) oil spill in the Gulf of Mexico (GoM) were unprecedented. The DWH disaster represents the largest accidental oil spill into the marine environment in history, discharging 4.1 million barrels of liquid hydrocarbons and 1.7×10^{11} g of natural gas into the deep ocean at ~1500 m water depth (McNutt et al. 2012). The emergency response to the DWH spill was also unique in that it incorporated the application of 7 million liters of chemical dispersants, mainly Corexit 9500 and 9527A, at the sea surface and at the discharging wellhead to prevent oil from reaching sensitive coastal ecosystems (Joye et al. 2016).

Approximately one-half of the oil discharged from the DWH blowout reached the ocean surface (Lubchenco et al. 2012), and an estimated 22,000 tons of weathered oil were transported to coastal ecosystems, where it contaminated approximately 1800 km of shoreline from East Texas to West Florida (Michel et al. 2013; Boufadel et al. 2014). Surfaced oil was either redeposited onto the seafloor of the coastal zone through the formation of marine snow (Passow et al. 2012; Brooks et al. 2015) or washed ashore (Michel et al. 2013). Oil was transported high onto the supratidal zone of beaches by waves and tides associated with storms (Michel et al. 2013), and a portion of the oil was deposited in the intertidal and subtidal zones. Because of the dynamic nature of coastal sediments, storms often resulted in the rapid burial of oil in the sediments. Submerged oil mats (SOMs), tens to hundreds of meters long and up to 20-cm thick, have been reported and likely still exist in the inner shelf of the Northern Gulf (Dalyander et al. 2014; Louchouarn et al. 2011; OSAT 2011). Surface residue balls (SRBs), typically 0.5–5 cm in diameter and containing 5–10% hydrocarbons by weight (Urbano et al. 2013) are washed up every day at northeastern GoM shores. Oil thus persists in submerged sublittoral sediments, tidally wetted intertidal sediments, and dry beach sands. Investigating and modeling the fate of buried oil are thus central for risk assessment associated with these hydrocarbons for environmental and human health, coastal food sources, and economic impacts.

Coastal benthic ecosystems are hotspots of biogeochemical activity that provide critical ecosystem services in the GoM (Huettel et al. 2014). These ecosystems drive the Gulf economy through tourism, provide a physical barrier protecting coastal municipalities from storms, and comprise an important habitat for commercially important fish and shellfish. Biodegradation mediated by indigenous microbial communities is the ultimate fate of the majority of oil hydrocarbon that enters the marine environment (Atlas 1995; Leahy and Colwell 1990; Prince 2010). Available oil biodegradation studies to date were primarily focused on the water column and/or deep-sea sediments, and less is known about the response or adaptation of microbial communities to oiling in nearshore or coastal ecosystems (see recent reviews by King et al. 2015; Joye et al. 2016).

Science is largely driven by technological improvements, and the scientific response to the DWH event illustrates this concept. At the time of the Exxon Valdez oil spill in 1989, environmental microbiology was a relatively nascent field, and the ability to determine the structure and functioning of microbial communities in nature was in its infancy. The DWH event was the first major oil spill that occurred after the advent of next-generation sequencing technologies. Prior to the DWH spill, relatively little baseline information was available from Gulf ecosystems. With newfound capabilities, microbiologists were able to effectively track the impacts of oil on microbial communities, and much progress has been made to determine the response of specific bacterial taxa to oil contamination in impacted Gulf ecosystems (see reviews of King et al. 2015 and Joye et al. 2016). However, beyond this descriptive understanding, very little quantitative information exists on the specific pathways and metabolites employed by microorganisms to break down oil and how the environmental conditions affect biodegradation rates. The majority of previous work on hydrocarbon-degrading bacterial communities in the marine environment has been conducted under enrichment conditions in laboratory microcosms, employing PCR (polymerase chain reaction) amplification and sequencing of SSU (small subunit) rRNA genes. A paucity of information exists on the impacts of oil contamination to the metabolic potential or functioning of indigenous bacterial communities under in situ or natural attenuation conditions. Addressing these knowledge gaps will lead to the identification of robust biomarkers of oil degradation and thereby, improvement in our ability to predict the fate of oil in nearshore ecosystems. Biomarkers that are representative of the different phases/stages in oil degradation, possibly including oil-sensitive organisms, can help site managers to monitor oil degradation and decide on the appropriate actions such as stimulating the biodegradation process (e.g., biostimulation, through manipulation of environmental conditions), with obvious benefits for restoring ecosystem functions and minimizing risk to human and animal health. To enable informed biostimulation of oil degradation, a thorough knowledge of the environmental controls of microbial decomposition processes is prerequisite.

In this chapter, the state of the field and overarching questions on the microbial response to oiling based on a case study conducted in shallow coastal sediments is reviewed. Due largely to their accessibility, coastal ecosystems provide an ideal natural laboratory to investigate the in situ effects of oil discharged from the DWH disaster. This review will center on advances to the field and lessons learned from these investigations.

11.2 Fate of Petroleum Hydrocarbons at Pensacola Municipal Beach

Oil washed ashore on Pensacola municipal beach (PB) in repeated pulses of deposition during a 1-month period from June to July of 2010, with total petroleum hydrocarbon (TPH) concentrations reaching up to ~2 kg per meter of beach (Huettel et al. 2018). Due to high ambient temperatures at this time of the year, stranded oil heated up and pooled over large swathes of the beach surface (Fig. 11.1). Beaches are dynamic environments, and over the course of the next few months, waves and storms acted to bury oiled sand layers deeper into the sediment column, with oiled sand grains and smaller oil particles mixed below the beach surface. By October 2010, the oiled sand layer had reached 70 cm below surface.

Responders of the Unified Area Command as well as stakeholders were concerned about the potential impacts of this buried oil to environmental and human health. Thus, BP initiated cleanup efforts termed "Operation Deep Clean" (ODP) designed to mechanically extract larger oil sand aggregates from beaches in Florida to Louisiana

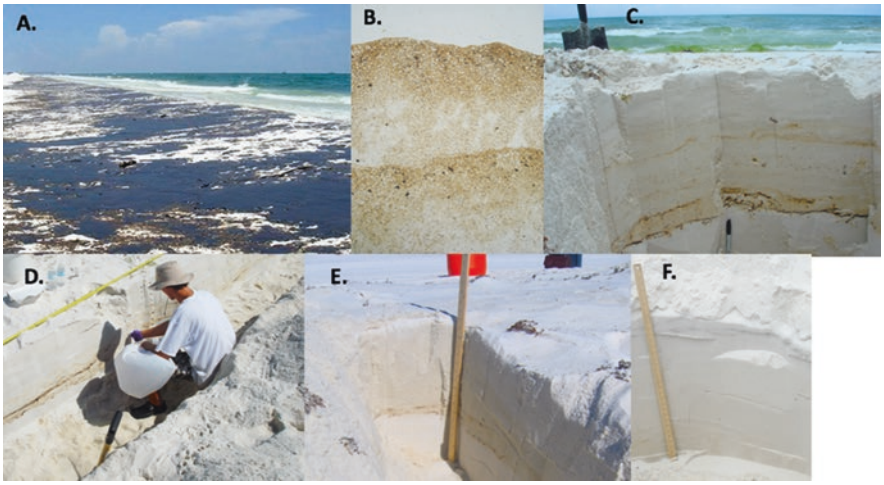

Fig. 11.1 DWH oil contamination at Pensacola Beach/Florida (30°19′32.08″N, 87°10′30.55″W). (**a**) The oil-contaminated beach on June 24, 2010 (image Florida DEP, public domain). (**b**) Oil film and small oil particles deposited on the beach surface by waves on July 1, 2010. The water containing oil drained through the permeable sand, leaving oil at the surface but also transporting small oil particles into the sediment. (**c**) Beach cross section on July 25, 2010, with a dark double layer produced by oil deposited during the nights of June 22 and June 23 at 45–50 cm depth. (**d**) Will Overholt sampling sediment on September 1, 2010, in a trench with a ~10-m long dark vein of buried oil. (**e**) Beach cross section on December 2, 2010, with a homogeneously brown-stained sand layer redeposited by ODC after removal and sifting. Some remains of the deep dark oil layers depicted in (**c**) were still present. (**f**) Beach cross section on April 21, 2011. No visible oil stains were left in the sediment. Gray layers near the surface are detrital material, not oil. (Reprinted from Huettel et al. (2018), Copyright (2018), with permission from Elsevier)

(Hayworth and Clement 2011). Using a machine dubbed the "Sand Shark," oiled sands were excavated, pulverized, sifted, mixed with clean sands, and redeposited onto the beach. ODC cleaning operations were strictly physical, with no chemical or biological treatment, removing sand to a depth of ~45 cm and separating out particles >2 mm from the sand. Despite this massive cleanup, little quantitative information was collected to track the oil contamination, and therefore the processes controlling buried oil decomposition and decay rates remained largely unquantified. This cleanup activity illustrates a disconnect between the emergency and scientific responses to the DWH disaster.

The fact that the MC-252 discharge represented an unprecedented release of oil in deep water (1500-m water depth; Atlas and Hazen 2011) as well as concerns for understudied deep-sea habitats led to a surge of research on offshore systems surrounding the wellhead (King et al. 2015). By contrast, coastal response efforts somewhat lagged behind studies conducted in the deep sea (Hayworth and Clement 2011). The role of permeable sand microbial communities in mediating ecosystem services was studied, such as carbon and nutrient cycling, in the Northern Gulf for a number of years (Huettel et al. 2014). It was hypothesized that the burial of the oil would trigger blooms of aerobic microbial communities, including hydrocarbon-degrading microbial groups, and these bacterial blooms would rapidly degrade buried petroleum hydrocarbons due to the constant replenishment of oxygen by tidal pumping. Therefore, the objectives of this research were to (1) determine the rates and mechanisms of microbially mediated hydrocarbon degradation, (2) assess the impacts to critical ecosystem functions, and (3) develop microbial indicators for the extent of biodegradation. The assessment of the microbial response closely combined state-of-the-art biogeochemical and microbiological approaches along with leveraging previous research at Pensacola Beach. Field efforts were intense, including sampling at monthly intervals over a nearly 2-year period. This research also represented one of the first large-scale applications of next-generation sequencing technologies to the understanding of microbial community dynamics in Gulf sediments.

Oxygen is a master chemical variable limiting hydrocarbon biodegradation (Head et al. 2006; Prince 2010). Half-lives of petroleum hydrocarbons range from days to months under aerobic conditions, whereas these same compound classes persist for years under oxygen-depleted conditions. Warm, wet, and mostly well-aerated Gulf beach sands in many respects represent ideal environments for microbial growth and metabolism. Field observations supported these assumptions. In the summer and fall of 2010, sediment temperatures ranged from 30 to 40 °C. Most of the oil was stranded in the supratidal zone, where sands maintained a moisture level of 2–7%. In this moist but unsaturated environment, sands remained aerobic, although oxygen concentrations of 50% saturation were measured in layers exposed to heavy oiling (Huettel et al. 2018). Petroleum hydrocarbons (PHCs) were rapidly degraded in beach sediments, with half-lives of aliphatic and aromatic hydrocarbons reaching 25 and 22 days, respectively (Fig. 11.2). The majority of PHCs were depleted within the first 4 months after oil came ashore, and by March of 2011, concentrations were not significantly different from those of pristine reference sites.

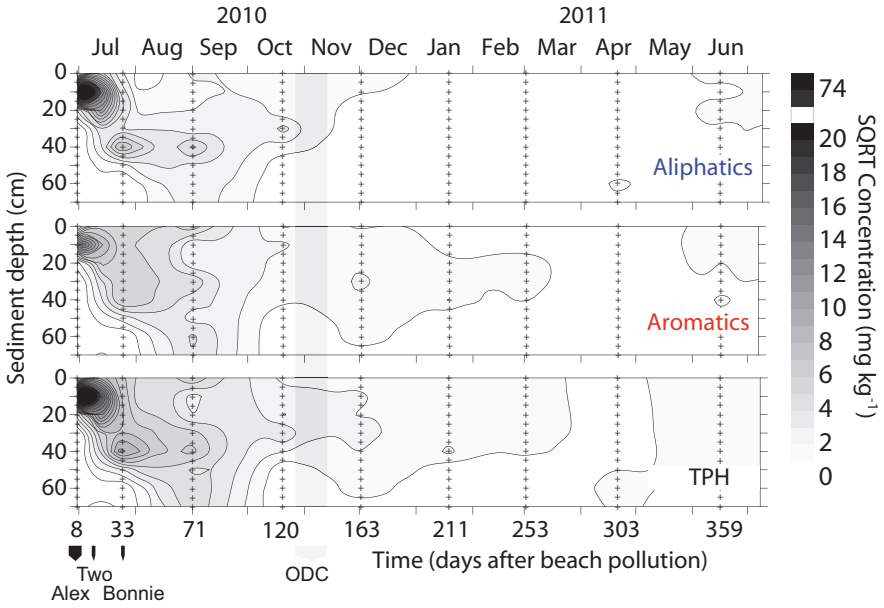

Fig. 11.2 Spatial and temporal distribution of buried oil concentrations in PB sand. Note that the concentrations were square root transformed to accommodate their full ranges. Small "+" symbols indicate sampling dates and depth intervals. The TPH panel depicts total petroleum hydrocarbon concentrations. Black arrows at the lower left (below numbered X-axis) indicate dates and durations of the tropical storms that affected Pensacola Beach. (Reprinted from Huettel et al. (2018), Copyright (2018), with permission from Elsevier)

11.3 Diagnosis of the Oil-Induced Bacterial Bloom Using Next-Generation Sequencing Methods

Prior to 2010, methodological limitations hampered the ability to characterize the dynamics of in situ bacterial communities responding to environmental perturbations such as the presence of oil contamination. The majority of previous work was conducted under enrichment conditions in laboratory microcosms, and microbial communities were investigated through cloning and sequencing of SSU rRNA genes. Little baseline information was available on microbial communities from sedimentary or planktonic environments in the Gulf.

Diagnosis of a large bacterial bloom in response to DWH oiling of PB sands and the subsequent succession of microbial populations were facilitated by next-generation sequencing technologies, mainly in terms of the scale and resolution of analysis. In a matter of months, hundreds of samples could be interrogated for abundance and community composition using PCR-based methods, and thousands of gene sequences per sample supported determination of taxonomic diversity. Herein, a description is provided on how these technological advances were employed in this PB case study.

Initial characterization after the spill supported previous work (Hunter et al. 2006; Mills et al. 2008; Gihring et al. 2009; Huettel et al. 2014) to demonstrate that permeable sands, which cover large portions of the shallow ocean globally, contain highly diverse bacterial communities that are predominated by members of the *Gammaproteobacteria* and *Alphaproteobacteria* (Kostka et al. 2011; Gobet et al. 2012). Microbial communities in Pensacola Beach sands were shown to be more diverse than marine bacterioplankton but not as diverse as the bacterial communities of marine muds. Once improved PCR primers were made available (Caporaso et al. 2010), abundant archaea were also observed in the PB sands (Huettel et al. 2018).

A series of field investigations demonstrated that buried oil at PB was degraded by a succession of hydrocarbon-degrading microbial populations (Kostka et al. 2011; Rodriguez-R et al. 2015; Huettel et al. 2018). Hydrocarbon degradation was concomitant over space and time with a large bacterial bloom (Fig. 11.3). Bacterial abundance increased by two to four orders of magnitude in buried oil layers in comparison to lightly oiled or unoiled sands, and moreover, the depth of the bacterial bloom moved deeper into the beach sand over time in parallel with the residual PHCs. RNA-based analyses as well as cultivation-based studies confirmed that predominant hydrocarbon-degrading bacterial groups were metabolically active in oiled sediment layers. Further, oiling exerted a strong selective pressure on benthic microbial communities, resulting in profound changes to taxonomic diversity and composition. Similar to bacterial abundance, taxonomic diversity declined in parallel with the concentration of PHCs in oiled sands and rebounded as hydrocarbons became depleted (Fig. 11.3). The distribution of microbial populations, soon after oil came ashore, reflected profound changes to community composition. In some cases, known hydrocarbon-degrading microbial groups such as *Marinobacter* comprised over 50% of the microbial community in heavily oiled sand layers (Huettel et al. 2018).

Oil perturbation selected for populations of winners and losers. Over a 1-year period, a succession of microbial populations, dominated by known aerobic hydrocarbon-degrading bacteria, was enriched and then declined concurrently with PHC concentrations. Microbial groups known to degrade aliphatic hydrocarbons, mostly members of the *Gammaproteobacteria* (*Alcanivorax*, *Marinobacter*), responded first to oil contamination and were then replaced after 3 months by populations of *Alphaproteobacteria* (*Hyphomonas*, *Parvibaculum*) capable of aromatic hydrocarbon decomposition (Fig. 11.3). After 1 year, a typical benthic microbial community had reestablished that showed little to no evidence of oil hydrocarbon degradation potential, but it differed significantly from the community present before the oil spill. Observations are generally corroborated by studies conducted at other Gulf beaches over the same period of time. In a study conducted at Elmer's Beach in Louisiana, Lamendella et al. (2014) found that microbial abundance increased by two orders of magnitude in oiled sands, with members of the *Alpha-* and *Gammaproteobacteria* dominating successional changes. Likewise, Newton et al. (2013) reported that members of the *Gammaproteobacteria* (*Alcanivorax*, *Alteromonas*, *Marinobacter*) exhibited the largest increase in relative abundance in oiled sands collected from beaches along the Mississippi, Alabama, and Florida coasts between June and November 2010.

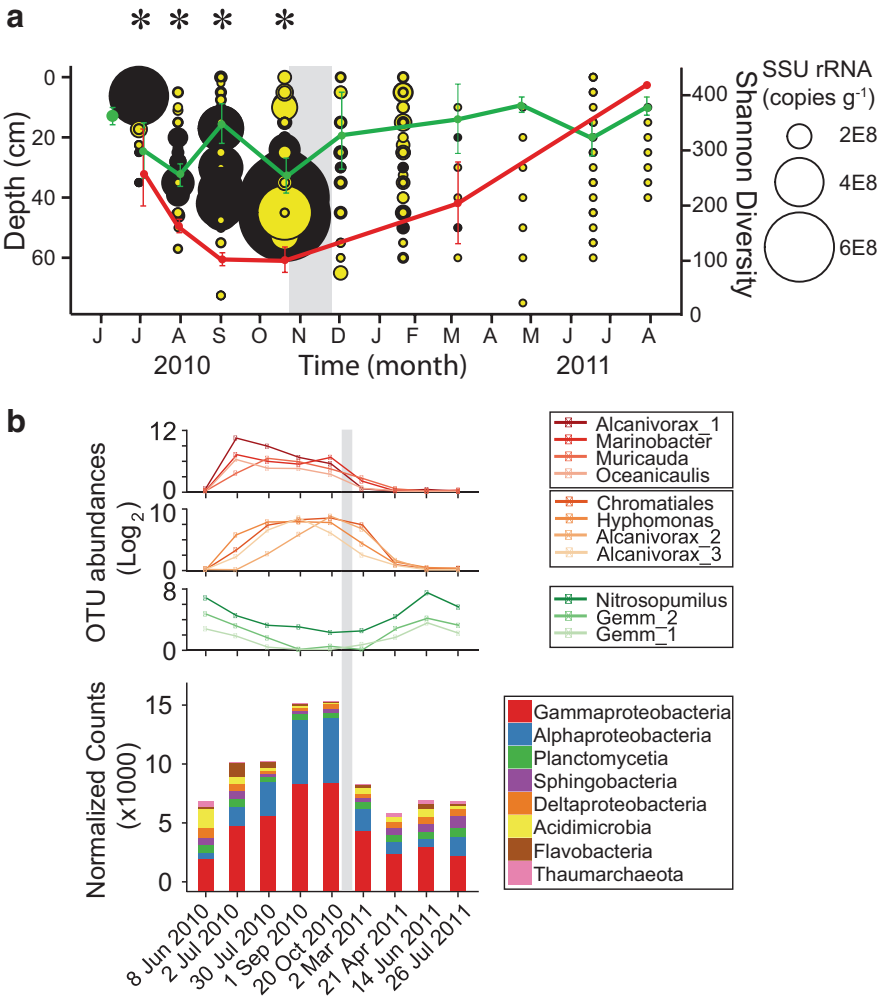

Fig. 11.3 Development of microbial communities in Pensacola Beach sands. (**a**) Abundances of bacterial small-subunit (SSU) rRNA genes in heavily contaminated sand (solid black circles) and in lightly contaminated sand (yellow circles). Asterisks indicate significant difference in SSU rRNA gene copies between heavily and lightly oiled sand (Welch's t-test, $p < 0.05$). The green circle in June 2010 represents diversity at the SGI reference site. The green line depicts the average Shannon diversity in OTU equivalents ($e^{H'}$, secondary y-axis) in the lightly oiled layer, and the red line represents Shannon diversity in the heavily oiled layer. After March 2011 all samples had no visible oil. Error bars represent standard error. (**b**) Time series of the abundances of oil-degrading bacteria that peaked in the first week after beach contamination. Upper line graph: *Marinobacter*, which dominated in June, had already decreased by July 2. Middle line graph: oil degraders that increased 1 week after beach contamination. Lower line graph: microbial groups that declined after oiling. Column graph: microbial community compositions in heavily and lightly oiled sand layers. Normalized counts independently agree with qPCR data shown in (**a**). The June 8, 2010, sample was collected prior to the beach oil contamination. The vertical gray bar in A and B depicts the time frame of ODC. (Reprinted from Huettel et al. (2018), Copyright (2018), with permission from Elsevier)

Clearly, the buried DWH oil enhanced microbial growth and metabolism in coastal sediments by acting as a carbon and energy source to heterotrophic bacteria. Although weathering during transport removed most short-chain (<14 C atoms) PHC from the oil before it was buried in the beach (Huettel et al. 2018), the oil from the Macondo well, a "light Louisiana Sweet Crude," was characterized by relatively high degradability (Reddy et al. 2012). Buried oil thus acted as a strong selective pressure on microbial communities and was rapidly degraded under close to ideal conditions, allowing recovery within 1 year.

11.4 Using Metagenomics to Determine the Functional Response to Oil Contamination

Although findings from next-generation sequencing of rRNA gene amplicons provided important insights on the benthic microbial community response to oiling, the pathways/controls of hydrocarbon degradation and specific impacts to ecosystem function remained mostly unknown. The use of metagenomic techniques catalyzed more fundamental discoveries in these areas.

Researchers generated what remains as the largest metagenomic time series available from the DWH response. This time series encompassed 16 samples, with at least triplicate metagenomes from 4 time points, and over 450 million gene sequences (Rodriguez-R et al. 2015). More importantly, the time course covered from pre-oiling to recovered microbial communities. Overall, metagenomic results supported observations based on next-generation sequencing of SSU rRNA genes (Fig. 11.4). Metagenomes from PB sands were more diverse than bacterioplankton and less diverse than fine-grained soils and sediments. The same abundant groups of known hydrocarbon-degrading bacteria were detected in metagenomes from oiled sands, and shifts in taxonomic diversity closely paralleled observations from studies of SSU rRNA genes. Novel observations were revealed in the functional diversity and metabolic potential of benthic microbial communities.

The pulsed inputs of weathered Macondo oil on PB can be considered as a press disturbance of the ecosystem. The ecological principles controlling the response of biological communities to disturbance were mainly studied previously in plants and animals, and the role of ecological theory in microbial ecology is in its infancy (Prosser et al. 2007; Prosser 2012). Rodriguez-R et al. (2015) posited that the response of PB sand microbial communities to oiling could be predicted by the specialization-disturbance hypothesis following previous observations in plant communities of other ecosystems (Vazquez and Simberloff 2002). This was surprising in that it was contrary to the expectations from most microbiology enrichment experiments. The hypothesis states that the majority of the microbial community is selected based on the ability to survive under disturbed conditions and the response to disturbance correlates negatively with the level of functional specialization. The result is that generalist microbial populations with traits selected by the disturbance, largely hydrocarbon-degrading bacteria in this case,

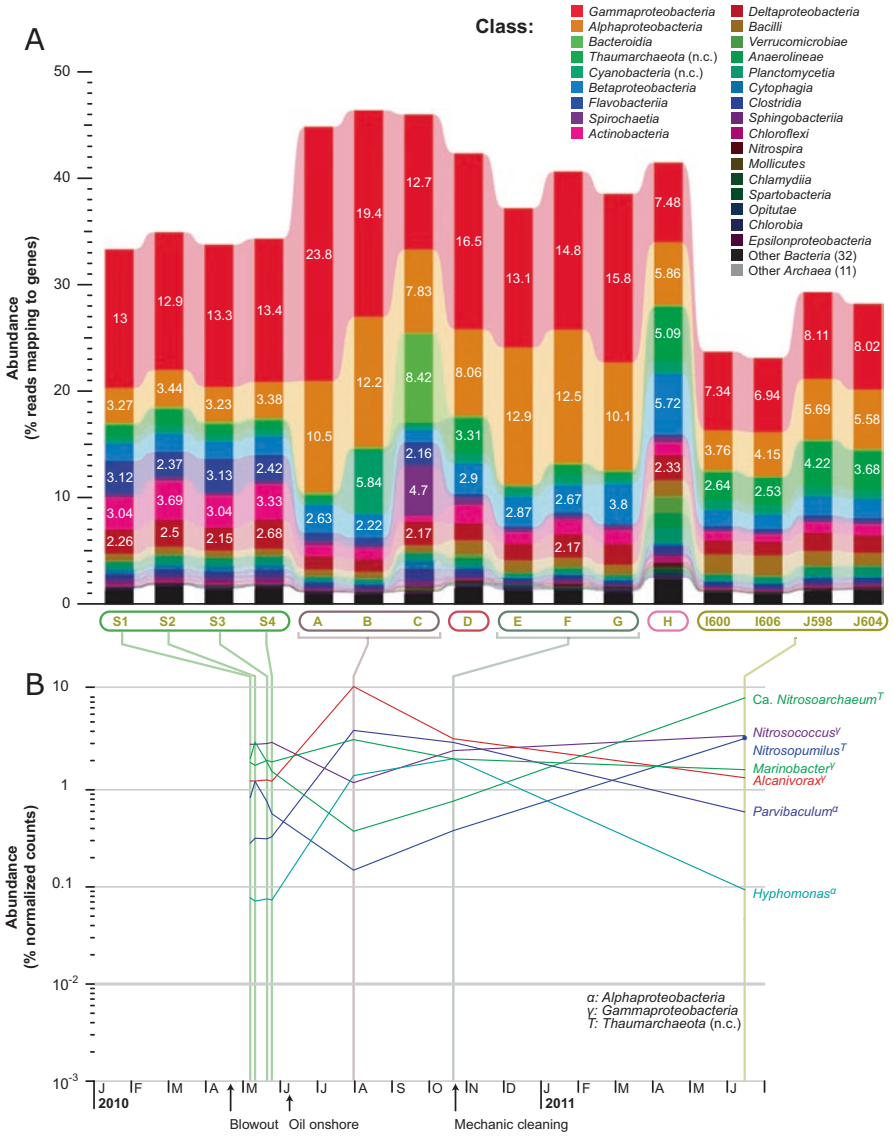

Fig. 11.4 Taxonomic shifts in the microbial community in response to oil. The distribution of metagenomic reads in (**a**) classes displayed for taxa that recruited more than 10% and 2% of the total reads, respectively (white numbers). (**b**) Genera with abundance above 0.1% and significantly different between pre-spill and oiled or between oiled and recovered samples (*P*-value adjusted, $p < 0.01$) are also displayed. The minimum and maximum abundance of each genus is indicated with open and filled circles, respectively, and the class is indicated with superscripts. (Reprinted by permission from Springer Nature: Rodriguez-R et al. (2015))

become highly abundant. Conversely, specialist taxa, adapted to relatively narrow niches, are selected against. Field observations from our metagenome time series supported the disturbance-specialization hypothesis. In contrast to taxonomic diversity, communities exhibited an increase in functional diversity in oiled samples with respect to pre-oiled samples and a reduction in functional diversity in recovered samples in comparison to oiled samples. It was concluded that specialists adapted to oligotrophic conditions, mainly chemolithoautotrophic nitrifiers, were outcompeted upon oil deposition. Sandy sediments are nutrient poor and would favor functional specialization in their pristine condition. Comprised of tens of thousands of different carbon compounds, oil input would likely stimulate fast-growing copiotrophic generalists during early succession, while toxic compounds would likely select against specialists. Indeed, fast-growing hydrocarbon-degraders (*Pseudomonas*, *Marinobacter*, *Parvibaculum*, *Hyphomonas*) dominated, and generation times calculated from metagenomic data were lower in oiled communities, whereas putative chemolithoautotrophic archaea (*Nitrosopumilus*, *Cenarchaeum*), presumably adapted to carbon-limited conditions, predominated in the pre-oil and recovered communities. Selection against nitrifying taxa suggests that critical ecosystem services provided by the microbial nitrogen cycle may be disrupted by oiling. These observations warrant further investigation under controlled conditions in the laboratory where the functioning of microbial communities can be better constrained.

Given the observations that oiling selected for generalist heterotrophs, the dominance of *Alcanivorax* in oiled sediments throughout these studies is somewhat puzzling. *Alcanivorax* is considered as an obligate hydrocarbonoclastic organism with a narrow range of carbon substrate utilization and therefore does not fit the definition of a generalist. Some evidence indicates that the utilization of PHCs is a strain-specific trait (Head et al. 2006). Perhaps, the *Alcanivorax* genus contains generalists that have not yet been cultivated or the definition of obligate hydrocarbonclastic bacteria requires revision (see below for further discussion). For example, Barbato et al. (2016) reported the capacity of *Alcanivorax* strains to utilize carbon sources alternative to hydrocarbons, which allows them to permanently colonize pristine marine environments. According to these authors, the differential transcriptomic responses to hydrocarbons in the different *Alcanivorax* strains make them a functionally redundant and plastic reservoir of oil-degrading players, able to activate in the case of oil-spill occurrence, sustaining natural attenuation and biostimulation-based cleanup processes.

Our metagenomic time series further revealed the pathways and controls of PHC degradation. Communities of oiled sands contained a statistically significant, higher abundance of gene annotations associated with hydrocarbon degradation in comparison to pre-oiled and recovered communities (Rodriguez-R et al. 2015; Fig. 11.5). Concurrent with the transition from alkane-degrading *Gammaproteobacteria* to *Alphaproteobacteria* capable of utilizing more recalcitrant aromatics, the relative abundance of genes associated with aliphatics degradation peaked in July and dropped from July to October 2010. Conversely, the abundance of genes associated

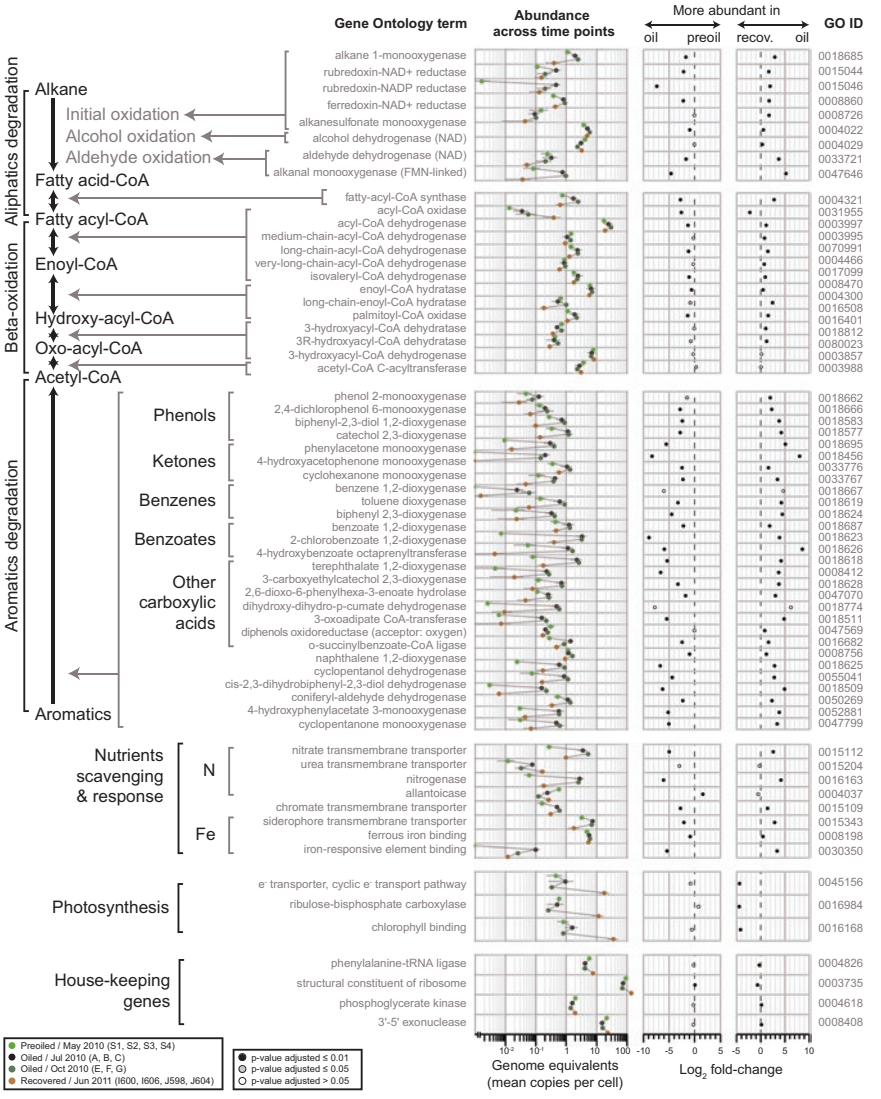

Fig. 11.5 Microbial community functional shifts in response to oil. Selected molecular functions related to hydrocarbon degradation, nutrient scavenging and response, photosynthesis, and some housekeeping genes are listed (left) along with the mean genome equivalents per group of samples (middle) and the log2 of pre-oil/oiled and oiled/recovered fold changes (right). The rightmost column indicates the GO ID of the terms. The abundance was assessed as average genome equivalents (mean copies per bacterial/archaeal cell) on each sampling time (downwards; see legend). The triangles indicate values below the plotted range. The log2-fold-change was estimated as the log2 of the ratio of normalized counts between pre-oiled samples (S1, S2, S3, S4) and oiled samples (A, B, C, E, F, G) and between oiled samples and recovered samples (I600, I606, J598, J604). P-values were estimated using a negative binomial test. (Reprinted by permission from Springer Nature: Rodriguez-R et al. (2015))

with aromatics degradation was maintained or increased from July to October. Genes associated with nutrient acquisition, such as genes encoding nitrogenase that catalyzes the reduction of atmospheric dinitrogen to ammonium, showed elevated abundance in oiled samples. These observations are corroborated by previous studies that indicate oil-contaminated environments are nutrient-limited (Joye et al. 2016). Moreover, the genomes of these key populations have been recovered, and the corresponding sequences are publicly available as part of NCBI's SRA database. These genomes are expected to greatly facilitate future studies such as the design of PCR assays to study in situ gene expression and activity. The great majority of these abundant populations during oiling were shown to represent novel species, if not genera, compared to the already described taxa (Rodriguez-R et al. 2015), indicating that several more mysteries remain to be solved in the not-so-distant future.

A key knowledge gap in oil spill science is the definition of baselines in biological communities. At PB, both SSU rRNA gene amplicon and metagenomic data indicated that after 1 year, microbial communities recovered to a state that resembled the pre-oil condition (Rodriguez-R et al. 2015; Huettel et al. 2018). However, significant differences were observed between the pre-oiled and recovered communities. Taxonomic diversity remained elevated in recovered communities, above that of the pre-oiled community, while functional diversity was lower in the recovered compared to the pre-oiled. Why and how are these recovered communities different? Recovered communities contained higher relative abundances of eukaryotic and archaeal taxa in comparison to pre-oiled and oiled communities. Such differences could be due to unrecognized long-term effects of disturbance, such as the emergence of new taxa, and stochastic environmental events such as changes in nutrient or carbon input. However, they may also be linked to patterns in seasonality and reflect the dynamic nature of beaches rather than long-term impacts. This is an open question that is actively being pursued as a legacy DWH issue. Future work such as laboratory incubations with beach sands that simulate well the in situ environment while circumventing the stochastic fluctuations are expected to offer new insights into the latter issues.

Another open question in the field is whether oil-contaminated environments are "primed" for hydrocarbon degradation. In other words, it has been hypothesized that microbial populations have evolved and adapted to degrade petroleum compounds in environments where these have been introduced on a regular basis, such as in natural hydrocarbon seeps in the Gulf. An alternative hypothesis states that since oil is a natural product and natural organic matter from recently dead plants/animals contains similar compounds (Lea-Smith et al. 2015), microbial populations that degrade petroleum hydrocarbons are ubiquitous in marine and terrestrial ecosystems. To investigate the evolutionary history of hydrocarbon degradation, genes encoding AlkB (alkane hydrolase) were characterized as a marker for alkane degradation. A large diversity of *alkB* genes was observed in PB sands that did not appear to be constrained by oiling. Alkane degradation was mediated by a large latent diversity of alkane-degraders that were already present in the sand prior to oiling, perhaps living off of residual oil or natural organic matter.

11.5 Linking Advances in Metagenomics to Cultivation

Metagenomics approaches have revolutionized the field of microbiology; nevertheless, these methods remain new and they should be employed as a part of a polyphasic approach. To completely verify the metabolism or function of a microorganism, it is necessary to bring that organism into pure culture. This case study demonstrates the need to employ a combination of cultivation-dependent approaches alongside cultivation-independent molecular techniques to fully characterize the microbial response to the input of petroleum hydrocarbons. Pure cultures were obtained for many of the predominant hydrocarbon-degrading genera which were detected in abundance with next-generation sequencing approaches in field samples (Kostka et al. 2011). Overholt et al. (2013) then sequenced the genomes of ten representative strains to facilitate their use as model organisms for further physiological studies in the laboratory. In parallel, Eren et al. (2015) leveraged our metagenomic time series to test a new bioinformatics platform, named Anvi'o, designed to analyze and visualize metagenomic data. Whereas previously published analysis involved assembly of metagenomic sequences without binning (Rodriguez-R et al. 2015), the Anvi'o platform was used to bin the sequences and construct genomes for individual microbial populations. This is now referred to as metagenome-assembled genomes (MAGs). Anvi'o detected a total of 56 MAGs from 33 genera, including a fungus and a cyanobacterium in PB sands. At a broader resolution, the taxonomy of the MAGs largely agreed with the results presented in Rodriguez-R et al. (2015). However, Eren et al. (2015) concluded that model pure cultures such as *Alcanivorax* sp. P2S70, though present in abundance, represented a minority of the hydrocarbon-degraders responding to oil input at PB. Rather, the genomes of uncharacterized members of the *Gammaproteobacteria* and *Alphaproteobacteria* showed the highest relative abundance in oil-impacted sediments. The results imply that characterization targeted to the sequencing of single taxonomic marker genes, such as SSU rRNA, is insufficient for the accurate determination of microbial community dynamics at high resolution. The fact that uncharacterized organisms are dominant indicates that there is much to learn about the physiology of microbial responders to oil spills. The conclusion that many of the important oil-degraders had been cultivated from PB beach turned out to be only partially correct. This calls for more cultivation-based studies directed by information on the putative metabolism of uncharacterized taxa gleaned from MAGs. In addition, whole genomes should be used, and further advances in bioinformatics are needed to fully investigate the metabolic potential of complex microbial communities that respond to oil.

Alcanivorax is arguably the best studied of hydrocarbon-degrading taxa, and the 15 described species of this group are considered as obligate hydrocarbonoclasts, with a narrow range of carbon substrate utilization (Yakimov et al. 2007). While there have been no detailed comparative genomics studies on this group, *Alcanivorax borkumensis* has been extensively studied as a model organism for the genus due to its cosmopolitan distribution, putative ecological role in oil-degrading consortia, and the ability for researchers to manipulate its genetic system (Schneiker et al. 2006;

Shao and Wang 2013; Yakimov et al. 2007). *A. borkumensis* is characterized by a highly restrictive growth profile and contains the features of oligotrophic bacteria with a large number of nutrient transporters that allow a rapid response to hydrocarbons under nutrient poor conditions (Schneiker et al. 2006; Yakimov et al. 2007). *A. borkumensis* grows on a diverse range of aliphatic hydrocarbons including n-alkanes (max n-C_{32}), long-chain isoprenoids, phytane, pristine, and alkyl aromatic-hydrocarbons (Yakimov et al. 2007). Members in this genus have a large number of alkane degradation systems under complex metabolic regulation associated with chemotaxis as well large changes in central metabolic networks (Sabirova et al. 2006, 2011; Schneiker et al. 2006; van Beilen and Funhoff 2007; Wang and Shao 2014; Barbato et al. 2016).

It is not well known how interacting *Alcanivorax* populations respond to hydrocarbons within an impacted community, and these case studies document multiple distinct groups. Of these, multiple investigations pointed to *Alcanivorax* sp. P2S70 as the most abundant characterized strain in oiled PB beach sands, and strain P2S70 showed the highest potential for oil degradation in pure culture studies (Overholt et al. 2016). Initial physiological characterization revealed contrasts between strains isolated from PB sands impacted by the DWH spill, suggesting niche specialization in carbon and major nutrient metabolism (Kostka et al. 2011). Another isolate from oiled PB sands, *Alcanivorax* strain PN3, showed a much lower potential for hydrocarbon degradation in culture. Detailed phylogenetic analysis of full-length rRNA genes shows that strain PN3 shares high sequence identity with *Alcanivorax dieselolei*, whereas P2S70 is more related to *A. nanhaiticus* (Fig. 11.6). Comparison of whole genomes using conserved single copy genes generally supports the interpretation based on SSU rRNA genes, although P2S70 is more closely related to the *A. borkumensis* genomes (Fig. 11.6). Strain PN3 is confirmed to be highly similar to the *A. dieseloli* group, sharing an average nucleic acid identity (ANI) of >99% to *A. xenomutans* and *A. dieseloli* KS-293 genomes as well as an ANI of 93% with *A. dieseloli B5* (the type strain). Moreover, genome sequencing revealed substantial variation in the assembly and number of hydrocarbon degradation genes between *Alcanivorax* strains, suggesting strain-specific differences in metabolism and hydrocarbon degradation potential (Overholt et al. 2013). P2S70 exhibited similar genome streamlining as seen in the *A. borkumensis* genomes with around 3000 genes, while PN3 and all *A. dieselolei* strains have 1 Mb larger genomes with over 4000 genes. Field observations corroborate these genotypic and phenotypic results from the laboratory to indicate that hydrocarbon degradation is a strain-specific trait (Head et al. 2006; Kostka et al. 2011; Huettel et al. 2018). At least three different dominant *Alcanivorax* OTUs were detected in our PB time series with contrasting ecological response strategies. One OTU, similar to P2S70, showed a maximum in abundance during the first few months after oil came ashore when lower molecular weight aliphatic compounds were degraded, whereas other *Alcanivorax* OTUs peaked in abundance later in the time course, concurrent with the depletion of more recalcitrant classes of hydrocarbon compounds. A similar pattern was evident in the Eren et al.'s (2015) study where two MAGs (P2S70 and one similar to *A. jadensis*) responded immediately following oiling and one followed later. However, follow-up

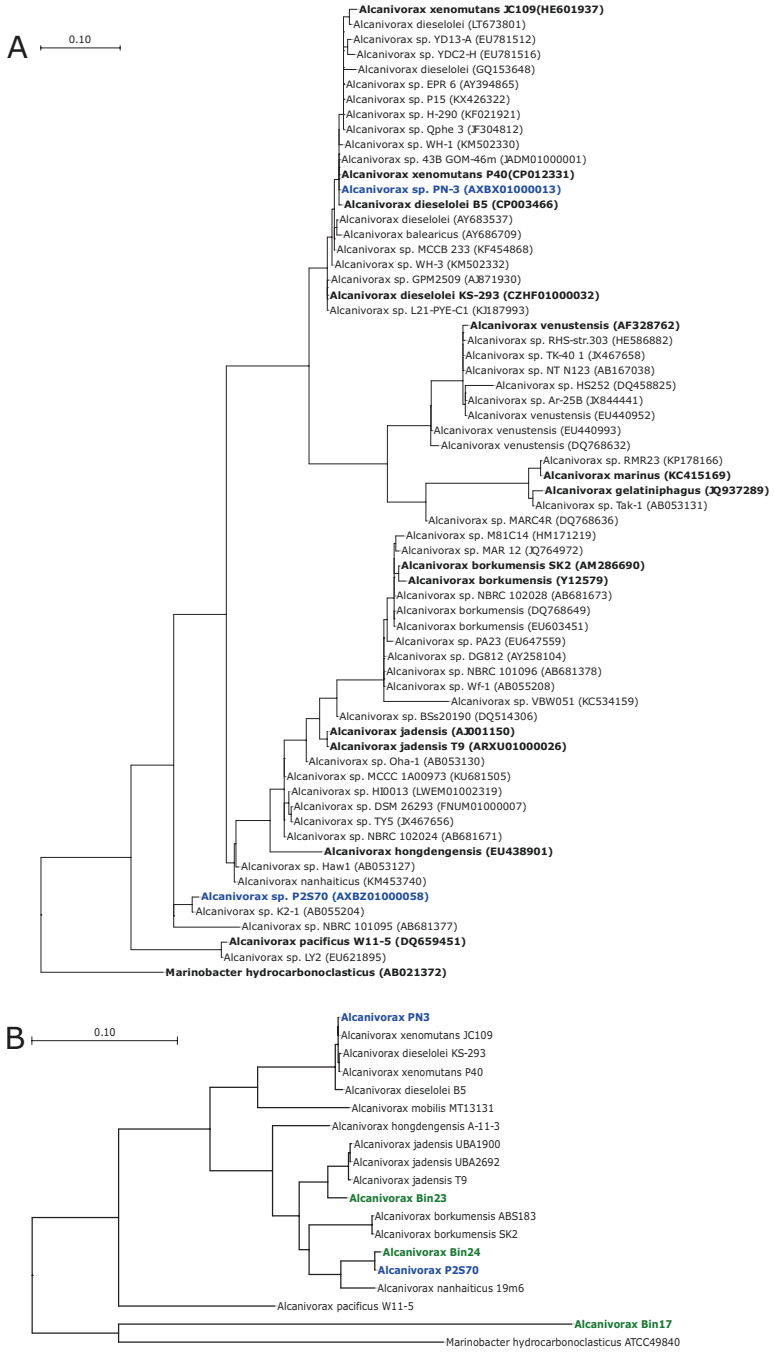

Fig. 11.6 Phylogenetic analysis of the characterized strains of the *Alcanivorax* genus. Isolates from Pensacola Beach are highlighted in blue, and type strains as well as strains with a whole genome available are bolded. (**a**) Full length, bootstrapped, maximum likelihood SSU rRNA gene tree generated from SILVA aligned sequences with the bacterial weighting mask available in ARB. (**b**) Whole genome tree generated according to the approach of Parks et al. (2018) from a concatenated alignment of single copy reference genes used by the Genome Taxonomy Database (Parks et al. 2018). The *Alcanivora*x subtree displayed is congruent with a whole genome tree generated from all orthologous genes (845), as well as a UPGMA dendrogram from average amino acid identities (AAI) across all genomes (data not depicted)

phylogenetic analysis suggests that the late responder (Bin17) is not with the *Alcanivorax* group and is instead affiliated with the order *Cellvibrionales* (Fig. 11.6, MiGA taxonomic assignment not shown). It is concluded that the *Alcanivorax* group exhibits a much larger genotypic and phenotypic plasticity than was previously perceived. *Alcanivorax* strains appear to exploit a larger range of niches, including the ability to metabolize more recalcitrant aromatic or aliphatic compounds along with alkanes.

11.6 Conclusions and Guidance for Future Emergency Response Efforts

Technological advances have enabled tremendous progress in the ability to identify the predominant microbial populations and their succession in response to oil perturbation. The emergence of metagenomics approaches has greatly facilitated the interpretation of the metabolic potential of microbial responders. The research community has a much better idea of "who's there," while it remains difficult to interpret "what they are doing there" and perhaps more importantly, "how fast and under what environmental conditions." At Pensacola Beach, results showed that oiling led to a large increase in the growth and metabolism of indigenous microbes in the form of a bacterial bloom. Oil contamination strongly selected for microbial groups capable of hydrocarbon degradation, leading to a drastic decline in taxonomic diversity, as has been observed in other oiled ecosystems. A succession of microbial populations was observed to parallel the chemical evolution of petroleum hydrocarbons. Oil was degraded, and benthic microbial communities returned to near-baseline levels, with little evidence of hydrocarbon-degrading bacteria, approximately 1 year after oil came ashore. Close coupling of biogeochemistry, next-generation sequencing, and metagenomics approaches provided evidence in support of the disturbance-specialization hypothesis. Surprisingly, the functional diversity of microbial communities increased during active degradation in oiled sand layers, indicating a selection for generalist copiotrophs and against specialist oligotrophs such as nitrifying prokaryotes. These observations comprise promising steps toward using ecological principles to predict the microbial response to major perturbations such as oil spills.

This case study indicates that benthic microbial communities contain a high potential for petroleum hydrocarbon biodegradation. Moreover, these results indicate that even when small oil particles (<1 cm) are buried in the coastal zone, biodegradation by indigenous microbial communities is sufficient for the rapid mitigation of oil contamination after a major spill, in the presence of sufficient levels of oxygen and nutrients. Larger sand-oil aggregates take longer to completely degrade because of their unfavorable surface to volume ratio. "Operation Deep Cleaning" removed these aggregates but also involved biostimulation insofar as many larger oil aggregates were broken down into smaller ones thereby increasing the surface area available for microbial degradation. For environmental managers, these results suggest that petroleum hydrocarbon degradation in beach sands is relatively rapid because oxygen can easily penetrate to the buried oil, and resources may be better placed elsewhere in environments where degradation is limited by

oxygen availability or physical access to hydrocarbons. Other remediation strategies such as bioaugmentation, which involves seeding the natural microbial communities with hydrocarbon-degrading bacteria, are unlikely to facilitate a more rapid biodegradation (AAM 2011). Further, specialist microbial groups such as chemolithoautotrophic nitrifiers show promise as microbial bioindicators of oil contamination in coastal marine ecosystems. However, more work is needed to further validate these biomarkers, especially under different environmental conditions and fluctuations.

Despite excellent progress, a predictive understanding remains hampered by challenges in interpreting the in situ activity and ecosystem response of benthic microbial populations. A polyphasic approach is encouraged that employs metagenomics in the field along with cultivation and microcosm or mesocosm experiments in the laboratory to further elucidate impacts to ecosystem function and the in situ metabolism of microbial communities that mediate hydrocarbon degradation. In particular, more information is needed about which microbes mediate degradation of individual classes of hydrocarbon carbon compounds and how oil impacts important ecosystem services provided by microbes, such as organic matter mineralization and nutrient cycling. Interpretation of microbial community dynamics based on SSU rRNA gene sequences alone, which was commonly done during the DWH response, may lead to conclusions that are not sufficiently supported or even incorrect and thus insufficient for predictive modeling. Next-generation sequencing of taxonomic genes is great for initial "range finding" of the microbial community response over large scales. However, amplicon-based studies should be supplemented by metagenomics and comparisons of metagenome-assembled genomes wherever possible. Hypotheses from field observations should be tested by experiments conducted under controlled conditions in the laboratory. Further, research during future disasters would be greatly facilitated by improved coordination between the emergency responders directing mitigation efforts and scientists investigating the success of those efforts.

Funding Information This research was made possible by grants from The Gulf of Mexico Research Initiative through its consortia: The Center for the Integrated Modeling and Analysis of the Gulf Ecosystem (C-IMAGE), Deep Sea to Coast Connectivity in the Eastern Gulf of Mexico (Deep-C). This research was also supported by grants from the National Science Foundation (to MH, JEK, WAO), the Florida Institute of Oceanography (to MH and JEK), and the Northern Gulf Institute (to MH and JEK).

References

American Academy of Microbiology (2011) FAQ: microbes & oil spills. http://www.asmscience.org/content/report/faq?order=date

Atlas RM (1995) Petroleum biodegradation and oil spill bioremediation. Mar Pollut Bull 31:178–182

Atlas RM, Hazen TC (2011) Oil biodegradation and bioremediation: a tale of the two worst spills in U.S. history. Environ Sci Technol 45(16):6709–6715. https://doi.org/10.1021/es2013227

Barbato M, Scoma A, Mapelli F, De Smet R, Banat IM, Daffonchio D, Boon N, Borin S (2016) Hydrocarbonoclastic alcanivorax isolates exhibit different physiological and expression responses to n-dodecane. Front Microbiol 7:2056

Boufadel MC, Abdollahi-Nasab A, Geng X, Galt J, Torlapati J (2014) Simulation of the landfall of the Deepwater Horizon oil on the shorelines of the Gulf of Mexico. Environ Sci Technol 48(16):9496–9505

Brooks GR, Larson RA, Schwing PT, Romero I, Moore C, Reichart GJ, Jilbert T, Chanton JP, Hastings DW, Overholt WA, Marks KP, Kostka JE, Holmes CW, Hollander D (2015) Sedimentation pulse in the NE Gulf of Mexico following the 2010 DWH blowout. PLoS One 10(7):e0132341

Caporaso JG, Bittinger K, Bushman FD, DeSantis TZ, Andersen GL, Knight R (2010) PyNAST: a flexible tool for aligning sequences to a template alignment. Bioinformatics 26:266–267

Dalyander PS, Long JW, Plant NG, Thompson DM (2014) Assessing mobility and redistribution patterns of sand and oil agglomerates in the surf zone. Mar Pollut Bull 80(1–2):200–209

Eren AM, Esen ÖC, Quince C, Vineis JH, Morrison HG, Sogin ML, Delmont TO (2015) Anvi'o: an advanced analysis and visualization platform for 'omics data. PeerJ 3:e1319

Gihring TM, Humphrys M, Mills HJ, Huette M, Kostka JE (2009) Identification of phytodetritus-degrading microbial communities in sublittoral Gulf of Mexico sands. Limnol Oceanogr 54(4):1073–1083

Gobet A, Böer SI, Huse SM, Van Beusekom JE, Quince C, Sogin ML, Boetius A, Ramette A (2012) Diversity and dynamics of rare and of resident bacterial populations in coastal sands. ISME J 6(3):542

Hayworth JS, Clement TP (2011) BP's operation deep clean-could dilution be the solution to beach pollution? Environ Sci Technol 45:4201–4202

Head IM, Jones DM, Roling WFM (2006) Marine microorganisms make a meal of oil. Nat Rev Microbiol 4:173–182

Huettel M, Berg P, Kostka JE (2014) Benthic exchange and biogeochemical cycling in permeable sediments. Annu Rev Mar Sci 6(1):23–51

Huettel M, Overholt WA, Kostka JE, Hagan C, Kaba J, Wells WB, Dudley S (2018) Degradation of Deepwater Horizon oil buried in a Florida beach influenced by tidal pumping. Mar Pollut Bull 126:488–500

Hunter EM, Mills HJ, Kostka JE (2006) Microbial community diversity associated with carbon and nitrogen cycling in permeable shelf sediments. Appl Environ Microbiol 72(9):5689–5701

Joye SB, Kleindienst S, Gilbert JA, Handley KM, Weisenhorn P, Overholt WA, Kostka JE (2016) Responses of microbial communities to hydrocarbon exposures. Oceanography 29(3):136–149

King GM, Kostka JE, Hazen TC, Sobecky PA (2015) Microbial responses to the Deepwater Horizon oil spill: from coastal wetlands to the deep sea. Annu Rev Mar Sci 7:377–401

Kostka JE, Prakash O, Overholt WA, Green S, Freyer G, Canion A, Delgardio J, Norton N, Hazen TC, Huettel M (2011) Hydrocarbon-degrading bacteria and the bacterial community response in Gulf of Mexico beach sands impacted by the Deepwater Horizon oil spill. Appl Environ Microbiol: AEM 77:7962–7974. https://doi.org/10.1128/AEM.05402-11

Lamendella R, Strutt S, Borglin SE, Chakraborty R, Tas N, Mason OU, Hultman J, Prestat E, Hazen TC, Jansson JK (2014) Assessment of the Deepwater Horizon oil spill impact on Gulf coast microbial communities. Front Microbiol 5:130

Leahy JG, Colwell RR (1990) Microbial-degradation of hydrocarbons in the environment. Microbiol Rev 54:305–315

Lea-Smith DJ, Biller SJ, Davey MP, Cotton CA, Sepulveda BMP, Turchyn AV, Scanlan DJ, Smith AG, Chisholm SW, Howe CJ (2015) Contribution of cyanobacterial alkane production to the ocean hydrocarbon cycle. Proc Natl Acad Sci 112(44):13591–13596

Louchouarn P, Yeager KM, Brunner CA, Briggs K, Guo L, Asper V, Coney N, Fortner C, Prouhet J, Schindler KJ, Martin KM, Zhou Z, Loeffler J, Jung A, Cruz V (2011) Deepwater Horizon: coastal ocean to Marsh margin sediment impacts. Abstracts of Papers of the American Chemical Society 241

Lubchenco J, McNutt MK, Dreyfus G, Murawski SA, Kennedy DM, Anastas PT, Chu S, Hunter T (2012) Science in support of the Deepwater Horizon response. Proc Natl Acad Sci 109(50):20212–20221

McNutt MK, Chu S, Lubchenco J, Hunter T, Dreyfus G, Murawski SA, Kennedy DM (2012) Applications of science and engineering to quantify and control the Deepwater Horizon oil spill. Proc Natl Acad Sci 109(50):20222–20228

Michel J, Owens EH, Zengel S, Graham A, Nixon Z, Allard T, Holton W, Reimer PD, Lamarche A, White M, Rutherford N (2013) Extent and degree of shoreline oiling: Deepwater Horizon oil spill, Gulf of Mexico, USA. PloS One 8(6):e65087

Mills HJ, Hunter E, Humphrys M, Kerkhof L, McGuinness L, Huettel M, Kostka JE (2008) Characterization of nitrifying, denitrifying, and overall bacterial communities in permeable marine sediments of the northeastern Gulf of Mexico. Appl Environ Microbiol 74(14):4440–4453

Newton RJ, Huse SM, Morrison HG, Peake CS, Sogin ML, McLellan SL (2013) Shifts in the microbial community composition of Gulf Coast beaches following beach oiling. PLoS One 8:e74265

OSAT (2011) Summary report for fate and effects of remnant oil in the beach environment, Operational Science Advisory Team (OSAT-2). Team, Gulf Coast Incident Management Team. In: OSAT reports. USCG

Overholt WA, Green SJ, Marks KP, Venkatraman R, Prakash O, Kostka JE (2013) Draft genome sequences for oil-degrading bacterial strains from beach sands impacted by the Deepwater Horizon oil spill. Genome Announc 1(6):e01015–e01013. https://doi.org/10.1128/genomeA.01015-13

Overholt WA, Marks KP, Romero IC, Hollander DJ, Snell TW, Kostka JE (2016) Hydrocarbon-degrading bacteria exhibit a species-specific response to dispersed oil while moderating ecotoxicity. Appl Environ Microbiol 82(2):518–527

Parks DH, Chuvochina M, Waite DW, Rinke C, Skarshewski A, Chaumeil PA, Hugenholtz P (2018) A standardized bacterial taxonomy based on genome phylogeny substantially revises the tree of life. Nat Biotechnol 36:996–1004

Passow U, Ziervogel K, Asper V, Diercks A (2012) Marine snow formation in the aftermath of the Deepwater Horizon oil spill in the Gulf of Mexico. Environ Res Lett 7(3):035301

Prince RC (2010) Bioremediation of marine oil spills. In: Timmis KN (ed) Handbook of hydrocarbon and lipid microbiology. Springer, Berlin Heidelberg, pp 2618–2626

Prosser JI (2012) Ecosystem processes and interactions in a morass of diversity. FEMS Microbiol Ecol 81(3):507–519

Prosser JI, Bohannan BJ, Curtis TP, Ellis RJ, Firestone MK, Freckleton RP, Green JL, Green LE, Killham K, Lennon JJ, Osborn AM (2007) The role of ecological theory in microbial ecology. Nat Rev Microbiol 5(5):384

Reddy CM, Arey JS, Seewald JS, Sylva SP, Lemkau KL, Nelson RK, Carmichael CA, McIntyre CP, Fenwick J, Ventura GT, Van Mooy B (2012) Composition and fate of gas and oil released to the water column during the Deepwater Horizon oil spill. Proc Natl Acad Sci 109(50):20229–20234

Rodriguez-R LM, Overholt WA, Hagan C, Huettel M, Kostka JE, Konstantinidis KT (2015) Microbial community successional patterns in beach sands impacted by the Deepwater Horizon oil spill. ISME J 9:1928–1940

Sabirova JS, Ferrer M, Regenhardt D, Timmis KN, Golyshin PN (2006) Proteomic insights into metabolic adaptations in Alcanivorax borkumensis induced by alkane utilization. J Bacteriol 188(11):3763–3773. https://doi.org/10.1128/JB.00072-06

Sabirova JS, Becker A, Lünsdorf H, Nicaud J-M, Timmis KN, Golyshin PN (2011) Transcriptional profiling of the marine oil-degrading bacterium Alcanivorax borkumensis during growth on n-alkanes. FEMS Microbiol Lett 319(2):160–168. https://doi.org/10.1111/j.1574-6968.2011.02279.x

Schneiker S, dos Santos VAM, Bartels D, Bekel T, Brecht M, Buhrmester J, Chernikova TN, Denaro R, Ferrer M, Gertler C, Goesmann A, Golyshina OV, Kaminski F, Khachane AM, Lang S, Linke B, McHardy AC, Meyer F, Mechitaylo T, Pühler A, Regenhardt D, Rupp O, Sabirova JS, Selbitschka W, Yakimov MM, Timmis KN, Jorhölter FJ, Weidner S, Kaiser O, Golyshin PN (2006) Genome sequence of the ubiquitous hydrocarbon-degrading marine bacterium Alcanivorax borkumensis. Nat Biotechnol 24(8):997–1004. https://doi.org/10.1038/nbt1232

Shao Z, Wang W (2013) Enzymes and genes involved in aerobic alkane degradation. Front Microbiol 4:116

Urbano M, Elango V, Pardue JH (2013) Biogeochemical characterization of MC252 oil:sand aggregates on a coastal headland beach. Mar Pollut Bull 77:183–191

van Beilen JB, Funhoff EG (2007) Alkane hydroxylases involved in microbial alkane degradation. Appl Microbiol Biotechnol 74(1):13–21. https://doi.org/10.1007/s00253-006-0748-0

Vázquez DP, Simberloff D (2002) Ecological specialization and susceptibility to disturbance: conjectures and refutations. Am Nat 159:606–623

Wang W, Shao Z (2014) The long-chain alkane metabolism network of Alcanivorax dieselolei. Nat Commun 5:5755

Yakimov MM, Timmis KN, Golyshin PN (2007) Obligate oil-degrading marine bacteria. Curr Opin Biotechnol 18:257–266

Chapter 12
Combining Isoscapes with Tissue-Specific Isotope Records to Recreate the Geographic Histories of Fish

Ernst B. Peebles and David J. Hollander

Abstract After the *Deepwater Horizon* (DWH) oil spill, interest in marine animal movement was heightened by recognition that some individual animals had been cryptically exposed to the oil, and that some of these exposed individuals later moved, introducing oil contamination to geographic areas that were beyond the initial domain of direct oil impact. Forensic methods based on internally recorded stable-isotope records can be used to address the issue of movement by contaminated individuals. Different tissues provide stable-isotope histories that reflect different periods in the individual's history, ranging from just a few recent days in the case of blood plasma to the entire lifetime in the case of eye lenses and otoliths. Isotopic offsets between tissue types (e.g., liver and muscle) within the same individual can be used to measure the relative site fidelities of different individuals. Among individuals that have low site fidelity, geographic movements can be estimated by comparing lifetime isotope trends with background maps of isotope variation (isoscapes). The process of isotope conservation within the vertebrate eye lens is described, and practical application of forensic methods and data interpretation are discussed.

Keywords Isoscapes · Isotope gradients · Site fidelity · Animal migration · Cryptic exposure · Tissue-specific isotope analysis · Eye-lens anatomy · Crystallins · Eye-lens isotopes · Compound-specific isotope analysis

12.1 Introduction

There are many reasons for investigating the geographic movement of animals, and most of these involve resource management. In the case of the *Deepwater Horizon* (DWH) oil spill, interest in marine animal movement was heightened by concerns that some animals would not or could not avoid contaminated waters and sediments,

E. B. Peebles (✉) · D. J. Hollander
University of South Florida, College of Marine Science, St. Petersburg, FL, USA
e-mail: epeebles@mail.usf.edu; davidh@usf.edu

S. A. Murawski et al. (eds.), *Scenarios and Responses to Future Deep Oil Spills*,
https://doi.org/10.1007/978-3-030-12963-7_12

and others would become contaminated and then move, introducing the contamination to areas that were beyond the initial domain of direct oil impact.

In cases of direct oiling of animals by crude oil floating at the sea surface, the general location and means of animal contamination are often readily apparent, as oiled animals are often directly observed to be near or within areas contaminated by surface oil. In contrast, the processes behind other more cryptic types of oil exposure are usually difficult or impossible to recognize visually. One cryptic process is body contact with crude oil in the form of its water-accommodated fractions (WAF). WAF includes both dissolved oil components and invisible microdroplets of oil that are not buoyant enough to overcome friction with seawater and thus remain suspended at depth in accordance with Stokes' law. Other forms of cryptic oil exposure include consumption of oil-exposed prey, ingestion of WAF while drinking seawater to maintain osmotic balance, and body contact between benthic animals and oil-contaminated sediments. Detection of cryptic oil exposures requires chemical analysis of soft tissues (e.g., muscle, liver), body fluids (e.g., blood, bile), or hard parts (e.g., otoliths, Granneman et al. 2017).

Once cryptic oil exposure has been detected, the question arises "Where did the exposure to oil take place?" This is a relevant question because there is an important distinction between a fish being exposed to oil elsewhere and then swimming into local waters and a fish being cryptically exposed within local waters. While neither outcome is desirable, the second outcome means there was a source of cryptic oil in local waters, even if no surface oil had been previously detected there [i.e., undetected oil could exist locally as invisible WAF, as sediments containing oil-bound marine snow (MOSSFA), as interstitial sediment porewater WAF, or as contaminated prey moving into local waters]. For example, Murawski et al. (2014) reported oil-related PAHs in red grouper from areas of the West Florida Shelf that had not been exposed to surface oil.

In the likely scenario where there is no artificial tagging program available that can recreate the individual geographic histories of fish that have had known, cryptic, exposure to oil, the researcher is left with forensic approaches for addressing the geographic exposure question. There are several hard and soft tissues that can be used to forensically recreate the lifetime histories of individual fish; these approaches were recently reviewed by Tzadik et al. (2017). One of the most promising forensic approaches involves stable-isotope analysis of various tissues. Different tissues provide stable-isotope histories that reflect different periods in the individual's history, ranging from just a few recent days in the case of blood plasma to the entire lifetime in the case of eye lenses and otoliths. During the course of recreating individual geographic histories, other information obtained from stable isotopes is likely to shed light on the individual's trophic position and basal-resource dependence (i.e., whether the individual ultimately depended on phytoplankton, benthic algae, or a mixture of these as biomass drivers at the base of its food web). All of this new insight has potential utility toward developing a process-based understanding of oil-spill impacts.

Once individual isotopic histories have been obtained, interpretation requires comparison of the individual's stable-isotope values with background values from the seascape around it. Maps of background stable isotopes are referred to as "isoscapes" (Fig. 12.1).

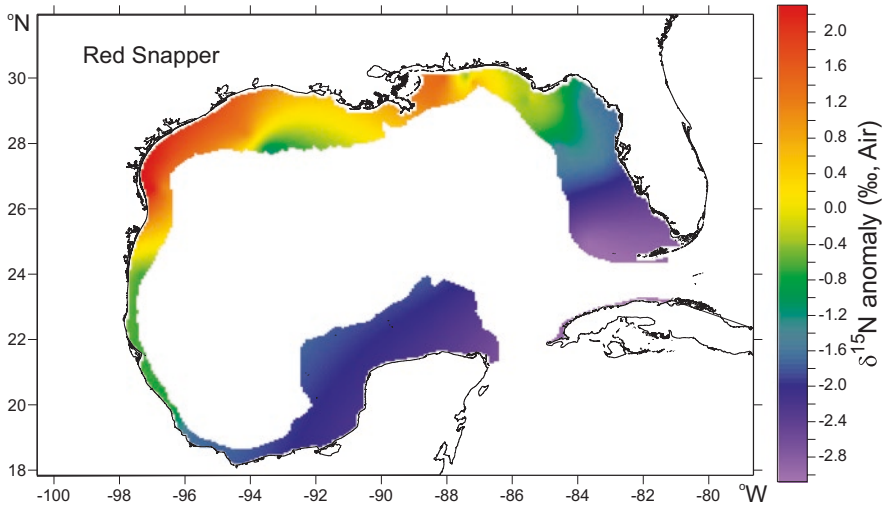

Fig. 12.1 Empirical isoscape (based on kriged data, not a statistical model) of continental shelf $\delta^{15}N$ based on red snapper (*Lutjanus campechanus*) muscle, expressed as differences from the grand mean value. The grand mean was subtracted because correlations between $\delta^{15}N$ and either fish weight or fish length were not significant. This isoscape is derived from 34 locations distributed around the perimeter of the Gulf of Mexico

12.2 Marine Isoscapes

As recently as the 2000s, marine isoscapes were unavailable for most of the world's oceans and coastal waters. The large-scale isoscapes that were produced (e.g., those presented by McMahon et al. 2013) were the products of correlative models that helped interpolate among empirical observations, and these empirical observations were often spaced far apart from each other. Although isoscape models may appear to provide detailed depictions of isoscapes across large areas of the world's oceans, they often do so in areas (such as the Gulf of Mexico (GoM)) where there were very few empirical observations to support the models. Given the lack of detailed, empirical isoscapes, marine ecologists began to create higher resolution isoscapes for their own geographic regions of interest, sometimes including assessments of seasonal and annual variation (e.g., Radabaugh et al. 2013; MacKenzie et al. 2014; Radabaugh and Peebles 2014). These isoscapes have focused on $\delta^{13}C$, $\delta^{15}N$, and to a lesser extent, $\delta^{18}O$, whereas terrestrial isoscapes, which have received far more research attention than marine isoscapes, have focused on $\delta^{2}H$ (deuterium) from precipitation in addition to vegetation-based $\delta^{13}C$, $\delta^{15}N$, and $\delta^{18}O$ (Hobson and Wassenaar 2007).

The precipitation-based $\delta^{2}H$ and $\delta^{18}O$ isoscapes used by terrestrial ecologists reflect predictable phase change, Raleigh distillation, and mixing-based offsets that generally coincide with latitude and climate ("meteoric" effect, Smith and Freeman 2006; West et al. 2010; note that $\delta^{2}H$ and $\delta^{18}O$ isoscapes can also be derived from plants). As precipitation-borne isotopes become incorporated into

animal tissues, including hard parts (i.e., bird feathers and mammal teeth and hooves), additional fractionations take place, and the resulting offsets are modeled using "transfer functions" to produce organism-specific isoscapes.

Most of these computations can be automated online by the IsoMAP program (https://isomap.rcac.purdue.edu/isomap/), which assigns geographic-origin probabilities (gridded map files) to each individual animal. The user must calibrate the transfer functions using empirical data specific to his or her study and may post-process IsoMAP's output to accommodate additional information not supported by IsoMAP's algorithms (Bowen et al. 2014). The methods for developing and using marine isoscapes are not as advanced as the methods associated with IsoMAP and terrestrial isoscapes. There is currently no marine equivalent of the IsoMAP online workspace, and IsoMAP offers little direct utility to the marine ecologist other than to provide an example of a successful, automated approach that could be mirrored for application to the marine environment.

Marine $\delta^{13}C$ and $\delta^{15}N$ isoscapes may be based on isotope measurements of primary producers (trophic position 1.0), herbivores (trophic position 2.0), or omnivores and predators (trophic position >2.0). Basing marine isoscapes on herbivores such as bivalves, sponges, tunicates, or sea urchins (Radabaugh et al. 2013) is particularly appealing because herbivores integrate short-term fluctuations in the primary-producer isotopic baseline, and, unlike phytoplankton, many are either stationary (sessile organisms) or slow-moving (sea urchins). Terrestrial ecologists often assume spatial stationarity (i.e., little or no spatial variation in isoscapes over time), whereas marine ecologists generally recognize that this assumption is more problematic in the marine realm, where dynamic processes prevail. In all cases, isoscapes can only be useful if they capture spatial variation, and isoscapes are most useful if the cause of spatial variation is understood.

12.3 Overview of Variation in $\delta^{13}C$ and $\delta^{15}N$ Isoscapes

In coastal ecosystems, prominent causes of variation in baseline $\delta^{13}C_{biomass}$ include freshwater runoff or tidal exchange with slow-moving backwaters (notably swamps and marshes), where DIC (dissolved inorganic carbon) evolving from microbial respiration of primary-producer detritus is more likely to be recycled into new primary production, causing a portion of the DIC molecules to undergo repeated photosynthetic fractionation, dramatically reducing $\delta^{13}C_{biomass}$ (photosynthetic fractionation is strongly negative) and contributing to a trend of progressively more depleted $\delta^{13}C_{DIC}$ (Keough et al. 1998). Low (<−22‰) and highly variable $\delta^{13}C$ values are associated with the DIC recycling process.

$\delta^{13}C_{biomass}$ is also indicative of the light environment, with primary producers from lower-light settings having higher $\delta^{13}C_{biomass}$ values (less photosynthetic fractionation) than those from higher-light settings (higher photosynthetic fractionation); at a global scale, benthic algae have about 5‰ higher $\delta^{13}C_{biomass}$ values than phytoplankton from the same location (Radabaugh et al. 2014 and references cited therein), and this difference gets passed on to higher trophic positions, providing an indication

of individuals' relative dependence on different basal resources (i.e., plankton-based vs. benthos-based primary producers). Benthic algae become unimportant beyond the outer continental shelf due to lack of light reaching the sea floor, and DIC recycling is less likely in the deep sea due to a relative lack of plant detritus and higher likelihood of CO_2 molecules fluxing into the global ocean and atmosphere as a result of turbulent water flows (i.e., thus becoming less available for local recycling). As a result, the $\delta^{13}C_{biomass}$ values of open-ocean phytoplankton tend to be somewhat monotonous over space and time, hovering between −19 to −22‰ (but can be as high as −16‰ and as low as −30‰, Rau et al. 1989) at most lower and middle latitudes (McMahon et al. 2013).

Finally, $\delta^{13}C$ is also strongly influenced by the type of vascular plant that contributes detritus to the food web (C3, C4, and CAM photosynthetic pathways). However, in the coastal ocean, these distinctions are only important at locations that receive vascular plant detritus from wetlands or from riverine inputs and at locations that define the transition between mangroves (C3) and *Spartina*-dominated (C4) coastal biomes.

$\delta^{15}N$ has particular utility in recreating individual trophic and geographic histories (Wallace et al. 2014; Quaeck 2017), as it has been demonstrated that geographic variation in $\delta^{15}N_{biomass}$ often exists as predictable gradients that are potentially useful for reconstructing the geographic histories of individual animals (McMahon et al. 2013; Radabaugh et al. 2013; Radabaugh and Peebles 2014). These $\delta^{15}N_{biomass}$ gradients exist between areas of the coastal ocean where the mass-balanced influences of surface runoff from land (and possibly denitrification, cf. Chang et al. 2002) result in elevated $\delta^{15}N$ and oligotrophic areas where nitrogen fixation is dominant and $\delta^{15}N_{biomass}$ is low (e.g., oceanic gyres and other nitrogen-poor seas). In fishes, individual histories for $\delta^{15}N$ are of particular interest because $\delta^{15}N$ is difficult to obtain from otoliths due to the otoliths' low nitrogen content, and thus the ability to obtain lifetime $\delta^{15}N$ histories for fishes is particularly novel.

12.4 Effects of Scale on Isoscapes

Given that the above causes of isotopic variation may vary at different spatial and temporal scales, it can be expected that the patterns observed within isoscapes may also be sensitive to the effects of scale. For example, at a scale of hundreds of kilometers in the eastern GoM (Fig. 12.1), the general trend in $\delta^{15}N$ is an increase from low values toward the southeast, where nitrogen fixation is more common, to higher values toward the northwest, where large riverine inputs are present (Atchafalaya/Mississippi/Mobile Rivers). Yet at a much smaller scale within this range, at a span of tens of kilometers, this trend is reversed as one moves northward away from the mouth of the Suwannee River, which has elevated $\delta^{15}N$ values (Michael Poniatowski, FWC, pers. comm.). The Suwannee River is a much smaller river than the others, and thus it does not contribute substantially to the larger-scale trend observed at the scale of hundreds of kilometers, yet it nevertheless creates its own localized trend, one that is recognizable at the smaller scale of tens of kilometers.

12.5 Tissue-Specific Isotope Analysis

When conducting stable-isotope studies, the primary reason for considering tissue type is selection of the time scale that is most relevant to the research question being addressed. Any vascularized tissue, even bone and teeth, can be expected to turn over (i.e., to have its mass partially or totally replaced by new tissue over time). Turnover rates are usually described as the length of time required to reach a specified percentage of turnover (e.g., the number of days required to reach 90% turnover). Different vascularized tissues (blood, liver, muscle, bone, etc.) typically have different turnover rates, generally ranging from a few days in the case of blood plasma to about a year in the case of bone (Gaston and Suthers 2004; Buchheister and Latour 2010; Heady and Moore 2013).Turnover rates can vary substantially with variation in the individual's growth and metabolic rates (MacNeil et al. 2006).

In stable-isotope studies of aquatic organisms, muscle has been the most commonly analyzed tissue type. At lower latitudes such as the GoM, isotopes from muscle represent conditions over a duration of several months, more or less, prior to the specimen's collection date. However, small organisms are often analyzed intact due to difficulty isolating enough mass of a given tissue type; this results in an isotope value that reflects the mass balance of the contributions of different tissue types to the overall dry weight of the analyzed sample. Very small organisms such as phytoplankton cells or zooplankton may be composited (i.e., multiple cells or individuals dried, ground to powder, and analyzed together). It should be noted that differences in the types of tissues analyzed can lead to the false perception of isotopic differences between organisms that do not actually exist.

12.6 Site Fidelity Based on Two or More Tissues (Tissue Comparison Method)

The fact that isotopic turnover rates are tissue-specific can be exploited to provide new insights. Given enough time after an isotopic diet shift, isotope values within different tissues will eventually equilibrate with the new diet but will do so at different rates, provided the tissues' turnover rates are different. Thus, if an individual animal moves to a new location that has an isotopically different dietary baseline, then its liver will reflect the new diet faster than its muscle because liver tissue has a faster turnover rate.

Isotopic offsets between tissue types within the same organism can therefore be used to measure the relative site fidelities of different individuals, species, sexes, or whatever factor the researcher chooses to evaluate. There is a major caveat when doing this, however. One cannot assume that all tissues come to the same equilibrium value after an isotopic diet switch. For example, muscle $\delta^{15}N$ from marine fishes equilibrates at a value that is approximately 1.8‰ higher than liver (Julie Vecchio, USF, pers. comm. of unpublished data). This equilibrium offset is a tissue-

specific constant that must be subtracted from original muscle-liver offsets in order to assign relative site fidelities. After making this correction, the researcher may compare the sign of the offset (i.e., whether it is positive or negative) to determine the likely direction of movement within the local isoscape's isotopic gradients.

Another caveat is that some tissues contain storage molecules. In fishes, lipids (fats and oils) may be stored in various tissues, including muscle, liver, and mesenteries. Oily fishes such as clupeids (herrings and sardines), scombrids (mackerels), and carangids (jacks and scads) store lipids within muscle, and this storage is dynamic, changing with the seasons, prior to spawning, or as feeding conditions change over space and time. This dynamic behavior in lipid storage creates problems with temporal interpretation of isotope results. To avoid this storage problem, it has become common practice to extract lipids from dried, powdered tissues prior to isotope analysis. Lipid extraction, which is achieved using various organic solvents such as dichloromethane (DCM) or a mixture of hexane and acetone, is sometimes automated using an accelerated solvent extractor (ASE). It is important to realize that lipid extraction not only removes storage lipids such as triacylglycerols (fats) but also removes more ubiquitous lipids such as sterols (associated with cell membranes). Lipids are hydrocarbons and thus have very high elemental C:N ratios. As an alternative to lipid extraction, empirical equations have been developed that allow the sample's elemental C:N value (i.e., its relative lipid content) to be used to adjust observed $\delta^{13}C$ to correct for the presence of lipids (Post et al. 2007). Note that $\delta^{15}N_{biomass}$ values are not affected by the presence of lipids, as lipids contain very little nitrogen. In fact, as hydrocarbons, lipids are generally considered to be devoid of nitrogen, yet nitrogen-bearing functional groups can be attached to certain lipid types (fatty acids, specifically). However, the contribution of these functional groups to $\delta^{15}N_{biomass}$ is considered negligible.

12.7 Lifetime Isotope Records from Eye Lenses

Eye-lens layers preserve lifetime isotopic records (Lynnerup et al. 2008; Nielsen et al. 2016; Tzadik et al. 2017). As an individual animal grows, new eye-lens layers (new laminae) form successively at the outside of the lens (Nicol 1989; Greiling and Clark 2012). During the initial part of new-lamina formation, the mass-dominant structural proteins produced within the lamina (crystallins) reflect dietary isotope ratios (Wistow and Piatigorsky 1988). However, final development of the new lamina involves attenuated apoptosis, which destroys organelles and genetic material that are required for new protein synthesis (Shi et al. 2009; Wride 2011). Attenuated apoptosis improves the optical properties of the newly formed lamina by removing these light-scattering materials, but it also halts new protein synthesis and traps existing isotopes that were originally associated with incipient formation of the new lamina. Likewise, formation of the next (outer) lamina incorporates the dietary isotopes of the next time period, and so forth.

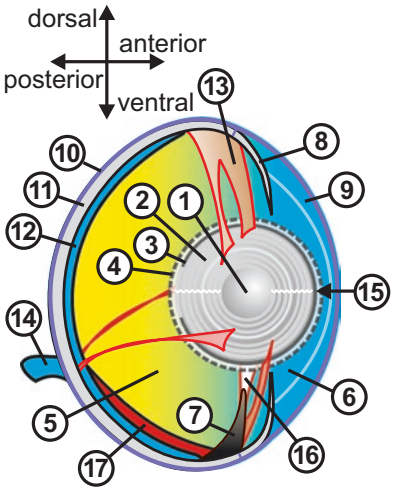

1. lens nucleus (primary fiber cells - embryonic)
2. lens cortex (secondary fiber cells)
3. lens epithelium
4. lens capsule
5. vitreous humor
6. aqueous humor
7. retractor lentis muscle
8. iris
9. cornea
10. sclera
11. choroid
12. retina
13. central suspensory ligament
14. optic nerve
15. anterior pole of lens, with suture line (white)
16. retractor lentis tendon
17. falciform process

Fig. 12.2 Anatomical features of the teleost (bony fish) eye. Except in very small specimens, the lens nucleus would be much smaller than depicted

Poor vascularization appears to be an important requirement for isotopic conservation within tissues of any type. In addition to the eye lens, examples of poorly vascularized soft tissues include cartilage, which is avascular, and ligaments and tendons, which contain avascular regions. During embryonic eye development in vertebrates, the hyaloid artery and its associated network of blood vessels (the tunica vasculosa lentis) nourish the newly developing eye lens and its primary fiber cells, but this system of blood vessels soon disintegrates during continued development, leaving the post-embryonic lens without a direct source of vascularization. The retractor lentis muscle (Fig. 12.2) is the most proximal vascular tissue to the post-embryonic lens; it is vascularized via the falciform process or via the retina in species where the falciform process is diminished or absent. However, the retractor lentis muscle is isolated from vascular communication with the eye lens by the poorly vascularized retractor lentis tendon (Fig. 12.2). In the absence of direct contact between the eye lens and vascularized tissues, most isotopic communication with the post-embryonic eye lens likely occurs through the vitreous and aqueous humors, which are clear, colorless fluids that bathe the lens capsule; the highly elastic lens capsule surrounds the lens epithelium and the newly forming laminae that are produced by the lens epithelium. One important function of the lens capsule is to influence molecular communication between humor fluid and the lens epithelium (Danysh and Duncan 2009).

As the result of interest in cataracts and other lens pathologies that affect the human eye, the physiology and biochemistry of mammalian lens maintenance have been the subject of extensive research, and much of this research has concentrated on the movement of proteins within the lens. Such protein movement, if present, could possibly interfere with isotope records by redistributing proteins along the

radial axes of the lens (centripetal diffusion). Protein diffusion during embryonic development of the lens nucleus is suspected of being somewhat isotropic, but there appears to be very little post-embryonic centripetal diffusion of proteins among laminae within the organelle-free zone (i.e., the post-apoptotic zone), which includes the lens nucleus and all post-apoptotic laminae within the lens cortex (Shi et al. 2009, Fig. 12.2). The small amount of centripetal diffusion that does occur within the organelle-free zone results in nominal isotopic deviations equivalent to 0.5–1.0% annual carbon turnover; this turnover appears to be limited to the water-soluble fraction of crystallins and is not of sufficient magnitude to mask the temporal details of the atmospheric bomb pulse recorded by eye-lens isotopes (Stewart et al. 2013). Eye-lens laminae are composed of bundles of secondary fiber cells that derive from the equatorial lens epithelium and elongate from this equatorial point of origin toward the two poles of the lens, at which point the secondary fiber cells meet and interdigitate with fiber cells from other "longitudes" within the epithelium, forming a "suture" that may have taxon-specific morphology. New protein synthesis allows new secondary fiber cells to elongate until they reach the suture near the poles, after which they undergo attenuated apoptosis (Shi et al. 2009; Wride 2011). During this period of fiber-cell elongation from the equatorial epithelium to the poles, proteins are exchanged among elongating cells, but this exchange appears to be limited to lateral (concentric) diffusion among cells of similar age, rather than centripetal diffusion among laminae (Shi et al. 2009).

Collectively, the above circumstances allow eye lenses to be used to recreate lifetime isotopic histories for a variety of organism types, including humans (Kjeldsen et al. 2010; Lynnerup et al. 2010; Stewart et al. 2013), sharks (Nielsen et al. 2016; Quaeck 2017; Quaeck-Davies et al. 2018), bony fishes (Wallace et al. 2014; Quaeck 2017; Quaeck-Davies et al. 2018), and cephalopods (Parry 2003; Hunsicker et al. 2010; Onthanks 2013). Human eye-lens-isotope applications have focused on matching lifetime trends in radiocarbon (^{14}C) to temporal trends in atmospheric radiocarbon that have resulted from nuclear bomb testing in the 1950–1960s (i.e., the "bomb pulse"). This approach was developed as a forensic tool for humans that provides a fairly accurate estimation of birth year (Lynnerup et al. 2010), but the method can also be applied to other long-lived vertebrates such as sharks (Nielsen et al. 2016). Parry (2003) provided an early example of the application of stable isotopes (vs. radiocarbon) to the recreation of individual isotopic histories for two species of squid, and his approach was successfully repeated by other cephalopod biologists (Hunsicker et al. 2010; Onthanks 2013; Meath et al. 2019). In comparison, the application of eye-lens isotopes to bony fishes is relatively recent (Wallace et al. 2014; Quaeck-Davies et al. 2018).

Due to practical limitations on experiments involving long-lived organisms or organisms that are difficult or impossible to keep captive for sufficient periods of time, experimental validation of isotopic conservation within eye lenses has not been widely attempted, with the exception of one recent study by Granneman (2018), who documented an eye-lens isotope shift that followed an isotopic diet switch in a captive bony fish (red drum, *Sciaenops ocellata*). She found that mean

90% assimilation of the new diet was achieved by about 54 days after the $\delta^{15}N$ of the diet had been reduced by 3‰.

The net effect of the above processes is the formation of (1) a conservative organic record within the lens nucleus and elsewhere within the organelle-free zone and (2) non-conservative organic records at the newly forming outermost laminae that become conservative once the outer laminae undergo attenuated apoptosis. Aside from differences in cellular organization (Greiling and Clark 2012), fish eye lenses have the same anatomical, cellular, and compositional features as mammalian eye lenses (Nicol 1989; Wride 2011). Notably, because the eye lens is protein-rich, it provides ready access to useful $\delta^{15}N$ records that are, by comparison, very difficult to obtain from largely inorganic hard parts such as otoliths (Tzadik et al. 2017).

It follows from this history of methods development that there are likely many other taxa to which this general approach can be applied. Cephalopods are unique among invertebrates in having a large eye lens that can be manually delaminated to create isotopic time series, whereas most vertebrate groups possess eye lenses that can be manually delaminated (exceptions being eyeless cave-dwelling/subterranean species). In particular, lower vertebrates (fishes, amphibians, reptiles) are particularly well suited to this approach because they undergo continuous and substantial eye-lens growth during life. In contrast, much of the eye-lens growth in higher vertebrates (birds, mammals) occurs while the organisms are still embryonic, and thus only the outermost lens contains post-embryonic information.

12.8 Practical Solutions for Eye-Lens Analysis

In most cases, fish eye lenses can be readily delaminated using two forceps and a stereomicroscope. Periodically adding small amounts of clean, fresh water facilitates the delamination process (dry method, Wallace et al. 2014), or, alternatively, the lens may be delaminated while immersed in water within a petri dish (wet method, Stewart et al. 2013). Although the wet method results in greater loss of water-soluble material from the lens, experiments with fish eye lenses, wherein the wet method was used for one eye of the individual and the dry method was used for the other eye, did not reveal any statistical difference between the two methods (Julie Vecchio and Amy Wallace, USF, pers. comm. of unpublished data). The wet method tends to be the faster of the two and results in better temporal resolution (more, thinner dissected laminae per lens).

Exceptions to convenient delamination involve very long-lived species, which may have naturally lost the most water-soluble crystallins from a large part of the central eye lens, causing it to become hardened and highly resistant to delamination. In such cases, one solution is to delaminate the lens as much as possible, and then section the remaining hardened core through its center using a slow-speed saw equipped with two or more diamond blades that are separated by appropriately sized

spacers (i.e., the same equipment used to section otoliths). The resulting thin section can then be carefully broken apart using a scalpel under a stereomicroscope, using water as needed (Kurth 2016).

Hardened lens cores also exist in smaller, shorter-lived species, but these tend to represent smaller proportions of the overall lifespan and thus may not require subdivision. Note that the term "core" is defined by practicality rather than anatomy, as the cores typically contain both the embryonic lens nucleus (primary fiber cells) as well as hardened, adjacent laminae (secondary fiber cells). In the event that the core from one eye is of insufficient mass to be analyzed by the available IRMS instrumentation, then cores of similar diameters from both eyes of the same individual can be composited to provide a larger sample, as both left and right eyes contain very similar, if not identical, isotope records (Wallace et al. 2014, Fig. 12.3).

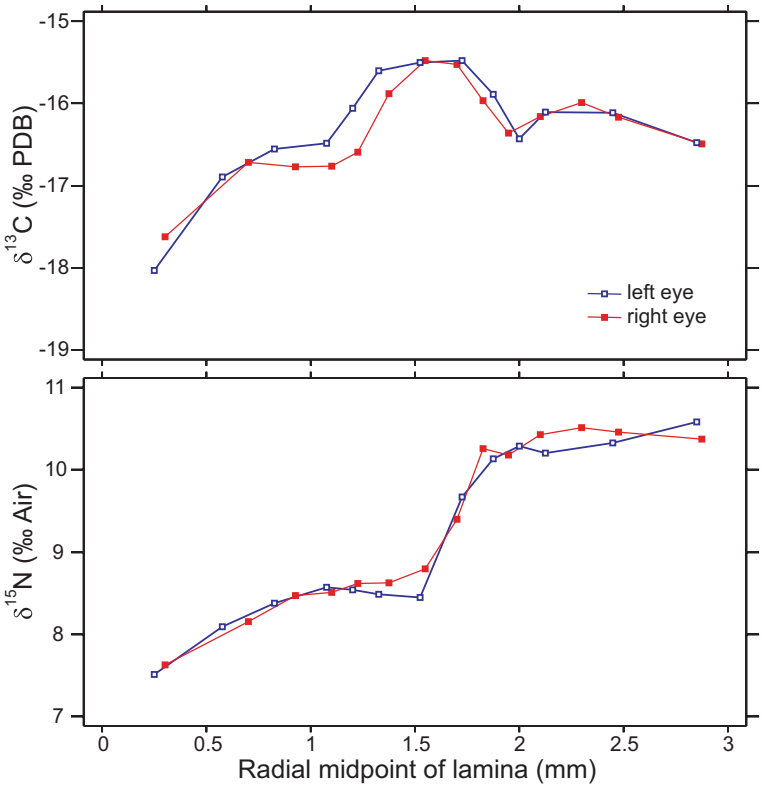

Fig. 12.3 Comparison of lifetime trends in $\delta^{13}C$ and $\delta^{15}N$ in the left and right eye lenses of a single white grunt (*Haemulon plumieri*). Early life is toward the left (from Wallace et al. 2014). In contrast, lifetime isotopic trends in tilefish (*Lopholatilus chamaeleonticeps*), a burrow-inhabiting (stationary) species, increase together in a more-or-less straight line from the lower left to the upper right, reflecting gradual increases in trophic position during life

Successively isolated laminae can be organized on aluminum foil placed on the lab countertop. Isolated laminae tend to dry very quickly at room temperature and do not typically require the use of a drying oven. Powdering is also relatively straightforward, as the dried laminae have a crystalline consistency that is highly friable, and either a mortar and pestle or a dental ball mill will work well to powder the samples.

While the laminated microstructure of the vertebrate eye lens suggests it can be interpreted in the same manner as otolith microstructure (i.e., by recognizing daily, annual, or other growth increments), this is difficult to do in practice. Comparisons with otolith-based ages reveal that individual laminae typically represent a time period of 3 months or less (and approximately 1 month in the case of the squid *Doryteuthis plei*; Meath et al. 2019). However, when an ocular micrometer is used to measure both lamina thickness and lamina position within two lenses from the same individual, it becomes evident that delaminations of the left and right eyes do not result in consistent, corresponding sequences of laminar thicknesses and positions (Wallace et al. 2014). Instead, lamina thickness appears to be influenced by the dexterity of the technician rather than by the locations of inherent, structural interfaces between adjacent laminae. Although inherent interfaces may be visually apparent within lens thin sections, exact separation at these interfaces can be difficult or impossible to achieve during manual delamination, and thus the radial midpoints (mm from lens center) of laminae dissected from the left and right eyes typically do not match (Fig. 12.3). If radial comparisons are to be made between left and right eyes or among eyes from different individuals, then an interpolation method such as cubic splining will be required first.

Given our present inability to directly interpret eye-lens microstructure as a chronometer, the relative positions of the laminae can be used instead to calibrate lifetime events. It is known that the center of the lens represents the embryonic stage and that its outer edge represents the time near collection, and so the relative positions of the laminae between these two points represent different times during life. The lens grows as the fish grows, and the shape of this relationship can be modeled. Specifically, an ocular micrometer can be used to determine laminar midpoints, and these can be converted to fish lengths using regressions that relate total lens diameter to fish length. Special care needs to be taken when interpreting the intercept of these relationships, however, just as special considerations are taken when otolith dimensions are related to fish length (see Campana and Jones 1992). In practice, lens diameter is measured before and after every lamina removal, and radial midpoints are calculated by averaging these pairs of measurements. In bony fishes, the lens diameter is very similar to the pupil diameter (Fig. 12.2), which is fixed (Walls 1942; Jagger 1997; Dahm et al. 2007). Measuring pupil diameters in bony fishes can be a practical alternative to dissecting and directly measuring lens diameters (a minor conversion factor may also be calculated and applied, if desired). At this point in time, the most defendable currency for representing points in life within eye-lens records is estimated fish length rather than estimated fish age.

12.9 Interpretation of Lifetime Isotopic Histories from Eye Lenses

The first consideration to make when interpreting lifetime isotopic records (Fig. 12.3) is to recognize that the synthesis of new eye-lens protein is proportionate to growth in some manner, which means that periods of slow growth or no growth will either not be represented or will be represented poorly. This can include important life-history events such as spawning migrations, wherein a fish could live and grow at an isotopically distinctive location, then make an energetically expensive spawning migration, and then return to feeding at the isotopically distinctive location. In such a scenario, there would be no isotopic record of the spawning migration.

Another consideration is that trends within isotopic records reflect both geographic movement and changing trophic relationships. Furthermore, regarding geographic movement, it can be very difficult to distinguish the movements of a predator from that of its prey, as either or both could result in isotopic shifts. However, different methods can be combined to address this question. For example, if a predator is known to have high site fidelity (e.g., from tagging studies or the tissue-comparison method described above), and the predator is also known to prey upon seasonally migrating coastal pelagic fishes (from diet studies), then it can be argued that the isotopic shift was more likely to originate from prey movement. In some cases, the tissue-comparison method could be applied to both predator and prey, with prey samples being obtained from recently ingested stomach contents or from a separate, dedicated collection effort.

Before addressing geographic movement, however, the issue of changing trophic relationships should be addressed, if at all possible. There are two primary conditions that cause trophic relationships to change at the predator level: changing baselines and changing trophic positions. In the case of $\delta^{15}N$, both of these issues can be addressed directly through isotopic analysis of source and trophic amino acids (compound-specific isotope analysis, CSIA; Chikaraishi et al. 2009; Ellis 2012; Layman et al. 2012). The $\delta^{15}N$ of source amino acids provides the isotopic baseline, after which the isotopic offset between the $\delta^{15}N$ of source and trophic amino acids can be used to calculate trophic position with relative precision. Moreover, it is entirely feasible to apply this CSIA approach to individual eye-lens laminae, thereby allowing the reconstruction of lifetime trends in baseline and trophic position. After accounting for these two effects, any remaining trends will be the result of geographic movement of predator or prey.

Finally, another promising approach would be to reconstruct individual isotopic histories for species that are already well-known (model species). Repeating this for a combination of model species that includes similar and disparate life-history types is likely to be particularly informative. Future work should also include additional efforts to validate eye-lens records under experimental conditions (e.g., Granneman 2018) and should explore novel combinations of approaches that are designed to overcome ambiguities in isotope-based results.

Acknowledgments This research was made possible in part by a grant from The Gulf of Mexico Research Initiative/C-IMAGE I, II, and III.

References

Bowen GJ, Zhongfang L, Vander Zanden HB, Zhao L, Takahashi G (2014) Geographic assignment with stable isotopes in IsoMAP. Methods Ecol Evol 5:201–206

Buchheister A, Latour RJ (2010) Turnover and fractionation of carbon and nitrogen stable isotopes in tissues of a migratory coastal predator, summer flounder (*Paralichthys dentatus*). Can J Fish Aquat Sci 67:445–461

Campana SE, Jones CM (1992) Analysis of otolith microstructure data. In: Stevenson DK, Campana SE (eds) Otolith microstructure examination and analysis, pp 73–100. Canadian Special Publication of Fisheries and Aquatic Sciences 117

Chang CCY, Kendall C, Silva SR, Battaglin WA, Campbell DH (2002) Nitrate stable isotopes: tools for determining nitrate sources among different land uses in the Mississippi River Basin. Can J Fish Aquat Sci 59:1874–1885. https://doi.org/10.1139/f02-153

Chikaraishi Y, Ogawa NO, Kashiyama Y, Takano Y, Suga H, Tomitani A, Miyashita H, Kitazato H, Ohkouchi N (2009) Determination of aquatic food-web structure based on compound-specific nitrogen isotopic composition of amino acids. Limnol Oceanogr Methods 7:740–750

Dahm R, Schonthaler HB, Soehn AS, van Marle J, Vrensen GFJM (2007) Development and adult morphology of the eye lens in the zebrafish. Exp Eye Res 85:74–89

Danysh BP, Duncan MK (2009) The lens capsule. Exp Eye Res 88:151–164

Ellis G (2012) Compound-specific stable isotopic analysis of protein amino acids: ecological applications in modern and ancient systems. Doctoral dissertation, University of South Florida, Tampa, FL

Gaston TF, Suthers IM (2004) Spatial variation in $\delta^{13}C$ and $\delta^{15}N$ of liver, muscle and bone in a rocky reef planktivorous fish: the relative contribution of sewage. J Exp Mar Biol Ecol 304:17–33

Granneman J (2018) Evaluation of trace-metal and isotopic records as techniques for tracking lifetime movement patterns in fishes. Doctoral dissertation, University of South Florida, Tampa, FL

Granneman J, Jones DL, Peebles EB (2017) Associations between metal exposure and lesion formation in offshore Gulf of Mexico fishes collected after the Deepwater Horizon oil spill. Mar Pollut Bull 117:462–477

Greiling TMS, Clark JI (2012) New insights into the mechanism of lens development using zebra fish. Int Rev Cell Mol Biol 296:1–61

Heady WN, Moore JW (2013) Tissue turnover and stable isotope clocks to quantify resource shifts in anadromous rainbow trout. Oecologia 172:21–34

Hobson KA, Wassenaar LI (2007) Tracking animal migration with stable isotopes. Academic Press, Amsterdam, 144 pp

Hunsicker ME, Essington TE, Aydin KY, Ishida B (2010) Predatory role of the commander squid *Berryteuthis magister* in the eastern Bering Sea: insights from stable isotopes and food habits. Mar Ecol Prog Ser 415:91–108

Jagger WS (1997) Chromatic and monochromatic optical resolution in the rainbow trout. Vis Res 37:1249–1254

Keough JR, Hagley CA, Ruzycki E, Sierszen M (1998) $\delta^{13}C$ composition of primary producers and role of detritus in a freshwater coastal ecosystem. Limnol Oceanogr 43:734–740

Kjeldsen H, Heinemeier J, Heegaard S, Jacobsen C, Lynnerup N (2010) Dating the time of birth: a radiocarbon calibration curve for human eye-lens crystallins. Nucl Instrum Methods Phys Res Sect B-Beam Interact Mater Atoms 268:1303–1306. https://doi.org/10.1016/j.nimb.2009.10.158

Kurth BN (2016) Trophic ecology and habitat use of Atlantic tarpon (*Megalops atlanticus*). Master's thesis, University of South Florida, Tampa, FL

Layman CA, Araujo MS, Boucek R, Hammerschlag-Peyer CM, Harrison E, Jud ZR, Matich P, Rosenblatt AE, Vaudo JJ, Yeager LA, Post DM, Bearhop S (2012) Applying stable isotopes to examine food-web structure: an overview of analytical tools. Biol Rev 87:545–562

Lynnerup N, Kjeldsen H, Heegaard S, Jacobsen C, Heinemeier J (2008) Radiocarbon dating of the human eye lens crystallins reveal proteins without carbon turnover throughout life. PLoS One. https://doi.org/10.1371/journal.pone.0001529

Lynnerup N, Kjeldsen H, Zweihoff R, Heegaard S, Jacobsen C, Heinemeier J (2010) Ascertaining year of birth/age at death in forensic cases: a review of conventional methods and methods allowing for absolute chronology. Forensic Sci Int 201:74–78. https://doi.org/10.1016/j.forsciint.2010.03.026

MacKenzie KM, Longmore C, Preece C, Lucas CH, Trueman CN (2014) Testing the long-term stability of marine isoscapes in shelf seas using jellyfish tissues. Biogeochemistry 121:441–454

MacNeil MA, Drouillard KG, Fisk AT (2006) Variable uptake and elimination of stable nitrogen isotopes between tissues in fish. Can J Fish Aquat Sci 63:345–353

Meath B, Peebles EB, Seibel BA, Judkins H (2019) Stable isotopes in the eye lenses of Doryteuthis plei (Blainville 1823): Exploring natal origins and migratory patterns in the eastern Gulf of Mexico. Cont Shelf Res 174:76–84

McMahon KW, Hamady LL, Thorrold SR (2013) Ocean ecogeochemistry: a review. Oceanogr Mar Biol Annu Rev 51:327–374

Murawski SA, Hogarth WT, Peebles EB, Barbieri L (2014) Prevalence of fish diseases in the Gulf of Mexico, post-Deepwater Horizon. Trans Am Fish Soc 143:1084–1097

Nicol JAC (1989) The eyes of fishes. Oxford University Press, Oxford, 308p

Nielsen J, Hedeholm RB, Heinemeier J, Bushnell PG, Christiansen JS, Olsen J, Ramsey CB, Brill RW, Simon M, Steffensen KF, Steffensen JF (2016) Eye lens radiocarbon reveals centuries of longevity in the Greenland shark (*Somniosus microcephalus*). Science 353:702–704. https://doi.org/10.1126/science.aaf1703

Onthank KL (2013) Exploring the life histories of cephalopods using stable isotope analysis of an archival tissue. Doctoral dissertation, Washington State University, Pullman, WA

Parry MP (2003) The trophic ecology of two ommastrephid squid species, *Ommastrephes bartramii* and *Sthenoteuthis oualaniensis*, in the North Pacific sub-tropical gyre. Doctoral dissertation, University of Hawaii at Manoa, Honolulu, HI

Post DM, Layman CA, Arrington DA, Takimoto G, Quattrochi J, Montaña CG (2007) Getting to the fat of the matter: models, methods and assumptions for dealing with lipids in stable isotope analyses. Oecologia 152:179–189

Quaeck K (2017) Stable isotope analysis of fish eye lenses: reconstruction of ontogenetic trends in spatial and trophic ecology of elasmobranchs and deep-water teleosts. Doctoral dissertation, University of Southampton, 209 pp

Quaeck-Davies K, Bendall VA, MacKenzie KM, Hetherington S, Newton J, Trueman CN (2018) Teleost and elasmobranch eye lenses as a target for life-history stable isotope analyses. PeerJ. https://doi.org/10.7717/peerj.4883

Radabaugh KR, Peebles EB (2014) Multiple regression models of $\delta^{13}C$ and $\delta^{15}N$ for fish populations in the eastern Gulf of Mexico. Cont Shelf Res 84:158–168

Radabaugh KR, Hollander DJ, Peebles EB (2013) Seasonal $\delta^{13}C$ and $\delta^{15}N$ isoscapes of fish populations along a continental shelf trophic gradient. Cont Shelf Res 68:112–122

Radabaugh KR, Malkin EM, Hollander DJ, Peebles EB (2014) Evidence for light-environment control of carbon isotope fractionation by benthic microalgal communities. Mar Ecol Prog Ser 495:77–90

Rau GH, Takahashi T, Des Marais DJ (1989) Latitudinal variations in plankton $\delta^{13}C$: implications for CO_2 and productivity in past oceans. Nature 341:516–518

Shi Y, Barton K, De Maria A, Petrash JM, Shiels A, Bassnett S (2009) The stratified syncytium of the vertebrate lens. J Cell Sci 122:1607–1615

Smith FA, Freeman KH (2006) Influence of physiology and climate on δD of leaf wax n-alkanes from C3 and C4 grasses. Geochim Cosmochim Acta 70:1172–1187

Stewart DN, Lango J, Nambiar KP, Falso MJS, Fitzgerald PG, Rocke DM, Hammock BD, Buchholz BD (2013) Carbon turnover in the water-soluble protein of the adult human lens. Mol Vis 19:463–475

Tzadik OE, Curtis JS, Granneman JE, Kurth BN, Pusack TJ, Wallace AA, Hollander DJ, Peebles EB, Stallings CD (2017) Chemical archives in fishes beyond otoliths: a review on the use of other body parts as chronological recorders of microchemical constituents for expanding interpretations of environmental, ecological, and life-history changes. Limnol Oceanogr Methods 15:238–263

Wallace AA, Hollander DJ, Peebles EB (2014) Stable isotopes in fish eye lenses as potential recorders of trophic and geographic history. PLoS One 9:1–8. https://doi.org/10.1371/journal.pone.0108935

Walls GL (1942) The vertebrate eye and its adaptive radiation. Hafner, New York

West JB, Bowen GJ, Dawson TE, Tu KP (2010) Isoscapes. Springer, Dordrecht, 487 pp

Wistow GJ, Piatigorsky J (1988) Lens crystallins: the evolution and expression of proteins for a highly specialized tissue. Annu Rev Biochem 57:479–504

Wride MA (2011) Lens fibre cell differentiation and organelle loss: many paths lead to clarity. Philos Trans R Soc B – Biol Sci 366:1219–1233

Chapter 13
The Utility of Stable and Radioisotopes in Fish Tissues as Biogeochemical Tracers of Marine Oil Spill Food Web Effects

William F. Patterson III, Jeffery P. Chanton, David J. Hollander, Ethan A. Goddard, Beverly K. Barnett, and Joseph H. Tarnecki

Abstract Direct exposure to petroleum compounds was widely reported for a variety of taxa following the DWH. Evidence of exposure ranged from oiling of skin, shells, or feathers, depending on the taxa, to observation of ingested oil in small translucent, invertebrates, to biomarkers of petroleum compounds within an organism's tissues, such as PAHs in the hepatopancreas of invertebrates or the liver of fishes, or metabolic products of PAH catabolism in the bile of various vertebrate taxa. Development of natural biogeochemical tracers to examine indirect effects, especially over long (months to years) time scales, can be much more problematic. In this chapter, we describe the utility of employing stable isotopes and radioisotopes to 1) examine whether food web effects can be inferred from shifts in stable isotope values measured in vertebrate taxa; 2) examine the assimilation and trophic transfer of petrocarbon in marine food webs; and, 3) serve as long-term biogeochemical tracers either of petrocarbon assimilation or trophic shifts that are indicative of food web effects of marine oil spills. Data and analyses are largely drawn from DWH-related studies but with broader implications to marine oil spills in general.

Keywords Petrocarbon · Reef fish · Stable isotopes · Radiocarbon

W. F. Patterson III (✉) · J. H. Tarnecki
University of Florida, Fisheries and Aquatic Sciences, Gainesville, FL, USA
e-mail: will.patterson@ufl.edu

J. P. Chanton
Florida State University, Department of Earth, Ocean and Atmospheric Science, Tallahassee, FL, USA
e-mail: jchanton@fsu.edu

D. J. Hollander · E. A. Goddard
University of South Florida, College of Marine Science, St. Petersburg, FL, USA
e-mail: davidh@usf.edu; egoddard@usf.edu

B. K. Barnett
University of Florida, Fisheries and Aquatic Sciences, Gainesville, FL, USA

National Marine Fisheries Service, Southeast Fisheries Science Center, Panama City Laboratory, Panama City, FL, USA
e-mail: beverly.barnett@noaa.gov

S. A. Murawski et al. (eds.), *Scenarios and Responses to Future Deep Oil Spills*,
https://doi.org/10.1007/978-3-030-12963-7_13

13.1 Introduction

Large-scale marine oil spills such as the *Deepwater Horizon* (DWH) oil spill have caused significant impacts to a broad diversity of taxa, from plankton to marine mammals, around the globe. Often, the impacts from these spills receiving the greatest attention are direct ones, such as mortality due to oiling of organisms or toxicological or physiological effects due to exposure to petroleum compounds, such as polycyclic aromatic hydrocarbons (PAHs). While the expression of direct impacts of spills is often acute, occurring in the minutes to days after a spill, other effects can be chronic and manifested for years thereafter.

Indirect effects of oil spills, such as altered food webs or the bioenergetic consequences of such changes, have received considerably less attention than direct effects (but see Gin et al. 2001; Peterson et al. 2003; McCann et al. 2017; Olin et al. 2018). This is likely due to the fact that direct effects are often easier to diagnose and track. One simply needs to find evidence of exposure to petroleum compounds, have an understanding of the toxicological or physiological consequences of that exposure, and then measure the response at the cellular, tissue, organ, or organismal level. Estimating indirect effects on organisms, populations, communities, or ecosystems is much less tractable for several reasons (Fodrie et al. 2014; Beyer et al. 2016). First, one must have baseline data to understand pre-spill conditions and natural variability (process error) in the parameters of interest. Then, one must have a way to measure and track indirect effects over time that is independent of the markers utilized to estimate direct exposure to petroleum compounds. Ideally, these markers would not be ephemeral but instead would have some level of permanence such that chronic impacts of indirect effects could be examined years to decades after a spill.

Evidence of direct exposure to petroleum compounds can range from oiling of skin, shells, or feathers, depending on the taxa, to observation of ingested oil in small translucent, invertebrates, to biomarkers of petroleum compounds within an organism's tissues, such as PAHs in the hepatopancreas of invertebrates or the liver of fishes, or metabolic products of PAH catabolism in the bile of various vertebrate taxa. Development of natural biogeochemical tracers to examine indirect effects, especially over long (months to years) time scales, can be much more problematic. However, natural biogeochemical tracers described in earlier chapters of this book, in the form of stable isotope ratios measured in tissues of various taxa, may be ideal for inferring changes in food web structure and prey resource availability following a marine oil spill. Furthermore, depleted $\Delta^{14}C$ values in tissues may indicate petrocarbon assimilated into and transferred through the marine food web, thus providing a natural tracer of the footprint of an oil spill's effects (e.g., Wilson et al. 2016). Therefore, the objectives of this chapter are to describe the utility of employing stable isotopes and radioisotopes to (1) examine whether food web effects can be inferred from shifts in stable isotope values measured in reef fishes, (2) examine the assimilation and trophic transfer of petrocarbon in marine food webs, and (3) serve as long-term biogeochemical tracers either of petrocarbon assimilation or trophic

shifts that are indicative of food web effects of marine oil spills. Data and analyses are drawn from DWH-related studies but with broader implications to marine oil spills in general.

13.2 Stable Isotopes Utilized to Infer Food Web Effects

Stable isotopes are widely utilized in marine ecology to infer sources of organic carbon, estimate trophic position, and examine food web connectivity (Fry 2006). The most widely utilized stable isotope ratios in ecology are those of C and N, expressed as the delta values $\delta^{13}C$ and $\delta^{15}N$. In each case, a stable isotope delta value is computed as the ratio of a lighter to heavier stable isotope of a given element in a sample relative to a standard with the following equation:

$$\delta X = \left[\left(R_{\text{sample}} / R_{\text{standard}}\right) - 1\right] * 10^3, \tag{13.1}$$

where $X = {}^{13}C$ or ${}^{15}N$, $R = {}^{13}C/{}^{12}C$ or ${}^{15}N/{}^{14}N$, standards are N in air ($\delta^{15}N_{Air}$) for $\delta^{15}N$ and Pee Dee Belemnite ($\delta^{13}C_{V\text{-}PBD}$) for $\delta^{13}C$, and units of δX are ‰ or per mille. For a given element, its stable isotopes only differ by the number of neutrons. Therefore, different stable isotopes for that element have different atomic masses but have slightly slower chemical reaction kinetics. In turn, this results in the products of reactions, including metabolic reactions in organisms, having different (heavier) isotopic ratios.

Physiological differences in primary producers drive differences in basal $\delta^{13}C$ values, which then can be utilized to distinguish different sources of organic C and trophic pathways in marine ecosystems. However, on the northern Gulf of Mexico (nGoM) shelf, the predominant primary producers are benthic microalgae (BMA, ~ −19‰) and phytoplankton (~ −21‰), which differ very little in $\delta^{13}C$ (Moncrieff and Sullivan 2001; Radabaugh et al. 2013; Tarnecki and Patterson 2015). Furthermore, there is no significant difference in the $\delta^{15}N$ values between nGoM phytoplankton and BMA (Radabaugh et al. 2013; Tarnecki and Patterson 2015), with mean basal $\delta^{15}N$ being 5.82‰ among baseline BMA and phytoplankton samples collected on the north central GoM shelf prior to the DWH (Tarnecki and Patterson 2015).

Having accurate estimates of basal $\delta^{13}C$ and $\delta^{15}N$ values is critical to examining food web dynamics with stable isotope ratios. As organic matter is consumed and assimilated by organisms at progressively higher trophic positions, $\delta^{13}C$ and $\delta^{15}N$ values increase due to the metabolic process of trophic fractionation (Fry 2006). Given that reaction kinetics of the lighter isotope, ${}^{12}C$ in the case of C and ${}^{14}N$ in the case of N, are slightly faster than with the heavier isotope (${}^{13}C$ or ${}^{15}N$), the metabolic processes of digestion and assimilation result in the isotopic ratios becoming enriched in the heavier isotopes of C and N, thus the $\delta^{13}C$ and $\delta^{15}N$ values increasing at progressively higher trophic positions. If one has an estimate of the basal values, particularly for $\delta^{15}N$, and an estimate of the trophic discrimination factor (TDF), or

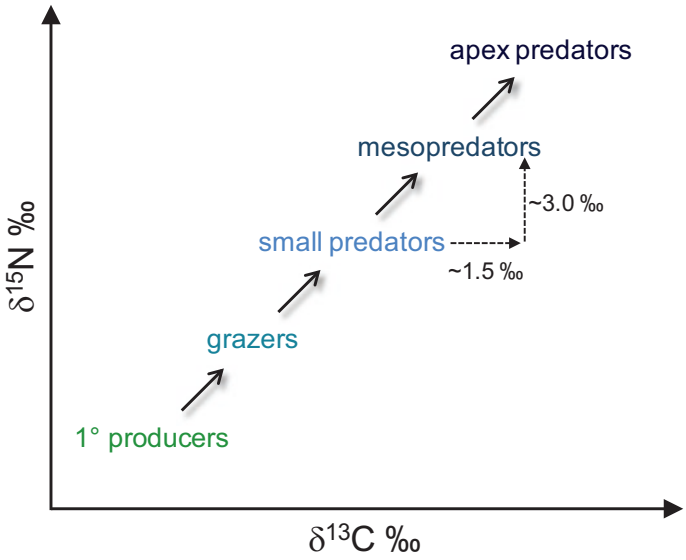

Fig. 13.1 Conceptual model of trophic fractionation of muscle tissue that occurs as organic matter is consumed and assimilated by organisms at progressively higher trophic levels. Trophic discrimination factor estimates are 3.0‰ for $\delta^{15}N$ and 1.5‰ for $\delta^{13}C$ (see text for details)

the per mille increase in $\delta^{15}N$ per trophic position, then one can estimate the trophic position of a given individual from its measured $\delta^{15}N$ value.

Trophic discrimination factors differ by element as well as by the tissue being examined. In marine ecology, muscle tissue is often analyzed due its relatively long (months) turnover time, which implies a trophic signature integrated over that time period. In the case of bony fish muscle, the TDF for $\delta^{13}C$ (Δ^{13}_{C}) estimated across a range of experiments and studies is approximately 1.5‰ (Sweeting et al. 2007). The TDF for $\delta^{15}N$ (Δ^{15}_{N}) is approximately 3.0‰, which is the mean measured for fishes feeding on high-protein diets (McCutchan et al. 2003; Vanderklift and Ponsard 2003; Rooker et al. 2006). Therefore, at progressively higher trophic levels, one would expect an increase in $\delta^{13}C$ of approximately 1.5‰ and an increase in $\delta^{15}N$ of approximately 3.0‰, resulting in a positive slope in the relationship between $\delta^{15}N$ and $\delta^{13}C$ when a bi-plot of those parameters is constructed across different trophic levels within a marine food web (Fig. 13.1).

13.2.1 Temporal Variability in Reef Fish Muscle Stable Isotopes

The general relationship between $\delta^{15}N$ and $\delta^{13}C$ enables the usage of stable isotopes to examine food web structure, as well as to examine shifts in that structure resulting from disturbance. For example, stable isotopes have been utilized to examine

marine trophic shifts due to eutrophic phytoplankton blooms and habitat degradation (Chasar et al. 2005), effects of chronic trawling and overfishing (Jennings et al. 2002), and large-scale aquaculture operations (Holmer et al. 2007). Therefore, as long as pre-disturbance stable isotope data are available, trophic shifts or food web effects can be inferred by examining stable isotopes in post-disturbance samples.

In the case of the DWH, Tarnecki and Patterson (2015) reported significant post-DWH diet shifts in red snapper, *Lutjanus campechanus*, a reef fish that is a ubiquitous member of natural and artificial reef communities in the nGoM. Red snapper are extreme generalists, with their diet ranging from swarming zooplankton to fish (McCawley et al. 2003; Tarnecki and Patterson 2015). Therefore, they are an ideal candidate to examine post-DWH diet shifts. Following the spill, plankton disappeared from red snapper diet, and benthic and demersal fishes constituted a much larger percentage of observed prey. These diet shifts were also apparent in white muscle stable isotope values, as $\delta^{15}N$ increased and $\delta^{34}S$ declined in post-DWH samples, although stable isotope shifts lagged behind diet shifts due to the turnover time in their white muscle tissue being approximately 6 months (Nelson et al. 2011). While $\delta^{15}N$ is indicative of trophic position, $\delta^{34}S$ serves as an effective biomarker of pelagic versus benthic production (Fry 2006). For example, nGoM phytoplankton $\delta^{34}S$ is approximately 20‰, while BMA has a value of approximately 10‰ (Moncrieff and Sullivan 2001; Tarnecki and Patterson 2015). These distinctive signatures are due to sulfate, SO_4^{2-}, being the predominant source of S in the water column, while it is reduced to sulfide (S^{2-}) by bacteria in the benthos (Fry and Chumchal 2011). Given only minimal trophic fractionation (~0.5‰ per trophic level) in $\delta^{34}S$, it effectively distinguishes pelagic versus benthic production sources (Fry 2006).

The red snapper white muscle stable isotope data reported by Tarnecki and Patterson (2015) were updated through April 2015 to demonstrate trends in $\delta^{15}N$ and $\delta^{13}C$ from the year prior to the DWH through 5 years post-spill. Adult red snapper samples were collected with hook-and-line sampling at natural and artificial reefs across the north central GoM shelf between 15 and 80 m water depths in a ~7500 km^2 region bracketed by 86° 14' W and 88° 59' W longitude. White muscle tissue was freeze-dried and analyzed for $\delta^{15}N$ and $\delta^{13}C$ with either a Europa Scientific GSL/Geo 20–20 stable isotope ratio-mass spectrometer (SIR-MS) or with a Thermo Delta+XL SIR-MS. Both SIR-MS instruments were coupled with elemental analyzers to estimate %C and %N, hence C:N, in each sample. Because lipids are depleted in ^{13}C relative to muscle protein, and C:N ratio serves as an effective proxy of lipid content in fish muscle samples, all $\delta^{13}C$ data reported below were first corrected for lipid content with the equation reported by Post et al. (2007):

$$\mathrm{CF} = -3.32 + \left(0.99 * \mathrm{C:N}\right), \tag{13.2}$$

where CF is the correction factor applied to $\delta^{13}C$ to account for percent lipid in dried muscle samples and C:N serves as a proxy for percent lipid.

There were 400 red snapper muscle tissue samples analyzed across 6 years (Table 13.1, Fig. 13.2a), with two trends apparent in the data. First, $\delta^{15}N$ increased approximately 0.7‰, or one-quarter of a trophic position, between the pre-spill period and year-3 post-DWH (Fig. 13.2a) and then returned to near pre-DWH levels.

Table 13.1 Sample sizes for northern Gulf of Mexico reef fish muscle tissue samples (n = 846) analyzed for $\delta^{15}N$ and $\delta^{13}C$ in the year prior to and the 5 years following the *Deepwater Horizon* oil spill

Species	Pre-DWH	Year-1	Year-2	Year-3	Year-4	Year-5	Total
gray triggerfish	8	28	40	18	15	6	115
red porgy	10	42	24	4	22	5	107
red snapper	52	133	71	43	76	25	400
tomtate	19	20	29	17	10	5	100
vermilion snapper	12	35	27	11	28	11	124

Sample locations were between 86° 14′ and 88° 59′ west longitude at depths of 15–80 m across the shelf

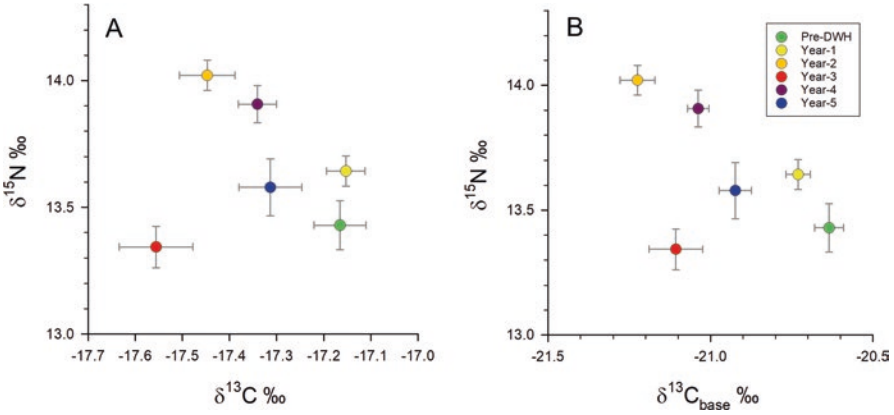

Fig. 13.2 Bi-plots of northern Gulf of Mexico red snapper muscle (**a**) $\delta^{15}N$ versus $\delta^{13}C$ for fish sampled the year prior to and during the 5 years following the *Deepwater Horizon* oil spill and (**b**) $\delta^{15}N$ versus $\delta^{13}C$ estimated at the base of the food web ($\delta^{13}C_{base}$) to account for shifts in trophic position inferred from shifts in $\delta^{15}N$ observed following the spill (see text for details). Error bars are ± standard error of the mean

Secondly, instead of $\delta^{13}C$ increasing with $\delta^{15}N$, which would follow the general pattern indicated in Fig. 13.1, $\delta^{13}C$ actually decreased (Fig. 13.2a), which indicates a lighter source of organic C in the system. Tarnecki and Patterson (2015) inferred this trend in $\delta^{13}C$ most likely resulted from the trophic transfer and assimilation of petrocarbon in the food web. However, understanding $\delta^{13}C$ dynamics is complicated due to trophic fractionation that occurs in $\delta^{13}C$. Therefore, trophic position was controlled for in $\delta^{13}C$ data, by estimating basal $\delta^{13}C$ ($\delta^{13}C_{base}$) for each muscle sample with the equation:

$$\delta^{13}C_{base} = \delta^{13}C_{muscle} - \left[\left(\text{trophic position} - 1\right) * \Delta_C\right], \tag{13.3}$$

where $\delta^{13}C_{muscle}$ is the measured $\delta^{13}C$ in a given muscle sample; trophic position is the trophic position of sample estimated from the measured $\delta^{15}N$ in the sample, a $\delta^{15}N_{base}$ value of 5.82‰, and $\Delta^{15}N$ = 3.0‰ per trophic level; and, $\Delta^{13}C$ = 1.5‰ per trophic level.

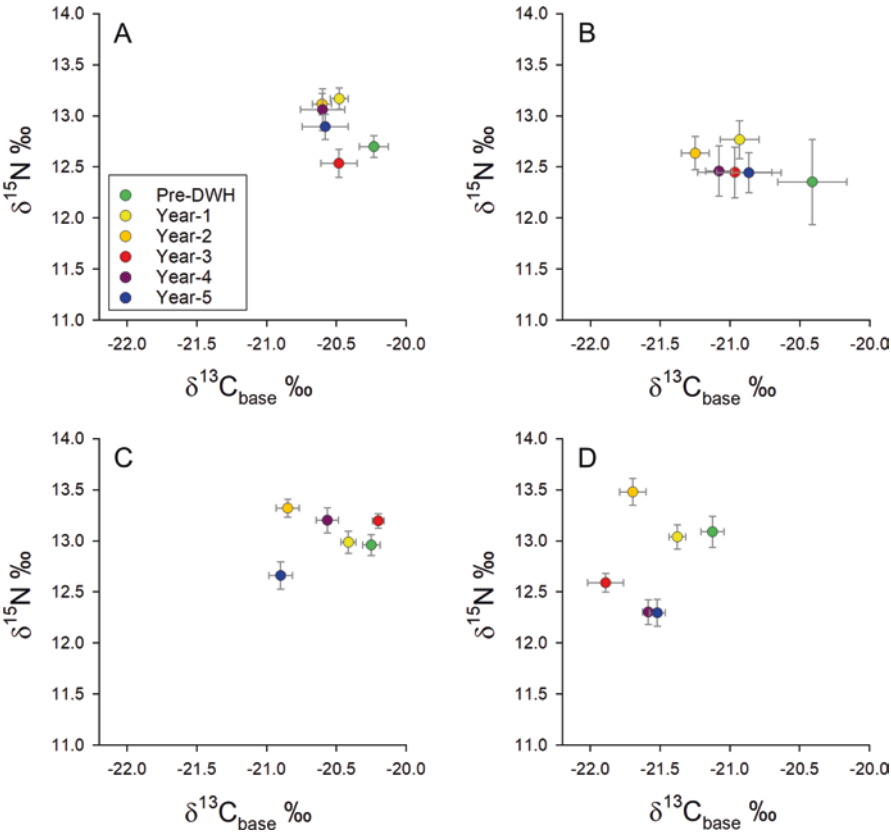

Fig. 13.3 Bi-plots of white muscle $\delta^{15}N$ versus $\delta^{13}C$ estimated at the base of the food web ($\delta^{13}C_{base}$) for northern Gulf of Mexico reef fishes: (**a**) gray triggerfish, (**b**) tomtate, (**c**) red porgy, and (**d**) vermilion snapper. Error bars are ± standard error of the mean

The trend in lighter $\delta^{13}C_{base}$ over the first 3 years post-DWH is more pronounced than that observed for red snapper muscle $\delta^{13}C$ without correcting for trophic position (Fig. 13.2), thus more clearly indicating ^{13}C depletion following the DWH. Norberg (2015) reported similar patterns for tomtate, *Haemulon aurolineatum*, another ubiquitous reef fish in the nGoM which is predominantly an invertivore (Sedberry 1985; Norberg 2015). The narrower diet of tomtate meant nonsignificant shifts in muscle $\delta^{15}N$ were observed, but post-DWH declines in $\delta^{13}C$ were similar to those reported by Tarnecki and Patterson (2015).

Here, we report $\delta^{15}N$ and $\delta^{13}C_{base}$ for muscle tissue from additional reef fish species sampled in the same study region and during the same period as described above for red snapper (Fig. 13.3). These include tomtate; gray triggerfish, *Balistes capriscus*, a demersal grazing invertivore with a diet comprised of benthic and encrusting invertebrates (Vose and Nelson 1994; Kurz 1995; Goldman et al. 2016); red porgy, *Pagrus pagrus*, a demersal reef omnivore (Manooch 1977; Goldman et al. 2016); and vermilion snapper, *Rhomboplites aurorubens*, a pelagic reef omnivore with a diet

nearly as broad as red snapper (Grimes 1979; Tarnecki et al. 2016). In all species, the shift in $\delta^{15}N$ was ~0.5‰ but was highest for vermilion snapper and lowest for tomtate (Fig. 13.3). Like red snapper, muscle $\delta^{15}N$ had generally returned to near pre-DWH values by year-4 post-spill for these other reef fishes as well. However, vermilion snapper muscle $\delta^{15}N$ actually decreased below the pre-spill mean (Fig. 13.3d). It is unclear what drove that result; however, only 12 pre-spill vermilion snapper were sampled, and they came from a somewhat restricted area on the western side of the study region. Therefore, it is possible these fish were not representative of the entire region.

The shift in $\delta^{13}C_{base}$ observed among the additional reef fish species ranged from approximately 0.5 to 1.0‰ in the years following the DWH (Fig. 13.3), which brackets the pattern observed in red snapper samples (Fig. 13.2). However, the overall patterns are most easily observed when simply plotting the mean shifts in $\delta^{15}N$ versus $\delta^{13}C_{base}$ (Fig. 13.4). Among all species, the decline in mean $\delta^{13}C_{base}$ was approximately 0.6‰ by year-3. A transition back toward pre-spill values occurred thereafter, but $\delta^{13}C_{base}$ never fully returned to pre-DWH values during the 5 post-spill years.

The observed difference in $\delta^{13}C_{base}$ between pre-DWH and year-5 data, which is consistent across species, could be explained by a number of possible scenarios. Phytoplankton could have contributed a greater proportion of primary production relative to BMA in the post-spill time period, hence the lower $\delta^{13}C_{base}$ values. The actual difference (~0.3‰) is so small that it could have been caused by any number of factors that potentially affect phytoplankton physiology (Leboulanger et al. 1995; Fry 2006). Lastly, if the decline in $\delta^{13}C_{base}$ observed between pre-DWH and year-3

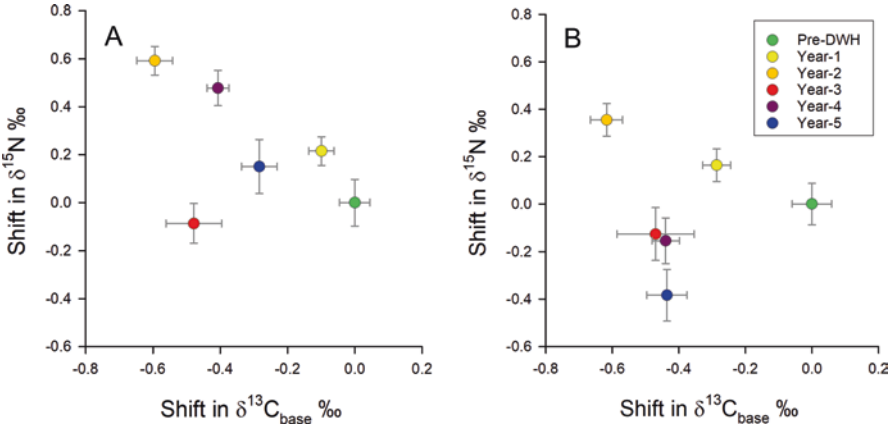

Fig. 13.4 Shifts in $\delta^{15}N$ versus those in $\delta^{13}C_{base}$ for (**a**) red snapper (n = 400) and (**b**) other reef fishes (gray triggerfish, n = 115; red porgy, n = 107; tomtate, n = 100; and vermilion snapper, n = 124) observed in the years following the *Deepwater Horizon* oil spill relative to pre-spill mean values. Among the samples depicted in panel B, species-specific shifts were computed relative to species-specific mean pre-spill values; then mean annual shifts among all samples across all species were computed. Error bars are ± standard error of the mean

samples was due to trophic transfer and assimilation of petrocarbon, then the persistence of organic carbon depleted in ^{13}C could be due to the retention and cycling of that signature in the nGoM food web. Evidence is presented below that supports the hypothesis that lower post-DWH $\delta^{13}C_{base}$ values in reef fish muscle tissue samples were in fact driven by the assimilation, trophic transfer, and retention of petrocarbon in the nGoM food web.

13.3 Petrocarbon Assimilation in the Gulf of Mexico Food Web

There are several lines of evidence demonstrating that petrocarbon was assimilated into lower trophic levels of the nGoM food web following the DWH. Micro-(1 μm–0.2 mm) and meso-(0.2–20 mm) zooplankton sampled off Alabama (i.e., the western edge of the reef fish sample region described above) had depleted $\delta^{13}C$ signatures in summer 2010 that coincided with the arrival of surface oil slicks during the DWH event (Graham et al. 2010). The hydrocarbons released during the DWH had a $\delta^{13}C$ value of −27.2‰ for petroleum (Graham et al. 2010) and −57.4‰ for methane (Chanton et al. 2012), while mean $\delta^{13}C$ of nGoM particulate organic carbon (POM), which is a proxy for phytoplankton, is ~20‰ (Chanton et al. 2020). Therefore, Graham et al. (2010) inferred $\delta^{13}C$ values depleted in ^{13}C by ~4‰ in microzooplankton and ~1‰ in mesozooplankton relative to pre-spill values were indicative of bacterial assimilation of petroleum that was then transferred to two levels of consumers: first to microzooplankters, such as ciliates, and then to mesozooplankters, such as copepods. The authors discounted the potential for freshwater input from Mobile Bay to have affected plankton $\delta^{13}C$ values given the sampling occurred during a low-flow period and lower zooplankton $\delta^{13}C$ values closely corresponded with the arrival of surface oil slicks.

Results of subsequent ^{14}C analysis of nGoM plankton samples provide yet stronger evidence of petrocarbon assimilation and transfer in the nGoM food web. Radiocarbon (^{14}C) is a radioisotope and thus undergoes radioactive decay. It is typically reported as $\Delta^{14}C$, which is a measure of the relative difference in ^{14}C activity in a sample versus the absolute international standard (base year 1950) and corrected for age and fractionation via $\delta^{13}C$ (Stuiver and Pollach 1977). Its usage as a biomarker for petrocarbon is reviewed earlier in this book by Chanton et al. (2020). Briefly, modern surface organic C has a $\Delta^{14}C$ value of ~40‰, while petrocarbon, which is a fossil carbon that has been buried for millions of years such that all of its ^{14}C has been lost to radioactive decay, has a value of −1000‰. Therefore, assimilated petrocarbon in nGoM biota following the DWH would cause a much greater depletion in $\Delta^{14}C$ than would be observed in $\delta^{13}C$ given the greater difference in $\Delta^{14}C$ versus $\delta^{13}C$ values of end-members (Wilson et al. 2016; Bosman et al. 2017).

Chanton et al. (2020) report utilizing $\Delta^{14}C$ as a biogeochemical tracer to examine petrocarbon in three different carbon pools in the nGoM: dissolved organic

carbon (DOC), sinking particulate organic carbon (POC_{sink}), and sedimentary organic matter (SOM). As they point out, these pools play important roles in carbon cycling in this ecosystem, as well as in nutrient cycling. However, our interest here is in yet another pool, which is assimilated carbon, specifically petrocarbon, in the biomass of living organisms (i.e., the food web). Toward that end, plankton sampled from the nGoM in 2010 and 2011 and analyzed by Chanton et al. (2012) for $\delta^{13}C$ with SIR-MS and for $\Delta^{14}C$ with accelerator mass spectrometry (AMS) produced a significant linear relationship between $\delta^{13}C$ and $\Delta^{14}C$ values. The authors concluded these results indicated an admixture existed in zooplankton biomass between ^{13}C- and ^{14}C-depleted material and modern organic carbon fixed by phytoplankton. Furthermore, they concluded their data supported the inference of Graham et al. (2010) that petrocarbon consumed and assimilated by bacteria had been transferred into the metazoan food web via mesozooplankton grazing on microzooplankters but suggested methane instead of petroleum might be the source of petrocarbon. Later, based on SIR-MS and AMS analysis of POC samples taken off the shelf to a depth of 1200 m, Cherrier et al. (2013) clearly demonstrated that methane was in fact the most likely source of petrocarbon found in nGoM plankton following the DWH. The questions that follow are whether DWH-derived petrocarbon was effectively transferred to higher trophic levels and whether more permanent biomarkers than muscle protein may have recorded this signal.

13.3.1 Radiocarbon Analysis of Reef Fish Muscle Tissue

The archive of freeze-dried reef fish muscle tissue samples described above provided an opportunity to examine whether petrocarbon assimilated into the nGoM microbial food web, and then transferred via grazing zooplankton into the metazoan food web, made it to the level of mesopredator reef fishes. To test this, red snapper muscle tissue samples ($n = 15$) were analyzed for $\delta^{13}C$ with SIR-MS and for $\Delta^{14}C$ with AMS at the Center for Applied Isotope Studies (CAIS) University of Georgia or the National Ocean Sciences Accelerator Mass Spectrometry (NOSAMS) at Woods Hole Oceanographic Institution. Samples were randomly selected from among the 400 dried tissues and transferred to CAIS or NOSAMS. They were first subjected to H_3PO_4 in closed, evacuated glass vessels. The produced CO_2 was then stripped and cryogenically purified from H_20 vapor and N_2. A portion of the purified CO_2 was analyzed for $\delta^{13}C$ with SIR-MS, and the remainder was transferred to a reaction tube and reduced to pure C (graphite) in the presence of H_2 gas and Fe as a catalyst. The graphite was then pressed into target cartridges and analyzed for ^{14}C with AMS. Results are reported as $\Delta^{14}C$, which was corrected for natural isotopic fractionation via $\delta^{13}C$.

There is a significant linear relationship between $\Delta^{14}C$ and $\delta^{13}C_{base}$ among archived red snapper muscle samples, with the regression's coefficient of determination (R^2) being 0.48 (Fig. 13.5). This relationship confirms the decline in $\delta^{13}C_{base}$ observed in reef fish muscle tissue was due to petrocarbon being assimilated and

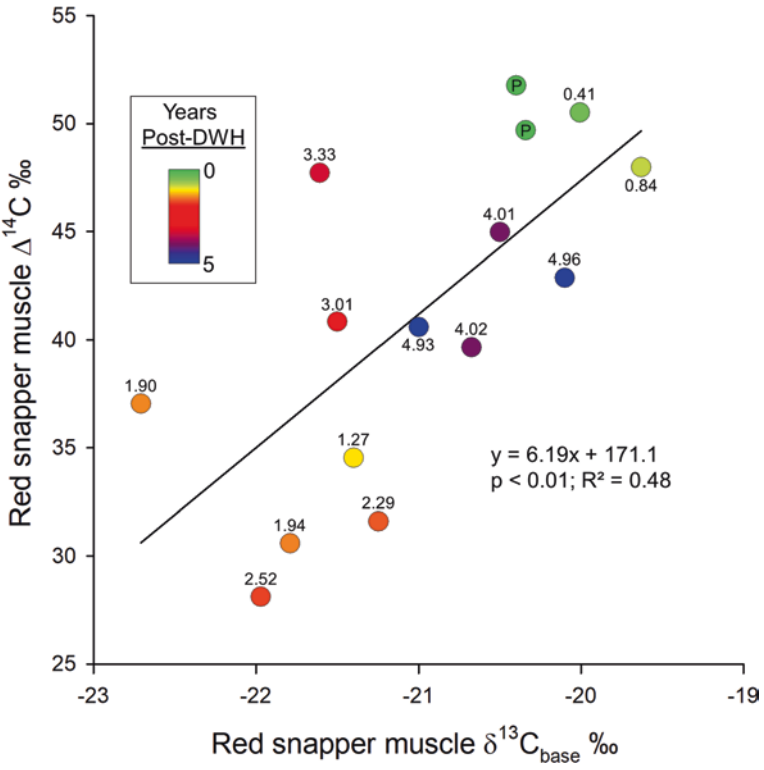

Fig. 13.5 Plot of red snapper muscle $\Delta^{14}C$ versus estimated $\delta^{13}C_{base}$ for fish sampled in the northern Gulf of Mexico the year before the *Deepwater Horizon* oil spill through 5 years post-spill. The legend indicates the timing of samples. Line indicates linear regression fit to the data. Numbers next to symbols on plot indicate years post-DWH; P = pre-spill samples

transferred up the metazoan food web. In fact, the relationship between red snapper muscle $\Delta^{14}C$ and $\delta^{13}C_{base}$ is actually slightly stronger than the one reported by Chanton et al. (2012) for nGoM zooplankton ($R^2 = 0.48$ versus 0.37). Furthermore, the slopes of the two relationships (6.2 for red snapper and 9.1 for plankton) are not significantly different, but that mostly owes to wide confidence intervals due to substantial unexplained variance in each model.

Red snapper muscle $\Delta^{14}C$ in the pre-spill period (2009 through early 2010) was higher (mean = 50.7‰) than mean $\Delta^{14}C$ reported by Chanton et al. (2012) for nGoM dissolved inorganic C (DIC, 41.0‰), which reflects complex dynamics in the system. For starters, shelf water DIC is affected by bomb ^{14}C that was input into the global ocean during nuclear weapon testing in the middle of the last century. The peak in $\Delta^{14}C$ occurred in ~1975, as inferred from coral records, with slight variation among ocean basins (Grottoli and Eakin 2007). There has been a linear decline since then (~2.6‰ per year in the nGoM; Barnett et al. 2018) due to mixing of bomb ^{14}C into the deep ocean. The fact that red snapper muscle tissue had higher $\Delta^{14}C$ than that of DIC reported by Chanton et al. (2012) is likely due to organic carbon

fixed with earlier DIC $\Delta^{14}C$ signatures being assimilated, transferred, and somewhat preserved in the standing stock of various taxa.

The trend in red snapper muscle $\Delta^{14}C$ suggests there was a lag of approximately 1 year between when zooplankton samples depleted in ^{14}C were first observed and when $\Delta^{14}C$ started declining in red snapper muscle tissue (Fig. 13.5). Furthermore, it was not until ~2.5 years post-spill that muscle $\Delta^{14}C$ values were at their lowest. Muscle $\Delta^{14}C$ increased during the last 2 years of the time series, but had not recovered to pre-DWH levels by 2014–2015, and no data currently exist to examine whether $\Delta^{14}C$ continued to increase after 2015. However, it may be that values of muscle $\Delta^{14}C$ observed in 2014–2015 did not increase further given $\Delta^{14}C$ was approximately 11‰ lower in 2014–2015 (year-5 post-DWH) than during 2009–2010, which is consistent with the predicted rate of decline in DIC $\Delta^{14}C$ over that time period (Barnett et al. 2018).

Red snapper muscle $\Delta^{14}C$ values have greater utility than simply certifying declines in reef fish muscle $\delta^{13}C_{base}$ resulted from petrocarbon or understanding the temporal progression of petrocarbon moving through the nGoM food web. Mixing models, such as those employed by Chanton et al. (2020), were applied to muscle $\Delta^{14}C$, as well as to $\delta^{13}C_{base}$, to estimate the percentage of carbon in red snapper muscle tissue derived from petrocarbon. The model employed to estimate percent petrocarbon from $\delta^{13}C_{base}$ for a given sample was:

$$\delta^{13}C_{base} = \left(f_1 * \delta^{13}C_{meta}\right) + \left(f_2 * \delta^{13}C_{petrocarbon}\right), \tag{13.4}$$

where $\delta^{13}C_{meta}$ is the $\delta^{13}C$ of metabolic carbon at the base of the food web for a given red snapper muscle sample, assumed here to be the mean of $\delta^{13}C_{base}$ estimated from the year prior to the DWH (−20.63‰); $\delta^{13}C_{petrocarbon}$ is $\delta^{13}C$ of petrocarbon [−57.4‰ for methane (Chanton et al. (2012) or −27.2‰ for petroleum (Graham et al. 2010)]; f_1 = fraction of $\delta^{13}C_{base}$ contributed by $\delta^{13}C_{meta}$; and f_2 = fraction of $\delta^{13}C_{base}$ contributed by petrocarbon, which equals $1 - f_1$. The model was solved for f_2 and then the percentage of $\delta^{13}C_{base}$ contributed by petrocarbon estimated as $100*f_2$. With respect to muscle $\Delta^{14}C$, a similar mixing model was utilized:

$$\Delta^{14}C_{muscle} = \left(f_1 * \Delta^{14}C_{meta}\right) + \left(f_2 * \Delta^{14}C_{petrocarbon}\right), \tag{13.5}$$

where $\Delta^{14}C_{muscle}$ is the $\Delta^{14}C$ measured in a given red snapper muscle tissue sample; $\Delta^{14}C_{meta}$ is the metabolic $\Delta^{14}C$ assimilated in prey ingested by red snapper, assumed here to be the mean of pre-DWH red snapper muscle $\Delta^{14}C$ (50.7‰) given there is no trophic fractionation in $\Delta^{14}C$; $\Delta^{14}C_{petrocarbon}$ is the $\Delta^{14}C$ of petrocarbon, which is −1000‰ whether the source is petroleum or methane; f_1 = fraction of $\Delta^{14}C_{muscle}$ contributed by $\Delta^{14}C_{meta}$; and f_2 = fraction of $\Delta^{14}C_{muscle}$ contributed by petrocarbon, which equals $1 - f_1$. The model was solved for f_2 and then the percentage of $\Delta^{14}C_{muscle}$ contributed by petrocarbon estimated as $100*f_2$.

The %petrocarbon in red snapper muscle tissue estimated with $\Delta^{14}C$ ranged from zero prior to the DWH to 2.2% ~2.5 years after the spill (Fig. 13.6a). One potential caveat is that utilizing mean pre-spill $\Delta^{14}C_{muscle}$ as one endpoint in the mixing model

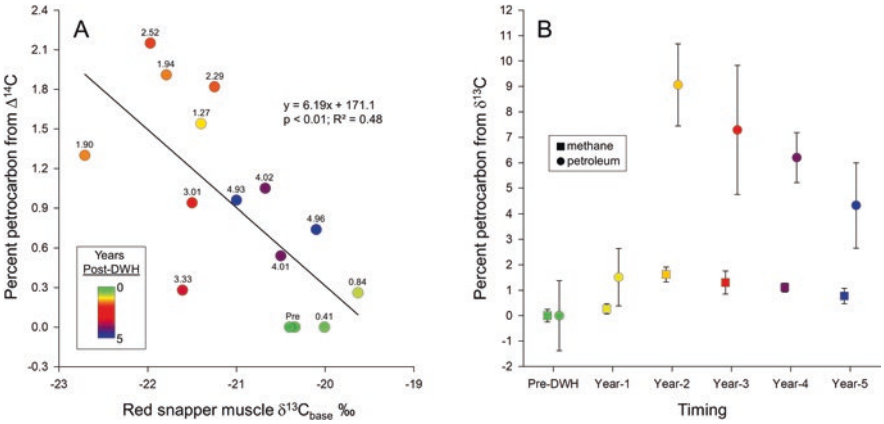

Fig. 13.6 The percentage (±95% CIs) of adult red snapper muscle carbon with a petrocarbon origin estimated with mixing models for (**a**) $\Delta^{14}C$ ($n = 15$) and (**b**) $\delta^{13}C_{base}$ ($n = 400$) values measured in muscle tissue samples. Numbers next to symbols on plot indicate years post-DWH; P = pre-spill samples. The legend in panel A indicates collection timing for a given sample. In panel B, mixing models were computed with both methane (−57.4‰) and petroleum (−27.2‰) as potential $\delta^{13}C$; see text for details

would result in an underestimate of red snapper muscle %petrocarbon if petrocarbon contributed some percentage of organic carbon assimilated by red snapper prior to the DWH. However, the close correspondence between the pre-DWH mean $\delta^{13}C_{base}$ (±95% CI) of −20.63‰ (±0.09‰) to $\delta^{13}C$ of offshore GoM surface DOC (−20.7‰; Walker et al. 2017), which is a proxy for phytoplankton $\delta^{13}C$, suggests the assumption that zero petrocarbon was assimilated in red snapper muscle in the year prior to the DWH is valid.

Clearly, different estimates of %petrocarbon in red snapper muscle tissue computed with $\delta^{13}C$ result whether methane (−57.4‰) or petroleum (−27.2‰) is assumed to be the source of assimilated petrocarbon (Fig. 13.6b). Given the shorter distance in isotope space between $\delta^{13}C_{base}$ and the $\delta^{13}C$ of petroleum, the shifts observed in $\delta^{13}C_{base}$ in the years following the DWH yield higher estimates of %petrocarbon with oil-derived carbon rather than if methane was the source. The peak in %petrocarbon occurred in year-2 regardless of the petrocarbon endmember, with a mean (±95% CI) of 1.62% (±0.29%) for methane versus 9.06% (±1.61%) for petroleum. The estimates produced with methane as an end-member most closely align with those produced with $\Delta^{14}C$; thus it is most likely that methane was the predominant source of petrocarbon assimilated in red snapper muscle tissue. Cherrier et al. (2013) similarly concluded that methane was the most likely contributor to petrocarbon in nGoM POC sampled in 2011 and 2012.

Overall, temporal shifts in red snapper muscle %petrocarbon were similar over the 6 study years whether $\delta^{13}C$ (assuming methane as the predominant petrocarbon source) or $\Delta^{14}C$ is examined. Both biomarkers produced peak estimates of ~2% petrocarbon contribution to the carbon assimilated in red snapper muscle tissue. Chanton et al. (2012) estimated nGoM plankton samples collected in 2010 and 2011

had a peak %petrocarbon of ~5%, while the greatest depletion in plankton $\delta^{13}C$ (−4‰) reported by Graham et al. (2010) in summer 2010 would yield a methane-based %petrocarbon estimate of ~10%. Among fish muscle samples, there was a 2- year lag between petrocarbon being assimilated by mesoplankton in summer 2010 and the peak in estimated red snapper muscle %petrocarbon, but the estimates for red snapper muscle suggest remarkable conservation of the petrocarbon signal through multiple trophic levels in the nGoM food web. This likely reflects not only the spatial extent of the spill and the volume of hydrocarbons released but also the duration of gas and oil availability to hydrocarbon-consuming bacteria (Joye et al. 2014). The time period of declining %petrocarbon in red snapper muscle, taking into account the ~6 month turnover time in the tissue (Nelson et al. 2011), is also consistent with the boom-bust cycle that was apparent in hydrocarbon-consuming bacteria populations in the years following the DWH (Dubinsky et al. 2013; Crespo-Medina et al. 2014; Joye et al. 2014).

13.3.2 Potential Long-Term Biomarkers

Muscle stable isotope or radioisotope signatures are ephemeral given tissue turnover; thus they are unable to provide a long-term biomarker of either trophic effects or the spatial extent of petroleum hydrocarbons in a marine ecosystem. Candidate structures in bony fishes that might be well suited for this purpose include otoliths or ear stones. Otoliths function in the acoustico-lateralis system of bony fishes where they occur in three pairs. The largest otoliths are the sagittae, which are routinely aged by counting annually formed opaque zones. Otoliths occur in a closed system, are principally composed (~95%) of aragonite (biogenic $CaCO_3$) in a protein matrix, and are metabolically inert once formed. The protein in otoliths has been extracted and its bulk and amino acid-specific $\delta^{13}C$ or $\delta^{15}N$ analyzed to estimate trophic position, habitat utilization, and food web structure (Huxam et al. 2007; McMahon et al. 2011; Lueders-Dumont et al. 2018). By mass, otoliths are ~10% C, with ~20–40% of that derived from metabolic carbon and the rest contributed by DIC (Høie et al. 2003; Tohse and Mugiya 2008). Given the time-keeping property of otoliths and the ability to discretely subsample growth zones with micromilling techniques (Barnett and Patterson 2010), otoliths may serve as ideal natural long-term biomarkers of trophic effects and petrocarbon assimilation following marine oil spills.

The potential for otoliths to serve as biomarkers of DWH-derived petrocarbon was tested with age-0 red snapper otoliths. Fish were sampled with trawls in October and November 2009–2013 (fish age ~120–150 days; Wells et al. 2008) on the nGoM shelf at water depths between 20 and 65 m. Samples were collected in two regions: the north central GoM in the region of the DWH spill (87° 30′ W to 88° 45′ W) and the southwest US GoM off Texas (94° 10′ W to 95° 50′ W). Fish were frozen in plastic bags and then stored in a freezer at −20 ° C. Later, fish ($n = 3$ per region per year) were thawed and their sagittal otoliths extracted with acid-leached glass

probes, rinsed of adhering tissue with double-deionized water, air dried under a class-10 clean hood, and stored dry in acid-leached polyethylene vials. The surface of dried otoliths was cleaned by immersion in 1% ultrapure HNO_3 for ~30 seconds and then repeatedly flooded with double-deionized water. Otoliths were again placed under a class-10 clean hood to air dry; then each was ground to a fine powder with an acid-leached mortar and pestle. Otolith powder (~10 mg) was transferred to glass vials that had been combusted at 500 ° C for 4 hours and then shipped to NOSAMS for $\delta^{13}C$ analysis with SIR-MS and $\Delta^{14}C$ analysis with AMS. Samples were processed for radiocarbon analysis as described above for muscle samples. Results are reported as $\Delta^{14}C$, which was corrected for natural isotopic fractionation via $\delta^{13}C$.

No red snapper samples were available for the north central GoM in fall 2011 due to poor red snapper recruitment in the eastern GoM the year following the DWH (SEDAR 2018). Otolith $\Delta^{14}C$ declined in both regions over the 5 study years, generally following the linear relationship reported by Barnett et al. (2018) for nGoM red snapper otolith $\Delta^{14}C$ versus year of formation (Fig. 13.7a). Observed otolith $\Delta^{14}C$ was subtracted from year-specific otolith $\Delta^{14}C$ values predicted from the Barnett et al. (2018) function to compute the residual value of individual samples (Fig. 13.7b). Ninety-five percent confidence intervals demonstrate mean $\Delta^{14}C$ residuals were not significantly different from zero (i.e., prediction) for both regions in all years, except for the north central GoM fish in 2010. In that year and region, age-0 red snapper had a mean (±95% CI) otolith $\Delta^{14}C$ residual value of −6.13‰ (±2.64‰). Age-0 red snapper otoliths have a mean %metabolic carbon of 34% (W. Patterson, *unpublished data*); thus the scaled total decline in metabolic $\Delta^{14}C$ would have been −18.0‰. Given mixing model end-members of −1000‰ for

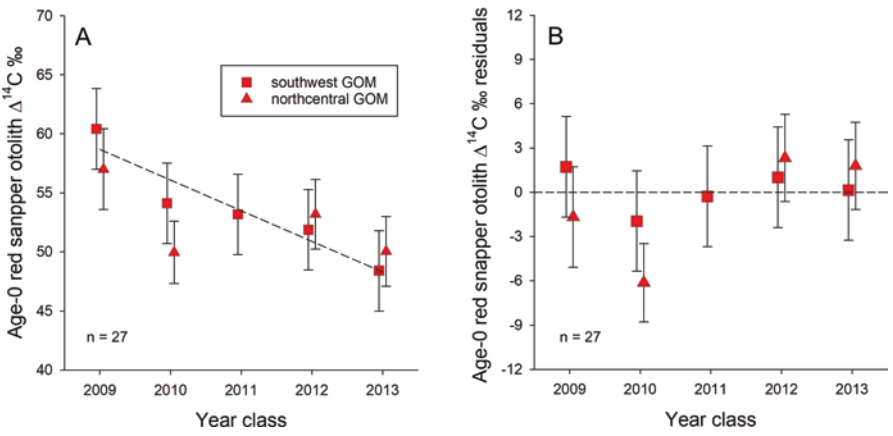

Fig. 13.7 (**a**) Plot of annual mean $\Delta^{14}C$ measured in whole age-0 red snapper otoliths (n = 3 per region per year) from the north central (88° 10′ to 88° 45′ west) and southwest (>94° 10′ west) US Gulf of Mexico from 2009 to 2013. Dashed line in panel A indicates the annual decline (−2.6‰ per year) in otolith core $\Delta^{14}C$ reported by Barnett et al. (2018) for northern Gulf of Mexico red snapper otoliths. (**b**) Residuals of annual mean age-0 otolith $\Delta^{14}C$ values relative to the predicted decline reported by Barnett et al. (2018) and plotted in panel A. Error bars in each panel are 95% confidence intervals

petrocarbon and approximately −40‰ for POM (Chanton et al. 2020), a scaled decline in $\Delta^{14}C$ of −18.0‰ would translate to petrocarbon constituting 1.73% of the metabolic carbon in fall 2010 north central GoM age-0 red snapper otoliths.

This estimated contribution of petrocarbon to age-0 red snapper otolith aragonite in fall 2010 is similar to that estimated for red snapper muscle 2–2.5 years after the DWH. This earlier incorporation of petrocarbon is likely due to age-0 red snapper feeding on lower trophic level prey, including plankton, that were already depleted in ^{14}C in summer and fall 2010 and also due to the fact that recently consumed metabolic carbon is precipitated on the rapidly growing otoliths of juvenile fishes (Høie et al. 2003; Tohse and Mugiya 2008). Therefore, there was no lag in petrocarbon incorporation in age-0 red snapper otoliths due to assimilation and tissue turnover processes like occurs with muscle or other tissues. It is unknown whether north central GoM age-0 red snapper had negative $\Delta^{14}C$ residual values in 2011 and if so whether they were similarly depleted or even to a greater extent than observed in fall 2010. One way to potentially examine that would be to analyze otolith cores of later-sampled subadult or adult north central GoM red snapper with 2010 birth years, but the older the fish, the greater the uncertainty they spent their early life in that region (Patterson 2007). What can be inferred from the otolith results is otolith $\Delta^{14}C$ appears to serve as an effective long-term biomarker of DWH petrocarbon. A larger sample, including some 2011 age-class fish from the north central GoM, would enable a more robust test of that premise, but results presented here are promising.

13.4 Summary and Implications for Future Marine Oil Spills

The clear petrocarbon signature in mesopredator reef fish muscle sampled from a broad (~7500 km^2) region of the north central GoM shelf in the years following the DWH provides strong support that $\Delta^{14}C$ and $\delta^{13}C$ can be utilized as natural biomarkers of the spatial extent of food web effects of marine oil spills. The advantages of utilizing $\Delta^{14}C$ as biomarker in this context are it providing higher resolution due to larger differences between tissue and petroleum endmember values, as well as having a common end-member value (−1000‰) regardless of the petrocarbon source. A key disadvantage is the cost of analysis (~$325US for $\Delta^{14}C$ versus ~$15US for $\delta^{13}C$ in 2018), given both stable carbon and radiocarbon isotopes can provide valuable information about the extent, timing, and duration of petrocarbon assimilation. While assimilation and trophic transfer of petrocarbon in the nGoM food web are not evidence, per se, of food web effects, they do indicate in the case of the DWH the persistent presence of petroleum hydrocarbons in the ecosystem in the years following the spill.

Trophic effects inferred from red snapper muscle $\delta^{15}N$ and $\delta^{34}S$, and from $\delta^{15}N$ alone in muscle samples from a suite of other reef fishes, do clearly demonstrate the overlap of food web effects and petrocarbon assimilation in the food web. Muscle tissue signatures are ephemeral, given tissue turnover, and thus did not provide a

long-term biomarker of either trophic effects or the spatial extent of petroleum hydrocarbons in the system. However, chemical signatures in otoliths likely do provide long-term trophic and petrocarbon biomarkers that could be utilized to examine temporal and spatial dynamics of DWH food web effects or those caused by other large-scale marine oil spills. Regardless of the question, or the tissue or structure utilized as a biogeochemical marker to examine it, results here clearly indicate the value of baseline data, without which no reference to assess potential post-spill shifts would be possible.

Acknowledgments Reef fish samples described herein were collected during cooperative research with for-hire recreational fishermen in the nGoM. We thank Captains Johnny Greene, Gary Jarvis, Sean Kelley, and Seth Wilson for their contributions, as well as numerous volunteers who helped procure samples. We thank Miaya Glabach and Samantha Bosman for processing samples for $\delta^{13}C$ and $\Delta^{14}C$ analysis and Sue Handwork, Kathy Elder, and Ann McNichol at WHOI-NOSAMS and Alexander Cherkinsky at UGA-CIAS for $\delta^{13}C$ and $\Delta^{14}C$ analysis.

Funding Information In addition to the Gulf of Mexico Research Initiative (GoMRI) funding through the C-IMAGE consortium, this research was also made possible by grants from the Florida Institute of Oceanography, a grant from the Florida Department of Environmental Protection, and a grant from the Florida Fish and Wildlife Research Institute. All data presented herein are publicly available through the Gulf of Mexico Research Initiative Information and Data Cooperative (GRIIDC): https://data.gulfresearchinitiative.org/data/Y1.x049.000:0007 and https://data.gulfresearchinitiative.org/data/R4.x267.180:0021).

References

Barnett BK, Patterson WF III (2010) The effect of coring and pulverizing juvenile red snapper, *Lutjanus campechanus*, otoliths on their chemical signatures. Environ Biol Fish 89(3–4):463–417. https://doi.org/10.1007/s10641-010-9697-7

Barnett BK, Thorton LR, Allman RJ, Chanton JP, Patterson WF III (2018) Linear decline in red snapper (*Lutjanus campechanus*) otolith $\Delta^{14}C$ extends the utility of the bomb radiocarbon chronometer for fish age validation in the Northern Gulf of Mexico. ICES J Mar Sci 75(5):1664–1771. https://doi.org/10.1093/icesjms/fsy043

Beyer J, Trannum HC, Bakke T, Hodson PV, Collier TK (2016) Environmental effects of the Deepwater Horizon oil spill: a review. Mar Pollut Bull 110:28–51. https://doi.org/10.1016/j.marpolbul.2016.06.027

Bosman SH, Chanton J, Rogers KL (2017) Using stable and radiocarbon analyses as a forensic tool to find evidence of oil in the particulates of the water column and on the seafloor following the 2010 Gulf of Mexico Oil Spill. In: Stout S, Wang Z (eds) Case studies in Oil Spill environmental forensics. Academic Press. https://doi.org/10.1016/B978-0-12-804434-6.00029-X

Chanton JP, Cherrier J, Wilson RM, Sarkodee-Adoo J, Bosman S, Mickel A, Graham WM (2012) Radiocarbon evidence that carbon from the Deepwater Horizon spill entered the planktonic food web of the Gulf of Mexico. Environ Res Lett 7:045303. https://doi.org/10.1088/1748-9326/7/4/045303

Chanton JP, Jaggi A, Radović JR, Rosenheim BE, Walker BD, Larter SR, Rogers K, Bosman S, Oldenburg TBP (2020) Mapping isotopic and dissolved organic matter baselines in waters and sediments of Gulf of Mexico (Chap. 10). In: Murawski SA, Ainsworth C, Gilbert S, Hollander D, Paris CB, Schlüter M, Wetzel D (eds) Scenarios and responses to future Deep Oil Spills – fighting the next war. Springer, Cham

Chasar LC, Chanton JP, Koenig CC, Coleman FC (2005) Evaluating the effect of environmental disturbance on the trophic structure of Florida Bay, USA: multiple stable isotope analyses of contemporary and historical specimens. Limnol Oceanogr 50(4):1059–1072. https://doi.org/10.4319/lo.2005.50.4.1059

Cherrier J, Sarkodee-Adoo J, Guilderson TP, Chanton JP (2013) Fossil carbon in particulate organic matter in the Gulf of Mexico following the Deepwater Horizon event. Environ Sci Tech Lett 2014(1):108–112. https://doi.org/10.1021/ez400149c

Crespo-Medina M, Meile CD, Hunter KS, Diercks AR, Asper VL, Orphan VJ, Tavormina PL, Nigro LM, Battles JJ, Chanton JP, Shiller AM, Joung DJ, Amon RMC, Bracco A, Montoya JP, Villareal TA, Wood AM, Joye SB (2014) The rise and fall of methanotrophy following a Deepwater oil-well blowout. Nat Geosci 7:423–427. https://doi.org/10.1038/NGEO2156

Dubinsky EA, Conrad ME, Chakraborty R, Bill M, Borglin SE, Hollibaugh JT, Mason OU, Piceno YM, Reid FC, Stringfellow WT, Tom LM, Hazen TC, Andersen GL (2013) Succession of hydrocarbon-degrading bacteria in the aftermath of the Deepwater Horizon Oil Spill in the Gulf of Mexico. Environ Sci Technol 47:10860–10867. https://doi.org/10.1021/es401676y

Fodrie FJ, Able KW, Galvez F, Heck KL Jr, Jensen OP, Lopez-Duarte PC, Martin CW, Turner RE, Whitehead A (2014) Integrating organismal and population responses of estuarine fishes in Macondo spill research. Bioscience 64:778–788. https://doi.org/10.1093/biosci/biu123

Fry B (2006) Stable isotope ecology. Springer-Verlag, New York

Fry B, Chumchal MC (2011) Sulfur stable isotope indicators of residency in estuarine fish. Limnol Oceanogr 56(5):1563–1576. https://doi.org/10.4319/lo.2011.56.5.1563

Gin KYH, Huda MK, Lim WK, Tkalich P (2001) An oil-spill food chain interaction model for coastal seas. Mar Pollut Bull 42(7):590–597. https://doi.org/10.1016/S0025-326X(00)00205-8

Goldman SF, Glasgow DM, Falk MM (2016) Feeding habits of 2 reef-associated fishes, red porgy (*Pagrus pagrus*) and gray triggerfish (*Balistes capriscus*), off the southeastern United States. US Fish Bullet 114(3):317–329. https://doi.org/10.7755/FB.114.3.5

Graham WM, Condon RH, Carmichael RH, D'Ambra I, Patterson HK, Linn LJ, Hernandez FJ Jr (2010) Oil carbon entered the coastal planktonic food web during the Deepwater Horizon oil spill. Environ Res Lett 5:045301. https://doi.org/10.1088/1748-9326/5/4/045301

Grimes CB (1979) Diet and feeding ecology of vermilion snapper, *Rhomboplites aurorubens* (Cuvier) from North Carolina and South Carolina waters. Bull Mar Sci 29(1):53–61

Grottoli AG, Eakin CM (2007) A review of modern coral $\delta^{18}O$ and $\Delta^{14}C$ proxy records. Earth Sci Rev 81:67–91. https://doi.org/10.1016/j.earscirev.2006.10.001

Høie H, Folkvord A, Otterlei E (2003) Effect of somatic and otolith growth rate on stable isotopic composition of early juvenile cod (*Gadus morhua* L) otoliths. J Exp Mar Biol Ecol 289:41–58. https://doi.org/10.1016/S0022-0981(03)00034-0

Holmer M, Marba N, Diaz-Almela E, Duarte CM, Tsapakis M, Danovaro R (2007) Sedimentation of organic matter from fish farms in oligotrophic Mediterranean assessed through bulk and stable isotope ($\delta^{13}C$ and $\delta^{15}N$) analyses. Aquaculture 262:268–280. https://doi.org/10.1016/j.aquaculture.2006.09.033

Huxam M, Kimani E, Newton J, Augley J (2007) Stable isotope records from otoliths as tracers of fish migration in a mangrove system. J Fish Biol 70:1554–1567. https://doi.org/10.1111/j.1095-8649.2007.01443.x

Jennings S, Greenstreet SPR, Hill L, Piet GJ, Pinnegar JK, Warr KJ (2002) Long-term trends in the trophic structure of the North Sea fish community: evidence from stable-isotope analysis, size-spectra and community metrics. Mar Biol 141:1085–1097. https://doi.org/10.1007/s00227-002-0905-7

Joye SB, Teske AP, Kostka JE (2014) Microbial dynamics following the Macondo oil well blowout across Gulf of Mexico environments. Bioscience 64:766. https://doi.org/10.1093/biosci/biu121

Kurz RC (1995) Predator-prey interactions between gray triggerfish (*Balistes capriscus* Gmelin) and a guild of sand dollars around artificial reefs in the northeastern Gulf of Mexico. Bull Mar Sci 56(1):150–160

Leboulanger C, Descolas-Gros C, Fontugne MR, Bentaleb HJ (1995) Interspecific variability and environmental influence on particulate organic carbon $\delta^{13}C$ in cultured marine phytoplankton. J Plankton Res 17(11):2079–2091

Lueders-Dumont JA, Wang XT, Jensen OP, Sigman DM, Ward BB (2018) Nitrogen isotopic analysis of carbonate-bound organic matter in modern and fossil fish otoliths. Geochim Cosmochim Acta 224:200–222. https://doi.org/10.1016/j.gca.2018.01.001

Manooch CS (1977) Foods of the red porgy, *Pagrus pagrus* Linnaeus (Pisces: Sparidae), from North Carolina and South Carolina. Bull Mar Sci 27(4):776–787

McCann MJ, Able KW, Christian RR, Fodrie FJ, Jensen OP, Johnson JJ, Lopez-Duarte PC, Martin CW, Olin JA, Polito MJ, Roberts BJ, Ziegler SL (2017) Key taxa in food web responses to stressors: the Deepwater Horizon oil spill. Front Ecol Environ 15(3):142–149. https://doi.org/10.1002/fee.1474

McCawley JR, Cowan JH Jr, Shipp RL (2003) Red snapper (*Lutjanus campechanus*) diet in the north-central Gulf of Mexico on Alabama artificial reefs. Proc Gulf Caribb Fish Inst 54:372–385

McCutchan JH Jr, Lewis WM Jr, Kendall C, McGrath CC (2003) Variation in trophic shift for stable isotope ratios of carbon, nitrogen, and sulfur. Oikos 102:378–390. https://doi.org/10.1034/j.1600-0706.2003.12098.x

McMahon KW, Fogel ML, Johnson BJ, Houghton LA, Thorrold SR (2011) A new method to reconstruct fish diet and movement patterns from $\delta^{13}C$ values in otolith amino acids. Can J Fish Aquat Sci 68:1330–1340. https://doi.org/10.1139/F2011-070

Moncrieff CA, Sullivan MJ (2001) Trophic importance of epiphytic algae in subtropical seagrass beds: evidence from multiple stable isotope analyses. Mar Ecol Prog Ser 215:93–106

Nelson J, Chanton J, Coleman F, Koenig C (2011) Patterns of stable carbon isotope turnover in gag, *Mycteroperca microlepis*, an economically important marine piscivore determined with a non-lethal surgical biopsy procedure. Environ Biol Fish 90(3):243–252. https://doi.org/10.1007/s10641-010-9736-4

Norberg MA (2015) Effects of the Deepwater Horizon Oil Spill and habitat type on the ecology of tomtate, *Haemulon aurolineatum*, in the northern Gulf of Mexico. University of South Alabama, Mobile, 81 pp

Olin JA, Bergeon Burns CM, Woltmann S, Taylor SS, Stouffer PC, Bam W, Hooper-Bui L, Turner RE (2018) Seaside Sparrows reveal contrasting food web responses to large-scale stressors in coastal Louisiana saltmarshes. Ecosphere 8(7):e01878. https://doi.org/10.1002/ecs2.1878

Patterson WF III (2007) A review of Gulf of Mexico red snapper movement studies: implications for population structure. Am Fish Soc Symp 60:221–236

Peterson CH, Rice SD, Short JW, Esler D, Bodkin JL, Ballachey BE, Irons DB (2003) Long-term ecosystem response to the Exxon Valdez Oil Spill. Science 302:2082–2086. https://doi.org/10.1126/science.1084282

Post DM, Layman CA, Arrington DA, Takimoto G, Quattrochi J, Montana CG (2007) Getting to the fat of the matter: models, methods and assumptions for dealing with lipids in stable isotope analyses. Oecologia 152:179–189. https://doi.org/10.1007/s00442-006-0630-x

Radabaugh KR, Hollander DJ, Peebles EB (2013) Seasonal $\delta^{13}C$ and $\delta^{15}N$ isoscapes of fish populations along a continental shelf trophic gradient. Cont Shelf Res 68:112–122. https://doi.org/10.1016/j.csr.2013.08.010

Rooker JR, Turner JP, Holt SA (2006) Trophic ecology of *Sargassum*-associated fishes in the Gulf of Mexico determined from stable isotopes and fatty acids. Mar Ecol Prog Ser 313:249–259

Sedberry GR (1985) Food and feeding of the tomtate, *Haemulon aurolineatum* (Pisces, Haemulidae), in the South Atlantic Bight. US Fish Bullet 83(3):461–466

Southeast Fishery Assessment and Review (SEDAR) (2018) SEDAR 52 stock assessment report Gulf of Mexico Red Snapper. South Atlantic Fishery Management Council, Charleston, South Carolina. 435 pp. http://sedarweb.org/sedar-52, Accessed 1 Oct 2018

Stuiver M, Pollach HA (1977) Discussions of reporting ^{14}C data. Radiocarbon 19:355–363

Sweeting CJ, Barry J, Barnes C, Polunin NVC, Jennings S (2007) Effects of body size and environment on diet-tissue $\delta^{15}N$ fractionation in fishes. J Exp Mar Biol Ecol 340:1–10. https://doi.org/10.1016/j.jembe.2006.07.023

Tarnecki JH, Patterson WF III (2015) Changes in red snapper, *Lutjanus campechanus*, diet and trophic ecology in the northern Gulf of Mexico following the Deepwater Horizon Oil Spill. Marine and Coastal Fisheries 7:135–147. https://doi.org/10.1080/19425120.2015.1020402

Tarnecki JH, Wallace A, Simons J, Ainsworth CH (2016) Progression of a Gulf of Mexico food web supporting Atlantis ecosystem model development. Fish Res 179:237–250. https://doi.org/10.1016/j.fishres.2016.02.023

Tohse H, Mugiya Y (2008) Sources of otolith carbonate: experimental determination of carbon incorporation rates from water and metabolic CO_2, and their diel variations. Aquat Biol 1:259–268. https://doi.org/10.3354/ab00029

Vanderklift MA, Ponsard S (2003) Sources of variation in consumer-diet $\delta^{15}N$ enrichment: a meta-analysis. Oecologia 136:169–182. https://doi.org/10.1007/s00442-003-1270-z

Vose FE, Nelson WG (1994) Gray triggerfish (*Balistes capriscus* Gmelin) feeding from artificial and natural substrate in shallow Atlantic waters of Florida. Bull Mar Sci 55(2–3):1316–1323

Walker BD, Druffel ERM, Kolasinski J, Roberts BJ, Xu X, Rosenheim BE (2017) Stable and radiocarbon isotopic composition of dissolved organic matter in the Gulf of Mexico. Geophys Res Lett 44:8424–8434. https://doi.org/10.1002/2017GL074155

Wells RJD, Cowan JH Jr, Patterson WF III, Walters CJ (2008) Effect of trawling on juvenile red snapper (*Lutjanus campechanus*) habitat selection and life history parameters. Can J Fish Aquat Sci 65(11):2399–2411. https://doi.org/10.1139/F08-145

Wilson RM, Cherrier J, Sarkodee-Adoo, Bosman S, Mickle A, Chanton JP (2016) Tracing the intrusion of fossil carbon into coastal Louisiana macrofauna using natural ^{14}C and ^{13}C abundances. Deep Sea Res II 129:89–95. https://doi.org/10.1016/j.dsr2.2015.05.014

Chapter 14
Modernizing Protocols for Aquatic Toxicity Testing of Oil and Dispersant

Carys L. Mitchelmore, Robert J. Griffitt, Gina M. Coelho, and Dana L. Wetzel

Abstract The goals of this chapter are to discuss, compare and contrast these new or altered protocols with the initial Chemical Response to Oil Spills: Ecological Effects Research Forum (CROSERF) methods. Although we do not advocate for any specific approach, we do provide a summary of updated guidelines and present recommendations for improvements to the standard protocols for future aquatic toxicity testing with oil and/or chemical dispersants.

Keywords CROSERF · CEWAF · WAF · Exposure · Chemical analyses · Toxicity testing

14.1 Introduction

Performing laboratory toxicity testing with complex hydrocarbon mixtures presents unique challenges due to inherent difficulties in preparing exposure media from two immiscible liquids and in quantifying and interpreting exposure concentrations (Coelho et al. 2013; Bejarano et al. 2014; Redman and Parkerton 2015).

C. L. Mitchelmore (✉)
University of Maryland Center for Environmental Science, Chesapeake Biological Laboratory, Solomons, MD, USA
e-mail: mitchelmore@umces.edu

R. J. Griffitt
University of Southern Mississippi, Division of Coastal Sciences, School of Ocean Science and Technology, Ocean Springs, MS, USA
e-mail: Joe.Griffitt@usm.edu

G. M. Coelho
Sponson Group Inc., Mansfield, TX, USA
e-mail: Ginacoelho@sponson.net

D. L. Wetzel
Mote Marine Laboratory, Sarasota, FL, USA
e-mail: dana@mote.org

S. A. Murawski et al. (eds.), *Scenarios and Responses to Future Deep Oil Spills*,
https://doi.org/10.1007/978-3-030-12963-7_14

In the mid-1990s, the Chemical Response to Oil Spills: Ecological Effects Research Forum (CROSERF) was established to develop standardized robust toxicity testing methodology for oil, chemical dispersants, and chemically dispersed oil. CROSERF was established to promote the development of comparable data sets across laboratories using environmentally realistic and validated methods that were acceptable to all stakeholders. This work resulted in the publication of a set of standardized protocols, which have been routinely used over the past couple of decades (Singer et al. 2000, 2001a, b; Aurand and Coelho 2005). These protocols were established with the best available science at the time, and since then, suggestions for modifications have been made, primarily due to new exposure scenarios, a greater understanding of exposure pathways, an increased understanding of toxicological mechanisms of action (MOAs) for classes of chemicals responsible for these toxicological perturbations, and advances in analytical chemistry (Barron and Ka'aihue 2003; NRC 2005; Incardona et al. 2013; Bejarano et al. 2014; Redman and Parkerton 2015; Sandoval et al. 2017; Adams et al. 2017; Forth et al. 2017a, b).

The *Deepwater Horizon* (DWH) incident also highlighted that the status quo for oil spill research methodologies is no longer adequate to address the new era of exposure studies needed to evaluate or predict environmental damage. Many modifications of, or additions to, the original CROSERF protocols were made by the responsible party, the trustees, and researchers carrying out DWH impact assessments. Protocol alterations have been made based on the specific questions asked, in order to (1) improve Natural Resource Damage Assessment (NRDA), (2) expand basic scientific knowledge regarding fate and effect, (3) provide data to inform operational decisions during a spill, and (4) populate toxicological models. The goals of this chapter are to discuss, compare, and contrast these new or altered protocols with the initial CROSERF methods. This chapter is not meant to be an exhaustive and extensive review of the literature as there are a number of recent reviews that provide more in-depth discussions (Barron and Ka'aihue 2003; NRC 2005; Bejarano et al. 2014; Redman and Parkerton 2015; Sandoval et al. 2017; Bejarano 2018). Although we do not advocate for any specific approach, we do provide a summary of updated guidelines and present recommendations for improvements to the standard protocols for future aquatic toxicity testing with oil and/or chemical dispersants.

14.2 Understanding the Objectives for Aquatic Toxicity Testing of Oil and Dispersants

The first extensive effort for aquatic toxicity testing of oil dates back to studies evaluating the application of degreasing agents for shoreline oil removal from the SS Torrey Canyon oil tanker spill off the coast of Great Britain in 1967. This

spill opened up a new field of study for oil and dispersed oil toxicity testing which was further supported by the legislation of the 1990 Oil Pollution Act (OPA), strengthening EPA's ability to respond to and even help prevent catastrophic oil spills.

There are several different research objectives for oil and chemical dispersants. At the simplest level, there is regulatory testing conducted to screen individual dispersant products for efficacy and aquatic toxicity. In the United States, the EPA approval of various dispersant products listed under the National Contingency Plan (NCP) Product Schedule (NCP Subpart J 2018) requires simple acute toxicity tests using dispersants and oil. While these tests help compare dispersant A to dispersant B, they provide no ecological relevance that can aid spill response decision-makers with assessing potential consequences of using dispersants on an oil spill, at environmentally realistic exposures observed in the field. On the opposite end of the research spectrum is scientific research associated with NRDA. This research is a critical line of scientific inquiry, needed to enhance comprehension of how oil and dispersed oil may affect individual organisms, species, assemblages, or ecosystems.

Laboratory and mesocosm-scale toxicity experiments exposing key representative organisms to various concentrations of oil and/or chemical dispersant and evaluating an array of biological endpoints have been utilized to assess environmental damage. The utility of this applied research is incumbent on the use of proven standard research protocols using environmentally relevant exposures that can generate consistent, comparable data, meeting or exceeding a minimum level of quality across multiple laboratories. Despite CROSERF, there are still widely varying methods of laboratory testing and extrapolation procedures that are not fully reliable for environmental assessments of oil spills or inclusion into toxicological models (Coelho et al. 2013; Bejarano et al. 2014; Bejarano 2018). There is often a severe lack of understanding by researchers, resulting in incorrect methodology for conducting appropriate toxicity tests to address specific research questions (i.e., toxicological comparisons between different oil mixtures, species, and life stages or how to emulate specific parameters unique to a new spill event). There can also be a mismatch between the generation of biological data (effects) and the actual chemical and physical parameters of the exposure.

Inadequate characterization of the exposure media leads to the likelihood of making significant errors (i.e., under- and overestimations of toxicity). These errors result from using invalid approaches for experimental design, chemical analysis of the exposure media, biological endpoint selection, and data analysis. Consequently, data generated from studies using unreliable methods and procedures can be difficult, if not impossible, to interpret in the context of real spill scenario conditions and can lead to a false narrative regarding exposure responses.

14.3 The Genesis of CROSERF Protocols

In 1994, the "Chemical Response to Oil Spills: Ecological Effects Research Forum," or CROSERF program, was established under funding from the American Petroleum Institute and various US federal and state agencies. The objectives of the CROSERF program were to evaluate ways to improve oil and dispersant toxicity tests and develop protocols which offered structure and detailed methodology for providing standards to achieve meaningful and consistent analytical chemistry, environmentally realistic exposure regimes, and methods for solution preparation (Aurand and Coelho 2005). The CROSERF working group held nine workshops between 1994 and 1999, during which research teams from several US laboratories and academic institutions endeavored to develop and vet standardized oil, dispersant, and dispersed oil aquatic toxicity testing protocols. The intent was to thoroughly evaluate all relevant aspects of a robust oil and dispersant toxicity testing design to generate universal standardized methods, applicable for use in most oil spill response assessment scenarios.

An overview of the program and final summary reports from all of the individual laboratories participating in the laboratory toxicity testing program were presented during the 2001 International Oil Spill Conference (Aurand and Kucklick 1995; Aurand and Coelho 1996; Coelho and Aurand 1996, 1997, 1998a, b; Aurand et al. 2001; Singer et al. 2001a, b; Clark et al. 2001; Fuller and Bonner 2001; Wetzel and Van Vleet 2001; Rhoton et al. 2001). A final workshop was held to review data from all participating laboratories, which resulted in a summary report on the program results (Aurand and Coelho 2005). These CROSERF protocols (Table 14.1, Aurand and Coelho 2005) have provided a baseline of standard procedures which have been used globally to develop scientifically defensible and comparable data sets and are still considered the gold standard in oil spill research today, against which all other protocols are compared.

14.4 Evolution and Modification of CROSERF Methods

CROSERF protocols have been successfully used not only for oil spill research in general but for NRDAs, including the DWH incident and during oil spill event net environmental benefit analyses (NEBA), for decisions regarding the selection of the most appropriate response options (Bejarano et al. 2014). Furthermore, results of these standard toxicity tests using CROSERF methods have been incorporated in numerous models of oil fate and effects (Di Toro et al. 2000; French-McKay 2002; Bejarano et al. 2015; Bejarano 2018). However, despite the existence of CROSERF protocols, some oil and dispersant toxicity experiments are still being conducted using atypical exposure methods, unrealistic concentrations, or improper chemical characterization rendering data that cannot be interpreted (NCR 2005; Coelho et al. 2013; Bejarano et al. 2014; Bejarano 2018). One of the most troubling aspects

Table 14.1 CROSERF protocols and definitions

CROSERF **solution preparation protocols**	
WAF Water-accommodated fraction	Solution derived from no vortex mixing using magnetic stir bar with 24-hr mixing and no settlement time
CE-WAF Chemically enhanced WAF	Solution derived from mixing (20–25% vortex) of oil and dispersant with 18–24-hr mixing and 3–6-hr settlement time. 1:10 dispersant-to-oil ratio
Loading rate or nominal concentration	The amount of oil and/or dispersant added to mixing media. Not acceptable as an actual exposure concentration
Variable loading	Uses a series of decreasing concentrations of oil to generate decreasing concentrations of WAF or CE-WAF
Other parameters	Defined the type of water, oil, vessel, headspace (20–25% by volume), mixing in the dark at test temperatures
Exposure terminology (as defined by CROSERF)	
Constant exposure	Refers to a constant exposure in which the aim is a constant concentration. The exposure may be flow-through, static nonrenewal, or static renewal
Continuous flow-through	Refers to a constant exposure with a constant concentration test solution (i.e., no dilution of the test solution occurs)
Spiked exposure	Refers to a beginning test solution concentration exposure followed by a slow dilution (declining concentration) with contaminant-free media
Pulsed exposure	Refers to a square-wave concentration exposure. In this type of exposure, organisms are placed in a closed, static chamber with no headspace above the test solution. The organisms are left in the solution for unspecified time period, then removed and placed in clean water
Static renewal	Refers to a constant exposure where the test solution is renewed at regular time intervals (typically 24 hrs) with fresh test solution made at the same concentration
Static nonrenewal	Refers to a constant exposure in which there is no test solution renewal
Additional parameters	Test design (number of treatments and replicates), exposure time, feeding, removal or dead organisms, laboratory lighting, standard water quality parameters
Analytical chemistry requirements	
Total petroleum hydrocarbon (TPH) concentration	The sum of the total extractable hydrocarbons analyzed by GC/FID through the integration of FID signal over the *n*-C_{10} to *n*-C_{36} hydrocarbon range
Total petroleum hydrocarbon concentration (TPH $_{(resolved)}$)	GC/FID integration of FID signal over the *n*-C_{10} to *n*-C_{36} hydrocarbon range corresponding to individual compounds (i.e., normal paraffin and other resolved, discrete peaks)
Total PAH (TPAH) concentration (optional)	PAHs including alkyl homologues by GC/MS
Volatiles (optional)	x < *n*-C_{10}
Corexit 9500 and 9527	UV spectroscopy

observed in some toxicity testing is the inappropriate reporting of nominal concentrations (or loading rate) of oil and dispersant as the measures of organismal exposure against which the biological endpoints are compared.

Furthermore, in order for these established protocols to remain useful, they must be periodically updated to reflect the latest advances in technology and to align with state-of-the-science understanding of oil spill exposure dynamics. Since its initial publication in 2005, modifications to the CROSERF protocols have been proposed by numerous working groups and researchers to address unique oil spill scenarios (e.g., deep-sea spills, arctic spills), incorporate advancements in analytical capabilities, and align with increased scientific understanding of toxicological MOAs. There have also been new insights into parameters that may lead to over- or underrepresentation of toxicity, especially concerning photo-enhanced toxicity issues and a disconnect between the analytical chemistry used and toxicological interpretations, e.g., the partitioning of chemicals between dissolved and particulate phases (Barron and Ka'aihue 2003; NRC 2005). In 2005 the National Research Council of the National Academy of Sciences "Committee on Understanding Oil Spill Dispersants: Efficacy and Effects" published its review of issues related to the potential for expanded dispersant use in the United States (NRC 2005).

As part of the review, the committee examined the CROSERF initiative and made various suggestions to refine the CROSERF protocols. The NAS Committee recommended to "…develop and implement a series of focused toxicity studies to: (1) provide data that can be used to parameterize models to predict photo-enhanced toxicity; (2) estimate the relative contribution of dissolved and particulate oil phases to toxicity with representative species, including sensitive species and life stages; and (3) expand toxicity tests to include an evaluation of delayed effects."

The discussion points for amending the CROSERF protocols (prior to DWH) included:

- Consider equal mixing energy (20–25% vortex) for both chemically enhanced water-accommodated fractions (CEWAF) and water-accommodated fractions (WAF).
- Improve documentation (i.e., specifying loading ratios of oil and/or dispersant, timing of samples for chemical analyses, and explaining how toxicological endpoints are calculated).
- Consider phototoxicity and the potential for the underestimation of toxicity if natural sunlight wavelengths and intensity are not used.
- Evaluate variable dilution (i.e., making one oil/water loading stock solution and preparing serial dilutions from this single stock solution for exposure ranges) versus variable loading (i.e., individually preparing each oil/water loading separately). Issues to consider would be a variable ratio of toxic components with variable loading (maximum solubility issues so no increase with increased oil after solubility threshold is reached) and in CEWAF/HEWAFs the potential for dissolution of components from oil droplets with dilutions.
- Expand chemical characterization to include measurements of components in both the dissolved phase and the particulate phase (microdroplets).

- Investigate the importance of oil droplets (size distribution and quantity) in the dissolution of oil components in test media and alternate exposure routes of oil/dispersants to organism.
- Expand chemical characterization of oil constituents (i.e., total PAH (TPAH) of up to 70 individual parent and alkyl PAHs, BTEX, etc.).

The process of predicting all future environmental oil spill scenarios and then accurately emulating them in laboratory-based toxicity studies is unrealistic. However, during the DWH damage assessment, researchers realized that, in addition to the recommended protocol changes previously described in the NAS report (e.g., media preparation, chemical analysis, and toxicological interpretations), CROSERF procedures were not designed to consider the conditions presented by a prolonged, large-scale subsea oil release being treated with dispersants under deep ocean conditions. The DWH spill underscored the limitations of using the CROSERF standard procedures alone, since they did not consider the deep ocean environments, controlling the fate, transport, and physiochemical characteristics of spilled oil and dispersed oil which need to be considered when designing toxicity exposure studies. Post DWH, the CROSERF protocols were modified to reflect the dynamics of this subsea spill, taking into account some of the prior recommendations. These modifications included new mixing regimes with different mixing intensities, durations, and settling times, such as the HEWAF preparation method (Carney et al. 2016; Forth et al. 2017a, b; Krasnec et al. 2016) intended to approximate deep-sea blowout conditions and subsea dispersant injection (SSDI). With advancements in analytical chemistry and greater understanding of toxicity MOA, it is evident that the chemical assessment of oil must now include the analysis of $\sum$50+ PAHs, the physical and chemical characterization of the compositional differences between dissolved and particulate fractions, and the quantity and size of oil droplets (Carney et al. 2016; Sandoval et al. 2017). A summary of the various modifications to media preparation, exposure design, and chemical/physical characterization of test media is shown in Table 14.2 (Krasnec et al. 2016; Sandoval et al. 2017; Carney et al. 2016; Forth et al. 2017a, b).

Some of the main deviations from the original CROSERF that were included in DWH-related studies are summarized as follows:

- The mixing energy used to make test solutions included additional energy regime protocol to mimic the high energy zones at the wellhead (HEWAFs). It also included the same mixing energy for preparing WAF and CEWAFs (i.e., 20–25% vortex).
- The majority of the WAF preparation methods used the variable dilution rather than the variable loading procedure for solution preparation. This approach, validated with rigorous analytical chemistry, was used in part to reduce the number of chemical analyses (Carney et al. 2016; Forth et al. 2017a, b).
- Given that dispersants were used at both the surface and subsea at varying dispersant-to-oil ratios (DOR), DORs ranged from 1:10 to 1:100.
- The use of a glass fiber filter approach to prepare filtered solutions to compare the chemistry and toxicity of filtered (i.e., dissolved phase) and unfiltered (i.e.,

Table 14.2 Modifications to CROSERF protocols after DWH

Solution preparation protocols	
ME-WAF Mid-energy WAF	Solution derived from vortex mixing (20–25%) using magnetic stir bar with 18–24-hr mixing and 2–8-hr settlement period
HE-WAF[1] High-energy WAF	Solution derived using the lowest speed with a food blender for a 30-sec blend and 1-hr settlement period
SHE-WAF[1,2] Super high-energy WAF	Solution derived from the lowest blending speed using a food blender with 120-sec blend and 1-hr settlement period
Variable dilution method	Solution of oil and water mixtures from which dilutions are prepared
Variable dispersant-to-oil ratios	Range of dispersant oil ratios used 1:10 to 1:100 DOR to reflect both surface and subsurface use
Other exposure media preparation	
Oil emulsion[1]	Solution derived from a low blending speed using a food blender with 30-sec blend and used in its entirety without settlement
Oiled sediment[1]	Sediments mixed with oil for 30 minutes at a moderate speed using either a large food preparation mixer or concrete mixer
Sediment-derived WAF[1]	Supernatant derived by adding water to contaminated sediments and then either stirring for 10 seconds followed by 2-hr settle or shaking at 300 RPM for 6 hrs with 12-hr settle
Exposure Regime	
Static renewal or nonrenewal	Refers to a constant exposure in which there is test solution renewal at regular time intervals (typically 24 hrs) with fresh test solution made at the same concentration or there is no test solution renewal
Co-stressors	Influence of co-stressors investigated (i.e., UV light, temperature, dissolved oxygen)
Chemistry	
Total PAH concentration (TPAH or ∑50PAH)	PAHs including alkyl homologues by GC/MS/SIM individually quantified and generally comprised of 50+ PAH compounds (MC 252 QAPP, 2011)
Chemical partitioning (dissolved/ particulate phases)	Pass test solution through 2 stacked GF (0.3um) filters[3–5] or glass wool and 1um GF/F and 0.7 GF/F[2] under gentle vacuum and analysis of filtrate and nonfiltered test solutions
Quantitation of droplets	Recommend analysis of size and distribution

[1]Krasnec et al. (2016), [2]Sandoval et al. (2017), [3]Carney et al. (2016), [4,5]Forth et al. 2017a,b

dissolved and particulate phase exposures) preparations (MC252 QAPP 2011; Forth et al. 2017a, b; Sandoval et al. 2017).

- Fluorescence detection was used by some laboratories as screening technique of the exposure concentrations of select test solutions during a test; however, full analytical chemistry was still done for the actual oil quantification results.
- Chemical and physical (droplet size and number) assessment of all oils (source oil, artificially weathered source oil, slick A and slick B) with and without dispersants using all WAF preparation techniques at various time points over a stan-

dard 96-hour acute toxicity test exposure time (Forth et al. 2017a, b; Sandoval et al. 2017).
- Expansion of chemical analytes measured and the use of new analytical techniques and methodologies (i.e., expansion of number of individual parent PAHs and their associated alkylated PAHs (i.e., 50+individual PAHs; MC252 QAPP 2011; Forth et al. 2017a, b; Sandoval et al. 2017)).
- Use of natural lighting regimes (UV light, not laboratory fluorescence) to control for photo-enhanced toxicity issues.
- Investigation in the use of passive samplers for estimating dissolved hydrocarbon components (i.e., polydimethylsiloxane (PDMS)-coated glass fibers (Redman and Parkerton 2015)).
- Toxicological models to predict oil/dispersant toxicity in understudied/sensitive species (Bejarano et al. 2014).

The DWH incident has highlighted the importance of updating the CROSERF protocols and periodically re-evaluating standard procedures for laboratory oil and dispersant toxicity testing based on current state of the science. Despite CROSERF's initial efforts to bring wholesale standardization of oil and dispersant toxicity testing guidelines to research, there continues to be toxicity tests conducted today that are deficient due to design and analytical flaws, poor biological endpoint selection, invalid data interpretations, and inadequate application of statistics (NRC 2005; Coelho et al. 2013; Bejarano et al. 2014). A recent review of studies for inclusion into dispersant toxicity models found that almost 25% of these studies were deemed of low reliability (Bejarano 2018). It should also be noted that standardizing sediment exposure toxicity tests was not completed under CROSERF but should be addressed since the long-term exposure to sediment-bound oil is an environmental concern.

14.5 Lessons Learned from the DWH Spill and Recommendations for Future Oil Spill Toxicology Research

The scientific response to the *Deepwater Horizon* oil spill was one of the largest coordinated response and research efforts in modern US history. The result was that many scientists approached the problem with creativity and innovation, but little understanding of prior scientific research procedures, and without communicating with subject matter experts in the field. It is not realistic to expect the scientific response to an event as large as the DWH oil spill to go smoothly, but here we present some possible lessons from the combined experiences of the authors, all of whom were intimately involved in the operational scientific monitoring or ongoing scientific research to understand the complex effects of the DWH event. A positive aspect of DWH was that there was an increased linkage between government management agencies and academic scientists, not just in the United States but

internationally. Scientists from around the world were eager to add their expertise to the response and scientific studies. The NRDA process brought together a group of government, industry, and academic scientists to identify critical research needs, design a plan to examine those questions, and develop revised protocols for toxicity testing and analytical chemistry. Depending on the priorities of each group, there were different scientific approaches used for academic scientists interested in looking at marine organismal responses to oil and/or dispersants and the management agencies that were interested in the applied effects of the release on fishery populations. These differences were evident in research conducted in laboratory settings versus field. However, refinements made pre-DWH to the CROSERF protocols were combined with creative ones pertinent to the DWH incident. These new procedures (Carney et al. 2016) were rapidly disseminated to researchers both nationally and internationally involved in DWH oil spill research allowing for more comparable toxicological data sets.

14.5.1 Recommendations for Modernizing of CROSERF Protocols

Although we must do everything possible to prevent them, oil spills happen. When they do, we need to be poised and ready to implement the most comprehensive but nimble plan of action, carefully curated with input from all stakeholders and disciplines: indigenous people and on-site spill responders, sociologists and resource managers, federal and state government, and communication experts. We need access to the best field and analytical/diagnostic tools, and we need to use all available expertise to minimize the social, economic, human, and environmental health impacts. After each spill event, we learn how to not only be better prepared for the next event, but we also learn how to better evaluate the consequences of a spill and the response options employed. Defining the timing for rapid spill or post-spill evaluation and determining the appropriate sensitive species/life stage/habitats or biological endpoints in need of protection are immensely important goals. Here, we make further recommendations toward helping to achieve those environmental impact assessment goals for future spills.

General recommendations include:

1. *Conducting oil/dispersant toxicity tests needs to consider the environmentally relevant exposure scenarios for that particular spill and response options.*
2. *Resource trustees and the scientific community should ensure that relevant local toxicity data is appropriately included in the Area Contingency Plans and individual site Oil Spill Response Plans,* via *the NEBA decision-making tools that use toxicity data.*

The decision-making tools used for net environmental benefit analysis to support response option selection (e.g., CERAs, SIMAs, and CRAs) should rely on the best

available local scientific information for relevant local species. Better use of databases such as DIVER can aid in connecting useful information to the Environmental Unit within the incident management team.

3. *Researchers have continued conferences and workshops dedicated to an interdisciplinary understanding of the effects of hydrocarbons on ecosystems.*

At a minimum, this would include chemists, ecologists, toxicologists, physical scientists, environmental managers, and modelers. Meeting in a format (likely not tied to the traditional research talk structure) that allows for a free and open exchange of ideas, priorities, experiences, and innovative approaches is critical.

4. *Toxicity assays must include natural variations in nonchemical stressors or variations from environmental norms as part of the experimental design.*

Salinity, temperature, UV light, and dissolved oxygen levels are examples of physical variables that are changing in a complex marine environment and known to affect biological uptake of oil.

5. *Extensive chemical characterization of exposure test media is critical, nominal doses are unacceptable, and a minimum criteria of chemical analytes depending upon the oil/dispersant in use (*i.e.*, 50+ individual PAH (TPAH), dispersant chemical analyses) should be conducted at appropriate and multiple time points during the test.*
6. *Investigations and chemical quantitation in dissolved and particulate phases (potentially including a physical assessment of oil droplet quantity and size) should be performed.*

A widely accepted and agreed upon method for performing analysis of oil mixtures is essential, as is the understanding that without a rigorous assessment of the oil composition (either in controlled laboratory exposures or in field collected samples), interpretation of biological responses is difficult and may be impossible.

7. *A minimum criteria and data quality requirement would provide more toxicological data points suitable for inclusion in toxicity models.*

We suggest that a good model for promoting interaction between field sampling data and laboratory exposure experiments is to adopt the framework of "Field sampling tells us what did happen, laboratory exposures tell us why it happened." The development of aquatic toxicity models such as PETROTOX (Redman et al. 2012) and the integration of toxicity data into the.

NOAA data repository known as DIVER (2017) have provided compelling reasons for these recommended changes in aquatic toxicity testing protocols. A revised set of testing protocols will help produce data for environmentally relevant exposures that can be used to inform and validate toxicity models while also helping the spill response community evaluate toxicity results in a consistent and meaningful way.

8. *An in-depth synthesis of all GoMRI studies to catalogue the methods and results of oil and /or dispersant toxicity tests to create an improved framework for future oil spill toxicity research.*

It is essential that the CROSERF protocols are updated so that future oil/dispersant toxicity tests provide meaningful data for use in NRDA, NEBA, and toxicity models.

References

Adams J, Charbonneau K, Tuori D, Brown RS, Hodson PV (2017) Review of methods for measuring the toxicity to aquatic organisms of the water accommodated fraction (WAF) and chemically-enhanced water accommodated fraction (CEWAF) of petroleum. Department of Fisheries and Oceans, Canadian Science Advisory Secretariat Research Document 2017/064. x + 108 p

Aurand DV, Coelho GM (1996) Proceedings of the fourth meeting of the chemical response to oil spills: ecological effects research forum. April 24–25, 1996 Santa Cruz, California, USA. Ecosystem Management & Associates, Purcellville, VA, Report 96–01, 50 p

Aurand D, Coelho G (2005) Cooperative aquatic toxicity testing of dispersed oil and the Chemical Response to Oil Spills: Ecological Effects Research Forum (CROSERF). Ecosystem Management & Associates, Inc. Lusby, MD. Technical Report 07–03, 105 p

Aurand D, Kucklick JH (Editors) (1995) Proceedings of the third meeting of the chemical response to oil spills: ecological effects research forum. Marine Spill Response Corporation, Washington, DC. Marine Spill Response Corporation Technical Report Series 95-018, 69 p

Aurand DV, Jamail R, Sowby M, Lessard RR, Steen A, Henderson G, Pearson L (2001) Goals, objectives, and the sponsors' perspective on the accomplishments of the chemical response to Oil Spills: ecological effects research forum (CROSERF). Proceedings, 2001 international oil spill conference. Global strategies for prevention, preparedness, response, and restoration. API Publication No. 4686B (same number used for the 1999 Proceedings). American Petroleum Institute, Washington, D.C. pp 1257–1261

Barron MG, Ka'aihue L (2003) Critical evaluation of CROSERF test methods for oil dispersant toxicity testing under subarctic conditions. Mar Pollut Bull 46:1191–1199

Bejarano AC (2018) Critical review and analysis of aquatic toxicity data on oil spill dispersants. Environ Toxicol Chem 37(12):2989–3001

Bejarano AC, Clark JR, Coelho GM (2014) Issues and challenges with oil toxicity data and implications for their use in decision making: a quantitative review. Environ Toxicol Chem 33(4):732–742

Bejarano AC, Farr JK, Jenne P, Chu V, Hielscher A (2015) The chemical aquatic fate and effects database (CAFÉ), a tool that supports assessments of chemical spills in aquatic environments. Environ Toxicol Chem 35(6):1576–1586

Carney MW, Forth HP, Krasnec MO, Takeshita R, Holmes JV, Morris JM (2016) Quality assurance project plan: *Deepwater Horizon* laboratory toxicity testing. DWH NRDA toxicity technical working group. Prepared for National Oceanic and Atmospheric Administration by Abt Associates, Boulder, CO

Clark JR, Bragin GE, Febbo EJ, Letinski DJ (2001) Toxicity of physically and chemically dispersed oils under continuous and environmentally realistic exposure conditions: applicability to dispersant use decisions in spill response planning. Proceedings, 2001 international oil spill conference. Global strategies for prevention, preparedness, response, and restoration. American Petroleum Institute Publication No. 4686B (same number used for the 1999 Proceedings). American Petroleum Institute, Washington, D.C. pp 1249–1255

Coelho GM, Aurand DV (1996) Proceeding of the fifth meeting of the chemical response to oil spills: ecological effects research forum. September 18–19, 1996. Corpus Christi, Texas, USA. Ecosystem Management & Associates, Purcellville, VA, Report 96–03, 60 p

Coelho GM, Aurand DV (1997) Proceedings of the sixth meeting of the chemical response to oil spills: ecological effects research forum. April 3–4, 1997. Fort Lauderdale, Florida, USA. Ecosystem Management & Associates, Purcellville, VA. Report 97–01, 69 p

Coelho GM, Aurand DV (1998a) Proceedings of the seventh meeting of the chemical response to oil spills: ecological effects research forum. November 13–14, 1997. Santa Cruz, California, USA. Ecosystem Management & Associates, Purcellville, VA, Report 97–02, 53 p

Coelho GM, Aurand DV (1998b) Proceedings of the eighth meeting of the chemical response to oil spills: ecological effects research forum. Ecosystem Management & Associates, Purcellville, VA. Technical Report 98–03, 30 p

Coelho G, Clark J, Aurand D (2013) Toxicity testing of dispersed oil requires adherence to standardized protocols to assess potential real world effects. Environ Pollut 177:185–188

Di Toro DM, McGrath JA, Hansen DJ (2000) Technical basis for narcotic chemicals and polycyclic aromatic hydrocarbon criteria. I. Water and tissue. J Environ Toxicol Chem 19:1951–1970

DIVER (2017) Web application: data integration visualization exploration and reporting application, National Oceanic and Atmospheric Administration. Retrieved: [July 23, 2018], from https://www.diver.orr.noaa.gov

Forth HP, Mitchelmore CL, Morris JM, Lay CR, Lipton J (2017a) Characterization of dissolved and particulate phases of water accommodated fractions used to conduct aquatic toxicity testing in support of the Deepwater Horizon natural resource damage assessment. Environ Toxicol Chem 36(6):1460–1472

Forth HP, Mitchelmore CL, Morris JM, Lipton J (2017b) Characterization of oil and water accommodated fractions used to conduct aquatic toxicity testing in support of the Deepwater Horizon natural resource damage assessment. Environ Toxicol Chem 36(6):1450–1459

French-McKay DP (2002) Development and application of an oil toxicity and exposure model, (OilToxEx). J Environ Toxicol Chem 21:2080–2094

Fuller C, Bonner JS (2001) Comparative toxicity of oil, dispersant, and dispersed oil to Texas marine Species. Proceedings, 2001 international oil spill conference. Global strategies for prevention, preparedness, response, and restoration. American Petroleum Institute Publication No.4686B (same number used for the 1999 Proceedings). American Petroleum Institute, Washington, D.C. pp 1243–1248

Incardona JP, Swarts TL, Edmunds RC, Linbo TL, Aquilina-Beck A, Sloan CA, Scholz NL (2013) Exxon Valdez to Deepwater Horizon: comparable toxicity of both crude oils to fish early life stages. Aquat Toxicol:142–143. https://doi.org/10.1016/j.aquatox.2013.08.011

Krasnec MO, Forth HP, Carney MW, Takeshita R,McFadden AK, Lipton I, Wallace B, Dean K, Lay CR, Cacela D, Holmes VJ, Lipton J, Morris JM (2016) General laboratory procedures and practices: *Deepwater Horizon* laboratory toxicity testing. DWH NRDA Toxicity Technical Working Group. Prepared for National Oceanic and Atmospheric Administration by Abt Associates, Boulder, CO

MC 252 (Deepwater Horizon) Natural Resource Damage Assessment. U.S. Department of Commerce National Oceanic and Atmospheric Administration. Analytical Assurance Plan. Version 3.0; 2011

National Contingency Plan Subpart J (2018) Retrieved 2018, September 19 from: https://www.epa.gov/emergency-response/national-contingency-plan-subpart-j#schedule

National Research Council (2005) Oil Spill dispersants: efficacy and effects. The National Academies Press, Washington, DC. https://doi.org/10.17226/11283

Redman AD, Parkerton TF (2015) Guidance for improving comparability and relevance of oil toxicity tests. Mar Pollut Bull 98(1–2):156–170

Redman A, Parkerton TF, McGrath JA, Di Toro DM (2012) PETROTOX: an aquatic toxicity model for petroleum substances. Environ Toxicol Chem 31:2498–2506

Rhoton SL, Perkins RA, Braddock JF, Behr-Andres C (2001) A cold-weather species' response to chemically dispersed fresh and weathered Alaska North Slope crude oil. Proceedings, 2001 international oil spill conference. Global strategies for prevention, preparedness, response, and restoration. API Publication No. 4686B (same number used for the 1999 Proceedings). American Petroleum Institute, Washington, D.C. pp 1231–1236

Sandoval K, Ding Y, Gardinali P (2017) Characterization and environmental relevance of oil water preparations of fresh and weathered MC-252 Macondo oils used in toxicology testing. Sci Total Environ 576:118–128

Singer M, Aurand DV, Bragin G, Clark J, Coelho G, Sowby M, Tjeerdema R (2000) Standardization of the preparation and quantitation of water-accommodated fractions of petroleum for toxicity testing. Mar Pollut Bull 40(11):1007–1016

Singer MM, Aurand DV, Coelho GM, Bragin GE, Clark JR, Jacobson S, Sowby M, Tjeerdema R (2001a) Making, measuring, and using water-accommodated fractions of petroleum for toxicity testing. Proceedings of the 2001 International Oil Spill Conference pp 1269–1274

Singer MM, Jacobson S, Tjeerdema RS, Sowby ML (2001b) Acute effects of fresh versus weathered oil to marine organisms: California findings. In: Proceedings of the 2001 international oil spill conference. American Petroleum Institute, Washington, D.C., pp 1263–1268

Wetzel DL, Van Vleet ES (2001) Cooperative Studies on the toxicity of dispersants and dispersed oil to marine organisms: a 3-year Florida study. Proceedings, 2001 international Oil Spill conference. Global strategies for prevention, preparedness, response, and restoration. API Publication No. 4686B (same number used for the 1999 Proceedings). American Petroleum Institute, Washington, D.C. pp 1237–1241

Chapter 15
Polycyclic Aromatic Hydrocarbon Baselines in Gulf of Mexico Fishes

Erin L. Pulster, Adolfo Gracia, Susan M. Snyder, Isabel C. Romero, Brigid Carr, Gerardo Toro-Farmer, and Steven A. Murawski

Abstract The lack of baseline data has hindered the assessment of impacts from large-scale oil spills throughout their history. Baseline data collected before an adverse event such as an oil spill are critical for quantifying impacts and understanding recovery rates to pre-spill levels. In the case of the two largest oil spills in the Gulf of Mexico (GoM), *Deepwater Horizon* and Ixtoc 1, the lack of comprehensive contaminant baselines limits our ability to project when the ecosystem will return to pre-spill conditions and assess the short- and long-term impacts of contamination on ecosystems. Beginning in 2011, we initiated comprehensive sampling in the GoM to develop broad-scale and Gulf-wide hydrocarbon contaminant baselines primarily targeting continental shelf fishes in the USA, Mexico, and Cuba. We also developed a time series of collections over 7 years from the region in which DWH occurred. In the event there is another oil spill in the GoM, the samples from these baselines will provide broad-scale but not installation-specific baseline information for the assessment of impact and recovery. This chapter provides a summary of historical sampling and current baseline data for pelagic, mesopelagic, and demersal fish in the GoM. Further, we outline the importance of ongoing and more specific collection of monitoring data for hydrocarbon pollution.

Keywords PAHs · Polycyclic aromatic hydrocarbons · Gulf of Mexico · Ixtoc 1 · *Deepwater Horizon* · Oil spill baselines

E. L. Pulster (✉) · S. M. Snyder · I. C. Romero · B. Carr · S. A. Murawski
University of South Florida, College of Marine Science, St. Petersburg, FL, USA
e-mail: epulster@mail.usf.edu; ssnyder4@mail.usf.edu; isabelromero@mail.usf.edu; becarr@mail.usf.edu; smurawski@usf.edu

A. Gracia
Universidad Nacional Autónoma de México, Instituto de Ciencias del Mar y Limnología, Ciudad de México, CDMX, Mexico
e-mail: gracia@unam.mx

G. Toro-Farmer
New College of Florida, Sarasota, FL, USA

University of South Florida, College of Marine Science, St. Petersburg, FL, USA
e-mail: gtoro-farmer@ncf.edu

S. A. Murawski et al. (eds.), *Scenarios and Responses to Future Deep Oil Spills*,
https://doi.org/10.1007/978-3-030-12963-7_15

15.1 Introduction

Assessments evaluating the extent, duration of elevated concentrations, and impacts of oil spills are heavily reliant on data collected prior to, during, and after such events. A chronological sedimentary history of oil deposition can be recorded in cores (e.g., dated through radioisotopes or other means), assuming oil is deposited proportionally to the quantity released, bioturbation does not disturb the chronological order, and bacterial degradation is relatively slow. However, for living resources, depending upon how long after the event sampling occurs, contaminants within the animals may be reduced over time (via decontamination) and transformed into other compounds (via metabolism), some of which may be more toxic than the original exposure. For long-duration, post-spill monitoring assessments (e.g., several decades post-oil spill), few animals will record such events owing to their life spans. The most direct way to assess the effects and impacts of such spills is to have obtained pre-spill baselines beforehand with which to compare contamination levels and toxic biomarkers post-spill. Assessments of the impacts of the subsurface well blowout of the Mexican oil well Ixtoc 1 in 1979 were inconclusive due in part to the lack of pre-spill contaminant data (Amezcua-Linares et al. 2015). Ten years later, pre-spill data was dubbed one of the "rarest of all commodities" for researchers following the 1989 *Exxon Valdez* oil spill (Shigenaka 2014). Furthermore, 21 years subsequent to EVOS, researchers assessing the *Deepwater Horizon* oil spill (DWH, NAS 2013) lamented the virtual lack of relevant comprehensive pre-spill baselines, especially for living resources (Murawski and Hogarth 2013; Murawski et al. 2014). For decades, the unavailability of baseline data and reference sites in the Gulf of Mexico (GoM) has hindered the evaluation and health assessments of both the biota and the environment (Kennicutt et al. 1988; Lewis et al. 2002; Ward and Tunnell Jr. 2017). This chapter summarizes the availability and adequacy of PAH contamination data from fish tissues collected before and after the two largest spills in the GoM, the DWH and Ixtoc 1.

15.2 Pre-*DWH* Polycyclic Aromatic Hydrocarbon Baselines in Fish

In the USA, all 50 US states, the District of Columbia, the US territories of American Samos and Guam, and 5 Native American tribes issue fish consumption guidelines for potential health risks from consuming contaminated fish caught in their waters (US EPA 2009). Only five bioaccumulative chemicals (mercury, PCBs, chlordane, dioxins, and DDT) constitute 97% of all advisories in effect. Additionally, all five states bordering the GoM have coastal fish consumption guidelines, yet given the amount of oil and gas activity in the GoM, there are no active advisories or closures for petroleum-derived compounds. Fishery closures were in place during and just after the DWH accident, but most closures were lifted following seafood safety

surveillance testing (Ylitalo et al. 2012). Importantly, while most fish tested post-spill were below levels of concern (LOC), there were little data with which to judge if contamination levels had risen beyond pre-spill levels after the spill or to assess species most at risk.

Several programs have collected PAH contaminant data prior to DWH either as part of surveillance programs or in response to specific events. The National Oceanographic and Atmospheric Administration's (NOAA) National Status and Trends (NS&T) program undertakes nationwide sampling (i.e., Mussel Watch) to describe the current status and trends in the environmental quality of our estuarine and near-coastal waters (Farrington et al. 2016). Sampling included biliary PAH data for six inshore fish species (hardhead catfish, *Ariopsis felis*; Atlantic croaker, *Micropogonias undulatus*; red drum, *Sciaenops ocellatus*; spot, *Leiostomus xanthurus*; black drum, *Pogonias cromis*; and sand seatrout, *Cynoscion arenarius*) collected from 1985 to 1991 from along the US Gulf coast. Total biliary PAHs ranged from 7,000 to 1,000,000 ng FACs/g bile for both low- and high-molecular-weight fluorescent aromatic compounds (FACs; NCCOS 2017). The highest concentrations were found in Atlantic croaker collected in 1989 from Barataria Bay, Louisiana. In general, the samples collected across all years from the northwest region of the GoM, along the Texas coast, had significantly higher biliary PAHs (300,000 ± 240,000 ng/g bile) than those collected in the north central region ($p = 0.0046$; Louisiana, Mississippi, Alabama: 160,000 ± 220,000 ng/g bile) and west Florida ($p = 0.0054$; 94,000 ± 100,000 ng/g bile).

In a separate study, hardhead catfish, Gulf killifish (*Fundulus grandis*), longnose killifish (*F. majalis*), and red drum were collected during 1990–1991 from Tampa and Sarasota bays to compare levels of organic contaminants between industrialized (Tampa Bay) and nonindustrialized areas (Sarasota Bay) (McCain et al. 1996). Mean biliary naphthalene equivalents ranged from 11,000 to 120,000 ng FAC/mg of biliary protein and 6,800 to 150,000 ng FAC/mg of biliary protein in the Tampa Bay and Sarasota Bay, respectively. Mean concentrations of the biliary naphthalene equivalents in hardhead catfish collected in Tampa Bay were all significantly higher than those collected from within Sarasota Bay. In addition, the biliary PAHs measured in fish collected within the more industrialized areas of Tampa Bay (i.e., Hillsborough Bay) were significantly higher than nearby nonindustrialized sites.

Edible muscle samples from hardhead catfish, channel catfish (*Ictalurus punctatus*), and largemouth bass (*Micropterus salmoides*) were surveyed in 1996 to compare the tissue quality between fish collected from wastewater-impacted areas and reference locations in northwestern Florida and southwestern Alabama (Lewis et al. 2002). Average muscle concentrations of PAHs ranged from 0.6 to 3.5 ng/g wet weight (w.w.). The results from this study indicated that total PAH concentrations averaged across fish collected from the wastewater-impacted areas (2.2 ± 3.3 ng/g w.w.) were similar to those collected at the reference sites (1.8 ± 1.6 ng/g w.w.). A regional assessment of whole-body concentrations in fish and shellfish across the west, northeast, southeast, and Gulf coasts were analyzed for chemical contaminants to evaluate compliance with the EPA fish meal recommended guidelines (Harvey et al. 2008). In general, PCBs accounted for the greatest percentage (31%)

of exceedances across all regions, followed by mercury (29%), PAHs (21%), and total DDTs (11%). In the Gulf region, mercury accounted for the highest percentage of exceedances (19%), followed by PCBs (11%), total DDTs (7%), PAHs (6%), toxaphene (2%), and cadmium (1%).

In the early 1990s, a study supported by the Minerals Management Service (MMS) evaluated biliary PAHs at several offshore gas rigs in the western GoM (McDonald et al. 1996). This study evaluated the impacts of oil contamination from specific rigs by evaluating fish collected near the rigs and those collected from several kilometers away. Biliary PAHs were evaluated for a variety of bottom-dwelling fishes, generally showing weak negative correlation with distances from the rigs (McDonald et al. 1996).

In the aftermath of Hurricane Katrina in 2005, Hom et al. (2008) evaluated the safety of seafood primarily in Mississippi Sound and offshore waters, examining Atlantic croaker, shrimps, and a few other species. No samples were found to exceed LOCs despite the strong storm surge from that hurricane.

Mesopelagic species were collected in 2007 over the slope of the north central GoM near cold-seep habitats to characterize species composition as well as distributions and determine PAH content in muscle tissues (Ross et al. 2010; Romero et al. 2018). Because of their proximity in time and space, PAH determinations from this dataset represent a serendipitous PAH baseline for DWH-based contamination of mesopelagic fishes in the northern GoM. Pre-spill PAH values ranged from 24 to 555 ng/g w.w., containing a few PAH compounds (mostly naphthalene). These values are relatively high compared to other more shallow-water communities, this trend of organic pollutants accumulating in the deep ocean (Froescheis et al. 2000; Koenig et al. 2013) is a pattern potentially explained by the natural seeps in the study area and likely due to a combination of biological factors intrinsic to mesopelagic communities (e.g., vertical migration, PAH metabolism).

15.3 Post-DWH and Ixtoc 1 Baselines in Fish

15.3.1 Seafood Safety

With the release of more than 200 million gallons of crude oil from DWH, there were concerns regarding the integrity and safety of the seafood supply for human consumption, resulting in intensive testing, federal and state fishery closures, risk assessments, and the inclusion of petroleum-related compounds in the 2011 National Listing of Fish Advisories (Ylitalo et al. 2012; US EPA 2013). Between April 28, 2010, and March 31, 2011, more than 8,000 seafood samples were collected and analyzed from within and around closure areas across the GoM for PAHs and the dispersant component dioctyl sodium sulfosuccinate (DOSS). Primarily edible tissues from fish (snappers, groupers, porgies, tuna, etc.) and shellfish contained low concentrations of PAH (<1 ng/g w.w.) and DOSS (0.05–0.29 μg/g w.w.) with both at least two orders of magnitude lower than the LOCs for human health risk (Ylitalo et al. 2012).

An independent assessment of seafood safety evaluated fishes obtained from within fishing closures along the Mississippi coast (Xia et al. 2012). Samples were collected and analyzed weekly from May 27, 2010, until October 2010 and then monthly until August 2011. Eleven fish species consisting of Atlantic croaker, black drum, red drum, cobia (*Rachycentron canadum*), Gulf menhaden (*Brevoortia patronus*), red snapper (*Lutjanus campechanus*), southern flounder (*Paralichthys lethostigma*), spotted seatrout (*Cynoscion nebulosus*), striped mullet (*Mugil cephalus*), tripletail (*Lobotes surinamensis*), and sand seatrout were analyzed for PAHs. Edible muscle composites were analyzed for 25 PAHs for each species. Overall, all PAHs were at least three orders of magnitude below the LOCs established by NOAA, the FDA, and the Gulf states. LOCs ranged from 35 ng/g for benzo[a]pyrene and dibenzo[a,h]anthracene to 490,000 ng/g w.w. for anthracene and phenanthrene. Maximum concentrations detected in fillets (muscle) ranged from nondetect to 20.1 ng/g for benzo[a]pyrene and anthracene/phenanthrene, respectively. The levels of total PAHs (average, 16 ng/g w.w.) were consistent until January 2011, and thereafter concentrations significantly declined ~44% to an average of 9 ng/g (w.w.).

15.3.2 Hepatobiliary and Extrahepatic PAH Levels in Fish

The most comprehensive Gulf-wide survey of the health of GoM fishes conducted to date is that by the Center for Integrated Modeling and Analysis of Gulf Ecosystems (C-IMAGE) wherein ~15,000 fishes were evaluated for disease frequencies and a subset sampled for PAH levels. The C-IMAGE sampling campaign focused on reef and deep-dwelling shelf species (e.g., snappers, tilefishes, groupers) collected from 2011 to 2017 (Fig. 15.1; Murawski et al. 2014, 2018). To date, over 1800 bile samples from 75 offshore species of finfish and sharks have been analyzed for fluorescent aromatic compounds (FACs) in fish bile (Snyder et al., 2015; Pulster et al. 2017a). These samples were collected between 2011 and 2017 from coastal regions from southwest Florida to the Yucatán Peninsula and Cuba. Preliminary biliary PAHs ranged from <1 to 1,900,000 ng/g bile for naphthalene and benzo[a]pyrene FACs (Pulster et al. 2017a). This represents a 90% increase in the maximum total biliary PAHs compared to those measured by the earlier studies conducted in the northern GoM between 1985 and 1991 (Pulster et al. 2017a; NCCOS 2017). Overall for the years 2011–2016, the north central region (39–1,900,000 ng FACs/g bile; 125,000 ± 190,000 ng FAC/g bile) of the GoM remained significantly higher in average total biliary FACs than the southwest region (<1–960,000 ng FAC/g; 73,000 ± 97,000 ng FAC/g bile; $p < 0.0001$), the west Florida shelf (1,500–360,000 ng FAC/g; 37,000 ± 59,000 ng FAC/g bile; $p < 0.0001$), and the northwest region (130–370,000 ng FAC/g; 90,000 ± 79,000 ng FAC/g bile; Fig. 15.2; Pulster et al. 2017a). The 2011–2016 preliminary biliary naphthalene and benzo[a]pyrene concentrations ranged from 410 to 1,900,000 ng/g and 0.073 to 9,600 ng/g, respectively (Fig. 15.2). The highest concentrations of biliary naphthalene and benzo[a]

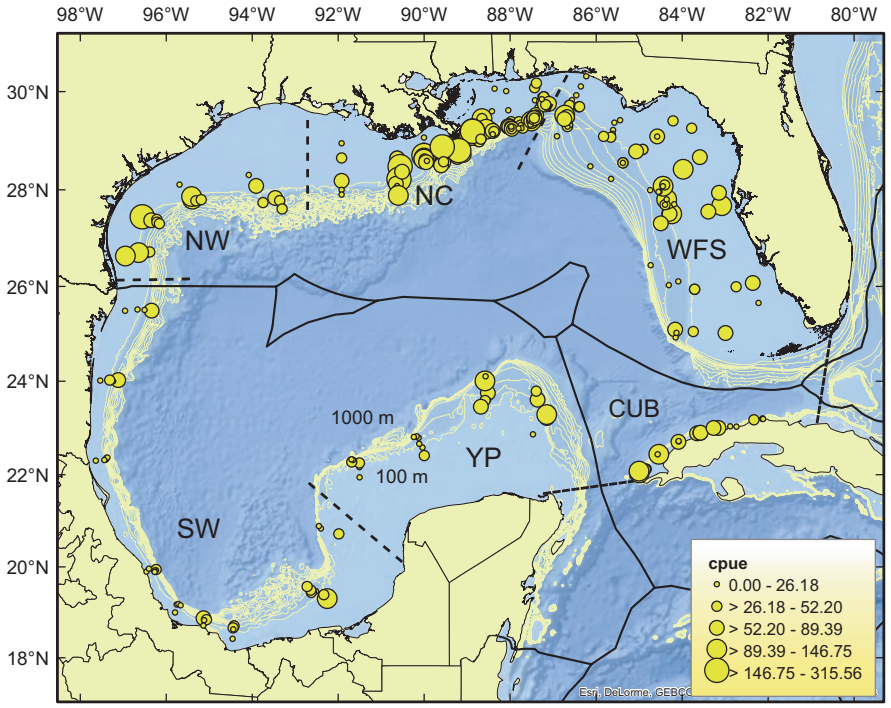

Fig. 15.1 Standardized catch rates (catch in numbers per 1000 hook-hours) of fishes sampled with demersal longlines, 2011–2017 (Murawski et al. 2018)

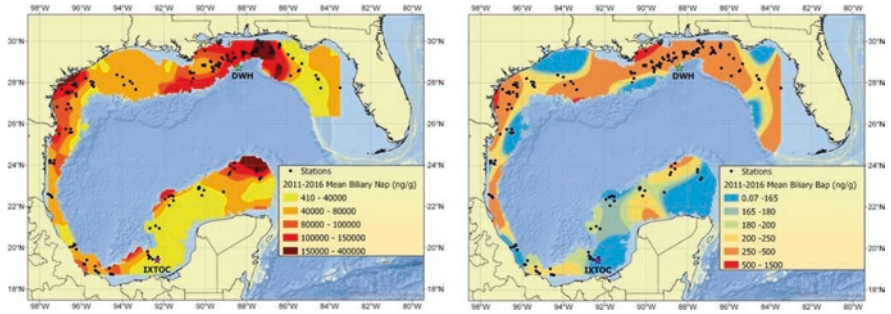

Fig. 15.2 Mean 2011–2016 biliary naphthalene (Nap ng/g) and benzo[a]pyrene (BaP ng/g) in fish collected in the Gulf of Mexico by the C-IMAGE Consortium (Pulster et al. 2017a). Black dots indicate station locations where fish were collected

pyrene were found in the north central region of the GoM (where DWH occurred). Additional "hot spots" of elevated levels of biliary FACs occurred near major shipping ports (i.e., Brownsville, Corpus Christi, Louisiana, Tampa), vessel shipping lanes, and rivers (i.e., Rio Grande, Mississippi, Coatzacoalcos).

Following the 2010 DWH oil spill, skin lesion frequencies and biliary FACs declined in a number of species collected from the north central region of the GoM (where DWH occurred), and this decline provides compelling evidence of the acute and episodic nature of PAH exposures from the DWH oil spill (Murawski et al. 2014; Snyder et al. 2015; Pulster et al. 2017a, 2020) and the impacts such exposures may have on fish health. Lesion frequencies in red snapper (*Lutjanus campechanus*) declined 53% between 2011 and 2012 (Murawski et al. 2014). In addition, 12 species that were repeatedly collected in the north central region of the GoM also demonstrated declines over time in total biliary PAHs in the years following DWH (2011–2015, Fig. 15.3, Pulster et al. 2017a). Total biliary PAHs declined by 15% in little gulpers (*Centrophorus uyato*) (2014–2015) to 90% in yellow conger eels (*Rhynchoconger flavus*) (2011–2015). As of 2015, 5 years after DWH, biliary PAH levels had continued to decline suggesting that levels were not yet reduced back to baseline or pre-spill levels.

Golden tilefish (*Lopholatilus chamaeleonticeps*) and a number of other species, including Gulf hake (*Urophycis cirrata*), snowy grouper (*Epinephelus niveatus*), yellowedge grouper (*Hyporthodus flavolimbatus*), red snapper, and red grouper (*Epinephelus morio*), all exhibited an increase in biliary PAHs between 2012/2013 and 2014 (Struch et al. unpublished; Pulster et al. 2017a, 2018; Snyder et al. 2015). This pattern of increasing PAH levels during the same time period (2012–2014) has also been observed in common loons, seaside sparrows, and sediments (Perez-Umphrey et al. 2018; Paruk et al. 2016; Turner et al. 2014). In Gulf menhaden, body burdens of PAH concentrations decreased, while benzo[a]pyrene toxic equivalents increased between 2012 and 2013 suggesting resuspension of oil residues rather than a new source (Olson et al. 2016). Changes in redox-sensitive elements,

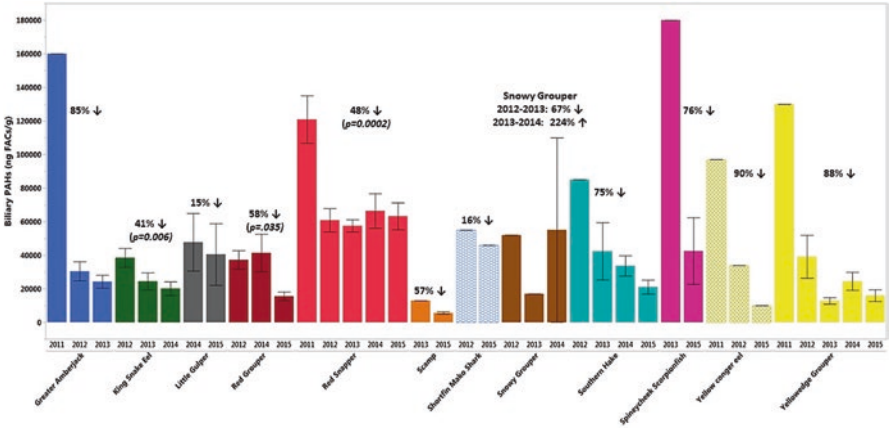

Fig. 15.3 Trends (2011–2015) in preliminary mean biliary PAHs (ng FACs/g bile) for multiple fish species collected from the north central Gulf of Mexico. Percent declines in biliary PAHs were calculated between the first and last year sampled for each species. Mean biliary PAHs are the sum of the naphthalene and benzo[a]pyrene fluorescent aromatic compounds (FACs). Error bars are ±1 standard error of the mean

radioisotope analyses, and in situ data from the GoM also provide supporting evidence for bioturbation, sedimentation pulses, and resuspension events during a similar time frame (Brooks et al. 2015; Hastings et al. 2016; Diercks et al. 2018). Resuspension events can be caused by a number of physical processes such as variation in subsurface currents, surface and internal waves, and storm-driven surges. An episodic large-scale resuspension event as the result of Hurricane Isaac in 2012 was identified from current meter data and sediment records in the northern GoM (Diercks et al. 2018). This is not surprising considering the GoM experiences frequent tropical storms, for instance, Tropical Storm Debby and Hurricane Isaac in 2012 and Tropical Storm Andrea and Tropical Storm Karen in 2013. The resuspension of sediments reintroduces contaminants into the water column (e.g., freely dissolved or sediment bound), thereby increasing bioavailability to biota. Suspended particles with associated sediment-bound contaminants, including PAHs, enhance the uptake rates and bioaccumulation in fish and other organisms (Zhai et al. 2018; Peterson et al. 1996; Leppänen and Kukkonen 1998; Menon and Menon 1999; Zhang et al. 2015).

Post-DWH, tissues from a number of fish species were also analyzed for PAHs from multiple regions within the GoM as part of the C-IMAGE Gulf-wide comprehensive fish survey (Murawski et al. 2014; Snyder et al. 2015, 2017; Carr et al. 2018; Pulster et al. 2018; Murawski et al. 2018). In 2011, concentrations of muscle and liver PAHs in red snapper collected in the north central region of the GoM were low (<35 ng/g w.w.) compared to the relatively high concentrations of PAH equivalents measured in the bile (41,000–470,000 ng FAC/g bile, Murawski et al. 2014). Despite the ability of fishes to quickly metabolize most PAHs, the PAH composition profiles in the liver samples had a significantly strong positive relationship ($r^2 = 0.82$, $p < 0.001$) with the profiles of the crude oil from the DWH wellhead (Fig. 15.4, Murawski et al. 2014).

Muscle tissues collected in 2011 from mesopelagic fish species in the north central region of the GoM contained PAH levels (330–2,350 ng/g w.w.; Romero et al. 2018) more than an order of magnitude higher than other species during the same time period (Murawski et al. 2014; Romero et al. 2018; Ylitalo et al. 2012; Xia et al. 2012). Similar to other species, the muscle concentrations in mesopelagic fish demonstrated significant increases between pre- and post-DWH levels, followed by a significant decline by 2015 (Romero et al. 2018). Romero et al. suggest the higher tissue concentrations in mesopelagic fish than shallower water species may be due to the increased frequency and duration of exposure periods due to their vertical migratory behaviors throughout the water column (Romero et al. 2018). However, in addition to species-specific differences in metabolic capacity, a number of additional critical environmental and physiochemical factors may partially explain the increased concentrations observed in mesopelagic fish. First, the fish in this study were collected (50–1,000 m) within similar depths of the continuous subsurface plume of oil residues (~1,000–1,200 m) that was identified post-DWH (Camilli et al. 2010). Although there is evidence that chemical cues can elicit habitat avoidance in fish (Pulster et al. 2020), the potential for increased and extended periods of exposure in 2010 exists due to the subsurface plume which persisted for

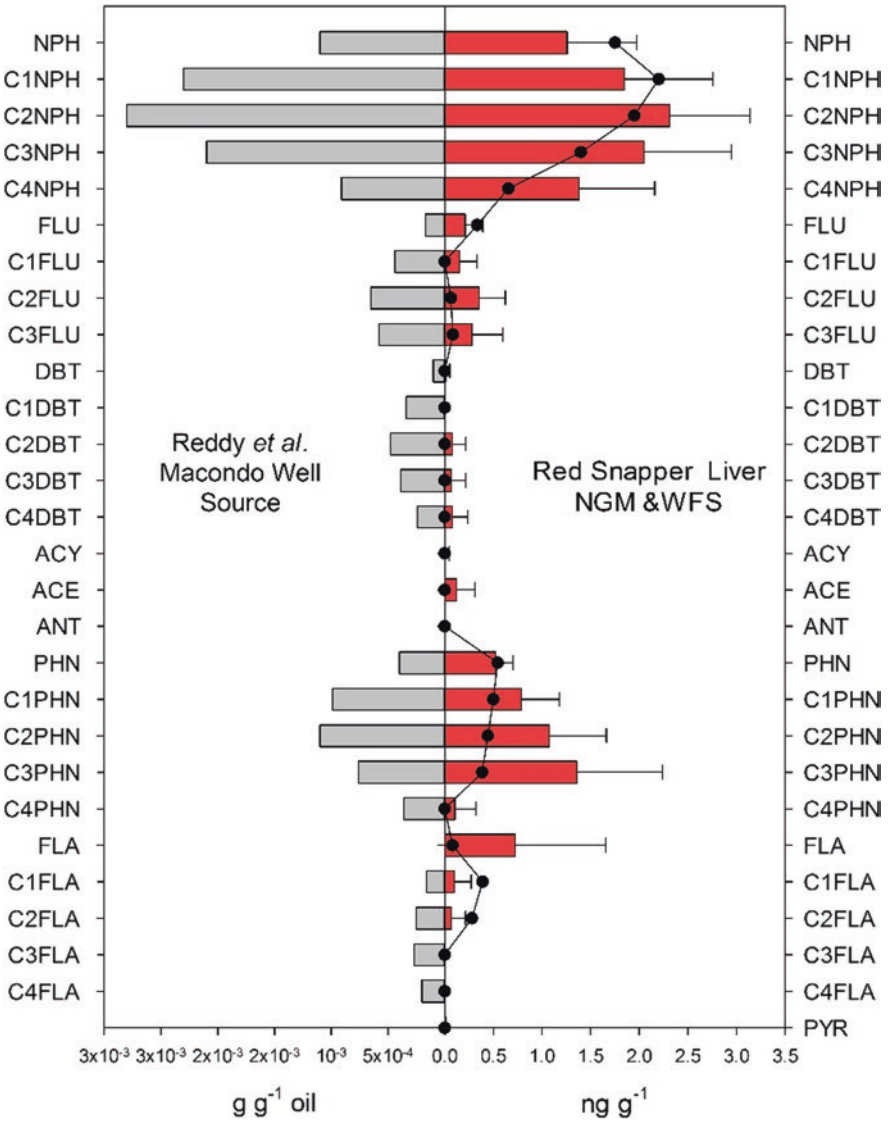

Fig. 15.4 Concentrations of some PAH parent compounds and alkylated homologues sampled from the Macondo (*Deepwater Horizon*) wellhead (Reddy et al. 2012; gray bars) and 2011 composite samples of red snapper livers collected from the Gulf of Mexico (red bars). (Reprinted with permission from Murawski et al. 2014)

months and continued water column contamination persisted in 2010, likely due to resuspended sediments. Furthermore, water temperatures decrease significantly with depth and are 15–20° lower at 1,000 m than at the surface, increasing the persistence and bioavailability of contaminants at deep pelagic depths. Specifically

to PAHs, low water temperatures promote their persistence in water due to lower volatilization and biodegradation which consequently decreases elimination rates further resulting in the retention of PAHs in fish tissues (Varanasi et al. 1981; Egaas and Varanasi 1982; Varanasi 1989). For example, starry flounders (*Platichthys stellatus*) held at temperatures (4 °C) similar to the temperatures at the depth of DWH in the GoM were found to have 26–34 times higher naphthalene concentrations than those held at 12 °C (Varanasi et al. 1981). The preliminary total PAHs in liver tissues collected ranged from 7.7 to 407 ng/g w.w. for hakes (*Urophycis* sp., 2012–2015; Struch et al. unpublished), 1200 to 195,000 ng/g w.w. for golden tilefish (2012–2016; Snyder et al. 2017, 2018), and 67.6 to 17,300 ng/g w.w. for groupers (*Epinephelus* sp., 2012–2016; Pulster et al. 2018). While there were a few species and site differences, in general the groupers collected within the north central region (2,350 ± 2,800 ng/g w.w.) had similar levels of total PAHs to those collected in the northwest region (1580 ± 2470 ng/g w.w.) yet significantly higher than those collected in the southwest region (983 ± 2,260 ng/g w.w.; $p < 0.0001$). In contrast to biliary PAHs, there appears to be an increasing trend over time in the liver concentrations of PAHs for a number of species. For instance, between 2012 and 2015, liver concentrations in yellowedge groupers from the north central region increased to 362% ($p = 0.036$) (Fig. 15.5). Similar trends were also observed in the southwest region for both snowy (237% increase) and yellowedge groupers (177% increase) from 2015 to 2016. In addition, PAH levels increased to 102% in hake livers between 2012 and 2015.

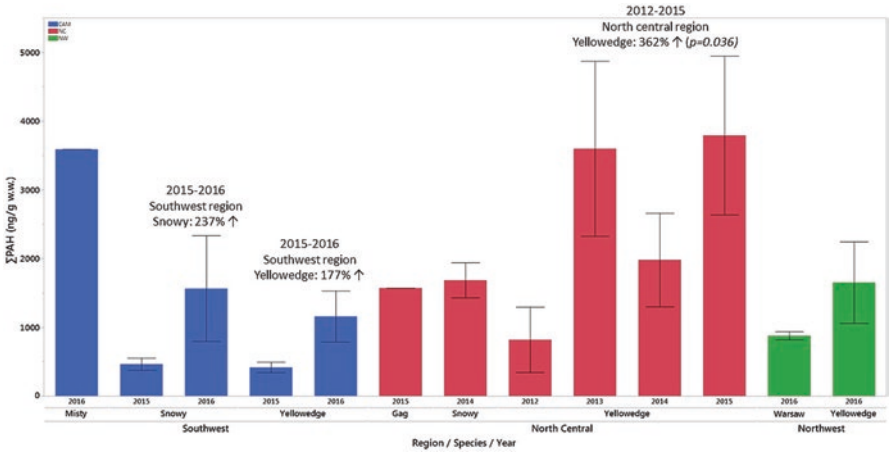

Fig. 15.5 Trends in preliminary mean liver concentrations of PAHs (ng/g wet weight) in grouper species collected from the southwest (blue bars), north central (red bars), and northwest (green bars) regions of the Gulf of Mexico (2011–2016). Percent increases in liver PAHs were calculated between the first and last year sampled for each species. The ∑PAHs is the sum of 46 parental PAHs and their alkylated homologues. Error bars are ±1 standard error of the mean

Preliminary concentrations of total PAHs in liver tissues from golden tilefish sampled between 2015 and 2016 were similar among regions but significantly higher in the northwest region offshore of Texas (31,000 ± 25,000 ng/g w.w.) than the southwest (21,000 ± 28,000 ng/g w.w.) and north central (16,000 ± 11,000 ng/g w.w.) regions (Snyder et al. 2017, 2018). The opposite pattern occurred for biliary PAHs. Biliary PAHs are higher in the north central region (470,000 ± 400,000 ng/g) than the southwest (170,000 ± 140,000 ng/g) and northwest regions (230,000 ± 88,000 ng/g). These results suggest the highest recent exposure to PAHs in the north central region, perhaps more efficient metabolism and elimination, and higher accumulation in the liver tissue in the southwest and northwest regions. As mentioned above, many species, including golden tilefish from the north central GoM, demonstrated increased biliary naphthalene metabolite concentrations between 2012 and 2015, possibly related to the resuspension of sedimented oil as discussed above. In contrast, total liver PAHs have remained relatively constant for golden tilefish sampled in 2012–2015.

In the southwest region, hardhead catfish collected in 2008 from along the Tabasco coast in Mexico had liver concentrations of PAHs ranging from 7,340 to 119,000 ng/g w.w., 1 year after the Kab-121 oil spill and 28 years post-Ixtoc 1 (Gold-Bouchot et al. 2014). Liver concentrations significantly declined to 1390–9470 ng/g w.w. within 3 months of the first sampling event. In 2010, Gracia (2010) analyzed the muscle content from 29 fish species collected at 30 sampling locations in the southwestern GoM near Ixtoc I spill area (off Veracruz, Tabasco, and Campeche states, Gracia 2010). The most frequent fish species sampled included hardhead catfish, Mexican flounder, sheepshead (*Archosargus probatocephalus*), gray triggerfish (*Balistes capriscus*), Atlantic croaker, and southern kingfish (*Menticirrhus americanus*). The highest value of PAH muscle concentrations (474 ng/g d.w.) was found in goliath grouper (*Epinephelus itajara*); however, relatively high concentrations of PAHs (100–474 ng/g d.w.) were also found in spotted weakfish (*Cynoscion nebulosus*), sand seatrout, sheepshead (*Archosargus probatocephalus*), and goliath grouper which were mainly found in coastal areas (Fig. 15.6; Gracia 2010). Anthracene (99 ng/g d.w.), fluoranthene (100 ng/g d.w.), and phenanthrene (98 ng/g d.w.) were the dominant PAHs in tissue content.

Fish surveys conducted in 2015 and 2016 by C-IMAGE in the southern GoM evaluated muscle tissues for PAH concentrations in 107 organisms from 16 species. The muscle concentrations of PAHs in red snapper and yellowedge grouper ranged from 10 to 493 ng/g d.w. (Gracia et al. 2018). Red snapper (59–83.4 ng/g d.w.) had higher mean muscle PAH concentrations than yellowedge grouper (53–37 ng/g d.w.), although not significantly so (Fig. 15.7). Muscle concentrations of PAHs in red snapper collected within the exclusion zone near where the Ixtoc 1 wellhead was located were relatively high; however, the highest levels were located off the Yucatán Peninsula where there are no known oil rigs or natural oil seeps (Fig. 15.8). The high levels of PAHs observed in multiple species in this location may be the result of proximity to major shipping channels and strong current systems (Snyder et al. 2017; Gracia et al. 2018). Yellowedge grouper showed high PAH muscle

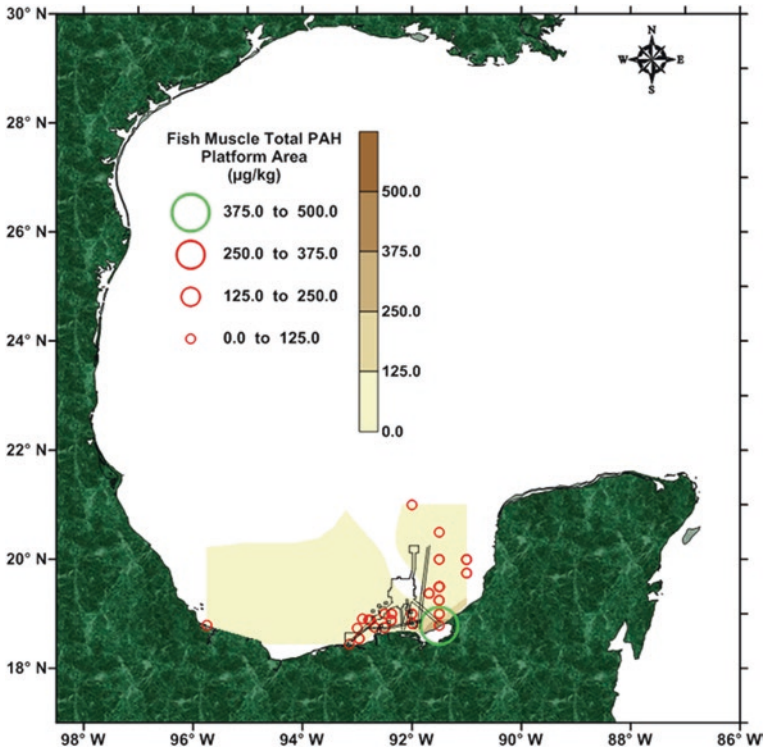

Fig. 15.6 Mean concentrations of PAHs (µg/g d.w.) in muscle tissues from fish (29 species) collected in 2010 from the southern Gulf of Mexico near oil infrastructure within the Ixtoc 1 zone

values in three main areas; however, similar to the red snapper, the concentrations off the Yucatán Peninsula were higher than those samples near the exclusion zone (Fig. 15.9; Gracia et al. 2018). However, the mean PAH muscle concentration of both species was very low with respect to US LOCs.

15.4 Conclusions

A complex interaction of physiochemical properties (e.g., molecular weight and octanol-water partition coefficients), species-specific life histories (e.g., habitat, diet), metabolic capacities, and environmental factors (e.g., temperature, salinity) regulates the chemical bioavailability, uptake, metabolic rates, and excretion rates of oil contaminant dynamics in fishes. Although fish have a relatively high capacity to rapidly metabolize PAHs, there is a potential for increased toxicity and bioaccumulation during the metabolic process as PAHs are hydrolyzed, reabsorbed, and returned through circulation (Lech and Vodicnik 1985; Kleinow et al. 1987; Varanasi et al. 1989).

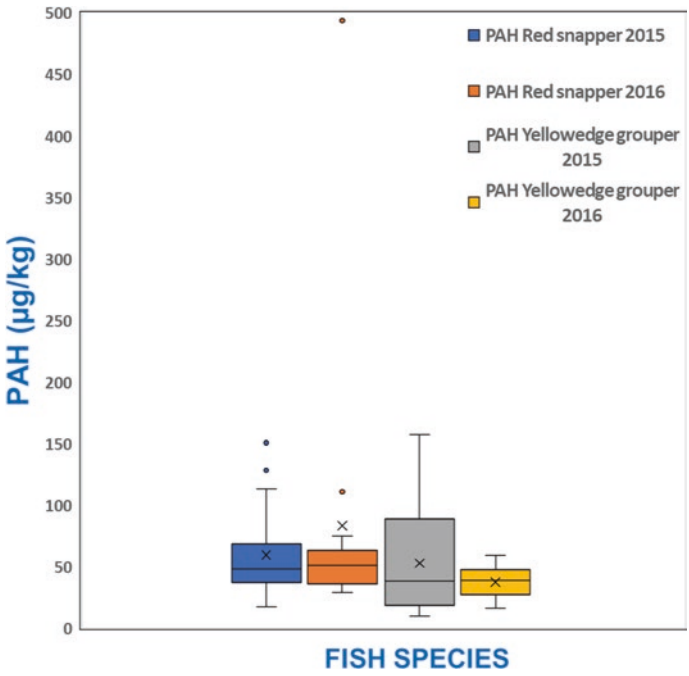

Fig. 15.7 Muscle concentrations of PAHs (µg/kg d.w.) measured in red snapper and yellowedge grouper collected in the southwestern Gulf of Mexico, 2015–2016

Studies have demonstrated that exposure routes have little effect on the biotransformation products of some compounds and the distribution of PAHs within tissues (Stein et al. 1984; Varanasi 1989; Pulster et al. 2017b). Rather, differences observed between muscle and liver concentrations are more likely due to chronic exposures and accumulation rates that are faster than the fishes' ability to metabolize and excrete xenobiotics. Importantly, chronically exposed fish have slower elimination and increased PAH levels than those exposed acutely (Varanasi 1989). This is evident in the increasing trend in baseline levels of biliary and tissue concentrations of PAHs in a number of fish species between pre-2000 and post-DWH data in the GoM that raises concern for the overall health of the Gulf ecosystem and its fish populations. The increasing oil production (especially in the northern GoM) and the higher fraction of oil derived from ultra-deep waters (>1500 m) mean that fish communities not traditionally exposed to oil contamination from oil extraction activities might now be at a higher risk (Romero et al. 2018). The increasing trend in oil accumulation in deepwater fishes and expansion of drilling into deeper waters warrants increased monitoring and fish health assessments and intensifies the need for more extensive and comprehensive offshore baseline data, since the majority of all baseline studies in the GoM prior to the DWH were for nearshore and shelf fishes.

Given the importance of the GoM to energy production in both the USA and Mexico (Murawski et al. 2020), the lack of coordinated, comprehensive, and

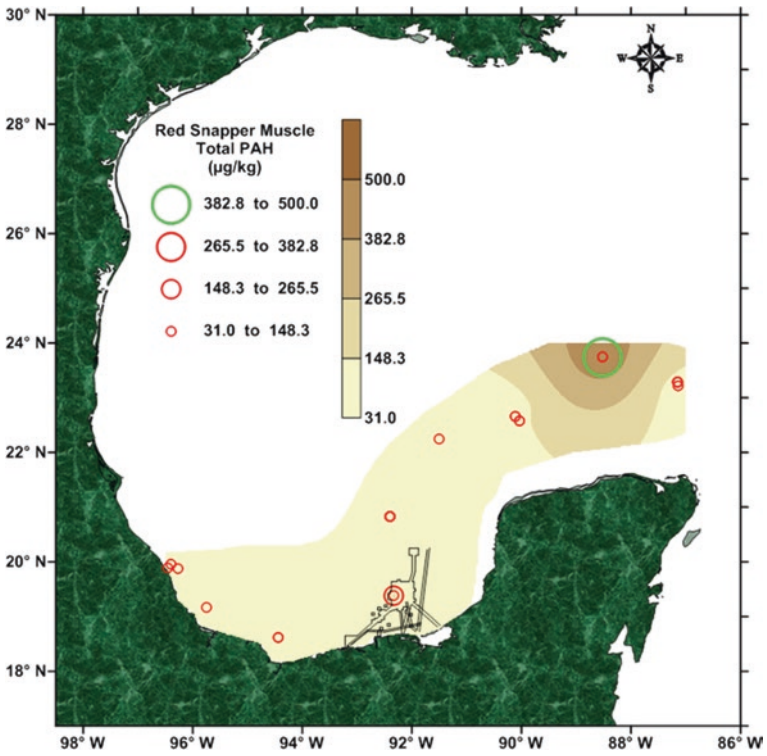

Fig. 15.8 Muscle concentrations of PAHs (µg/kg d.w.) in red snapper collected in the southwestern Gulf of Mexico, 2015–2016

continuous monitoring of oil-related pollution in sediments, fishes, and waters from these facilities is remarkable. Other than the post-DWH assessment activities, primarily supported by private foundation funding, there is no specific program in the USA to understand and assess pollution related to oil production and transportation activities. The advantages of developing such a program are numerous. Assessing the impacts of pollution from a specific infrastructure failure is the obvious primary advantage, but such data can also identify the interactions between pollution from natural sources (e.g., cold seeps) in relation to the entirety of the marine oil budget.

Pre-Ixtoc 1 data from Mexican waters are virtually nonexistent, and there is at least a 10-year data gap between the pre- and post-DWH data for PAH concentrations in fish from US waters. Given that the GoM is a highly dynamic system with numerous and expanding sources of anthropogenically derived pollution, collection of baseline data at shorter time intervals is critical for assessing and evaluating sources of pollution. Baseline data and long-term trends are essential to monitor the health of the GoM, changing environmental conditions, and the interactions of natural systems with anthropogenic activities. In the context of a future oil spill and changing environmental conditions in the GoM, continued monitoring is required for the assessment of impact, resilience, and recovery from future events.

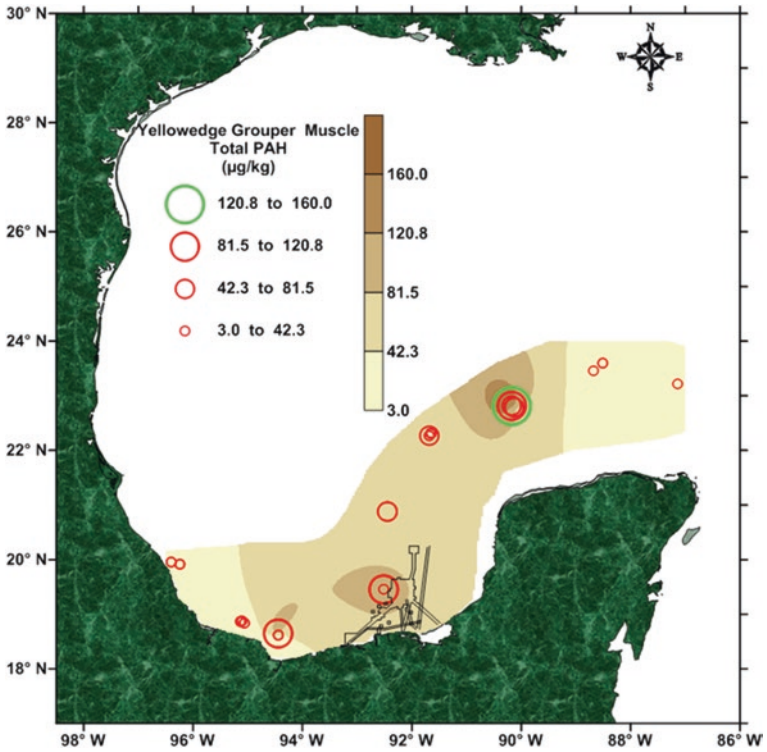

Fig. 15.9 Distributions of muscle concentrations of PAHs (µg/kg d.w.) in yellowedge grouper collected in the southwestern Gulf of Mexico, 2015–2016

Acknowledgments This research was made possible by a grant from the Gulf of Mexico Research Initiative/C-IMAGE I, II, and III. Preliminary data will be publicly available once validated and finalized. Final data are publicly available through the Gulf of Mexico Research Initiative Information and Data Cooperative (GRIIDC) at https://data.gulfresearchinitiative.org (R6.x805.000:0048, R6.x805.000:0052, R6.x805.000:0049, R6.x805.000:0051).

References

Amezcua-Linares F, Amezcua F, Gil-Manrique B (2015) Effects of the Ixtoc 1 oil spill on fish assemblages in the Southern Gulf of Mexico. In: Alford JB, Peterson MS, Green CC (eds) Impacts of Oil Spill disasters on marine habitats and fisheries in North America. CRC Press, Boca Raton, pp 209–236

Brooks GR, Larson RA, Schwing PT, Romero I, Moore C, Reichart G-J, Jilbert T, Chanton JP, Hastings DW, Overholt WA, Marks KP, Kostka JE, Holmes CW, Hollander D (2015) Sedimentation pulse in the NE Gulf of Mexico following the 2010 DWH Blowout. PLoS One 10(7):e0132341. https://doi.org/10.1371/journal.pone.0132341

Camilli R, Reddy CM, Yoerger DR, Van Mooy BAS, Jakuba MV, Kinsey JC, McIntyre CP, Sylva SP, Maloney JV (2010) Tracking hydrocarbon plume transport and biodegradation at *Deepwater Horizon*. Science 330:201–204. https://doi.org/10.1126/science.1195223

Carr BE, Pulster EL, Gracia A, Armenteros M, Murawski SA (2018) A spatiotemporal analysis of hepatic and biliary PAHs in groupers from around the Gulf of Mexico. In: Gulf of Mexico Oil Spill and ecosystem science, New Orleans

Diercks AR, Dike C, Asper VL, DiMarco SF, Chanton JP, Passow U (2018) Scales of seafloor sediment resuspension in the northern Gulf of Mexico. Elementa Sci Anthropocene 6. https://doi.org/10.1525/elementa.285

Egaas E, Varanasi U (1982) Effects of polychlorinated biphenyls and environmental temperature on in vitro formation of benzo[a]pyrene metabolites by liver of trout (*Salmo gairdneri*). Biochem Pharmacol 31:561–566. https://doi.org/10.1016/0006-2952(82)90160-5

Farrington JW, Tripp BW, Tanabe S, Subramanian A, Sericano JL, Wade TL, Knap AH (2016) Edward D. Goldberg's proposal of "the Mussel Watch": reflections after 40 years. Mar Pollut Bull 110:501–510

Froescheis O, Looser R, Cailliet GM, Jarman WM, Ballschmiter K (2000) The deep-sea as a final global sink of semivolatile persistent organic pollutants? Part I: PCBs in surface and deep-sea dwelling fish of the North and South Atlantic and the Monterey Bay Canyon (California). Chemosphere 40:651–660. https://doi.org/10.1016/S0045-6535(99)00461-0

Gold-Bouchot G, Ceja-Moreno V, Chan-Cocom E, Zapata-Perez O (2014) Petroleum hydrocarbons, fluorescent aromatic compounds in fish bile and organochlorine pesticides from areas surrounding the spill of the Kab121 well, in the Southern Gulf of Mexico: a case study. J Environ Biol 35:147–156

Gracia A (2010) Campaña Oceanográfica (SGM-2010). Informe Final. Gerencia de Seguridad Industrial, Protección Ambiental y Calidad Región Marina Noreste, PEMEX - EXPLORACIÓN – PRODUCCIÓN. Instituto de Ciencias del Mar y Limnología, UNAM, México

Gracia A, Murawski SA, Alexander-Valdés RM, Vázquez-Bader AR, Snyder S, LópezDurán IM, Ortega-Tenorio P, Pulster EL, Frausto-Castillo JA (2018) Fish stock resiliency to environmental PAH. Presentation at: Gulf of Mexico Oil Spill & ecosystem science conference, New Orleans, LA, February 6–9 2018

Harvey J, Harwell L, Summers JK (2008) Contaminant concentrations in whole-body fish and shellfish from US estuaries. Environ Monit Assess 137:403–412. https://doi.org/10.1007/s10661-007-9776-1

Hastings DW, Schwing PT, Brooks GR, Larson RA, Morford JL, Roeder T, Quinn KA, Bartlett T, Romero IC, Hollander DJ (2016) Changes in sediment redox conditions following the BP DWH blowout event. Deep Sea Res II Top Stud Oceanogr 129:167–178. https://doi.org/10.1016/j.dsr2.2014.12.009

Hom T, Collier TK, Krahn MM, Strom MS, Ylitalo GM, Nilsson WB, Paranjpye RN, Varanasi U (2008) Assessing seafood safety in the aftermath of Hurricane Katrina. Am Fish Soc Symp 64:73–93

Kennicutt MC, Brooks JM, Atlas EL, Giam CS (1988) Organic compounds of environmental concern in the Gulf of Mexico: a review. Aquat Toxicol 11:191–212. https://doi.org/10.1016/0166-445X(88)90013-6

Kleinow KM, Melancon MJ, Lech JJ (1987) Biotransformation and induction: implications for toxicity, bioaccumulation and monitoring of environmental xenobiotics in fish. Environ Health Perspect 71:105–119. https://doi.org/10.2307/3430418

Koenig S, Fernández P, Company JB, Huertas D, Solé M (2013) Are deep-sea organisms dwelling within a submarine canyon more at risk from anthropogenic contamination than those from the adjacent open slope? a case study of Blanes canyon (NW Mediterranean). Prog Oceanogr 118:249–259. https://doi.org/10.1016/j.pocean.2013.07.016

Lech JJ, Vodicnik MJ (1985) Biotransformation. In: Rand GM, Petrocelli SR (eds) Fundamentals of aquatic toxicology: methods and applications. Hemisphere, New York, pp 526–557

Leppänen MT, Kukkonen JVK (1998) Relative importance of ingested sediment and pore water as bioaccumulation routes for pyrene to oligochaete (*Lumbriculus variegatus*, Müller). Environ Sci Technol 32:1503–1508. https://doi.org/10.1021/es970941k

Lewis MA, Scott GI, Bearden DW, Quarles RL, Moore J, Strozier ED, Sivertsen SK, Dias AR, Sanders M (2002) Fish tissue quality in near-coastal areas of the Gulf of Mexico receiving point source discharges. Sci Total Environ 284:249–261. https://doi.org/10.1016/S0048-9697(01)00891-9

McCain BB, Brown DW, Hom T, Myers MS, Pierce SM, Collier TK, Stein JE, Chan SL, Varanasi U (1996) Chemical contaminant exposure and effects in four fish species from Tampa Bay, Florida. Estuaries 19:86–104. https://doi.org/10.2307/1352655

McDonald SJ, Willett KL, Thomsen J, Beatty KB, Connor K, Narasimhan TR, Erickson CM, Safe SH (1996) Sublethal detoxification responses to contaminant exposure associated with offshore oil production. Can J Fish Aquat Sci 53:2606–2617

Menon NN, Menon NR (1999) Uptake of polycyclic aromatic hydrocarbons from suspended oil borne sediments by the marine bivalve *Sunetta scripta*. Aquat Toxicol 45:63–69. https://doi.org/10.1016/s0166-445x(98)00092-7

Murawski SA, Hogarth WT (2013) Enhancing the ocean observing system to meet restoration challenges in the Gulf of Mexico. Oceanography 26:10–16

Murawski SA, Hogarth WT, Peebles EB, Barbieri L (2014) Prevalence of external skin lesions and polycyclic aromatic hydrocarbon concentrations in Gulf of Mexico Fishes, post-*Deepwater Horizon*. Trans Am Fish Soc 143:1084–1097. https://doi.org/10.1080/00028487.2014.911205

Murawski SA, Peebles EB, Gracia A, Tunnell JW, Armenteros M (2018) Comparative abundance, species composition, and demographics of continental shelf fish assemblages throughout the Gulf of Mexico. Mar Coast Fish 10:325–346. https://doi.org/10.1002/mcf2.10033

Murawski SA, Hollander D, Gilbert S, Gracia A (2020) Deep-water oil and gas production in the Gulf of Mexico, and related global trends (Chap. 2). In: Murawski SA, Ainsworth C, Gilbert S, Hollander D, Paris CB, Schlüter M, Wetzel D (eds) Scenarios and responses to future Deep Oil Spills – fighting the next war. Springer, Cham

NAS (2013) An ecosystem services approach to assessing the impacts of the Deepwater Horizon oil spill in the Gulf of Mexico. National Academies Press, Washington, DC

NCCOS (2017) NOAA's National status and trends data. National Centers for Coastal Ocean Science. 2018

Olson GM, Meyer BM, Portier RJ (2016) Assessment of the toxic potential of polycyclic aromatic hydrocarbons (PAHs) affecting Gulf Menhaden (*Brevoortia patronus*) harvested from waters impacted by the BP *Deepwater Horizon* Spill. Chemosphere 145:322–328. https://doi.org/10.1016/j.chemosphere.2015.11.087

Paruk JD, Adams EM, Uher-Koch H, Kovach KA, Long D, Perkins C, Schoch N, Evers DC (2016) Polycyclic aromatic hydrocarbons in blood related to lower body mass in common loons. Sci Total Environ 565:360–368. https://doi.org/10.1016/j.scitotenv.2016.04.150

Perez-Umphrey AA, Bergeon Burns CM, Stouffer PC, Woltmann S, Taylor SS (2018) Polycyclic aromatic hydrocarbon exposure in seaside sparrows (*Ammodramus maritimus*) following the 2010 *Deepwater Horizon* oil spill. Sci Total Environ 630:1086–1094. https://doi.org/10.1016/j.scitotenv.2018.02.281

Peterson CH, Kennicutt MC II, Green RH, Montagna P, Harper DE Jr, Powell EN, Roscigno PF (1996) Ecological consequences of environmental perturbations associated with offshore hydrocarbon production: a perspective on long-term exposure in the Gulf of Mexico. Can J Fish Aquat Sci 53:2637–2654

Pulster EL, Snyder S, Struch R, Carr B, Toro-Farmer GA, Gracia A, Murawski SA (2017a) What can bile tell us about the environmental health of the Gulf of Mexico? Presentation at: Gulf of Mexico Oil Spill and Ecosystem Science, New Orleans, LA

Pulster EL, Main K, Wetzel D, Murawski S (2017b) Species-specific metabolism of naphthalene and phenanthrene in 3 species of marine teleosts exposed to *Deepwater Horizon* crude oil. Environ Toxicol Chem 36:3168–3176. https://doi.org/10.1002/etc.3898

Pulster EL, Carr B, Murawski SA (2018, October) Spatiotemporal trends in hepatobiliary levels of polycyclic aromatic hydrocarbons in Gulf of Mexico groupers. University of South Florida, Presentation at: MARCUBA 2018, Havana Cuba

Pulster EL, Gracia A, Snyder SM, Deak K, Fogleson S, Murawski SA (2020) Chronic sublethal effects observed in wild caught fish following two major oil spills in the Gulf of Mexico: *Deepwater Horizon* and Ixtoc 1 (Chap. 24). In: Murawski SA, Ainsworth C, Gilbert S, Hollander D, Paris CB, Schlüter M, Wetzel D (eds) Deep Oil Spills: facts, fate and effects. Springer International, Cham

Reddy CM, Arey JS, Seewald JS, Sylva SP, Lemkau KL, Nelson RK, Carmichael CA, McIntyre CP, Fenwick J, Ventura GT, Van Mooy BAS, Camilli R (2012) Composition and fate of gas and oil released to the water column during the Deepwater Horizon oil spill. Proc Natl Acad Sci 109(50):20229–20234

Romero IC, Sutton T, Carr B, Quintana-Rizzo E, Ross SW, Hollander DJ, Torres JJ (2018) Decadal assessment of polycyclic aromatic hydrocarbons in mesopelagic fishes from the Gulf of Mexico reveals Exposure to oil-derived Sources. Environ Sci Technol. https://doi.org/10.1021/acs.est.8b02243

Ross SW, Quattrini AM, Roa-Varón AY, McClain JP (2010) Species composition and distributions of mesopelagic fishes over the slope of the north-central Gulf of Mexico. Deep Sea Res II Top Stud Oceanogr 57:1926–1956. https://doi.org/10.1016/j.dsr2.2010.05.008

Shigenaka G (2014) Twenty-five years after the *Exxon Valdez* Oil Spill: NOAA's Scientific Support, Monitoring, and Research. NOAA Office of Response and Restoration, Seattle

Snyder S, Pulster EL, Murawski SA (2017) Gulf-wide analysis of PAH exposure and accumulation in Golden Tilefish. Presented at: American Fisheries Society Annual Meeting, Tampa, FL

Snyder SM, Pulster EL, Fogelson SB (2018) Murawski SA Hepatic accumulation of PAHs and prevalence of hepatic lesions in Golden Tilefish from the northern Gulf of Mexico. Presentation at: Gulf of Mexico Oil Spill & Ecosystem Science Conference, New Orleans

Snyder SM, Pulster EL, Wetzel DL, Murawski SA (2015) PAH exposure in Gulf of Mexico demersal fishes, post-*Deepwater Horizon*. Environ Sci Technol 49:8786–8795. https://doi.org/10.1021/acs.est.5b01870

Stein JE, Hom T, Varanasi U (1984) Simultaneous exposure of English sole (*Parophrys vetulus*) to sediment-associated xenobiotics: part 1—uptake and disposition of 14C-polychlorinated biphenyls and 3H-benzo[a]pyrene. Mar Environ Res 13:97–119. https://doi.org/10.1016/0141-1136(84)90021-7

Turner RE, Overton EB, Meyer BM, Miles MS, McClenachan G, Hooper-Bui L, Engel AS, Swenson EM, Lee JM, Milan CS, Gao H (2014) Distribution and recovery trajectory of Macondo (Mississippi Canyon 252) oil in Louisiana coastal wetlands. Mar Pollut Bull 87:57–67. https://doi.org/10.1016/j.marpolbul.2014.08.011

US EPA (2009) 2008 Biennial National Listing of Fish Advisories. Washington, D.C.

US EPA (2013) 2011 National Listing of Fish Advisories. United States Environmental Protection Agency, Washington, D.C.

Varanasi U (ed) (1989) Metabolism of polycyclic aromatic hydrocarbons in the aquatic environment. CRC Press, Boca Raton

Varanasi U, Gmur DJ, Reichert WL (1981) Effect of environmental temperature on naphthalene metabolism by Juvenile Starry flounder (*Platichthys stellatus*). Arch Environ Contam Toxicol 10:203–214. https://doi.org/10.1007/bf01055622

Varanasi U, Stein JE, Nishimoto M (1989) Biotransformation and disposition of polycyclic aromatic hydrocarbons (PAH) in fish. In: Varanasi U (ed) Metabolism of polycyclic aromatic hydrocarbons in the aquatic environment. CRC Press, Boca Raton, pp 94–140

Ward CH, Tunnell JW Jr (2017) Habitats and biota of the Gulf of Mexico: An overview. In: Ward CH (ed) Habitats and Biota of the Gulf of Mexico: before the *Deepwater Horizon* Oil Spill, vol I. Springer Nature, New York

Xia K, Hagood G, Childers C, Atkins J, Rogers B, Ware L, Armbrust K, Jewell J, Diaz D, Gatian N, Folmer H (2012) Polycyclic aromatic hydrocarbons (PAHs) in Mississippi seafood from areas affected by the *Deepwater Horizon* oil spill. Environ Sci Technol 46:5310–5318. https://doi.org/10.1021/es2042433

Ylitalo GM, Krahn MM, Dickhoff WW, Stein JE, Walker CC, Lassitter CL, Garrett ES, Desfosse LL, Mitchell KM, Noble BT, Wilson S, Beck NB, Benner RA, Koufopoulos PN, Dickey RW

(2012) Federal seafood safety response to the *Deepwater Horizon* oil spill. Proc Nat Acad Sci USA 109:20274–20279. https://doi.org/10.1073/pnas.1108886109

Zhai Y, Xia X, Xiong X, Xia L, Guo X, Gan J (2018) Role of fluoranthene and pyrene associated with suspended particles in their bioaccumulation by zebrafish (*Danio rerio*). Ecotoxicol Environ Saf 157:89–94. https://doi.org/10.1016/j.ecoenv.2018.03.065

Zhang X, Xia X, Li H, Zhu B, Dong J (2015) Bioavailability of pyrene associated with suspended sediment of different grain sizes to *Daphnia magna* as investigated by passive dosing devices. Environ Sci Technol 49:10127–10135. https://doi.org/10.1021/acs.est.5b02045

Chapter 16
Case Study: Using a Combined Laboratory, Field, and Modeling Approach to Assess Oil Spill Impacts

Sandy Raimondo, Jill A. Awkerman, Susan Yee, and Mace G. Barron

Abstract The *Deepwater Horizon* (DWH) spill was the largest oil spill in US history, requiring an assessment of injuries to nearshore habitats and estuarine organisms. Developing a model of appropriate complexity is critical in an environmental assessment; models should be complex enough to adequately address the assessment objectives without being more complex than is needed. We present an approach that starts with a sensitivity analysis of an initial assumption-based model to prioritize model parameters and focus research efforts to reduce model uncertainty. We then develop a targeted research strategy that utilized laboratory, field, and intermediate modeling efforts to parameterize a final set of models of varying complexity to evaluate risk. We demonstrate this process in a case study of the small estuarine fish, the sheepshead minnow (*Cyprinodon variegatus*), exposed to weathered oil in Barataria Bay, LA, following the DWH oil spill.

Keywords Population-level risk assessment · Model complexity · Uncertainty · Spatially explicit

16.1 Introduction

The *Deepwater Horizon* (DWH) spill was the largest oil spill in US history, with 507 million L of oil released over a period of 87 days beginning April 22, 2010 (Barron 2012). The salt marshes of Louisiana were among the most heavily oiled habitats, with the greatest oiling occurring in northern Barataria Bay (Michel et al. 2013). Sediments, shorelines, and marsh vegetation mats and substrates remained heavily oiled in areas of Barataria Bay beyond 2011 (Lin and Mendelssohn 2012;

S. Raimondo (✉) · J. A. Awkerman · S. Yee · M. G. Barron
US Environmental Protection Agency, Gulf Ecology Division, Gulf Breeze, FL, USA
e-mail: Raimondo.sandy@epa.gov; Awkerman.jill@epa.gov; yee.susan@epa.gov; barron.mace@epa.gov

S. A. Murawski et al. (eds.), *Scenarios and Responses to Future Deep Oil Spills*,
https://doi.org/10.1007/978-3-030-12963-7_16

Silliman et al. 2012; Michel et al. 2013) and provided exposure routes to estuarine fish and other organisms (Awkerman et al. 2016; Brown-Peterson et al. 2017). For the DWH natural resource damage assessment, injuries to nearshore habitats and estuarine organisms were previously assessed using a hypothesis-driven approach of determining exposure, observing field effects, testing toxicity, and inferring impacts (Baker et al. 2017).

For complex assessments such as those for DWH, moving beyond deterministic approaches toward predictive, population-level assessments has been advocated (US EPA 2009). Ecological complexities (e.g., heterogeneous habitat and contaminant distribution) require models that include relevant scenarios and an understanding of the associated uncertainty. Coupled with sensitivity analyses, which identify the parameters with the largest influence on model outcome, predictive models have the potential to provide assessors a known confidence space in which decisions can be made (Lehuta et al. 2010).

Developing a model of appropriate complexity is a critical first step in an environmental assessment; models should be complex enough to adequately address the assessment objectives without being more complex than is needed (Schmolke et al. 2010). Model complexity can be either quantitative (e.g., empirical functions fit to observed data) or qualitative (e.g., categorical inclusion lacking empirical underpinnings), and the level of model complexity represents trade-offs in generality, realism, and precision (Raimondo et al. 2018). Qualitative complexity increases when functions are added to a general model that increases environmental realism, whereas quantitative complexity increases the precision in model output. Additional data may provide both qualitative and quantitative complexity, increasing both realism and precision, while other functions may increase model realism without the ability to evaluate confidence of the prediction. Understanding the trade-offs of generality, realism, and precision in developing a model of appropriate complexity is necessary to ensure the model appropriately addresses the objectives of the assessment.

As an assessor develops a model of appropriate complexity, they must identify important elements to include in the model and obtain the best data available to inform those functions or estimates. We present an approach that starts with a sensitivity analysis of an initial assumption-based model (herein, initial model) to prioritize model parameters on which to focus research efforts and reduce model uncertainty. We then develop a targeted research project that combines laboratory, field, and intermediate modeling efforts to parameterize a final set of models of varying complexity to evaluate risk. We demonstrate this process in a case study of the small estuarine fish, the sheepshead minnow (*Cyprinodon variegatus*), exposed to weathered oil in Barataria Bay, LA, following the DWH oil spill. Sheepshead minnows were selected because of their small home ranges (high site fidelity) and high levels of exposure from heavy oiling, due to close association with sediments (Raimondo et al. 2016).

16.2 Case Study Overview

16.2.1 Target Species

The sheepshead minnow is a euryhaline, eurothermic fish in the family Cyprinodontidae commonly found in estuarine areas along the Atlantic coast and in the Gulf of Mexico and may be the most abundant fish in some estuaries (Haney 1999). Sheepshead minnow burrow in the substrate and are highly territorial, with males displaying courtship behavior to attract females. Abundant toxicity information is available for this model species, and population models have been developed based on laboratory observations and experiments (Raimondo et al. 2009). The sheepshead minnow life cycle comprises four life stages representing embryo (within egg), larval (hatchling to development of swim bladder), juvenile (through sexual maturation), and adult. Fish life stages may be determined by size, age, or environment; however, size is most clearly linked to maturation (Kinne and Kinne 1962; Hardy 1978; Nordlie 2000; Cripe et al. 2009). The average size of fish at the larval-juvenile and juvenile-adult life stage transitions are 1.5 cm and 2.6 cm, respectively (Cripe et al. 2009; Nordlie 2000). Adults range from >2.6 to approximately 5.5 cm in size.

16.2.2 Conceptual Model

An initial model was developed for the sheepshead minnow in Gulf Coast estuaries that included layers for habitat suitability, distribution of a hypothetical contaminant, concentration response, and population dynamics. Initial fish distribution in the spatially explicit model was determined from pre-existing layers of salinity, temperature, dissolved oxygen, depth, and the observed range of their values, for sheepshead minnow obtained from the literature (Hardy 1978; Bennett and Beitinger 1997). A spatial layer of hypothetical contaminant distribution was used as input for hypothetical concentration-response curves to estimate the effect of exposure on fecundity, survival, and growth rates. Functions reflected percent reductions of individuals "exposed" to varying degrees of contamination relative to "unexposed" individuals.

A deterministic stage-based matrix population model captured population dynamics of sheepshead minnow with data derived from the control treatment of a laboratory toxicity study (Raimondo et al. 2009). The model has a 5-day time step corresponding to the duration of the shortest life stage (embryo), with the population growth rate, λ, determined as the dominant eigenvalue of the matrix (Caswell 2001). The matrix includes the estimated probability of survival within each of the four life stages (embryo, larval, juvenile, and adult), as well as the probability of transitioning to the next stage for each of the three developmental stages. The derivation of these parameters followed Caswell (2001) and is discussed in detail in

Raimondo et al. (2009). The estuary was divided into 90x90 m grids, with a fraction of the population moving between cells in each time step. Migration was modeled as the probability of fish moving between grids based on a decreasing function of habitat suitability. Density dependence was added to survival, reproduction, and movement, as both a ceiling on abundance (100 fish/m^2) and as an exponential relationship, in which fecundity and survival were dependent on habitat suitability.

16.2.3 Sensitivity Analysis

Model simulations with and without the contaminant were run to include interactions between all the model layers as appropriate. A global sensitivity analysis revealed which parameters and model assumptions had the strongest impacts on model predictions. A Monte Carlo analysis was performed that randomly drew parameters from ±10% of their model value. All parameters were modified simultaneously since some parameters are autocorrelated. The sensitivity of each parameter is defined as the proportional change in model outcome relative to the proportional change in the parameter.

Results of the sensitivity analysis are shown in Fig. 16.1. Larger values indicate that small changes in the parameter had large impacts on the model outcome. The analyses indicated that, in the absence of a contaminant, habitat suitability and density-dependent survival had the largest impacts on model predictions. Other parameters, including movement, larval survival, and larval development, also had strong impacts on model predictions. When the contaminant was included in the model, predictions also depended strongly on habitat suitability and larval survival, as well as the spatial distribution of the contaminant.

16.2.4 Developing a Targeted Research Strategy

Based on the results of the sensitivity analysis of the initial model, a targeted research strategy was developed to obtain the best available data from field, laboratory, or intermediate modeling to use in parameterizing a final set of models. The strategy included field observations to inform habitat suitability, contaminant distribution, and polycyclic aromatic hydrocarbon (PAH) composition, laboratory research to inform concentration-response relationships of each life stage exposed to weathered oil and density-dependent relationships, a hybrid field-laboratory study to identify differences in basic life history parameters (fecundity, size) in fish from laboratory and natural populations, and intermediate modeling to evaluate the interaction of density dependence and contaminant exposure and the influence of seasonally varying demographic rates.

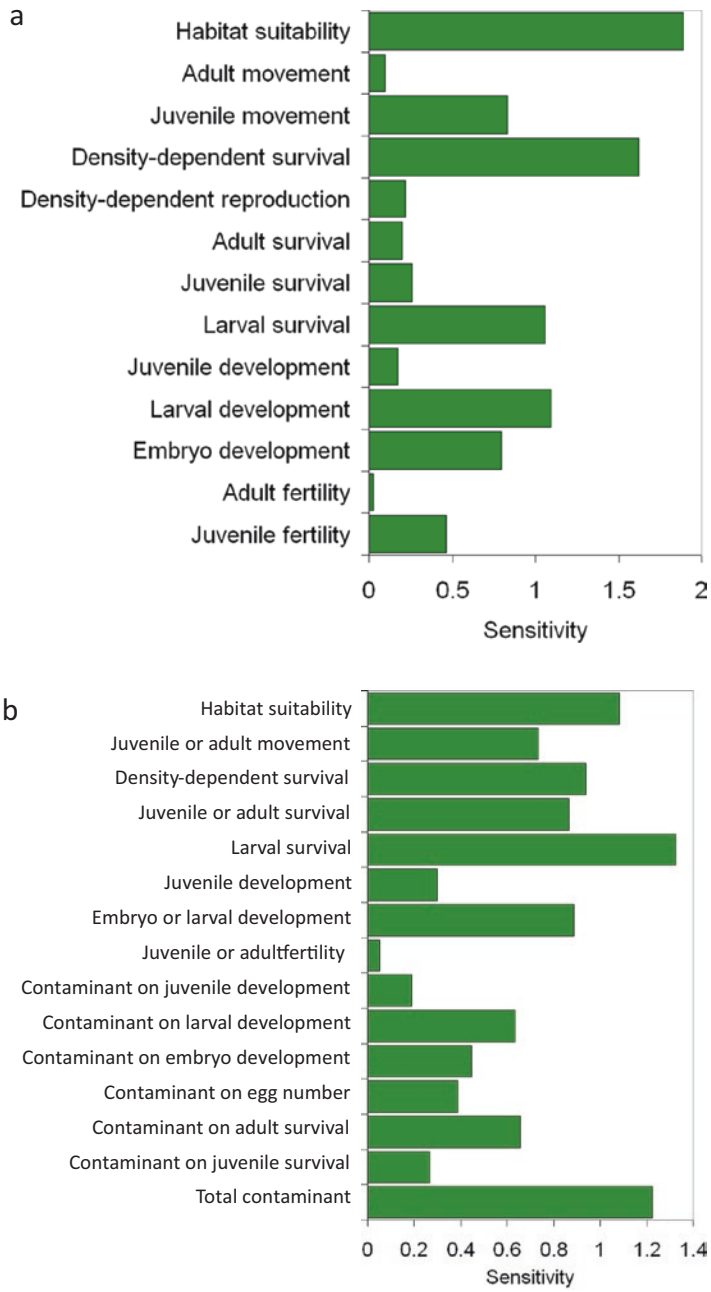

Fig. 16.1 Sensitivity analysis of initial models for fish dynamics (**a**) without contaminant exposure and (**b**) with contaminant exposure

16.3 Targeted Research

16.3.1 Field Research

16.3.1.1 Habitat suitability

A field study was conducted to develop a habitat suitability model for the sheepshead minnow in Gulf Coast estuaries. Data from areas classified as "Estuarine or Marine Wetland" by National Wetland Inventory Project in Pensacola Bay, Santa Rosa Sound, and Choctawhatchee Bay were used to determine habitat suitability based on sheepshead minnow abundance measured at these sites. Drop trap ($1m^2$) sampling was used to determine fish presence or absence (Rozas and Minello 1997) from over 300 sites across the estuarine systems. A generalized linear model (GLM) with binomial distribution and logit link was then fit to a model with habitat variables expected to be associated with presence of sheepshead minnows that were available as spatial layers for Barataria Bay (kriged values of bathymetry, salinity, and dissolved oxygen data). Sheepshead minnow was more probable in shallow areas with lower salinity and dissolved oxygen, and gridded locations within Barataria Bay were assigned habitat suitability scores using this model.

16.3.1.2 Contaminant Distribution and Composition

Sediment sampling locations were selected using a generalized random-tessellation stratified design, in which random sampling locations throughout Barataria Bay were chosen to be uniformly distributed within five Shoreline Cleanup Assessment Technique (SCAT) categories representing coastal oiling severity (no oil, very light, light, moderate, heavy). Sediment samples were collected in December 2010 and analyzed for PAHs, saturated hydrocarbons (SHC), and petroleum biomarkers. The relative ranking of PAH concentrations in collected samples did not always correspond with the SCAT observations in closest proximity at the time of sampling (Awkerman et al. 2016). Because PAHs were highly variable at finer spatial resolution, SCAT categories were used to define PAH concentrations in model simulations in two separate ways after gridded locations in our simulations had been categorized according to the closest SCAT observation for each time step. First, PAH concentrations were randomly chosen from empirical sediment sample values classified within the same SCAT category at the time of sampling, even though concentrations varied widely among categories. Data included all sediment samples analyzed within a year of the oil spill and documented in the Deepwater Horizon Information Management Portal. Second, the PAH range of sampled sediment was divided into quantiles, and the median value of each quantile was used to represent probabilistic exposure associated with each SCAT category. PAH estimates were then used in the final set of models as a basis from which to modify growth and survival rates of early life stage fish, using dose-response curves generated from laboratory exposures to weathered oiled sediment (Awkerman et al. 2016).

16.3.2 Laboratory Research

16.3.2.1 Toxicity Effects

Toxicity effects were determined from a life cycle exposure (from larvae through adult reproduction) of sheepshead minnows to laboratory-oiled sediment (Raimondo et al. 2016) and an embryonic development test using zebrafish as a surrogate (Raimondo et al. 2014). Both tests examined the impacts on fish exposed to sediment contaminated with weathered oil since oil binds to the sediment and burrowing fish, such as the sheepshead minnow, are most at risk through exposure to contaminated sediment. For both experiments, reference (uncontaminated) sediment was spiked with laboratory-weathered South Louisiana crude (SLC) oil at various concentrations to derive dose-response relationships of exposure and effects at each life stage. Zebrafish embryos were also exposed to sediment collected from an oiled site in Barataria Bay, Louisiana, in December 2010.

The embryonic development test is described in detail in Raimondo et al. (2014). Briefly, oiled sediment caused developmental malformations in embryos including yolk sac and pericardial edema, craniofacial and spinal defects, and tissue degeneration. No toxicity was observed in Barataria sediment, which contained 2 mg TPAH/kg 1% OC. Raimondo et al. (2016) described a 19-week complete life cycle experiment exposing sheepshead minnow to five concentrations of spiked sediment as well as one unspiked sediment control and one seawater (no sediment) control. The test was initiated with newly hatched larvae and ran through the reproductively active adult phase, measuring hatch rate, growth (e.g., length, weight), survival, and reproduction. Significant effects included reduced larval and juvenile standard length and wet weight and reduced fecundity. Dose-response relationships from both the embryonic and life cycle studies were used to describe the effects of oil in the final set of models.

16.3.2.2 Demographic Endpoints

Sheepshead minnow growth, survival, and reproduction for the initial model were estimated from cultured populations, which may not be representative of rates in wild populations. Rutter et al. (2012) compared four standard health condition metrics (hepatosomatic index, HSI; gonadosomatic index, GSI; fecundity, condition factor) between cultured and wild caught sheepshead minnow to determine if laboratory cultured fish were representative of wild populations. Wild fish yielded fewer eggs per female per unit body weight and were more robust (e.g., higher condition factor) than cultured fish. Fecundity estimates used in the final set of models were adjusted to reflect those from wild populations.

16.3.2.3 Density Dependence

The interaction between density dependence and contaminants can result in responses that range from compensatory to synergistic impacts to population growth (Raimondo et al. 2013). Density dependence (DD) was identified as a critical model component in the sensitivity analysis of the initial model but is difficult to quantify in field studies. A combination of laboratory and modeling research was conducted to quantify density dependence in sheepshead minnow and the potential interactions with chemical stressors. Influence of density on sheepshead minnow survival, growth, maturation, and reproduction was measured in a series of four laboratory studies (Raimondo et al. 2013). Sexual maturation was significantly affected by density but was not related to size, indicating that maturation is a function of both the presence and the density of adults. Fecundity was also density dependent, with significantly less fecund females in the mid-range and high densities compared to the lowest densities tested. Juvenile growth was only affected at extremely high densities (>500 fish m^{-2}), and there was no evidence of density-dependent influences on survival of any life stage. The highest observed field densities of fish in marsh sites were at levels that altered sexual maturation and fecundity in laboratory fish, but not at densities corresponding to laboratory impacts on juvenile growth (Awkerman et al. 2016).

16.3.3 Modeling

16.3.3.1 Interaction of Density Dependence and Contaminant Effects

Following the development of laboratory-based density dependence relationships, intermediate modeling efforts were conducted to evaluate whether density dependence and contaminant effects had additive, compensatory, or synergistic interactions (Raimondo 2013). In these simulations, density interacted with stressors in compensatory and synergistic ways, which were based on the DD functions used in the model and the organism-level impacts of the stressor. For example, the strongest compensation occurred where survival was both DD and impacted by the stressor. When no DD survival was included, DD fecundity and growth had limited compensatory influence. Since laboratory studies showed no evidence of DD survival in sheepshead minnow (Raimondo et al. 2013), compensatory mechanisms were not included in the final set of models, which applied a ceiling-type density dependence based on field data (Awkerman et al. 2016).

16.3.3.2 Temperature-Dependent Demographic Rates

Variation in survival and reproduction, including that attributed to seasonality, can be a large source of prediction uncertainty in models (Nordlie 2000; Raimondo et al. 2009). Temperature-driven functions for survival and reproduction were

derived for the sheepshead minnow to account for seasonal variation in these demographic parameters (Raimondo 2012). A temperature-dependent growth rate function was developed for the von Bertalanffy constant, K, measured at various temperatures and fit to a logistic curve to estimate duration of larval and juvenile life stages at different temperatures. Stage-specific mortality was then modeled as a power function of size that included a temperature-dependent modification. Seasonal reproduction was then determined from temperature-dependent functions of embryo survival and stage duration (Raimondo 2012). The temperature-dependent functions for determining survival of immature life stages were then used in the final set of models that simulated population-level effects of sheepshead minnow exposed to weathered oil (Awkerman et al. 2016).

16.4 Assessing Risk Using Models of Varying Complexity

16.4.1 Models to Evaluate Risk

A final set of models were developed from the research described in the previous sections to evaluate the role of model complexity in assessing risk (Table 16.1; Awkerman et al. 2016). For all models in the final set, sheepshead minnow life cycle was divided into three stages based on documentation of length thresholds for juveniles and breeding adults (Nordlie 2000; Raimondo 2012). The set of population models incorporated early life stage oil exposure effects at three different levels of spatial and temporal complexity. The first and most simple assessment was based on a deterministic matrix model used to represent a single exposure event ("simple matrix model"). Relative differences in fish population growth rates at different

Table 16.1 Model scenarios for which simulations were run to compare model complexity and outcome relative to potential application

	Fish dynamics				Oil dynamics	
Model scenario	Fish population	Seasonal fluctuations	Movement	Behavioral response	Temporal	Spatial
Simple matrix model	X					
Seasonal matrix model	X	X			X	
SEPM[a] no oil	X	X	X			
SEPM homogenous oil	X	X	X		X	
SEPM SCAT oil	X	X	X		X	X
SEPM oil avoidance	X	X	X	X	X	X

[a]Spatially explicit population model

exposure concentrations provide an indication of relative impacts but offer no long-term perspective. A second approach repeated the simple matrix model over time with seasonal variation in vital rates based on temperature flux ("seasonal matrix model"; Raimondo 2012) and changing coastal oiling categorization. The extended projection allowed interpretation of exposure effects over time and simulated potential recovery of the population. The third and final approach included more spatial context, recognizing that contaminant distribution varied throughout the bay as well as over time. Spatially explicit population models (SEPM) were developed for four different scenarios: (1) a baseline "SEPM no oil" simulation, (2) a "SEPM homogenous oil" simulation in which exposure throughout the bay is based on a single observation in Bay Jimmy, (3) a "SEPM SCAT oil" simulation in which the nearest observed coastal oiling category was used to determine probable range of PAH exposure, and (4) a "SEPM oil avoidance" simulation in which habitat-based movement criteria were modified to include preference for less oiled locations.

For the spatially explicit population models, migration was incorporated as the probability of staying at a location during each time step, which was determined by an exponential function of habitat suitability (see above), based on sheepshead minnow movement rates documented in the field (Sutton 2002; Chitty and Able 2004). Avoidance of oiled habitat was simulated by applying criteria that included movement to less oiled locations within the same range during each time step. For each model scenario, observed average temperature for each 2-week time step was used to determine rates of growth, survival, and reproduction. Initial distribution of sheepshead minnow population prior to simulations was determined by running the model for 10 years using the 5-year average temperature (from Oct 2009 to Sept 2014) for each 2-week time step.

16.4.2 Model Outcomes

Deterministic models indicated dramatic differences in population growth rate for a single exposure event, based on reduced growth and survival of larval sheepshead minnows (Fig. 16.2a). With longer-term perspective of a seasonally varying model, these impacts are most pronounced during periods of higher reproductive activity, in the summer, and are less detrimental over time as coastal oiling effects are reduced (Fig. 16.2b). Spatially explicit models show minimal long-term impacts on sheepshead minnow abundance when the population dynamics throughout the bay are incorporated with effects corresponding to local oiling severity, suggesting the potential for compensatory effect by areas that are less impacted by oil exposure (Fig. 16.2c).

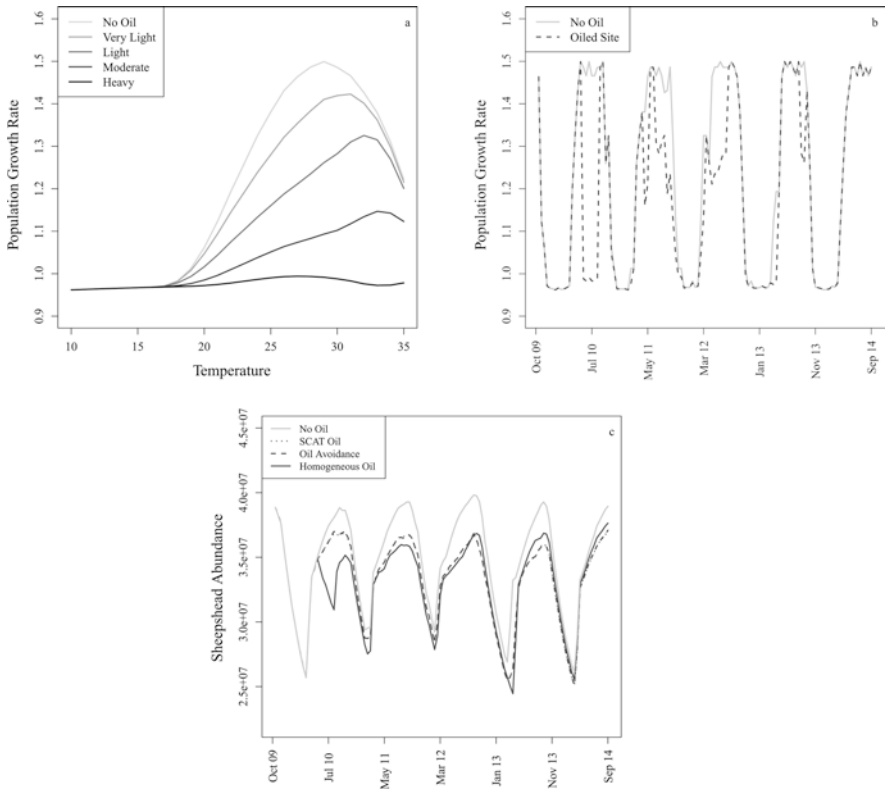

Fig. 16.2 Three approaches to modeling oil exposure effects in sheepshead minnow population: (**a**) including effects of temperature and PAH concentration on population growth rate, (**b**) comparing population growth rate of exposure representing maximally and minimally oiled sites with seasonal temperature variation, (**c**) simulating four spatial scenarios in which no oil is present, SCAT observations indicate spatial and temporal differences in PAH exposure, fish avoid oiled habitat, and PAH concentration from a single oiled site assumes homogenous oil distribution and is used to estimate a potential worst case scenario

16.5 Summary and Recommendations for Future Studies

Weathered DWH oil entered Barataria Bay during the 4 months of the spill and impacted sediments, shorelines, and marsh vegetation habitats (Michel et al. 2013). Oil distribution within the bay was heterogeneous, controlled by the small tidal range and high spatial variability in shoreline geography and density of vegetation. Additional factors affecting oil distribution included variability in composition, degree of weathering and viscosity of the weathered oil, and redistribution of hydrocarbons from storm events (Michel et al. 2013). Sediment PAH concentrations in Barataria Bay were extremely heterogeneous, ranging from non-detectable to greater than 100 mg/Kg (e.g., Turner et al. 2014; Awkerman et al. 2016). The aliphatic and lighter aromatic components of oil were more rapidly biodegraded,

whereas higher molecular weight PAHs persisted in sediments for multiple years (e.g., Mahmoudi et al. 2013; Turner et al. 2014).

The relatively data-rich, spatially explicit models of post-spill impacts on estuarine fish populations improved model interpretations from a cost/benefit perspective. The spatial and temporal extent of contaminant data were a rare commodity and yet spatial data still lacked the resolution to adequately incorporate fine-scale modifications to movement based on patchy and variable contaminant distribution. Different levels of model complexity offer endpoints of varying utility – from immediate impacts as estimated in a deterministic matrix model to long-term projections of potential recovery and overall population abundance. Resources are seldom available to empirically analyze changing contaminant distribution and potential impacts in a timely fashion; however, simulations like the examples presented offer a way of assessing different scenarios to establish a range of potential outcomes that could inform the relative impact of contamination effects as well as response strategies.

Acknowledgments We thank Alex Almario, George Craven, Geraldine Cripe, Adam Glahn, Becky Hemmer, Julie Krzywka, Crystal Lilivois, Bob Quarles, Hannah Rutter, and Deborah Vivian for their support during the research described here. The views expressed in this chapter are those of the authors and do not necessarily reflect the views or policies of the US Environmental Protection Agency.

References

Awkerman JA, Hemmer B, Almario A, Jackson CR, Barron MG, Raimondo S (2016) Spatially explicit risk assessment of estuarine fish after Deepwater Horizon Oil spill: trade-off in complexity and parsimony. Ecol Appl 26:1708–1720

Baker MC, Steinhoff MA, Fricano GF (2017) Integrated effects of the Deepwater Horizon oil spill on nearshore ecosystems. Mar Ecol Prog Ser 576:219–234

Barron MG (2012) Ecological impacts of the Deepwater Horizon oil spill: implications for immunotoxicity. Toxicol Pathways 40:315–320

Bennett WA, Beitinger TL (1997) Temperature tolerance of the sheepshead minnow, *Cyprinodon variegatus*. Copeia 1997:77–87

Brown-Peterson NJ, Krasnec MO, Lay CR, Morris JM, Griffitt RJ (2017) Responses of juvenile southern flounder exposed to Deepwater Horizon oil-contaminated sediment. Environ Toxicol Chem 36:1067–1076

Caswell H (2001) Matrix population models. Sinauer Associates, Inc, Sunderland, MA

Chitty JD, Able KW (2004) Habitat use, movements and growth of the sheepshead minnow, *Cyprinodon variegates*, in a restored salt marsh in Delaware Bay. Bull New Jersey Acad Sci 49:1–8

Cripe GM, Hemmer BL, Goodman LR, Fournie JW, Raimondo S, Vennari JC, Danner RL, Smith K, Manfredonia BR, Kulaw DH, Hemmer MJ (2009) Multigenerational exposure of the estuarine sheepshead minnow (*Cyprinodon variegates*) to 17a-estradiol. I. Organism-level effects over three generations. Environ Toxicol Chem 28:2397–2408

Haney DC (1999) Osmoregulation in the sheepshead minnow, *Cyprinodon variegatus*: Influence of a fluctuating salinity regime. Estuaries 22:1071–1077

Hardy JD (1978) Development of fishes of the mid-Atlantic Bight. An atlas of egg, larval and juvenile stages. Volume II. Anguillidae through Syngnathida. FWS/OBS-78/12. Final Report. U.S. Fish and Wildlife Service, Washington, DC

Kinne O, Kinne EM (1962) Rates of development in embryos of the cyprinodont fish exposed to different temperature-salinity-oxygen combinations. Can J Zool 40:231–253
Lehuta S, Mahevas S, Petitgas P, Pelletier D (2010) Combining sensitivity and uncertainty analysis to evaluate the impact of management measures with ISIS – Fish: marine protected areas for the Bay of Biscay anchovy (*Engraulis encrasicolus*) fishery. ICES J Mar Sci 67(5):1063–1075
Lin Q, Mendelssohn IA (2012) Impacts and recovery of the Deepwater Horizon oil spill on vegetation structure and function of coastal salt marshes in the Northern Gulf of Mexico. Environ Sci Technol 46:3737–3743
Mahmoudi N, Porter TM, Zimmerman AR, Fulthorpe RR, Kasozi GN, Silliman BR, Slater GF (2013) Rapid degradation of Deepwater Horizon spilled oil by indigenous microbial communities in Louisiana saltmarsh sediments. Environ Sci Technol 47:13303–13312
Michel J, Owens EH, Zengel S, Graham A, Nixon Z et al (2013) Extent and degree of shoreline oiling: Deepwater Horizon Oil Spill, Gulf of Mexico, USA. PLoS One 8(6):e65087
Nordlie FG (2000) Patterns of Reproduction and development of selected resident teleosts in Florida salt marshes. Hydrobiologia 434:165–182
Raimondo S (2012) Incorporating temperature-driven seasonal variation in survival, growth, and reproduction into population models for small fish. Mar Ecol Prog Ser 469:101–112
Raimondo S (2013) Density dependent functional forms drive compensation in populations exposed to stressors. Ecol Model 265:149–157
Raimondo S, Hemmer BL, Goodman LR, Cripe GM (2009) Multigenerational exposure of the estuarine sheepshead minnow (*Cyprinodon variegates*) to 17a-estradiol. II. Population-level effects through two life cycles. Environ Toxicol Chem 28:2409–2415
Raimondo S, Rutter H, Jackson CR, Hemmer BL, Cripe GM (2013) The influence of density on adults and juveniles of the estuarine fish, the sheepshead minnow (*Cyprinodon variegatus*). J Exp Mar Biol Ecol 439:69–75
Raimondo S, Jackson CR, Krzykwa J, Hemmer BL, Barron MG (2014) Developmental toxicity of Louisiana crude oiled-spiked sediment to zebrafish. Ecotoxicol Environ Saf 108:265–272
Raimondo S, Hemmer BL, Jackson CR, Krzykwa J, Almario A, Awkerman JA, Barron MG (2016) Effects of Louisiana crude oil on the sheepshead minnow (*Cyprinodon variegatus*) during a life-cycle exposure to laboratory oiled sediment. Environ Toxicol 31:1627–1639
Raimondo S, Etterson M, Pollesch N, Garber K, Kanarek A, Lehmann W, Awkerman J (2018) A framework for linking population model development with ecological risk assessment objectives. Integr Environ Assess Manag 14:369–380
Rozas LP, Minello TJ (1997) Estimating densities of small fishes and decapod crustaceans in shallow estuarine habitats: A review of sampling design with focus on gear selection. Estuaries 20:199–213
Rutter H, Norberg M, Raimondo S (2012) Comparison of cultured and wild sheepshead minnow (*Cyprinodon variegatus*) health condition metrics used in toxicity effects assessment. Gulf Mexico Sci 30(1–2):60–64
Schmolke A, Thorbek P, DeAngelis DL, Grimm V (2010) Ecological models supporting environmental decision making: a strategy for the future. Trends Ecol Evol 25:479–486
Silliman BR, van de Koppel J, McCoy MW, Diller J, Kasozi GN, Earl K, Adams PN, Zimmerman AR (2012) Degradation and resilience in Louisiana salt marshes after the BP–Deepwater Horizon oil spill. Proc Natl Acad Sci. https://doi.org/10.1073/pnas.1204922109
Sutton RJ (2002) Summer movements of desert pupfish among habitats at the Salton Sea. In: Barnum DA, Elder JF, Stephens D, Friend M (eds) The Salton Sea. Developments in hydrobiology, vol 161. Springer, Dordrecht, pp 223–228
Turner RE, Overton EB, Meyer BM, Miles MS, McClenachan G, Hooper-Bui L, Engel AS, Swenson EM, Lee JM, Milan CS, Gao H (2014) Distribution and recovery trajectory of Macondo (Mississippi Canyon 252) oil in Louisiana coastal wetlands. Mar Pollut Bull 87:57–67
US EPA (2009) Summary report: risk assessment forum technical workshop on population-level ecological risk assessment. EPA/100/R-09/006. US Environmental Protection Agency, Washington, DC

Part III
Simulations of Future Deep Spills

Teri Navajo
Misfortune Teller
Acrylic and ink on Canvas
24” × 24”

Chapter 17
Testing the Effect of MOSSFA (Marine Oil Snow Sedimentation and Flocculent Accumulation) Events in Benthic Microcosms

Edwin M. Foekema, Justine S. van Eenennaam, David J. Hollander, Alette M. Langenhoff, Thomas B. P. Oldenburg, Jagoš R. Radović, Melissa Rohal, Isabel C. Romero, Patrick T. Schwing, and Albertinka J. Murk

Abstract In multispecies experiments performed in microcosms with natural sediment, it was investigated how the presence of marine snow affects the fate and ecological impact of deposited oil residues. The response of different taxonomic groups like nematodes, foraminifera, crustaceans and molluscs onto the presence of marine snow with or without oil was compared with the impact of deposited oil residues without marine snow. Also the effect of the presence of marine snow on oil biodegradation and transfer of oil-derived compounds to selected biota was studied. Although not designed to mimic the specific deep sea conditions in the Gulf of Mexico, the outcome of the experiments gave new insights in how a MOSSFA event can affect the benthic community. In general the experiments indicate that at field realistic oil-derived compound concentrations, the adverse impact of the marine snow on the sediment surface has a stronger impact on the benthic ecosystem than

E. M. Foekema (✉)
Wageningen University & Research, Marine Animal Ecology Group, Wageningen, The Netherlands

Wageningen Marine Research, Den Helder, The Netherlands
e-mail: Edwin.foekema@wur.nl

J. S. van Eenennaam
Wageningen University & Research, Sub-department of Environmental Technology, Wageningen, The Netherlands

Regulatory Affairs Department, Safety Assessment, Charles River Laboratories, 's-Hertogenbosch, The Netherlands
e-mail: justine.vaneenennaam@wur.nl

D. J. Hollander · I. C. Romero · P. T. Schwing
University of South Florida, College of Marine Science, St. Petersburg, FL, USA
e-mail: davidh@usf.ued; isabelromero@mail.usf.edu; pschwing@mail.usf.edu

S. A. Murawski et al. (eds.), *Scenarios and Responses to Future Deep Oil Spills*,
https://doi.org/10.1007/978-3-030-12963-7_17

the oil's toxicity on its own. In addition, the presence of marine snow reduces the degradation of the oil and can create an exposure route for animals that consume oiled marine snow and thus potentially enhances the ecological impact further.

Keywords MOSSFA · Ecological impact · Sediment · Macroinvertebrates · Meiofauna

17.1 Introduction

During the *Deepwater Horizon* (DWH) spill, oil residues were brought to the seafloor by what was referred to as the MOSSFA (Marine Oil Snow Sedimentation and Flocculent Accumulation) event that occurred due to a combination of local factors. Apart from the presence of oil and dispersants, these factors included relatively high concentrations of phytoplankton and suspended mineral particles (Bianchi et al. 2011; Daly et al. 2016; Hu et al. 2011; O'Connor, 2013; Passow et al. 2012; van Eenennaam et al. 2016). Under the stressful conditions, the microbial/phytoplankton community produced extracellular polymeric substances (EPS) that were observed in large volumes during the spill (Dell'Amore 2010; Passow et al. 2012). After aggregation with oil and suspended mineral particles, the EPS sank to the seafloor. The sedimentation rates during the spill increased up to ten times (Brooks et al. 2015). Deposition of oil residues at depths greater than 200 m was estimated to cover an area of ~76,000 km^2, of which ~294 km^2 received more than 1 g oil residues/m^2 with a maximum of 43 g oil residues/m^2 (Romero et al. 2017).

In order to increase insight into the impact of MOSSFA on the fate (i.e. biodegradation) and the ecological effects of oil, a series of experiments were performed in benthic multispecies test systems (microcosms). The experiments were per-

A. M. Langenhoff
Wageningen University & Research, Sub-department of Environmental Technology, Wageningen, The Netherlands
e-mail: Alette.langenhoff@wur.nl

T. B. P. Oldenburg · J. R. Radović
University of Calgary, PRG, Department of Geoscience, Calgary, Canada
e-mail: toldenbu@ucalgary.ca; jagos.radovic@ucalgary.ca

M. Rohal
Texas A&M University – Corpus Christi, Harte Research Institute for Gulf of Mexico Studies, Unit 5869, Corpus Christi, TX, USA
e-mail: melissa.rohal@tamucc.edu

A. J. Murk
Wageningen University & Research, Marine Animal Ecology Group, Wageningen, The Netherlands
e-mail: Tinka.murk@wur.nl

formed at ambient pressure and with sediment and organisms collected from shallow water and were not intended to mimic the actual conditions in the deep sea of the GoM, but rather to give insight into the general mechanisms and processes that could play a role during a MOSSFA event.

17.2 Experimental Setup

The results described in this chapter are based on a series of three experiments (Exp-I, Exp-II and Exp-III) that are described in detail in Rahsepar et al. (unpublished), van Eenennaam et al. (2018) and van Eenennaam et al. (2019). The general setup that was followed in all experiments is briefly described below and summarized in Table 17.1. The major differences were that invertebrates were not added in Exp-I, and treatments were administred at once in Exp-I and II, and spread over 4 days in Exp-III.

Table 17.1 Some characteristics of the described experiments

	Exp-I	Exp-II	Exp-III
Control (n replicates)	3	3	6
Clay 0 g/m (n replicates)	3	3	6
Clay 3 g/m (n replicates)	–	–	6
Clay 10 g/m (n replicates)	3	6	6
Snow 0 g/m (n replicates)	3	3	6
Snow 3 g/m (n replicates)	–	–	6
Snow 10 g/m (n replicates)	3	6	6
C. volutator (n/microcosm)	–	40	40
P. ulvae (n/microcosm)	–	20	20
M. balthica (n/microcosm)	–	20	–
Foraminifera analysed?	–	Y	Y
Nematode/copepod analysed?	–	–	Y
Test duration biota (d)	–	16	42, 80
Test duration biodegradation (d)	42	42	42, 80
References	Rahsepar et al. *unpub.*	Van Eenennaam et al. (2018)	Van Eenennaam et al. (2019)
			Rohal et al. *unpub.* Schwing et al. *unpub.*

17.2.1 Test Systems

All experiments were performed in glass aquaria (25 × 25 × 25 cm, 15 L) stocked with 5 cm of natural fine organic-rich (6% OM) sediment and natural seawater, situated in a climate-controlled room with day-night light regime. Exp-I focused on the biodegradation of oil without influence of bioturbation, and therefore macroinvertebrates were not introduced. In the following experiments, the ecological impact was studied, and therefore 40 individuals of *Corophium volutator* (a sediment-dwelling amphipod) and 20 individuals of *Hydrobia ulvae* (an epifaunal deposit-feeding and grazing gastropod) were introduced to each microcosm prior to the treatment. For Exp-II an additional 20 individual juvenile *Macoma balthica* (a sediment-dwelling bivalve) were added. Organisms and sediments were collected during low tide from a tidal flat located near the laboratory in Den Helder, the Netherlands, where the experiments were performed.

17.2.2 Treatments

Although it is possible to produce natural marine snow under controlled conditions (van Eenennaam et al. 2016), we used artificial marine snow for our experiments for reasons of time efficiency and controllability. This artificial marine snow contained all ingredients considered essential in the MOSSFA process in the field situation (Daly et al. 2016): alginate-like exopolysaccharides (van Eenennaam et al. 2016), phytoplankton biomass (Hu et al. 2011; O'Connor, 2013) and mineral particles (Bianchi et al. 2011). The complete 'recipe' can be found in van Eenennaam et al. (2018) and results in a flake-like substance containing an organic fraction composed of dead phytoplankton and alginate and a mineral fraction (kaolin clay). During preparation the snow can be loaded with the required amount of oil, in this case 'surrogate Macondo oil' chemically similar to DWH oil (BP Gulf Science Data 2017).

The artificial snow was distributed over the microcosms in such a way that the sediment surface was homogenously covered. For treatments without marine snow, oiled clay (kaolin) was applied. The oil exposure levels tested were equivalent to 3 and 10 grams/m^2 (reported here as '3 g/m' and '10 g/m', respectively), reflecting the highly exposed area of 294 km^2 with oil residue concentrations of 1–43 g/m^2 as indicated by Romero et al. (2017). Both clay and snow treatments were also tested without oil. Together with the control systems without snow or clay, this resulted in five (Exp-I and II) or seven (Exp-III) treatments.

17.2.3 Analyses

Test duration ranged from 16 to 80 days. Standard parameters were temperature, salinity, dissolved oxygen concentration and pH and measured in the water column on a regular basis, combined with observations of biota behaviour and the

appearance of the sediment, e.g. the thickness of the oxidized layer. From microcosms with focus on oil biodegradation, sediment cores were collected during the trial for chemical analyses. In order to prevent resuspension of sediment, these samples were collected from the inside of a bigger core that was placed just before sampling and kept in place for the remainder of the test (see van Eenennaam et al. (2018) for a detailed description).

At termination of the test, sediment samples were collected for analyses of foraminifera and copepods/nematodes when appropriate. The remaining sediment was sieved to collect macroinvertebrates.

17.3 Experimental Results

Water characteristics were similar for all three experiments performed (salinity 33–35.5, water temperature 14.1–14.4°C, pH 8.3–8.5), and the general developments and outcomes were consistent between experiments. Below relevant test results will be described in general and illustrated with examples from individual experiments or combinations.

17.3.1 Oxygen Levels

Even though the water column was continuously aerated, the development of the dissolved oxygen concentration clearly reflected impact of the treatments (Fig. 17.1). The most pronounced is the reduction of the oxygen levels that began almost immediately after the addition of marine snow. It is obvious that the organic fraction in the snow stimulates microbial activity and accelerates oxygen consumption. This was observed in all snow treatments and not affected by oil concentration. The clay treatments show that the presence of the oil itself also had some impact on the oxygen concentration, as it can be expected as the oil components can be used as nutrients by oil-degrading bacteria. However, in the presence of marine snow, the contribution of oil is insignificant. After about a week, the peak in oxygen consumption declined in all treatments, and oxygen concentrations had reached control levels after 4 weeks.

The increased oxygen consumption of the marine snow led to oxygen depletion at the sediment surface as illustrated by the thickness of the oxygenated sediment layer (Fig. 17.2). In the control microcosms, this layer was between 2 and 4 mm thick throughout the experiment. After addition of marine snow, this layer disappeared indicating that the sediment that was covered with marine snow became completely anoxic. These observations were independent of the oil concentration. After 4 weeks signs of recovery were observed. Without oil it took about 40 days for the sediment to recover to the control situation. In both treatments with oil-contaminated snow, recovery was still not reached after 80 days indicating that the presence of oil hindered benthic recovery.

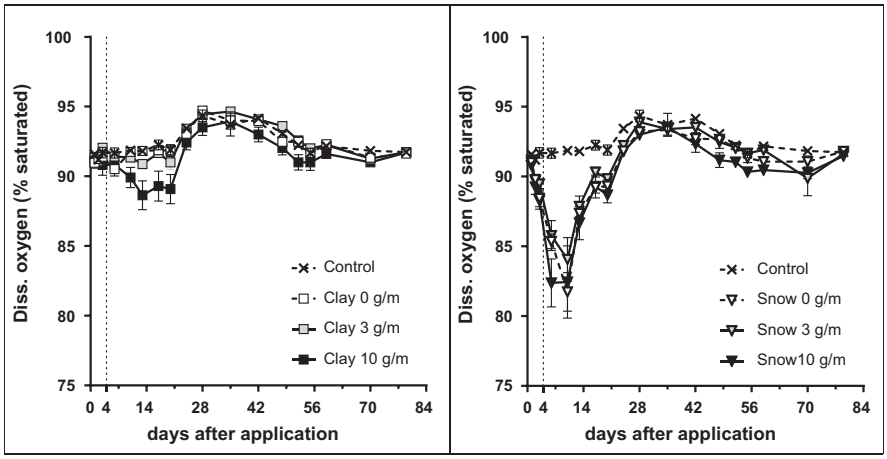

Fig. 17.1 Concentrations of dissolved oxygen over time in the water column of the test systems with clay (left) and snow (right) treatments with different oil concentrations. For reason of comparison, control treatments are shown in both figures. Snow and clay were added between day 0 and day 4 (vertical line). (Data from Experiment III van Eenennaam et al. 2019)

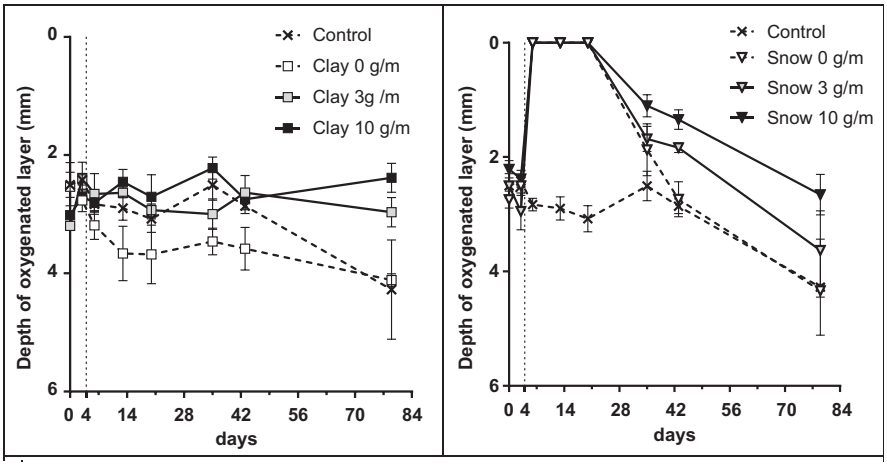

Fig. 17.2 Depth of the oxygenated sediment layer over time of the test systems with clay (left) and snow (right) treatments with different oil concentrations. For reason of comparison, control treatments are shown in both figures. Snow and clay were added between day 0 and day 4 (vertical line). Note that the Y-axis is reversed: 0 indicates the sediment surface. (Data from Experiment III van Eenennaam et al. 2019)

17.3.2 Macroinvertebrates

The benthic community is affected by the deposition of the oil-contaminated marine snow in various ways: (1) a sudden change in the structure of the top layer of the sediment, (2) the depletion of dissolved oxygen in/near the sediment surface and (3) the exposure to toxic compounds from the oil. The impact of the treatments on the macroinvertebrates depends largely on specific traits of the species.

The amphipods *C. volutator* showed their natural behaviour in the control microcosms, creating burrows in the top layer of the sediment. Deposition of marine snow affected this behaviour, especially in Exp-II when the 1-cm-thick snow layer was administered at once. The amphipods were not able to maintain their burrows and were observed escaping from the sediment swimming in the water column or resting on top of the layer of marine snow. The organisms were better capable of coping with the exposure scenario of Exp-III where the same amount of material was deposited over a 4-day period. This was also reflected by the higher numbers of individuals that were recovered from the snow 0 g/m treatments at the end of experiments (Fig. 17.3). The impact of the oil-contaminated treatments on *C. volutator* however was not changed by the exposure scenarios nor by the matrix (clay or snow).

The gastropod *H. ulvae* had the capability to escape the sediment by climbing the microcosm walls. This avoidance behaviour was observed in all snow treatments and in the oiled clay treatments. This could explain why the survival of *H. ulvae* was not affected by the presence of the oil in the clay treatments. In combination with marine snow however, the highest oiled concentration resulted in reduced survival, which could suggest that *H. ulvae* is exposed by feeding on the contaminated marine snow.

Compared to the macroinvertebrates previously mentioned, the sediment-dwelling bivalve *M. balthica* had no option to escape from the sediment cover. The deposition of a small layer of clay did not affect survival, and even when contaminated with oil, the impact was limited. However, when the same amount of oil was added associated with marine snow, it caused high mortality among the bivalves. This strong impact may have been partly due to the oxygen depletion that was caused by the presence of the marine snow.

17.3.3 Foraminifera

Exp-II indicated that the mortality of benthic foraminifera increased in all snow treatments and in the clay 10 g/m treatment (Fig. 17.3). Results indicate that the benthic foraminifera are both affected by (the oxygen depletion caused by) the presence of snow and the presence of oil, and the combination of both has a synergistic impact.

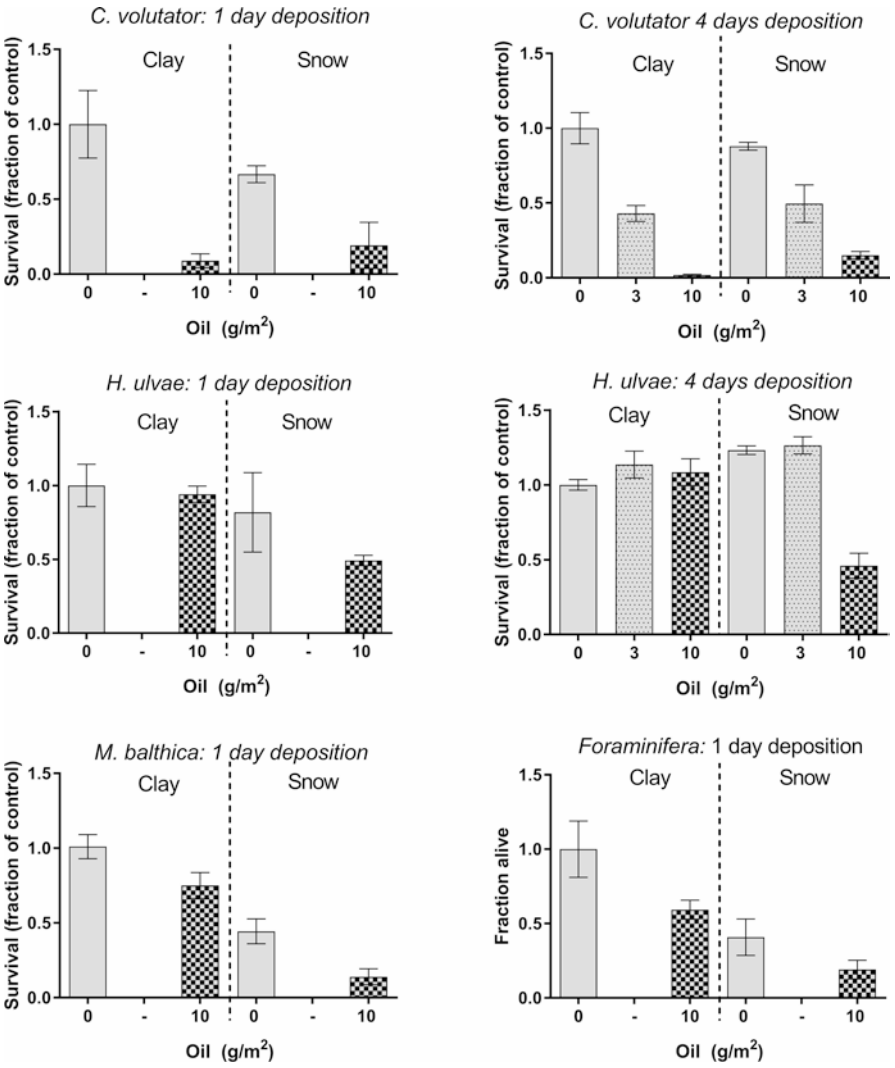

Fig. 17.3 Survival of selected organisms in test systems at the end of microcosm tests with treatments administered in 1 day ('1-day deposition') or spread over a 4-day period ('4-day deposition'). (Data from Exp-II (Van Eenennaam et al. 2018) and Exp-III (Van Eenennaam et al. 2019)

In Exp-III the response of individual benthic foraminifera species was characterized through changes in benthic foraminifera density and diversity indices. Overall, clay, snow and oil were all determined to be drivers of variability in benthic foraminifera diversity indices, but not necessarily density (Schwing et al. *in prep*). Also the effects of the treatments on the stable carbon and oxygen isotope ($\delta^{13}C$, $\delta^{18}O$) composition of benthic foraminifera shells (tests) were examined. The $\delta^{18}O$ in the tests from the snow treatments was depleted relative to the controls and enriched

relative to the clay treatments. This depletion was likely caused by differential oxygen fractionation of metabolic oxygen related to the physical properties of the snow (relatively high porosity, permeability) and clay treatments (low porosity, high tortuosity, low permeability).

17.3.4 Nematode/Copepod Ratio

The nematode/copepod ratio (N:C) is used to indicate polluted locations (Raffaelli and Mason 1981). As copepods are more sensitive to pollutants, a low N:C ratio is an indication of a contaminated situation. However, at the end of Exp-III, the nematode/copepod ratio (N:C) was lower in the presence of snow and oil (Fig. 17.4) than in the controls (Rohal et al. unpub.). The lowest ratios were observed in snow treatments of 10 g/m. The reduction in the ratio was due to the increase in the number of copepods. There was little change in the number of nematodes. The increase in the number of copepods was likely attributed to feeding conditions that were positively affected by the organic material in the snow. For practical reasons only samples were collected for this analysis during the final sampling of Exp-III. This was 76 days after the final administration of the treatment, when other endpoints show that the systems were partly recovered. It cannot be excluded that the N:C ratio also reflects (some) recovery.

17.3.5 Oil Degradation

Substantial biodegradation of oil will only occur in the presence of sufficient amounts of oxygen. Marine snow contains easily degradable carbon compounds in the form of dead organic matter that is biodegraded relatively quickly. This is

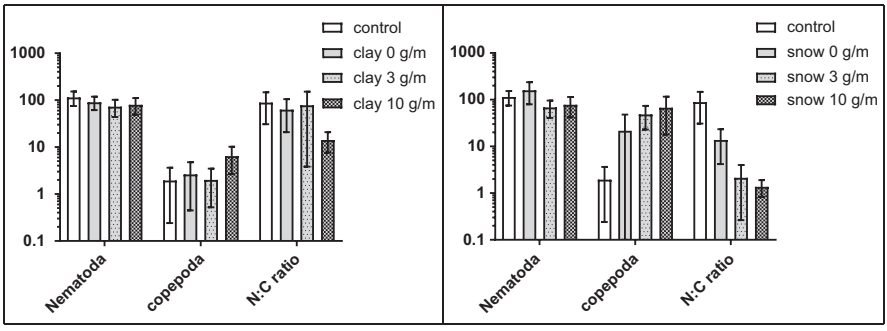

Fig. 17.4 Densities of nematodes and copepods and their ratio (N:C) in the sediment of microcosms 80 days after the start of the clay (left figure) or snow treatment (right figure) of selected organisms in test systems. (Data from Exp-III. For details see Rohal et al. unpub.)

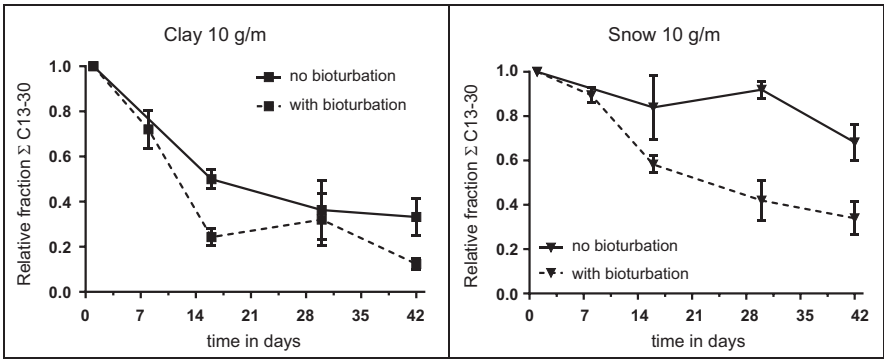

Fig. 17.5 Degradation of the oil in microcosm sediment without (no bioturbation) and with (with bioturbation) macroinvertebrates treated with clay (left figure) or marine snow (right figure) all with an initial oil content of 10 g/m^2. (Data from Exp-I, Rahsepar et al. in prep and Exp-II, van Eenennaam et al. 2018)

illustrated by the depletion of the oxygen in the sediment surface almost instantly after the deposition of marine snow. When marine snow and oil are both present, a competition for the available oxygen will occur. As oil compounds can be considered much more recalcitrant than the organic fraction of marine snow, lack of oxygen will slow down biodegradation of the oil. In the absence of bioturbating organisms in Exp-I, the presence of marine snow reduced the biodegradation of oil-derived alkanes by 40% (Fig. 17.5 'no bioturbation'). When the top layer of the sediment, including the layer of contaminated marine snow, is actively turned over by bioturbating organisms, oxygen penetration improves resulting in a faster biodegradation of oil-derived compounds (Fig. 17.5 'with bioturbation'). This positive effect of bioturbation is most pronounced in situations with marine snow present.

17.4 Conclusions on the Effect of MOSSFA on Oil Fate and Impact

The observations from the microcosm experiments show that MOSSFA enhances the potential negative impact of an oil spill on a benthic community, not only by transporting oil residues to the sediment but also by providing a surplus of readily degradable organic matter on the sediment surface. The latter results in oxygen depletion with direct impact on sessile sedentary organisms. In addition, the lack of oxygen hampers biodegradation of the oil residues, which is even stronger when bioturbation is minimized through the impact on the benthic community.

These observations are in line with findings of research that was conducted on field samples collected in the Gulf of Mexico after the DWH oil spill. Hastings et al. (2016) reported an increased intensity of anaerobic conditions in the sediment layer that lasted for years after the DWH event. Montagna et al. (2013), Baguley et al.

(2015), Washburn et al. (2017) and Schwing et al. (2015, 2017, 2018) reported reduced abundance and biodiversity of the benthic community. Brooks et al. (2015) found indications for reduced bioturbation in the sediment structure and sediment cores collected in the years after the spill that confirm the persistency of the oil residues in the sediments.

Findings from the microcosm experiments show that oil-contaminated marine snow can be used as food source by specific species, which could form the onset for further uptake of toxic compounds in the food chain.

MOSSFA thus not only enhances the impact of the oil spill on the benthic community but also its duration and perhaps even its outreach. In future oil spills, the likelihood that a MOSSFA event could develop under given local circumstances should be taken into consideration when deciding on the most effective mitigation plans.

Acknowledgements This research was made possible by a grant from the Gulf of Mexico Research Initiative/C-IMAGE I, II and III. Data are publicly available through the Gulf of Mexico Research Initiative Information & Data Cooperative (GRIIDC) at https://data.gulfresearchinitiative.org (doi: [10.7266/n7-bpgc-0b13, 10.7266/N74J0CRK, 10.7266/N7T72FJK])

References

Baguley JG, Montagna PA, Cooksey C, Hyland JL, Bang HW, Morrison C, Kamikawa A, Bennetts P, Saiyo G, Parsons E, Herdener M, Ricci M (2015) Community response of the deep-sea soft-sediment metazoan meiofauna to the Deepwater Horizon blowout and oil spill. Mar Ecol Prog Ser 528:127–140. https://doi.org/10.3354/meps11290

Bianchi TS, Cook RL, Perdue EM, Kolic PE, Green N, Zhang Y, Smith RW, Kolker AS, Ameen A, King G, Ojwang LM, Schneider CL, Normand AE, Hetland R (2011) Impacts of diverted freshwater on dissolved organic matter and microbial communities in Barataria Bay, Louisiana, U.S.A. Mar Environ Res 72:248–257. https://doi.org/10.1016/j.marenvres.2011.09.007

BP Gulf Science Data (2017) Application of dispersants to surface oil slicks by aircraft and by boat in approved areas of the Gulf of Mexico from April 22, 2010 to final application on July 19, 2010. Distributed by: Gulf of Mexico Research Initiative Information and Data Cooperative (GRIIDC), Harte Research Institute, Texas A&M University-Corpus Christi. Available from: http://data.gulfresearchinitiative.org/data/BP.x750.000:0017

Brooks GR, Larson RA, Schwing PT, Romero I, Moore C, Reichart G-J, Jilbert T, Chanton JP, Hastings DW, Overholt WA, Marks KP, Kostka JE, Holmes CW, Hollander D (2015) Sedimentation Pulse in the NE Gulf of Mexico following the 2010 DWH Blowout. PLoS One 10:e0132341. https://doi.org/10.1371/journal.pone.0132341

Daly KL, Passow U, Chanton J, Hollander D (2016) Assessing the impacts of oil-associated marine snow formation and sedimentation during and after the Deepwater Horizon oil spill. Anthropocene 13:18–33. https://doi.org/10.1016/j.ancene.2016.01.006

Dell'Amore C (2010) "Sea Snot" explosion caused by Gulf Oil Spill? Retrieved from http://news.nationalgeographic.com/news/2010/09/100916-sea-snot-gulf-bp-oil-spill-marine-snow-science-environment/

Hastings DW, Schwing PT, Brooks GR, Larson RA, Morford JL, Roeder T, Quinn KA, Bartlett T, Romero IC, Hollander DJ (2016) Changes in sediment redox conditions following the BP DWH blowout event. Deep-Sea Res Part II Top Stud Oceanogr 129:167–178. https://doi.org/10.1016/j.dsr2.2014.12.009

Hu C, Weisberg RH, Liu Y, Zheng L, Daly KL, English DC, Zhao J, Vargo GA (2011) Did the northeastern Gulf of Mexico become greener after the Deepwater Horizon oil spill? Geophys Res Lett 38:L09601. https://doi.org/10.1029/2011gl047184

Montagna PA, Baguley JG, Cooksey C, Hartwell I, Hyde LJ, Hyland JL, Kalke RD, Kracker LM, Reuscher M, Rhodes ACE (2013) Deep-Sea benthic footprint of the Deepwater Horizon Blowout. PLoS One 8(8):e70540

O'Connor B (2013) Impacts of the anomalous Mississippi River discharge and diversions on phytoplankton blooming in Northeastern Gulf of Mexico. University of South Florida. http://scholarcommons.usf.edu/etd/4736/

Passow U, Ziervogel K, Asper V, Diercks A (2012) Marine snow formation in the aftermath of the Deepwater Horizon oil spill in the Gulf of Mexico. Environ Res Lett 7:035301. https://doi.org/10.1088/1748-9326/7/3/035301

Raffaelli DG, Mason CF (1981) Pollution monitoring with meiofauna, using the ratio of nematodes to copepods. Mar Pollut Bull 12:158–163

Romero IC, Toro-Farmer G, Diercks A-R, Schwing P, Muller-Karger F, Murawski S, Hollander DJ (2017) Large-scale deposition of weathered oil in the Gulf of Mexico following a deep-water oil spill. Environ Pollut 228:179–189. https://doi.org/10.1016/j.envpol.2017.05.019

Schwing PT, Romero IC, Brooks GR (2015) A decline in deep-sea benthic foraminifera following the Deepwater Horizon event in the Northeastern Gulf of Mexico. PLOS One 10(3):e0120565. https://doi.org/10.1371/journal.pone.0120565

Schwing PT, O'Malley BJ, Romero IC (2017) Characterizing the variability of benthic foraminifera in the northeastern Gulf of Mexico following the Deepwater Horizon event (2010–2012). Environ Sci Pollut Res. https://doi.org/10.1016/j.ecolind.2017.09.044

Schwing PT, O'Malley BJ, Hollander DJ (2018) Resilience of benthic foraminifera in the Northern Gulf of Mexico Following the Deepwater Horizon Event (2011–2015). Ecol Indic 84:753–764. https://doi.org/10.1016/j.ecolind.2017.09.044

Van Eenennaam JS, Wei YZ, Grolle KCF, Foekema EM, Murk AJ (2016) Oil spill dispersants induce formation of marine snow by phytoplankton-associated bacteria. Mar Pollut Bull 104:294–302. https://doi.org/10.1016/j.marpolbul.2016.01.005

Van Eenennaam JS, Rahsepar S, Radović JR, Oldenburg TBP, Wonink J, Langenhoff AAM, Murk AJ, Foekema EM (2018) Marine snow increases the adverse effects of oil on benthic invertebrates. Mar Pollut Bull 126:339–348. https://doi.org/10.1016/j.marpolbul.2017.11.028

Van Eenennaam JS, Rohal M, Montagna PA, Radović JR, Oldenburg TBP, Romero IC, Murk AJ, Foekema EM (2019) Ecotoxicological benthic impacts of experimental oil-contaminated marine snow deposition Mar Pollut Bull 141:164–175. https://doi.org/10.1016/j.marpolbul.2019.02.025

Washburn TW, Reuscher MG, Montagna PA, Cooksey C, Hyland JL (2017) Macrobenthic community structure in the deep Gulf of Mexico one year after the Deepwater Horizon blowout. Deep-Sea Res I Oceanogr Res Pap 127(2017):21–30. https://doi.org/10.1016/j.dsr.2017.06.001

Chapter 18
Physical Processes Influencing the Sedimentation and Lateral Transport of MOSSFA in the NE Gulf of Mexico

Kendra L. Daly, Ana C. Vaz, and Claire B. Paris

Abstract Accurate predictions of the transport and fate of oil spilled in the marine environment are essential for response and mitigation efforts. The sedimentation of oil-associated marine snow (MOS) has been shown to be an important pathway by which *Deepwater Horizon* (DWH) oil was removed from the water column; thus, information is needed on the vertical and lateral dispersion of MOS. Here, we simulated the physical environment in the NE Gulf of Mexico using the Connectivity Modeling System (Paris et al., Environ Model Softw 42:47–54, 2013). Field measurements of marine snow provided initial conditions for the simulations. High Mississippi River (MR) discharge during 2010 and 2013 resulted in strong eastward flowing fronts along the shelf break to the east of the MR, and an anticyclonic eddy at the shelf break retained and aggregated particles, which acted to enhance MOS sedimentation. Forward simulations suggested that particles with high sinking rates (200 m $d^{-1)}$ reached the seafloor within <5–15 days and settled within 0–30 km of their origin, while particles with low sinking rates (30 m d^{-1}) were dispersed up to 110 km away from their origin. Suspended particles (no sedimentation rate) may be transported over 300 km from their origin.

Keywords Deepwater Horizon oil spill · Marine snow · Marine oil snow (MOS) · Ocean circulation · Fate of oil

K. L. Daly (✉)
University of South Florida, College of Marine Science, St. Petersburg, FL, USA
e-mail: kdaly@mail.usf.edu

A. C. Vaz · C. B. Paris
University of Miami, Rosentiel School of Marine and Atmospheric Science, Coral Gables, FL, USA
e-mail: avaz@rsmas.miami.edu; cparis@rsmas.miami.edu

S. A. Murawski et al. (eds.), *Scenarios and Responses to Future Deep Oil Spills*,
https://doi.org/10.1007/978-3-030-12963-7_18

18.1 Introduction

The 2010 *Deepwater Horizon* (DWH) oil spill in the northeast Gulf of Mexico (NEGOM) (Fig. 18.1) was exceptional because the oil originated from an ultra-deep well at 1500 m, the total volume of oil released was the largest on record (about 4.9 million barrels or 779 million L), a large amount of dispersants (Corexit EC9500A and EC9527A; about 2.1 million gallons or 7.9 million L) were released in deep water and at the sea surface (Kujawinski et al. 2011; McNutt et al. 2012; Lubchenco et al. 2012), and there was an unexpected and prolonged sedimentation event of oil-associated marine snow (MOS) to the seafloor (Passow 2014; Brooks et al. 2015; Daly et al. 2016). The term MOSSFA (Marine Oil Snow Sedimentation and Flocculent Accumulation) refers to the entire process related to coagulation of marine snow aggregates and oil droplets and the subsequent gravitation settling of the MOS aggregates. Overall, Romero et al. (2017) estimated that 21% ± 10% of the non-recovered oil sank to the seafloor. The largest pulse of MOS sedimentation occurred in August and September 2010, with elevated sedimentation rates likely into December 2010 (Brooks et al. 2015; Yan et al. 2016).

The formation and sedimentation of marine snow is a natural process that occurs everywhere in the world's oceans (Alldredge and Silver 1988), including the Gulf of Mexico (Walsh and Gardner 1992; Diercks and Asper 1997). Marine snow aggregates range in size from >0.5 mm to 10s of cm and consist of organic and inorganic particles, such as bacteria, phytoplankton, microzooplankton, zooplankton fecal pellets and feeding structures, detritus, and terrestrially derived lithogenic particles. The processes impacting the formation and sinking rates of MOS have been described in Passow et al. (2012), Passow (2014), and Daly et al. (2016). Field observations and experimental results indicated that large (mm to cm) mucus-rich aggregates were formed at the surface by bacterial mediation within weeks after the beginning of the oil spill (Passow 2014). Phytoplankton aggregates also incorporated oil droplets. An anomalously large phytoplankton bloom, which occurred in the vicinity of the oil spill during August 2010 over a 11,000 km^2 area (Hu et al. 2011), likely contributed to the large MOS flux observed in a sediment trap and on the seafloor (Brooks et al. 2015; Yan et al. 2016).

Field and model results have been used to investigate the sedimentation of MOS. Laboratory experiments using large marine snow aggregates (equivalent spherical diameters (ESD) ~ 2–7 mm) collected near visible oil during May 2010 had sinking velocities ranging from about 70 to 550 m d^{-1} (Passow et al. 2012). Dissanayake et al. (2018) adapted a one-dimensional model using coagulation theory to simulate the formation of MOS and predict the depth distribution of aggregates based on field data collected during the DWH oil spill in May 2010. Model results indicated that the terminal velocity of particles is initially negative, due to the presence of oil, but as ballast material is added to the aggregates, the average velocity was between 30 and 40 m d^{-1}. In addition, Dike (2015) reported average sinking velocities of 30–42 m d^{-1} for particles with an average diameter of 0.59–0.61 mm based on a field study in the NEGOM after the oil spill. Thus, larger MOS and

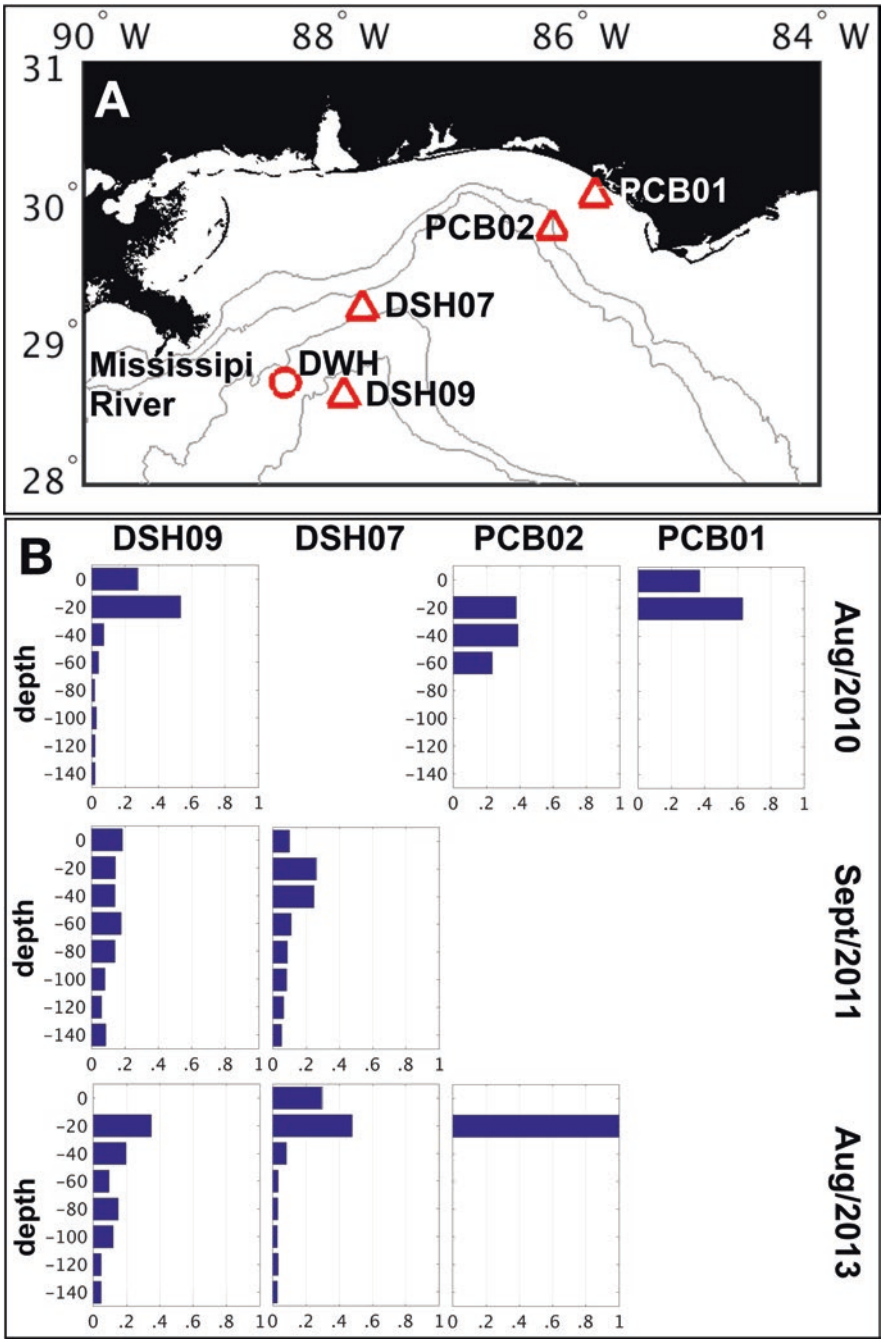

Fig. 18.1 Location of MOSSFA cruise stations (**a**), and the vertical distribution of aggregates (proportion of aggregates at each depth), used in simulations (**b**)

marine snow aggregates may sink very rapidly to the seafloor in a matter of days, whereas small particles may take about a month or longer. Given the range in sedimentation rates, little is known about the interaction of sinking particles with physical ocean processes, and, therefore, there is scant information on transport rates of marine snow or MOS.

Physical processes that may impact marine snow formation and particle transport in the NEGOM include Mississippi River discharge, which increases nutrients regionally, affects stratification over large areas, and influences the formation and strength of wind-driven coastal jets along frontal boundaries (Morey et al. 2003; Jochens and DiMarco 2008). The Loop Current and its associated anticyclonic eddies are a major energy source driving circulation in the eastern GOM. The extent of its northern penetration, however, is highly variable between years. Cyclonic and anticyclonic eddies are often present over the shelf slope in the NEGOM, which may act to aggregate particles locally. Upwelling in the De Soto Canyon on the west Florida shelf also may affect particle formation and transport in this region.

Here, our goals are to (1) estimate the vertical and lateral transport of marine snow and MOS particles based on the physical environment in the NEGOM during and after the DWH oil spill, (2) characterize the impacts of interannual environmental variability on particle fluxes, and (3) discuss major circulation features influencing the transport of marine oil snow particles. The physical environment was simulated using the Connectivity Modeling System (Paris et al. 2013) in order to investigate the region of origin of particles (backwards simulations), as well as the extent of transport of MOS from observed sites (forward simulations) to help explain the observed patterns of MOS seafloor sedimentation, as no field measurements are available on the lateral transport of MOS.

18.2 Methods

18.2.1 Field Program

We use 3 years of water column profiling data collected from four stations (DSH07, DSH09, PCB01, and PCB02) during August/September 2010, 2011, and 2013 on board the R/V *Weatherbird* (Fig. 18.1a). Stations, DSH07 and DSH09, were located over the shelf slope, south of Mobile Bay (DSH07), and to the east of the mouth of the Mississippi River at the base of the shelf slope (DSH09). These stations were 86 and 51 km east of the DWH wellhead site and at 400 and 2300 m depth, respectively. Stations PCB01 (25 m) and PCB02 (50 m) were located on the shallow west Florida shelf, adjacent to the De Soto Canyon. Measureable DWH oil was still present during August 2010 at the DSH07 and DSH09 sites.

Marine snow particles were observed using the Shadowed Image Particle Profiling Evaluation Recorder (SIPPER) camera imaging system (Remsen et al. 2004), while temperature, salinity, density, and chlorophyll fluorescence profiles

were obtained with a CTD rosette. Particle images greater than 0.1 mm equivalent spherical diameter (ESD) were extracted, automatically classified, and entered into a searchable image database using a customized software package called Plankton Image Classification and Extraction Software or PICES (Kramer 2010). Classified images were visually validated, and abundances were normalized to the volume sampled at each 1 m depth interval based on flowmeter data. A final classification was done using a dual classifier: multi-class support vector machine (SVM) and a binary feature selection SVM (Kramer et al. 2011).

18.2.2 Modeling

The Connectivity Modeling System (CMS, Paris et al. 2013) was used to simulate the advection and mixing of marine oil and marine snow particles in the Gulf of Mexico during and after the DWH oil spill. We implemented a new module in the model, which allowed us to include sedimentation rates for individual particles. At each time step, the particle vertical velocity is given by a sum of the deterministic movement from the vertical component of the velocity field, a random displacement to simulate submesoscale turbulence (Paris et al. 2013), and a prescribed sedimentation rate. Environmental variables (horizontal and vertical components of the velocity, temperature, and salinity) were obtained from the Gulf of Mexico HYCOM hindcast (0.04° degree horizontal resolution and 20 vertical layers). Nutrient fields were not included in this model. The GOM HYCOM is forced by the Navy Operational Global Atmospheric Prediction System (NOGAPS) winds and surface fluxes, by large-scale model fields at the Atlantic boundary, and by data assimilation with the Navy Coupled Ocean Data Assimilation (NCODA) system.

We conducted two separate sets of simulations: (1) backward simulations to estimate the origin of the water mass containing the aggregates observed at the cruise stations, extending for the 30 days preceding sampling, and (2) forward simulations, tracking the dispersal and sedimentation of aggregates for 30 days, to investigate how different sedimentation rates impact their distribution on the water column and sediments. For all experiments, the number of particles (maximum: 10,000) released in the vertical for each station (every 20 m from 0 to 140 m) was scaled based on SIPPER observations of the abundance and vertical distribution of marine snow (Daly GRIIDC dataset) (Fig. 18.1b). In the back-track simulations, the origin of particles from the four stations (PCB01, PCB02, DSH07, and DSH09) collected during August or September in 2010, 2011, and 2013 is shown for 10, 20, and 30 days prior to sampling.

For back-track simulations, we used the velocity fields for the first 300 m of the water column, since our preliminary results show that aggregates with no associated sedimentation rate remained above 240 m during the time period of the simulation (Fig. 18.2). The origin of particles for DSH09 is shown for August 2010, September 2011, and August 2013 for 10, 20, and 30 days prior to sampling (Fig. 18.3). The forward simulations focus on the summer of 2010, during the DWH oil spill, at

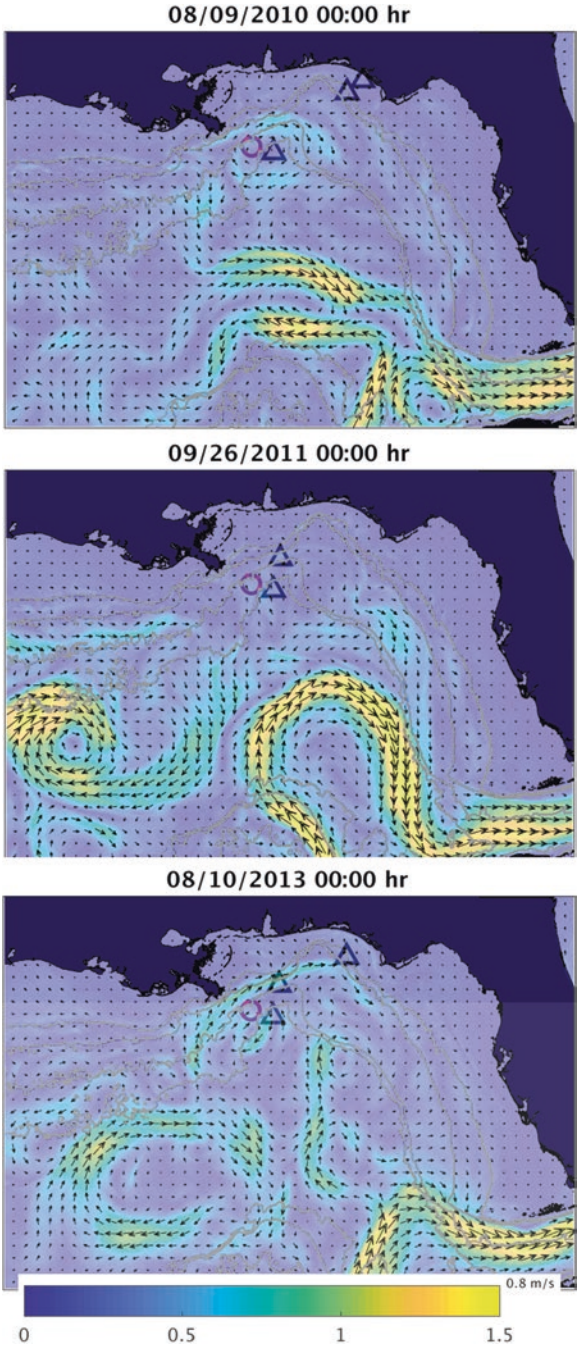

Fig. 18.2 Snapshots of the surface velocity field from the GOM HYCOM during cruise dates: August 9, 2010, September 26, 2011, and August 10, 2013. Arrows represent the direction and magnitude of the velocity field (m/s). Triangles show the location of stations sampled in each year

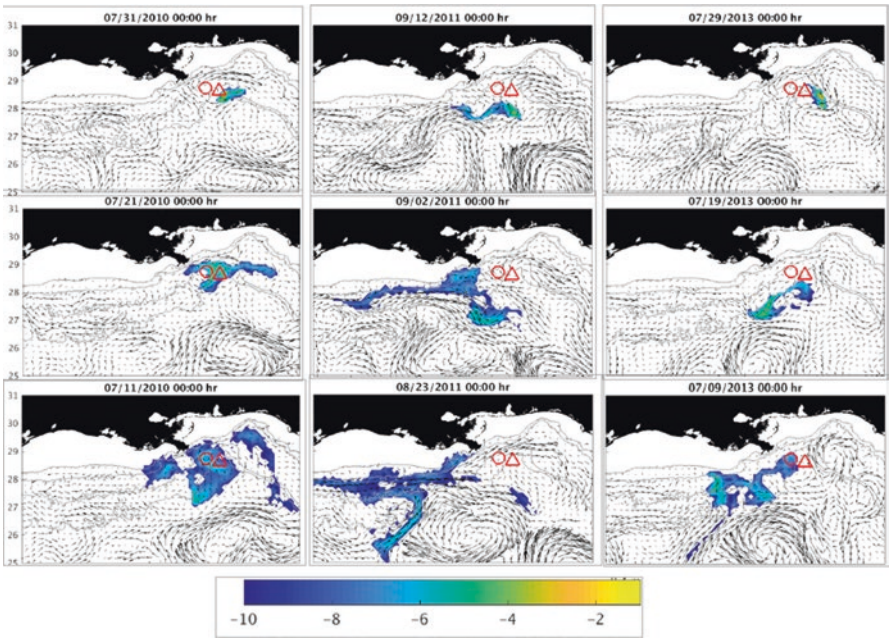

Fig. 18.3 Back-track simulations showing the origin of marine snow particles observed at DSH09 during August 2010 (left column), September 2011 (middle column), and August 2013 (right column). Probability density functions (PDFs) of particulate distributions and GOM HYCOM velocity fields at 20 m for 10, 20, and 30 days prior to cruise sampling. Upper panel shows 10-day, middle panel shows 20-day, and lower panel shows 30-day back-track simulations. PDFs are calculated using the particulate distributions binned over a 0.5° × 0.5° grid, where larger numbers represent a larger number of particles and the lowest value corresponds to a very low concentration of particles. A total of 60,000 particles were released per cruise date. The circle represents the position of the DWH wellhead, while the triangle represents the sampling station and release site (DSH09)

stations PCB01, PCB02, and DSH09 (Fig. 18.4). Here, we used the full 3D velocity field for these simulations in order to capture bottom deposition and considered three different scenarios regarding aggregate sedimentation rates: (1) neutrally buoyant, where particles sediment only when encountering the bathymetry (i.e., bathtub ring theory), (2) low sedimentation rate (30 m d^{-1}), and (3) high sedimentation rate (200 m d^{-1}) (Fig. 18.5). These MOS sinking rates bracketed those of field observations reported for MOS and marine snow in the NEGOM (Passow et al. 2012; Dike 2015). Aggregation, disaggregation, and remineralization of particles were not considered for these simulations.

To characterize the most common pathways of dispersal, we calculated the probability density function (PDF) of particle trajectories. PDFs are computed from the CMS Lagrangian output by binning particle trajectories into a 0.05° by 0.05° grid. By combining the daily PDFs of particle trajectories with the environment velocity, we create animations, which illustrate the evolution of the flow with the particle's

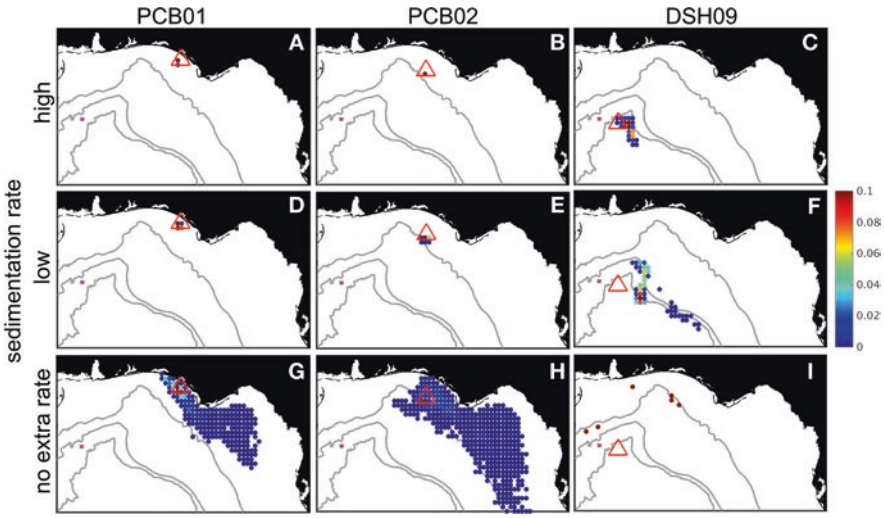

Fig. 18.4 Distribution of sedimented MOSSFA aggregates in August 2010 for stations PCB01 (left column), PCB02 (middle column), and DSH09 (right column), for different sedimentation rates: (1) high sedimentation rate (top row), (2) low sedimentation rate (middle row), and (3) neutrally buoyant particles (bottom row). A total of 60,000 particles were released per site/experiment and are forward tracked for 30 days. Triangles represent the position of the sampling station and release site. Values are given in probability of sedimented particles

distribution, allowing the identification of physical features influencing dispersal and retention of aggregates. For all simulations, we computed lateral and vertical transport rates, by calculating dispersal kernels of the particulate material for each station and depth, and then calculated the standard deviation of these rates for each scenario and year. For forward simulations, we identified the particles' fate and the concentration of particles sedimented on the GOM seafloor, in order to elucidate how the physical environment associated with sedimentation processes can together influence the lateral transport of MOSSFA and its signature on benthic depositions.

18.3 Results

Snapshots of the NEGOM velocity field at the ocean surface, based on the output of the GOM HYCOM model, are shown in Fig. 18.2. The surface velocity fields illustrate the complex oceanographic circulation features in this region. The physical circulation features that are evident in surface waters also show similar patterns at 50, 100, and 150 m depth (not shown); thus, most circulation features remain coherent through the upper 150 m of the water column. The Loop Current is visible as the yellow regions of higher current flow (>1 m/s) during all years. A Loop Current eddy is visible in 2011 and 2013, to the west of the Loop Current. During the time

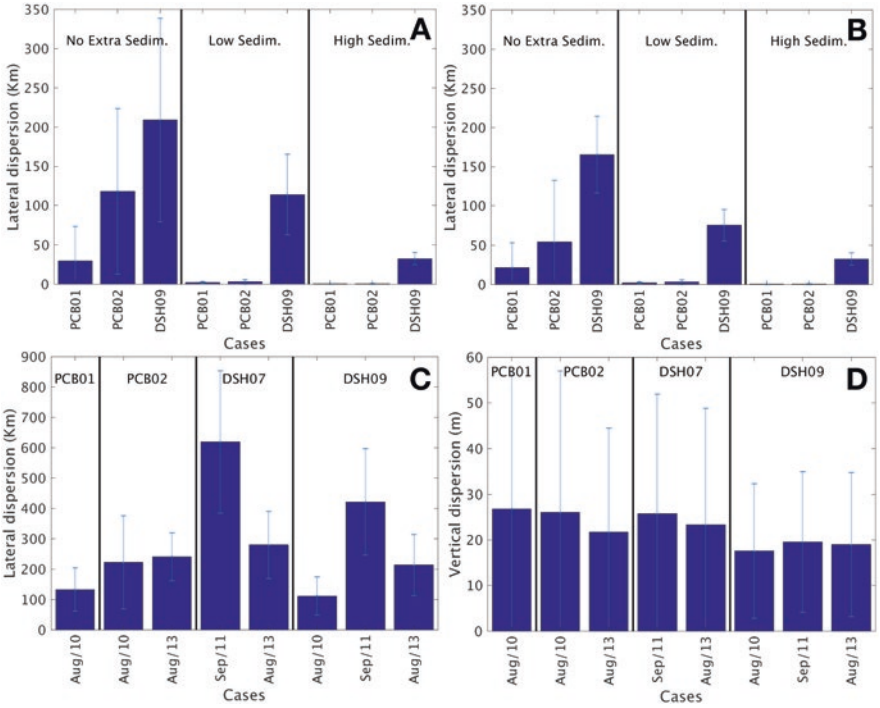

Fig. 18.5 Mean and standard deviation of lateral dispersion, in kilometers (**a**–**c**), and vertical dispersion, in meters (**d**). Forward experiments showing the mean and standard deviations of lateral dispersion rates for 2010 stations for particles having three sedimentation rates (neutrally buoyant, low, and high sedimentation): all particles (suspended and sedimenting) in each simulation (**a**) and only sedimented particles (**b**). Mean and standard deviations of lateral (**c**) and vertical (**d**) dispersion rates also are shown for each station and year for all particles

periods shown in this figure, the Loop Current did not appear to have had a major impact on the regional circulation in the NEGOM, although particles at the southern edge of the NEGOM and to the west of the Mississippi River delta were transported southward and eventually entrained into the Loop Current. During the summer of 2010, there is evidence of an eddy to the east of the mouth of the Mississippi River surrounding the DWH and DSH09 sites, which would act to retain particles in the region. In addition, 2010 had strong eastward flowing fronts along the shelf break. Model animations also indicate that upwelling occurred in this region during 2010. The year 2011 did not show strong flow patterns, while 2013 circulation was more similar to that observed in 2010, with a relatively strong current flow to the east along the shelf break and a shelf slope eddy slightly to the southwest of the DWH and DSH09 sites.

Depth profiles of normalized vertical MOS particle concentrations observed during August 2010 are shown in Fig. 18.1b. Particle concentrations were particularly high in August 2010 and 2013 at DSH07 and DSH09 in near-surface waters, coin-

cident with low salinity water indicating enhanced discharge from the Mississippi River. The back-track simulations (Fig. 18.3) suggest that vertical advection was constrained by the mixed layer depth (<100 m) and that MOS and marine snow particles were transported primarily along bathymetric lines from areas both to the east and to the west of the stations and by the smaller mesoscale eddies present in the NEGOM. MOS particles observed at DSH09 likely originated from the area covered by surface oil in the previous 10–30 days. The high Mississippi River discharge and resulting low salinity lens observed in surface waters at the DSH stations during 2010 and 2013 (Daly unpublished) did not appear to create a barrier to surface transport. On the other hand, the presence of eddies did influence particle transport, particularly the eddy observed east of the Mississippi River that occurred along the shelf break. In our 2010 and 2013 back-track and forward simulations, particles were entrained and retained in and around the core of the eddy. There also was indication of vertical and lateral transport on eddy filaments and in currents on the outer boundaries of the eddy. In general, our simulations suggest that there was a trend of higher transport in surface waters and lower transport at depth (data not shown). In 2011, the source of particles was primarily from the west, and in 2013, particles were transported from the eastern shelf slope region initially (10 day) and then from southwest of the DWH and DSH09 sites over 20- and 30-day time scales.

The forward simulations focused on the vertical and lateral transport of MOS during August 2010 (Figs. 18.4 and 18.5) in order to investigate the distance particles would be advected if they were (1) suspended particles (no sedimentation rate or neutrally buoyant), (2) had a low sinking rate (30 m d^{-1}), or (3) had a high sinking rate (200 m d^{-1}). The lateral dispersion for forward simulations is represented in Fig. 18.5a, b, which depicts the mean and standard deviation of the lateral dispersion for each station and sinking rate scenario. On panel A, the lateral dispersion of all aggregates is shown, independent of their fate, while on panel B, only the dispersion of the sedimented aggregates is calculated. A comparison of the transport of all aggregates versus only the sedimented aggregates shows that both follow the same patterns. Generally, the deeper stations present higher transport. The introduction of particles having high sinking rates decreases the extent of lateral transport at all stations. Particles with high sinking rates may reach the sea floor between <5 days (PCB01 and PCB02) and 15 days (DSH09); thus, the sedimentation time to the seafloor depended on the bottom depth of the site. Particles with high sinking rates sedimented within 30 km from their source. Particles with lower sinking rates also reached the seafloor within about 5 days at the shallow PCB01 and PCB02 sites, whereas buoyant particles often remained suspended at the end of the 30-day simulation. Marine snow particles originating from PCB01 and PCB02 and having high sinking rates were deposited at or within 35 km of their source, while slower sinking or buoyant particles sedimented during transport southward over the shallow west Florida shelf (Fig. 18.4). At the deepwater DSH09 station, MOS particles with high sinking rates primarily settled near the station, but a proportion of the aggregates were transported up to 45 km away, while particles with low sinking rates were advected up to about 110 km away. Suspended particles (no sedimentation rate) eventually may be deposited on the seafloor when its water mass comes in contact

with the seafloor along the shelf slope ("bathtub ring" hypothesis), with intermittent sedimentation on the shallow northern shelf of the NEGOM, as shown by the red dots spread along the 50 m bathymetric contour lines in Fig. 18.4I. In general, particles from DSH09 were deposited near the station, in the De Soto Canyon area, or further south following bathymetric contour lines. Buoyant particles may be transported over 300 km from their site of origin and outside the model domain. In particular, suspended particles showed increased lateral advection with distance from the shore (greater dispersion at DSH09 than PCB01). Some intermittent deposition along shallower bathymetric lines also was observed from all stations. The highest lateral dispersion rates occurred during September 2011, when current velocities were relatively low, but no eddies were present (Fig. 18.1). Vertical dispersion rates tended to be higher and more variable at shelf stations than deepwater sites.

Interannual variability in the extent of lateral dispersion was observed in the forward simulations (Fig. 18.5c). Lateral dispersion at the shallow shelf stations (PCB01, PCB02) did not show significant differences between 2010 and 2013, suggesting that shallow depth was the primary process governing deposition during high river flow years in that region. In contrast, the lateral dispersion at the shelf break (DSH07) and in deep water (DSH09) showed significant interannual variability, with the highest transport occurring during summer 2011, when the mean transport was 650 km and 450 km for DSH07 and DSH09, respectively. This may have been due to the presence of a large eddy associated with the Loop Current located to the south of the study area and strong coastal jet along the shelf slope off the west Florida shelf and Tampa Bay (Fig. 18.3, middle panel). In 2010 and 2013, the presence of smaller mesoscale eddies in the vicinity of the deeper stations likely decreased particle transport.

18.4 Discussion

Our model results indicated that riverine influence on mesoscale circulation and cross shelf transport are important processes affecting particle transport in the NEGOM. Riverine processes were particularly strong during the DWH oil spill. Emergency responders opened freshwater diversions along the lower Mississippi River with the intent to reduce the impact of oil on nearby sensitive estuaries and wetlands (Bianchi et al. 2011). Thus, river discharge rates were unusually high between June and September 2010 (Kourafalou and Androulidakis 2013) and, in combination with eastward upwelling-favorable winds, resulted in low salinity surface water overlying large regions to the east of the river delta (O'Connor et al. 2016). This led to increased buoyancy-driven currents and frontal zones, which contributed to the transport of surface oil and presumably MOS to Mississippi-Alabama-Florida shelf regions and into the vicinity of the De Soto Canyon in late July and August 2010 (Kourafalou and Androulidakis 2013; Weisberg et al. 2014). Model simulations by Schiller et al. (2011) also demonstrated that eastward currents

resulted in large freshwater transport from the Mississippi River plume toward the De Soto Canyon. Furthermore, eddies, ranging from 50 to 130 km in diameter, interacted with the plume and entrained riverine water. Overall, these observed environmental conditions were similar to the results demonstrated in our model simulations during 2010 and 2013.

The Loop Current is a major feature that impacts circulation in the NEGOM. Goni et al. (2015) noted that the Loop Current was at its northern most extent, about 150 km to the south of the oil spill, in early May 2010. It then shed an eddy (Eddy Franklin) and moved southward. By early August, Eddy Franklin reattached to the Loop Current off the southern west Florida shelf. As a result, only a small amount of oil may have been entrained into the Loop Current system. Extreme weather events also will impact particle transport. High winds from Hurricane Alex at the end of June and early July pushed surface oil onto the coastal shelves. A tropical storm occurred during August 2010, but the impacts of the short duration event would not have been evident due to the longer time period of the simulations.

Phytoplankton are a major contributor to marine snow formation. Hu et al. (2011) reported that an anonymously large phytoplankton bloom occurred in the NEGOM in summer 2010 and attributed it to the oil spill, while O'Connor et al. (2016) reported that the bloom was solely due to the enhanced river discharge and wind-driven currents moving the river plume eastward. These hypotheses are not mutually exclusive, and both may have contributed to the elevated ocean color observed by the MODIS satellite. Oil plumes from natural seeps in the NEGOM also have been shown to increase local chlorophyll concentrations (D'souza et al. 2016). Our simulation results further suggest that eddies likely entrained particles, thereby increasing the concentration of phytoplankton and marine snow in the DWH region, beyond in situ production levels. The higher eddy-entrained marine snow densities would have interacted with oil and led to enhanced MOS sedimentation rates.

The fastest sinking aggregates in the model essentially sank at their point of origin at shallow shelf sites (PCB01, PCB02) and, on average, within 25 km at the deepwater station (DSH09). Slower sinking and suspended particles may be transported up to 200 km away, and shelf particles may be dispersed 600 km. Vertical currents over the shallow shelf region would have resulted in additional deposition beyond that of sinking particles. Also deposition of neutrally buoyant particles released at DSH09 supports the hypothesis of a "bathtub ring" effect, since aggregates settled after impinging on shallow bathymetry. Romero et al. (2017) analyzed DWH seafloor hydrocarbon data and determined that DWH oil was observed up to 180 km from the drill rig in deep water and up to 517 km in coastal and shelf regions, which is consistent with our results of MOS lateral dispersion. A residual hydrocarbon deposition map showed that the largest area of oil deposition was at the DWH wellhead and to the southwest of the wellhead (Romero et al. 2017), possibly a result of the anticyclonic eddy flow in that area. ^{234}Thorium inventories from sediment cores indicated that oil and particulate matter were deposited in a sedimentation pulse over a 4–5-month period during and after the oil spill (Brooks et al. 2015).

Thus, in order to predict the origin and sedimentation of MOS for the entire DWH MOSSFA event, high-resolution sampling of MOS aggregates would be needed during the duration of the oil spill, as well as simulations spanning several months during and after the oil spill.

Two other modeling efforts have investigated the sedimentation of marine snow in the NEGOM. Dissanayake et al. (2018) used a marine snow coagulation model to simulate the formation and sinking of MOS, which included parameters for oil, mineral sediments, disaggregation processes, and particle characteristics, such as settling velocity. Sensitivity analyses indicated that particle characteristics, such as fractal dimension and stickiness, were important measurements for which there is little information. These authors also noted that coupling the model to a hydrographic model would improve understanding of the advection of settling MOS in this system. In addition, Liu et al. (2018) assessed the role of mesoscale eddies and fronts on lateral transport of sinking particles with vertical velocities of 20, 30, 50, and 100 m d^{-1}, using a Regional Ocean Modeling System (ROMS) to backtrack particle origins. The goal was to determine the catchment area for two sediment traps deployed to the southwest of the DWH site in 2012 to better understand the observed particle variability in the traps. Their results indicated that lateral transport of particles was on the order of 70–350 km, similar to our results. The authors concluded that particles reached the seafloor faster than would be expected based solely on sinking speeds, due to downwelling of particles aggregated in submesoscale convergence zones in the mixed layer, which was also observed in our results.

In conclusion, accurate predictions of the transport and fate of oil spilled in the marine environment are essential for response and mitigation efforts. Since MOS may be one significant pathway for the fate of oil, mechanistic models of MOS formation and sedimentation coupled to circulation models need to be developed for use as a tool to manage risk and improve our ability to predict the magnitude of MOSSFA events under varying environmental conditions. The model results reported here are a first step in understanding the extent of lateral transport of sedimenting MOS. Future models should combine a coagulation model that uses particle characteristics and sinking rates to simulate MOS formation, with mesoscale-resolving hydrographic models to better understand the vertical and lateral dispersion of sinking MOS.

Funding Information This research was made possible by grants from the Gulf of Mexico Research Initiative through its consortia: the Center for the Integrated Modeling and Analysis of the Gulf Ecosystems (C-IMAGE) to K.L.D and C.B.P. and Oil-Marine Snow-Mineral Aggregate Interaction and Sedimentation during the BP Oil Spill Project to K.L.D. We also acknowledge funding from the University of South Florida Division of Sponsored Research and the Florida Institute of Oceanography (FIO)/BP to K.L.D. Marine snow data are publicly available through the Gulf of Mexico Research Initiative Information and Data Cooperative (GRIIDC) at https://data.gulfresearchinitiative.org/data/doi:10.7266/N78P5XFP; doi: 10.7266/N76T0JKS.

References

Alldredge AL, Silver MW (1988) Characteristics: dynamics and significance of marine snow. Prog Oceanogr 20:41–82

Bianchi TS, Cook RL, Perdue EM, Kolic PE, Green N, Zhang Y, Smith RW, Kolker AS, Ameen A, King G, Ojwang LM, Schneider CL, Normand AE, Hetland R (2011) Impacts of diverted freshwater on dissolved organic matter and microbial communities in Barataria Bay, Louisiana, U. S. A. Mar Environ Res 72:248–257

Brooks GR, Larson RA, Schwing PT, Romero I, Moore C, Reichart G-J, Jilbert T, Chanton JP, Hastings DW, Overholt W, Marks KP, Kostka JE, Holmes CW, Hollander D (2015) Sedimentation pulse in the NE Gulf of Mexico following the 2010 DWH Blowout. PLoS One 10(7):e0132341. https://doi.org/10.1371/journal.pone.0132341

D'souza NA, Subramaniam A, Juhl AR, Hafez M, Chekalyuk A, Phan S, Yan B, MacDonald IR, Weber SC, Montoya JP (2016) Elevated surface chlorophyll associated with natural oil seeps in the Gulf of Mexico. Nat Geosci 9:215–218

Daly KL, Passow U, Chanton J, Hollander D (2016) Assessing the impacts of oil-associated marine snow formation and sedimentation during and after the Deepwater Horizon oil spill. Anthropocene 13:18–33. https://doi.org/10.1016/j.ancene.2016.01.006

Diercks A-R, Asper VL (1997) In situ settling speeds of marine snow aggregates below the mixed layer: Black Sea and Gulf of Mexico. Deep-Sea Res I 44(3):385–398

Dike CH (2015) Marine snow settling velocities at an oil spill site and a control site in the northern Gulf of Mexico. Master's Theses 107, University of Southern Mississippi, http://aquila.usm.edu/masters_theses/107

Dissanayake AL, Burd AB, Daly KL, Francis S, Passow U (2018) Numerical modeling of the interactions of oil, marine snow, and riverine sediments in the ocean. J Geophys Res Oceans 123. https://doi.org/10.1029/2018JC013790

Goni GJ, Trinanes JA, MacFadyen A, Streett D, Olascoaga MJ, MImhoff ML, Muller-Karger F, Roffer MA (2015) Variability of the Deep Water Horizon oil pill extent and its relationship to varying ocean currents and extreme weather conditions. In:Ehrhardt M (ed) Mathematical modelling and numerical simulation of oil pollution problems, The Reacting Atmosphere 2, Springer. https://doi.org/10.1007/978-3-319-16459-5_1

Hu C, Weisberg RH, Liu Y, Zheng L, Daly KL, English DC, Zhao J, Vargo GA (2011) Did the northeastern Gulf of Mexico become greener after the Deepwater Horizon oil spill? Geophys Res Lett 38:L09601. https://doi.org/10.1029/2011GL047184

Jochens AE, DiMarco SF (2008) Physical oceanographic conditions in the Deepwater Gulf of Mexico in summer 2000–2002. Deep-Sea Res II 55:2541–2554

Kourafalou VH, Androulidakis YS (2013) Influence of Mississippi River induced circulation on the Deepwater Horizon oil spill transport. J Geophys Res Oceans 118:3823–3842

Kramer K (2010) System for Identifying Plankton from the SIPPER Instrument Platform. PhD Dissertation, University of South Florida, 115 pp

Kramer K, Goldgof DB, Hall LO, Remsen A (2011) Increased classification accuracy and speedup through pair-wise feature selection for support vector machines. In Computational Intelligence and Data Mining (CIDM) IEEE Symposium, pp 318–324

Kujawinski EB, Kido Soule MC, Valentine DL, Boysen AK, Longnecker K, Redmond MC (2011) Fate of dispersants associated with the Deepwater Horizon oil spill. Environ Sci Technol 45:1298–1306

Liu G, Bracco A, Passow U (2018) The influence of mesoscale and submesoscale circulation on sinking particles in the northern Gulf of Mexico. Elementa Sci Anthrop 6:36. https://doi.org/10.1525/elementa.292

Lubchenco J, McNutt MK, Dreyfus G, Murawski SA, Kenedy DM, Anastas PT, Chu S, Hunter T (2012) Science in support of the Deepwater Horizon response. Proc Natl Acad Sci 109(50):20212–20221

McNutt MK, Chen S, Lubchenco J, Hunter T, Dreyfus G, Murawski SA, Kennedy DM (2012) Applications of science and engineering to quantify and control the Deepwater Horizon oil spill. Proc Natl Acad Sci 109(50):20222–20228

Morey SL, Schroeder WW, O'Brien JJ, Zavala-Hidalgo J (2003) The annual cycle of riverine influence in the eastern Gulf of Mexico basin. Geophys Res Lett 30(16). https://doi.org/10.1029/2003GL017348

O'Connor B, Muller-Karger FE, Nero RW, Hu C, Peebles EB (2016) The role of Mississippi River discharge in offshore phytoplankton blooming in the northeastern Gulf of Mexico during August 2010. Remote Sens Environ 173:133–144

Paris CB, Helgers J, Van Sebille E, Srinivasan A (2013) Connectivity modeling system: a probabilistic modeling tool for the multi-scale tracking of biotic and abiotic variability in the ocean. Environ Model Softw 42:47–54

Passow U (2014) Formation of rapidly-sinking, oil-associated marine snow. Deep-Sea Res II. https://doi.org/10.1016/j.dsr2.2014.10.001

Passow U, Ziervogel K, Asper V, Dierks A (2012) Marine snow formation in the aftermath of the Deepwater Horizon oil spill in the Gulf of Mexico. Environ Res Lett 7:11. https://doi.org/10.1088/1748-9326/7/3/035301

Remsen A, Hopkins TL, Samson S (2004) What you see is not what you catch: a comparison of concurrently collected net, optical plankton counter, and shadowed image particle profiling evaluation recorder data from the Northeast Gulf of Mexico. Deep-Sea Res I Oceanogr Res Pap 51(1):129–151

Romero IC, Toro-Farmer G, Diercks A-R, Schwing P, Muller-Karger F, Murawski S, Hollander DJ (2017) Large-scale deposition of weathered oil in the Gulf of Mexico following a deep-water oil spill. Environ Pollut 228:179–189

Schiller RV, Kourafalou VH, Hogan P, Walker ND (2011) The dynamics of the Mississippi River plume: impact of topography, wind and offshore forcing on the fate of plume waters. J Geophys Res 116:C06029. https://doi.org/10.1029/2010JC006883

Walsh ID, Gardner WD (1992) A comparison of aggregate profiles with sediment trap fluxes. Deep-Sea Res 19(11–12):1817–1834

Weisberg RH, Zheng L, Liu Y, Murawski S, Hu C, Paul J (2014) Did Deepwater Horizon hydrocarbons transit to the West Florida continental shelf? Deep-Sea Res II 129:259–272

Yan B, Passow U, Chanton J, Nöthig E-M, Asper V, Sweet J, Pitiranggon M, Diercks A, Pak D (2016) Sustained deposition of contaminants from the Deepwater Horizon oil spill. PNAS:E3332–E3340. https://doi.org/10.1073/pnas.1513156113

Chapter 19
Simulating Deep Oil Spills Beyond the Gulf of Mexico

Claire B. Paris, Ana C. Vaz, Igal Berenshtein, Natalie Perlin, Robin Faillettaz, Zachary M. Aman, and Steven A. Murawski

Abstract As deep-sea oil exploitation increases worldwide, the probability of another *Deepwater Horizon* (DWH) blowout also increases. The DWH disaster directly impacted the coastal communities of the Gulf of Mexico (GoM) with 11 deaths and the release of 172.2 million gallons of gas-saturated oil, covering over 1000 miles of coastline and contaminating an estimated 300,000 million cubic meters of GoM water. In the aftermath of the DWH blowout, the question of what a similar event would look like outside the GoM is of fundamental importance. Anticipating the extent and potential environmental impact of major spills in other locations becomes important for effective oil preparedness and response, including coordination of emergency response between neighboring countries. Avoiding deep-sea drilling in environmentally sensitive and some of the world's most biodiverse and productive fishing areas is also of upmost importance. The west coasts of Cuba and West Africa may be two of the most environmentally sensitive areas across the North Atlantic, yet exploitation of deepwater oil reservoirs has already started or is imminent. Northwest Cuba holds abundant coral reefs characterized by uniquely high diversity and fish biomass, and the region is also home of multi-species spawning aggregations, crucial for the persistence of fish populations. In addition, this area contains Cuba's most important lobster fishery grounds. A major oil spill occurring in NW Cuba is thus likely to have deleterious impacts on the biodiversity and seafood resources of the region. The West African

C. B. Paris (✉) · A. C. Vaz · I. Berenshtein · N. Perlin · R. Faillettaz
University of Miami, Rosenstiel School of Marine and Atmospheric Science, Miami, FL, USA
e-mail: cparis@rsmas.miami.edu; avaz@rsmas.miami.edu; iberenshtein@rsmas.miami.edu; nperlin@rsmas.miami.edu; robin.faillettaz@rsmas.miami.edu

Z. M. Aman
The University of Western Australia, Fluid Science and Resources Division, Department of Chemical Engineering, Perth, WA, Australia
e-mail: zachary.aman@uwa.edu.au

S. A. Murawski
University of South Florida, College of Marine Science, St. Petersburg, FL, USA
e-mail: smurawski@usf.edu

S. A. Murawski et al. (eds.), *Scenarios and Responses to Future Deep Oil Spills*,
https://doi.org/10.1007/978-3-030-12963-7_19

coastal upwelling system is an extremely productive area, harboring one of the world's main "hot spots" in terms of fish abundance and biomass. This important system is most likely also a crucial mechanism regulating the climate, and an oil spill in this area could thus have severe local and global impacts.

Here we simulate a DWH-like spill in two deepwater prospect blocks offshore Cuba and Senegal, West Africa, and evaluate their extent and impact against the DHW oil spill hindcast as a benchmark. These two hypothetical spills are not locally contained and are both severe, yet we find distinctive differences between their impact on the coastline, the seafloor, and the water column. Overall, the Senegal deep blowout scenario seems to be the most impactful with the highest sedimented and beached oil mass; the Cuba deep blowout scenario is the second worst, with the highest impact in terms of oiled area and volume. In this context, our study demonstrates that if another DWH occurred in a different region, poorly regulated emergency responses for international waters at the time of the spill could result in more detrimental impacts on marine ecosystems and coastal communities compared to the DWH. Here, we bring forward, quantify, and visualize the possible outcomes of another mega-spill similar to the DWH in two strategic locations to increase the awareness of decision-makers and the public to such implications. Since oil exploration is not expected to decrease in the near future, we urge governments to focus on establishing international agreements protecting sensitive marine resources and areas.

Keywords World Ocean · Ultra-deep exploration · Deep-sea blowout · Oil spill modeling · Deep-sea blowout · Cuba · Senegal · West Africa · Cayar Canyon · Pelagic fisheries · Upwelling · Productivity · Marine biodiversity · Spawning aggregations · Ecosystem impact

19.1 Introduction

As disastrous as the *Deepwater Horizon* (DWH) spill was, it was fortunately located in the semi-enclosed Gulf of Mexico, constraining the overall extent of the spill. The strong jet of the Loop Current entering the Gulf through the Yucatan Straits and exiting into the Florida Straits could have contributed to significant transport of oil toward the Florida Keys and the Southeastern United States (e.g., Fall DWH blowout scenario, Perlin et al. 2020). But the timing of the blowout coincided with the separation of the Loop Current Eddy Franklin that formed just south of the DWH location. This helped contain most of the Macondo oil within the GoM (Paris et al. 2012).

In the aftermath of the DWH blowout, a loss of well control at offshore platforms remains as the largest single risk factor to cause an oil spill. The question of what a similar event would look like outside the Gulf of Mexico (GoM) is highly relevant. Anticipating the extent and potential environmental impact of major spills in other locations becomes important for effective oil preparedness and response, including

coordination of emergency response teams of neighboring countries (e.g., deployment of coast guards, state-of-the-art forecast modeling, and reliable capping stacks at close proximity to the drilling sites). Avoiding deep-sea drilling in environmentally sensitive and the world's most biodiverse and productive fishing areas is also of upmost importance.

The west coasts of Cuba and West Africa, where exploitation of deepwater oil reservoirs has already started or is planned, may be two of the most environmentally sensitive areas across the North Atlantic. Senegal's ultra-deep offshore block exploration drilling is expected to start imminently. Cuba represents the under-explored southeast (SE) margin of the GoM petroleum mega province with estimate reserves up to 4.6 billion barrels in the north Cuba Basin (US Geological Survey 2005). The development of deepwater petroleum reserves so close to the United States is of special concern (Nerurkar and Sullivan 2011). On the other side of the Atlantic, Senegal's ultra-deep offshore block drilling will also start imminently. The "Cayar Profond" deep block, located in the new world-class gas and oil province discovered offshore in Senegal, is also located in one of the largest and most productive West African fishing grounds, extending from Senegal to Mauritania. Operational exploitation of ultra-deep reserves of Cayar Profound could be a concern for the entire region; there is no published review, however, on the impact of such activities on this iconic ecosystem.

19.1.1 Western Cuba

Physical attributes – Cuba is the largest Caribbean island, situated just below the Tropic of Cancer (19° 9′N-23° 10′N, 74° 7′W-84° 57′W) between the Caribbean Sea and the North Atlantic, and has hundreds of smaller islands, keys, and islets. The main island's coastline is ca. 5746 km long, and most of the continental shelf is surrounded by extensive reefs that have been exposed to relatively few anthropogenic effects. Exceptions are in the north central (NC) and southeast (SE) areas which were impacted by tourism-driven coastal development and agricultural chemical runoff, especially effluents from the sugar industry (Claro et al. 2001). The western point of Cuba is more pristine due to its relative isolation and to the confluence of various currents (Paris et al. 2005). This makes it a critically sensitive area. The bathymetry of this region is very steep with a near vertical (70–90 degree) shelf drop-off down to 150 m and a second abrupt incline (60–70 degree) to ca. 600 m. The westerly Caribbean Current impinges on the island, forcing mean westerly flows both on the south and north coasts (Claro et al. 2001). These coastal flows converge at the western end of Cuba and create a complex and variable current system: a mesoscale anticyclonic eddy bounded by the Cayman ridge sheds and smaller cyclonic and anticyclonic eddies on the edge of the shallow Gulf of Batabanó, southwest (SW) Cuba, while sub-mesoscale anticyclones moving eastward along the northwest (NW) Cuban coast form when the Florida Current meanders northward (Kourafalou et al. 2017). Importantly, this eddy activity is influenced by

wind-induced upwelling events and is connected to the evolution of the Loop Current and cyclonic eddies on the northern Florida Current front (Kourafalou et al. 2017). A major oil spill occurring on the NW Cuban deep slope is thus likely to have various pathways, including being upwelled off the Cuban coast and reaching Florida, swept across the straits by dominant southeasterly winds, and/or entrained in the Cuban Countercurrent and retained SW Cuba in the Cayman Sea for months before reentering the Florida Straits.

Biological attributes The Gulfs of Guanahacabibes (a biosphere reserve) and of Batabanó in NW and SW Cuban shelves, respectively, are two of the four broader shelf sections of the island. They hold abundant coral reef crests and patches with approximately 41 and 55 species of stony and gorgonian corals, 160 sponge species, 526 species of macro algae, and large areas of seagrass beds and mangroves (Claro et al. 2001). There, coral reef-fish diversity and biomass surpass that of the largest Cuban NC and SE archipelagos and of other Caribbean islands, from the Lesser Antilles to the Florida Keys (Claro and Parenti 2001). Western Cuba is also home of multi-species spawning aggregations (eight on the SW shelf bordering the Gulf of Batabanó, two in the NW) for five species of snapper and three species of grouper (Claro and Lindeman 2003; Paris et al. 2005). Such fish spawning aggregations (FSAs) are crucial for the persistence of fish populations and have a disproportionate conservation value, much comparable to high biodiversity coral reefs (Erisman et al. 2017) and warrant protection (Lindeman et al. 2018). In addition to holding important demersal and small pelagic fishery resources, the Gulf of Batabanó is Cuba's major lobster fishery ground. A major oil spill occurring in NW Cuba could thus have enormous impacts on the biodiversity and valuable fishery resources of the region.

19.1.2 Cayar Canyon, Senegal, West Africa

Physical attributes Senegal is the westernmost country of Africa with a very long coastline to the Atlantic with hundreds of fishing villages; in fact, the name Senegal, or "Sunou Gaal" in Wolof, translates to "Our Pirogue." Senegal also shares maritime boarders with the Cape Verde islands. With a Sahelian climate, fishery is a major economic sector, together with top peanut production after the United States. The continental shelf is 80 km wide in Casamance at the southern border and narrows toward the northern part of the country, with the narrowest portion (1 km) at Cayar submarine canyon, just north of the Cap Vert Peninsula. The submarine canyon itself is ca. 9 km wide, 3300 m at its deepest, and extends over 200 km in an elongate horseshoe-shaped pattern north of Cayar and Little Cayar Seamounts (Jacobi and Hayes 1982; Diop 1990). Downslope turbidity currents from the Cayar Canyon extends from the shelf break to southeast of the Cape Verde Islands, *ca.* 570 km west (Jacobi and Hayes 1982).

The offshore oceanographic environment is characterized by the prevailing southward Canary Current further connected to the North Atlantic Equatorial Current. Cold surface waters with temperature from 4 to 14 °C reveal the presence of a very strong upwelling in the region, especially from February to May when the trade winds pick up strength (5–7 m/s) (Barry-Gerard 1990). Due to planetary rotation and the easterly winds in tropical and subtropical areas, strong upwelling occurs off the western coast of continents. Compared to the "well-studied" Peruvian upwelling system, little is known about the Western African upwelling and its trophic webs. The West African upwelling and primary production dynamic are unique since dust from the Sahel may play an important role through iron fertilization. Upwelling is somewhat weaker during the first part of the cold season, from November to January. Two distinct upwelling zones are separated by a convergence zone at the Cayar submarine canyon. The warm season (June to August) is characterized by the arrival on the shelf of warmer and saltier waters from the Equatorial Counter Current. An unstable warm season with variable currents follows until the arrival of the trade wind setting up the cold, upwelling season again. Upwellings are the most productive systems in the oceans where the food webs are accelerated and produce seafood for healthy consumption (Bakun 1990). Large diatoms, profiting from upwelled nutrient rich cold waters, flourish in the upper ocean and are directly grazed by anchovies and sardines. These small pelagic organisms are essential food, not only for tunas and other large pelagic fish but also for their tremendous commercial value since they contain omega 3, a vitamin for the human brain. In our study region, maximum upwelling intensity occurs from March to April. Strong upwelling currents could interfere with the formation of a deep intrusion due to the lack of ambient stratification (Adams and Sococlofsky 2005) and entrain microdroplets to the sea surface. In the process, PAH contamination of the entire water column would presumably suppress primary production. A mega oil spill like the DWH occurring during the upwelling season could therefore be disastrous.

Biological attributes The Cayar Canyon plays an important ecological role and is one of the most abundant fishing zones of the country for highly migratory pelagic, small pelagic, and grouper species. In addition, the historically largest fishing village of the country, the Cayar Profond (*Fosse de Cayar*), has been designated as a marine protected area (MPA). Recent fish surveys revealed that the MPA is populated with large fish over 80 cm in fork length and 25–50 cm on average (Diankha 2018). Higher fish biodiversity occurs during the transition from cold to warm waters, while highest fish abundance occurs during the upwelling season when subsurface waters are cold and enriched with nutrients (Diankha et al. 2018). However, these fish surveys showed a negative trend in the total number of species observed between 2015 (223 species) and 2017 (160 species). It is noteworthy that this survey started in 2015, shortly before the first phase of a multi-well exploration drilling program period (Kosmos Energy 2016).

The complex formed by the Cayar submarine canyon and the Cape Verde Peninsula is known as a topographical and hydrological barrier to fish migration along the Senegalese coast. The canyon and peninsula complex forms a convergence

zone for small pelagic like sardines, resulting in crucial feeding and reproductive grounds for large pelagic such as sailfish (Limouzy and Cayre 1981). The entire coastline between Mauritania and Senegal represents important nursery grounds for many other pelagic and demersal species, including the white grouper (*Epinephelus aeneus*, or Thiof fish for the traditional thieboudienne meal) that can reach over 120 cm in fork length and migrate to form spawning aggregations in May–June (Diop 1990).

Here, we take a numerical approach to explore the extent and impact of a "what-if" deep-sea oil spill scenario in NW Cuba and Senegal. We simulate a DWH-like spill in two deepwater prospect well locations (Table 19.1) and evaluate their potential extent and impact to the shorelines, the seafloor, and the water column against the DHW oil spill hindcast as a benchmark (Berenshtein et al. 2020). The quantitative analyses include the relative distribution of the total petroleum hydrocarbons (TPH) suspended in the subsea and the upper ocean, the physical factors (i.e., hydrodynamical and geomorphological) that determine the volume of oil in the water column, and distribution on the seafloor and the coastline from such spills. The Cuban prospect well belongs to the western offshore blocks of the North Cuba Fold and thrust belt structures (US Geological Survey 2005). The Senegalese "Cayar Profond" deep block is located in the grand Cayar Canyon that incises the shelf at fisherman village of the same name, historically representing the most productive West African fishing grounds (Ruffan et al. 2018). We discuss the physical and biological factors that determine the volume and distribution of oil from such spills and their unprecedented potential impact on local and regional ecosystem diversity and fisheries.

Table 19.1 Summary of deep-sea blowout (DB) oil spill numerical experiments. All the scenarios have the following characteristics: 3000 particles are released bi-hourly; horizontal post-processing grid is 0.02 degree; surface evaporation half-life is 250 h; horizontal diffusivity is 10 m^2/s

Model simulation	Spill location	Initial conditions
DB_DWH	*Deepwater horizon* 28.736 N, 88.365 W Macondo depth = 1522 m	Start/end: April 20–July 15, 2010 Spill duration: 87 days; 167-day oil tracking Flow rate Q = 50,000–70,000 barrels/day (McNutt 2012) 1 < DSD < 500 μm, d_{50} = 109 μm (Perlin et al. 2020)
DB_Cuba	NW Cuba 22.08 N, 85.1 W Block N54 depth = 1500 m	Start/end: April 20–July 15, 2010 Spill duration: 87 days; 167-day oil tracking Flow rate Q = 50,000–70,000 barrels/day (McNutt 2012) 1 < DSD < 500 μm, d_{50} = 109 μm (Perlin et al. 2020)
DB_Senegal	Senegal 15.55 N, 17.6 W Cayar Profond depth = 1500 m	Start/end: April 20–July 15, 2010 Spill duration: 87 days; 167-day oil tracking Flow rate Q = 50,000–70,000 barrels/d (McNutt 2012) 1 < DSD < 500 μm, d_{50} = 109 μm (Perlin et al. 2020)

19.2 Methods

19.2.1 Oil Model Setup, Numerical Experiments, and Output Analyses

We use the DWH deep-sea blowout (*DB_DWH*) as an example to initialize a hydrodynamic model coupled to the proprietary oil application of the open-source Lagrangian application of the Connectivity Modeling System (CMS, Paris et al. 2013). The NW Cuba (*DB_Cuba*) and Senegal (*DB_Senegal*) simulations assume a similar blowout in timing (April 20, 2010), duration (87 days), oil type (light crude oil), oil pseudo-fractions and biodegradation, sedimentation, well depth (ca. 1500 m) and trap height (300 m), and flow rate (total oil mass) to the *DB_DWH*. The main differences are, therefore, the geomorphology and oceanography of the regions across the Atlantic, including winds, upwelling and subduction currents, and temperature and salinity gradients that drive the buoyancy and rising velocity of the oil droplets (Paris et al. 2012). Three thousand virtual oil droplets are released in the model on April 20, 2010, at the trap height every 2 hours for 87 days until July 15, 2010, using the same release scheme as in the "control" *DB_DWH* run (Perlin et al. 2020). The oil droplets are tracked for another 80 days, until September 30, 2010. The hypothetical wellhead locations and initial conditions are reported in Table 19.1, and details of the parameterization can be found in Perlin et al. (2020).

The CMS model trajectory output and oil concentrations are computed for grid boxes of 0.02° in the horizontal direction and 20 m in the vertical direction, except for the top 20 m that is split into two layers of 0–1 m and 1–20 m. Model output and post-processing algorithm are outlined in Perlin et al. (2020). Here, we chose to use various visualization techniques to qualitatively compare the output of the two new scenarios and understand the processes driving the oil transport and patterns of sedimentation. In addition, to quantitatively compare the different scenarios' outputs, we employed the method developed by Berenshtein et al. (2020).

19.2.2 Ocean Circulation Models

Northwest Cuba hydrodynamics For the Cuban oil spill simulations, we use two nested oceanographic fields within the Connectivity Modeling System Lagrangian framework (CMS, Paris et al. 2013): (i) the large-scale currents from the Global (GLBv.8) HYbrid Coordinate Ocean Model (HYCOM; Chassignet et al. 2003) with a 1/12°(ca. 8 km) horizontal grid and (ii) the regional HYCOM Gulf of Mexico hindcast GoMvI0.04 expt_31.0 on a 1/25° (ca. 4 km) horizontal grid. This hydrodynamic model setup provides diagnostic output from 20 vertical levels for GoM-HYCOM and 40 vertical levels for GlB-HYCOM, spanning from the surface down to 5500 m in a domain ranging from 100°W to 75°W and

from 15°N to 35°N. The GoM-HYCOM is forced by the Navy Operational Global Atmospheric Prediction System (NOGAPS) winds and surface fluxes, by large-scale HYCOM model fields at the Atlantic boundary and by data assimilation with the Navy Coupled Ocean Data Assimilation (NCODA) system, which assimilates available satellite altimeter observations, satellite and in situ sea surface temperature (SST) observations, as well as available in situ temperature and salinity profiles from moored buoys, XBTs, and Argo floats (Cummings 2005; Cummings and Smedstad 2013). The GBL-HYCOM also employs data assimilation using NCODA. GBL- and GoM-HYCOM oceanographic variables used as input for oil spill simulations include the horizontal and vertical velocity components and the seawater temperature and salinity fields.

West Africa hydrodynamics For the Senegalese oil spill simulations, we also use two nested oceanographic fields nested within the CMS Lagrangian framework: (i) the large-scale currents from GLB-HYCOM, as described above but with a domain restricted from 37°W to 12°W and from 9°N to 22.3°N and (ii) a high Regional Ocean Modeling System (ROMS) v3.7 hindcast model (Haidvogel et al. 2008). The ROMSv3.7 terrain-following vertical coordinate system results in accurate modeling of areas of variable bathymetry, which is ideal to resolve the coastal area for the NW Africa regional domain (27.47°W–15.92°W, 12.42°N–22.22°N) with a horizontal grid resolution of ca. 6 km and 30 vertical layers. Bathymetry to setup the model domains is derived in house by processing and combining data from the General Bathymetric Charts of the Oceans (GEBCO) global database (Weatherall et al. 2015) and Electronic Nautical Charts (ENCs). The atmospheric forcing dataset used to run the model consists of hourly mean sea level pressure, winds, and atmospheric fluxes extracted from the Climate Forecast System Reanalysis CFSR/CFSv2 (Saha et al. 2010). Freshwater contribution of two major river systems, the Gambia and Senegal Rivers, was included in the hindcast modeling. River discharges are assumed to be constant throughout each of the monthly runs and equal to their reported monthly climatological averages (peaks from August to November) obtained from the Research Data Archive (RDA) at the National Center for Atmospheric Research (NCAR) (Global Runoff Data Center et al. 2001). ROMS oceanographic fields were provided by MetOcean Solutions (2018) and were formerly calibrated with data from current meters. We use the horizontal component of the velocity, temperature, and salinity from April to December of 2010. The vertical component of the velocity was calculated offline, based on the continuity equation (Paris et al. 2012). To account for oil drift induced by the wind and wind-generated features (waves, Langmuir circulation), we incorporate a wind component in the surface velocities, as described in Le Henaff et al. (2012) and based on the global Blended Sea Winds dataset with a 0.25° resolution (Zhang et al. 2006; Peng et al. 2013; available at http://www.ncdc.noaa.gov/oa/rsad/blendedseawinds.html).

19.3 Results

19.3.1 Northwest Cuba Blowout Scenario

Simulation of the cumulative oil concentration across time and depth (Fig. 19.1a) for an 87-day DWH-like blowout in SW Cuba results in oil transported in all possible directions using three main pathways (Fig. 19.1b): (1) the oil enters the GoM via the Loop Current shedding eddies to the northern and western GoM, (2) the Florida Strait Current brings oil to the SE United States and farther out of the study domain into the North Atlantic, and (3) the Antilles Current spin-off gyres redistribute the oil into the Caribbean Sea that accumulates SW Cuba. The Loop Current position was at this time coinciding with the separation of the Loop Current Eddy Franklin, helping contain most of the Macondo oil within the GoM (Paris et al. 2012). Surprisingly, there is more oil spreading from Cuba into all the regions of the GoM than from the DWH location; only Campeche Bay in the SW Gulf is spared (Fig. 19.1b). This is unexpected since the Gulf presents well-defined dynamical oceanographic provinces with long residence times (see Paris et al. 2020). We note that the drifter data used to define the oceanographic provinces have no drifters released at the *DOB_Cuba* location, and

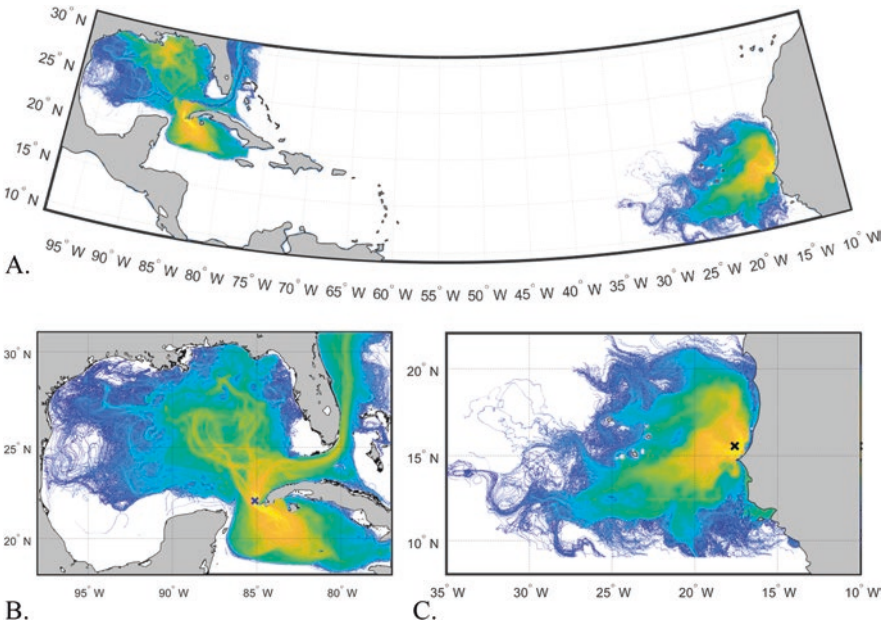

Fig. 19.1 Cumulative oil concentrations across time and depth for (**a**) the combined *Deepwater Horizon* (*DB_DWH*), DWH-like Cuban blowout (*DB_Cuba*), and DWH-like Senegalese blowout (*DB_Senegal*) scenarios, (**b**) *DB_Cuba*, and (**c**) *DB_Senegal*. The locations of the hypothetical oil spill sites are marked with the black x marks; refer to Table 19.1 for the simulation labeling conventions

only few drifter trajectories pass nearby the blowout site (see "spaghetti" plot, Miron et al. 2017). Indeed, Cuba is beyond the GoM, and the results of a blowout there are different from any possible oil spill within the GoM.

The vertical structure of horizontally cumulative suspended oil mass tracked over a 90-day period for the *DB_WH* control scenario (Fig. 19.2a) indicates that the highest

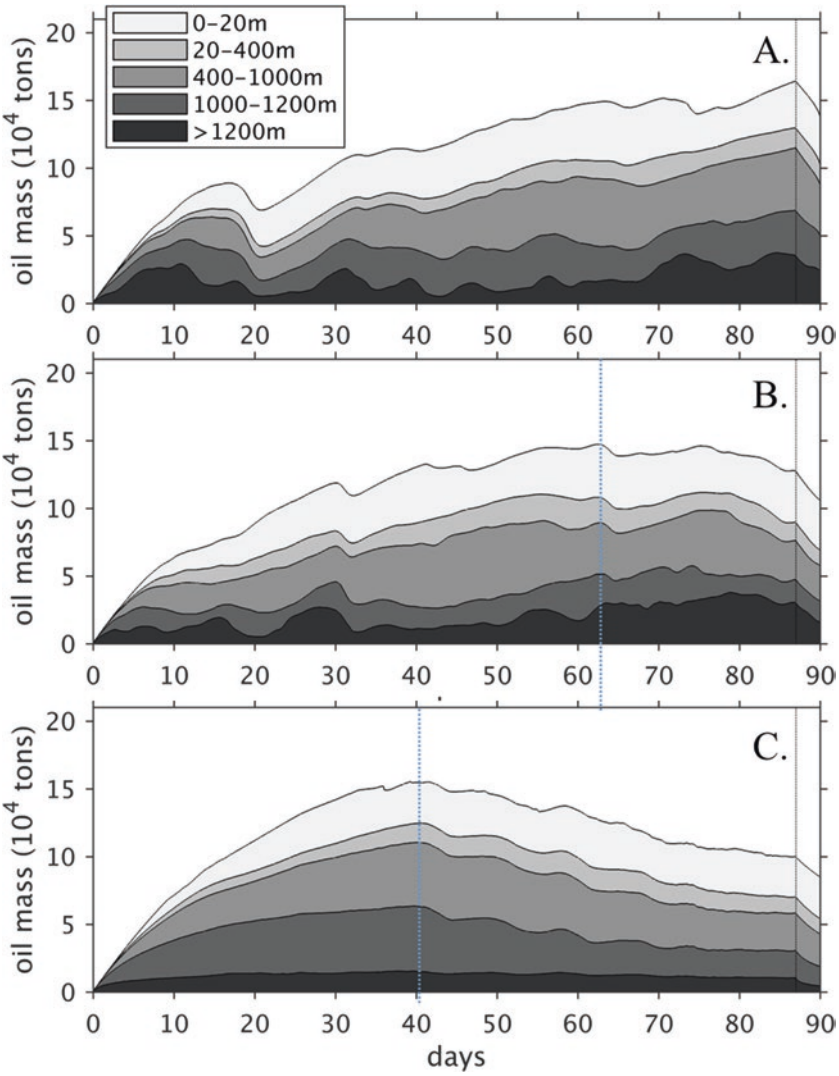

Fig. 19.2 Area-cumulative oil mass suspended in five vertical layers for the (**a**) Deepwater Horizon case scenario *DB_DWH*, (**b**) DWH-like Cuban blowout (*DB_Cuba*), and (**c**) DWH-like Senegalese blowout (*DB_Senegal*) simulations, for every 2-h output time intervals, over the duration of the run (days in the x-axis). Oil mass in layers are stacked, so the sum of all the layers shows the total oil mass in a water column. The dotted black lines indicate the end of the simulated spill at day 87; blue dotted lines indicate maximum oil mass, after which it stabilizes (*DB_Cuba*) or decreases (*DB_Senegal*) despite live oil still spewing for the simulated deep-sea blowout

oil content is found primarily in the subsea below 400 m and secondary in the upper 0–20 m layer. These results corroborate BP Gulf Science Data observations (Paris et al. 2018). This pattern is also true for *DB_Cuba*. Yet the temporal dynamic is different: the maximum oil mass occurs at day 63, before the wellhead is capped (Fig. 19.2a). Because there is lower sedimented and beached oil for *DB_Cuba* (Fig. 19.3a, b) than from *DB_DWH* or *DB_Senegal*, it is logical to assume the missing oil left the north boundary of the study domain into the North Atlantic (Fig. 19.1b). Importantly, a large fraction of the oil remains suspended in the water column, contaminating nearly the entire GoM and the Cayman basin (Fig. 19.1b), which is the most important pelagic nursery zone in the Caribbean for spiny lobster larvae (Kough et al. 2013).

The modeled 3-D evolution of *DB_Cuba* reveals a very dynamic spill with decoupled motion of the subsea plume and surface slick transport (Fig. 19.4a). The higher oil concentrations (black, Fig. 19.4a) reveal the well location between

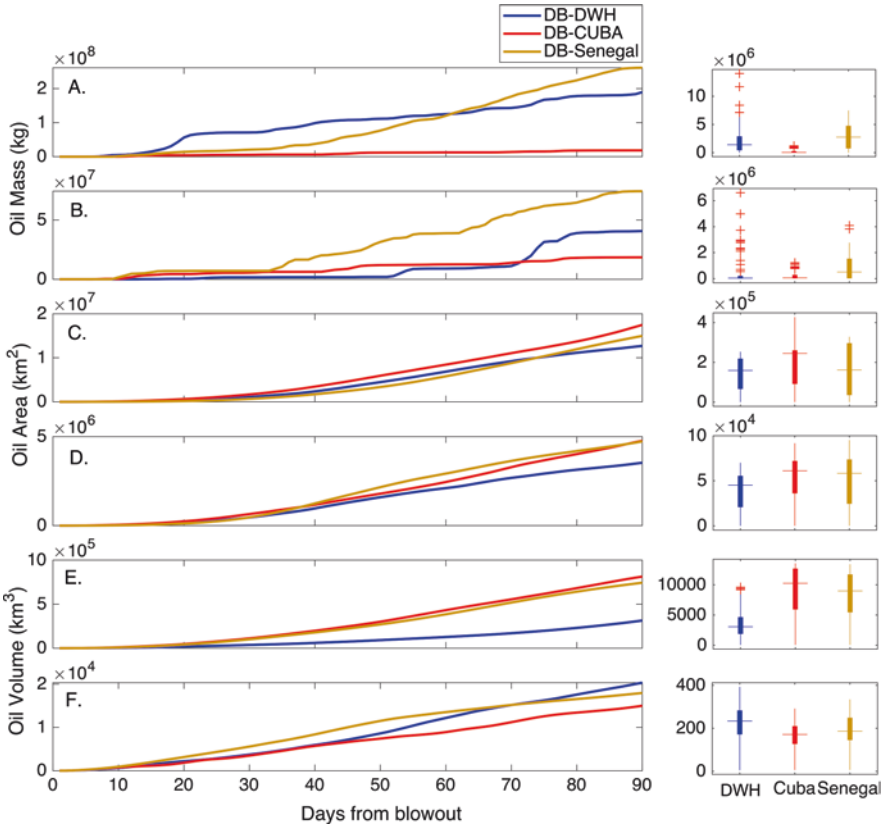

Fig. 19.3 Ninety-day time series of cumulative (**a**) sedimented oil mass; (**b**) beached oil mass; (**c**) area of total petroleum (greater than background TPH >1 ppb); (**d**) area that contains toxic concentrations (surface PAH > 0.5 ppb, subsurface PAH > 1 ppb toxic to biota); (**e**) seawater volume with TPH >1 ppb; (**f**) seawater volume with PAH > 0.5 ppb toxic to biota; right panels are boxplots of the time series (noncumulative) data. Data presented are for the four scenarios: *DB_DWH* (blue), *DB_Cuba* (red), and *DB_Senegal* (orange)

the steep bathymetry of the western point of Cuba and a seamount. The seamount seems to steer the deep currents, constraining the extent of the oil plume that never crosses the Yucatan Straits. In contrast, oil slicks freely cross the Straits toward the Yucatan peninsula and the Florida Keys (Fig. 19.4a). During the first 23 days, the deep plume is transported to SW Cuba, and then shifts back and forth from SW to NW Cuba. The formation of a deep intrusion with very high oil concentrations (orange plume of 100 ppb) is clear in all the daily snapshots. After the well is capped

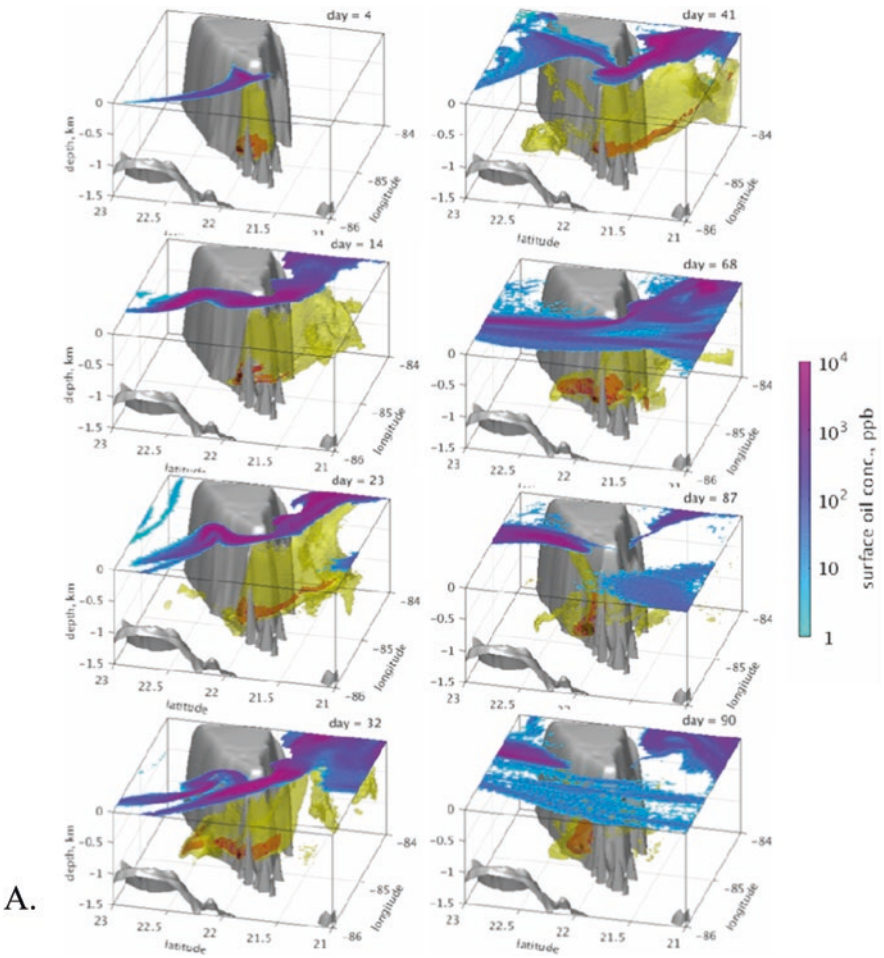

Fig. 19.4 Modeled 3-D evolution of the deep plume and oil slicks for two *Deepwater Horizon* oil spill scenarios: (**a**) Cuban blowout (*DB_Cuba*); (**b**) Senegalese blowout (*DB_Senegal*). Isosurfaces of the daily average subsea oil concentrations of 1000 ppb (black), 100 ppb (orange), 10 ppb (yellow), and surface concentration gradient (cyan-magenta) for 8 snapshot days as indicated in each panel; the surface concentrations shown are for the top 1 m of water. The red- and yellow-colored isosurfaces are semitransparent to allow seeing the internal structure of the plume and patches. Gray isosurface in the background is the bathymetry; see Table 19.1 for details on the simulated blowout locations and initial conditions

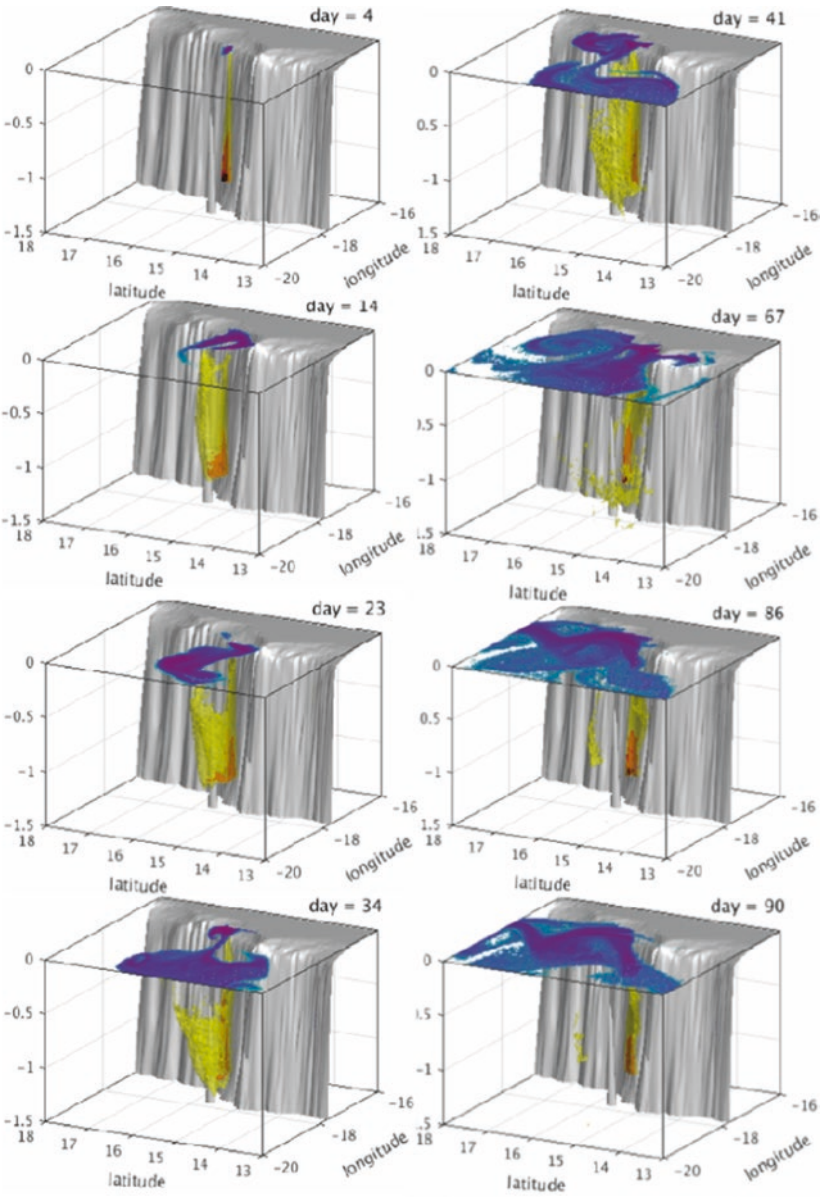

Fig. 19.4 (continued)

(day 87), the largest oil mass remains at proximity of the wellhead between the seamount and the SW Cuba slope (Fig. 19.4a).

The oil residue deposit for the *DB_Cuba* scenario (Fig. 19.6a) is marginal in comparison to *DB_DBW* (Perlin et al. 2020) and *DB_Senegal* (Fig. 19.6b). Having relatively little sedimented oil mass is expected, given the steep slope of the bathymetry (ca. 90°). Nevertheless, weathered oil accumulates in historical spawning

aggregation sites at the promontory of Cabo Corrientes on the western point of Cuba and in the Cayman Islands, as well as in the Gulf of Batabanó (a major spiny lobster fishing grounds), and from the upper Florida Keys to Biscayne Bay, and further on the southeast Florida coast.

19.3.2 Cayar Canyon: Senegal Blowout Scenario

Simulation of the cumulative oil concentration across time and depth for an 87-day DWH-like blowout in Senegal results in a monstrous oil footprint: the oil spreading north to south along the Mauritania coastline to the north, Gambia and Guinee-Bissau to the south, and offshore westward beyond the Cape Verde islands (Fig. 19.1b). The vertical structure of horizontally cumulative suspended oil mass tracked over a 90-day period (Fig. 19.2c) indicates that the highest oil content is still found primarily in the subsea below 400 m. Interestingly, while the two intermediate layers between 400 and 1200 m hold most of the suspended oil, the layer below 1200 m remains low in suspended oil mass. In addition, the temporal dynamic is significantly different from the *DB_DWH,* when the oil mass decreases only after the capping of the well (87 d): the maximum oil mass occurs early on at day 40 (Fig. 19.2c). Unlike the Cuba case, Fig. 19.1c shows that no oil is escaping the study domain, suggesting that the oil is sedimented and/or beached. Indeed, this blowout case has the highest amount of sedimented and beached oil, exceeding at the end of 90 days by ca. 100 and 250 million kg of oil mass sedimented and beached from that of the DWH scenario (*DB_DWH*) and by 200 and 500 million kg from the Cuban scenario (*DB_Cuba*) (Fig. 19.3a, b).

The modeled 3-D evolution of *DB_Senegal* reveals a much less dynamic deep plume than *DB_Cuba*, still with a decoupled motion from the surface oil transport (Fig. 19.4b). The surface slicks are moved by the mesoscale eddy field and expand quickly over the entire domain in Fig. 19.4b. The higher oil concentrations (black, Fig. 19.4b) reveal the wellhead location between the Cayar Canyon and the Cayar Seamount. The deep plume has a contained conical shape from the trap height up to the surface, as expected during the strong upwelling season in the region. A top view of the deep plume shows the subsea oil mass revolving around the Cayar Seamount in an anticyclonic motion for over 41 days (Fig. 19.5). Note the plume rotation as inferred by the trailing yellow region that follows a more subtle spin of the main plume (days 14, 23, 32, 41). The formation of a deep intrusion is evident early on (see day 14) and persists throughout the blowout. At day 68, the anticyclone is disorganized, and the deep intrusion is transported with the southward prevailing flow in the region. The largest oil mass remains at proximity of the wellhead between the visibly large Cayar Seamount and Canyon (Fig. 19.5).

The oil residue deposit for the *DB_Senegal* case (Fig. 19.6b) is enormous in comparison to *DB_Cuba* (Fig. 19.6a) and even to *DB_DBW* (Perlin et al. 2020). Here, heavy loads of sedimented oil cover the seafloor from the surf zone to beyond the 500 m isobath from the Cap Vert Peninsula to the north of Mauritania. In addition, strong interaction of the oil plume revolving around the seamount results in highest sedimentation directly on the Cayar Seamount and in the Cayar

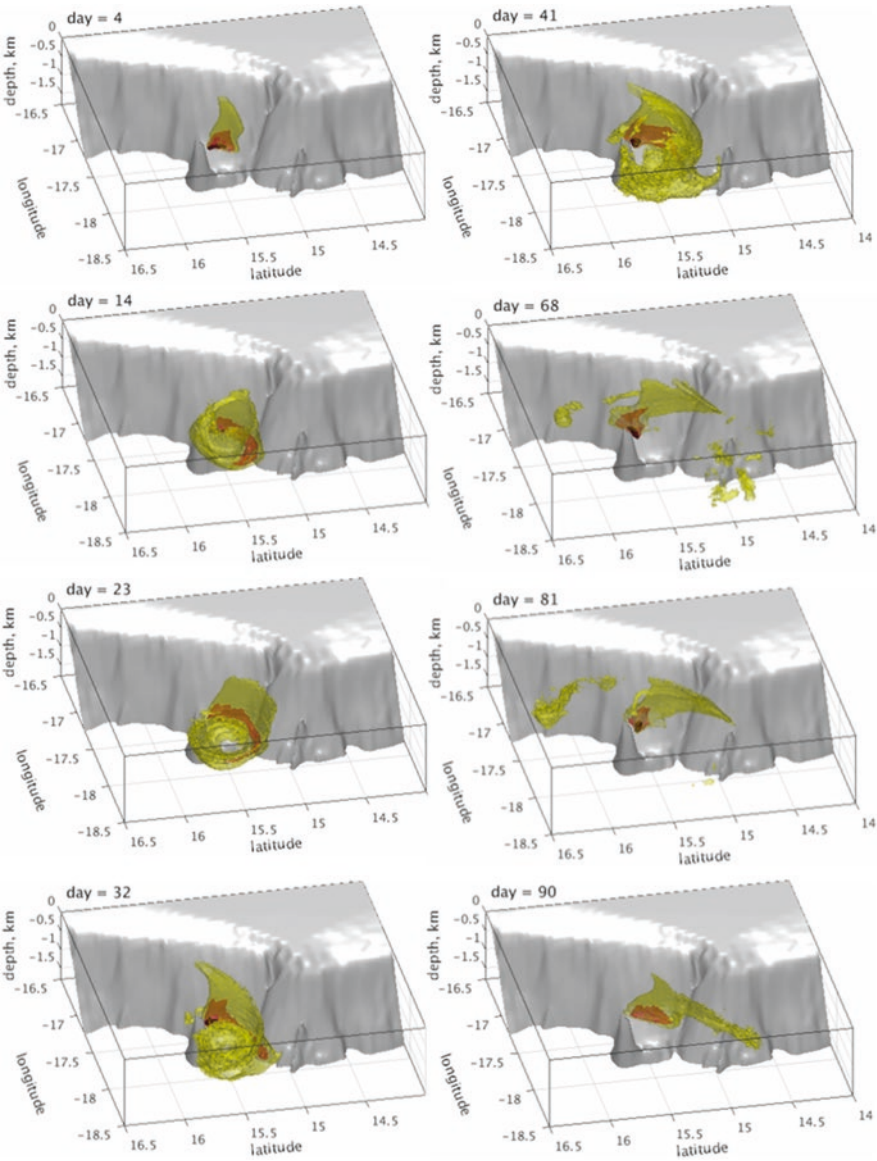

Fig. 19.5 Modeled 3-D evolution of the deep plume from the Senegalese blowout scenario (*DB_Senegal*). Isosurfaces of the daily average subsea oil concentrations of 1000 ppb (black), 100 ppb (orange), 10 ppb (yellow). The red- and yellow-colored isosurfaces are semitransparent to allow seeing the internal structure of the plume and patches. Gray isosurface in the background is the bathymetry; see Table 19.1 for details on the simulated blowout locations and initial conditions

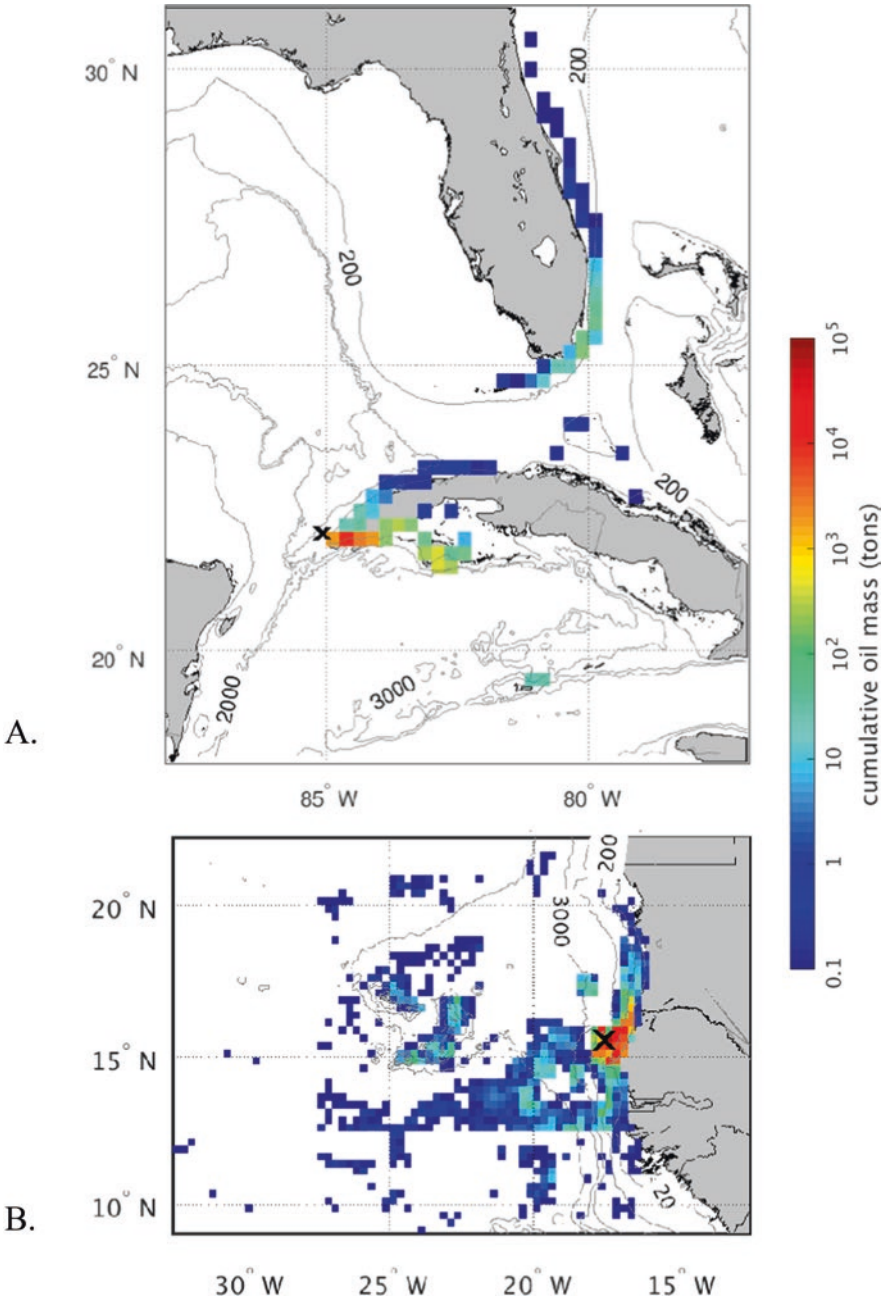

Fig. 19.6 Sedimented weathered oil mass on a 0.5° horizontal grid at the end of the model simulations (167 days) during hypothetical *Deepwater Horizon* oil spills: (**a**) Cuban blowout scenario (*DB_Cuba*); (**b**) Senegalese blowout scenario (*DB_Senegal*). See Table 19.1 for detail on spill location, duration, and initial conditions

Canyon (Fig. 19.6b). Weathered oil also accumulates in the Cape Verde islands and the neighboring seamounts, hot spots of fish abundance and marine biodiversity, and also along one of the world's largest fishing grounds operated by both local and international fisheries for sardines, tunas, and large pelagics. The benthic habitat along the Senegal-Mauritania coast also represents important reproductive and nursery grounds for numerous demersal species, including six species of grouper (Diop 1990).

19.3.3 Study Cases' Dynamical Comparison

The time series analysis indicates a few distinctive differences between the spills (Fig. 19.3). For example, the sedimented and beached oil mass of *DB_Cuba* were substantially lower than that of *DB_Senegal* and *DB_DWH*. The reason for that seems to be the difference in bathymetric structures and the coastline geomorphology. The NW Cuba hypothetical spill is located on a topographic saddle with steep slopes and the deepwaters of the Yucatan channel at proximity of the N54 block (Table 19.1). The strong inflow of the Caribbean current through the Yucatan channel generates strong currents at proximity of the spill across the water column. That strong flow, combined with deep bathymetry, prevents the oil from interacting with the bottom and substantially reduces the sedimented and beached oil mass. In contrast, the *DB_Senegal* and *DB_DWH* cases are characterized by a strong interaction of the oil with the bathymetry, as both are located on wide slopes with which the oil interacts. In addition, in the Senegal spill, a substantial amount of oil interacted the Cape Verde islands, which increased the sedimentation and beaching mass, as evident in the increase in beached oil mass around day 64 (Fig. 19.3b). The abrupt increase in beached mass in the *DB_DWH* around day 72 is attributed to Hurricane Alex that generated strong southeasterly winds which pushed much of the oil toward the northern beaches of the GoM (Louisiana, Alabama, Mississippi, and Northwest Florida). Another distinctive difference is the total volume of the *DB_DWH* oil spill compared to *DB_Cuba* and *DB_Senegal*. This difference is attributed to the relatively weak currents across the water column in the GoM – a semi-enclosed basin, which is "protected" from strong oceanic currents. In contrast, in the *DB_Cuba* and *DB_Senegal* cases, oil was subjected to stronger oceanic currents, the Caribbean and Canary Currents, which substantially increased the total volume affected by oil (see 3-D view, Fig. 19.4).

19.4 Discussion and Conclusions

Potential ecological impacts of deep oil spills beyond the Gulf of Mexico – None of the simulated spills stay local, and both were even more severe than the DWH (Table 19.2). In the case of the DWH spill, the oil was more contained (in terms of volume of water contaminated, Fig. 19.3e) for several reasons. First and foremost,

Table 19.2 Rank table from least to most impactful (1–3; white to dark gray), for the tested scenarios and variables

Blowout scenario	Sedimented oil mass	Beached oil mass	Oiled area	Toxic oiled area	Oiled volume	Toxic volume	Mean
DB_DWH	2	2	1	1	1	3	1.7
DB_Cuba	1	1	3	3	3	1	2.0
DB_Senegal	3	3	2	2	2	2	2.3

the gulf is a semi-enclosed sea where the ambient deep currents are relatively slow (i.e., in the order of a few cm/s). Secondly, deep cyclonic currents with periods up to 100 days also contributed to retain the oil in the deep ocean. These subsea eddies are attributed to the wall of the Loop Current interactions with the escarpment of the West Florida Shelf. In comparison, the blowout simulation in Senegal predicts the highest sedimented and beached oil mass due to strong and large upwelling system in the region. The NW Cuba blowout simulation predicts the highest concentrations of suspended oil in area and volume due to complex interactions of the Caribbean Currents with the steep topography of the island. Based on the background on the physical and biological attributes of the two putative blowout regions provided above (Sect. 19.1), it is safe to say that a major oil spill occurring in NW Cuba and Senegal could have severe impacts on the biodiversity and valuable fishery resources of the region. (Claro et al. 2009) Moreover, such disasters could precipitate long-lasting changes in the marine and coastal ecosystems, including the legacy of the Senegalese fishing villages and community, so ingrained in the Senegalese culture.

The impact of major spills needs to be seriously evaluated as it could not only be devastating for the marine environment but have serious socioeconomical consequences. Without this information any major spill in the region will likely be disastrous; we further suggest that damage assessment should be carried out internationally. We have not quantified here the impact of these deep-sea spills on neighboring countries, but we anticipate that any impact on the Caribbean spiny lobster metapopulation, for example (Kough et al. 2016), or on highly migratory species gathering in the Cayar Canyon and seamounts, could have international outcomes. Establishing international management agreements that recognize the risks of major spills and focus on protecting sensitive coastal and pelagic nurseries and reproductive grounds from well exploration and drilling programs should be a priority. Indeed, the safest solution to avoid similar disasters is to prevent deepwater drilling in sensitive areas; a more risky but suitable solution is to enforce the regulations for capping stacks worldwide.

Deep-sea oil exploitation rules and regulations Today, no one disclaims the dramatic impact oil spills have on the environment. The DWH spill was unprecedented by the depth of the well (about 5000 feet under the sea surface) that rendered the responses particularly difficult and slow, and overall, ineffective (Paris et al. 2018). While several response strategies have been undertaken by BP and others, such as the massive application of subsea chemical dispersant or the cementing of the well, the spill was only contained after 87 days by setting a “capping stack.” The Taylor

Energy platform that has been spilling up to 700 barrels per day for the last 14 years (i.e., between 855, 000 and 3.9 M gallons in total) is another example of the inherent risks of subsurface drilling activities (BSEE 2017).

The poor management of these oil spills highlighted the importance of robust, operationally validated safety regulations prior to drilling activities and led the US government to enforce the "Blowout Preventer Systems and Well Control" (BOP) in July 2016 (Rule 81 FR 25887; April 29, 2016). These new rules and regulations require the companies to have a capping stack operation before the start of drilling activities, as its rapid installation is by far as the safest responses to protect workers and the environment. However, and regardless of these recent scandals, the recently implemented "America-First Offshore Energy Strategy" aims to "reduce unnecessary procedures" and "provide more flexibility" to the oil-exploiting companies for the validation and certification of oil spill response tools (Order No. 3350; May 1, 2017). The most notable change implies that companies can now have their oil spill response plan validated by a third-party agency, cutting off the previously required authorization from the Bureau of Safety and Environmental Enforcement (BSEE). During the public campaign, the order received about 47,000 comments, highlighting how sensitive this topic is (regulations.gov/BSEE-2018-0002).

Due to the continuous growth of oil demand and the decrease in the level of historical wells over the last decade, oil companies are exerting a strong pressure to explore new oil-rich grounds around the world and particularly in the oceans. For instance, exploratory drilling activities are planned off the South African eastern coast, close to highly sensitive habitats such as the once-considered-extinct coelacanth (Stevens and Bungartz 2018). The Arctic Ocean is also under extreme pressure due to large amounts of oil present under the seafloor, and so is the US Atlantic coast since the US government offered to launch new exploitation leases as part of the "America-first Offshore Energy Strategy." In this context, our study demonstrates that if "another DWH" occurred in a different region, the poorly regulated emergency responses at the time of the spill would result in an impact much worse on marine ecosystems and coastal communities. Since oil exploration will not decrease in the near future, we urge governments, such as of Senegal or South Africa, to focus on implementing safe and operational regulations before selling new exploitation leases. This may likely be the only way to protect sensitive ecosystems and the coastal communities relying on them. Partnership deals with foreign oil companies are typically 1/9 (90% foreign), and any short-term economic benefits will be swamped by the long-term impact on seafood resources and tourism industry. For historical fishing nations such as Senegal, there is no tangible benefit from ultra-deep sea oil exploration.

Continued protection of sensitive areas worldwide is vital. Scientific communication and collaboration becomes critical. In the case of Cuba, we clearly have strong oceanographic and biophysical connections. In the case of Senegal, our connection is at a broader level; a mega oil spill occurring during the upwelling season could have global repercussions.

Jean Rostand – "The obligation to endure gives us the right to know."

Acknowledgments This research was made possible by a grant from the Gulf of Mexico Research Initiative/C-IMAGE II-III to Steve Murawski. Data are publicly available through the Gulf of Mexico Research Initiative Information and Data Cooperative (GRIIDC) at https://data.gulfresearchinitiative.org/data/R6.x805.000:0060 and https://data.gulfresearchinitiative.org/data/R6.x805.000:0059.

References

Adams EE, Sococlofsky SA (2005) Review of deep oil spill modeling activity. Technical Report, submitted to the DeepSpill JIP and Offshore Operators Committee, February 2004

Bakun A (1990) Global climate change and intensification of coastal ocean upwelling. Science 247(4939):198–201

Barry-Gerard M (1990) Le complexe fosse de kayak-presqu'ile du Cap Vert constitue-t-il un obstacle aux migrations de poissons le long des cotes Senegalaises? CRODT ISSN 0850-1602. Document Scientifique 119:32 pp

Berenshtein I, Perlin N, Ainsworth CH, Ortega-Ortiz J, Vaz AC, Paris CB (2020) Comparison of the spatial extent, impacts to shorelines, and ecosystem and four-dimensional characteristics of simulated oil spills (Chap. 20). In: Murawski SA, Ainsworth C, Gilbert S, Hollander D, Paris CB, Schlüter M, Wetzel D (eds) Scenarios and responses to future deep oil spills – fighting the next war. Springer, Cham

Bureau of Safety and Environmental Enforcement (BSEE) and Bureau of Ocean Energy, Management (BOEM) (2017) Incident Archive - Taylor Energy Oil Discharge at MC-20 Site and Ongoing Response Efforts [WWW Document]. https://www.bsee.gov/newsroom/library/incident-archive/taylor-energy-mississippi-canyon/ongoing-response-efforts. Accessed 24 Oct 2018

Chassignet EP, Smith LT, Halliwell GR, Bleck R (2003) North Atlantic simulations with the hybrid coordinate ocean model (HYCOM): impact of vertical coordinate choice, reference pressure and thermobaricity. J Phys Oceanogr 33:2504–2526

Claro R, Lindeman KC (2003) Spawning aggregation sites of snapper and grouper species (Lutjanidae and Serranidae) on the insular shelf of Cuba. Gulf Caribbean Res 14:91–106

Claro R, Parenti LR (2001) The marine ichthyofauna of Cuba, pp. 21–57. In: Claro R, Lindeman K, Parenti LR (eds) Ecology of the marine fishes of Cuba. The Smithsonian Institution Press, pp. 253, Washington D.C.

Claro R, Reshetnikov YS, Alcolado PM (2001) Physical attributes of coastal Cuba, pp. 1–20. In: Claro R, Lindeman K, Parenti LR (eds) Ecology of the marine fishes of Cuba. The Smithsonian Institution Press, pp. 253

Claro R, de Mitcheson YS, Lindeman KC, García-Cagide AR (2009) Historical analysis of Cuban commercial fishing effort and the effects of management interventions on important reef fishes from 1960–2005. Fish Res 99:7–16

Cummings JA (2005) Operational multivariate ocean data assimilation. Q. J. R. Meteorological Society Part C 131:3583–3604

Cummings JA, Smedstad OM (2013) Variational data assimilation for the global ocean. Data Assimilation for Atmospheric, Oceanic and Hydrologic Applications, Vol. II, chapter 13, 303–343

Diankha O (2018) Peuplements Halieutiques Du Réseau D'AMP Du Sénégal en 2017. Rapport technique DAMCP/MEDD, Sénégal, 86 pp.

Diankha O, Fatima BA, Sarr A, Diadhiou HD, Diop M, Ndiaye N, Brehmer P (2018) Preliminary study of fish assemblage structure of the marine protected area of Cayar in Senegal. J Mar Biol Oceanograp 7:1. https://doi.org/10.4172/2324-8661.1000184

Diop S (1990) La côte ouest-africaine. Du Saloum (Sénégal) à la Mellacorée (Rép. De Guinée). Editions ORSTOM, Paris, 379 p

Erisman B, Heyman W, Kobara S, Ezer T, Pittman S, Aburto-Oropeza O, Nemeth RS (2017) Fish spawning aggregations: where well-placed management actions can yield big benefits for fisheries and conservation. Fish Fish 18:128–144

Global Runoff Data Center, Federal Institute of Hydrology, S. International Hydrological Programme, United Nations Educational, and C. Organization (2001), Augmented monthly flow rates of world rivers (except former soviet union)

Haidvogel DB, Arango H, Budgell WP, Cornuelle BD, Di Lorenzo E, Fennel K, Geyer WR, Hermann AJ, Lanerolle L, Levin J, McWilliams JC, Miller AJ, Moore AM, Powell TM, Shchepetkin AF, Sherwood CR, Signell RP, Warner JC, Wilkin J (2008) Ocean forecasting in terrain-following coordinates: formulation and skill assessment of the Regional Ocean modeling system. J Comput Phys 227(7):3595–3624. https://doi.org/10.1016/j.jcp.2007.06.016

Jacobi RD, Hayes DE (1982) Bathymetry, microphysiography and reflectivity characteristics of the West African margin between Sierra Leone and Mauritania. In: von Rad U, Hinz K, Sarnthein M, Seibold E (eds) Geology of the Northwest African continental margin. Springer, Berlin, Heidelberg

Kosmos Energy (2016). https://www.offshore-mag.com/articles/2016/05/kosmos-energy-finds-more-deepwater-gas-offshore-senegal.html

Kough AS, Paris CB, Butler MJ (2013) Larval connectivity and the International Management of Fisheries. PLoS ONE 10:1371. https://doi.org/10.1371/journal.pone.0064970

Kourafalou, V.H., Androulidakis, Y.S., Kang, H., Le Hénaff, M., 2017. The dynamics of Cuba anticyclones (CubANs) and interaction with the Loop Current/Florida Current system. J. Geophys. Res. Oceans. https://doi.org/10.1002/2017JC012928

Kourafalou V, Androulidakis Y, Le Hénaff M, Kang HS (2017) The dynamics of Cuba Anticyclones (CubANs) and interaction with the loop current/Florida current system. J Geophys Res Oceans 122(10):7897–7923

Kough AS, Claro R, Lindeman K, Paris CB (2016) Decadal analysis of larval connectivity from Cuban snapper (Lutjanidae) spawning aggregations based on biophysical modeling. Mar Ecol Prog Ser 550:175–190

Le Hénaff M, Kourafalou VH, Morel Y, Srinivasan A (2012) Simulating the dynamics and intensification of cyclonic loop current frontal eddies in the Gulf of Mexico. J Geophys Res Oceans 117(C2).

Limouzy C, Cayre P (1981) Peche et aspects de la biology du Voilier de l'Atlantique (*Istiophorus platypterus*) sur les cotes Sénégalaises. ICCAT XV SRCS/80/55:361–371

Lindeman K, Claro R, Kough AS, Paris CB (2018) Biophysical connectivity of snapper spawning aggregations and marine protected area management alternatives in Cuba. Fish Oceanogr. https://doi.org/10.1111/fog.12384

MetOcean Solutions (2018) Senegal-Mauritania wave and hydrodynamic hindcast models now available. http://www.metocean.co.nz/news/2018/5/16/senegal-mauritania-wave-and-hydrodynamic-hindcast-models-now-available. Accessed 3 June 2018

Miron PF, Beron-Vera FJ, Olascoaga MJ, Sheinbaum J, Pérez-Brunius P, Froyland G (2017) Lagrangian dynamical geography of the Gulf of Mexico. Sci Rep 7:7021

Nerurkar N, Sullivan MP (2011) Cuba's Offshore Oil Development: Background and U.S. Policy Considerations, Congressional Research Service 7–5700. www.crs.gov, R41522, pp. 24

Paris CB, Cowen RK, Claro R, Lindeman KC (2005) Larval transport pathways from Cuban spawning aggregations (Snappers; Lutjanidae) based on biophysical modeling. Mar Ecol Prog Ser 296:93–106

Paris CB, Le Hénaff M, Aman ZM, Subramaniam A, Helgers J, Wang D-P, Kourafalou VH, Srinivasan A (2012) Evolution of the Macondo well blowout: simulating the effects of the circulation and synthetic dispersants on the subsea oil transport. Environ Sci Technol 46:13293–13302. https://doi.org/10.1021/es303197h

Paris CB, Helgers J, Van Sebille E, Srinivasan A (2013) Connectivity modeling system: a probabilistic modeling tool for the multi-scale tracking of biotic and abiotic variability in the ocean. Environ Model Softw 42:47–54. https://doi.org/10.1016/j.envsoft.2012.12.006

Paris CB, Berenshtein I, Trillo ML, Faillettaz R, Olascoaga MJ, Aman ZM, Schlüter M, Joye SB (2018) BP gulf science data reveals ineffectual sub-sea dispersant injection for the Macondo blowout. Front Mar Sci 5:389. https://doi.org/10.3389/FMARS.2018.00389

Paris CB, Murawski SA, Olascoaga MJ, Vaz AC, Berenshtein I, Beron-Vera FJ, Miron P, Faillettaz R (2020) Connectivity of the Gulf of Mexico continental shelf fish populations and implications of simulated oil spills (Chap. 22). In: Murawski SA, Ainsworth C, Gilbert S, Hollander D, Paris CB, Schlüter M, Wetzel D (eds) Scenarios and responses to future deep oil spills – fighting the next war. Springer, Cham

Peng G, Zhang HM, Frank HP, Bidlot JR, Higaki M, Stevens S, Hankins WR (2013) Evaluation of various surface wind products with OceanSITES buoy measurements. Weather Forecast 28:1281–1303. https://doi.org/10.1175/WAF-D-12-00086.1

Perlin N, Paris CB, Berenshtein I, Vaz AC, Faillettaz R, Aman ZM, Schwing PT, Romero IC, Schlüter M, Liese A, Noirungsee N, Hackbusch S (2020) Far-field modeling of a deep-sea blowout: sensitivity studies of initial conditions, biodegradation, sedimentation and subsurface dispersant injection on surface slicks and oil plume concentrations (Vol. 1, Chap. 11). In: Murawski SA, Ainsworth C, Gilbert S, Hollander D, Paris CB, Schlüter M, Wetzel D (eds) Deep oil spills – facts, fate and effects. Springer, Cham

Ruffan A, Meagher L, Stewart JMG, Monohan D (2018) Multi-disciplinary survey of Senegal/Gambia continental margin. Int Hydrogr Rev, Monaco LVI(1):81–106

Saha S, Moorthi D, Pan H-L, Wu X, Wang J, Nadiga S, Tripp P, Kistler R, Woollen J, Behringer D, Liu H, Stokes D, Grumbine R, Gayno G, Wang J, Hou Y-T, Chuang H-Y, Juang H-M H, Sela J, Iredell M, Treadon R, Kleist D, Van Delst P, Keyser D, Derber J, Ek M, Meng J, Wei H, Yang R, Lord S, Van Den Dool H, Kumar A, Wang W, Long C, Chelliah M, Xue Y, Huang B, Schemm J-K, Ebisuzaki W, Lin R, Xie P, Chen M, Zhou S, Higgins W, Zou C-Z, Liu Q, Chen Y, Han Y, Cucurull L, Reynolds RW, Rutledge G, Goldberg M (2010) The NCEP climate forecast system reanalysis. Bull Am Meteorol Soc 91(8):1015–1057. https://doi.org/10.1175/2010BAMS3001.1

Stevens V, Bungartz L (2018) Exploration drilling within block ER236, off the East Coast of South Africa – draft environmental impact assessment report V1

U.S. Geological Survey (2005) Assessment of Undiscovered Oil and Gas Resources of the North Cuba Basin, 2004, (February 2005). http://walrus.wr.usgs.gov/infobank/programs/html/factsheets/pdfs/2005_3009.pdf

Weatherall P, Marks KM, Jakobsson M, Schmitt T, Tani S, Arndt JE, Rovere M, Chayes D, Ferrini V, Wigley R (2015) A new digital bathymetric model of the world's oceans. Earth Space Sci 2(8):331–345. https://doi.org/10.1002/2015EA000107, 2015EA000107

Zhang H-M, Bates JJ, Reynolds RW (2006) Assessment of composite global sampling: sea surface wind speed. Geophys Res Lett 33:L17714. https://doi.org/10.1029/2006GL027086

Part IV
Comparisons of Likely Impacts from Simulated Spills

Curtis Whitwam
Wolf Pack
Watercolor on Aquaboard
20” × 16”

Chapter 20
Comparison of the Spatial Extent, Impacts to Shorelines, and Ecosystem and Four-Dimensional Characteristics of Simulated Oil Spills

Igal Berenshtein, Natalie Perlin, Cameron H. Ainsworth, Joel G. Ortega-Ortiz, Ana C. Vaz, and Claire B. Paris

Abstract The ever-growing increase in deep-sea oil explorations in the Gulf of Mexico (GoM) has been raising concerns with regard to future oil spills. Major oil spills in the GoM such as the *Deepwater Horizon* (DWH 2010) and the Ixtoc 1 (1979) resulted in extensive pollution of the pelagic, sea-floor, and coastal ecosystems. Oil spill transport and fate models are effective tools which allow a spatiotemporally explicit reconstruction of oil spills, while accounting for key processes such as evaporation, sedimentation, biodegradation, and dissolution. Oil transport data can be fed into an ecosystem model to help estimate system-scale changes in biodiversity and impacts on the delivery of ecosystem services. The increase in deep-sea oil-drilling endeavors warrants an evaluation of the potential outcomes and effects of oil spills. However, each spill scenario is a complex 4-D problem, spanning over wide spatiotemporal dimensions, affecting various media (water, sediments, coast, air); hence it is difficult to effectively evaluate the differences between various oil spill scenarios.

In the current chapter, we examine quantifiable variables, which enable an effective comparison of the outcomes of four different scenarios: the DWH (DB_control), the DWH occurring during the fall (DB_Fall), east GoM scenario (DB_AL2), and west GoM scenario (DB_AL3). Specifically, we evaluate the total area and volume of oil-affected waters, the total water area and volume affected by toxic oil

Electronic supplementary material The online version of this chapter (https://doi.org/10.1007/978-3-030-12963-7_20) contains supplementary material, which is available to authorized users.

I. Berenshtein (✉) · N. Perlin · A. C. Vaz · C. B. Paris
University of Miami, Rosenstiel School of Marine and Atmospheric Science, Department of Ocean Sciences, Miami, FL, USA
e-mail: iberenshtein@rsmas.miami.edu; nperlin@rsmas.miami.edu; avaz@rsmas.miami.edu; cparis@rsmas.miami.edu

C. H. Ainsworth · J. G. Ortega-Ortiz
University of South Florida, College of Marine Science, St. Petersburg, FL, USA
e-mail: ainsworth@usf.edu; jortegaortiz@mail.usf.edu

S. A. Murawski et al. (eds.), *Scenarios and Responses to Future Deep Oil Spills*,
https://doi.org/10.1007/978-3-030-12963-7_20

concentrations, the length of the shoreline affected by oil, and the total area of the sedimented oil. The oil transport model is coupled to Atlantis, a biogeochemical ecosystem model, to examine changes in the ecosystem biota. The depth and location of the oil vary with each scenario and so affect different habitats, species, and life stages. We consider relative impacts on pelagic and demersal food webs, shifts in age structure, changes in diet, and impacts on the sustainability of exploited species. We report the differences between the different oil spills and discuss their implications. Overall, the results differed slightly and not significantly between the four scenarios, ranked from most to least impactful: DB_AL2 > DB_control > DWH_Fall > DB_AL3. This work suggests that a "DWH" occurring at a different time or place in the GoM would result in impact fairly similar to that occurred during the actual DWH. This is relevant given the extensive petroleum-related activity in the GoM.

Keywords Oil spill impacts · Gulf of Mexico · Deepwater Horizon · Oil transport model

20.1 Introduction

Global offshore gas and oil production have been growing continuously, along with population growth and its associated energetic requirements (Energy Information Administration 2018). Consequently, oil explorations have been consistently moving to deeper waters, which are more complicated for containment in case of a spill or an uncontrolled blowout similar to the DWH (Lubchenco et al. 2012). Despite constant improvement in the safety protocols and spill containment efficiency (Fingas 2011), the overall increase in production, and deeper water explorations in specific, encompasses considerable risks of oil spills, specifically, risks to human physical (Gohlke et al. 2011) and mental (Osofsky et al. 2011) health, to the ecosystem (Beyer et al. 2016), and to the economy (Sumaila et al. 2012).

The Gulf of Mexico (GoM) is a highly productive region consisting of more than 95% of the offshore gas and oil production in the USA and providing livelihood to hundreds of thousands of people around the GoM states. Specifically, there are nearly 2600 active leases, more than half of which are deeper than 1000 m (BOEM 2018). Therefore, it is not surprising that since 2005 there were 19 oil spills in the GoM. Six other significant oil spills occurred in the GoM before the DWH: Ixtoc 1 (1979), Burmah Agate (1979), Mega Borg (1990), Alvenus (1984), Ocean 255 (1993), and Hurricane Katrina (2005), spilling between 65,000 and 8.1 million gallons of oil to the GoM waters (Office of Response and Restoration 2012). The recent "Delta House oil spill" occurred in October 2017 released approximately 320,000 gallons of oil to the GoM.

A basic component of oil spill management is the realistic estimation of a given oil spill extent before, during, and after it occurs, using this extent to evaluate

trade-off between the energetic and economical merits of the well, against the risks associated with a possible oil spill (Boehm and Page 2007; Deepwater Horizon Natural Resource Damage Assessment Trustees 2016; Beyer et al. 2016; Nelson and Grubesic 2018a). The progress dynamics of this field are based on damage assessments and reconstruction of past events and assimilation of that knowledge into the current risk assessments of potential spills (Fingas 2011).

Such analyses normally include vulnerability, risk, and direct impact analyses (Nelson and Grubesic 2018b). Vulnerability analysis normally quantifies the expected damage to shorelines following oiling and often includes an environmental sensitivity index (ESI) considering the type of habitat or creating vulnerability scores considering environmental, economic, and social assets. Risk analysis includes mainly the computation of probability that an oil spill will impact a given area. A recent work by Nelson and Grubesic (2018b) evaluated the potential impact of a major blowout in ten nearshore and offshore locations in the West Florida shelf (WFS), taking into account the risk of hazard and spatially specific sensitivity in the domain.

In the current chapter, we develop geographic and ecological variables for comparison between possible oil spills by coupling the oil application of the Connectivity Modeling System (CMS, Paris et al. 2013) and Atlantis (Ainsworth et al. 2015) models. We analyze the difference in these variables to gauge the effect of spatio-temporal variability in oceanic conditions on the oil spill outcome. Specifically, we focus on the DWH, and we simulate three other scenarios which use the same chemo-physical characteristics of the oil spill, i.e., the amount of oil discharge, oil composition, spill's depth, and duration, but at different locations or time of year. We then compare the following variables between the spills: toxic and nontoxic spill area and volume, shoreline length affected by oil, sedimented area, guild-specific biomass loss, estimated years to guild recovery, and net guild biomass change after 20 years. Importantly, the coupled oil-CMS and Atlantis models provide a more holistic approach considering second-order effects in addition to first-order immediate impact (Ainsworth et al. 2018).

20.2 Methods

20.2.1 General Method Approach

In the current chapter, we examined the differences between the outcomes of four different oil spill scenarios in the GoM. Our methodological approach is composed of three parts: (1) an oil transport and fate model, which predicts the 4-D concentrations of a given oil spill; (2) a spatially explicit ecosystem model which can compute the effect of a given oil spill on the ecosystem, incorporating ocean physics, chemistry, and biology; and (3) an extensive post-processing of the modeling outputs to produce a meaningful comparison and outcome evaluation.

20.2.1.1 Oil Transport and Fate Model: Oil-CMS

Our study implements the existing oil application (Perlin et al. 2020; Paris et al. 2012) of the Connectivity Modeling System (CMS; Paris et al. 2013) to compute the transport and fate of the live oil spilled during the DWH blowout. The oil-CMS performs Lagrangian particle tracking of oil droplets released at the trap height above the well location. Particle transport calculations take into account ocean 3-D currents, temperature, salinity, multi-fractional droplet buoyancy, biodegradation, dissolution, and surface oil evaporation. The fourth-order Runge-Kutta integration scheme forms the basis for particle advection in the model. Computations of the vertical terminal velocity of a droplet are based on its density and size, its Reynolds number, as well as other ambient conditions such as water temperature, salinity, density, and kinematic viscosity (Zheng et al. 2003).

The model output is saved every 2 hours and includes oil droplets' effective density, size, location, and depth. The oil-CMS applies a multi-fraction droplet approach in which each droplet includes multiple hydrocarbon fractions (Lindo-Atichati et al. 2016). The biodegradation dynamics of the present study are based on high-pressure experiments and apply different decay rates for the different fractions. This allows the model to account for dissolution processes where droplets dissolve with the partitioning of oil compounds in the water column (Jaggi et al. 2017). Post-processing algorithms translate model output into oil concentrations (Perlin et al. 2020).

20.2.1.2 Oil Spill Scenarios

The different scenarios are given in Table 20.1. They aim at studying the effects of DHW-like blowouts under different times (DB_FALL) and locations (DB_AL2, DB_AL3) (Table 20.1).

The simulation DB_FALL assumes a blowout at the same location as the DWH but occurring later in the season starting September 1, 2010, under a different ocean state. Simulations DB_AL2 and DB_AL3 were designed for alternative locations of the deep-sea blowout in the GoM. The locations were chosen such that the water depth was similar to that of the DWH accident. We used two alternative location

Table 20.1 Simulation details of the four spill scenarios

Scenario	Location	Start date
DB_Control	28.736° N, 88.365° W	April 20, 2010
DB_Fall	28.736° N, 88.365° W	September 1, 2010
DB_AL2	27.000° N, 85.168° W	April 20, 2010
DB_AL3	26.660° N, 93.190° W	April 20, 2010

The DB_Control represents the actual DWH blowout in terms of location, date, and blowout characteristics. The DB_Fall location is similar to DB_Control but occurs at a different time of the year, during the Fall. DB_AL2 and DB_AL3 represent DWH-like spills in the east and west GoM respectively.

spill scenarios (Table 20.1), one in the eastern and one in the western GoM under similar conditions of the DHW blowout.

The DB_AL2 site is located in the eastern part of the GoM closer to the Florida peninsula and over the continental shelf break, in the "the elbow" leasing block – an area which was recently proposed for oil exploration and production (US Department of the Interior 2018). The DB_AL3 site is located in the western part of the Gulf, over the area with less steep bathymetry gradients, within the "Keathley Canyon" leasing block, an oil-rich area in which multiple oil companies have leased the rights to drill (Smith 2010).

20.2.1.3 Experimental Approach

Three thousand oil droplets were released above the blowout location (Table 20.1; Perlin et al. 2020) every 2 hours for 87 days and are tracked for 90 days. The release depth is 1222 m, or 300 m above the Macondo well depth, the estimated height of oil and gas separation above the wellhead, similarly to the DWH accident (Socolofsky et al. 2011). Initial droplet diameters are drawn from a uniform distribution between 1 and 500 microns. Each droplet released by the oil-CMS model contains three pseudo-components (fractions) accounting for the differential oil density as follows: 10% of light oil with the density of 800 kg/m^3, 75% of intermediate oil with 840 kg/m^3, and 15% of heavy oil with 950 kg/m^3 density. The biodegradation half-life rates for the light, intermediate, and heavy fractions were set to 30, 40, and 180 hours based on laboratory and observation studies (Hazen et al. 2010; Schedler et al. 2014; Lindo-atichati et al. 2016). Evaporation half-life rate was set to 250 hours (de Gouw et al. 2011). Horizontal diffusion was set to 10 m^2/s.

Ocean hydrodynamic forcing for the present study used daily output from the Hybrid Coordinate Ocean Model (HYCOM, Chassignet et al. 2003) for the GoM region on a 0.04-degree horizontal grid, including 40 vertical levels spanning from the surface to 5500 m (for more details see Perlin et al. 2020). The simulation included parameterization of the effects of the surface wind drift, the importance of which was emphasized by Le Hénaff et al. (2012). Wind stress components from the 0.5-degree Navy Operational Global Atmospheric Prediction System (NOGAPS) are interpolated into HYCOM GoM 0.04-degree grid, and 3% of their values are added to the top level ocean velocity horizontal components taking into account the wind stress rotation. The corrected ocean velocity fields are then implemented in the oil-CMS.

20.2.1.4 Oil Mass and Concentration Estimates

To obtain oil mass and concentrations from the oil-CMS model output of the droplet properties and locations, information about the oil flow rate is needed. In a simplified case of the constant flow rate during the oil spill event, a given number of total droplets released in the simulation, the estimated 7.3×10^5 tons of crude oil are represented by the total of 3.132×10^6 droplets. These values translate into the

233 kg of oil represented by a single oil droplet at each release time in the oil-CMS model. We approximate the droplet size distribution (DSD) using the binned approach, with droplets in the same bin representing similar mass of oil per droplet. We further compute the scaling factor (S_f) for each droplet as the ratio between the current and the initial masses. Mass is estimated from the droplet diameter and effective density given the time span. Oil mass at each output time is then scaled to obtain effective mass at a given location and summed for all the droplets found in each post-processing grid cell at a given time step.

The 3-D post-processing domain is of 0.02-degree resolution, with 126 vertical layers of 0–1 m (surface layer), 2–20 m, 20–40 m,…, 2480–2500 m. Concentrations are obtained by normalizing the total oil mass to the mass of water in the corresponding grid box, producing 4-D (time and space) concentrations and/or mass matrices. For more information, refer to Perlin et al. (2020).

20.2.1.5 Toxicity Computation for the oil-CMS

Toxicity computations for the CMS were based on the recent finding of the toxicity amplification due to the combined effect of PAH and UV radiation (Lay et al. 2015), with PAH becoming toxic to fish early life stages from a concentration of PAH = 0.5 ppb at the surface and PAH = 1 ppb at deeper waters (Deepwater Horizon Natural Resource Damage Assessment Trustees 2016). We applied linear regression to compute the PAH-TPH linear relationship from the BP Gulf Science Data (GSD; BP Gulf Science Data, 2016). Since total petroleum hydrocarbons (TPH) account for ~97% of oil (Overton et al. 2016), we multiplied the mass by 0.97 to obtain TPH. Linear regression indicated a significant relationship ($p < 0.001$, $R^2 = 0.9$, $n = 34$) between TPH and PAH such that:

$$\log_{10}(\mathrm{TPH}+1) = 1.733 + 1.0074 \times \log_{10}(\mathrm{PAH}+1) \quad \text{for surface waters}(\mathrm{Depth} \le 1\ \mathrm{m}) \tag{20.1}$$

Linear regression for deeper waters (depth >1 m) for TPH and PAH concentrations from GSD indicated a significant linear relationship ($p < 0.001$, $R^2 = 0.3$, $n = 641$), such that:

$$\log_{10}(\mathrm{TPH}+1) = 1.58357 + 0.85257 \times \log_{10}(\mathrm{PAH}+1) \quad \text{for deeper waters}(\mathrm{Depth} > 1\mathrm{m}) \tag{20.2}$$

20.2.2 Atlantis Ecosystem Model

Ecological effects of the different oil spill scenarios were simulated with the Atlantis ecosystem model of the GoM described in Ainsworth et al. (2015). Briefly, the spatially explicit biogeochemical end-to-end model divides the study

area into polygons, tracks flow of nitrogen through groups of species aggregated by niche and life history, and is coupled to a hydrodynamic model of currents, temperature, and salinity (Fulton et al. 2004, 2011; Ainsworth et al. 2015). The model has 91 functional groups and divides the GoM into 66 polygons, each with a sediment layer and up to six water column depth layers. Polygon geometry reflects physical processes, habitat, exploitation patterns, and management divisions. Atlantis sub-models calculate production, respiration, consumption, reproduction, and movement of functional groups based on pre-defined parameters (initial abundance, growth, vertical movement, seasonal migration, diet matrix, mortality, and fisheries catch).

We followed the approach of Ainsworth et al. (2018) to use the oil concentrations from the oil-CMS model and dose-response models developed by Dornberger et al. (2016) to estimate fish growth and mortality rates. Oil concentrations were integrated over the water column to match depth layers (partitioned at 10 m, 20 m, 50 m, 200 m, and 2000 m) in the Atlantis model. Emergency fisheries closures were implemented and updated on a daily basis as reported by the National Centers for Environmental Information (2016) (see Dornberger 2018 for additional information). Results from Atlantis functional groups were aggregated into eight guilds: snappers (Family: Lutjanidae), groupers (Family: Serranidae), Sciaenidae, elasmobranchs, large pelagic fish, small pelagic fish, small demersal and reef fish, and large demersal fish. Simulations operate on 12-hour time steps and were run for 20 years, starting on January 1, 2010.

20.2.3 Computation of Comparison Variables

Sedimented mass was computed as the cumulative mass of oil that sank to the sediment across the simulation span for a grid of 0.25 degree. Shoreline mass was computed as the mass (>10 kg) that reached grid cells with a depth shallower than 10 m. Shoreline length was computed by summing the edges' lengths of each grid cell that contained more than 10 kg of sedimented oil. For total oiled area, the maximum oil concentrations were computed across time and depth, obtaining a 2D matrix; then, all grid cells which contained oil concentrations higher than 1 ppb were considered as oiled area grid cells. Similarly, to compute the toxic area, the 2D matrix of maximum oil concentrations across time was transformed to PAH concentrations using Eqs. (20.1) and (20.2) for surface and water column. Then grid cells that had concentrations higher than the toxic thresholds were summed daily. For the computation of the total and toxic oil volumes, we used a similar method of that for the area, with the only difference that here the daily matrix of maximum oil concentrations was 3-D. From the Atlantis model, the guild-specific biomass loss, estimated years to guild recovery, and net guild biomass change after 20 years were considered as variables for comparison.

20.2.4 Comparison Between the Scenarios

To examine how the scenarios differ, we ranked their performance from the smallest to the largest effects (1–4) per each variable. To examine possible similarities and trade-offs between the different variables, we applied a pairwise Pearson correlation analysis.

20.3 Results

20.3.1 Spatial Extent of the Spill Scenarios

The oil spill extents demonstrate a wide footprint for all four scenarios, with DB_AL2 and DB_Fall extending across the widest area in the GoM. DB_AL2 provides the most substantial input to the Gulf Stream, while DB_AL3 extent is limited to the western part of the GoM, not reaching the WFS, and the Gulf stream. Sedimentation patterns (Fig. 20.1 lower panels) match the cumulative extents but with DB_AL2 demonstrating an exceptionally high extent of sedimentation due to the interaction of the DB_AL2 oil with a small anticyclonic eddy at the southern part of the Loop Current between days 20 and 45 after blowout (see video 20.1 in the Electronic Supplementary Material). In the other three scenarios, the oil did not interact with that eddy.

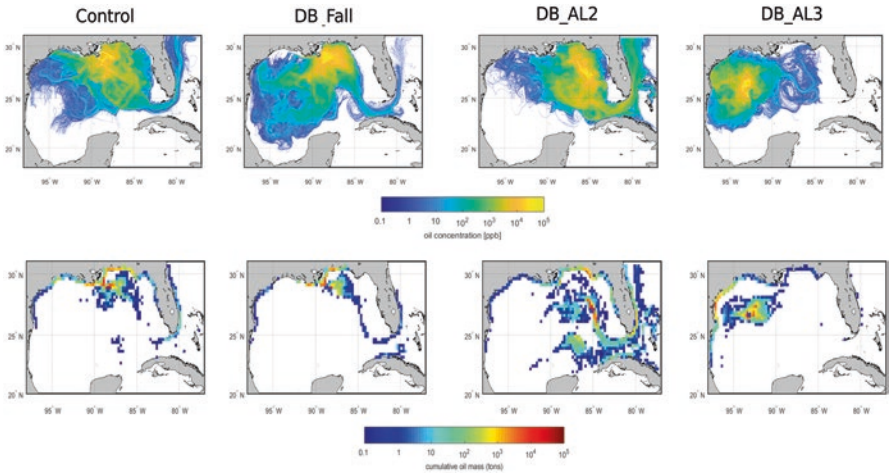

Fig. 20.1 Cumulative surface oil concentrations (upper panels) and cumulative sedimentation mass (lower panels) integrated across time for the four scenarios: DB_control, DB_FALL, DB_AL2, and DB_AL3

20.3.2 Oil-CMS Comparison Variables Across Time

The cumulative time-series plots demonstrate that there was no single scenario which had the strongest impact across all variables (Fig. 20.2). A few abrupt changes are evident across time. The increase in sedimented mass for the DB_control after day 15 and in shoreline oil mass around day 55 was a result of northerly wind-driven surface currents which pushed a substantial amount of oil toward the northern GoM coastal bathymetry (see animation in the Electronic Supplementary Material 20.1). Another increase in the sedimented mass, area, and shoreline length was observed around day 70–80 for the DB_control due to northerly surface currents associated with Hurricane Alex (Fig. 20.2, see animation in the Electronic Supplementary Material Image 20.1). The other scenarios were less affected by these winds as the oil location was further southward at that time (Fig. 20.1).

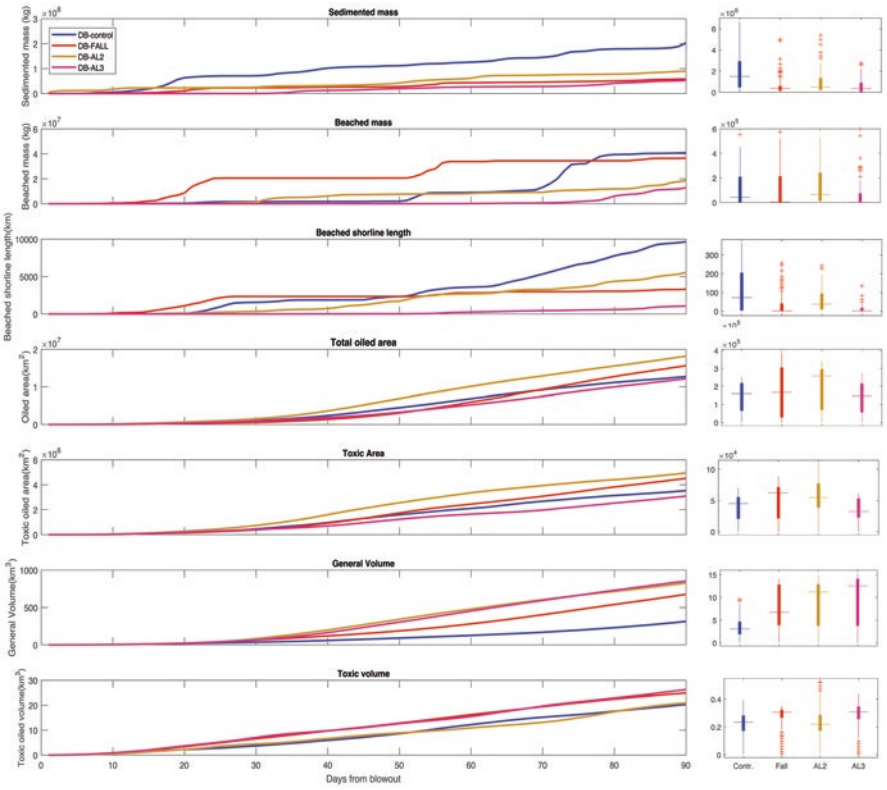

Fig. 20.2 Time series of cumulative sedimented mass, beached mass, oiled shoreline length, total sea area and volume affected by oil, sea area, and volume affected by toxic oil concentrations, for the four scenarios: DB_Control, DB_FALL, DB_AL2, and DB_AL3. Right panels are boxplots of the time series (noncumulative daily data)

Lastly, the relative low volume of oil in the water column for the DB_control is attributed to weak and circular currents across the water column, which retained the 3D extent of the oil, compared to the other scenarios, where directional currents resulted in higher 3D extents. From day 70 and onward, there is a substantial increase in oil spill volume of DB_control, following the strengthening of deep currents associated with Hurricane Alex (see animation in the Electronic Supplementary Material Image 20.2).

20.3.3 Atlantis Model Results

Atlantis simulations produced similar effects between the different scenarios with all the fish guilds having a significant decrease of biomass within the first year after the oil spill (Table 20.2). DB_AL2 scenario caused the most biomass decrease for most guilds. Between the different guilds, demersal fish guilds, both small and large, had the highest sensitivity to oil. Snappers were the least sensitive but, in the case of the DB_AL2 scenario, did not return to their original biomass and reached a new equilibrium with biomass 17% lower than the no-oil scenario at the end of the 20-year simulation. Biomass for the grouper guild did not recover in any scenario and reached a new equilibrium at 10–24% less biomass than the no-oil simulation. Sciaenidae, pelagic fish, and elasmobranchs had gradual and consistent biomass recovery, although the large pelagic and elasmobranchs had not fully recovered to within 99% of the no-oil biomass at the end of the 20-year simulations (Table 20.2).

20.3.4 Synthesis of Results

Overall, despite the spatial and temporal variation between the four scenarios, their outcome in terms of oil spill effects is rather similar. Still, DB_AL3 had the least impact, whereas DB_AL2 had the strongest impact (Table 20.3). Similarities and dissimilarities in ranks are evident across the variables, for example, DB_Control and DB_AL3 are first and last in terms of impact in sediment mass, beached mass, and shoreline length; and this trend reverses when we look at the volume variables, which is due to the fact that oil that was not sedimented is present in the water column.

20.4 Discussion

Our results demonstrate that had DWH occurred in other locations and time in the GoM, it would inflict impact in a similar scale compared to the actual DWH (Figs. 20.1 and 20.2). This is in agreement with the findings of Nelson and Grubesic

Table 20.2 Biomass change, relative to no-oil Atlantis simulation, for fish guilds under four oil spill scenarios

Fish guild		DB_ Control	DB_ Fall	DB_ AL2	DB_ AL3
Snappers	Minimum biomass (relative to no-oil)	71%	80%	69%	71%
	Years after spill to minimum biomass	0.58	0.58	0.58	0.58
	Years to 99% biomass recovery	DNR	7.70	DNR	DNR
	Net biomass change after 20 years	−4%	0	−17%	−5%
Large pelagic	Minimum biomass (relative to no-oil)	41%	44%	40%	44%
	Years after spill to minimum biomass	0.58	0.90	0.58	0.58
	Years to 99% biomass recovery	DNR	DNR	DNR	DNR
	Net biomass change after 20 years	−6%	−4%	−9%	−4%
Small demersal	Minimum biomass (relative to no-oil)	37%	37%	32%	41%
	Years after spill to minimum biomass	1.23	0.82	1.23	0.58
	Years to 99% biomass recovery	6.20	6.70	6.70	13.60
	Net biomass change after 20 years	−2%	0	−9%	−2%
Elasmobranchs	Minimum biomass (relative to no-oil)	54%	60%	54%	61%
	Years after spill to minimum biomass	0.99	0.58	0.99	0.99
	Years to 99% biomass recovery	DNR	20.30	DNR	DNR
	Net biomass change after 20 years	−9%	−1%	−11%	−5%
Groupers	Minimum biomass (relative to no-oil)	72%	72%	73%	70%
	Years after spill to minimum biomass	0.58	0.58	0.58	0.58
	Years to 99% biomass recovery	DNR	DNR	DNR	DNR
	Net biomass change after 20 years	−14%	−10%	−24%	−12%
Small pelagic	Minimum biomass (relative to no-oil)	62%	66%	59%	67%
	Years after spill to minimum biomass	0.58	0.58	0.58	0.58
	Years to 99% biomass recovery	10.00	10.20	3.70	3.50
	Net biomass change after 20 years	−2%	−2%	−2%	−1%
Sciaenidae	Minimum biomass (relative to no-oil)	58%	64%	59%	57%
	Years after spill to minimum biomass	0.58	0.58	0.58	0.58
	Years to 99% biomass recovery	6.60	6.80	DNR	7.00
	Net biomass change after 20 years	−1%	0	−3%	0%
Large demersal	Minimum biomass (relative to no-oil)	35%	45%	28%	36%
	Years after spill to minimum biomass	0.58	0.66	0.58	0.58
	Years to 99% biomass recovery	DNR	DNR	DNR	DNR
	Net biomass change after 20 years	−4%	−2%	−11%	−5%

DNR Did not recover

(2018a) which simulated spills at various locations across the WFS and found comparable results between their scenarios. The difference in spatial extents between the DB_AL3 and the rest of the scenarios also highlights the relative oceanographic isolation of the western GoM from the rest of the GoM (Miron et al. 2017), which has important implications for the oil spill dynamics and spatial extent (Fig. 20.1). Similarly, the DB_AL2 and the DB_ FALL scenarios highlight the difference in oil spill dynamics due to the variation in the Loop Current state (Fig. 20.1).

Table 20.3 (A) Rank table from least to most impactful (1–4, color coded green to red), for the tested scenarios and variables. (B) Rank (Pearson) correlation coefficients between the different variables in terms of scenarios' ranks, color coded from blue (negative) to red (positive)

(A)

	Sediment mass	Beached mass	Shoreline length	Oiled area	Toxic area	Oiled volume	Toxic volume	Min Biomass	Years to Min	Biomass Change	Mean
DB Cont.	4	4	4	2	2	1	1	3	3.5	3	2.8
DB FALL	1	3	2	3	4	2	3	1	2	1	2.2
DB AL2	3	2	3	4	3	3	2	4	3.5	4	3.2
DB AL3	2	1	1	1	1	4	4	2	1	2	1.9

(B)

	Sediment mass	Beached mass	Beached length	Oiled area	Toxic area	Oiled volume	Toxic volume	Min. Biomass	Years to min.
Beached mass	0.4								
Beached length	0.8	0.8							
Oiled area	0	0.2	0.4						
Toxic area	-0.4	0.4	0.2	0.8					
Oiled volume	-0.4	-1	-0.8	-0.2	-0.4				
Toxic volume	-0.8	-0.8	-1	-0.4	-0.2	0.8			
Min. Biomass	0.8	0	0.6	0.4	-0.2	0	-0.6		
Years to min.	0.7	0.6	0.9	0.6	0.3	-0.6	-0.9	0.7	
BiomassChange	0.8	0	0.6	0.4	-0.2	0	-0.6	1	0.7

Determining the relative importance of the different variables and their realistic effects is a complex task, concerning ecology, conservation, economics, and social sciences. These could be narrowed down to a few basic questions: Which assets are at risk? Which assets are more important? To whom? And how do we gauge the different effects on these assets? These questions, which do not have a single correct answer, are required to be addressed when considering drilling locations and are beyond the scope of current chapter. Ideally a comprehensive potential impact assessment includes vulnerability, risk, and direct and indirect impact analyses (Nelson and Grubesic 2018b). Vulnerability analysis normally quantifies the expected damage to shorelines following oiling and often includes environmental sensitivity index (ESI) considering the type of habitat or creating vulnerability scores considering environmental, economic, and social assets.

Here, we quantify and present a combination of geographic and ecological meaningful variables in a clear and reader-friendly manner, which facilitates an efficient use of data and results. In addition, we provide a simple comparison between these scenarios, which can highlight possible trends and trade-offs between the considered variables (Table 20.3). The ranking analysis used in this chapter does not explicitly indicate which scenario is worst but instead directs and focuses the reader on main trends in the spills comparison. While the results here indicate that DB_AL2 scenario is the most impactful, it is not necessarily the case in some perspectives. For example, for the groupers guild for DB_AL2 was actually the least damaging scenario in terms of minimum biomass relative to no-spill scenario (Table 20.2). Similarly, DB_AL2 exhibited the lowest volume of toxic oil concentrations but with very slight differences from the other scenarios (Fig. 20.2).

The results also demonstrate that while some variables are naturally positively correlated (e.g., coastline oiling mass vs. coastline oiling length; Table 20.3), other scenarios are negatively correlated (e.g., oiled volume vs. beached mass; Table 20.3B). This makes sense as the more oil there is in the open sea, the less oil is reaching the shores (Table 20.3). This means that the impact of the different scenarios should be discussed in the context of threatened assets and their value. For example to coastal communities, the degree of oiled shorelines is of greatest importance; however for the fisheries industry, the area impacted by toxic oil concentrations – which translates to fisheries closures – is perhaps of greater importance. Similarly, the toxic volume directly affects the number of pelagic organisms harmed including fish larvae and planktonic organisms which account for the basis of the food web.

This chapter advanced our understanding on how different locations and time of year may affect DWH-like oil spill outcome, and we present a user-friendly method of exploring these results and provide a preliminary ranking of the impact of the different scenarios. The coupling of the oil-CMS with the Atlantis model provides a powerful tool for assessing the impact of different oil spill scenarios, which could be useful for management purposes when planning future deep and ultra-deep drilling locations.

Funding Information This research was made possible by a grant from The Gulf of Mexico Research Initiative/C-IMAGE III, No. SA 18-16. Data are publicly available through the Gulf of Mexico Research Initiative Information & Data Cooperative (GRIIDC) at https://data.gulfresearchinitiative.org (doi: [10.7266/N7GM85C0, 10.7266/N76D5RCB, 10.7266/N7G44NQX, 10.7266/N7KD1WDB]).

References

Ainsworth CH, Schirripa MJ, Morzaria Luna HN (eds) (2015) An Atlantis ecosystem model for the northern Gulf of Mexico supporting integrated ecosystem management. U.S. Dept. Commer., NOAA Techical Memorandum NMFS-SEFSC-TM-676. https://doi.org/10.7289/V5X63JVH

Ainsworth CH, Paris CB, Perlin N, Dornberger LN, Patterson WF, Chancellor E, Murawski S, Hollander D, Daly K, Romero IC, Coleman F, Perryman H (2018) Impacts of the Deepwater Horizon oil spill evaluated using an end-to-end ecosystem model. PLoS One 13:e0190840. https://doi.org/10.1371/journal.pone.0190840

Beyer J, Trannum HC, Bakke T, Hodson P, Collier T (2016) Environmental effects of the Deepwater Horizon oil spill: a review. Mar Pollut Bull 110:28–51. https://doi.org/10.1016/j.marpolbul.2016.06.027

Boehm PD, Page DS (2007) Exposure elements in oil spill risk and natural resource damage assessments: a review. Hum Ecol Risk Assess Int J 13:418–448. https://doi.org/10.1080/10807030701226293

BOEM (2018) Offshore statistics by water depth. In: Leasing Data Center https://www.data.boem.gov/Leasing/OffshoreStatsbyWD/Default.aspx. Accessed 14 Aug 2018

Chassignet EP, Smith LT, Halliwell GR, Bleck R (2003) North Atlantic Simulations with the Hybrid Coordinate Ocean Model (HYCOM): impact of the vertical coordinate choice, reference pressure, and thermobaricity. J Phys Oceanogr 33:2504–2526. https://doi.org/10.1175/1520-0485(2003)033<2504:NASWTH>2.0.CO;2

De Gouw JA, Middlebrook AM, Warneke C, Ahmadov R, Atlas EL, Bahreini R, Blake DR, Brock CA, Brioude J, Fahey DW, Fehsenfeld FC, Holloway JS, Le Henaff M, Lueb RA, McKeen

SA, Meagher JF, Murphy DM, Paris C, Parrish DD, Perring AE, Pollack IB, Ravishankara AR, Robinson AL, Ryerson TB, Schwarz JP, Spackman JR, Srinivasan A, Watts LA (2011) Organic aerosol formation downwind from the Deepwater Horizon oil spill. Science (80-) 331:1295–1299. https://doi.org/10.1126/science.1200320

Deepwater Horizon Natural Resource Damage Assessment Trustees (2016) Deepwater Horizon oil spill: final programmatic damage assessment and restoration plan and final programmatic environmental impact statement. National Oceanic and Atmospheric Administration, Silver Spring

Dornberger L (2018) Using ecosystem-based modeling to describe an oil spill and assess the long-term effects. PhD Dissertation, University of South Florida, Tampa, 78 pp

Dornberger L, Ainsworth C, Gosnell S, Coleman F (2016) Developing a polycyclic aromatic hydrocarbon exposure dose-response model for fish health and growth. Mar Pollut Bull 109(1):259–266. https://doi.org/10.1016/j.marpolbul.2016.05.072

Fingas MF (2011) Oil spill science and technology : prevention, response, and clean up. Gulf Professional Pub./Elsevier, Burlington

Fulton EA, Parslow JS, Smith ADM, Johnson CR (2004) Biogeochemical marine ecosystem models II: the effect of physiological detail on model performance. Ecol Model 173(4):371–406. https://doi.org/10.1016/j.ecolmodel.2003.09.024

Fulton EA, Link JS, Kaplan IC, Savina-Rolland M, Johnson P, Ainsworth C, Horne P, Gorton R, Gamble RJ, Smith ADM, Smith DC (2011) Lessons in modelling and management of marine ecosystems: the Atlantis experience. Fish Fish 12(2):171–188. https://doi.org/10.1111/j.1467-2979.2011.00412.x

Gohlke JM, Doke D, Tipre M, Leader M, Fitzgerald T (2011) A review of seafood safety after the Deepwater Horizon blowout. Environ Health Perspect 119:1062–1069. https://doi.org/10.1289/ehp.1103507

Hazen T, Dubinsky E, DeSantis T (2010) Deep-sea oil plume enriches indigenous oil-degrading bacteria. Science 330:204–208

Jaggi A, Snowdon R, Stopford A, Radović J (2017) Experimental simulation of crude oil-water partitioning behavior of BTEX compounds during a deep submarine oil spill. Org Geochem 108:1–8. http://dx.doi.org/10.1016/j.orggeochem.2017.03.006

Lay CR, Morris JM, Takeshita R, Forth HP, Travers CL, Roberts AP, Alloy M, McFadden A, Garner TR, Overturf C (2015) The effect of ultraviolet (UV) radiation on the toxicity of Deepwater Horizon oil. Boulder, DWH Toxicity NRDA Technical Working Group Report

Le Hénaff M, Kourafalou VH, Paris CB, Helgers J, Aman ZM, Hogan PJ, Srinivasan A (2012) Surface evolution of the Deepwater Horizon oil spill patch: combined effects of circulation and wind-induced drift. Environ Sci Technol 46:7267–7273. https://doi.org/10.1021/es301570w

Lindo-atichati D, Paris CB, Le Henaff M (2016) Simulating the effects of droplet size, high-pressure biodegradation, and variable flow rate on the subsea evolution of deep plumes from the Macondo blowout. Deep Sea Res Part II 129:301–310. https://doi.org/10.1016/j.dsr2.2014.01.011

Lubchenco J, McNutt MK, Dreyfus G, Murawski SA, Kennedy DM, Anastas PT, Chu S, Hunter T (2012) Science in support of the Deepwater Horizon response. Proc Nat Acad Sci USA 109:20212–20221. https://doi.org/10.1073/pnas.1204729109

Miron P, Beron-Vera FJ, Olascoaga MJ, Sheinbaum J, Pérez-Brunius P, Froyland G (2017) Lagrangian dynamical geography of the Gulf of Mexico. Sci Rep 7:7021. https://doi.org/10.1038/s41598-017-07177-w

NCEI (2016) Fisheries closures: Deepwater Horizon support. National Centers for Environmental Information. National Oceanic and Atmospheric Administration. Accessed Sept 2016

Nelson JR, Grubesic TH (2018a) The implications of oil exploration off the Gulf Coast of Florida. J Mar Sci Eng 6:30. https://doi.org/10.3390/jmse6020030

Nelson JR, Grubesic TH (2018b) Oil spill modeling. Prog Phys Geogr: Earth Environ 42:112–127. https://doi.org/10.1177/0309133317744737

Office of Response and Restoration (2012). http://sero.nmfs.noaa.gov/deepwater_horizon/documents/pdfs/fact_sheets/historical_spills_gulf_of_mexico.pdf. Accessed 14 Aug 2018

Osofsky HJ, Osofsky JD, Hansel TC (2011) Deepwater Horizon oil spill: mental health effects on residents in heavily affected areas. Disaster Med Public Health Prep 5:280–286. https://doi.org/10.1001/dmp.2011.85

Overton E, Wade T, Radovic J, Meyer B, Miles MS, Larter S (2016) Chemical composition of Macondo and other crude oils and compositional alterations during oil spills. Oceanography 29:50–63. https://doi.org/10.5670/oceanog.2016.62

Paris CB, Le Hénaff M, Aman ZM, Subramaniam A, Helgers J, Wang DP, Kourafalou VH, Srinivasan A (2012) Evolution of the Macondo well blowout: simulating the effects of the circulation and synthetic dispersants on the subsea oil transport. Environ Sci Technol 46:13293–13302. https://doi.org/10.1021/es303197h

Paris CB, Helgers J, Van Sebille E, Srinivasan A (2013) Connectivity modeling system: a probabilistic modeling tool for the multi-scale tracking of biotic and abiotic variability in the ocean. Environ Model Softw 42:47–54. https://doi.org/10.1016/j.envsoft.2012.12.006

Perlin N, Paris CB, Berenshtein I, Vaz AC, Faillettaz R, Aman ZM, Schwing PT, Romero IC, Schlüter M, Liese A, Noirungsee N, Hackbusch S (2020) Far-field modeling of a deep-sea blowout: sensitivity studies of initial conditions, biodegradation, sedimentation and subsurface dispersant injection on surface slicks and oil plume concentrations (Chap. 11). In: Murawski SA, Ainsworth C, Gilbert S, Hollander D, Paris CB, Schlüter M, Wetzel D (eds) Deep oil spills – facts, fate and effects. Springer, Cham

Schedler M, Hiessl R, Valladares Juárez AG, Gust G, Müller R (2014) Effect of high pressure on hydrocarbon-degrading bacteria. AMB Express 4:77. https://doi.org/10.1186/s13568-014-0077-0

Smith T (2010) GOM: More Giant Oil Discoveries. GeoExPro: 62. https://www.geoexpro.com/magazine/vol-7-no-2. Accessed 18 Sep 2018

Socolofsky SA, Adams EE, Sherwood CR (2011) Formation dynamics of subsurface hydrocarbon intrusions following the Deepwater Horizon blowout. Geophys Res Lett 38. https://doi.org/10.1029/2011GL047174

Sumaila UR, Cisneros-Montemayor AM, Dyck A, Huang L, Cheung W, Jacquet J, Kleisner K, Lam V, McCrea-Strub A, Swartz W, Watson R, Zeller D, Pauly D (2012) Impact of the *Deepwater Horizon* well blowout on the economics of US Gulf fisheries. Can J Fish Aquat Sci 69:499–510. https://doi.org/10.1139/f2011-171

U.S. Energy Information Administration (2018) Residential consumption report. http://www.eia.gov/consumption/residential/reports/electronics.cfm. Accessed 10 Aug 2018

U.S. Department of the Interior. 2018. Secretary Zinke Announces Plan For Unleashing America's Offshore Oil and Gas Potential | U.S. Department of the Interior. https://www.doi.gov/press-releases/secretary-zinkeannounces-plan-unleashing-americas-offshore-oil-and-gas-potential. Accessed 18 Sep 2018

Zheng L, Yapa PD, Chen F (2003) A model for simulating deepwater oil and gas blowouts – Part I: theory and model formulation. J Hydraul Res 41:339–351. https://doi.org/10.1080/00221680309499980

Chapter 21
A Predictive Strategy for Mapping Locations Where Future MOSSFA Events Are Expected

Albertinka J. Murk, David J. Hollander, Shuangling Chen, Chuanmin Hu, Yongxue Liu, Sophie M. Vonk, Patrick T. Schwing, Sherryl Gilbert, and Edwin M. Foekema

Abstract A MOSSFA (marine oil snow sedimentation and flocculent accumulation) event was the reason that substantial amounts of the spilled oil were transported to the seafloor during the *Deepwater Horizon* (DWH) oil well blowout. The region-wide sinking and flocculent accumulation of marine oil snow on the sediment surface changed redox conditions, slowed down the biodegradation of the oil, and increased the spatial and temporal impacts on the benthic community and habitat suitability. Recent field research has confirmed that, in addition to the DWH MOSSFA event in the northern Gulf of Mexico (nGoM), another extensive MOSSFA event occurred in a biologically sensitive area in the southern Gulf of Mexico (sGoM) during the 1979–1980 Ixtoc 1 oil well blowout. Thus, MOSSFA events are not unexpected and have the potential to not only alter sediment chemical conditions but also to extend, expand, and intensify the ecological impact of an oil spill. Consequently this risk should be taken into consideration when preparing response

A. J. Murk (✉) · S. M. Vonk
Wageningen University, Wageningen University & Research, Marine Animal Ecology Group, Wageningen, The Netherlands
e-mail: tinka.murk@wur.nl; sophie_vonk@hotmail.com

D. J. Hollander · S. Chen · C. Hu · P. T. Schwing · S. Gilbert
University of South Florida, College of Marine Science, St. Petersburg, FL, USA
e-mail: davidh@usf.edu; shuangling@mail.usf.edu; huc@usf.edu; pschwing@mail.usf.edu; sherryl@usf.edu

Y. Liu
Nanjing University, Department of Geographic Information Science, Nanjing, Jiangsu Province, People's Republic of China
e-mail: yongxue@nju.edu.cn

E. M. Foekema
Wageningen University, Wageningen University & Research, Marine Animal Ecology Group, Wageningen, The Netherlands

Wageningen Marine Research, Wageningen University & Research, Den Helder, The Netherlands
e-mail: edwin.foekema@wur.nl

S. A. Murawski et al. (eds.), *Scenarios and Responses to Future Deep Oil Spills*,
https://doi.org/10.1007/978-3-030-12963-7_21

strategies for potential future oil spills and subsurface oil well blowouts. To illustrate this approach, MOSSFA-sensitive areas were identified in offshore areas where deepwater oil production and exploration are occurring. Based on the newly gained insights into the factors that can initiate and contribute to a MOSSFA event, global maps showing the presence of oil/gas platforms, phytoplankton biomass, and suspended mineral matter are developed in order to infer the probability that future MOSSFA events are likely to occur. These maps are of particular importance for oil spill responders who will be deciding locations and which oil spill response strategies (i.e., applying large volumes of dispersants, burning in situ burnings, increasing riverine inputs of nutrients, and fine-grained clay particles) would result in the development of a MOSSFA event.

Keywords MOSSFA · DWH · Ixtoc 1 · Prediction · Satellite imagery · Oil spill response

21.1 Introduction: Marine Oil Snow Sedimentation and Flocculent Accumulation (MOSSFA)

The pervasive assumption prior to the *Deepwater Horizon* (DWH) event was that spilled oil, with a density lower than water, forms floating layers on the water surface and that direct sediment contamination mainly occurs when the oil is washed ashore due to wave activity, wind direction, and/or tidal movement. Other mechanisms leading to oil sedimentation require that the oil changes its physical-chemical characteristics (evaporation or burning of lighter oil fractions, oil weathering) or has direct interaction with negatively buoyant particles (particulate matter from rivers, atmosphere, melting ice, or suspended sediments) and oil sedimentation via contaminated zooplankton fecal pellets (Passow and Ziervogel 2016 and references therein). An exhaustive review of over 50 large marine oil spills by Vonk et al. (2015) found that oil contamination on the seafloor was not considered a significant response concern at these spill sites and thus sedimentary oil was never adequately addressed. From this perspective, it is logical that benthic impact and recovery on the seafloor after oil spills received comparatively little attention in the past.

This earlier thinking was in stark contrast to the DWH events where significant amounts of oil sedimentation were described and observed during and after the DWH event (cf. Daly et al. 2016; Passow and Hetland 2016; Quigg et al. 2020). One of the legacy lessons learned from the DWH oil spill was that in certain circumstances a substantial fraction of spilled oil can reach the seafloor at great depths and cause significant and prolonged benthic community impacts (Montagna et al. 2013; Valentine et al. 2014; Chanton et al. 2015; Romero et al. 2015, 2017; Baguley et al. 2015; Washburn et al. 2017; Schwing et al. 2015, 2017a, b, 2018a, b; Schwing and Machain-Castillo 2020). This chapter first defines a MOSSFA event and identifies some of the critical components and processes needed for marine oil snow (MOS) formation. We then demonstrate that the DWH MOSSFA event was not unique but

also occurred during the 1979–1980 Ixtoc 1 blowout in the Bay of Campeche in the southern Gulf of Mexico (sGoM) (Schwing et al. 2020). We further discuss how MOSSFA events cause chemical changes in the sediments and long-term impacts to the benthic biological communities. This chapter then focuses on using satellite imagery to develop a predictive tool for evaluating, in active petroleum exploration areas around the globe, where MOSSFA events could likely occur. Taking into consideration the location of potential MOSSFA events can provide first responders with critical information to determine the best response strategy in case of large future oil spills and oil well blowouts.

21.2 Marine Oil Snow (MOS) Formation, Sedimentation, and Benthic Impacts

In an attempt to keep oil released from the DWH oil well blowout offshore, Mississippi River diversionary channels were opened (Bianchi et al. 2014). The input of nutrients to the offshore regions resulted in widespread phytoplankton blooms (Hu et al. 2011). The continuous Mississippi River outflow (regardless of diversionary channels) also delivered fine-grained terrigenous sediments throughout much of the area affected by surface oil during the DWH oil well blowout. Simultaneously, field-based studies around the surface oiled regions identified the widespread production and sinking of a mucilaginous and sticky material (extracellular polymeric substances (EPS)) that was produced as a toxic stress response to the presence of oil by blooming organisms (cf. Passow et al. 2012; Daly et al. 2016; Quigg et al. 2020). The large amounts of this MOS observed during the DWH spill were thought to be predominantly from oil-degrading bacteria, phytoplankton, and zooplankton and their interaction with weathered oil (Passow et al. 2012; Daly et al. 2016; Quigg et al. 2020). Another process of EPS production has also been observed in experimental studies when marine phytoplankton are exposed to dispersants only, in the absence of oil (Van Eenennaam et al. 2016). This further supports that the application of dispersants, if not essential, could help to facilitate the formation of EPS. These scenarios of EPS production created a situation where excess organic matter and oil together with clay-sized particles/mineral phases led to the widespread coagulation and aggregation and sinking of MOS (Passow and Hetland 2016; Daly et al. 2016; Quigg et al. 2020).

The rapid sinking of MOS and its accumulation over a significant area of the seafloor in the northern Gulf of Mexico (nGoM) was one of the unexpected events associated with the DWH oil spill (Valentine et al. 2014; Chanton et al. 2015; Brooks et al. 2015; Romero et al. 2015, 2017; Schwing et al. 2017b; Stout and German 2015; Brooks et al. 2015; Yan et al. 2016; Larson et al. 2020). The existence of a new mechanism for oil sedimentation, termed MOSSFA, led to many new lines of research and discovery focused on MOS formation, chemical characterization and distribution of sedimentary oil, and changes to sedimentary chemical environments and their impacts on benthic biological communities (cf. Daly et al. 2016).

The recognition that a MOSSFA event would manifest itself as a large sediment depositional event covering over thousands of square kilometers was one of the critically important findings of the Gulf of Mexico Research Initiative (GoMRI) studies of the DWH event (Valentine et al. 2014; Chanton et al. 2015; Brooks et al. 2015; Romero et al. 2015, 2017; Schwing et al. 2017b; Yan et al. 2016; Larson et al. 2020).

With vast amounts of MOS deposited on the seafloor, significant impacts are expected to a broad range of benthic organisms including infauna and epifauna and potentially demersal fish populations (Montagna et al. 2013; Valentine et al. 2014; Murawski et al. 2014; Chanton et al. 2015; Romero et al. 2015, 2017; Baguley et al. 2015; Washburn et al. 2017; Schwing et al. 2015, 2017a, b, 2018a, b, Schwing and Machain-Castillo 2020; Fisher et al. 2016). Significant amounts of labile organic matter will accelerate the sediment microbial decomposition and result in rapid changes to sediment redox conditions leading to the development and intensification of low-oxygen and anaerobic chemical environments (Hastings et al. 2016, 2020). Although oiling of the sedimentary environments can directly cause a toxic response, simultaneous changes brought on by excess sedimentation and the onset of anaerobic (oxygen depleted) conditions can lead to devastating impacts to all benthic organisms. The onset of anaerobic conditions will further reduce oil and organic matter decomposition rates and, thus, increase the time that the benthic environments will be impaired. Benthic ecosystem experimental studies that simulate oil, excess organic matter, and lithogenic sediment deposition show that rapid development of low-oxygen conditions results in slower oil degradation rates and significant benthic community impacts (Rahsepar et al. 2016; Van Eenennaam et al. 2018; Foekema et al. 2020; Langenhoff et al. 2020). Less mobile benthic organisms such as foraminifera and bivalves are not able to escape, while the larger burrowing organisms, such as worms, die and are unable to bioturbate the sediments further slowing benthic system habitat recovery (Van Eenennaam et al. 2018; Schwing et al. 2018a). Long-term studies of redox conditions in the nGoM sediments have revealed that DWH postdepositional sedimentary chemical environments remained anaerobic for a minimum of 3 years (Hastings et al. 2016). It has taken 3–5 years since the DWH MOSSFA event before a more region-wide recovery occurred (Hastings et al. 2016, 2020; Schwing et al. 2018b; Schwing and Machain-Castillo 2020).

21.3 Was the DWH MOSSFA Event Unique?

A natural question would be: did MOSSFA events occur in the past and can they be predicted in the future? Based on the meta-analysis of 51 large historical oil spills, Vonk et al. (2015) suggested that another blowout had the critical conditions and components for a MOSSFA event: the Ixtoc 1 blowout in the sGoM from 1979 to 1980. The Bay of Campeche in the sGoM is a sensitive biological region, fed seasonally by a river system containing abundant fine-grained clay mineral and is an

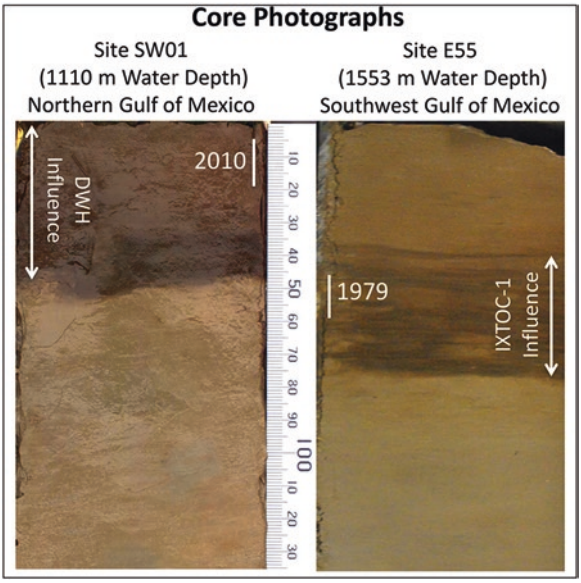

Fig. 21.1 Sediment core photographs comparing records (site SW01, collected at 1110 m water depth, photo credit: Rebekka Larson) from the northern Gulf of Mexico and the southern Gulf of Mexico (site E55, collected at 1553 m water depth, photo credit: Maria Machain). The white arrows are the depth interval influenced by the *Deepwater Horizon* event in the northern Gulf of Mexico and by Ixtoc 1 in the southern Gulf of Mexico, respectively. The white lines are the depth interval corresponding to the year 2010 in the northern Gulf of Mexico and 1979 in the Southern Gulf of Mexico, respectively, determined by short-lived radioisotope chronology (Brooks et al. 2015; Sanchez-Cabeza 2016). Influences seen above and below the actual date of each event are due to carbon loading, redox processes, and redeposition. (Copied from Schwing et al. 2020)

area of extensive oil production and deepwater exploration (Gracia et al. 2013; Murawski et al. 2018). Initiated by the insights from the DWH research, sediment cores were collected from the surrounding area where the Ixtoc 1 oil spill took place 40 years earlier (Fig. 21.1). A comparison between cores from the nGoM and the sGoM strongly suggests that a MOSSFA event occurred during both the Ixtoc 1 and the DWH spills (Schwing et al. 2020). The sediment in both cores document coeval redox changes (Hastings et al. 2016, 2020) and a sharp decline in benthic foraminifera diversity and abundance (Machain-Castillo et al. unpublished). Apparently the oiled layer was never mixed with younger sediment layers, as would normally happen by bioturbation (Fig. 21.1). It was not until a thick enough new layer of uncontaminated sediment had been deposited on the oiled layer, a process of years to decades, that the benthic life could recolonize the sediment. The analysis of benthic foraminifera from the Ixtoc 1 impacted sites shows that recovery took about 3–7 years, similar to that observed during the DWH MOSSFA event in the nGoM (Machain-Castillo et al. in review; Schwing and Machain-Castillo 2020). The comparison between the DWH and Ixtoc 1 events document that MOSSFA events are preserved in the sediment record, that they are not unique to the nGoM, and that MOSSFA events can potentially be predicted.

21.4 Mapping of Conditions Needed to Predict Future MOSSFA Events

High phytoplankton densities and suspended mineral particles (such as clay) should be present in sufficient amounts in the water column to give the oiled marine snow complexes the negative buoyancy that facilitates settlement. Riverine input forms the most continuous source of such particles, but also clay from melting ice or atmospheric dust input could possibly make the oiled snow complexes sink. Based on these insights it is possible to identify areas that, perhaps for a certain time period of the year, can be considered vulnerable for a MOSSFA event in the case of a large oil spill.

Where the analyses of Vonk et al. (2015) concluded that it is very likely that MOSSFA events have occurred unnoticed during a number of historic oil spills, this chapter aims to forecast the vulnerability of potential future oil spill locations (worldwide) for a MOSSFA event. This exercise will be done by combining indications of critical environmental conditions and oil production regions based on global maps, as an example of how this could be approached in more detail by responsible local institutes.

MOSSFA events are likely to occur in locations and periods when biological processes are active (to facilitate formation of marine snows) and inorganic particulate matter are abundant (to facilitate sinking of marine snows). We used satellite-derived data products to determine the optimal locations meeting these conditions. Specifically, MODIS/Aqua global data products from the period of July 2002 to August 2018 were used to create global maps of phytoplankton biomass expressed as chlorophyll concentration (Chl, mg m^{-3}), and the concentration of suspended mineral matter expressed as particulate inorganic carbon (PIC, mol m^{-3}) (Fig. 21.2).

Only <10% of the global oceans have surface Chl > 0.5 mg m^{-3} and was therefore selected as a threshold, above which the water is regarded as being biologically active. Because biological activity is expected to be different between growth period and decaying period, a derivative analysis was carried out for each location to

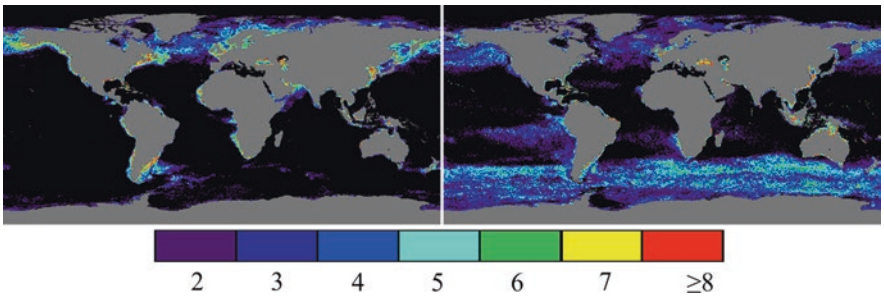

Fig. 21.2 Total number of months of chlorophyll (Chl, left) and particulate inorganic carbon (PIC, right) exceeding the predefined thresholds in both growth periods of a climatological year, based on MODIS data between July 2002 and August 2018 binned to 0.5-degree grids

determine whether the location meeting the >0.5 mg m^{-3} criteria is during a growth period (i.e., positive derivative value). In many locations there are two growth periods, and both were counted in statistics. To remove speckle noise, the original 9-km data were binned to 0.5° resolution. Figure 21.2 (left) shows the total number of months of MODIS Chl exceeding the 0.5 mg m^{-3} during a climatological year. Note that because MODIS Chl in productive waters was estimated using an empirical algorithm to convert the ratio of blue/green reflectance to Chl (O'Reilly et al. 2000), the data product also contains information on colored dissolved organic matter and non-phytoplankton particles because they both impact the blue/green reflectance ratio.

Abundant particulate inorganic particles can facilitate sinking of marine snow. Unfortunately there is no such satellite data product to provide this information. The best proxy is perhaps the particulate inorganic carbon (PIC) data product, derived from MODIS/Aqua measurements using combined algorithms of Gordon et al. (2001) and Balch et al. (2005) where both empirical lookup tables (LUTs) and semi-analytical inversions are used to convert the spectral reflectance to PIC concentrations. For PIC the threshold was determined as the mean PIC value within a 1 × 1 degree box centered at the DWH site from daily MODIS images in the month before the oil spill (March 20 to April 19, 2010). Above this threshold of 7.12×10^{-5} mol m^{-3}, the condition is regarded as being optimal for particle sinking (i.e., formation of MOSSFA). Figure 21.2 (right) shows the total number of months within a year during which PIC exceeded this predefined threshold.

The maps (Fig. 21.2) show that phytoplankton blooms occur for at least 50% of the time along the majority of the coasts of the northern hemisphere, including the cold waters near Alaska and Siberia. At the southern hemisphere, algal blooms are less frequent in general. At specific locations, however, like the West coasts of Africa and around the southern tip of America, elevated phytoplankton densities can be found for at least 6 months per year.

PIC concentrations are above the estimated threshold level for about 5 months a year in the whole lower half of the southern hemisphere and for a longer period just along the coastlines. Especially along the coasts of Southeast Asia and Northern Australia, PIC thresholds are exceeded during a major part of the year. In the northern hemisphere, PIC thresholds are in general less often exceeded, with exception of the European North Sea and the waters near Alaska.

21.5 Mapping Sites of Potential MOSSFA Events with Active Deep-Sea Oil Exploration and Production

Ideally, a compiled database of global distributions of oil/gas platforms can provide critical information on potential oil spills. However, such a database simply does not exist due to lack of coordinated efforts across political boundaries. Therefore, platform locations have been determined from remote sensing data using the

time-series remote sensing (TSRS) approach detailed in Liu et al. (2018). Briefly, tens of thousands of medium-resolution optical and radar images have been used to determine temporally persistent anomalies over the same locations and determined to be a fixed platform. The uncertainties were generally <10%. Figure 21.3 shows the density of offshore platforms on a global scale.

Unlike accidents with oil tankers or broken oil pipelines, deep-sea oil production areas are at risk for MOSSFA events because blowout scenarios are likely to result in longer lasting and high volume spills. Four subregions are indicated in Fig. 21.3 where both a high platform density and deep water nearby are present. In these subregions, deepwater drilling already takes place or is likely to start in the near future. For each of these subregions, detailed graphs (Figs. 21.4, 21.5, 21.6, and 21.7) are plotted to discuss the sensitivity of that area for a MOSSFA event. Be aware that these graphs are presented only as a demonstration of the concept and assumes that the Chl and PIC data that were used are indeed a good proxy for phytoplankton biomass and suspended mineral matter in the water column.

1. Gulf of Mexico (Fig. 21.4): Especially along the northern coast, including the area of the DWH spill, Chl and PIC are above the threshold for more than 6 months per year indicating a high sensitivity for a MOSSFA event.
2. East coast of South America (Fig. 21.5): PIC thresholds are regularly exceeded, but exceedance of the Chl threshold seems less frequent. This could indicate a moderate sensitivity for a MOSSFA event but, given the high density of suspended mineral particles sedimentation of oil, could still occur without marine snow formation.

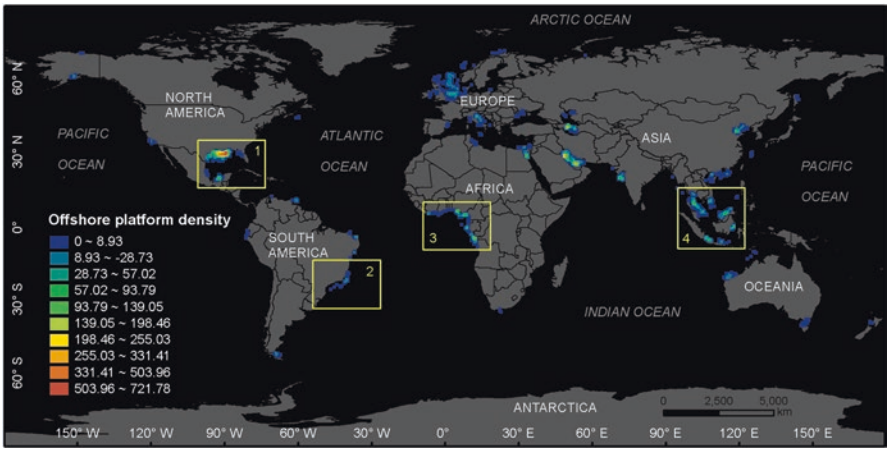

Fig. 21.3 Oil/gas platform density generated from satellite data. Yellow boxes indicate sub regions with high offshore activity where deepwater oil exploration is in progress or can be expected in the near future. For these four regions, the MOSSFA risk information is shown in more detail in Figs. 21.4, 21.5, 21.6, and 21.7

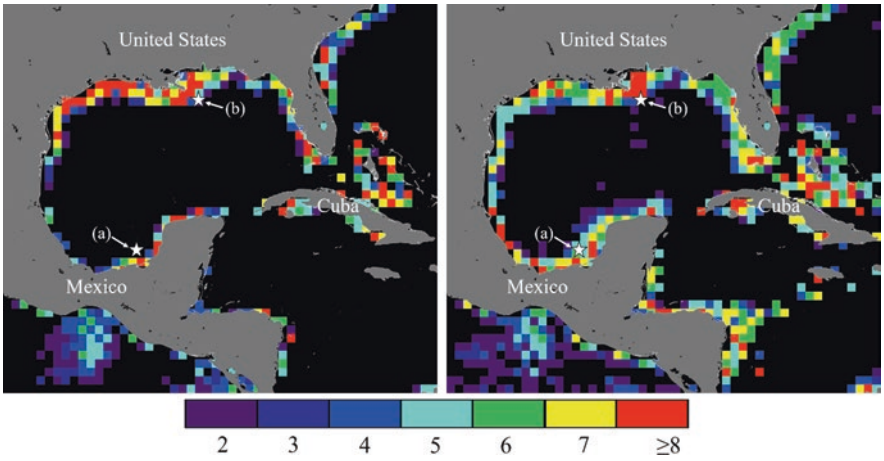

Fig. 21.4 Total number of months of Chl (left) and PIC (right) exceeding the predefined thresholds in both growth periods of a climatological year in subregion 1 of Fig. 21.2 (11.0°N~34.2°N, 100.0°W~74.0°W). The two proven MOSSFA locations are indicated with a letter: Ixtoc 1 (**a**) and DWH (**b**)

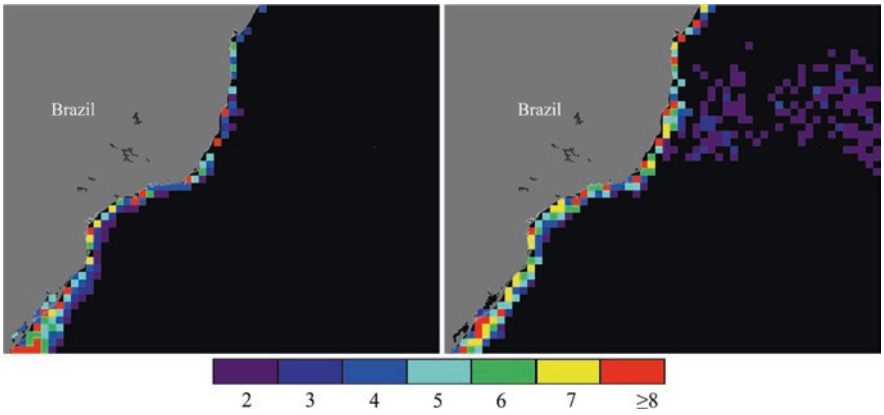

Fig. 21.5 Total number of months of Chl (left) and PIC (right) exceeding the predefined thresholds in both growth periods of a climatological year in subregion 2 of Fig. 21.2 (34.3°S~11.0°S, 54.2°W~25.0°W)

3. West coast of Africa (Fig. 21.6): Local algal blooming occurs frequently, but PIC threshold levels are only rarely exceeded. A MOSSFA event is not likely to occur under these circumstances. The phytoplankton can be induced to produce EPS, but given the lack of mineral particles, the oiled EPS will probably stay buoyant.
4. Malaysia (Fig. 21.7): Especially the PIC threshold, but also Chl threshold, is frequently exceeded. This makes this region sensitive for a MOSSFA event.

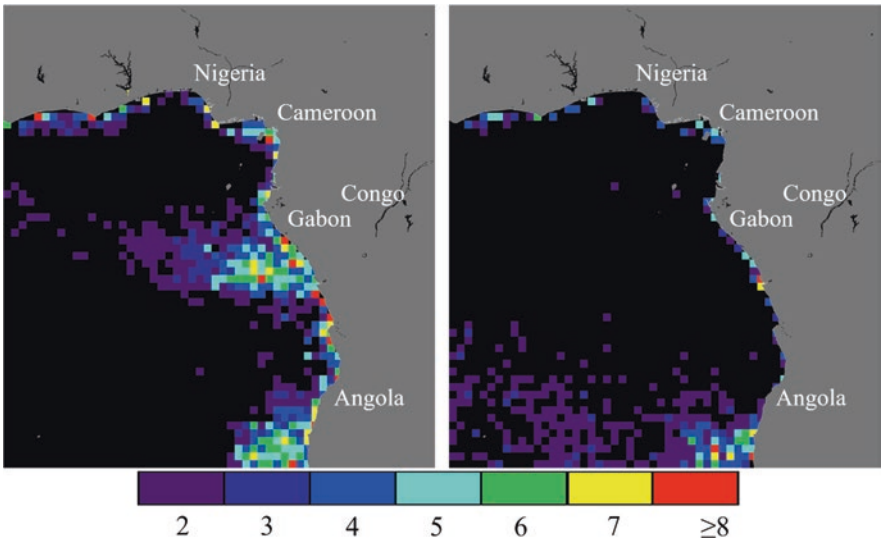

Fig. 21.6 Total number of months of Chl (left) and PIC (right) exceeding the predefined thresholds in both growth periods of a climatological year in subregion 3 of Fig. 21.2 (18.0°S~12.0°N, 8.0°W~20.0°E)

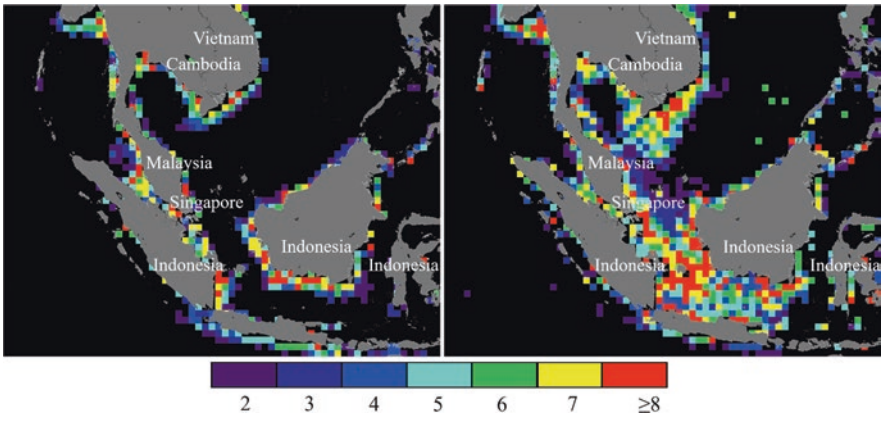

Fig. 21.7 Total number of months of Chl (left) and PIC (right) exceeding the predefined thresholds in both growth periods of a climatological year in subregion 4 of Fig. 21.2 (9.5°S~17.0°N, 90.0°E~123.0°E)

21.6 Conclusions and Implications

As mentioned earlier, the outcome of the analyses of the four subregions should only be considered as a demonstration of the concept. In order to assess the actual MOSSFA sensitivity of an area, more detailed information should be obtained about

the vital phytoplankton biomass, proximity of river systems, concentration of suspended mineral matter in the water column, and additional relevant factors such as local currents, climate patterns, and rainfall. In addition the threshold levels still need to be validated, both in general regional terms and specifically for the local conditions including phytoplankton species and mineral type. The intensity of EPS formation may also vary depending on the circumstances, like temperature, light intensity, and nutrient availability that both directly affect the phytoplankton community and the likelihood of EPS formation by their symbiotic bacteria.

Despite these current uncertainties, we believe that the approach used can help to create awareness about the fact that some regions may require alternative response strategies that limit MOS formation and avoid potential MOSSFA events. In potentially MOSSFA-prone areas, the actual local conditions should be included in oil fate modeling to assist the decision-makers (e.g., dispersant application, modifying river discharge). Moreover, this approach may find that it is necessary to prepare alternative oil spill response options. This could include scenarios of (1) limited in situ burning, dispersant application and freshwater discharge; (2) intensifying mechanical cleanup; (3) use of alternative chemical oil spill response approaches (Tamis et al. 2011) such as oil gelling or solidifying agents, oil herding agents, de-emulsfifiers, sorbents, and booms; or (4) having no response as the best option (Zeinstra-Helfrich et al. 2015, 2017). It has been shown in several cases that surface dispersant application may have actually increased the oil-polluted surface area while not enhancing oil dispersion (Zeinstra-Helfrich et al. 2015, 2016, 2017).

Finally we want to note that based on our general maps, the Arctic region could be extremely sensitive to a MOSSFA event. The impact of a large-scale MOSSFA event in the Arctic (at the scale of the DWH spill) would likely be more long lasting as the temperatures are lower and biodegradation rates slower. Also the Arctic food chain could be at risk due to its dependence on a healthy benthic ecosystem. Although arctic conditions are unlike those in the GoM, where MOSSFA was first identified, it is advisable to study the potential risk of an Arctic MOSSFA event and to include this risk in oil spill response planning before starting large-scale oil exploration and production.

Acknowledgments This research was made possible by a grant from the Gulf of Mexico Research Initiative/C-IMAGE III. Data from Figs. 21.2–21.7 are currently not available through GRIIDC.

References

Baguley J, Montagna P, Cooksey C, Hyland JL, Bang HW, Morrison C, Kamikawa A, Bennetts P, Saiyo G, Parsons E, Herdener M, Ricci M (2015) Community response of deep-sea soft-sediment metazoan meiofauna to the Deepwater Horizon blowout and oil spill. Mar Ecol Prog Ser 528:127–140. https://doi.org/10.3354/meps11290

Balch WM, Gordon HR, Bowler BC, Drapeau DT, Booth ES (2005) Calcium carbonate measurements in the surface global ocean based on moderate-resolution imaging spectroradiometer data. J Geophys Res 110:C07001. https://doi.org/10.1029/2004JC002560

Brooks GR, Larson RA, Schwing PT, Romero I, Moore C, Reichart GJ, Jilbert T, Chanton JP, Hastings DW, Overholt WA, Marks KP, Kostka JE, Holmes CW, Hollander D (2015) Sediment pulse in the NE Gulf of Mexico following the 2010 DWH blowout. PLoS One 10(7):e0132341. https://doi.org/10.1371/journal.pone.0132341

Bianchi TS, Osburn C, Shields MR, Yvon-Lewis S, Young J, Guo L, Zhou L (2014) Deepwater horizon oil in Gulf of Mexico waters after 2 years: transformation into the dissolved organic matter pool. Environ Sci Technol 48(16):9288–9297. https://doi.org/10.1021/es501547b

Chanton J, Zhao T, Rosenheim BE, Joye S, Bosman S, Brunner C, Hollander D (2015) Using natural abundance radiocarbon to trace the flux of petrocarbon to the seafloor following the Deepwater Horizon oil spill. Environ Sci Technol 49:847–854

Daly KL, Passow U, Chanton J, Hollander D (2016) Assessing the impacts of oil-associated marine snow formation and sedimentation during and after the Deepwater Horizon oil spill. Anthropocene 13:18–33. https://doi.org/10.1016/j.ancene.2016.01.006

Fisher CR, Montagna PA, Sutton TT (2016) How did the Deepwater Horizon oil spill impact deep-sea ecosystems? Oceanography 29(3):182–195. https://doi.org/10.5670/oceanog.2016.82

Foekema EM, van Eenennaam JS, Hollander DJ, Langenhoff AM, Oldenburg TBP, Radović JR, Roha M, Romero IC, Schwing PT, Murk AJ (2020) Testing the effect of MOSSFA (marine oil snow sedimentation and flocculent accumulation) events in benthic microcosms (Chap. 17). In: Murawski SA, Ainsworth C, Gilbert S, Hollander D, Paris CB, Schlüter M, Wetzel D (eds) Scenarios and responses to future deep oil spills – fighting the next war. Springer, Cham

Gordon HR, Boynton GC, Balch WM, Groom SB, Harbour DS, Smyth TJ (2001) Retrieval of coccolithophore calcite concentration from SeaWiFS imagery. Geophys Res Lett 28(8):1587–1590

Gracia A, Enciso Sánchez G, Alexander Valdés HM (2013) Composición y volúmen de contaminantes de las descargas costeras al Golfo de México. In: Botello AV, Rendón von Osten J, Benítez J, Gold-Boucht G (eds) Golfo de México. Contaminación e impacto ambiental: diagnóstico y tendencias. uac, unam-icmyl, cinvestav-Unidad Mérida

Hastings DW, Schwing PT, Brooks GR, Larson RA, Morford JL, Roeder T, Quinn KA, Bartlett T, Romero IC, Hollander DJ (2016) Changes in sediment redox conditions following the BP DWH Blowout event. Deep-Sea Res II 129:167. https://doi.org/10.1016/j.dsr2.2014.12.009

Hastings DW, Bartlett T, Brooks GR, Larson RA, Quinn KA, Razionale D, Schwing PT, Pérez Bernal LH, Ruiz-Fernández AC, Sánchez-Cabeza JA, Hollander DJ (2020) Changes in redox conditions of surface sediments following the *Deepwater Horizon* and Ixtoc 1 events (Chap. 16). In: Murawski SA, Ainsworth C, Gilbert S, Hollander D, Paris CB, Schlüter M, Wetzel D (eds) Deep oil spills – facts, fate and effects. Springer, Cham

Hu C, Weisberg RH, Liu Y, Zheng L, Daly K, English D, Zhao J, Vargo G (2011) Did the northeastern Gulf of Mexico become greener after the Deepwater Horizon oil spill? Geophys Res Lett 38:L09601. https://doi.org/10.1029/2011GL047184

Langenhoff AM, Rahsepar S, van Eenennaam JS, Radović JR, Oldenburg TPP, Foekema E, Murk AJ (2020) Effect of marine snow on microbial oil degradation (Chap. 18). In: Murawski SA, Ainsworth C, Gilbert S, Hollander D, Paris CB, Schlüter M, Wetzel D (eds) Deep oil spills – facts, fate and effects. Springer, Cham

Larson RA, Brooks Gregg GR, Schwing PT, Diercks AR, Holmes CW, Chanton JP, Diaz-Asencio M, Hollander DJ (2020) Characterization of the sedimentation associated with the *Deepwater Horizon* blowout: depositional pulse, initial response, and stabilization (Chap. 14). In: Murawski SA, Ainsworth C, Gilbert S, Hollander D, Paris CB, Schlüter M, Wetzel D (eds) Deep oil spills – facts, fate and effects. Springer, Cham

Liu Y, Hu C, Sun C, Zhan W, Sun S, Xu B, Dong Y (2018) Assessment of offshore oil/gas platform status in the northern Gulf of Mexico using multi-source satellite time-series images. Remote Sens Environ 208:63–81. https://doi.org/10.1016/j.rse.2018.02.003

Montagna PA, Baguley JG, Cooksey C, Hartwell I, Hyde LJ, Hyland JL, Kalke RD, Kracker LM, Reuscher M, Rhodes ACE (2013) Deep-sea benthic footprint of the Deepwater Horizon blowout. PLoS One 8(8):e70540. https://doi.org/10.1371/journal.pone.0070540

Murawski SA, Hogarth WT, Peebles EB, Barbieri L (2014) Prevalence of external skin lesions and polycyclic aromatic hydrocarbon concentrations in Gulf of Mexico fishes, post Deepwater Horizon. Trans Am Fish Soc 143(4):1084–1097. https://doi.org/10.1080/00028487.2014.911205

Murawski SA, Peebles EB, Gracia A, Tunnell JW Jr, Armenteros M (2018) Comparative abundance species composition , and demographics of continental shelf fish assemblages throughout the Gulf of Mexico. Mar Coast Fish: Dyn Manage Ecosyst Sci 10(3):325–346. https://doi.org/10.1002/mcf2.10033

O'Reilly JE, Maritorena S, Siegel D, O'Brien MO, Toole D, Mitchell BG (2000) Ocean color chlorophyll a algorithms for SeaWiFS, OC2 and OC4: Version 4. In Hooker SB, Firestone ER (eds) SeaWiFS Postlaunch calibration and validation analyses (NASA Tech. Memo. 2000–206892, vol 11, pp 9–23). NASA Goddard Space Flight Center, Greenbelt

Passow U, Ziervogel K (2016) Marine snow sedimented oil released during the Deepwater Horizon spill. Oceanography 29:118–125

Passow U, Hetland RD (2016) What happened to all of the oil? Oceanography 29(3):88–95. https://doi.org/10.5670/oceanog.2016.73

Passow U, Ziervogel K, Asper V, Diercks A (2012) Marine snow formation in the aftermath of the Deepwater Horizon oil spill in the Gulf of Mexico. Environ Res Lett 7:11. https://doi.org/10.1088/1748-9326/7/3/035301

Quigg A, Passow U, Daly KL, Burd A, Hollander DJ, Schwing PT, Lee K (2020) Marine oil snow sedimentation and flocculent accumulation (MOSSFA) events: learning from the past to predict the future (Chap. 12). In: Murawski SA, Ainsworth C, Gilbert S, Hollander D, Paris CB, Schlüter M, Wetzel D (eds) Deep oil spills – facts, fate and effects. Springer, Cham

Rahsepar S, Smit MPJ, Murk AJ, Rijnaarts HHM, Langenhoff AAM (2016) Chemical dispersants: oil biodegradation friend or foe? Mar Pollut Bull 108(1–2):113–119. https://doi.org/10.1016/j.marpolbul.2016.04.044

Romero IC, Schwing PT, Brooks GR, Larson RA, Hastings DW, Ellis G, Goddard EA, Hollander DJ (2015) Hydrocarbons in deep-sea sediments following the 2010 Deepwater Horizon Blowout in the northeast Gulf of Mexico. PLoS One. https://doi.org/10.1371/journal.pone.0128371, 23 pp

Romero IC, Toro-Farmer G, Diercks A-R, Schwing P, Muller-Karger F, Murawski S, Hollander DJ (2017) Large-scale deposition of weathered oil in the Gulf of Mexico following a deep-water oil spill. Environ Pollut 228:179–189

Sanchez-Cabeza JA (2016) Recent sedimentation in the southern Gulf of Mexico. In: Proceedings of the Gulf of Mexico oil spill and ecosystem science conference, Tampa, FL

Schwing PT, Machain-Castillo MA (2020) Impact and resilience of benthic foraminifera in the aftermath of the *Deepwater Horizon* and Ixtoc 1 oil spills (Chap. 23). In: Murawski SA, Ainsworth C, Gilbert S, Hollander D, Paris CB, Schlüter M, Wetzel D (eds) Deep oil spills – facts, fate and effects. Springer, Cham

Schwing PT, Romero IC, Brooks GR, Hastings DW, Larson RA, Hollander DJ (2015) A decline in deep-sea benthic foraminifera following the Deepwater Horizon event in the northeastern Gulf of Mexico. PloS One 10(3):e0120565. https://doi.org/10.1371/journal.pone.0120565

Schwing PT, O'Malley BJ, Romero IC, Martinez-Colon M, Hastings DW, Glabach MA, Hladky EM, Greco A, Hollander DJ (2017a) Characterizing the variability of benthic foraminifera in the northeastern Gulf of Mexico following the Deepwater Horizon event (2010–2012). Environ Sci Pollut Res 24:2754. https://doi.org/10.1007/s11356-016-7996-z

Schwing PT, Brooks GR, Larson RA, Holmes CW, O'Malley BJ, Hollander DJ (2017b) Constraining the spatial extent of the marine oil snow sedimentation and accumulation (MOSSFA) following the DWH event using a 210Pbxs inventory approach. Environ Sci Technol 51:5962–5968. https://doi.org/10.1021/acs.est.7b00450

Schwing PT, O'Malley BJ, Hollander DJ (2018a) Resilience of benthic foraminifera in the northern Gulf of Mexico following the Deepwater Horizon event (2011–2015). Ecol Indic 84:753–764. https://doi.org/10.1016/j.ecolind.2017.09.044

Schwing PT, Chanton JP, Romero IC, Hollander DJ, Goddard EA, Brooks GR, Larson RA (2018b) Tracing the incorporation of petroleum carbon into benthic foraminiferal calcite following the Deepwater Horizon event. Environ Pollut 237:424–429. https://doi.org/10.1016/j.envpol.2018.02.066

Schwing PT, Hollander DJ, Brooks GR, Larson RA, Hastings DW, Chanton JP, Lincoln SA, Radović JR, Langenhoff A (2020) The sedimentary record of MOSSFA events in the Gulf of Mexico: a comparison of the *Deepwater Horizon* (2010) and Ixtoc 1 (1979) oil spills (Chap. 13). In: Murawski SA, Ainsworth C, Gilbert S, Hollander D, Paris CB, Schlüter M, Wetzel D (eds) Deep oil spills – facts, fate and effects. Springer, Cham

Stout SA, German CR (2015) Characterization and flux of marine oil snow in the Viosca Knoll (Lophelia Reef) area due to the Deepwater Horizon oil spill Newfields, Rockland, MA. https://www.fws.gov/doiddata/dwh-ar-documents/946/DWH-AR0039084.pdf

Tamis JE, Jongbloed RH, Karman CC, Koops W, Murk AJ (2011) Rational application of chemicals in response to oil spills may reduce environmental damage. Integr Environ Assess Manag 8:231–241

Valentine DL, Fisher GB, Bagby SC, Nelson RK, Reddy CM, Sylva SP, Woo M (2014) Fallout plume of submerged oil from Deepwater Horizon. Proc Natl Acad Sci U S A 111(45):15906–15911. https://doi.org/10.1073/pnas.1414873111

Van Eenennaam JS, Wei Y, Grolle KCF, Foekema EM, Murk AJ (2016) Oil spill dispersants induce formation of marine snow by phytoplankton-associated bacteria. Mar Pollut Bull 104(1–2):94–302

Van Eenennaam JS, Rahsepar S, Radović JR, Oldenburg TBP, Wonink J, Langenhoff AAM, Foekema EM (2018) Marine snow increases the adverse effects of oil on benthic invertebrates. Mar Pollut Bull 126:339–348. https://doi.org/10.1016/j.marpolbul.2017.11.028

Vonk SM, Hollander DJ, Murk AJ (2015) Was the extreme and wide-spread marine oil-snow sedimentation and flocculent accumulation (MOSSFA) event during the Deepwater Horizon blowout unique? Mar Pollut Bull 100(1):5–12. https://doi.org/10.1016/j.marpolbul.2015.08.023

Washburn TW, Reuscher MG, Montagna PA, Cooksey C, Hyland JL (2017) Macrobenthic community structure in the deep Gulf of Mexico one year after the Deepwater Horizon blowout. Deep Sea Res Part 1 Oceanogr Res Pap 127:21–30. https://doi.org/10.1016/j.dsr.2017.06.001

Yan B, Passow U, Chanton J, Nöthig E-M, Asper V, Sweet J, Pitiranggon M, Diercks A, Pak D (2016) Sustained deposition of contaminants from the Deepwater Horizon oil spill. Proc Natl Acad Sci USA 113:E3332–E3340. www.pnas.org/cgi/doi/10.1073/pnas.1513156113

Zeinstra-Helfrich M, Koops W, Murk AJ (2015) The NET effect of dispersants—a critical review of testing and modelling of surface oil dispersion. Mar Pollut Bull 100(1):102–111. https://doi.org/10.1016/j.marpolbul.2015.09.022

Zeinstra-Helfrich M, Koops W, Murk AJ (2016) How oil properties and layer thickness determine the entrainment of spilled surface oil. Mar Pollut Bull 110:184–193. https://doi.org/10.1016/j.marpolbul.2016.06.063

Zeinstra-Helfrich M, Koops W, Murk AJ (2017) Predicting the consequence of natural and chemical dispersion for oil slick size over time. J Geophys Res Oceans 122:7312–7324. https://doi.org/10.1002/2017JC012789

Chapter 22
Connectivity of the Gulf of Mexico Continental Shelf Fish Populations and Implications of Simulated Oil Spills

Claire B. Paris, Steven A. Murawski, Maria Josefina Olascoaga, Ana C. Vaz, Igal Berenshtein, Philippe Miron, and Francisco Javier Beron-Vera

Abstract The Gulf of Mexico (GoM) marine ecosystem is experiencing acute stressors. Natural (e.g., hurricanes, harmful algal blooms) or anthropogenic (e.g., oil spills), these stressors have the potential to impact fish populations and decrease biodiversity that may be difficult to recover unless the ecosystem is resilient.

One of the most effective factors governing the resilience capacity of sensitive Gulf fish species is the degree of connectivity and network modularity among spatial sub-units of species occupying the continental shelf. This chapter is a meta-study that looks at the relationship between the Lagrangian dynamical geography of the GoM regions, the community structure of demersal fish, and the potential for larval connectivity. We use adult fish movement from tagging data, larval fish migration from biophysical modeling, and oceanographic patterns from satellite-tracked Lagrangian drifters to quantify the degree of connectivity and modularity of the GoM ecosystem. We evaluate the biophysical model output with 20+ years of data from the Southeast Area Monitoring and Assessment Program (SEAMAP) ichthyoplankton survey and use the drifter inferred dynamics provinces to access mechanisms underlying retention or exchange for each species and GoM province. The tagging analyses reveal a modular network structure consistent with the Lagrangian oceanographic provinces. While the oceanographic dynamic patterns drive self-recruitment levels and the size and location of these provinces, they do not constrain connectivity patterns between distant locations within the GoM. In contrast, larval transport and migration between the provinces and subregions drive the patterns of connectivity and community structure similarity. Ultimately, it is the combination

C. B. Paris (✉) · M. J. Olascoaga · A. C. Vaz · I. Berenshtein · P. Miron · F. J. Beron-Vera
University of Miami, Department of Ocean Sciences, Rosenstiel School of Marine & Atmospheric Science, Miami, FL, USA
e-mail: cparis@rsmas.miami.edu; jolascoaga@rsmas.miami.edu; avaz@rsmas.miami.edu; iberenshtein@rsmas.miami.edu; pmiron@rsmas.miami.edu; fberon@rsmas.miami.edu

S. A. Murawski
University of South Florida, College of Marine Science, St. Petersburg, FL, USA
e-mail: smurawski@usf.edu

S. A. Murawski et al. (eds.), *Scenarios and Responses to Future Deep Oil Spills*,
https://doi.org/10.1007/978-3-030-12963-7_22

of within-scale functional redundancy and cross-scale species connectivity that can amplify resilience and speed of recovery and minimize the potential for catastrophic regime shifts in ecological meta-communities such as in the GoM. The importance of such studies to natural resource management and oil spill preparedness outcomes is discussed.

Keywords Connectivity · Ecosystem modularity · Larval dispersal · Biophysical modeling · SEAMAP · Gulf of Mexico · Oil spill effects

22.1 Introduction

Among the attributes of complex ecosystems that may mitigate the effect of acute but relatively localized perturbations (such as oil spills) is the degree of modularity and connectivity among spatial sub-units of species occupying complex systems (Grilli et al. 2016; Gilarranz et al. 2017). As with power grids, global financial networks and other nested systems, a high degree of ecosystem connectivity may result in widespread, cascading impacts from localized perturbations (Gilarranz et al. 2017), whereas a high degree of ecosystem modularity may undermine resiliency, owing to the lack of species redundancy to restore affected areas (Zamora et al. 2010; Grilli et al. 2016). Following disturbance, the potential for receiving beneficial spillover of biota from adjacent areas, thus reestablishing richness and diversity and increasing abundances, is likely to be proportionate to the number of species shared (Hersperger and Forman 2003; Zamora et al. 2010). In the advent of significant species depletion, larval transport and recruitment or directed movement of juveniles and/or adults of species from adjacent areas would likely affect the trajectory of recovery, and thus the degree of shared species is a potentially important factor contributing to the overall resilience of an ecosystem.

Continental shelf fish communities in the Gulf of Mexico (GoM) are structured by water depth and subregions with different patterns of species association (Murawski et al. 2018). Insights into how species populations may be connected between subregions need further understanding of linkages maintained by dispersal and migration of individuals at all life history stages. Adult fishes may exhibit specific movements between subregions of the GoM, but for most benthic fish species, the only opportunity to migrate is as fish larvae that may be transported by the currents among subregions. Patterns of species associations are thus likely influenced by both the pelagic and demersal environments, such as oceanography eddies and boundaries and habitat types on Gulf shelves upon which juvenile fish settle. Recent work involving drifter trajectories describes weak oceanographic connectivity between provinces of the GoM, providing an important step furthering the understanding of physical mechanisms underlying oceanographic connectivity in the region (Miron et al. 2017). However, the biophysical complexity of larval dispersal is often underappreciated and may differ significantly from passive pathways of surface drifters (Paris et al. 2007). Therefore, association of these findings with larval

fish connectivity needs to be further assessed by biophysical modeling taking into account adult spawning strategy as well as larval traits and swimming behavior (Kough and Paris 2015; Staaterman and Paris 2014). Importantly, the distribution of juveniles and adults of a species occurring in a structured ecosystem could be used to cross-check the results of hydrodynamic modeling of larval transport (Karnauskas et al. 2013). If such projections forecast occurrences that do not occur in nature, then there may be mechanisms other than larval supply dictating recruitment dynamics, such as the presence of proper settlement habitat.

Here, we take an integrated approach utilizing the dynamical Lagrangian geography of the GoM, subregional fish communities, and the exchange of fish species at all stages. Our goals are to understand the connectivity and thus resilience potential of the continental shelf fish populations in the GoM. Special objectives are to investigate (1) the factors determining observed patterns of species distribution and apparent connectivity in the GoM, (2) the relationship between the structure of fish communities and the oceanographic provinces in the GoM, and (3) the biophysical drivers and constraints of continental shelf fish population connectivity in the GoM.

22.2 Methods

We use the locations and catch per unit effort (CPUE)-adjusted abundances of major functional groups of fish species collected on the GoM continental shelf between 20 and 500 m depth collected over 7 years (Murawski et al. 2018), to initialize a GoM-HYCOM hydrodynamic model coupled to the open-source Lagrangian application of the Connectivity Modeling System (CMS). We evaluate the model output with 20+ years of data from the South Area Monitoring and Assessment Program (SEAMAP) ichthyoplankton survey and use the drifter inferred dynamics provinces to access what biophysical mechanisms are underlying retention or exchange for each species and GoM province.

22.2.1 Similarities Among Demersal Communities in the Gulf of Mexico (GoM)

In order to assess the distribution and thus the modularity of fish resources in the GoM, we used fish assemblage data described in Murawski et al. (2018). Briefly, six provinces were defined based on predominant fish assemblages sampled during comprehensive long-line surveys on continental shelves throughout the GoM (Fig. 22.1). A consistent sampling of demersal fish communities in the continental shelf waters (~40–300 m deep) of the GoM and in waters of Mexico and Cuba (343 sites) was carried out during 2011–2017. We determined the extent to which each pair of GoM provinces shared common species (Fig. 22.2) by computing the

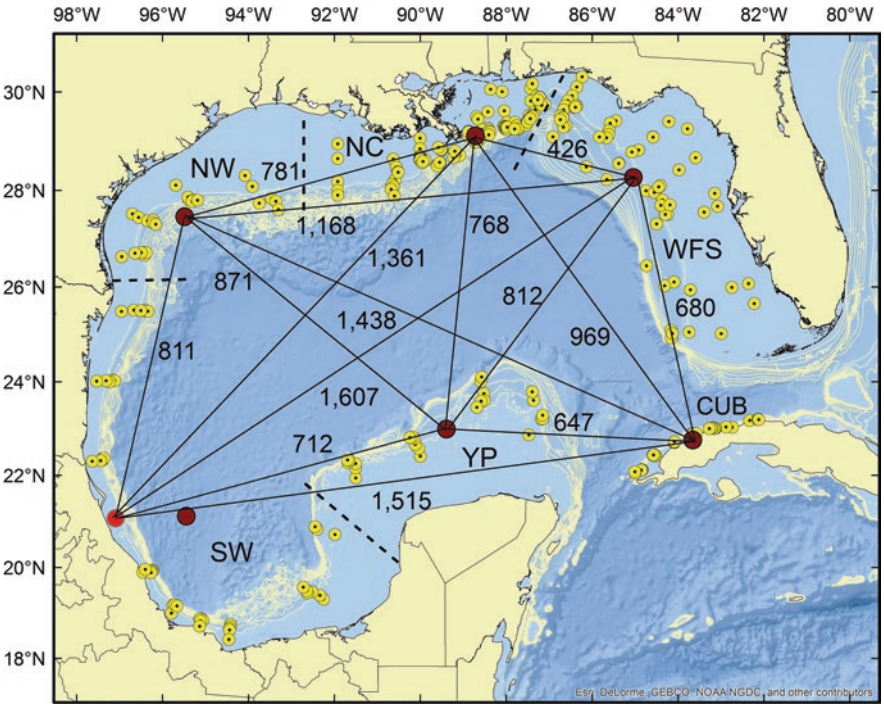

Fig. 22.1 Locations (circles) of demersal long-line sampling stations from surveys conducted by Murawski et al. (2018). The latitude-longitude centroids of the stations comprising six previously identified GoM subregions are plotted as the minimum linear distances (km) between the respective centroids. For the SW sub-area, two centroids are plotted: the arithmetic centroid is off the continental shelf, and an alternative centroid on the shelf is plotted and used for distance calculations. Numbers are the linear distances (km) between pairs of centroids of the six subregions. Subregional designations are NC north central, NW northwest, SW southwest, YP Yucatan Peninsula, CUB Cuba, WFS west Florida shelf

number of species observed in each province, the number and percentage of extant species unique to each, and the number of species shared among all pairs of provinces (Table 22.1).

22.2.2 Connectivity Inferred by Surface Ocean Drifters (OCE)

Using historical (1994–2016) surface drifting buoy trajectory data, we conduct a probabilistic Lagrangian circulation study which sheds light on the oceanographic connectivity within the GoM. At a first step, the GoM is partitioned into a grid of N-connected boxes $\{B_1, \ldots, B_N\}$. As described in Miron et al. (2017), we use 25-km-side boxes covering the GoM and 2-day-long drifter trajectory pieces, which may begin on any day. We construct a transition matrix $P = P_{ij} \approx$ (# of drifters in B_i at any

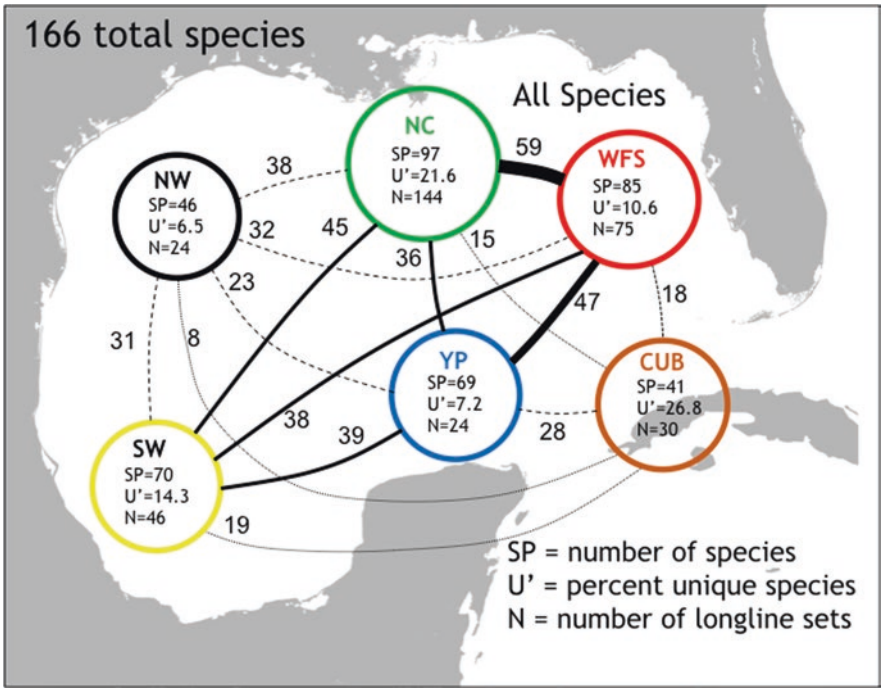

Fig. 22.2 Numbers of shared fish species occurring in six identified subregions of the Gulf of Mexico (Fig. 22.1), based on demersal long-line sampling (Murawski et al. 2018). Thickness of the lines is proportional to the number of shared species. The number of sampling stations in each region is N, U′ is the percent of species unique to each sub-area, and SP = the total number of species encountered

Table 22.1 Numbers of species observed in demersal long-line sampling (Murawski et al. 2018) that occurred in one to all six subregions of the Gulf of Mexico (GoM; Fig. 22.4)

Number of subregions of the GoM (N)	Number of species occurring in N subregions
1	59
2	39
3	28
4	18
5	17
6	5

Total number of species sampled was 166

t that evolves to B_j at $t + T$)/(# of drifters in B_i at any t). The matrix P defines a Markov chain representation of the dynamics, with the entries P_{ij} equal to the conditional transition probabilities between boxes, which represent the states of the chain. This allows one to leverage the well-established machinery of Markov chains to assess motion through a chain and thus estimate the evolution of Lagrangian tracers. For instance, regions of the domain where Lagrangian trajectories accumulate

(almost-invariant attracting sets) and regions where those trajectories originate (basins of attraction) are revealed by the dominant left and right eigenvectors of the transition matrix P, respectively. The forward evolution of the discrete representation of a tracer f (x), $\mathbf{f} = (f_1, \ldots, f_N)$, is calculated under left multiplication, that is, $\mathbf{f}^{(k)} = \mathbf{f}\mathrm{P}^k$, $k = 1, 2, \ldots$.

22.2.3 Biophysical Modeling of Larval Connectivity (CMS)

Oceanographic module To simulate larval dispersal of continental fish species, we use the open-source probabilistic Connectivity Modeling System (CMS, Paris et al. 2013) and environmental variables (i.e., horizontal and vertical components of the velocity, temperature, and salinity) from the Gulf of Mexico-HYCOM hindcast (0.04° horizontal resolution and 20 vertical layers). The GoM-HYCOM is forced at the surface by the Navy Operational Global Atmospheric Prediction System (NOGAPS) winds and surface fluxes, at the Atlantic boundary by large-scale model fields, and by data assimilation with the Navy Coupled Ocean Data Assimilation (NCODA) system (Chassignet et al. 2007).

Target species and biological module configuration Based on grouping of species and their depth gradient of occurrence of fish collected on the GoM continental shelf between 20 and 500 m depth over 7 years (Murawski et al. 2018), we select the following three representative demersal species and one epipelagic taxa: red grouper (*Epinephelus morio*), red snapper (*Lutjanus campechanus*), golden tilefish (*Lopholatilus chamaeleonticeps*), and tuna (Scombridae). The CMS is configured with the species biological traits including the adults spawning seasonality and depth, areas of occurrence in the GoM (Murawski et al. 2018), as well as the larval traits such as pelagic larval duration (PLD), competence period, and behavior (Table 22.1). Release points are the sampling stations from Murawski et al. (2018), divided into six provinces defined by multivariate analysis of species associations and spatial groupings of stations: (1) west Florida shelf (WFS), (2) north central (NC) and (3) northwest (NW) GoM, (4) southwest (SW) GoM, (5) Yucatan Peninsula (YP), and (6) Cuba (CUB). We evaluate the biophysical model output with 20+ years of data from the South Area Monitoring and Assessment Program (SEAMAP) ichthyoplankton survey (Fig. 22.5) and use the drifter inferred dynamics provinces to access what biophysical mechanisms are underlying retention or exchange for each species and GoM province.

22.2.4 Connectivity Matrices and Statistical Analyses

To elucidate the patterns of connectivity across the GoM, we calculate connectivity matrices, which show the probability of connections between each geographic province. We then use a linear distance matrices regression to examine the relationship

between the computed connectivity matrices and the degree of province similarity in terms of community structure, for both the oceanographic connectivity (OCE; see Sect. 22.2.2) and larval connectivity (CMS, Sect. 22.2.3) methods. The assumption is that OCE connectivity should have a good fit with the degree of province similarity for epipelagic tuna larvae, while CMS connectivity matrices are expected to have a good fit for both epipelagic and deep-dwelling species with larvae undergoing ontogenetic vertical migration (Paris and Cowen 2004). We also performed a graph theoretical network analyses to identify ecological corridors among the spawning and settlement sites and calculated the betweenness centrality of all sites to identify multigenerational connections. Betweenness centrality is defined as the fractions of shortest paths between pairs of sites, passing through each of them. This analysis includes information of both direct and indirect connections (Treml et al. 2008; Treml and Halpin 2012), making it relevant for broad ecological questions such as species distribution and community structure. Graphs and calculations were based on the MatlabBGL package (downloaded from https://github.com/dgleich/matlab-bgl).

To compare the different types of matrices, connectivity, distance, community similarity, etc., we ranked the values per each matrix since the relationship between the different variables cannot be assumed to be linear (or any other type of relationship for that matter). We used Kendall rank correlation coefficients (τ) of Mantel tests to examine the pairwise correlation between the various matrices in the connectivity synthesis. To specifically examine the relationship between the computed connectivity matrices (CMS and OCE) and the degree of province similarity in terms of community structure, we used a linear regression on the ranked distance matrices using the permutation-based MRM function from Ecodist library (Goslee and Urban 2007).

22.3 Results

22.3.1 Connectivity Inferred by Adult Fish Distribution and Movement Data

Highest numbers of shared species occurred between NC and WFS (59 shared species) and between WFS and YP (47 shared species), despite a deep channel separating the subregions in the latter case (Fig. 22.1). Conversely, the CUB region had the lowest number of species overall (41 shared species), and relatively low numbers of species in common with the other five provinces (Fig. 22.2). However, while the number of species sampled in demersal longlines of NW Cuba was low, the CUB province had the highest percentage of unique species (26.8%), whereas the NW (6.5%) and the Yucatan Peninsula (7.2%) were regions with the lowest percentages of unique species sampled. Only 36% of species were unique to one province (Table 22.1) indicating a relatively high degree of potential connectivity among provinces (Fig. 22.2) and conversely low to moderate levels of ecosystem modularity.

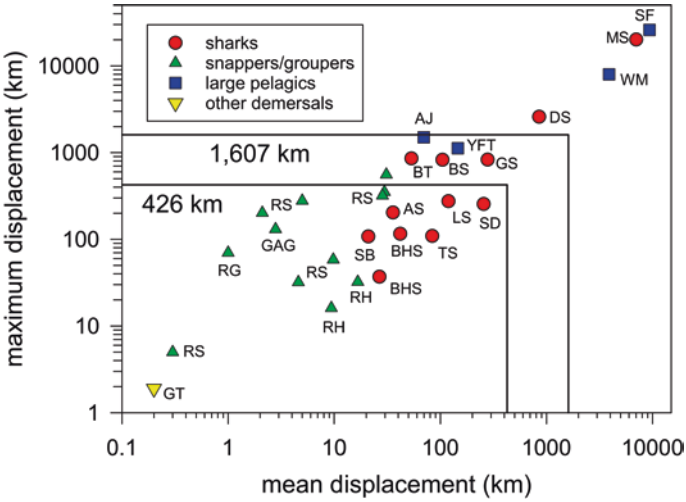

Fig. 22.3 Relationships between mean and maximum displacement for tagged and recaptured fish species. Abbeviations are GT golden tilefish, RS red snapper, GAG gag grouper, BHS bonnethead shark, TS tiger shark, DS dusky shark, SF sailfish, MS mako shark, AJ, greater amberjack, BT blacktip shark, BS bull shark, LS lemon shark, SD smooth gogfish, RG red grouper, WM white marlin, GS Gulf smoothhound shark, AS Atlantic sharpnose shark, YFT yellowfin tuna, SB sandbar shark, RH red hind. Boxes represent the minimum and maximum distances between the centroids of six subregions of the Gulf of Mexico (Fig. 22.2). For GT, a small positive distance traveled was included because of the use of logged axes

While the fractions of unique species were relatively low in any one province, thus indicating the potential connectivity of the GoM as a whole, only 5 of 166 species (3%; Table 22.1) occurred in all six sub-areas, indicating that these sub-areas are not completely redundant. Of the five species found in all six regions, three were sharks, one is a deepwater snapper, and one is a large pelagic species: smooth dogfish, tiger shark, sharpnose sevengill shark, wenchman, and greater amberjack. Because sharks are ovoviviparous, their distribution potential is completely dictated by juvenile and adult migratory potential (Fig. 22.3).

With respect to the distribution potential of species to repopulate provinces subjected to rapid depletion, an important question is the degree to which juveniles and adults of species are capable of directed movements over the scales that would connect sub-areas of the GoM (Fig. 22.1). Obviously, there is a high variation of adult fish movement distances across species. Species characterized by a limited displacement (e.g., tilefish; Grimes et al. 1983) could not repopulate to adjacent sub-areas relatively quickly. Conversely, large pelagic species such as dusky shark (Hoffmayer et al. 2014) and yellowfin tuna (Hoolihan et al. 2014) can cross hundreds of km in days to weeks and thus range across several sub-areas. The locations of the centroids of the sampling station within each of the six GoM provinces were calculated (Fig. 22.2) to illustrate scales of movement necessary for repopulation via adult migration to occur. While movements across shared sub-area boundaries can occur for species with limited dispersal capacity, this would require "stepping

stone" movements to eventually populate whole subregion in the case of non-peripatetic species. Further analyses would require to (1) examine if the species adult displacement is a good predictor for the occupancy of provinces, geographic range of occurrences, and (2) if PLD is a good predictor for the occupancy of provinces, geographic range of occurrences.

We conducted a meta-analysis of tagging studies for GoM species to assess the degree of movement potential of economically important and geographically abundant species. The mean and maximum distances traveled by a variety of relatively sedentary to highly migratory species are plotted in Fig. 22.3. Data included in the analysis (Fig. 22.2) were derived from Schirripa et al. (1999), Patterson III et al. (2001), Tyminski et al. (2005), Addis et al. (2007), Patterson (2007), Oritz et al. (2009), Murie et al. (2011), Hedon et al. (2013), Bethea and Driggers (2014), Hoffmayer et al. (2014), Hoolihan et al. (2014), Center for Sportfish Science and Conservation (2018), and the Guy Harvey Research Institute (2018). Tagging results from two out-of-basin studies were included since they represent species found in the GoM (Grimes et al. 1983; Nemeth et al. 2007), but for which no regional tagging studies have been reported.

A significant linear trend between the mean and maximum observed movement distances is evident at scales ranging essentially from zero (tilefish) to thousands of km (sailfish, mako shark, white marlin). For the important snapper and grouper complex, maximum movements ranged from ~10 m to about 200 km, much less than the minimum linear distance between the centroids of the WFS and NC provinces—the closest of the 15 pairwise province distances (Figs. 22.1, 22.2, and 22.3). None of the small-bodied sharks are capable of covering the distance between two centroids. Only large-bodied sharks and several large pelagic species are capable of minimum centroid-spanning movements and fewer yet capable of swimming the maximum centroid distance of 1607 km (WFS to SW, Fig. 22.3). These data show that for most bony fish, the process of recolonization of regions significantly impacted by large-scale perturbations will occur primarily via egg drift, larval transport, and "chain migration" comprised of several sequential movements across boundaries.

22.3.2 Surface Connectivity Inferred by Surface Ocean Drifters (OCE)

The oceanographic province partitioning is slightly different from the partitioning emerged from the community structure analysis. For example, the west Florida shelf, and the southern west Florida shelf (WFS) are separated , but are one province in the community structure analysis, whereas the NW and CN GoM provinces are separated in the community structure analysis, but represent a single province (LaTex province; Fig. 22.4b). The boundaries between the provinces are determined by the Lagrangian circulation itself, rather than by arbitrary geographical

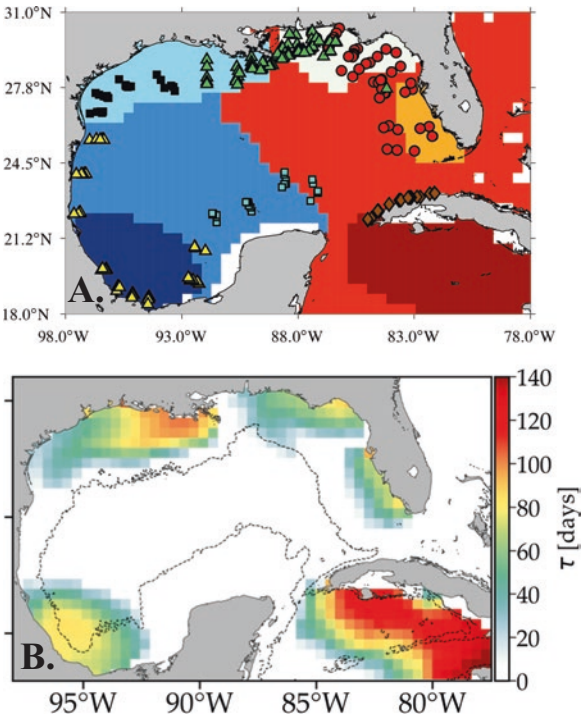

Fig. 22.4 Dynamical geographies with weakly Lagrangian interacting subregions and locations of station grouped via similarities of species compositions: (**a**) six dynamical provinces roughly spanning the northern west Florida shelf, the southern west Florida shelf (WFS), the Louisiana-Texas shelf (LaTex), the Bay of Campeche (Yucatan Peninsula), and a region over the Cuban Caribbean Sea. These provinces are WFS (orange); NC, north central GoM (yellow); YP Yucatan Peninsula (blue), SW southwestern GoM (dark blue), NW northwestern GoM (LaTex, light blue), CUB Cuba (dark red). (**b**) Tracers initially within these provinces will spend more time moving and eventually temporarily accumulating in regions within them than dispersing across their boundaries. These dynamical provinces thereby set the way that distant regions in the GoM are weakly connected by tracer motion

demarcations. Tracers initially released within these provinces (Fig. 22.5a) will spend more time moving and eventually temporarily accumulating in regions within them than dispersing across their boundaries. These dynamical provinces thereby set the way that distant regions in the GoM are weakly connected by tracer motion. The Lagrangian dynamics control the biological connectivity in the GoM as it is evident by comparing with the independently inferred biological geography described in the previous section. We evolve a tracer starting in each of these provinces where each of the species was found and taking into account the different PLD for tuna (15 days), red snapper (26 days), red grouper (40 days), and golden tilefish (100 days; Table 22.2). The connectivity matrices for each of the species show the connectivity between provinces (Fig. 22.6a). The oceanographic connectivity reveals the spatial scales of subregional retention, which in turn influence the degree

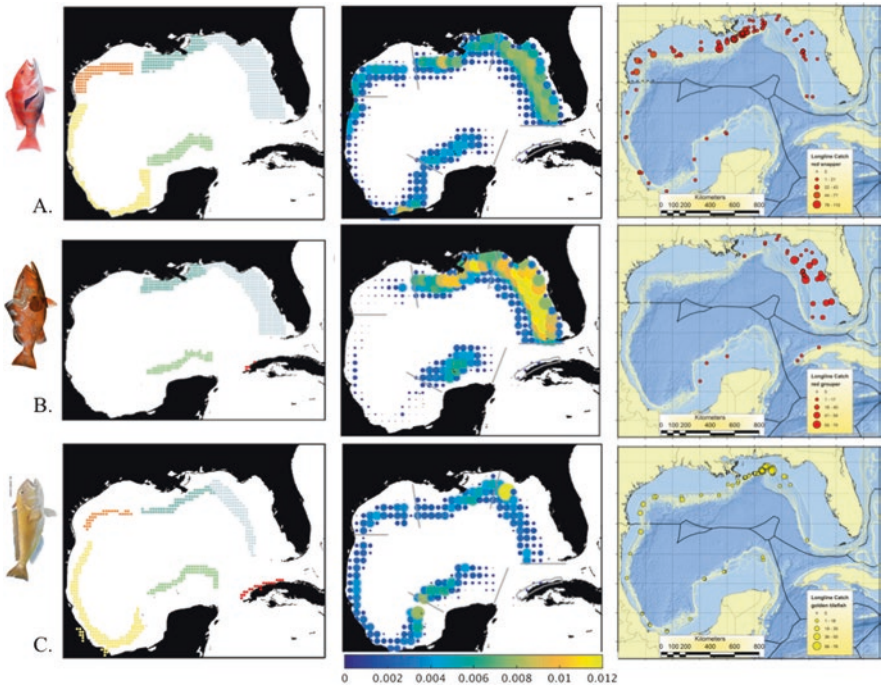

Fig. 22.5 Modeled larval distributions for (**a**) red snapper, (**b**) red grouper, and (**c**) golden tilefish. Release locations in the CMS are color-coded by the six provinces and correspond to a grid extrapolated between the locations of demersal long-line sampling (see Fig. 22.1) where each species were caught (left panels); the probability of expected larval settlement (middle panel) agrees with the observed catches of the longline surveys (right panel)

of modularity of the ecosystem. The provinces delineated by the drifters can be considered as retentive areas—at least for the upper 15 m of the GoM surface—and in fact the provinces are all relatively shallow regions. The Lagrangian dynamics as inferred from satellite-tracked drifters impose strong constraints on biological retention in the GoM.

22.3.3 Larval Connectivity Inferred by Biophysical Modeling (CMS)

There is good correspondence between mutual species and rank of similarity between regions (Table 22.3), thus similarity matrix is a good proxy for the modularity of the subregions in terms of species composition and number of mutual species. We find that larval connectivity (CMS) is correlated with drifter connectivity (OCE) (Table 22.3) since both drifters and biophysical modeling predict high self-recruitment among provinces (Fig. 22.6). Moreover, both CMS and OCE connectivity matrices have a significant linear relationship with species similarity (CMS: linear

Table 22.2 Configuration and parameterization of the Connectivity Modeling System (CMS) to simulate the larval transport and connectivity of the species representative of the Gulf of Mexico (GoM) continental shelf community

Species	Max PLD (d)	Release frequency	Depth of adult occurrence (m)	Larval vertical behavior	Habitat subregion	Source
Tuna (*Scombridae*)	15	Every 15 days from April to September	All ranges	15 m	GoM	
Golden tilefish (*L. chamaeleonticeps*)	100	Every 15 days from April to September	>200	OVM	WFS, NC, YP, SW, NW	Harris et al. (2004)
Red snapper (*Lutjanus campechanus*)	26–30	Every 15 days from February to November	<200	OVM	WFS, NC, YP, SW, CUB	Brule et al. (2010)
Red grouper (*Epinephelus morio*)	40–60	Every 15 days from November to August	<100	Buoyancy 1d, OVM afterward	WFS, NC, YP, SW, CUB	Coleman et al. (1996, 2010), Brulé et al. (2010), Coleman and Koenig (2010), Burgos et al. (2015), Lowerre-Barbieri et al. (2016)

PLD pelagic larval duration; habitat is defined as the following subregions (Fig. 19.4): *WFS* west Florida shelf, *NC* north central, *NW* northwest GoM, *SW* southwest GoM, *YP* Yucatan Peninsula, *CUB* Cuba, *OVM* Ontogenetic vertical migration

regression on distance matrices, $R^2 = 0.52$, $F = 20$, $p < 0.05$; OCE: linear regression on distance matrices, $R^2 = 0.41$, $F = 5.33$, $p < 0.05$). Yet CMS performed better in predicting connectivity between provinces (Fig. 22.6b) by explaining a higher amount of variation (R^2) in the community structure (Fig. 22.7).

The first order of the fish community structure is the spatial extent of the larval retention for the adults that are less mobile (Fig. 22.3). The second order of the structure is the larval exchange driven by the larval traits and in particular larval vertical migration, allowing the crossing of these boundaries. Most of larvae spawned in the provinces remain in the provinces. The connectivity occurs at a lower order of magnitude, yet is significantly correlated to the community structure similarity and to the number of mutual species (Table 22.3).

Table 22.3 Kendall rank correlation coefficients (τ) of Mantel tests between various matrices in the connectivity synthesis and, cells are color-coded (blue to red) in increasing and decreasing order, respectively

·	Com Sim	Mut Sp	Ge Dist	Grouper OCE	Snapper OCE	Tilefish OCE	Tuna OCE	Grouper CMS	Snapper CMS	Tilefish CMS	Tuna CMS	OCE mean
Mutual Sp	0.81											
GeoDist	0.18	0.30										
Grouper OCE	0.12	0.24	0.26									
Snapper OCE	0.41	0.45	0.50	0.37								
Tilefish OCE	0.47	0.50	0.37	0.31	0.75							
Tuna OCE	0.33	0.49	0.47	0.41	0.54	0.49						
Grouper CMS	0.27	0.35	0.29	0.75	0.48	0.50	0.43					
Snapper CMS	0.52	0.60	0.39	0.37	0.73	0.75	0.62	0.58				
Tilefish CMS	0.54	0.62	0.30	0.24	0.71	0.85	0.49	0.46	0.83			
Tuna CMS	0.60	0.68	0.31	0.37	0.70	0.83	0.54	0.56	0.85	0.87		
OCE mean	0.41	0.52	0.43	0.60	0.62	0.71	0.66	0.56	0.66	0.60	0.70	
CMS mean	0.58	0.66	0.33	0.31	0.71	0.81	0.52	0.54	0.90	0.92	0.94	0.68

ComSim community similarity, *MutSp* mutual species, *GeoDist* geographic distance. "OCE" refers to simulations done using the Lagrangian methods; "CMS" refers to larval simulations done with the Connectivity Modeling System (CMS). "Mean" refers to the mean matrix of the simulation type (CMS, OCE)

Connectivity networks reveal that the SW province is central since it connects the western provinces together, keeping the Yucatan from being isolated from the NW GoM (Fig. 22.8). It is also essential to connect the western and eastern Gulf. The WFS province has the highest proportion of regional self-recruitment for the GoM and is the second most central node (Fig. 22.8). This analysis corresponds well with the number of shared fish species based on demersal long-line sampling (Murawski et al. 2018; Fig. 22.2). Acute disturbances such as oil spill in these two critical provinces would therefore threaten the resilience of the GoM ecosystem. It is important to note that fish species with the continental shelf communities have different dispersal potentials and connectivity networks (Fig. 22.9), which suggests that their populations will react uniquely to perturbation or conservation actions.

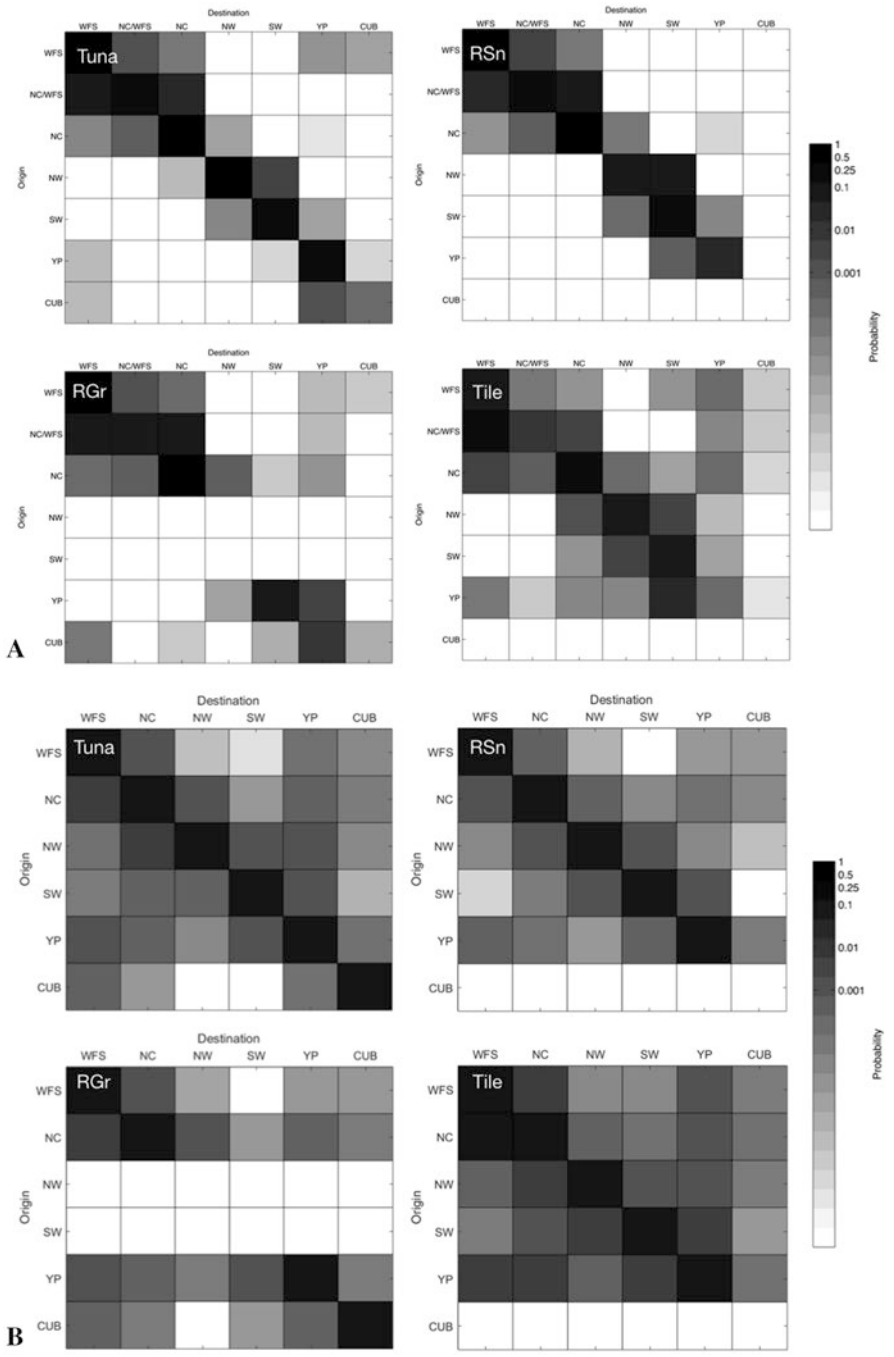

Fig. 22.6 Connectivity in the Gulf of Mexico (GoM)—(**a**) oceanographic connectivity from drifters (OCE) and (**b**) larval connectivity from biophysical modeling (CMS). Matrices are shown for tuna, red snapper (RSn), red grouper (RGr), and golden tilefish (Tile). Source (y-axis) and destination (x-axis) provinces are western Florida shelf (WFS), north central (NC), north western (NW), and south western (SW) GoM, Yucatan Peninsula (YP), Cuba (CUB); the diagonal represents self-recruitment (source province = destination province)

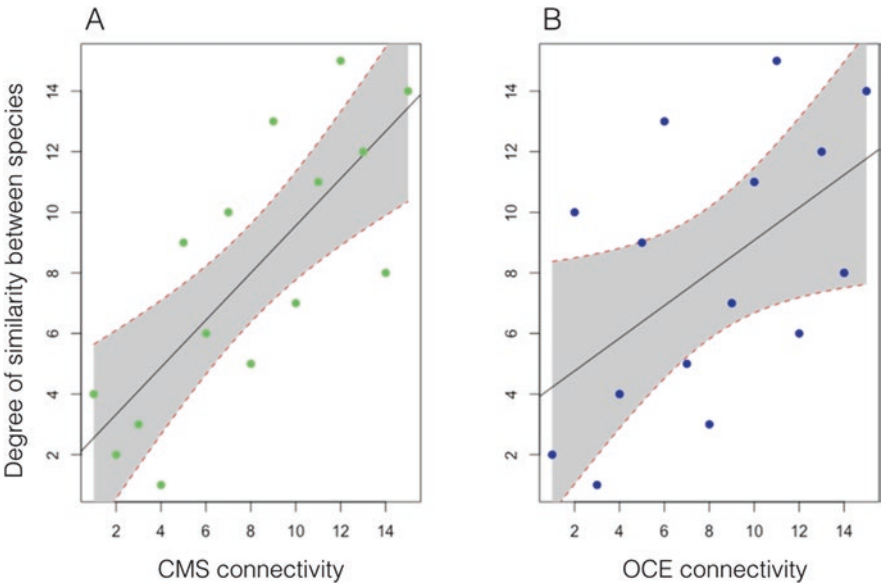

Fig. 22.7 Relationship between connectivity matrices among subregions (i.e., ranked number of connections per province) and the matrix of ranked species similarity among provinces for (**a**) the larval connectivity matrix (CMS; linear regression on distance matrices, $R^2 = 0.52$, $F = 20$, $p = 0.02$) and (**b**) the oceanographic connectivity matrix (OCE; linear regression on distance matrices, $R^2 = 0.41$, $F = 5.33$ $p = 0.01$). We find a better fit between the larval connectivity and the species similarity, suggesting that modularity is driven by the pelagic larval stage of fishes

22.4 Discussion

In the past decades, large-scale acute and chronic stressors in marine ecosystems have the potential to cause regime shifts from which ecosystems may not be capable of rapid recovery. In addition, nonlinear responses to stressors make predictions of their impact on the fisheries difficult. The resilience of perturbed marine ecosystems depends on the interconnected species populations. Here the high degree of cross-regional connectivity of fish species among GoM subregions is maintained by a combination of water mass movements transporting free-floating teleost eggs and larvae (DiMarco et al. 2005; Miron et al. 2017) and migratory patterns of large juvenile and adult fishes (Fig. 22.3). However, the degree of connectivity is not uniform among subregions (Fig. 22.6), and understanding the physical and biological mechanisms that result in differing patterns of meta-community connectivity among subregions is thus a high priority for understanding how systems might recover from catastrophic perturbations. We can assess the degree to which individual species co-occur among spatial modules. However, understanding the pathways, probabilities, and frequency of connections among modules requires the use of hydrodynamics coupled to larval dispersal modeling together with the use of additional adult fish movement data to fully discern how the observed patterns of

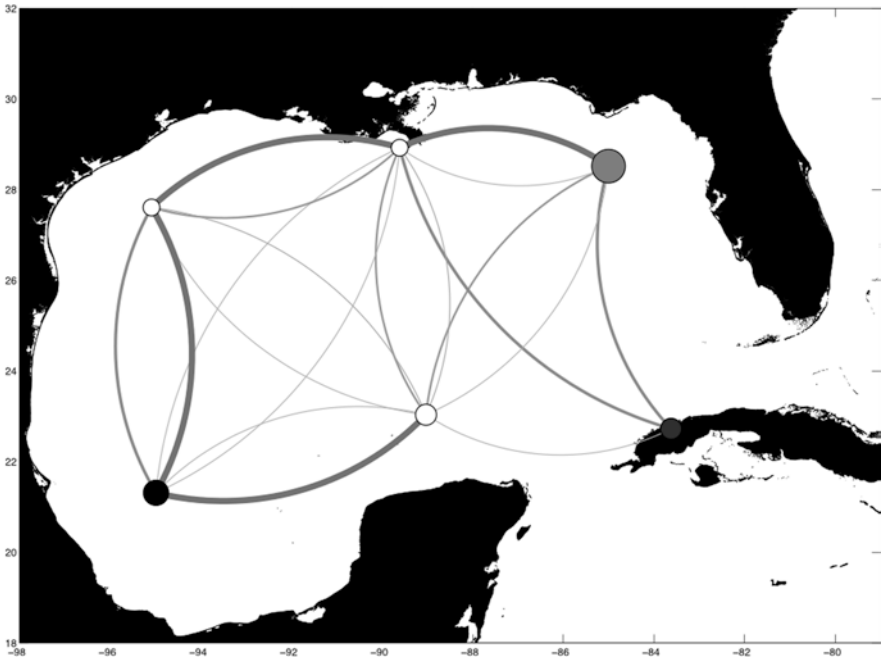

Fig. 22.8 Modularity of the Gulf of Mexico (GoM) continental shelf fish community based on larval dispersal. Connectivity network between the GoM subregions represented by nodes, edges represent larval exchanges (clockwise along arc), size of the node indicates the proportion of regional self-recruitment, and shade of the node indicates betweenness centrality, with darker shades for higher values. The thickness of the edge represents the probability of larval migration (threshold of 0.001 to illustrate connections of demographic significance)

species similarity are maintained. This extends also to genetic connectivity within species and structure of meta-populations.

Because most of the oil production in the GoM now occurs in ultra-deep waters beyond continental shelves (Murawski et al. 2020), should another significant blow-out occur there, the most direct impacts will likely be on meso- and epipelagic resources (Sutton et al. 2020). While data on movement potential of large, economically valuable epipelagic species exists (e.g., Sutton et al. 2020; Fig. 22.3), for the majority of species in the open ocean, no such data are available. Assessing the recovery potential of pelagic fish resources from offshore spills is thus an important research priority as is collecting abundance, distribution, and movement ecology information from a broader cross-section of these open-ocean species. The situation is also complicated by the vertical migrations undertaken by many of the mesopelagic species (Romero et al. 2018) which connects mesopelagic prey and epipelagic predators.

Our analyses reveal a weakly modular (subregional) network structure with shared species in the GoM. Genomic analyses conducted at appropriate spatial

scales for shared species can reveal the relative frequency at which interstock intermingling occurs. Modularity can buffer impacts on the network as a whole when individual modules are perturbed (Gilarranz et al. 2017) and aid in recovery of impacted nodes subject to acute stressors. Ultimately, it is the combination of within-scale functional redundancy and cross-scale species connectivity that can amplify resilience, aid population recovery, and minimize the potential for catastrophic regime shifts in ecological meta-communities such as in the GoM (Gunderson 2000; Ocean Studies Board 2013).

22.5 Conclusions

The clustering of stations agrees well with the dynamic provinces delineated by the surface currents (OCE), suggesting that the fish larvae of the species considered here (with up to 100 days PLD) may not cross these oceanographic boundaries with the surface currents (Fig. 22.6a). Thus passive drifters cannot serve as a proxy of larval dispersal and migration. In contrast, the CMS simulations that incorporate ontogenetic vertical migration indicate that larval behavior allows exchange between regions (Fig. 22.6b). Connectivity is thus determined by the larval exchange and agrees well with the subregion community structure (Fig. 22.7). The analysis restricted to species (tuna, red snapper, red grouper, golden tilefish) showed mixed results (Table 22.3). Discrepancies with independently inferred biological larval transport (i.e., OCE) are attributed to ignoring larval behavior (e.g., ontogenetic vertical migration, settlement behavior). Unresolved details of the Lagrangian dynamics from the drifter data (OCE), such as seasonal variability, can also play a role. Complementing these results with the ones from biophysical larval modeling (CMS) match better and help to understand the observed patterns (Fig. 22.7, 22.8, and 22.9).

We find that the dynamical oceanographic provinces are not isolated from the neighboring regions, but they are well-defined regions with “long” residence time. We conclude that the first-order fish determinant of community structure is the spatial extent of the larval retention (except for sharks) since adults are sedentary or migrate over shallow continental shelf. The second order is the larval exchange driven by larval traits and in particular, ontogenetic vertical migration, allowing the crossing of the surface water mass boundaries. Oceanographic provinces revealed by the OCE connectivity may be seen as larval retention areas and dictate the regional scales of self-recruitment. The bulk of larvae spawned in the oceanographic provinces remain there—describing the degree of modularity. Connectivity happens at a lower order of magnitude, yet is significantly correlated to the community structure similarity and to the number of mutual species. Modularity can buffer impacts on the network as a whole when individual modules are perturbed and aid in recovery of impacted nodes subject to acute stressors.

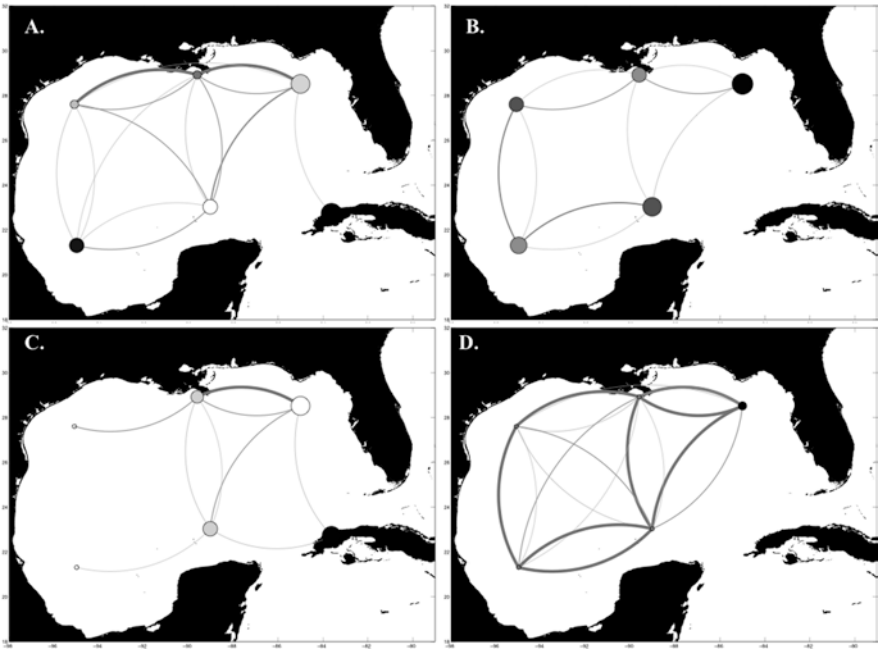

Fig. 22.9 Subregional Gulf of Mexico larval connectivity networks: (**a**) tuna, (**b**) red snapper, (**c**) red grouper, and (**d**) golden tilefish. The subregional connectivity patterns are species specific, while betweenness centrality is the highest for red snapper in the SWF; the probability of migration across the GoM is higher for the golden tilefish

Acknowledgments This research was made possible by a grant from the Gulf of Mexico Research Initiative, CIMAGE II/III. We appreciate the assistance of Kesley Gibson and Greg Stunz of the Center for Sportfish Science and Conservation, Harte Research Institute for Gulf of Mexico Studies, for sharing preliminary shark tagging data for the western Gulf of Mexico, and Mandy Karnauskas from NOAA for sharing Red snapper model parameterization data. We also appreciate the permission to use fish image drawings granted by the artist Diane Peebles. Data are publicly availble at https://data.gulfresearchinitiative.org/data/R4.x267.000:0039 for the longline surveys and R6.x805.000:0075 for the connectivity and similarity matrices.

References

Addis DT, Patterson III WF, Dance MA (2007) Site fidelity and movement of reef fishes tagged at unreported artificial reef Sites off NW Florida. In: Proceedings of the 60th Gulf and Caribbean Fisheries Institute November 5–9, 2007, pp 297–304

Bethea DM, Driggers WB (2014) Tag and recapture data for smoothhound sharks, *Mustelus* spp., in the Gulf of Mexico and US South Atlantic: 1998–2012. SEDAR39-DW-01. SEDAR, North Charleston, SC, 11 pp

Brulé T, Colás-Marrufo T, Pérez-Díaz E, Sámano-Zapata JC (2010) Red snapper reproductive biology in the southern Gulf of Mexico. Trans Am Fish Soc 139:957–968. https://doi.org/10.1577/T09-125.1

Burgos JM, Sedberry GR, Wyanski GR, Harris PJ (2015) Life history of red grouper, (*Epinephelus morio*) off the coasts of North Carolina and South Carolina. SEDAR42-RD-04 July 2015

Chassignet EP, Hurlburt HE, Smedstad OM, Halliwell GR, Hogan PJ, Wallcraft AJ, Baraille R, Bleck R (2007) The HYCOM (HYbrid Coordinate Ocean Model) data assimilative system. J Mar Syst 65:60–83

Center for Sportfish Science and Conservation (2018) Results from shark tagging studies. Harte Research Institute for Gulf of Mexico Studies https://www.harteresearchinstitute.org/collaboration/tracking-sharks-gulf-mexico

Coleman FC, Koenig CC (2010) The effects of fishing, climate change, and other anthropogenic disturbances on red grouper and other reef fishes in the Gulf of Mexico. Integr Comp Biol 50:201–212. https://doi.org/10.1093/icb/icq072

Coleman FC, Koenigi CC, Collins LA (1996) Reproductive styles of shallow-water groupers (Pisces: Serranidae) in the eastern Gulf of Mexico and the consequences of fishing spawning aggregations. Environ Biol Fish 47:129–141

Coleman FC, Koenig CC, Scanlon KM, Heppell S, Heppell S, Miller MW (2010) Benthic habitat modification through excavation by red grouper, *Epinephelus morio*, in the northeastern Gulf of Mexico. Open Fish Sci J 3:1. https://doi.org/10.2174/1874401X01003010001

DiMarco SF, Nowlin Jr WD, Reid RO (2005) A statistical description of the velocity fields from upper ocean drifters in the Gulf of Mexico, pp 101–110. In: Sturges W, Lugo-Fernandez A (eds) Circulation in the Gulf of Mexico: observations and models. American Geophysical Union Monograph Series 161, 347 pp

Gilarranz LJ, Rayfield B, Liñán-Cembrano G, Bascompte J, Gonzalez A (2017) Effects of network modularity on the spread of perturbation impact in experimental metapopulations. Science 357:199–201

Goslee SC, Urban DL (2007) The ecodist package for dissimilarity-based analysis of ecological data. J Stat Softw 22:1–19

Grilli J, Rogers T, Allesina S (2016) Modularity and stability in ecological communities. Nat Commun 7:1–10

Grimes CB, Turner SC, Able KW (1983) A technique for tagging deepwater fish. Fish Bull (US) 81:663–666

Gunderson LH, Holling CS, Allen CR (2009) The evolution of an idea – the past, present and future of ecological resilience In: Gunderson LH, Allen CR, Holling CS (eds) Foundations of Ecological Resilience. Island Press, Washington, DC, 2009) pp. 423–444

Gunderson LH (2000) Ecological resilience – in theory and application. Annu Rev Ecol Syst 31:425–439

Guy Harvey Research Institute (2018) http://www.ghritracking.org/

Harris PJ, Wyanski DM, Mikell PTP (2004) Age, growth, and reproductive biology of Blueline tilefish along the southeastern coast of the United States, 1982–1999. Trans Am Fish Soc 133:1190–1204. https://doi.org/10.1577/T02-158.1

Hendon JM, Hoffmayer ER, Parsons GR (2013) Tag and recapture data for Atlantic sharpnose, Rhizoprionodon terraenovae, and bonnethead, Sphyrna tiburo, sharks caught in the northern Gulf of Mexico from 1998-2011. SEDAR34-WP-33. SEDAR, North Charleston, SC. 6 pp

Hersperger A, Forman RTT (2003) Adjacency arrangement effects on plant diversity and composition in woodland patches. Oikos 101:279–290

Hoffmayer ER, Franks JS, Driggers WB III, McKinney JA, Hendon JM, Quattro JM (2014) Habitat, movements and environmental preferences of dusky sharks, *Carcharhinus obscurus*, in the northern Gulf of Mexico. Mar Biol 161:911–924. https://doi.org/10.1007/s00227-014-2391-0

Hoolihan JP, Wells RJD, Luo J, Falterman B, Prince ED, Rooker JR (2014) Vertical and horizontal movements of yellowfin tuna in the Gulf of Mexico. Mar Coast Fish 6:211–222. https://doi.org/10.1080/19425120.2014.935900

Karnauskas M, Walter III JF, Paris CB (2013) Use of the connectivity modeling system to estimate movements of red snapper (*Lutjanus campechanus*) recruits in the northern Gulf of Mexico. SEDAR31-AW10. SEDAR, North Charleston, SC, 20 pp

Kough SA, Paris CB (2015) The influence of spawning periodicity on population connectivity. Coral Reefs 34:753–757. https://doi.org/10.1007/s00338-015-1311-1

Lowerre-Barbieri SL, Crabtree R, Switzer T, Walters-Burnsed S, Guenther C (2016) Age truncation and reproductive resilience of red snapper (*Lutjanus Campechanus*) in Florida east coast waters. SEDAR41- DW07. SEDAR, North Charleston, SC

Miron PF, Beron-Vera FJ, Olascoaga MJ, Sheinbaum J, Pérez-Brunius P, Froyland G (2017) Lagrangian dynamical geography of the Gulf of Mexico. Sci Rep 7:7021

Murawski SA, Peebles EB, Gracia A, Tunnell JW Jr, Armenteros M (2018) Comparative abundance, species composition, and demographics of continental shelf fish assemblages throughout the Gulf of Mexico. Mar Coast Fish: Dyn Manage Ecosyst Sci 10:325–346

Murawski SA, Hollander DJ, Gilbert S, Gracia A (2020) Deep-water oil and gas production in the Gulf of Mexico, and related global trends (Chap. 2). In: Murawski SA, Ainsworth C, Gilbert S, Hollander D, Paris CB, Schlüter M, Wetzel D (eds) Scenarios and responses to future deep oil spills – fighting the next war. Springer, Cham

Murie DJ, Parkyn DC, Austin J (2011) Seasonal movement and mixing rates of greater amberjack in the Gulf of Mexico and assessment of exchange with the South Atlantic spawning stock. SEDAR33-DW12. SEDAR, North Charleston, SC, 46 pp

Nemeth RC, Blondeau J, Herzlieb S, Kadison E (2007) Spatial and temporal patterns of movement and migration at spawning aggregations of red hind, *Epinephelus guttatus*, in the U.S. Virgin Islands. Environ Biol Fish 78:365–381

Ocean Studies Board, National Research Council (2013) An ecosystem services approach to assessing the impacts of the deepwater horizon oil spill in the Gulf of Mexico. National Academies Press, Washington, DC, 246 pp

Ortiz M, Burns K, Sprinkel J (2009) Review of tagging data for gag grouper (Mycteroperca microlepis) from the southeastern Gulf of Mexico region 1985-2005. SEDAR 10 DW- 08. SEDAR, North Charleston, SC. 18 pp.

Paris CB, Cowen RK (2004) Direct evidence of a biophysical retention mechanism for coral reef fish larvae. Limnol Oceanogr 49:1964–1979

Paris CB, Cherubin LM, Cowen RK (2007) Surfing, diving or spinning from reef to reef: effects on population connectivity. Mar Ecol Prog Ser 347:285–300

Paris CB, Helgers J, Van Sebille E, Srinivasan A (2013) Connectivity modeling system: a probabilistic modeling tool for the multi-scale tracking of biotic and abiotic variability in the ocean. Environ Model Softw 42:47–54. https://doi.org/10.1016/j.envsoft.2012.12.006

Patterson WF (2007) A review of movement in Gulf of Mexico red snapper: implications for population structure. Am Fish Soc Symp 60:221–235

Patterson WF III, Watterson JC, Shipp RL, Cowan JH Jr (2001) Movement of tagged red snapper in the northern Gulf of Mexico. Trans Am Fish Soc 130:533–545. https://doi.org/10.1577/1548-8659(2001)130<0533:MOTRSI>2.0.CO;2

Romero IC, Sutton T, Carr B, Quintana-Rizzo E, Ross SW, Hollander DJ, Torres JJ (2018) Decadal assessment of polycyclic aromatic hydrocarbons in mesopelagic fishes from the Gulf of Mexico reveals exposure to oil-derived sources. Environ Sci Technol (Published online) 52:10985. https://doi.org/10.1021/acs.est.8b02243

Schirripa MJ, Legault CM, Ortiz M (1999) The red grouper fishery of the Gulf of Mexico: assessment 3.0. National Marine Fisheries Service, Southeast Fisheries Science Center, Sustainable Fisheries Division Contribution No. SFD-98/99-56

Staaterman E, Paris CB (2014) Modeling larval fish navigation: the way forward. ICES J Mar Sci 71:918–924. https://doi.org/10.1093/icesjms/fst103

Sutton T, Frank T, Judkins H, Romero IC (2020) As Gulf oil extraction goes deeper, who is at risk? Community structure, distribution, and connectivity of the deep-pelagic fauna (Chap.

24). In: Murawski SA, Ainsworth C, Gilbert S, Hollander D, Paris CB, Schlüter M, Wetzel D (eds) Scenarios and responses to future deep oil spills – fighting the next war. Springer, Cham

Tyminski J, Simpfendorfer C, Hueter R (2005) Results of Mote Marine Laboratory shark tagging program for blacktip (*Carcharhinus limbatus*) and sandbar (*C. plumbeus*) sharks SEDAR LCS Data Workshop 34. SEDAR, North Charleston, SC

Treml EA, Halpin PN, Urban DL, Pratson LF (2008) Modeling population con- nectivity by ocean currents, a graph-theoretic approach for marine conservation. Landsc Ecol 23:19e36

Treml EA, Halpin PN (2012) Marine population connectivity identifies ecological neighbors for conservation planning in the Coral Triangle. Conservation Letters. 2012; https://doi.org/10.1111/j.1755-263X.2012.00260.x

Zamora R, Hodar JA, Matias L, Mendoza I (2010) Positive adjacency effects mediated by seed disperser birds in pine plantations. Ecol Appl 20:1053–1060

Chapter 23
Evaluating the Effectiveness of Fishery Closures for Deep Oil Spills Using a Four-Dimensional Model

Igal Berenshtein, Natalie Perlin, Steven A. Murawski, Samatha B. Joye, and Claire B. Paris

Abstract During the *Deepwater Horizon* (DWH) oil spill, extensive areas of the Gulf of Mexico (GoM) were closed for fishing due to the risk of seafood contamination and fishers' health. The closures were determined daily according to the estimated extent of the spill relying mainly on satellite imaging. These closures were largely limited to the northern GoM. Yet, evidence from the field indicates a presence of oil beyond the closures, in some cases at toxic concentrations. With the advancement of oil transport modeling, together with the availability of new in situ data, we examine the 4D extent of the DWH spill, along with the effectiveness of the fishery closures in capturing the oil spill extent. We use the oil application of the Connectivity Modeling System (oil-CMS), cross-checked against in situ BP Gulf Science Data (GSD) and other published studies. The oil-CMS indicates that DWH extended well beyond the satellite footprint and fishery closures, with the closures capturing only ~55% of the total extent of the spill. With an increasing global shift toward deep-sea drilling, our findings are important for the safety of coastal communities and marine ecosystems around deep-sea drilling areas.

Keywords Deepwater Horizon · Fishery closures · Oil spill · Marine pollution · Resource management · Spill response

I. Berenshtein (✉) · N. Perlin · C. B. Paris
University of Miami, Department of Ocean Sciences, Rosenstiel School of Marine and Atmospheric Science, Miami, FL, USA
e-mail: iberenshtein@rsmas.miami.edu; nperlin@rsmas.miami.edu; cparis@rsmas.miami.edu

S. A. Murawski
University of South Florida College of Marine Science, St. Petersburg, FL, USA
e-mail: smurawski@usf.edu

S. B. Joye
University of Georgia, Department of Marine Sciences, Athens, GA, USA
e-mail: mjoye@uga.edu

S. A. Murawski et al. (eds.), *Scenarios and Responses to Future Deep Oil Spills*,
https://doi.org/10.1007/978-3-030-12963-7_23

23.1 Introduction

The *Deepwater Horizon* (DWH) oil spill was a major catastrophe spilling 795 million liters of oil into the Gulf of Mexico (GoM) with oil slicks covering a cumulative estimated area of 149,000 km^2 (MacDonald et al. 2015). As a result, vast areas of the GoM were closed for fishing covering more than a third of the US national exclusive economic zone. Daily fishery closures were applied based on satellite and areal imagery by NOAA National Environmental Satellite, Data, and Information Service (NESDIS) Satellite Analysis Branch (SAB) utilizing mainly synthetic aperture radar (SAR), multispectral satellite imagery, and forward-in-time tracking of the satellite footprint for up to 72 h. These closures successfully diminished the risk of seafood poisoning and fishers' health (Ylitalo et al. 2012).

The cumulative satellite imagery footprint was largely accepted as the DWH oil spill extent from scientific, public, and management perspectives (MacDonald et al. 2015; Deepwater Horizon Natural Resource Damage Assessment Trustees 2016; Özgökmen et al. 2016; Wilson et al. 2016). Yet, multiple field studies support a much wider extent of the DWH spill extending beyond the fishery closures, reaching the west Florida shelf (WFS), the Texas shores (TXS), Loop Current (LC) system, and the Florida Keys (FK).

Specifically, in the WFS studies indicate high concentrations of oil (Sammarco et al. 2013), including toxic and mutagenic levels, in the water (Paul et al. 2013), in sediments (Harding et al. 2016), in sand patties (McDaniel et al. 2015), and on the coast (Nixon et al. 2016). Furthermore, Murawski et al. (2014) indicated that Macondo oil (i.e., oil associated with DWH) penetrated the WFS food web with high levels of polycyclic aromatic hydrocarbons (PAH) in red snappers' liver, which co-occurred with high frequency of skin lesions in bottom-dwelling fish. Lastly, Weisberg et al. (2016) used satellite imagery and particle tracking to show that an oil slick present east of Pensacola (north WFS) was transported southeast along the WFS, reaching Tampa and the Dry Tortugas (FK) within a few weeks. In the TXS, studies using water (Murawski et al. 2016) and sediment (Romero et al. 2017) samples demonstrated that oil reached the Texas coastal and continental shelf area, part of which were at toxic levels (Sammarco et al. 2013). The presence of DWH oil in the LC area was reported by the European Space Agency in May 2010 (European Space Agency 2010). Later, during early June, NOAA satellite imagery revealed the presence of 12 oil slicks in the area of the LC system, stretching from FK to the GoM interior, covering a cumulative area of 381 km^2. Wade et al. (2011b) reported high concentrations of oil in the LC, west of the fishery closures during late June till mid-July 2010; yet, the source of the oil could not be determined. The occurrence of a deep intrusion extending southwest ~400 km from the Macondo well was documented by Diercks et al. (2010) and successfully reconstructed by the oil transport model in Paris et al. (2012). The deep plume which exceeded ~300 km beyond the closure areas contained high and toxic levels of oil concentration within 13 km from the wellhead (Diercks et al. 2010).

Numerous modeling efforts were carried out in an attempt to reconstruct spatiotemporal dynamics of the DWH oil spill. Lagrangian coherent structure (LCS) core analysis modeled the movement of oil on the surface at short time scales, successfully reconstructing the oil footprint from the satellite imagery (Olascoaga and Haller 2012). Similarly, the 3D oil application of the Connectivity Modeling Systems (CMS) (Paris et al. 2013) and the General NOAA Operational Modeling Environment (GNOME) (Boufadel et al. 2014) simulated the oiled coastline areas, both successfully reconstructing the observed beaching patterns (Nixon et al. 2016). The GNOME was also used to conduct probabilistic Monte Carlo simulations, running hundreds of oil transport scenarios based on historical wind and currents data (Barker 2011).

Given the capabilities and knowledge available during the DWH, the fishery closures were successful in capturing the bulk of the satellite footprint and diminishing seafood poisoning risk (Ylitalo et al. 2012). Yet with the advancement of oil transport modeling (de Gouw et al. 2011; Paris et al. 2012; Olascoaga and Haller 2012; Le Hénaff et al. 2012; Boufadel et al. 2014; North et al. 2015; Lindo-atichati et al. 2016) and the accumulation of spatially explicit observational data (e.g., BP Gulf Science Data 2016a, b), a more comprehensive examination of the 3D extent of the oil spill is now possible. The purpose of the current chapter is to examine (1) the 3D DWH oil spill extent cross-checked against in situ data and (2) to assess the effectiveness of the fishery closures in capturing that extent.

23.2 Methods

23.2.1 General Methods Approach

The methods approach in the current chapter is composed of two components: (1) spatial extent comparison from satellite imagery, in situ observations, and oil transport modeling and (2) quantifying the effectiveness of the fishery closures in capturing the oil spill extent, specifically, the daily portion of oil mass and total area which were encompassed by the fishery closures. We used MATLAB 2017a (The MathWorks, INC) to compute the spatial analyses related to the oil-CMS output and R software version 3.03 (R Foundation 2017) for all data and statistical analyses.

23.2.2 In Situ Water and Sediment Samples

To examine the DWH spatiotemporal extent of the oil spill from in situ measurements, we used the British Petroleum (BP) Gulf Science Data (GSD) (BP Gulf Science Data 2016a, b), which includes more than 25,000 water and sediment samples from at least 67 Response and Natural Resource Damage Assessment (NRDA)

studies collected by multiple response agencies, trustees, and BP(BP Gulf Science Data 2016a, b). We used TPH (C9-C44) and PAH50 concentrations (μg L^{-1}), representing the summed concentrations of 50 main PAH components. Water samples data included only unfiltered samples, therefore concentrations account for both the dissolved and the particulate phases of hydrocarbons. Concentrations were blank corrected with values below method detection limit (MDL) set to zero. Background PAH thresholds for water and sediment samples were 0.056 ppb (Wade et al. 2016) and 300 ppb (Kennicutt 2017), respectively. The spatial extent of the modeled oil spill was compared visually against the distribution of higher-than-background water and sediment concentrations. The rationale for this comparison was the non-uniform sampling effort and the patchy nature of oil in the water. In other words, sampling of high concentrations is a rare event due to patchiness in time and space; hence, higher-than-background concentrations indicate the presence of oil, but a sample with zero oil concentration does not necessarily indicate lack of oil in the vicinity of the sample.

23.2.3 Satellite and Areal Imagery: National Environmental Satellite, Data, and Information Service (NESDIS) Anomaly

NESDIS anomaly data represents Synthetic aperture radar (SAR), high-resolution visible/multispectral imagery and/or other types of ancillary data sources representing the estimated areas with oil slicks on the water surface during the DWH (http://www.ssd.noaa.gov/PS/MPS/about.html), utilizing mainly SAR. The NESDIS anomaly together with daily fishery closures data were downloaded from the Environmental Response and Management Application (ERMA) web page: https://erma.noaa.gov/gulfofmexico/. ArcMap (ESRI) software was used for computing the area of the NESDIS anomaly daily composites and for computing the daily intersected regions between the NESDIS footprint and the fishery closures. State waters which covered less than 2% of the domain were omitted from the spatial analysis due to limited data availability; thus, only federal closures were considered.

23.2.4 Oil Transport Model: Oil-CMS

We implemented the existing oil application (Paris et al. 2012) of the Connectivity Modeling System (CMS; Paris et al. 2013) to compute the transport and fate of the live oil spilled during the DWH blowout. The oil-CMS performs Lagrangian particle tracking of oil droplets released at the trap height above the well location. Particle transport calculations consider ocean 3D currents, temperature, salinity,

multi-fractional droplet buoyancy, biodegradation, and surface oil evaporation (de Gouw et al. 2011; Paris et al. 2012, 2013; Le Hénaff et al. 2012; Lindo-atichati et al. 2016). The 4th-order Runge-Kutta integration scheme forms the basis for particle advection in the model. Computations of the vertical terminal velocity of a droplet is based on the droplet's density and size, its Reynolds number, as well as water temperature, salinity, density, and kinematic viscosity (Paris et al. 2012, 2013; Le Hénaff et al. 2012; Lindo-atichati et al. 2016). The model output is saved every 2 h and includes droplets' effective density, size, location, and depth. The oil-CMS horizontal grid spacing is of 0.04° and includes 20 vertical layers. The oil-CMS applies a multi-fraction droplet approach in which each droplet includes multiple hydrocarbon fractions (Lindo-atichati et al. 2016). The biodegradation dynamics of the present study are based on high-pressure experiments and apply different decay rates for the different fractions (Lindo-atichati et al. 2016). This allows to account for dissolution processes where the droplet shrinks with the partitioning of the oil compounds in the water column (Jaggi et al. 2017). Post-processing algorithms translate model output into oil concentrations.

Three thousand oil droplets were released above the blowout location (28.736°N, 88.365°W) every 2 h for 87 days until July 15, 2010 – the day of successful capping of the oil well. The release depth is 1222 m, i.e., 300 m above the Macondo well depth, which is the estimated height of oil and gas separation above the wellhead (Paris et al. 2012). Initial droplet diameters are drawn from a uniform distribution between 1 and 500 μm. Each droplet released by the CMS model contains three pseudo-components (fractions) accounting for the differential oil densities as follows: 10% of light oil with the density of 800 kg m^{-3}, 75% of intermediate oil with 840 kg m^{-3}, and 15% of heavy oil with 950 kg m^{-3} density. The biodegradation half-life rates for the light, intermediate, and heavy fractions were set to 30, 40, and 180 h based on laboratory and observation studies (Lindo-atichati et al. 2016). Evaporation half-life rate was set to 250 h (de Gouw et al. 2011; Paris et al. 2012). Horizontal diffusion was set to 10 m^2 s^{-1}.

Ocean hydrodynamic forcing for the present study used daily output from the Hybrid Coordinate Ocean Model (HYCOM) for the GoM region on a 0.04° horizontal grid, including 40 vertical levels spanning from the surface to 5500 m. HYCOM model employs data assimilation using the Navy Coupled Ocean Data Assimilation (NCODA), which assimilates available satellite altimeter and sea surface temperature (SST) observations, as well as available temperature and salinity profiles from moored buoys and drifting hydrographic floats. HYCOM output variables used for CMS simulations included horizontal and vertical velocity components, temperature, and salinity.

The simulation included parameterization of the surface wind-drift effects (Le Hénaff et al. 2012). Wind stress components from the 0.5° Navy Operational Global Atmospheric Prediction System (NOGAPS) are interpolated into HYCOM Gulf of Mexico 0.04° grid, and 3% of their values are added to the top-level ocean velocity horizontal components taking into account the wind stress rotation. The corrected ocean velocity fields are then implemented in the oil-CMS. Flow rate was modeled

as a simplified case of a constant rate during the oil spill event. The estimated 7.3×10^5 tons of crude oil, which corresponds to ~5.0 million barrels of oil (McNutt et al. 2012), are represented by a total of 3.132×10^6 droplets. These values translate into the 233 kg of oil represented by a single oil droplet at each release time in the CMS model.

The DSD distribution was approximated using the binned approach, with droplets in the same bin representing similar mass of oil per droplet. We further compute the scaling factor for each droplet as the ratio between the current and the initial masses. Mass is estimated from the droplet diameter and effective density. Oil mass at each output time is then scaled to obtain effective oil mass at a given location and then summed for all the droplets found in each postprocessing domain 3D grid cell and at a given time step.

23.3 Results

23.3.1 Spatial DWH Cumulative Extents

The simulated cumulative oil spill extent, integrated across time and depth, spreads well beyond the areas denoted by NESDIS anomaly footprint and the fishery closures. In contrast, the spatial extent of the NESDIS anomaly footprint was substantially smaller and was nearly fully contained by the fishery closures (Fig. 23.1a, b). Specifically, the oil extended beyond the NESDIS anomaly footprint to TXS, WFS, LC, and FK and along the Gulf stream toward the east Florida shelf. This spatial distribution is in agreement with the higher-than-background GSD PAH samples (Fig. 23.1a), as well as with the spatially explicit information reported in previous studies for Apalachee Bay (AB) (Nixon et al. 2016), WFS(Harding et al. 2016), TXS (Sammarco et al. 2013; Romero et al. 2017), LC (Wade et al. 2011b), and deep plume (DP) (Payne and Driskell 2015) (Fig. 23.1b). NESDIS anomaly also confirmed the presence of multiple oil patches in the LC and the FK (Fig. 23.1a). Notably, the spatial shape and location of the NESDIS anomaly correspond to the regions containing the highest simulated cumulative oil concentrations (Fig. 23.1a, b).

23.3.2 The Effectiveness of the Fishery Closures

The oil-CMS transport model indicated that the fishery closures captured 82 ± 19% (SD) of the total oil mass in the domain (Fig. 23.2a), 54 ± 20% (SD) of the total area covered by oil (Fig. 23.2b). In contrast, the fishery closures captured 94 ± 9% (SD) of the NESDIS anomaly (Fig. 23.2c). The areas where the closures failed to capture the oil spill extent according to oil-CMS model were primarily TXS, LC, and WFS. Specifically, the oil-CMS indicated expansions of the spill extent on

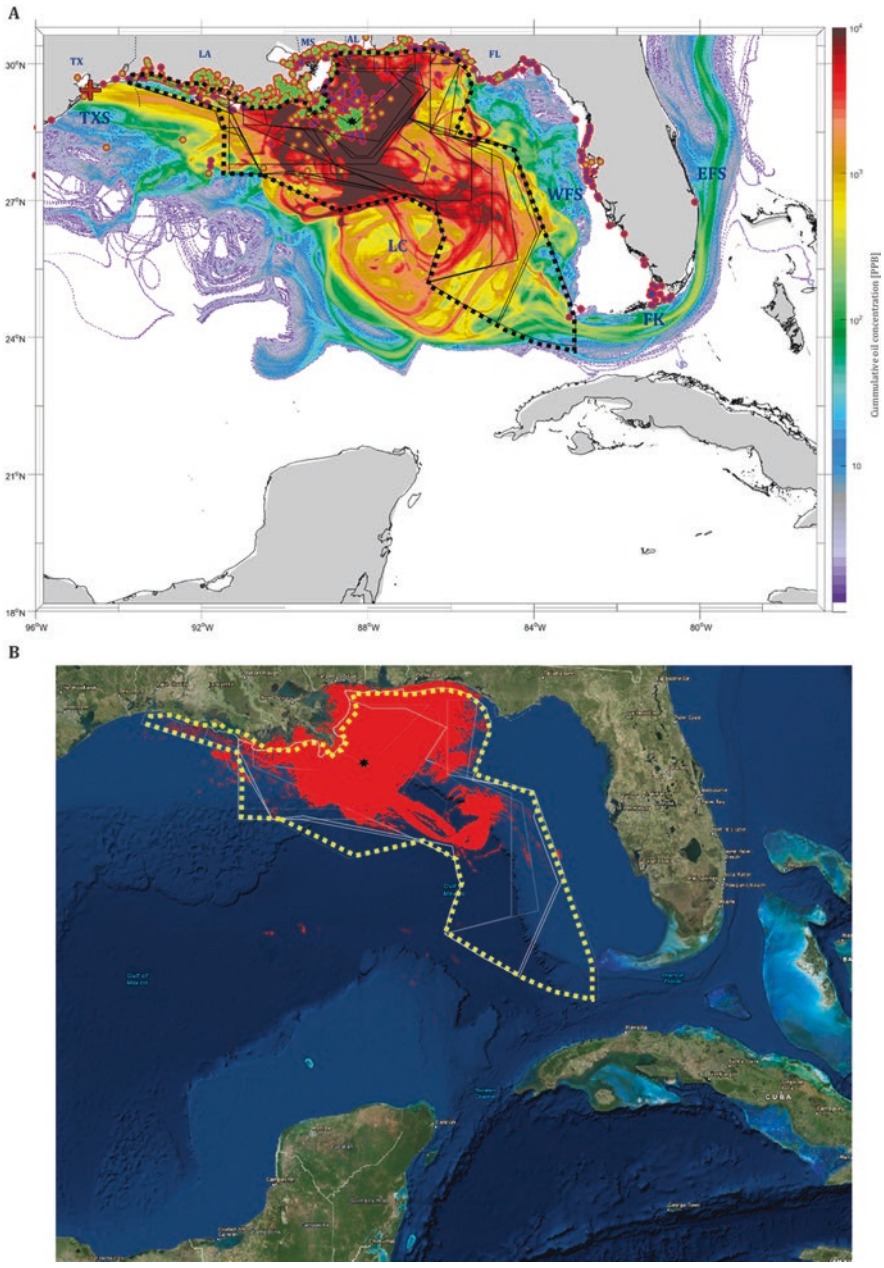

Fig. 23.1 Spatial DWH cumulative extents. (**a**) Cumulative daily oil concentrations (ppb), integrated from April 20, 2010, to July 21, 2010, and across water depths. Vertical layers are 0–1 m, 1–20 m, and in 20 m increments down to 2500 m. Sediment and water samples with higher-than-background concentration are marked in green and blue circles, respectively. Daily fishery closures are marked with thin black polygons; cumulative fishing closure area is marked with a dotted

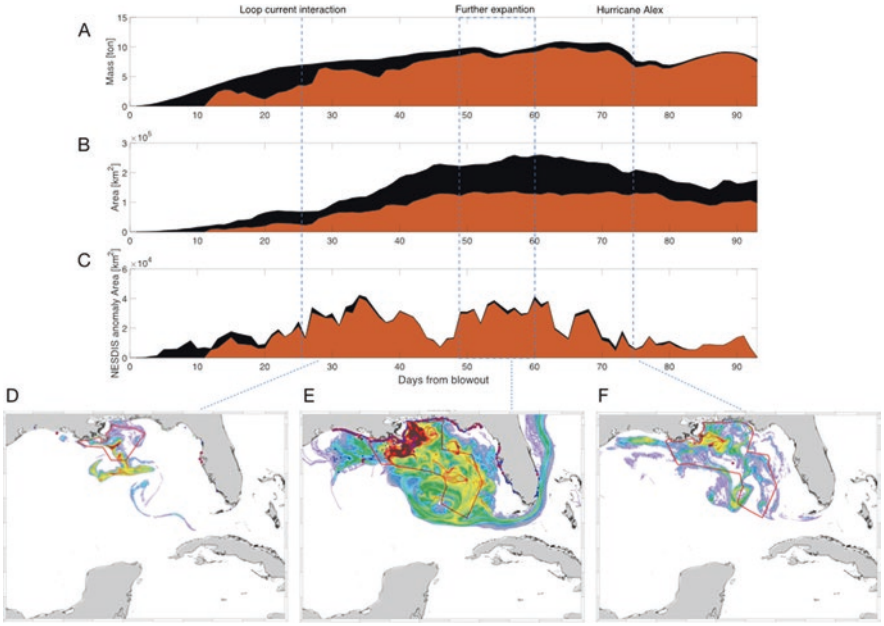

Fig. 23.2 The effectiveness of the fishery closures. (**a**) Mass, (**b**) area of total oil spill, and (**c**) area of National Environmental Satellite, Data, and Information Service (NESDIS) anomaly footprint, captured by the fishery closures (brown) with respect to the total (black) present in the domain across 93 days from blowout. The oil-CMS during May 15, 2010 (**d**), cumulative across June 6–18, 2010 (**e**), and July 2–10, 2010 (**f**). Purple, green, blue, orange, and red colors in (**d**–**f**) represent oil concentrations of 1, 10, 10^2,10^3, and $>10^4$ ppb, respectively. Sediment and water samples from the Gulf Science Data (GSD) are marked in green and blue circles, respectively, with red outlines representing samples with higher-than-background concentrations

May 15, 2010, toward TXS and toward the LC (Fig. 23.2e), which is in agreement with the European Space Agency report for that same date (European Space Agency 2010). As the spill evolved during June 2010, the oil extended further west, south, and east reaching the WFS in addition to TXS and LC, which agrees with the GSD in situ water and sediment samples (Fig. 23.2e). Between June 28 and July 2, 2010, hurricane Alex swept through the GoM, with strong southeasterly winds and waves enhancing the weathering, mixing, and beaching of the DWH oil, causing a decline in oil area and mass and spatial extent for the following day (July, 3) (Fig. 23.2a–c, f).

Fig. 23.1 (continued) black polygon. TXS: Texas shore, LC: Loop Current system, WFS: west Florida shelf, EFS: east Florida shelf, FK: Florida Keys, DP: deep plume, AB: Apalachee Bay. Red-edged points represent higher-than-background in situ water (blue) and sediment (green) samples. (**b**) Cumulative National Environmental Satellite, Data, and Information Service (NESDIS) anomaly daily composites integrated from April 20, 2010, to July 21, 2010. Daily fishing closures are marked with thin gray polygons; cumulative fishing closure area is marked with a dotted yellow polygon. Black stars represent the location of the DWH blowout in (a) and (b)

23.4 Discussion

The spatial synthesis of previously published studies (European Space Agency 2010; Wade et al. 2011b; Sammarco et al. 2013; Murawski et al. 2014; Payne and Driskell 2015; McDaniel et al. 2015; Harding et al. 2016; Nixon et al. 2016; Weisberg et al. 2016; Romero et al. 2017), combined with the GSD water and sediment samples (BP Gulf Science Data 2016a, b), clearly demonstrates that DWH oil spill has extended beyond the satellite detection and the fishery closures' limits, reaching TXS, WFS, DP, and LC (Fig 23.1). Our results from the oil-CMS agree with that extent, providing the oil transport context for these observations, and resolving an apparent spatial discrepancy between satellite footprint and field studies. Previous spatial modeling efforts of DWH provided similar spatial extents to that of the oil-CMS. NOAA's GNOME produced a nearly identical spatial probability heat map to that of the oil-CMS (Fig. 23.1a) (Barker 2011), as well as other modeling studies using LCS core analysis and particle tracking (Maltrud et al. 2010; Olascoaga 2011) indicating that Macondo oil reached TX, WFS, LC, and FK.

The GoM is highly active in terms of both oil drillings and oil seeps (MacDonald et al. 2015); therefore, it is possible that some samples contained non-Macondo oil. Yet, few methods aid in determining the pollution source. Explicit forensic analyses were applied in samples of sediments (Romero et al. 2017), sand patties (McDaniel et al. 2015), and animal tissues (Murawski et al. 2014), demonstrating that Macondo oil was the source of contamination. For water samples, due to quick degradation of many compounds, a forensic fingerprinting analysis was not possible, yet spatial kriging interpolation methods (Murawski et al. 2016) demonstrated a clear concentration gradient from the Macondo well, further supporting the DWH as the pollution source. Moreover, due to the patchy nature of the oil distribution in both time and space, many observations from multiple studies found no evidence of oil. In fact, even within 10 km of the Macondo well during the oil spill, ~52% of the water samples were below PAH background level (BP Gulf Science Data 2016a). This is important when weighing "no indication of oil" versus "positive indication of oil."

Notably, the fishery closures captured the bulk of the oil mass and satellite footprint (Figs. 23.1 and 23.2). Moreover, the ultimate purpose of the fishery closures is not necessarily to encompass the entire oil spill but rather to prevent capturing contaminated seafood and prevent health risk for the fishers. While large areas of the spill were not covered by the closures, whether or not these areas imposed risk of seafood contamination are unclear. Moreover, there is little information regarding the ambient oil concentrations at which bioaccumulation rate leads to seafood contamination above the level of concern.

A possible approach for determining fishery closures in real time is to use the toxic-to-biota thresholds of oil concentrations in seawater as the benchmark determining the closures boundaries. In such approach, in situ sampling effort should be pre-allocated for the purpose of determining the true boundaries of the oil spill and should be applied on a pre-gridded domain, similarly to the protocol applied in the reopening of fishery closures (Ylitalo et al. 2012). When overlaying the fishery closures and GSD water sample locations, it is evident that there is a poor representation of in situ oil concentration samples along the fishery closure boundaries (Fig. 23.3a)

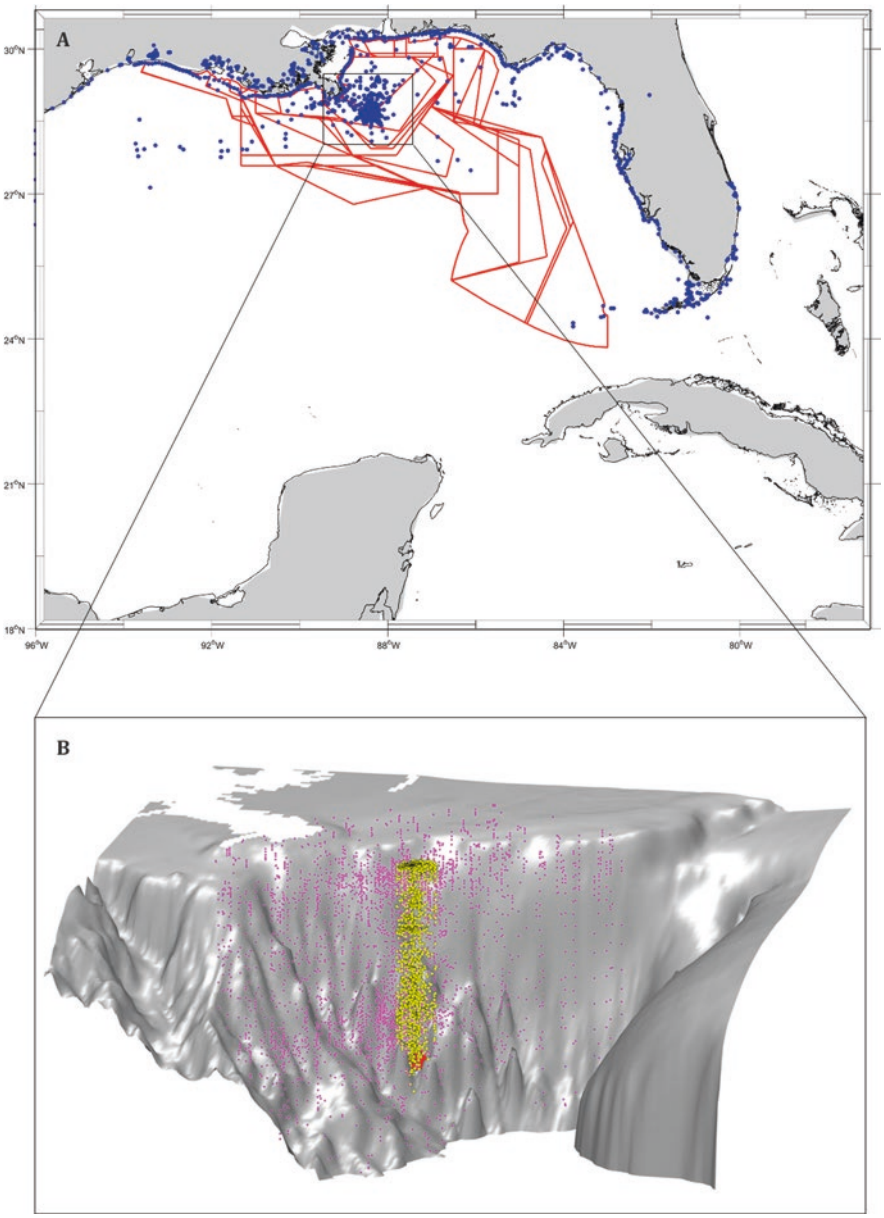

Fig. 23.3 (**a**) Blue circles represent in situ water samples from BP Gulf Science Data sampled between April 20, 2010, and July 21, 2010. Red polygons are fishery closures. (**b**) Zoom-in on an area within approximately 100 km from the wellhead (red). Magenta and yellow circles represent in situ water samples from BP Gulf Science Data within 100 km and 10 km from the wellhead

and that the bulk of the samples fell within 100 km from the spill (Fig. 23.3b). With the rapid increase in global deep-sea drilling efforts and petroleum-related activities, it is important to consider these findings in future oil spill response and management.

Funding Information This research was made possible by grants from the Gulf of Mexico Research Initiative through its consortia: The Center for the Integrated Modeling and Analysis of the Gulf Ecosystem (C-IMAGE), National Academy of Sciences grant (to C. B. P. and S. M.). Data are publicly available through the Gulf of Mexico Research Initiative Information & Data Cooperative (GRIIDC) at https://data.gulfresearchinitiative.org (doi: [10.7266/N7GM85C0, 10.7266/N76D5RCB, 10.7266/N7G44NQX, 10.7266/N7KD1WDB]).

References

Barker CH (2011) A statistical outlook for the Deepwater Horizon oil spill. American Geophysical Union (AGU), pp 237–244. https://doi.org/10.1029/2011GM001129

Boufadel MC, Abdollahi-Nasab A, Geng X, Galt J, Torlapati J (2014) Simulation of the landfall of the Deepwater Horizon oil on the shorelines of the Gulf of Mexico. Environ Sci Technol 48:9496–9505. https://doi.org/10.1021/es5012862

BP Gulf Science Data (2016a) Chemistry data associated with water column samples collected in the Gulf of Mexico from May 2010 through July 2012. http://dx.doi.org/10.7266/N747489X

BP Gulf Science Data (2016b) Chemistry data associated with submerged sediment samples collected in the Gulf of Mexico from April 2010 through December 2011. http://dx.doi.org/10.7266/N73J3BC2

de Gouw JA, Middlebrook AM, Warneke C, Ahmadov R, Atlas EL, Bahreini R, Blake DR, Brock CA (2011) Organic aerosol formation downwind from the Deepwater Horizon oil spill. Science 331:1295–1299. https://doi.org/10.1126/science.1200320

Deepwater Horizon Natural Resource Damage Assessment Trustees (2016) Deepwater Horizon oil spill: final programmatic damage assessment and restoration plan and final programmatic environmental impact statement. National Oceanic and Atmospheric Administration, Silver Spring

Diercks AR, Highsmith RC, Asper VL, Joung DJ, Zhou Z, Guo L, Shiller AM, Joye SB, Teske AP, Guinasso N, Wade TL, Lohrenz SE (2010) Characterization of subsurface polycyclic aromatic hydrocarbons at the Deepwater Horizon site. Geophys Res Lett 37:L20602. https://doi.org/10.1029/2010GL045046

European Space Agency (2010) Gulf of Mexico oil spill in the loop current. In: ScienceDaily. https://www.sciencedaily.com/releases/2010/05/100519112721.htm. Accessed 9 Feb 2018

Harding V, Camp J, Morgan LJ, Gryko J (2016) Oil residue contamination of continental shelf sediments of the Gulf of Mexico. Mar Pollut Bull 113:488–495. https://doi.org/10.1016/j.marpolbul.2016.07.032

Jaggi A, Snowdon RW, Stopford A, Radović JR, Oldenburg TBP, Larter SR (2017) Experimental simulation of crude oil-water partitioning behavior of BTEX compounds during a deep submarine oil spill. Org Geochem 108:1–8. https://doi.org/10.1016/j.orggeochem.2017.03.006

Kennicutt MC (2017) Sediment contaminants of the Gulf of Mexico. In: Habitats and biota of the Gulf of Mexico: before the Deepwater Horizon oil spill. Springer, New York, pp 217–273

Le Hénaff M, Kourafalou VH, Paris CB, Helgers J, Aman ZM, Hogan PJ, Srinivasan A (2012) Surface evolution of the Deepwater Horizon oil spill patch: combined effects of circulation and wind-induced drift. Environ Sci Technol 46:7267–7273. https://doi.org/10.1021/es301570w

Lindo-atichati D, Paris CB, Le HM (2016) Simulating the effects of droplet size , high- pressure biodegradation , and variable flow rate on the subsea evolution of deep plumes from the Macondo blowout. Deep Sea Res Part II 129:301–310. https://doi.org/10.1016/j.dsr2.2014.01.011

MacDonald IR, Garcia-Pineda O, Beet A, Daneshgar Asl S, Feng L, Graettinger G, French-McCay D, Holmes J, Hu C, Huffer F, Leifer I, Muller-Karger F, Solow A, Silva M, Swayze G (2015) Natural and unnatural oil slicks in the Gulf of Mexico. J Geophys Res Oceans 120:8364–8380. https://doi.org/10.1002/2015JC011062

Maltrud M, Peacock S, Visbeck M (2010) On the possible long-term fate of oil released in the Deepwater Horizon incident, estimated using ensembles of dye release simulations. Environ Res Lett 5:035301. https://doi.org/10.1088/1748-9326/5/3/035301

McDaniel LD, Basso J, Pulster E, Paul JH (2015) Sand patties provide evidence for the presence of Deepwater Horizon oil on the beaches of the west Florida shelf. Mar Pollut Bull 97:67–77. https://doi.org/10.1016/J.MARPOLBUL.2015.06.032

McNutt MK, Camilli R, Crone TJ, Guthrie GD, Hsieh PA, Ryerson TB, Savas O, Shaffer F (2012) Review of flow rate estimates of the Deepwater Horizon oil spill. Proc Natl Acad Sci 109:20260–20267. https://doi.org/10.1073/pnas.1112139108

Murawski SA, Hogarth WT, Peebles EB, Barbeiri L (2014) Prevalence of external skin lesions and polycyclic aromatic hydrocarbon concentrations in Gulf of Mexico fishes, post-Deepwater Horizon. Trans Am Fish Soc 143:1084–1097. https://doi.org/10.1080/00028487.2014.911205

Murawski SA, Fleeger JW, Patterson WF III, Hu C, Daly K, Romero I, Toro-Farmer GA (2016) How did the oil spill affect coastal and continental Deepwater Horizon shelf ecosystems of the Gulf of Mexico? Oceanography 29:160–173. https://doi.org/10.5670/oceanog.2016.80

Nixon Z, Zengel S, Baker M, Steinhoff M, Fricanod G, Rouhanie S, Michela J (2016) Shoreline oiling from the Deepwater Horizon oil spill. Mar Pollut Bull 107:170–178. https://doi.org/10.1016/J.MARPOLBUL.2016.04.003

North EW, Adams EE, Thessen AE, Schlag Z, He R, Socolofsky SA, Masutani SM, Peckham SD (2015) The influence of droplet size and biodegradation on the transport of subsurface oil droplets during the Deepwater Horizon spill: a model sensitivity study. Environ Res Lett 10. https://doi.org/10.1088/1748-9326/10/2/024016

Olascoaga MJ (2011) Physical oceanography division – monitoring the Gulf of Mexico conditions – simulated flow trajectories. In: NOAA website. http://www.aoml.noaa.gov/phod/dhos/lcs.php. Accessed 6 Aug 2018

Olascoaga MJ, Haller G (2012) Forecasting sudden changes in environmental pollution patterns. Proc Natl Acad Sci 109:4738–4743. https://doi.org/10.1073/pnas.1118574109

Özgökmen T, Chassignet E, Dawson CN, Dukhovskoy D, Jacobs G, Ledwell J, Garcia-Pineda O, MacDonald IR, Morey SL, Olascoaga MJ, Poje AC, Reed M, Skancke J (2016) Over what area did the oil and gas spread during the 2010 Deepwater Horizon oil spill? Oceanography 29:96–107. https://doi.org/10.5670/oceanog.2016.74

Paris CB, Le Hénaff M, Aman ZM, Subramaniam A, Helgers J, Wang DP, Kourafalou VH, Srinivasan A (2012) Evolution of the Macondo well blowout: simulating the effects of the circulation and synthetic dispersants on the subsea oil transport. Environ Sci Technol 46:13293–13302. https://doi.org/10.1021/es303197h

Paris CB, Helgers J, Van Sebille E, Srinivasan A (2013) Connectivity modeling system: a probabilistic modeling tool for the multi-scale tracking of biotic and abiotic variability in the ocean. Environ Model Softw 42:47–54. https://doi.org/10.1016/j.envsoft.2012.12.006

Paul JH, Hollander D, Coble P, Daly KL, Murasko S, English D, Basso J, Delaney J, McDaniel L, Kovach CW (2013) Toxicity and mutagenicity of Gulf of Mexico waters during and after the Deepwater Horizon oil spill. Environ Sci Technol 47:9651–9659. https://doi.org/10.1021/es401761h

Payne JR, Driskell W (2015) 2010 DWH offshore water column samples – forensic assessments and oil exposures. (CHEM_TR.18). Seattle. DWH Natural Resource Exposure NRDA Technical Working Group Report

R Foundation (2017) The R project for statistical computing. https://www.r-project.org/. Accessed 9 Apr 2018

Romero IC, Toro-Farmer G, Diercks A-R, Schwing P, Muller-Karger F, Murawski S, Hollander DJ (2017) Large-scale deposition of weathered oil in the Gulf of Mexico following a deep-water oil spill. Environ Pollut 228:179–189. https://doi.org/10.1016/J.ENVPOL.2017.05.019

Sammarco PW, Kolian SR, Warby RAF, Bouldin JL, Subra WA, Porter SA (2013) Distribution and concentrations of petroleum hydrocarbons associated with the BP/Deepwater Horizon oil spill, Gulf of Mexico. Mar Pollut Bull 73:129–143. https://doi.org/10.1016/j.marpolbul.2013.05.029

Wade TL, Sweet ST, Sericano JL, Guinasso Jr NL, Diercks A-R, Highsmith RC, Asper VL, Joung DJ, Shiller AM, Lohrenz SE, Joye SB (2011a) Analyses of water samples from the Deepwater Horizon oil spill: documentation of the subsurface plume. In: Monitoring and modeling the Deepwater Horizon oil spill: a record breaking enterprise, pp 77–82. https://doi.org/10.1029/2011GM001103

Wade TL, Sweet ST, Walpert JN, Sericano JL, Singer JJ, Guinasso Jr NL (2011b) Evaluation of possible inputs of oil from the Deepwater Horizon spill to the loop current and associated eddies in the Gulf of Mexico. In: Monitoring and modeling the Deepwater Horizon oil spill: a record breaking enterprise, pp 83–90. https://doi.org/10.1029/2011GM001095

Wade TL, Sericano JL, Sweet ST, Knap AH, Guinasso NL Jr (2016) Spatial and temporal distribution of water column total polycyclic aromatic hydrocarbons (PAH) and total petroleum hydrocarbons (TPH) from the Deepwater Horizon (Macondo) incident. Mar Pollut Bull 103:286–293. https://doi.org/10.1016/j.marpolbul.2015.12.002

Weisberg RH, Zheng L, Liu Y, Murawski S, Hu C, Paul J (2016) Did Deepwater Horizon hydrocarbons transit to the west Florida continental shelf? Deep Sea Res Part II Top Stud Oceanogr 129:259–272. https://doi.org/10.1016/J.DSR2.2014.02.002

Wilson M, Graham L, Hale C (2016) Persistence, fate, and effectiveness of dispersants used during the Deepwater Horizon oil spill. Sea Grant Programs. doi: GOMSG-G-15-004

Ylitalo GM, Krahn MM, Dickhoff WW, Stein JE, Walker CC, Lassitter CL, Garrett ES, Desfosse LL, Mitchell KM, Noble BT, Wilson S, Beck NB, Benner RA, Koufopoulos PN, Dickey RW (2012) Federal seafood safety response to the Deepwater Horizon oil spill. Proc Natl Acad Sci USA 109:20274–20279. https://doi.org/10.1073/pnas.1108886109

Chapter 24
As Gulf Oil Extraction Goes Deeper, Who Is at Risk? Community Structure, Distribution, and Connectivity of the Deep-Pelagic Fauna

Tracey T. Sutton, Tamara Frank, Heather Judkins, and Isabel C. Romero

Abstract The habitat and biota most affected by ultra-deep oil spills in the Gulf of Mexico (GoM) will necessarily be in the deep-pelagic domain. This domain represents ~91% of the GoM's volume and almost certainly contains the majority of its metazoan inhabitants. Ultra-deep oil spills may or may not reach the surface or the seafloor but will occur entirely within the deepwater column domain at some point and likely for the longest duration. Recent research has shown the deep-pelagic GoM to be extremely rich in biodiversity, both taxonomic and functional. Indeed, the GoM is one of the four "hyperdiverse" midwater ecosystems in the World Ocean. This biodiversity is functionally important. For example, well over half (58%) of all fish species known to exist in the GoM spend all or part of their lives in the oceanic domain. Recent research has also shown the deep-pelagic GoM to be highly connected vertically, as well as horizontally (onshore-offshore). This vertical connectivity provides an increasingly valued ecosystem service in the form of atmospheric carbon sequestration via the "biological pump." In this chapter, we summarize the GoM deep-pelagic nekton (fishes, macrocrustaceans, and cephalopods) that have been, and would be, affected by ultra-deep oil spills. We also discuss key aspects of distribution and behavior (e.g., vertical migration). These behaviors and distributions are key elements of ecosystem assessments before and after oil spills.

T. T. Sutton (✉) · T. Frank
Nova Southeastern University, Halmos College of Natural Sciences and Oceanography, Dania Beach, FL, USA
e-mail: tsutton1@nova.edu; tfrank1@nova.edu

H. Judkins
University of South Florida St. Petersburg, Department of Biological Sciences, St. Petersburg, FL, USA
e-mail: Judkins@mail.usf.edu

I. C. Romero
University of South Florida, College of Marine Science, St. Petersburg, FL, USA
e-mail: isabelromero@mail.usf.edu

S. A. Murawski et al. (eds.), *Scenarios and Responses to Future Deep Oil Spills*,
https://doi.org/10.1007/978-3-030-12963-7_24

For example, some deep-pelagic taxa show affinities for oceanic rim habitats (i.e., continental slopes), where ultra-deep drilling is most intense. Lastly, we summarize what is known about hydrocarbon contamination in the deep-pelagic biota and its possible ecosystem consequences.

Keywords Epipelagic · Mesopelagic · Bathypelagic · Biodiversity · Vertical distribution · Connectivity

24.1 Introduction

As oil extraction efforts in the Gulf of Mexico (GoM) proceed inexorably deeper, with ultra-deep (>1500 m water depth) wells now representing the majority of GoM production (Murawski et al. 2020), an imminent need exists to quantify and understand the faunal composition and dynamics of the deep-pelagic domain (i.e., midwater depths from 200 m and deeper to just above the seafloor). Given the buoyant nature of oil and oil-associated sinking processes, and natural weathering processes affecting oil bioavailability in the water column (Ryerson et al. 2012; Murawski et al. 2016; Romero et al. 2017), the deep-pelagic domain would be the largest ecosystem component affected in any ultra-deep oil spill scenario.

The deep-pelagic domain comprises the mesopelagic (200–1000 m) and bathypelagic (>1000 m) depth zones. The majority of the mesopelagic fauna conduct diel vertical migrations, residing deep (~400–1000 m) during the day and swimming up into the epipelagic (0–200 m) at night to feed (reviewed in Sutton 2013). Thus, the epi- and mesopelagic zones are tightly connected ecologically. Likewise, most bathypelagic nekton (fishes, macrocrustaceans, cephalopods) have epi-/mesopelagic early life history stages, and the majority of bathypelagic species also occur in the mesopelagic (Sutton et al. 2010); thus, the meso- and bathypelagic zones are also interconnected in this manner. Finally, early life history stages of many coastal species, including GoM reef fishes, are prevalent members of the oceanic epipelagic fauna, demonstrating onshore-offshore connectivity (Sutton et al. in prep). In summary, the oceanic domain of the GoM, from the surface to great depths, represents a continuum of ecological processes.

One of the legacies of the *Deepwater Horizon* oil spill (DWHOS) may prove to be the use of sub-surface dispersant injection at the wellhead as an effective response technique during ultra-deep oil spills to mitigate oil at the sea surface (French-McCay et al. 2018). A prerequisite for evaluating the environmental benefits of sequestering oil at depth via dispersant application is information on the ecosystem services provided by the fauna that this dispersant and dispersed oil would affect. The main challenges in this evaluation are the many knowledge gaps around the functioning of deep-sea ecosystems, including those of the GoM, and the prevalence of intermediate services relative to final services (Armstrong et al. 2012). Intermediate services include nutrient cycling, resilience and resistance, and biologically induced mixing (Jobstvogt et al. 2014), whereas final services include carbon

storage and sequestration, food provision, genetic resources, and waste absorption and detoxification (Ramirez-Lodra et al. 2011; Jobstvogt et al. 2014; Thurber et al. 2014). The loss of biodiversity is correlated to an exponential decline in deep-sea ecosystem functioning (e.g., nutrient and carbon cycling; Danavaro et al. 2008) and reduces the resilience of deep-sea ecosystems and their ability to respond to disturbance (Levin and Dayton 2009; Leduc et al. 2012). Globally the deep-pelagic domain is a primary engine of the biological pump, which absorbs ~ 25% of anthropogenic carbon emissions (Canadell et al. 2007; Sabine and Feely 2007), a critical service influencing climate. Recent research has also shown that the trophic interactions of deep-pelagic and deep-demersal fishes in slope ecosystems play an important role in the ocean carbon cycle, bypassing the detrital particle flux and transferring carbon to deep long-term storage (Trueman et al. 2014). In addition to their trophic significance, estimates suggest that fishes are important contributors of oceanic carbonate production (up to 15%, produced in their intestines; Wilson et al. 2009), and deep-pelagic fishes comprise the majority of Earth's fish biomass (Irigoien et al. 2014). Fish carbonate production may rise in response to rising environmental carbon dioxide, becoming an increasingly important part of the inorganic carbonate cycle (Wilson et al. 2009). In the deep-pelagic GoM, one important ecosystem service is the provision of foraging grounds for commercially valuable epipelagic fishes (e.g., bluefin tuna, *Thunnus thynnus*) and federally protected cetaceans (Allain 2005). As oil extraction expands into deeper waters, it will be important to consider ecosystem service frameworks that can be used to quantify the economic value of the deep-pelagic domain.

Knowledge of global deep-pelagic biodiversity, particularly water depths below 1000 m, lags that of coastal ecosystems by orders of magnitude (Webb et al. 2010; Sutton et al. 2017). That said, intensive sampling and analysis since the DWHOS have made the GoM one of the most, if not the most, known deep-pelagic ecosystems in the World Ocean. In this chapter, we summarize the current state of knowledge of deep-pelagic fish, macrocrustacean, and cephalopod assemblages in the GoM, summarize the major patterns of vertical distribution, and emphasize the elements of connectivity from the lens of future oil spill impacts.

24.2 Biodiversity and Faunal Composition

Two large-scale deep-pelagic sampling programs have been conducted in the GoM since the DWHOS. The first was the Offshore Nekton Sampling and Analysis Program (ONSAP), designed and executed by T. Sutton at the request of NOAA as part of their Natural Resource Damage Assessment (NRDA). This program, conducted from Nov 2010 to Sep 2011, utilized two ships and two gear types: (1) a large (162 m^2 mouth area), dual-warp, high-speed rope trawl, fished from the NOAA vessel *Pisces* and (2) a 10 m^2 mouth area MOCNESS (Multiple Opening Closing Net and Environmental Sensing System) rectangular midwater trawl, fished from the M/V *Meg Skansi*. The former net allowed sampling of large volumes of water

and larger, more mobile fauna, while the latter allowed discrete-depth, metered (quantitative) sampling, especially of the smaller, numerically dominant, "micronektonic" (2–20 cm size range) fauna. The latter fauna is the primary component of the ubiquitous "deep scattering layer," found in the GoM and throughout the world's oceanic ecosystems (D'Elia et al. 2016). Both sampling programs fished from the surface to 1500 m depth, with discrete-depth sampling dividing the water column into five depth bins: 0–200 m, 200–600 m, 600–1000 m, 1000–1200 m, and 1200–1500 m. The second large-scale, post-DWHOS sampling program was conducted from 2015 to 2018 by the GoMRI-funded DEEPEND (Deep-Pelagic Nekton Dynamics) consortium (www.deependconsortium.org). This program followed the NRDA *Meg Skansi* sampling protocols precisely, with MOCNESS sampling at the same depth intervals and sampling stations. Together these programs produced one of (if not the) the largest sample sets and faunal inventories of deep-pelagic nekton in oceanographic history. In the following sections, we briefly summarize these results with the goal of identifying the fauna at risk during simulation and future oil spills in the GoM.

24.2.1 Deep-Pelagic Fishes

Among the taxa of deep-pelagic micronekton and nekton, fishes are the numerically and biomass-dominant constituents (Herring 2001) globally, though in some locations macrocrustaceans can dominate (Feagans-Bartow and Sutton 2014). To date, ONSAP and DEEPEND sampling and analysis have identified 897 species, of which 186 are new records for the Gulf and 21 putatively new to science (Sutton et al. in prep). This represents 12% increase in the fish diversity records of the GoM prior to these programs. Functionally, 3% of these fish species are primarily epipelagic, 29% mesopelagic, 10% meso−/bathypelagic (spanners), 13% bathypelagic, 30% coastal juveniles, and 16% deep benthic/demersal juveniles. Of the coastal taxa, the species richness of larval benthic eels was exceptional, with 109 species (vs. 7 species of truly pelagic eels). Numerically, fishes of the order Stomiiformes (e.g., Gonostomatidae, Stomiidae, Sternoptychidae) are the overwhelmingly dominant order, representing about 75% of all deep-pelagic fishes (owing largely to the dominance of the single genus *Cyclothone*). Lanternfishes of the order Myctophiformes are the next most abundant, comprising approximately 15%. The order Perciformes, which dominate the coastal GoM, are much less abundant offshore, ranking third with a numerical contribution between 2% and 6%. Anguilliformes (mainly eel leptocephalus larvae, which have long pelagic residence times), Stephanoberyciformes and Aulopiformes are the remaining deep-pelagic orders contributing more than 1% of total numbers. These results depict the overall Gulf ichthyofauna as being highly speciose, oceanic, and vertically and horizontally connected, befitting its status as the "American Mediterranean." Examples of the most abundant orders of fishes are presented in Fig. 24.1. These findings confirm the GoM as one of the four most speciose mesopelagic ecoregions in the World Ocean (Sutton et al. 2017).

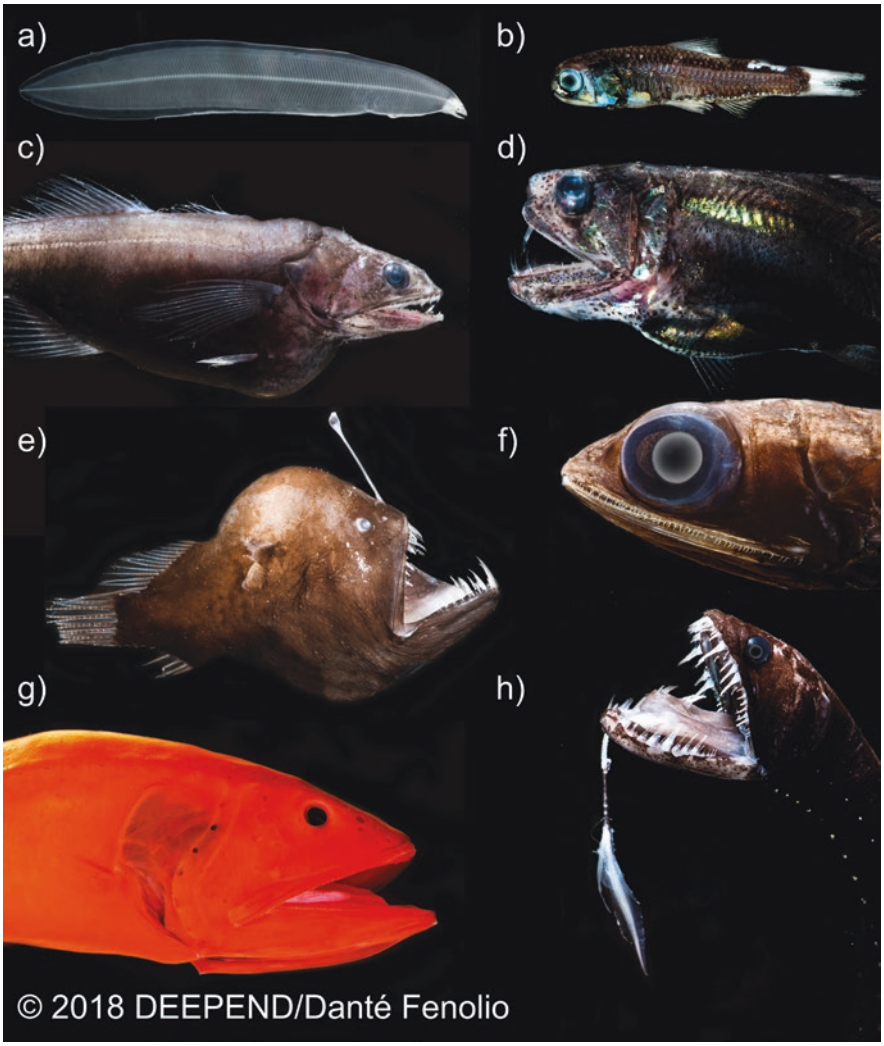

Fig. 24.1 The dominant deep-pelagic fish orders in the Gulf of Mexico: (**a**) Anguilliformes (*Gymnothorax kolpos*), (**b**) Myctophiformes (*Diaphus mollis*), (**c**) Perciformes (*Chiasmodon braueri*), (**d**) Aulopiformes (*Coccorella atlantica*), (**e**) Lophiiformes (*Melanocetus murrayi*), (**f**) Osmeriformes (*Bathylaco nigricans*), (**g**) Stephanoberyciformes (*Barbourisia rufa*), and (**h**) Stomiiformes (*Idiacanthus fasciola*)

24.2.2 Deep-Pelagic Macrocrustaceans

Macrocrustaceans have significant roles and contributions to the food web and biomass of pelagic nekton in all deep-sea communities (Pearcy and Forss 1966; Hopkins et al. 1994.). In the GoM, there are approximately 120 species spread

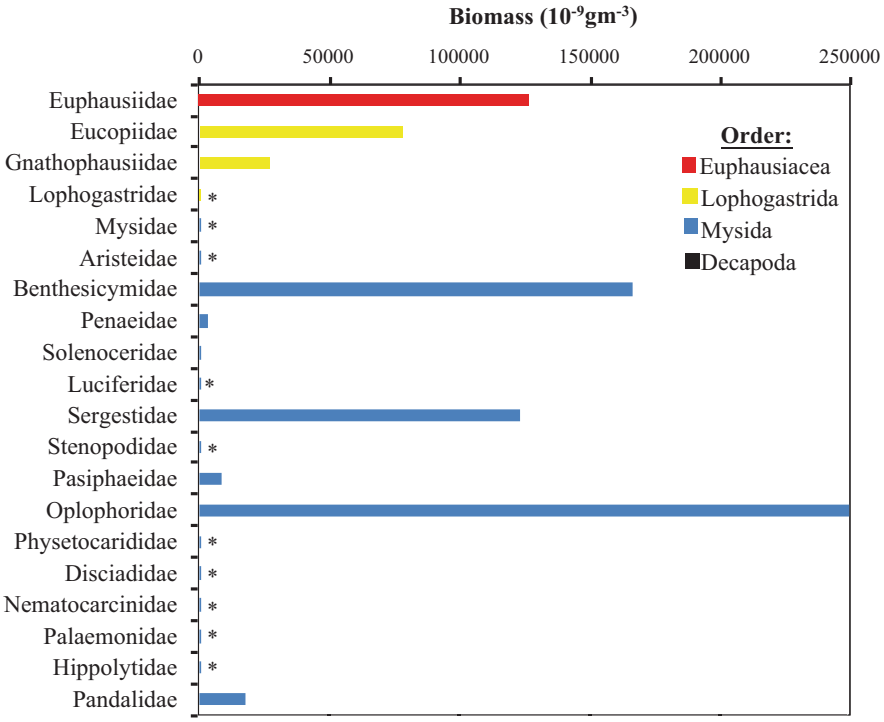

Fig. 24.2 Biomass ($\times 10^{-9}$ g m^{-3}) of crustacean families by order in the Gulf of Mexico. * indicates biomass values too small to show. (Modified from Burdett 2016)

across 21 families living between 0 and 1500 m water depth. In terms of biomass, the assemblage is dominated by five families: (1) Oplophoridae, (2) Benthesicymidae, (3) Euphausiidae, (4) Sergestidae, and (5) Eucopidae (Fig. 24.2). Together, these five families comprise approximately 90% of the total pelagic macrocrustacean biomass and 95% of the total abundance.

24.2.3 Deep-Pelagic Cephalopods

There are approximately 800 extant cephalopod species reported worldwide (Judkins and Vecchione 2016; Uribe and Zardoya 2017) inhabiting all marine habitats where salinity is higher than 17.5 psu, with 89 species known specifically in the GoM (Judkins 2009). Since 2009, there have been species with new geographic range extensions (Judkins et al. 2016) and new species discovered (Judkins et al. in prep) in the northern GoM, yielding an updated total of 94 known species. Cephalopod depth ranges extend from the intertidal zone to deeper than 5000 m. Many GoM coastal species have been examined due to their accessibility (Voss 1956, 1973; Laroe 1967; Lipka 1975), while the deep-sea species are more difficult to study because of net avoidance and other escape tactics (Passerella 1990).

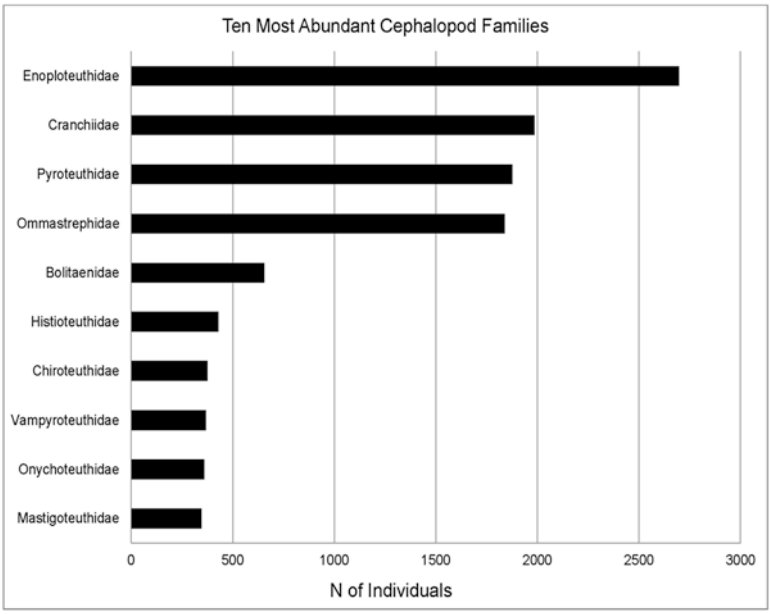

Fig. 24.3 Relative abundance of the dominant oceanic cephalopod families of the Gulf of Mexico

During ONSAP and DEEPEND efforts, over 12,000 cephalopod specimens were collected using two net types (large commercial trawl and smaller rectangular research trawl), generating one of the largest deep-sea cephalopod datasets to date (Judkins and Vecchione 2016). Over 80 documented cephalopod species have been collected through these efforts. The ten most collected cephalopod families are shown in Fig. 24.3 (from Judkins and Vecchione 2016). *Pyroteuthis* and *Pterygioteuthis* were the most abundant genera caught within the family Pyroteuthidae, followed by the Cranchiidae, with *Cranchia scabra* being the most abundant species. Rare species were also collected through these efforts (e.g., *Magnapinna pacifica*, *Planctoteuthis danae*), which highlight the importance of using multiple gear types to collect different life history stages of the deep midwater faunal groups (Judkins and Vecchione 2016).

24.3 Distribution, Vertical Migration, and Reproductive Seasonality

24.3.1 Horizontal Spatial Distributions

Spatial analyses of fishes in the northern GoM did not reveal spatial coherence with the continental shelf break (Milligan and Sutton submitted), arguing against the existence of a "boundary community," at least for fishes. However, fish assemblages

did differ on the mesoscale, with species composition and vertical distribution patterns varying in response to the presence of the Loop Current and Loop Current/warm-core eddies.

Horizontal/geographic spatial analyses were conducted for the crustacean families Oplophoridae (Burdett et al. 2017) and Euphausiidae (Fine 2016), comparing the assemblage structure on the landward side of the 1000 m shelf break (henceforth referred to as slope stations) to the oceanic side (henceforth referred to as offshore stations). Overall, the abundance and biomass of both the Oplophoridae and Euphausiidae were higher in slope stations vs. offshore stations, although these differences were not statistically significant. While the oplophorid diversity was similar between the two regions, the offshore assemblage of the euphausiids was significantly more diverse than the near-slope assemblage, at all depths and times of day, except for the epipelagic daytime assemblage, which was significantly more diverse over the slope. When looking at individual species, two species of Oplophoridae and eight species of Euphausiidae were significantly more abundant in shelf break stations, while two oplophorid species and one euphausiid species were significantly more abundant in offshore stations. Although studies on relationships between slope and offshore fauna are relatively uncommon, evidence of differences have been reported for the Oplophoridae in the Hawaiian Islands (Reid et al. 1991) and the Mediterranean Sea (Aguzzi and Company 2010).

Spatial distributions of cephalopods span from coastal to pelagic zones in the northern GoM (Judkins 2009). The DEEPEND program examined pelagic faunal trends associated with warm-core eddies, including inside, on the edge, and outside of these features. Preliminary findings suggest that cephalopods are least abundant within these eddies or when there is an extended Mississippi River outflow (Judkins unpublished) in the northern GoM.

24.3.2 Vertical Distributions and Diel Vertical Migration

Vertical distribution patterns have been constructed for 151 of the most common species of offshore fishes of the GoM (Milligan and Sutton, submitted; Sutton et al. in prep). Of all of the patterns characterized, 24-hour occupation of the epipelagic zone (0–200-m depth) was demonstrated by the highest number of taxa, largely due to the preponderance of early life history stages (e.g., flatfish, tuna, eels, and coastal reef fish larvae/juveniles). The next pattern is synchronous diel migration, where nearly all individuals migrate from mesopelagic depths into the epipelagic at night. This pattern characterized 24 taxa, primarily zooplanktivorous myctophids. Asynchronous migration, where only part of a species' local population migrates each night, was prevalent both in the mesopelagic and deep-meso−/bathypelagic zones, with roughly equal taxonomic representation (25 and 23 taxa, respectively). Non-migration, where no individual of a species local population significantly changes depth on a diel basis, was prevalent in the lower meso- and bathypelagial, but most of the taxa (other than *Cyclothone* spp.) are uncommon or rare.

Considering macrocrustaceans, approximately 75% of the species from the five dominant families are considered vertical migrators, either strong (>50% of the assemblage migrated into shallower waters at night) or weak (15–50% of the assemblage migrated), while the other 25% were considered non-migrators (<15% of the assemblage migrated). Most of the non-migrating taxa had daytime depth distributions in the lower mesopelagic (600–1000 m) or bathypelagic (1000–1500 m) zone. These data indicate that the micronektonic crustaceans could be significant vectors of contamination in deeper waters, such as oil residues from the DWHOS, into surface waters. Given that micronektonic crustaceans are prey of numerous predatory species (Borodulina 1972; Hopkins et al. 1994), oil residues ingested at deeper depths would be transported through the food webs at all depths.

Past studies have examined midwater cephalopod depth distributions and vertical migration patterns (Roper and Young 1975; Young 1978; Lu and Roper 1979). These studies were based on few individuals in some cases and localized, for example, to the area surrounding Hawaii (Young 1978). To date, 31 cephalopod vertical migration plots have been created from the current study to examine patterns. The top ten most abundant cephalopod families (Fig. 24.3) exhibit a wide variety of migration patterns: from synchronous migrators (e.g., enoploteuthids, pyroteuthids) to those who do not vertically migrate or descend through ontogenic shifts (e.g., Vampyroteuthidae, Bolitaenidae, Mastigoteuthidae) (Judkins et al. in prep). Every depth zone is utilized by multiple cephalopod species at various times throughout a 24-hour cycle in this midwater region of the GoM. Future studies of the ONSAP/DEEPEND dataset include examining seasonality patterns of cephalopods and fishes.

24.3.3 Reproductive Seasonality

Although little is known about seasonality of reproduction in deep-sea species, analyses have been conducted for those GoM species of Oplophoridae (12) and Euphausiidae (5) that carry eggs during part of their reproductive cycle (Burdett et al. 2017; Fine 2016). All 12 species of Oplophoridae had gravid females in the fall, while 8 of these had no gravid females in the spring. Three species of oplophorids had substantially more gravid females in the spring as well as the smallest percentage of gravid females in the fall. The euphausiids appeared to prefer the spring; all five species had gravid females during the spring, and only one species had substantially more gravid females in the fall. What these data suggest is that the timing of an event like oil spills may have significantly different effects on different families, depending on their preferred season of reproduction. Interestingly, the one species (*Acanthephyra stylorostratis)* that showed no seasonality among the Oplophoridae is also the deepest-living species, with no individuals found shallower than 600 m; the bulk of the population reside between 1000 and 1200 m, with no evidence of vertical migrations. All the species of Oplophoridae and Euphausiidae that show evidence of seasonality migrate into the epipelagic zone at night.

24.4 Petrogenic Contamination

24.4.1 Water Column

The DWHOS occurred at ~1500 m depth, affecting the water column during vertical transport of oil residues to the surface and to the seafloor (sinking/sedimentation processes) as well as by the formation of submerged plumes (Romero et al. 2015, 2017; Yan et al. 2016). These different transport pathways weathered the oil in the water column, with most soluble hydrocarbons entrained at depth (~69% of the deep plume mass), while undissolved hydrocarbon mixtures (e.g., oil droplets) formed surface oil slicks (Ryerson et al. 2012). In the water column, soluble hydrocarbon compounds such as polycyclic aromatic hydrocarbons (PAHs) are of main concern due to their high bioavailability and toxic characteristics, even though only ~4% by weight is found in the DWHOS oil (Reddy et al. 2011). The majority of the water samples collected in 2010 (from surface to just above the seafloor) showed PAH concentrations higher than 0.3 μg/L (Murawski et al. 2016; Romero et al. 2018), with high levels and fluxes at depth still observed in 2011 (Yan et al. 2016; Romero et al. 2018). Exposure to PAHs as low as 0.3 μg/L was demonstrated to cause lethal and sublethal effects in marine fishes (Carls et al. 1999; Heintz et al. 1999, 2000; Whitehead et al. 2012). Therefore, the high concentrations of PAHs observed after the DWHOS suggest a potential impact to the deep-pelagic fauna. Moreover, lower concentrations found in the following years (2011 to 2013; Adhikari et al. 2015; Romero et al. 2018) suggest a slow but consistent recovery of the water column after the spill. However, transformation products from the DWHOS were still observed in 2015 (Walker et al. 2017), indicating a longer persistence of DWHOS residues at depth, longer than previously thought. Natural processes such as resuspension and downslope transport of contaminated sediments (Ziervogel et al. 2015; Romero et al. 2017) may redistribute hydrocarbons at depth, hence affecting the water column chemistry and the deep-pelagic inhabitants for years (~decades) after an accidental oil spill at depth.

24.4.2 Mesopelagic Fishes

While ongoing efforts are attempting to determine the community-level effects of the DWHOS on the mesopelagic fauna via time series analysis, the incorporation of carbon from the DWHOS into the mesopelagic food web was demonstrated by Quintana-Rizzo et al. (2015). These authors concluded that since most of the mesopelagic community is planktivorous (or feeds directly on zooplanktivores) in the upper 200 m at night (Hopkins and Sutton 1998 and references therein), the shift detected in their isotopic signatures likely resulted from consumption of prey rich in depleted carbon from the dispersed oil. This hypothesis is supported by other studies showing the introduction of oil-derived carbon into the planktonic food web in

2010 and 2011 (Graham et al. 2010; Chanton et al. 2012). Moreover, data collected 5 years after the spill indicate recovery of the system to pre-DWHOS conditions based on the isotopic carbon composition of *Chauliodus sloani* from different studies (Quintana-Rizzo et al. 2015; Richards et al. 2018). This incorporation of oil residues in the food web indicates that at the least, sublethal effects of the DWHOS were present in the deep-pelagic domain as shown by a decadal study of PAHs (Romero et al. 2018).

Exposure to PAHs in shallower-living fish species has been linked to early mortality, embryonic abnormalities, and several sublethal effects in adult fishes, such as swimming impairment, lesions in gills, reproductive impairment, and DNA damage (Carls et al. 1999; Heintz et al. 1999; Barron et al. 2004; Sundberg et al. 2006; Whitehead et al. 2012; Murawski et al. 2014; West et al. 2014; Millemann et al. 2015; Sørhus et al. 2017). These effects have been observed within the range of PAH concentrations measured after the DWHOS in muscle (2010–2011) and unhatched eggs (2015–2016) of mesopelagic fish species (Romero et al. 2018). PAHs in 2010–2011 were seven- to tenfold higher than in 2007, with a composition similar to DWH-derived PAHs (Fig. 24.4). In 2015–2016, PAH composition was similar to 2010–2011, but concentrations were near the levels measured in 2007 samples (Fig. 24.4). Biological factors (e.g., diet, habitat, life span) and inputs from natural sources (e.g., Mississippi River, natural seeps) do not explain the temporal

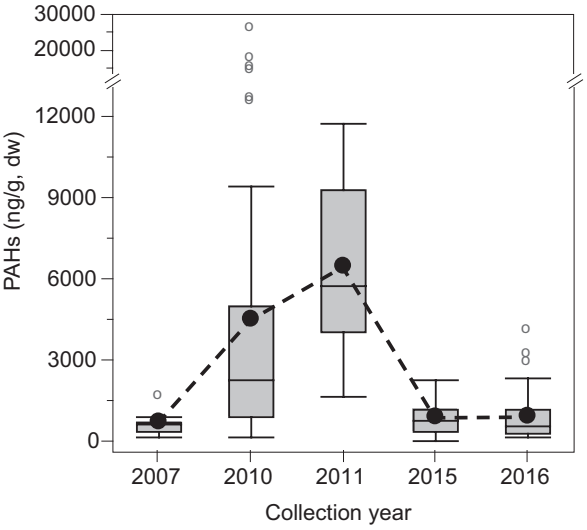

Fig. 24.4 Time series assessment of PAH concentration in the muscle tissues of mesopelagic fishes collected in the northern Gulf of Mexico. Sampling years: pre-spill (2007), post-spill (2010–2011), and recovery (2015–2016). PAHs refer to the sum of 2–6 rings, including alkylated homologues. Graph shows shaded boxes as the interquartile ranges with horizontal lines indicating median values and whiskers representing the 10th and 90th percentiles. Black and white circles denote mean and outlier values, respectively. (Reprinted with permission from Romero et al. 2018, Copyright 2018 American Chemical Society)

variability of PAHs observed from 2007 to 2016. Therefore, this trend suggests an episodic contamination event in 2010 that continued through 2011, and a recovery period after 2015. Also, bioaccumulation was found to be driven by dietary intake and maternal transfer of PAHs, explaining the elevated PAH levels in unhatched eggs in 2015–2016.

Results also indicate that a longer-term sink for oil in deep-pelagic organisms occurs, potentially higher than shallower counterparts, due to oil residue tendency to be more available at depth (see the previous section "Water Column"), combined with higher exposure to contaminants caused by their vertical migratory behaviors. This is supported by a similar composition of PAHs in the muscle tissue of mesopelagic fishes and oil residues in the water column from 2007 (primarily indicating seep sources) to 2016 (weathered oil from the DWHOS) (Romero et al. 2018). Overall, results from Romero et al. (2018) demonstrated the importance of monitoring the persistence of organic contaminants in the deep-pelagic GoM to better understand acute and chronic PAH exposures and bioaccumulation patterns in mesopelagic fishes. However, trends and gaps in the datasets also emphasize the need for longer time scale ecosystem-based management efforts of the deep-pelagic ocean.

24.5 Summary

Recent research efforts in the GoM have greatly enhanced our understanding of the deep-pelagic domain. Biodiversity is quite high, with a concomitant variety of vertical distribution patterns, including diel migrations. Reproductive seasonality has been demonstrated for some crustacean groups, and analyses are ongoing for fish and cephalopod species. PAH contamination in the midwater taxa highlights the need for long-term monitoring to quantify effects of large oil spills. These effects may persist for decades, given that high concentrations of PAHs within the range observed to cause mortality and sublethal effects in embryonic and juveniles fishes were found 5–6 years after the DWHOS. The extent to which the DWHOS affected the diversity, growth patterns, and reproduction of the deep-pelagic fauna is unclear, given the lack of a pre-spill baseline, but should be investigated further to understand the long-term resilience of this important ecosystem domain, as oil extraction efforts are now concentrated toward >1500 m depth in the GoM.

Acknowledgements This research was made possible by a grant from The Gulf of Mexico Research Initiative through the DEEPEND and C-IMAGE II and C-IMAGE III consortia. Data are publicly available through the Gulf of Mexico Research Initiative Information & Data Cooperative (GRIIDC) at https://data.gulfresearchinitiative.org (doi: [10.7266/N7VX0DK2, 10.7266/N7R49NTN]).

References

Adhikari PL, Maiti K, Overton EB (2015) Vertical fluxes of polycyclic aromatic hydrocarbons in the Northern Gulf of Mexico. Mar Chem 168:60–68

Aguzzi J, Company JB (2010) Chronobiology of deep-water decapod crustaceans on continental margins. Adv Mar Biol 58:155–226. https://doi.org/10.1016/B978-0-12-381015-1.00003-4

Allain V (2005) Diet of four tuna species of the Western and Central Pacific Ocean. Fish Newslett S Pac Commission 114:30

Armstrong CW, Foley NS, Tinch R, van den Hove S (2012) Services from the deep: steps towards valuation of deep-sea goods and services. Ecosyst Serv 2:2–13. https://doi.org/10.1016/j.ecoser.2012.07.001

Barron MG, Carls MG, Heintz R, Rice SD (2004) Evaluation of fish early life-stage toxicity models of chronic embryonic exposures to complex polycyclic aromatic hydrocarbon mixtures. Toxicol Sci 78:60–67. https://doi.org/10.1093/toxsci/kfh051

Borodulina OD (1972) The feeding of mesopelagic predatory fish in the open ocean. J Ichthyol 12:692–703

Burdett EA (2016) Geographic and depth distributions of decapod shrimps (Caridea: Oplophoridae) from the northeastern Gulf of Mexico with notes on ontogeny and reproductive seasonality. Master's Thesis. Nova Southeastern University. Retrieved from NSUWorks, https://nsuworks.nova.edu/occ_stuetd/409

Burdett EA, Fine CD, Sutton TT, Cook AB, Frank TM (2017) Geographic and depth distributions, ontogeny and reproductive seasonality of decapod shrimps (Caridea: Oplophoridae) from the northeastern Gulf of Mexico. Bull Mar Sci 93(3):743–767. https://doi.org/10.5343/bms.2016.1083

Canadell JG, Le Quéré C, Raupach MR, Field CB, Buitenhuis ET, Ciais P, Conway TJ, Gillett NP, Houghton RA, Marland G (2007) Contributions to accelerating atmospheric CO2 growth from economic activity, carbon intensity, and efficiency of natural sinks. Proc Natl Acad Sci 104(47):18,866–18,870. https://doi.org/10.1073/pnas.0702737104

Carls MG, Rice SD, Hose JE (1999) Sensitivity of fish embryos to weathered crude oil: part I. Low-level exposure during incubation causes malformations, genetic damage, and mortality in larval pacific herring (*Clupea pallasii*). Environ Toxicol Chem 18:481–493

Chanton JP, Cherrier J, Wilson RM, Sarkodee-Adoo J, Bosman S, Mickle A, Graham WM (2012) Radiocarbon evidence that carbon from the Deepwater Horizon spill entered the planktonic food web of the Gulf of Mexico. Environ Res Lett 7:045303. https://doi.org/10.1088/1748-9326/7/4/045303

Danovaro R, Gambi C, Dell'Anno A, Corinaldesi C, Fraschetti S, Vanreusel A, Vincx M, Gooday AJ (2008) Exponential decline of deep-sea ecosystem functioning linked to benthic biodiversity loss. Curr Biol 18(1):1–8. https://doi.org/10.1016/j.cub.2007.11.056

D'Elia M, Warren JD, Rodriguez-Pinto I, Sutton TT, Cook A, Boswell KM (2016) Diel variation in the vertical distribution of deep-water scattering layers in the Gulf of Mexico. Deep-Sea Res I 115:91–102

Feagans-Bartow JN, Sutton TT (2014) Ecology of the oceanic rim: pelagic eels as key ecosystem components. Mar Ecol Prog Ser 502:257–266

Fine CD (2016) The vertical and horizontal distribution of deep-sea crustaceans of the order Euphausiacea (Malacostraca: Eucarida) from the northern Gulf of Mexico with notes on reproductive seasonality. Master's thesis. Nova Southeastern University. Retrieved from NSUWorks. https://nsuworks.nova.edu/occ_stuetd/432

French-McCay D, Crowley D, Rowe JJ, Bock M, Robinson H, Wenning R, Hayward Walker A, Joeckel J, Nedwed TJ, Parkerton TF (2018) Comparative risk assessment of spill response options for a Deepwater oil well blowout: part 1. Oil spill modeling. Mar Pollut Bull 133:1001–1015

Graham WM, Condon RH, Carmichael RH, D'Ambra I, Patterson HK, Linn LJ, Hernandez FJ Jr (2010) Oil carbon entered the coastal Planktonic Food Web during the Deepwater Horizon Oil Spill. Environ Res Lett 5(4):045301

Heintz RA, Short JW, Rice SD (1999) Sensitivity of fish embryos to weathered crude oil: part 2. Increased mortality of Pink Salmon (*Oncorhynchus gorbuscha*) embryos incubating downstream from weathered Exxon Valdez crude oil. Environ Toxicol Chem 18:494–503

Heintz RA, Rice SD, Wertheimer AC, Bradshaw RF, Thrower FP, Joyce JE, Short JW (2000) Delayed effects on growth and marine survival of Pink Salmon *Oncorhynchus gorbuscha* after exposure to crude oil during embryonic development. Mar Ecol Prog Ser 208:205–216

Herring P (2001) The biology of the deep ocean. OUP, Oxford

Hopkins TL, Sutton TT (1998) Midwater fishes and shrimps as competitors in low latitude oligotrophic ecosystems. Mar Ecol Prog Ser 164:37–45

Hopkins TL, Flock ME, Gartner JV, Torres JJ (1994) Structure and trophic ecology of a low latitude midwater decapod and mysid assemblage. Mar Ecol Prog Ser 109:143–156. https://doi.org/10.3354/meps109143

Irigoien X, Klevjer TA, Røstad A, Martinez U, Boyra G, Acuña JL, Bode A, Echevarria F, González-Gordillo JI, Hernandez-Leon S, Agusti S (2014) Large mesopelagic fishes biomass and trophic efficiency in the open ocean. Nat Commun 5:Article number: 3271

Jobstvogt N, Townsend M, Witte U, Hanley N (2014) How can we identify and communicate the ecological value of deep-sea ecosystem services? PLoS One 9(7):e100646. https://doi.org/10.1371/journal.pone.0100646

Judkins HL (2009) Cephalopods of the Broad Caribbean: distribution, abundance, and ecological importance. (Torres J, Vecchione M Eds.). University of South Florida

Judkins H, Vecchione M (2016) Diversity of midwater cephalopods in the northern Gulf of Mexico: comparison of two collecting methods. Mar Biodivers:1–11. https://doi.org/10.1007/s12526-016-0597-8

Judkins H, Vecchione M, Rosario K (2016) Morphological and molecular evidence of *Heteroteuthis dagamensis* in the Gulf of Mexico. Bull Mar Sci. https://doi.org/10.5343/bms.2015.1061

Judkins H, Lindgren A, Villanueva R, Clark K, Vecchione M (in prep.) A description of three new bathyteuthid squid species from the North Atlantic and Gulf of Mexico.

LaRoe ET (1967) A contribution to the biology of the Loliginidae (Cephalopoda: Myopsida) of the Tropical Western Atlantic. Master of Science thesis; University of Miami, Coral Gables

Leduc D, Rowden AA, Bowden DA, Probert PK, Pilditch CA, Nodder SD (2012) Unimodal relationship between biomass and species richness of deep-sea nematodes: implications for the link between productivity and diversity. Mar Ecol Prog Ser 454:53–64. https://doi.org/10.3354/meps09609

Levin LA, Dayton PK (2009) Ecological theory and continental margins: where shallow meets deep. Trends Ecol Evol 24:606–61.7. https://doi.org/10.1016/j.tree.2009.04.012

Lipka DA (1975) The systematics and zoogeography of cephalopods of the Gulf of Mexico. PhD. Dissertation, Texas A&M University, 204 p

Lu CC, Roper CFE (1979) Cephalopods from Deepwater Dumpsite 106 (Western Atlantic): vertical distribution and seasonal abundance; Smithsonian Contributions to Zoology, n. 288; Smithsonian Institution Press, 36p

Millemann DR, Portier RJ, Olson G, Bentivegna CS, Cooper KR (2015) Particulate accumulations in the vital organs of wild *Brevoortia patronus* from the northern Gulf of Mexico after the Deepwater Horizon oil spill. Ecotoxicology 24:1831–1847. https://doi.org/10.1007/s10646-015-1520-y

Milligan RE, Sutton TT (submitted) An overview of the species composition, abundance, and vertical distribution of the mesopelagic fish family Myctophidae in the northern Gulf of Mexico. Deep-Sea Res I

Murawski SA, Hogarth WT, Peebles EB, Barbeiri L (2014) Prevalence of external skin lesions and polycyclic aromatic hydrocarbon concentrations in Gulf of Mexico fishes, post-Deepwater Horizon. Trans Am Fish Soc 143:37–41. https://doi.org/10.1080/00028487.2014.911205

Murawski SA, Fleeger JW, Patterson WF, Hu C, Daly K, Romero I, Toro-Farmer GA (2016) How did the Deepwater Horizon oil spill affect coastal and continental shelf ecosystems of the Gulf of Mexico? Oceanography 29. https://doi.org/10.5670/oceanog.2016.80

Murawski SA, Hollander DJ, Gilbert S, Gracia A (2020) Deep-water oil and gas production in the Gulf of Mexico, and related global trends (Chap. 2). In: Murawski SA, Ainsworth C, Gilbert S, Hollander D, Paris CB, Schlüter M, Wetzel D (eds) Scenarios and responses to future Deep Oil Spills – fighting the next war. Springer, Cham

Passarella KC (1990) Oceanic cephalopod assemblage in the Eastern Gulf of Mexico. Department of Marine Science. University of South Florida, St. Petersburg. 50p

Pearcy WG, Forss CA (1966) Depth distribution of oceanic shrimps (Decapoda; *Natantia*) off Oregon. J Fish Res Bull Can 23(8):1135–1143. https://doi.org/10.1139/f66-106

Quintana-Rizzo E, Torres JJ, Ross SW, Romero I, Watson K, Goddard E, Hollander D (2015) $\delta^{13}C$ and $\delta^{15}N$ in deep-living fishes and shrimps after the *Deepwater Horizon* Oil Spill, Gulf of Mexico. Mar Pollut Bull 94(1–2):241–250

Ramirez-Llodra E, Tyler PA, Baker MC, Bergstad OA, Clark MR, Escobar E, Levin LA, Menot L, Rowden AA, Smith CR, Van Dover CL (2011) Man and the last great wilderness: human impact on the deep sea. PLoS One 6(7):e22588. https://doi.org/10.1371/journal.pone.0022588

Reddy CM, Arey JS, Seewald JS, Sylva SP, Lemkau KL, Nelson RK, Carmichael C, McIntyre CP, Fenwick J, Ventura GT, Van Mooy BAS, Camilli R (2011) Composition and fate of gas and oil released to the water column during the Deepwater Horizon oil spill. Proc Natl Acad Sci 109:20229–20234. https://doi.org/10.1073/pnas.1101242108

Reid SB, Hirota J, Young RE, Hallacher LE (1991) Mesopelagic-boundary community in Hawaii: micronekton at the interface between neritic and oceanic ecosystems. Mar Biol 109(3):427–440. https://doi.org/10.1007/BF01313508

Richards TM, Gipson EE, Cook A, Sutton TT, Wells RJD (2018) Trophic ecology of meso- and bathypelagic predatory fishes in the Gulf of Mexico. ICES J Mar Sci. https://doi.org/10.1093/icesjms/fsy077

Romero IC, Schwing PT, Brooks GR, Larson RA, Hastings DW, Flower BP, Goddard EA, Hollander DJ (2015) Hydrocarbons in deep-sea sediments following the 2010 Deepwater Horizon Blowout in the Northeast Gulf of Mexico. PLoS One 10:1–23. https://doi.org/10.1371/journal.pone.0128371

Romero IC, Toro-farmer G, Diercks A, Schwing P, Muller-Karger F, Murawski S, Hollander DJ (2017) Large-scale deposition of weathered oil in the Gulf of Mexico following a deep-water oil spill. Environ Pollut 228:179–189. https://doi.org/10.1016/j.envpol.2017.05.019

Romero IC, Sutton TT, Carr B, Quintana-Rizzo E, Ross SW, Hollander DJ, Torres JJ (2018) Decadal assessment of polycyclic aromatic hydrocarbons in mesopelagic fishes from the Gulf of Mexico reveals exposure to oil-derived sources. Environ Sci Technol. https://doi.org/10.1021/acs.est.8b02243

Roper CFE, Young YR (1975) Vertical distribution of pelagic cephalopods; Smithsonian contributions to zoology n. 209; Smithsonian Institution Press, 51p

Ryerson TB, Camilli R, Kessler JD, Kujawinski EB, Reddy CM, Valentine DL, Atlas E, Blake DR, de Gouw J, Meinardi S, Parrish DD, Peischl J, Seewald JS, Warneke C (2012) Chemical data quantify Deepwater Horizon hydrocarbon flow rate and environmental distribution. Proc Natl Acad Sci U S A 109:20246–20253. https://doi.org/10.1073/pnas.1110564109

Sabine CL, Feely RA (2007) The oceanic sink for carbon dioxide. In: Reay D, Hewitt CN, Smith K, Grace J (eds) Greenhouse gas sinks. CAB International, Oxfordshire, pp 31–46

Sørhus E, Incardona JP, Furmanek T, Goetz GW, Scholz NL, Meier S, Edvardsen RB, Jentoft S (2017) Novel adverse outcome pathways revealed by chemical genetics in a developing marine fish. elife 6:e20707:1–30. https://doi.org/10.7554/eLife.20707

Sundberg H, Ishaq R, Tjärnlund U, Åkerman G, Grunder K, Bandh C, Broman D, Balk L (2006) Contribution of commonly analyzed polycyclic aromatic hydrocarbons (PAHs) to potential toxicity in early life stages of rainbow trout (*Oncorhynchus mykiss*). Can J Fish Aquat Sci 1333:1320–1333. https://doi.org/10.1139/F06-034

Sutton TT (2013) Vertical ecology of the pelagic ocean: classical patterns and new perspectives. J Fish Biol 83:1508–1527

Sutton TT, Wiebe PH, Madin LP, Bucklin A (2010) Diversity and community structure of pelagic fishes to 5000 m depth in the Sargasso Sea. Deep-Sea Res II 57:2220–2233

Sutton TT, Clark MR, Dunn DC, Halpin PN, Rogers AD, Guinotte J, Bograd SJ, Angel MV, Perez JA, Wishner K, Haedrich RL, Lindsay DJ, Drazen JC, Vereshchaka A, Piatkowski U, Morato T, Blachowiak-Samolyk K, Robison BH, Gjerde KM, Pierrot-Bults A, Bernal P, Reygondeau G, Heino M (2017) A global biogeographic classification of the mesopelagic zone. Deep-Sea Res I 126:85–102

Sutton TT, Moore JA, Cook AB, Pruzinsky N (in prep.) Oceanic fishes of the Gulf of Mexico: the DEEPEND synthesis.

Thurber AR, Sweetman AK, Narayanaswamy BE, Jones DOB, Ingels J, Hansman RL (2014) Ecosystem function and services provided by the deep sea. Biogeosciences 11(14):3,941–3,963. https://doi.org/10.5194/bg-11-3941-2014

Trueman CN, Johnston G, O'Hea B, MacKenzie KM (2014) Trophic interactions of fish communities at midwater depths enhance long-term carbon storage and benthic production on continental slopes. Proc. R. Soc. B 281:20140669.

Uribe JE, Zardoya R (2017) Revisiting the phylogeny of Cephalopoda using complete mitochondrial genomes. J Molluscan Stud 83(2):133–144. https://doi.org/10.1093/mollus/eyw052

Voss GL (1956) A review of the cephalopods of the Gulf of Mexico. Bull Mar Sci 6(2):85–178

Voss GL (1973) The potentially commercial species of octopus and squid of Florida, the Gulf of Mexico and the Caribbean Sea. Univ. Miami Sea Grant Program, Miami, FL

Walker BD, Druffel ERM, Kolasinski J, Roberts BJ, Xu X, Rosenheim BE (2017) Stable and radiocarbon isotopic composition of dissolved organic matter in the Gulf of Mexico. Geophys Res Lett 44(16):8424–8434

Webb TJ, Berghe EV, O'Dor R (2010) Biodiversity's big wet secret: the global distribution of marine biological records reveals chronic under-exploration of the deep pelagic ocean. PLoS One 2:5(8):e10223

West JE, Neill SMO, Ylitalo GM, Incardona JP, Doty DC, Dutch ME (2014) An evaluation of background levels and sources of polycyclic aromatic hydrocarbons in naturally spawned embryos of Pacific herring (*Clupea pallasii*) from Puget Sound, Washington, USA. Sci Total Environ 499:114–124. https://doi.org/10.1016/j.scitotenv.2014.08.042

Whitehead A, Dubansky B, Bodinier C, Garcia TI, Miles S, Pilley C, Raghunathan V, Roach JL, Walker N, Walter RB, Rice CD, Galvez F (2012) Genomic and physiological footprint of the Deepwater Horizon oil spill on resident marsh fishes. Proc Natl Acad Sci 109:20298–20302. https://doi.org/10.1073/pnas.1109545108

Wilson RW, Millero FJ, Taylor JR, Walsh PJ, Christensen V, Jennings S, Grosell M (2009) Contribution of fish to the marine inorganic carbon cycle. Science 323(5912):359–362

Yan B, Passow U, Chanton JP, Nöthig E-M, Asper V, Sweet J, Pitiranggon M, Diercks A, Pak D (2016) Sustained deposition of contaminants from the Deepwater Horizon spill. Proc Natl Acad Sci 113:E3332–E3340. https://doi.org/10.1073/pnas.1513156113

Young RE (1978) Vertical distribution and photosensitive vesicle of pelagic cephalopods from Hawaiian waters. Fish Bull 76(3):583–615

Ziervogel K, Dike C, Asper V, Montoya J, Battles J, D'souza N, Passow U, Diercks A, Esch M, Joye S, Dewald C, Arnosti C (2015) Enhanced particle fluxes and heterotrophic bacterial activities in Gulf of Mexico bottom waters following storm-induced sediment resuspension. Deep-Sea Res II Top Stud Oceanogr 129:77–88. https://doi.org/10.1016/j.dsr2.2015.06.017

Chapter 25
Evaluating Impacts of Deep Oil Spills on Oceanic Marine Mammals

Kaitlin E. Frasier

Abstract The *Deepwater Horizon* (DWH) oil spill may be indicative of future large, deep spills that may occur in the coming decades. Given that future deepwater spills are possible, critical considerations include (1) establishing baselines for oceanic marine mammal and populations in at-risk areas, (2) understanding the implications of response choices for oceanic marine mammals, (3) designing studies with adequate coverage for post-spill monitoring, and (4) identifying effective strategies for oceanic marine mammal restoration. In this chapter, we consider these four stages in the context of a series of hypothetical oil spill scenarios, identifying ways that lessons learned from the DWH oil spill and prior events can be applied to future disasters.

Keywords Marine mammal · Sperm whale · Beaked whale · Dolphin · Passive acoustic monitoring (PAM) · Megafauna · Mammal · Odontocete · Bryde's whale · Spotted dolphin · *Stenella* · *Kogia* · Echolocation · Visual survey · Ship strike · Noise · Air gun · HARP · Mississippi Canyon · Green Canyon · Risso's dolphin · Pilot whale · Tag · Aerial survey · Habitat model · Loop Current · AUV · Satellite · Genetic · Monitoring · Dispersant · Hazing · Deterrent · NRDA · Cetacean · Disturbance · NOAA · Stock · Restoration · Mexico · Seismic

25.1 Introduction

The *Deepwater Horizon* (DWH) event differed from previous spills in that it occurred in deep water at an offshore location (1525 m deep, 66 km from the nearest shoreline). As a result it affected offshore marine megafauna in oceanic (>200 m bottom depth) habitats where prior study and monitoring efforts were sparse and infrequent. To characterize the effect of the event on marine mammals, the focus

K. E. Frasier (✉)
University of California San Diego, Scripps Institution of Oceanography, Marine Physical Laboratory, La Jolla, CA, USA
e-mail: kfrasier@ucsd.edu

S. A. Murawski et al. (eds.), *Scenarios and Responses to Future Deep Oil Spills*,
https://doi.org/10.1007/978-3-030-12963-7_25

turned to coastal impacts and tractable nearshore surrogate species (Trustees 2016), because it was determined to be "unrealistic" to quantify offshore impacts directly. However, bay, sound, and estuary (BSE) bottlenose dolphins (the oceanic marine mammal surrogate) are weak proxies for the diverse, wide-ranging, and deep-diving oceanic species affected by the event. The true impacts of the DWH event on oceanic marine mammals and their offshore habitats may never be fully quantified.

As oil extraction operations deepen and extend into increasingly inaccessible locations, the difficulties of measuring spill impacts will likely increase. Future deep spills may affect deep waters of the Northern Gulf of Mexico (GOM) and Northeastern Atlantic, as well as Arctic waters (Huntington 2009; Cordes et al. 2016). As in the case of the DWH spill, effects of these events on marine mammal populations will likely be challenging to observe. Nonetheless, the ability to characterize the nature and magnitude of the impacts of these events is necessary for response, damage assessment, and restoration activities.

We discuss preparation strategies for future spills in at-risk regions. Based on the lessons from the DWH event, we ask what measures could be taken before, during, and after an offshore spill to characterize oceanic marine mammal populations, incorporate potential effects on marine mammals as a consideration in disaster response decisions, quantitatively evaluate population-level impacts of oil spills, and support population recovery.

25.2 Before a Spill: Establishing Baselines

The lack of precise pre-spill estimates of GOM marine mammal distributions and abundances severely limited efforts to evaluate the impacts of the DWH spill on oceanic megafauna. Measuring baseline marine mammal population sizes and distributions in at-risk areas is clearly a critical part of preparing for future oil spills; however it is rare to have this type of data prior to an event (Bonebrake et al. 2010). Monitoring an area the size of the GOM is expensive and logistically challenging, particularly with the level of readiness required to quantify impacts at an unknown time and location. Furthermore, standard survey methods are unlikely to achieve adequately precise density and abundance estimates or provide the level of spatiotemporal resolution needed to quantify exposure (Taylor et al. 2007). Practical approaches for long-term monitoring of large oceanic marine ecosystems with enough spatiotemporal resolution to quantify impacts of future spills at unknown times and locations on marine mammals have not been demonstrated.

Marine mammals are wide-ranging and capable of transiting long distances over large time scales (e.g., Jochens et al. 2008); therefore any monitoring strategy must account for population mobility and migration within and beyond the study region. Many GOM marine mammal species appear to migrate or shift their distributions seasonally, while others appear to be year-round residents (Hildebrand et al. 2015; Frasier 2015). Tropical and subtropical species may seek different habitat conditions. In the GOM, transient Loop Current features including cold- and warm-core eddies,

as well as the loop itself, have a strong influence on regional oceanographic conditions and likely affect GOM marine mammal distributions (Davis et al. 2002). Interpreting these distributions is further complicated by the fact that surveys are typically limited to the US EEZ, which accounts for only 35% of the GOM ecosystem. Distinguishing between population declines and population shifts is challenging because it is unclear how some species move throughout the GOM.

A combination of in situ monitoring and modeling is likely the most realistic approach for establishing abundance and distribution baselines in large regions of concern. In situ monitoring data can be used to develop habitat models used to interpolate marine mammal distributions between measurements across space and time. In the case of a disaster, models can use observed historical relationships between seasonal and oceanographic drivers and marine mammal encounters (Redfern et al. 2006; Roberts et al. 2016) to estimate exposure at the event location. However, developing robust models requires extensive monitoring effort for species of concern across seasons, habitats, and regional oceanographic variability (Kaschner et al. 2012) and may require integration of multiple observation methods to achieve sufficient predictive power.

25.2.1 In Situ Monitoring Strategies

Visual Surveys

Shipboard line transect surveys with visual observers are the standard method for estimating baseline abundance and describing the distributions of oceanic cetaceans (Davis et al. 1998; Mullin and Hoggard 2000; Fulling et al. 2003; Mullin and Fulling 2003, 2004; Barlow and Forney 2007). This method relies on animal sightings at the sea surface. Visual surveys provide broad spatial coverage of a region at brief snapshots in time (roughly 0.5 hours/10 km transect segment). Some temporal coverage can be obtained if surveys are repeated on a regular schedule; however visual methods are resource intensive, requiring extensive vessel and personnel time; therefore they may not be conducted often enough to provide precise estimates. Visual surveys also rely on fair weather conditions; therefore in the GOM, most visual survey effort has occurred in summer months (Maze-Foley and Mullin 2007; Mullin 2007).

To provide adequate data for training habitat models with broad spatial and temporal predictive capabilities, visual survey methods must cover a large surface area, survey across a variety of oceanographic features, occur in multiple seasons, and develop species-specific sighting rate estimates (Buckland et al. 2007). Given that marine mammals only spend a fraction of their time at the sea surface, visual survey data tend to be sparse (~1 sighting per 50 km of NOAA shipboard pelagic visual survey effort in the GOM, 2002–2014), requiring extensive survey effort to produce robust models. Double-blind visual surveys with two independent visual teams are typically used to accurately estimate sighting probabilities for different species (Palka 2006), as each species has a different probability of seen by observers: The

tall blows of sperm whales or large groups of dolphins are more likely to be sighted than cryptic species such as beaked whales and *Kogia* species. Sighting rates are further influenced by survey platform height; therefore survey vessels are not interchangeable and must be calibrated (e.g., Palka 2006). Recent field studies have also found evidence of vessel avoidance by marine mammals (Cholewiak et al. 2017) which may lead to underestimates of marine mammal densities if not accounted for. In general, the low precision of abundance estimates from large-scale visual surveys prevents estimation of long-term population trends and precludes detection of all but the most catastrophic population-level impacts (Williams et al. 2011; Taylor et al. 2007).

Shipboard visual surveys for oceanic marine mammals were conducted in the GOM prior to the DWH spill (Waring et al. 2009), but due to the expense and limitations of the method, the population size estimates were too imprecise to allow damages to be quantified by comparison with post-spill survey results. Unless Gulf-wide surveys could be conducted frequently across a range of seasons, visual surveys alone would likely remain insufficient for determining the effects of a future spill (Jewell et al. 2012; Taylor et al. 2007). Aerial visual surveys in the GOM typically focus on the expansive continental shelf region (Fulling et al. 2003) and are not used to survey oceanic populations. Unmanned aerial vehicles (UAVs) may become a viable low-cost solution for coastal surveys (Bevan et al. 2016); however the current range and battery life limitations of commercial AUVs limit their use for pelagic monitoring.

Passive Acoustic Monitoring

Static passive acoustic monitoring (PAM) provides an alternative modality for cetacean monitoring; this approach employs acoustic sensors at fixed sites but can provide a nearly continuous record of animal presence at monitored locations (Wiggins and Hildebrand 2007) regardless of time of day or weather. This method relies on underwater detection of species-specific vocalizations; therefore monitored species must be classifiable based on features of their acoustic signals. Passive acoustic monitoring data have been collected in the GOM nearly continuously using fixed seafloor sensors since 2010 (Hildebrand et al. 2015; Hildebrand et al. 2019). The time series from acoustic monitoring sites provides high-resolution temporal coverage; however spatial coverage is limited because sensor locations are fixed, and detection ranges are restricted by the acoustic characteristics of the vocalizations monitored (Frasier et al. 2016; Hildebrand et al. 2015).

PAM tends to result in higher detection rates than visual surveys because they rely on sounds produced during foraging and social behaviors rather than surface sightings. This type of data can provide strong support for habitat modeling efforts (Soldevilla et al. 2011). Because the sensors are generally stationary, they must monitor over long periods (months to years) in order to capture the full range of environmental conditions and variability that visual surveys achieve in part by surveying along transect lines. Despite their stationarity, fixed PAM can monitor across a remarkably wide range of oceanographic conditions due to the dynamic nature of the marine environment (Fig. 25.1).

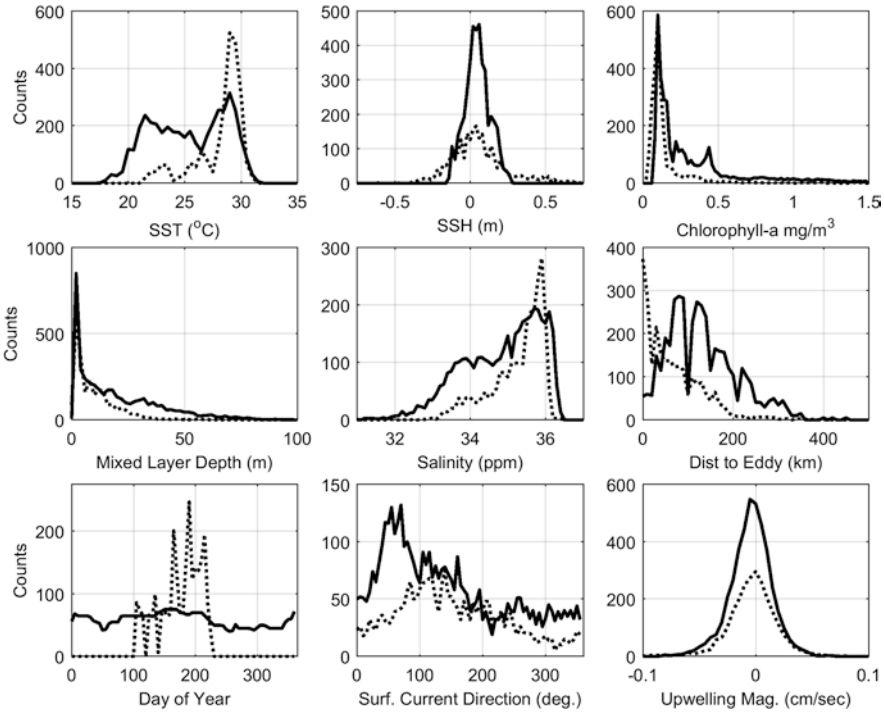

Fig. 25.1 A comparison of environmental parameter distributions observed at static PAM sites (black line) and those traversed by a NOAA visual survey vessel (dashed line). PAM data represents five static sites monitored continuously for 3 years as part of the GOM HARP project. Visual survey data represents five shipboard surveys conducted by NOAA in spring or summer of 2002, 2003, 2009, 2012, and 2014

Mobile passive acoustic sensors can combine some of the advantages of visual surveys (spatial coverage) with the autonomous advantage of PAM (Klinck et al. 2012; Moore et al. 2007; Mellinger et al. 2007). However these sensors come with their own set of challenges that may complicate their use for quantitative density and abundance estimation, including signal distortion and surface noise for near-surface sensor types, variable signal detection probabilities for profiling sensors, self-noise (e.g., electrical noise, onboard pumps, and flow noise), and limited navigational ability in regions with significant currents (Hildebrand et al. 2013). At the time of the DWH event, these systems were not a reliable option for large-scale monitoring, but mobile autonomous PAM may become a viable tool for future monitoring of at-risk regions.

Tagging

Marine mammal tag technology is a rapidly advancing field capable of providing insights to individual animal behaviors, home ranges, and migratory patterns (Jochens et al. 2008). However, insights gained individual animal tracks, and behaviors can be difficult to generalize to a population or species level and can

require significant effort for even a limited sample size. Various tag designs exist, each with different strengths. Long-term implanted tags typically have GPS sensors and remain affixed to the animal for many months (Mate et al. 2007). Most long-term tags are not designed to be recovered; therefore data collection is typically limited to what can be transmitted via satellite, such as location of surface intervals. Satellite tagging studies may be particularly useful for understanding the degree to which populations flow in and out of an area of concern, as in the GOM. For instance, tag data showing seasonal migrations could fill in knowledge gaps related to large-scale distribution shifts, seasonal patterns, and migratory corridors (Costa et al. 2010; Baird et al. 2010). Shorter-term tags designed to be retrieved once they separate from the animal can store more information, such as underwater movement (body rotation, foraging lunges, acoustic recordings, and video footage), but must be recovered to acquire the data (Johnson et al. 2009; Calambokidis et al. 2007). Short-term archival tags are useful for obtaining information on behavior (Soldevilla et al. 2017). Low Impact Minimally Percutaneous Electronic Transmitter (LIMPET) tags are medium-duration option capable of supporting a range of sensors (Baird et al. 2010). Suction cups are another common short-term mounting method, typically remaining attached for a few hours to a few days. Beaked whales and dolphins have been successfully tagged with suction cup and LIMPET tags; however tags are most readily applied to large whales.

Other Methods

Satellite imagery has been proposed as a possible tool for marine mammal population monitoring (Fretwell et al. 2014). This strategy may be a viable option for large whales under favorable conditions (low glare, low Beaufort scale); however the resolution of publicly available satellite imagery is currently too low to detect or identify most marine mammal species. Satellite imagery might be a viable option in the future for studying distributions of large whales (Fretwell et al. 2014), depending on image resolution and the development of methods to account for poor detection conditions and other factors influencing detectability.

Genetic studies can also provide estimates of population sizes (Frankham 1996) and identify possible periods of population expansion or contraction (De Bruyn et al. 2009). These methods use biological samples such as tissue or skin to look at genetic diversity and drift. Genetic approaches have been used to estimate past and current population sizes and to quantify the impacts of historic events such as whaling; however sources of uncertainty including mutation rates, reproductive success, and effects of selection at individual loci can lead to low precision in population size estimates when used in isolation (Harris and Allendorf 1989; Alter et al. 2007). This method is most appropriate for studies over longer time scales but may be used to evaluate long-term effects of historic events when earlier data are not available. Genetic information has been used to identify distinct bottlenose dolphin stocks in the GOM (Sellas et al. 2005), allowing impact assessments to be limited to affected stocks. Similar efforts to delineate stocks for oceanic species could help narrow the focus of future damage assessments.

25.2.2 Complementary Monitoring Data Sources

Given the size of the survey areas, and unknown locations of future disasters, it is unlikely that any of these individual monitoring methods alone can cover space and time well enough to produce the data needed for baseline population size estimates or provide the spatiotemporal resolution required for large-scale disaster preparedness. Habitat models capable of predicting marine mammal density distributions as a function of environmental drivers (Redfern et al. 2006) may provide a mechanism for estimating marine mammal exposure to future events. Habitat models have been developed for the GOM based on visual survey data following the DWH oil spill (Roberts et al. 2016) however they do not currently cover all seasons or achieve high enough confidence to fulfill future damage assessment needs. Since no individual method seems capable of fully censusing mobile and migratory populations, the best approach may involve integrating multiple data sources (Fujioka et al. 2014). In particular, visual surveys and passive acoustics may be able to accomplish the task in combination by leveraging the spatial coverage of one and the temporal coverage of the other.

25.3 During a Spill: Megafauna and Response Efforts

There is no evidence that marine mammals avoid oil (Goodale et al. 1981; Geraci 1990; Vander Zanden et al. 2016; Wilkin et al. 2017); therefore it must be assumed that animals present during an oil spill are injured by the event and that response choices including dispersant use, noise, and vessel activity directly affect marine mammals.

25.3.1 Response Activities

Dispersants

Chemical dispersants have been applied at the sea surface in oil spill responses as early as 1967 (Torrey Canyon spill response; Southward and Southward 1978). The DWH response represented the first use of dispersants at depth, where they were applied directly to the oil outflow (Kujawinski et al. 2011). The use of deep dispersants as part of the DWH response has largely been viewed as a success: Approximately 50% of the spilled oil remained at depth (Joye 2015), never reaching the sea surface where it would have increased slick size, required further cleanup actions, and potentially reached coastlines. Managers have indicated that they would use deep dispersant applications in future response efforts (French-McCay

et al. 2018). However, the trade-offs of deep and surface applications of dispersant approach with respect to implications for pelagic marine organism health are largely unknown. The application of dispersants at depth is thought to increase oil residence times in the water column and increase the influence of subsurface currents on oil transport (Testa et al. 2016). In Frasier et al. (2020) we reviewed the sparse literature on dispersant effects on marine mammal health, which relies on surrogate species and cell cultures. There appears to be little consensus on whether dispersants or dispersed oil are more or less toxic to marine organisms than undispersed oil. Dispersing oil in a deep subsurface plume likely increases routes of exposure for many oceanic marine mammals. Indirect impacts of deep dispersant applications via deposition of large amounts of oil on the seafloor are also a concern (Fisher et al. 2016). Deposited oil has the potential to smother benthic communities and negatively affect pelagic food webs with long-term implications for marine mammal populations.

Although the use of dispersants has been considered a success so far, there is not enough data to conclude that dispersant use results in safer conditions for marine mammal populations. In a future spill scenario, the presence and density of deep-diving marine mammals may need to be considered as a risk factor when weighing the trade-offs of applications of dispersants at depth.

Vessels

Vessel activity was very high in the Mississippi Canyon region during the DWH oil spill response and oil slick cleanup effort. Elevated ship noise, echosounders, and underwater communication signals associated with response activities dominated the acoustic soundscape during the response period. Noise associated with seismic surveys and shipping is generally high in the GOM; therefore distinguishing between the response-associated noise and chronic noise impacts may be challenging. Increased ship traffic raises the risk of marine mammals being struck by vessels (Carrillo and Ritter 2010). Anthropogenic noise has been associated with a wide range of injuries to marine mammal species, ranging from disruption of foraging to possible death (Cox et al. 2006; Tyack 2008). Cleanup activities such as skimming and burning increase the potential for entanglement in deployed gear and reduce air quality and the sea surface for air-breathing marine mammals.

Deterrents

Deterrence or “hazing” strategies aimed at discouraging marine mammal presence in oiled areas do not appear to have been used during the DWH oil spill response but have since been proposed as strategies for future events (NOAA 2014). These strategies use sounds from underwater discharges (“seal bombs”), Oikami pipes, or helicopters to herd or move animals out of affected areas and have the potential to reduce direct exposure during a spill. However, these methods constitute illegal harassment outside of an emergency; therefore they should be viewed with extreme caution and require specific authorization (NMFS 2017).

25.4 After a Spill

25.4.1 Damage Assessment

NOAA's natural resource damage assessment (NRDA) process is the primary framework for estimating impacts on marine megafauna following an oil spill. In the DWH case, the injury assessment phase of the NRDA spanned from 2010 to 2015 (Trustees 2016). However the effects on these long-lived species likely play out over a much longer period (Schwacke et al. 2017; Ackleh et al. 2018; Matkin et al. 2008); therefore the full magnitude of the impacts may not be immediately measurable during an NRDA. This leads to a mismatch between the time frame in which damages are assessed (a few years) and the time frame over which the damage may appear (possibly decades).

Models may be necessary to predict the extent of future damage within the time frame of the NRDA. Following the DWH an effort was made to develop life history models to estimate the magnitude of the impacts in terms of "lost cetacean years" (Schwacke et al. 2017) for BSE bottlenose dolphins. These models rely on knowledge of life history traits such as average life span, typical mortality across different age classes, reproductive rates etc., which are difficult to establish for oceanic species (King et al. 2015). Targeted studies to establish these parameters for populations of concern would likely facilitate future damage assessment estimates. Population recovery models may not fully account for cumulative impacts when estimating recovery times (Williams et al. 2016). Even if pre-spill data do exist, some marine mammal populations may not be at their stable or optimal size at the time of an event (e.g., recovering from a prior event or declining due to other impacts), causing models to incorrectly estimate the time to full population recovery. Following the DWH event coordinated efforts began to develop models capable of estimating population-level effects of chronic disturbance (Pirotta et al. 2018) which may be incorporated into future recovery estimation efforts.

As previously discussed, effective short-term damage assessment requires knowledge of the types and numbers of animals impacted by the disaster and a comparison of pre- and post-spill numbers to account for any loss. If habitat models (e.g., Roberts et al. 2016) exist for a region prior to a spill, these could be used to predict the magnitude of exposure based on the location, timing, and oceanographic conditions during the event (Gregr et al. 2013). Surveying or monitoring during the event could be conducted to validate the model predictions. In the case of the DWH, the GOM HARP project (a long-term passive acoustic monitoring effort; Hildebrand et al. 2015) began monitoring 19 days after the beginning of the spill, allowing for high temporal resolution monitoring of the wellhead region. NOAA shipboard oceanic marine mammal visual surveys were conducted during June through August and October through November 2010 (SEFSC 2018). Although these were relatively rapid responses, the initial exposure period was not recorded; therefore some immediate effects may have been missed. Preparedness plans for rapid deployment

of monitoring tools following future oil spills could decrease the time lag between event and initial monitoring effort, which could in turn decrease uncertainty around short-term exposure.

25.4.2 Long-Term Monitoring

After a spill, long-term monitoring is necessary to establish trends and assess recovery progress at affected locations. Marine mammal presence varies on fine timescales as animals seek out prey and favorable conditions; follow mobile, ephemeral mesoscale features; and appear to respond to drivers ranging from lunar cycles to human activities (Davis et al. 2002; Simonis et al. 2017; Ellison et al. 2012). The mechanisms that drive oceanic marine mammal spatial distributions and variability are poorly understood, in part because many probable contributing factors such as prey availability and oceanographic conditions at depth are not readily measured on the broad spatial and temporal scales over which monitoring occurs. Indirect drivers such as sea surface conditions, primary productivity, and general ocean conditions, though widely available from satellite data and physical models, typically have only weak explanatory power with respect to oceanic marine mammal occurrence (Forney et al. 2012; Roberts et al. 2016). Unexplained variability in marine mammal distributions complicates interpretation of long-term trends from monitoring data, because short- and long-term population movements and true population size changes are convolved.

Targeted, carefully designed monitoring programs (Taylor et al. 2007; Jewell et al. 2012; Kaschner et al. 2012) are necessary to provide the spatial and temporal coverage required to achieve a level of precision high enough to confidently measure population-level changes on a reasonable time scale (years rather than decades or centuries). Considerations include coverage of the full range of habitats of interest, accounting for possible non-uniform species distributions across the monitored area, surveying across the full range of seasons, and taking measures to reduce inherent uncertainty in parameters such as animal availability for detection, method-specific probability of detection, avoidance or attraction effects, and multipliers used to convert detections into numbers of animals (e.g., cue rates, group size estimates) (Buckland et al. 2007). Although visual surveys are the most common oceanic marine mammal monitoring method, simply increasing the frequency of surveys may not result in more precise population estimates (Jewell et al. 2012). PAM is likely one of the more effective strategies for collecting enough data to resolve long-term trends despite short-term (weeks to months) and inter-annual variability at impacted sites. Where available, identification of impacted stocks can limit the spatial extent of survey effort needed (e.g., BSE bottlenose dolphin stocks in the GOM), but oceanic marine mammal stocks are typically large and poorly defined.

25.4.3 Restoration

Following the DWH oil spill, restoration of large, mobile marine megafauna appeared to be an intractable problem, given the scale of their habitat, the complexity, and length of their life cycles. Direct actions to increase marine mammal populations are not a viable option. However, there appears to be a growing consensus that indirect restoration actions aimed at mitigating the chronic impacts that weaken population resilience (Wright et al. 2011) may support population recovery and reduce harm from possible future events.

We suggest that a potential approach to restoration is addressing the chronic impacts that compromise marine mammal population resilience and reduce their ability to withstand and recover from disasters. Chronic impacts including sublethal stressors can have cumulative effects on survival, reducing reproduction rates, shortening life spans, and increasing sensitivity to disease or unfavorable environmental conditions (Wright et al. 2011). Chronic anthropogenic impacts to marine mammals in the GOM include noise, ship strikes, exposure to pollutants, entanglement, ingestion of debris, bycatch, and reduced prey quality and quantity (see Frasier et al. 2020). In the aftermath of an oil spill, restoration efforts could conceivably consist of identifying, quantifying, and mitigating these threats. For instance, if bycatch is considered a significant stressor in a region of concern, then a restoration strategy might include quantifying the extent of the bycatch issue across fisheries via an observer program, identifying high risk cases, and implementing mitigation strategies (equipment, regulation). Similarly if noise exposure was a concern, then areas of highest exposure could be identified by reviewing species distributions in relation to major shipping corridors and seismic surveys and taking actions to reduce vessel noise (via vessel quieting or speed limits) and move shipping lanes or timing seismic surveys to occur during windows of low expected densities in affected areas. Such efforts to reduce chronic impacts could increase population resilience and indirectly support recovery in the event of future oil spills.

25.5 Putting It into Practice: Alternate Spill Scenarios

Below, we step through three alternate oil spill scenarios to examine possible differences between the impacts of the hypothetical case and the DWH oil spill on oceanic marine mammals. Differences in species exposure are discussed, and implications of these differences for response and damage assessment processes are considered. Given the potential for GOM-wide population connectivity of oceanic marine mammal populations, coupled with how little is known regarding the processes that drive changes in GOM marine mammal densities and distributions, long-term monitoring needs would likely be comparable under all three scenarios, therefore recommendations are only detailed under Scenario 1. Restoration efforts would likely also be comparable; however, we highlight cases where certain species might benefit from targeted management actions.

25.5.1 Scenario 1

In this scenario, a hypothetical spill of similar origin, magnitude, and duration to the DWH event would have occurred during the fall of 2010 (beginning September 1), instead of during spring. Oil release from the well would have occurred over a 90-day period from September through November 2010.

25.5.1.1 Impacts and Damage Assessment

Based on seasonal trends observed in long-term monitoring data collected during the GOM HARP project, the expected presence of Risso's dolphins, mid-frequency (presumed *Stenella* species) dolphins, and *Kogia* spp. would have been lower in the fall scenario than during the spring (Fig. 25.2); therefore potential exposure of these species might have been lower. It is not known where these populations tend to go during winter months, only that occurrence appears to decrease at northern GOM HARP monitoring locations along the continental slope. Some populations may migrate into deeper waters or into the southern GOM during winter months. Sperm whale and low-frequency dolphin (presumed to be primarily short-finned pilot whale) presence are typically somewhat higher in the PAM record during fall at northern monitoring locations; therefore exposure might have been higher for these species. Gervais' beaked whale presence is not strongly seasonal at this site; therefore expected exposure under this scenario would be similar to the spring event. Cuvier's beaked whales are typically only detected in winter at this location; therefore expected exposure would be low but increasing at the very end of the oil spill period.

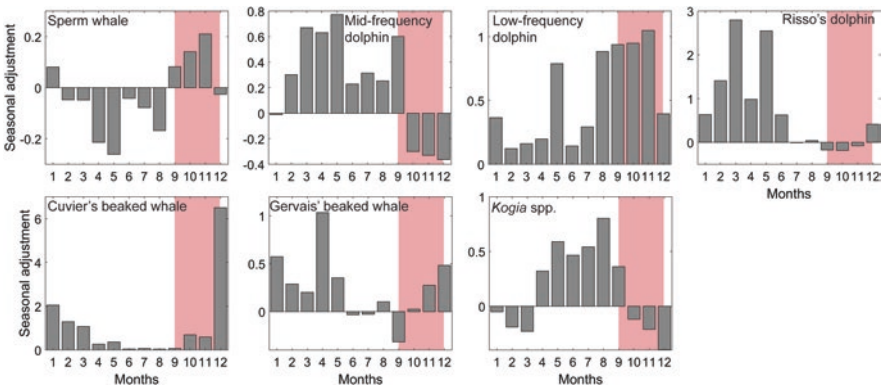

Fig. 25.2 Seasonal patterns in marine mammal presence at a passive acoustic monitoring site in Mississippi Canyon, located approximately 10 km from the DWH wellhead. The vertical axis indicates the factor by which seasonal presence varies relative to mean presence. Higher values indicate stronger seasonality. Pink shading indicates the months of the hypothetical oil spill examined in Scenario 1

Similarly to the DWH case, there would not have been enough survey data to estimate pre-spill population sizes or to develop models capable of estimating the magnitude of marine mammal exposure. Moreover, between 1992 and 2010, NOAA visual surveys were conducted no later than August; therefore there would have been no marine mammal observations for fall months in pre-spill data (Waring et al. 2009). *Stenella* dolphins, particularly pantropical spotted dolphins (*Stenella longirostris*), are the most abundant oceanic marine mammals in the northern GOM based on summer visual survey data (Waring et al. 2015). If *Stenella* dolphins do shift away from the Mississippi Canyon area in fall and winter as suggested by the PAM data, then the overall number of animals directly exposed to oil, dispersants, and response activities would have been significantly lower. The northern GOM appears to be a nursing ground for sperm whales (Jochens et al. 2008); therefore higher exposure might have had larger effects on the population as a whole. A focused effort on estimating sperm whale life history parameters to estimate lost sperm whale years would have been particularly useful under this scenario for quantifying impacts with potential long-lasting, population-level implications.

25.5.1.2 Long-Term Monitoring

Oceanic GOM marine mammal populations are typically classified by NOAA as single oceanic stocks, because no information exists to support more fine-scale structure. The degree to which populations flow between US waters in the north and Mexican waters in the south is unknown, but exchange between the northern and southern GOM is likely. A long-term monitoring strategy for oceanic GOM marine mammals likely needs to cover both US and Mexican waters, monitor year-round, and achieve high enough precision to detect impacts from large-scale events and/or restoration activities. A viable strategy involves the use of static PAM at a combination of permanent and temporary sites in the entire GOM. Temporary sites would be moved periodically across a grid of short-term (<1 year) monitoring locations to provide coverage of the full range of habitats and environmental conditions in the GOM, while long-term sites would be monitored continuously over many years as reference points. Using this type of dataset, habitat models could be produced to interpolate marine mammal density distributions across the entire region such that changes and effects could be evaluated on a gulf-wide scale. Further, impacts of future events could be inferred from modeled density surfaces. Model precision would be dictated by the number of sensors and monitoring locations occupied and the duration of the effort.

25.5.1.3 Restoration

Mississippi Canyon appears to be a hot spot of biological activity in the northern GOM; therefore restoration actions to support biodiversity might be particularly appropriate. The Mississippi River plays a dominant role in shaping offshore

northern GOM ecosystems, by bringing in nutrients that fuel high productivity. Although these nutrients contribute to the creation of a seasonal hypoxic zone on the continental shelf, they also likely form the foundation of the rich food web that appears to sustain high marine mammal presence in the Mississippi Canyon region. One set of management actions to support marine recovery in the region might include minimizing upstream contaminant inputs from agricultural activities. Nitrate from fertilizers is the most abundant and problematic (Rabalais et al. 1996) contaminant found in these riverine inputs, along with pesticides and herbicides (Goolsby and Pereira 1996; Pereira and Hostettler 1993). Recent research also indicates an increase in Mississippi River salinity (Kaushal et al. 2018) which could have impacts on the offshore food web. Pollutants are also derived from oil and gas extraction in the region (Neff 1990; Neff et al. 2011a, b). A second avenue for restoration would include limiting and tightly regulating the activity of increasingly deep drilling rigs which may increase the risks of impacts of future incidents on recovering populations.

25.5.2 Scenario 2

In this scenario the origin of the hypothetical spill would have been at a location along the west Florida shelf (27.0° N, 85.168° W) with oil escaping over a period of 90 days beginning April 20, 2010, and ending July 19, 2010.

25.5.2.1 Impacts and Damage Assessment

This scenario would likely have had greater impacts on beaked whales, which have been recorded at very high densities at a west Florida shelf site relative to other GOM monitoring locations (Hildebrand et al. 2015). However, the PAM site nearest this hypothetical spill location for the GOM HARP project was located further south along the west Florida shelf, and the degree of generalizability of beaked whale habitat preferences based on these observations remains unclear. A PAM study focused on the Mississippi Canyon region (Sidorovskaia et al. 2016) suggested that neighboring sites (50 nm apart) could have quite different beaked whale species compositions. Patchiness in beaked whale distributions may be related to their deep-dive capabilities which could enable them to interact with and take advantage of seafloor features which are not available to shallow-diving species. Applications of deep dispersants might have an outsized impact on beaked whales at this location by increasing oil deposition in their benthic foraging grounds. Beaked whales are also sensitive to anthropogenic noise (particularly echosounders) and might have been repelled or stranded in response to high-frequency anthropogenic noise (communications and echosounders) associated with the response (Weilgart 2007). Densities of Risso's dolphin are also higher in the region but tend to peak in the fall; therefore Risso's might avoid the majority of direct exposure under this scenario.

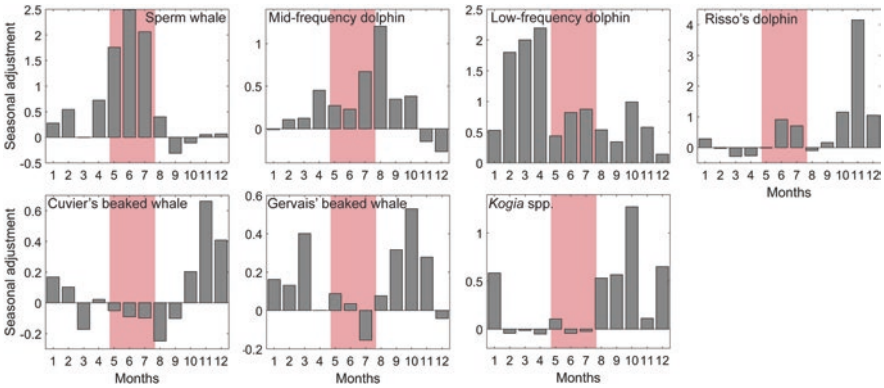

Fig. 25.3 Seasonal patterns in marine mammal presence at a passive acoustic monitoring site on the west Florida shelf. The vertical axis indicates the factor by which seasonal presence varies relative to mean presence. Higher values indicate stronger seasonality. Pink shading indicates the months of the hypothetical oil spill examined in Scenario 2

Direct impacts on female and juvenile GOM sperm whales might also have been reduced because overall sperm whale densities are likely to be lower in this region relative to Mississippi Canyon; however migratory males moving through the area in summer months might have been more strongly affected (Fig. 25.3).

One population of particular concern under this spill scenario is the very small GOM Bryde's whale population (proposed to be listed as endangered; NMFS 2015). GOM Bryde's whale core habitat is located just north of the origin of this hypothetical oil spill. This population appears to be an endemic GOM subspecies and consists of an estimated 33 animals (Hayes et al. 2018). Although the reasons behind its current small population size are largely unknown, Soldevilla et al. (2017) proposed based on a tagged animal that this species may be particularly vulnerable to ship strikes. The tagged individual showed a repetitive behavior of resting at night at the sea surface and foraging near or at the seafloor during the day. These two behaviors, if they are characteristic of the population (subsequent unpublished data suggests that they are), might put the species at high risk of exposure to surface and deposited oil, as well as increased risk being struck by response vessels (Soldevilla et al. 2017). Given the small size of this population, the potential impacts from an oil spill overlapping its core habitat could threaten the long-term survival of GOM Bryde's whales.

As in other scenarios, there would have been limited pre-spill visual survey data for this region of the GOM. Entrainment of oil into the Loop Current and possibly the Gulf Stream would open up the possibility of oil exposure to an even greater number of marine mammal species in the Western Atlantic where marine mammal diversity and densities are fairly high. Marine mammal survey effort in the NE Atlantic (US EEZ) has been more extensive than in the GOM, but habitat models were not available at the time. They have been published since using pre-spill data (Roberts et al. 2016) but lack certainty for many species. Given that beaked whales

might have been particularly affected under this scenario, the ability to quantify impacts to beaked whales in terms of "lost beaked whale years" would be an important tool in estimating the extent of the damage in this scenario. These are particularly cryptic, difficult animals to study; therefore it would be very difficult to establish accurate life history parameters for damage assessment purposes.

25.5.2.2 Restoration

Key restoration actions for Bryde's whales would likely involve vessel restrictions in their core habitat. Restricting vessel speeds and prohibiting nighttime transits through the area would likely be an effective restoration strategy (Carrillo and Ritter 2010). Beaked whale-oriented restoration efforts might include taking action to minimize acoustic disturbance from echosounders, fish-finders, and sonar. Preliminary research suggests that male sperm whales may transit through this region, but it is unclear where they are coming from. Undertaking tagging efforts to better understand the connectivity between the apparently resident northern GOM population of sperm whales (primarily females and juveniles) with mature males observed in the broader Atlantic might help inform management actions to support recovery of this population. Sperm whales, particularly large males, were highly targeted by the whaling industry; therefore it cannot be assumed that the pre-spill GOM sperm whale numbers reflected a healthy or stable population size.

25.5.3 Scenario 3

In this scenario, an oil spill of similar magnitude, depth, and duration to the DWH event would have occurred in the northwestern GOM (26.66° N, 93.19° W), from April 20 to July 19, 2010.

25.5.3.1 Impacts and Damage Assessment

The oceanography of the northwestern GOM differs significantly from the eastern GOM. Instead of the clearly defined continental slope regions typical of the northeastern GOM, the seafloor in the northwestern GOM gradually deepens from 40 to 2000 meters deep over hundreds of kilometers across a complex network of salt domes and other geological features. Oil and gas infrastructure is more prevalent in the western half of the northern GOM (BOEM 2018), and the Port of Houston, one of the busiest ports in the USA, is associated with high vessel traffic through the region (BOEM 2015). Visual survey and PAM data indicate that overall marine mammal occurrence may be lower in this region, but marine mammal survey effort has also been lower.

The relative influence of differences in habitat, infrastructure, human activity, and marine mammal survey effort on perceived lower marine mammal occurrence

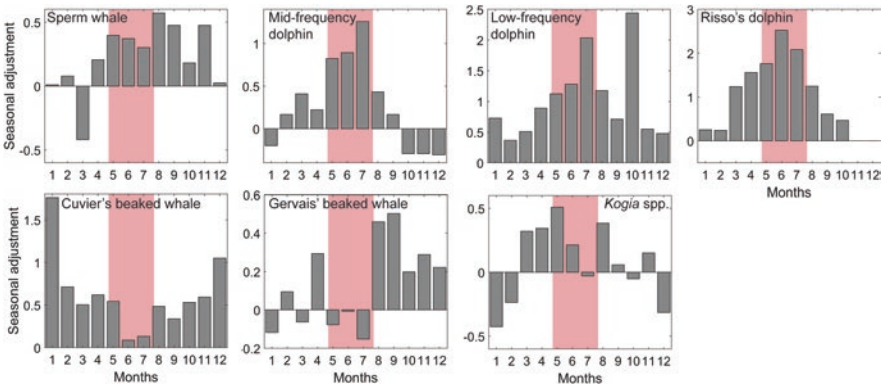

Fig. 25.4 Seasonal patterns in marine mammal presence at a passive acoustic monitoring site in Green Canyon, the western-most year-round monitoring location for toothed whales in the GOM. The vertical axis indicates the factor by which seasonal presence varies relative to mean presence. Higher values indicate stronger seasonality. Pink shading indicates the months of the hypothetical oil spill examined in Scenario 3

in the western GOM is unknown. The westernmost sensor deployed by the GOM HARP project was located near Green Canyon (27.56° N, 91.17° W); however this location was selected as an un-oiled comparison with Mississippi Canyon and does not necessarily represent average western GOM conditions. PAM data from that location indicated somewhat lower occurrence of marine mammals relative to the Mississippi Canyon site. Sperm whales, *Stenella* dolphins, pilot whales, *Kogia* spp., and Risso's dolphins would likely have been directly exposed to oil and response activities (Fig. 25.4). Insufficient monitoring data are available to estimate the extent of the potential exposure. Oil spills of various sizes are not uncommon in the western GOM; therefore it might be particularly difficult to distinguish the effect of one event from impacts from other sources.

25.5.3.2 Restoration

Given the comparatively high risk of future oil spills in the western GOM and the challenges of measuring new impacts in a highly exploited context, a proportional increase in marine mammal monitoring effort relative to the western GOM may be appropriate to establish robust baselines and fill in extensive knowledge gaps. However current marine mammal population sizes and distributions in the western GOM are unlikely to represent historic extents given the clear human footprint on the region. For example, data suggest that the GOM Bryde's whale population's home range, now restricted to the eastern GOM, may have previously extended into the western GOM (Soldevilla et al. 2017).

A particularly common source of disturbance in the western GOM are seismic surveys, in which explosive releases of air are used to produce high amplitude sounds waves to map the seafloor and search for oil deposits. Noise generated by these

surveys dominates the low-frequency soundscape in the GOM. Research into the effects of seismic surveys on marine mammals is ongoing; however studies have reported a range of effects including no perceived response, decreased foraging, and displacement (Mate et al. 1994; Miller et al. 2009; Stone and Tasker 2006). Determining seasonal trends in marine mammal abundance and distributions in the GOM might reveal strategies for minimizing spatiotemporal overlap between seismic surveys and critical habitat. Measures taken to quiet container ships could also significantly reduce noise-related stressors on GOM marine mammals (Malakoff 2010).

25.6 Conclusions

Direct measurement of impacts will become more difficult as spills get deeper, further offshore, and in less accessible locations. Robust baselines are needed to measure impacts to oceanic megafauna. A multi-pronged approach to monitoring utilizing visual surveys and passive acoustic monitoring is likely the best method for quantifying injury to and measuring recovery of oceanic marine mammal populations. Marine mammal species are wide-ranging, with long, complex, poorly understood life cycles. Direct restoration of marine mammal populations is unlikely; however management actions aimed at limiting chronic stressors such as ship strikes, pollution, noise, bycatch, entanglement, or actions taken to restore and protect oceanic food webs would likely increase marine mammal population resilience and improve long-term outcomes.

Acknowledgements Collaborators John A. Hildebrand and Alba Solsona Berga from the Scripps Institution of Oceanography contributed substantially to the ideas discussed in this review.

This research was made possible by a grant from The Gulf of Mexico Research Initiative/C-IMAGE I, II, and III. Funding for HARP data collection and analysis was also provided by the Natural Resource Damage Assessment partners (20105138), the US Marine Mammal Commission (20104755/E4061753), the Southeast Fisheries Science Center under the Cooperative Institute for Marine Ecosystems and Climate (NA10OAR4320156) with support through Interagency Agreement #M11PG00041 between the Bureau of Offshore Energy Management, Environmental Studies Program, and the National Marine Fisheries Service, Southeast Fisheries Science Center. The analyses and opinions expressed are those of the authors and not necessarily those of the funding entities. The data used for this study are archived by the Gulf of Mexico Research Initiative at https://data.gulfresearchinitiative.org/data/R4.x267.180:0011 maintained by the Gulf Research Initiative Information and Data Cooperative.

References

Ackleh A, Caswell H, Chiquet R, Tang T, Veprauskas A (2018) Sensitivity analysis of the recovery time for a population under the impact of an environmental disturbance. Nat Resour Model:e12166

Alter SE, Rynes E, Palumbi SR (2007) DNA evidence for historic population size and past ecosystem impacts of gray whales. Proc Natl Acad Sci 104(38):15162–15167

Baird RW, Schorr GS, Webster DL, McSweeney DJ, Hanson MB, Andrews RD (2010) Movements and habitat use of satellite-tagged false killer whales around the main Hawaiian Islands. Endanger Species Res 10:107–121

Barlow J, Forney KA (2007) Abundance and population density of cetaceans in the California Current ecosystem. Fish Bull 105(4):509–526

Bevan E, Wibbels T, Navarro E, Rosas M, Najera BM, Sarti L, Illescas F, Montano J, Peña LJ, Burchfield P (2016) Using unmanned aerial vehicle (UAV) technology for locating, identifying, and monitoring courtship and mating behaviour in the green turtle (*Chelonia mydas*). Herpetol Rev 47:27–32

BOEM Data Center (2018) https://www.data.boem.gov/Mapping/Files/platform.zip; https://www.data.boem.gov/Mapping/Files/wells.zip. Accessed 26 June 2018

BOEM, NOAA (2015) Commercial vessel density October 2009–2010 AIS National. marinecadastre.gov/data. Accessed 9/15/2018

Bonebrake TC, Christensen J, Boggs CL, Ehrlich PR (2010) Population decline assessment, historical baselines, and conservation. Conserv Lett 3(6):371–378

Buckland ST, Anderson DR, Burnham KP, Laake JL, Borchers DL, Thomas L (2007) Advanced distance sampling: estimating abundance of biological populations, Oxford

Calambokidis J, Schorr GS, Steiger GH, Francis J, Bakhtiari M, Marshall G, Oleson EM, Gendron D, Robertson K (2007) Insights into the underwater diving, feeding, and calling behavior of blue whales from a suction-cup-attached video-imaging tag (CRITTERCAM). Mar Technol Soc J 41(4):19–29

Carrillo M, Ritter F (2010) Increasing numbers of ship strikes in the Canary Islands: proposals for immediate action to reduce risk of vessel-whale collisions. J Cetacean Res Manag 11(2):131–138

Cholewiak D, DeAngelis AI, Palka D, Corkeron PJ, Van Parijs SM (2017) Beaked whales demonstrate a marked acoustic response to the use of shipboard echosounders. R Soc Open Sci 4(12):170940

Cordes EE, Jones DO, Schlacher TA, Amon DJ, Bernardino AF, Brooke S, Carney R, DeLeo DM, Dunlop KM, Escobar-Briones EG (2016) Environmental impacts of the deep-water oil and gas industry: a review to guide management strategies. Front Environ Sci 4:58

Costa DP, Block B, Bograd S, Fedak MA, Gunn JS (2010) TOPP as a marine life observatory: using electronic tags to monitor the movements, behaviour and habitats of marine vertebrates. Proce OceanObs 9:21–25

Cox TM, Ragen T, Read A, Vos E, Baird R, Balcomb K, Barlow J, Caldwell J, Cranford T, Crum L (2006) Understanding the impacts of anthropogenic sound on beaked whales. SPACE AND NAVAL WARFARE SYSTEMS CENTER SAN DIEGO CA

Davis RW, Fargion GS, May N, Leming TD, Baumgartner M, Evans WE, Hansen LJ, Mullin K (1998) Physical habitat of cetaceans along the continental slope in the northcentral and western Gulf of Mexico. Mar Mamm Sci 14(3):490–507

Davis RW, Ortega-Ortiz JG, Ribic CA, Evans WE, Biggs DC, Ressler PH, Cady RB, Leben RR, Mullin KD, Wursig B (2002) Cetacean habitat in the northern oceanic Gulf of Mexico. Deep-Sea Res I Oceanogr Res Pap 49(1):121–142. https://doi.org/10.1016/S0967-0637(01)00035-8

De Bruyn M, Hall BL, Chauke LF, Baroni C, Koch PL, Hoelzel AR (2009) Rapid response of a marine mammal species to Holocene climate and habitat change. PLoS Genet 5(7):e1000554

Ellison W, Southall B, Clark C, Frankel A (2012) A new context-based approach to assess marine mammal behavioral responses to anthropogenic sounds. Conserv Biol 26(1):21–28

Fisher CR, Montagna PA, Sutton TT (2016) How did the Deepwater Horizon oil spill impact deep-sea ecosystems? Oceanography 29(3):182–195

Forney KA, Ferguson MC, Becker EA, Fiedler PC, Redfern JV, Barlow J, Vilchis IL, Ballance LT (2012) Habitat-based spatial models of cetacean density in the eastern Pacific Ocean. Endanger Species Res 16(2):113–133

Frankham R (1996) Relationship of genetic variation to population size in wildlife. Conserv Biol 10(6):1500–1508

Frasier KE (2015) Density estimation of delphinids using passive acoustics: a case study in the Gulf of Mexico. Ph.D. Thesis, The University of California San Diego, La Jolla, CA

Frasier KE, Wiggins SM, Harris D, Marques TA, Thomas L, Hildebrand JA (2016) Delphinid echolocation click detection probability on near-seafloor sensors. J Acoust Soc Am 140(3):1918–1930. https://doi.org/10.1121/1.4962279

Frasier KE, Solsona-Berga A, Stokes L, Hildebrand JA (2020) Impacts of the Deepwater Horizon oil spill on marine mammals and sea turtles (Chap. 26). In: Murawski SA, Ainsworth C, Gilbert S, Hollander D, Paris CB, Schlüter M, Wetzel D (eds) Deep Oil Spills – facts, fate and effects. Springer, Cham

French-McCay D, Crowley D, Rowe JJ, Bock M, Robinson H, Wenning R, Walker AH, Joeckel J, Nedwed TJ, Parkerton TF (2018) Comparative risk assessment of spill response options for a Deepwater oil well blowout: part 1. Oil spill modeling. Mar Pollut Bull 133:1001–1015

Fretwell PT, Staniland IJ, Forcada J (2014) Whales from space: counting southern right whales by satellite. PLoS One 9(2):e88655

Fujioka E, Kot CY, Wallace BP, Best BD, Moxley J, Cleary J, Donnelly B, Halpin PN (2014) Data integration for conservation: leveraging multiple data types to advance ecological assessments and habitat modeling for marine megavertebrates using OBIS-SEAMAP. Eco Inform 20:13–26. https://doi.org/10.1016/j.ecoinf.2014.01.003

Fulling GL, Mullin KD, Hubard CW (2003) Abundance and distribution of cetaceans in outer continental shelf waters of the US Gulf of Mexico. Fish Bull 101(4):923–932

Geraci JR (1990) Physiologic and toxic effects on cetaceans. In: Geraci JR, St. Aubin DJ (eds) Sea mammals and oil: confronting the risks. Academic Press, Inc., San Diego, pp 167–192

Goodale DR, Hyman MA, Winn HE, Edkel R, Tyrell M (1981) Cetacean responses in association with the Regal Sword oil spill. Cetacean and Turtle Assessment Program, University of Rhode Island, Annual Report 1979. U.S. Dept. of the Interior, Washington, D. C

Goolsby DA, Pereira WE (1996) Pesticides in the Mississippi river. US GEOLOGICAL SURVEY CIRCULAR USGS CIRC:87–102

Gregr EJ, Baumgartner MF, Laidre KL, Palacios DM (2013) Marine mammal habitat models come of age: the emergence of ecological and management relevance. Endanger Species Res 22(3):205–212

Harris RB, Allendorf FW (1989) Genetically effective population size of large mammals: an assessment of estimators. Conserv Biol 3(2):181–191

Hayes S, Josephson E, Maze-Foley K, Rosel P, Byrd B, Chavez-Rosales S, Col T, Engleby L, Garrison L, Hatch J, Henry A, Horstman S, Litz J, Lyssikatos M, Mullin K, Orphanides C, Pace R, Palka D, Soldevilla M, Wenzel F (2018) TM 245 US Atlantic and Gulf of Mexico Marine Mammal Stock Assessments - 2017

Hildebrand JA, Gentes ZE, Johnson SC, Frasier KE, Merkens KP, Thayre BJ, Wiggins SM (2013) Acoustic monitoring of Cetaceans in the Northern Gulf of Mexico using wave gliders equipped with high-frequency acoustic recording packages. MPL Tech Memo 539:35

Hildebrand J, Baumann-Pickering S, Frasier K, Tricky J, Merkens K, Wiggins S, M M, Harris D, T M, Thomas L (2015) Passive acoustic monitoring of beaked whale densities in the Gulf of Mexico during and after the Deepwater Horizon oil spill. Nat Sci Rep 5:16343

Hildebrand JA, Frasier KE, Baumann-Pickering S, Wiggins SM, Merkens KP, Garrison LP, Soldevilla MS, McDonald MA (2019) Assessing seasonality and density from passive acoustic monitoring of signals presumed to be from pygmy and dwarf sperm whales in the gulf of mexico. Front Mar Sci 6

Huntington HP (2009) A preliminary assessment of threats to arctic marine mammals and their conservation in the coming decades. Mar Policy 33(1):77–82

Jewell R, Thomas L, Harris CM, Kaschner K, Wiff R, Hammond PS, Quick NJ (2012) Global analysis of cetacean line-transect surveys: detecting trends in cetacean density. Mar Ecol Prog Ser 453:227–240

Jochens A, Biggs D, Benoit-Bird K, Engelhaupt D, Gordon J, Hu C, Jaquet N, Johnson M, Leben R, Mate B, Miller P, Ortega-Ortiz J, Thode A, Tyack P, Würsig B (2008) Sperm whale seismic study in the Gulf of Mexico: synthesis report, vol OCS Study MMS 2008–006. US Dept. of Interior, Minerals Management Service, Gulf of Mexico OCS Region, New Orleans, LA

Johnson M, de Soto NA, Madsen PT (2009) Studying the behaviour and sensory ecology of marine mammals using acoustic recording tags: a review. Mar Ecol Prog Ser 395:55–73
Joye SB (2015) Deepwater Horizon, 5 years on. Science 349(6248):592–593
Kaschner K, Quick NJ, Jewell R, Williams R, Harris CM (2012) Global coverage of cetacean line-transect surveys: status quo, data gaps and future challenges. PLoS One 7(9):e44075
Kaushal SS, Likens GE, Pace ML, Utz RM, Haq S, Gorman J, Grese M (2018) Freshwater salinization syndrome on a continental scale. Proc Natl Acad Sci:201711234
King SL, Schick RS, Donovan C, Booth CG, Burgman M, Thomas L, Harwood J (2015) An interim framework for assessing the population consequences of disturbance. Methods Ecol Evol 6(10):1150–1158
Klinck H, Mellinger DK, Klinck K, Bogue NM, Luby JC, Jump WA, Shilling GB, Litchendorf T, Wood AS, Schorr GS, Baird RW (2012) Near-real-time acoustic monitoring of beaked whales and other cetaceans using a seaglider (TM). PLoS One 7(5). https://doi.org/10.1371/journal.pone.0036128
Kujawinski E, Soule M, Valentine D, Boysen A, Longnecker K, Redmond M (2011) Fate of dispersants associated with the Deepwater Horizon Oil Spill. Environ Sci Technol 45(4):1298–1306. https://doi.org/10.1021/es103838p
Malakoff D (2010) A push for quieter ships. Science 328:1502–1503
Mate BR, Stafford KM, Ljungblad DK (1994) A change in sperm whale (*Physeter macrocephalus*) distribution correlated to seismic surveys in the Gulf of Mexico. J Acoust Soc Am 96(5):3268–3269
Mate B, Mesecar R, Lagerquist B (2007) The evolution of satellite-monitored radio tags for large whales: one laboratory's experience. Deep-Sea Res II Top Stud Oceanogr 54(3–4):224–247
Matkin CO, Saulifis EL, Ellis GM, Olesiuk P, Rice SD (2008) Ongoing population-level impacts on killer whales *Orcinus orca* following the Exxon Valdez oil spill in Prince William sound, Alaska. Mar Ecol Prog Ser 356:269–281
Maze-Foley K, Mullin K (2007) Cetaceans of the oceanic northern Gulf of Mexico: distributions, group sizes and interspecific associations. J Cetacean Res Manag 8(2):203
Mellinger DK, Stafford KM, Moore SE, Dziak RP, Matsumoto H (2007) An overview of fixed passive acoustic observation methods for cetaceans. Oceanography 20(4):36–45. https://doi.org/10.5670/oceanog.2007.03
Miller PJ, Johnson M, Madsen PT, Biassoni N, Quero M, Tyack P (2009) Using at-sea experiments to study the effects of airguns on the foraging behavior of sperm whales in the Gulf of Mexico. Deep-Sea Res I Oceanogr Res Pap 56(7):1168–1181
Moore SE, Howe BM, Stafford KM, Boyd ML (2007) Including whale call detection in standard ocean measurements: application of acoustic Seagliders. Mar Technol Soc J 41(4):53–57
Mullin KD (2007) Abundance of cetaceans in the oceanic Gulf of Mexico based on 2003–2004 ship surveys. Available from: NMFS, Southeast Fisheries Science Center, PO Drawer 1207
Mullin KD, Fulling GL (2003) Abundance of cetaceans in the southern US North Atlantic Ocean during summer 1998. Fish Bull 101(3):603–613
Mullin KD, Fulling GL (2004) Abundance of cetaceans in the oceanic northern Gulf of Mexico, 1996-2001. Mar Mamm Sci 20(4):787–807. https://doi.org/10.1111/j.1748-7692.2004.tb01193.x
Mullin KD, Hoggard W (2000) Visual surveys of cetaceans and sea turtles from aircraft and ships. In: Davis R, WE, Wursig B (eds) Cetaceans, sea turtles and seabirds in the northern Gulf of Mexico: distribution, abundance and habitat associations, vol 2. Vol II Tech Rep. OCS Study MMS 96–0027. USGS/BRD/CR-1999-0006. , Minerals Management Service, Gulf of Mexico OCS Region, New Orleans, LA, p 111–172
Neff JM (1990) Composition and fate of petroleum and spill-treating agents in the marine environment. In: Sea mammals in oil: confronting the risks. Academic Press, Inc, San Diego, pp 1–33
Neff J, Lee K, DeBlois EM (2011a) Produced water: overview of composition, fates, and effects. In: Produced water. Springer, pp 3–54
Neff J, Sauer TC, Hart AD (2011b) Bioaccumulation of hydrocarbons from produced water discharged to offshore waters of the US Gulf of Mexico. In: Produced water. Springer, pp 441–477

NMFS (2015) Endangered and threatened wildlife; 90-day finding on a petition to list the Gulf of Mexico Bryde's whale as threatened or endangered under the endangered species act. vol 80 FR 18343

NMFS (2017) NMFS Arctic marine mammal disaster response guidelines. NOAA Tech. Memo. U.S. Dep. Commer. https://doi.org/10.7289/V5/TM-F/AKR-16

NOAA (2014) Oil Spill emergency response killer whale - hazing implementation plan. NOAA Fisheries West Coast Region,

Palka DL (2006) Summer abundance estimates of cetaceans in US North Atlantic navy operating areas. Northeast Fisheries Science Center Ref Doc:06–03

Pereira WE, Hostettler FD (1993) Nonpoint source contamination of the Mississippi River and its tributaries by herbicides. Environ Sci Technol 27(8):1542–1552

Pirotta E, Booth CG, Costa DP, Fleishman E, Kraus SD, Lusseau D, Moretti D, New LF, Schick RS, Schwarz LK (2018) Understanding the population consequences of disturbance. Ecol Evol 8(19):9934–9946

Rabalais NN, Turner RE, Justic D, Dortch Q, Wiseman WJ, SenGupta BK (1996) Nutrient changes in the Mississippi River and system responses on the adjacent continental shelf. Estuaries 19(2B):386–407

Redfern JV, Ferguson MC, Becker EA, Hyrenbach KD, Good CP, Barlow J, Kaschner K, Baumgartner MF, Forney KA, Ballance LT (2006) Techniques for cetacean–habitat modeling. Mar Ecol Press Ser 310:271–195

Roberts JJ, Best BD, Mannocci L, Fujioka E, Halpin PN, Palka DL, Garrison LP, Mullin KD, Cole TV, Khan CB (2016) Habitat-based cetacean density models for the US Atlantic and Gulf of Mexico. Sci Rep 6

Schwacke LH, Thomas L, Wells RS, McFee WE, Hohn AA, Mullin KD, Zolman ES, Quigley BM, Rowles TK, Schwacke JH (2017) Quantifying injury to common bottlenose dolphins from the Deepwater Horizon oil spill using an age-, sex-and class-structured population model. Endanger Species Res 33:265–279

SEFSC (2018) Gulf of Mexico marine mammal vessel surveys - NRDA. Retrieved from https://inport.nmfs.noaa.gov/inport/item/26499

Sellas AB, Wells RS, Rosel PE (2005) Mitochondrial and nuclear DNA analyses reveal fine scale geographic structure in bottlenose dolphins (*Tursiops truncatus*) in the Gulf of Mexico. Conserv Genet 6(5):715–728

Sidorovskaia N, Li K, Tiemann C, Ackleh A, Tang T (2016) Long-term spatially distributed observations of deep diving marine mammals in the Northern Gulf of Mexico using passive acoustic monitoring. J Acoust Soc Am 140(4):3073–3073

Simonis AE, Roch MA, Bailey B, Barlow J, Clemesha RE, Iacobellis S, Hildebrand JA, Baumann-Pickering S (2017) Lunar cycles affect common dolphin *Delphinus delphis* foraging in the Southern California bight. Mar Ecol Prog Ser 577:221–235

Soldevilla MS, Wiggins SM, Hildebrand JA, Oleson EM, Ferguson MC (2011) Risso's and Pacific white-sided dolphin habitat modeling from passive acoustic monitoring. Mar Ecol Prog Ser 423:247–260

Soldevilla MS, Hildebrand JA, Frasier KE, Dias LA, Martinez A, Mullin KD, Rosel PE, Garrison LP (2017) Spatial distribution and dive behavior of Gulf of Mexico Bryde's whales: potential risk of vessel strikes and fisheries interactions. J Endanger Species Res 32:533–550

Southward A, Southward EC (1978) Recolonization of rocky shores in Cornwall after use of toxic dispersants to clean up the Torrey Canyon spill. J Fish Res Board Can 35(5):682–706

Stone CJ, Tasker ML (2006) The effects of seismic airguns on cetaceans in UK waters. J Cetacean Res Manag 8(3):255

Taylor BL, Martinez M, Gerrodette T, Barlow J, Hrovat YN (2007) Lessons from monitoring trends in abundance of marine mammals. Mar Mamm Sci 23(1):157–175

Testa JM, Eric Adams E, North EW, He R (2016) Modeling the influence of deep water application of dispersants on the surface expression of oil: a sensitivity study. J Geophys Res Oceans 121(8):5995–6008. https://doi.org/10.1002/2015JC011571

Trustees DHNRDA (2016) Injury to natural resources. In: Final Programmatic Damage Assessment and Restoration (PDARP) plan and final Programmatic Environmental Impact Statement (PEIS). Retrieved from http://www.gulfspillrestoration.noaa.gov/restoration-planning/gulf-plan, p 516

Tyack PL (2008) Implications for marine mammals of large-scale changes in the marine acoustic environment. J Mammal 89(3):549–558

Vander Zanden HB, Bolten AB, Tucker AD, Hart KM, Lamont MM, Fujisaki I, Reich KJ, Addison DS, Mansfield KL, Phillips KF (2016) Biomarkers reveal sea turtles remained in oiled areas following the Deepwater Horizon oil spill. Ecol Appl 26(7):2145–2155

Waring GT, Josephson E, Fairfield-Walsh CP, Maze-Foley K (2009) US Atlantic and Gulf of Mexico marine mammal stock assessments - 2008. NOAA Tech Memo NMFS NE 210(440):11.10

Waring GT, Josephson E, Maze-Foley K, Rosel PE (2015) US Atlantic and Gulf of Mexico marine mammal stock assessments - 2014. NOAA Tech Memo NMFS NE 231:361

Weilgart LS (2007) The impacts of anthropogenic ocean noise on cetaceans and implications for management. Can J Zool 85(11):1091–1116

Wiggins SM, Hildebrand JA (2007) High-frequency Acoustic Recording Package (HARP) for broad-band, long-term marine mammal monitoring. Institute of Electrical and Electronics Engineers, Tokyo, Japan., International Symposium on Underwater Technology 2007 and International Workshop on Scientific Use of Submarine Cables & Related Technologies 2007

Wilkin SM, Rowles TK, Stratton E, Adimey N, Field CL, Wissmann S, Shigenaka G, Fougères E, Mase B, Network SRS (2017) Marine mammal response operations during the Deepwater Horizon oil spill. Endanger Species Res 33:107–118

Williams R, Gero S, Bejder L, Calambokidis J, Kraus SD, Lusseau D, Read AJ, Robbins J (2011) Underestimating the damage: interpreting cetacean carcass recoveries in the context of the Deepwater Horizon/BP incident. Conserv Lett 4(3):228–233

Williams R, Thomas L, Ashe E, Clark CW, Hammond PS (2016) Gauging allowable harm limits to cumulative, sub-lethal effects of human activities on wildlife: a case-study approach using two whale populations. Mar Policy 70:58–64

Wright AJ, Deak T, Parsons E (2011) Size matters: management of stress responses and chronic stress in beaked whales and other marine mammals may require larger exclusion zones. Mar Pollut Bull 63(1–4):5–9

Chapter 26
Comparative Environmental Sensitivity of Offshore Gulf of Mexico Waters Potentially Impacted by Ultra-Deep Oil Well Blowouts

Emily Chancellor, Steven A. Murawski, Claire B. Paris, Larry Perruso, and Natalie Perlin

Abstract Environmental sensitivity indices (ESIs) have long been used to identify coastal and shoreline resources particularly vulnerable to oil spills and ensuing mitigation measures. In the Gulf of Mexico, oil production by the United States and Mexico has increasingly focused on deepwater sources. As oil exploration and production continue further offshore, deepwater and open ocean pelagic resources increasingly become the focus of susceptibility to oil well blowouts. Methodologies are proposed to spatially quantify ESIs specifically for offshore living marine resources. A multi-attribute utility model is proposed to integrate biological resource sensitivity measures and measures of potential economic losses to define spatially explicit environmental sensitivity. Model sensitivity is examined using three weighting schemes for various environmental attributes. The relative environmental sensitivities of four simulated deepwater blowouts in the Gulf of Mexico were analyzed and compared. While differences were found between four oil well blowout scenarios in terms of the overall sensitivity and to the individual attributes, results were relatively insensitive to the weights assigned to various attributes. The uses of ESIs in optimizing oil production locations to minimize potential impacts on sensitive ecological resources and economic uses are discussed.

E. Chancellor (✉) · S. A. Murawski
University of South Florida, College of Marine Science, St. Petersburg, FL, USA
e-mail: echancellor@mail.usf.edu; smurawski@usf.edu

C. B. Paris · N. Perlin
University of Miami, Department of Ocean Sciences, Rosenstiel School of Marine and Atmospheric Science, Miami, FL, USA
e-mail: cparis@rsmas.miami.edu; nperlin@rsmas.miami.edu

L. Perruso
National Marine Fisheries Service, Southeast Fisheries Science Center, Miami, FL, USA
e-mail: larry.perruso@noaa.gov

S. A. Murawski et al. (eds.), *Scenarios and Responses to Future Deep Oil Spills*,
https://doi.org/10.1007/978-3-030-12963-7_26

Keywords Environmental sensitivity indices · ESI · Multi-attribute utility theory · Gulf of Mexico

26.1 Introduction

The Gulf of Mexico (GoM) provides almost all of the offshore oil production in the United States (~97%; EIA 2018) with estimated oil reserves of over 3.67 billion barrels (Kazanis et al. 2015). In the GoM, US and Mexico oil production has increasingly focused on deepwater sources to maintain and increase volumes as these deepwater sources are more productive than shallower fields (i.e., depth has a positive logarithmic relationship with production, Murawski et al. 2020, Fig. 2.5). Additionally, deepwater areas in the eastern GoM that are currently under moratorium for drilling under the GoM Energy Security Act of 2007 (Sissine 2007) have been included in future proposals for oil exploration and production (DOI Press 2018). The significant offshore movement of marine oil and gas production challenges traditional paradigms for habitat and species sensitivity considerations as being purely coastal issues. As oil production drilling continues to move further offshore, offshore marine resources become increasingly susceptible to oil well blowouts.

Potential biological and human use resource losses to coastal areas and shorelines have been estimated by various methods including the use of environmental sensitivity indices (ESIs; Jensen et al. 1990). ESIs for the offshore areas can estimate the potential losses of these offshore marine resources and can serve as valuable input for resource planning for offshore drilling (identification of particularly sensitive areas) and for prioritization of response efforts in the event of future deepwater oil well blowouts.

In this chapter, we explore methodologies to spatially quantify the relative sensitivity of offshore marine resources in the northern GoM using ESIs and illustrate this methodology using a subset of relevant ecological and economic data. A multi-attribute utility model (Huber 1974) is proposed to integrate biological resource sensitivity and economic loss potential to define overall spatial and temporal sensitivity. This chapter outlines methodologies for ESIs, creates a preliminary ESI matrix for the northern GoM based on several biological and economic datasets, and uses these ESIs to compare sensitivities for four simulated deepwater oil well blowouts in the GoM. We outline additional relative ecological datasets and propose optimization modeling approaches to quantify trade-offs between production and environmental protection that may be useful in the oil well siting process.

26.2 History of Environmental Sensitivity Indices in Oil Spill Response

Historically, ESIs have been created to identify environmentally sensitive coastal areas for the prioritization of oil spill cleanup (Jensen et al. 1990, 1998). The National Oceanic and Atmospheric Administration (NOAA) has published guidelines for

creating shoreline ESIs consisting of an index with three components; shoreline type, biological resources, and human uses of resources (Petersen et al. 2002; NOAA Response and Restoration 2018). The shoreline type is classified into one of eight categories based on published NOAA criteria. Biological components include areas with many distinct species, areas of large overall abundance of biological organisms, and areas where vulnerable species are present (e.g., seabirds, turtles, and other endangered species). Human use components include historical sites and public use areas such as parks and recreational beaches. ESIs created under these guidelines are graphical and largely qualitative, as areas are marked as sensitive or not, and can be marked sensitive due to meeting only one of the three above criteria. Sensitive areas defined under this process are not quantitative in the relative sense or necessarily comparable across landscapes.

Site-specific geographic information system (GIS)-based ESIs have been published for much of the shoreline of the United States including the GoM (Knudsen and Druyor 2009; NOAA ORR 2018). Categorical and quantitative ESIs have been created for shoreline sensitivity to offshore spills in many areas and for marine spatial planning specific to locations in the Mediterranean Sea (Kassomenos 2004; Adler and Inbar 2007; Castañedo et al. 2008; Fattal et al. 2010; Santos et al. 2013; Olita et al. 2012; Alves et al. 2014; Maitieg et al. 2018) GoM (Nelson et al. 2015; Nelson and Grubesic 2018), Brazil (Carmona et al. 2004; Szlafsztein and Sterr 2007; Romero et al. 2013), and Asia (Lan et al. 2015; Lee and Jung 2015; Kankara et al. 2016). Environmental sensitivity is also regularly calculated using ESI methods by the Bureau of Ocean Energy Management (BOEM) for Oil and Natural Gas Planning Program Assessment (BOEM 2018; Niedoroda et al. 2014). However, these analyses may not be spatially disaggregated enough to identify discrete, sensitive areas worthy of increased scrutiny. This chapter differs from the previous research by moving the focus from exclusively shoreline areas to deeper regions and resources and developing the ESIs at a finer spatial scale of resolution: 1° latitude × 1° longitude resolution for offshore areas of the northern GoM.

26.3 The Need for an Offshore ESI

Like the coastal areas, offshore waters contain biological resources and human use patterns threatened during an oil well blowout. The offshore waters of the GoM are biologically important as they are home to multiple species of economically important fish and shellfish (Pulster et al. 2020; Sutton et al. 2020; Perlin et al. 2020). As well, offshore areas support ecologically important forage species and other animals of concern including mammals, turtles, seabirds, and deep-sea corals which all experience lethal and sublethal effects from exposure to oil (Antonio et al. 2011; Carmichael et al. 2012; Schwacke et al. 2013; Tran et al. 2014; Haney et al. 2014; Etnoyer et al. 2016; Frasier 2020). Many economically important fish species spawn

in open waters, and their larval life stages are particularly vulnerable to oil. Up to half of known fish species in the GoM occur in mesopelagic deep waters, and new species are being encountered there (Sutton et al. 2017, 2020). Human uses of resources in offshore waters include commercial and recreational fisheries, commercial shipping and cruise lines, military exercise areas, oil and gas leases, renewable energy infrastructure, and other uses (McCrea-Strub et al. 2011; BOEM Offshore Statistics by Water Depth 2018).

This chapter defines quantitative ESI scores via a multi-attribute utility model (MAUM; Huber 1974). In a MAUM, the overall value, or utility, is calculated by the weighted sum or product of the individual utility values of a set of attributes. The definition of this overall utility then allows for comparisons to be made between different sets of attributes, particularly focusing on the sensitivity of the relative weights assigned to each attribute. In the health industry, for example, MUAMs are used to assign patients an overall health index based on several independent health attributes, e.g., vision, hearing, speech, ambulation, dexterity, emotion, cognition, and pain/discomfort. Coefficients for the attributes are calculated from surveys of the importance of the listed attributes. Individual patients are then assigned a semi-quantitative value of 0–6 in each of the health attributes, and these attribute scores are then substituted into the utility function in order to give an overall health index per patient (Feeny et al. 2002). We develop a similar methodology for the creation of the ESIs for the offshore areas in the GoM.

Similar to the human health example above, the environmental sensitivity of a marine geographic location can be determined both by the biological attributes extant at that location and human dependence on the region that might be compromised by an oil well blow out or other significant events resulting in biological and/or economic losses. To illustrate these issues, we develop a MAUM based on three ecological variables and three economic (human use) indicators. Using results from the systematic SEAMAP larval sampling program (Chancellor 2015), we focus on the diversity of larval fishes in both offshore and coastal areas. Larval fish are highly sensitive to oil-related pollution as they are susceptible to physiological defects and mortality at exceedingly low concentrations of oil exposure (Carls et al. 1999; Incardona et al. 2004, 2013; Hicken et al. 2011). Pollution from oil well blowouts would likely impact survival of a variety of species, varying seasonally (Chancellor 2015). We gridded the results of the larval diversity, estimated species richness, and overall abundance data into 1° latitude × 1° longitude rectangles for the northern GoM (Figs. 26.1 and 26.2). In addition to larval measures, we computed measures of economic dependence assigned to the same 1° grid rectangles using estimated offshore (pelagic) ex-vessel revenues and species composition based on vessel logbook information made available from the National Marine Fisheries Service. These data are compared with similar revenue estimates derived from vessel logbook data for coastal reef fishes, coastal migratory pelagic species, and shrimp fisheries.

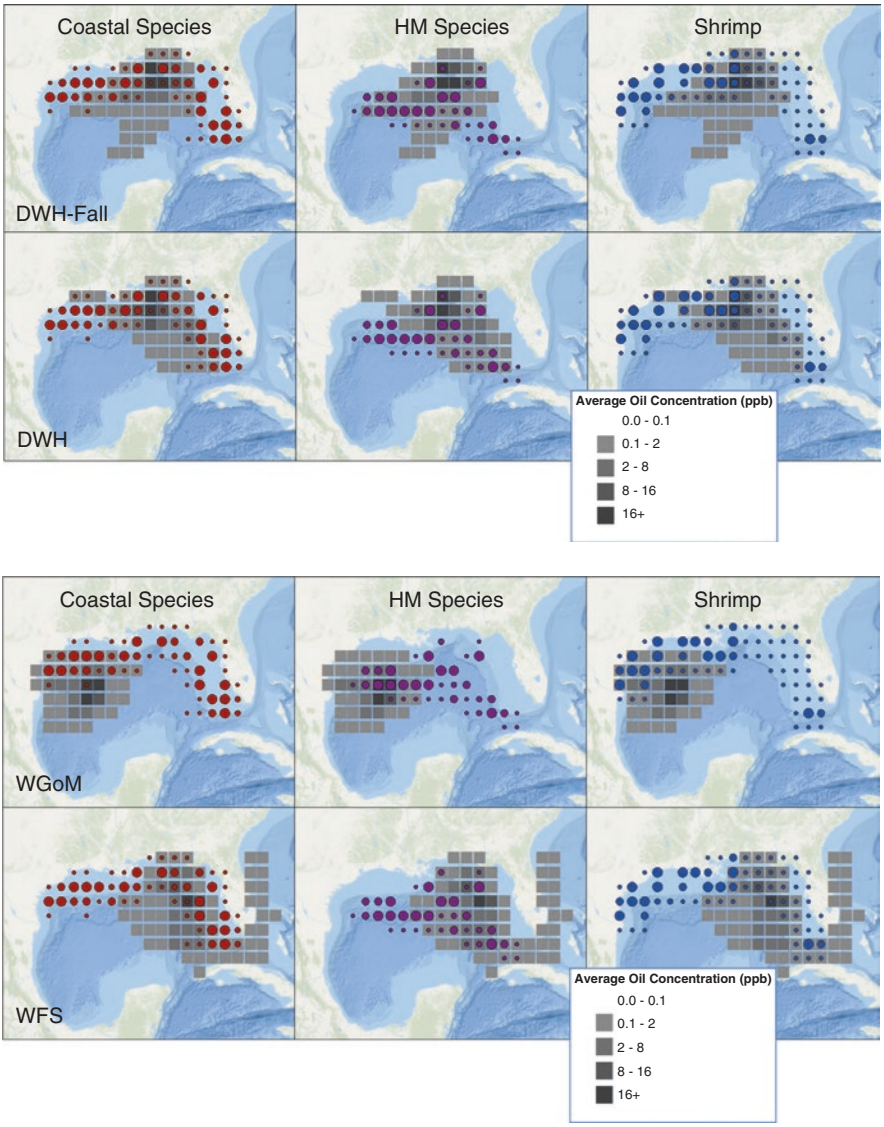

Fig. 26.1 (**upper**) Indexed values for the sensitivity attributes of coastal species fishery catches, HMS fishery catches, and shrimp fishery catches (left to right) spatially mapped against two simulated blowouts (top to bottom), DWH-Fall = the *Deepwater Horizon* spill but starting in September (vs. April) and DWH = the *Deepwater Horizon* scenario. (**lower**) Indexed values for the sensitivity attributes of coastal species fishery catches, HMS fishery catches, and shrimp fishery catches (left to right) spatially mapped against two simulated blowouts (top to bottom), WGoM Western Gulf of Mexico, WFS West Florida Slope

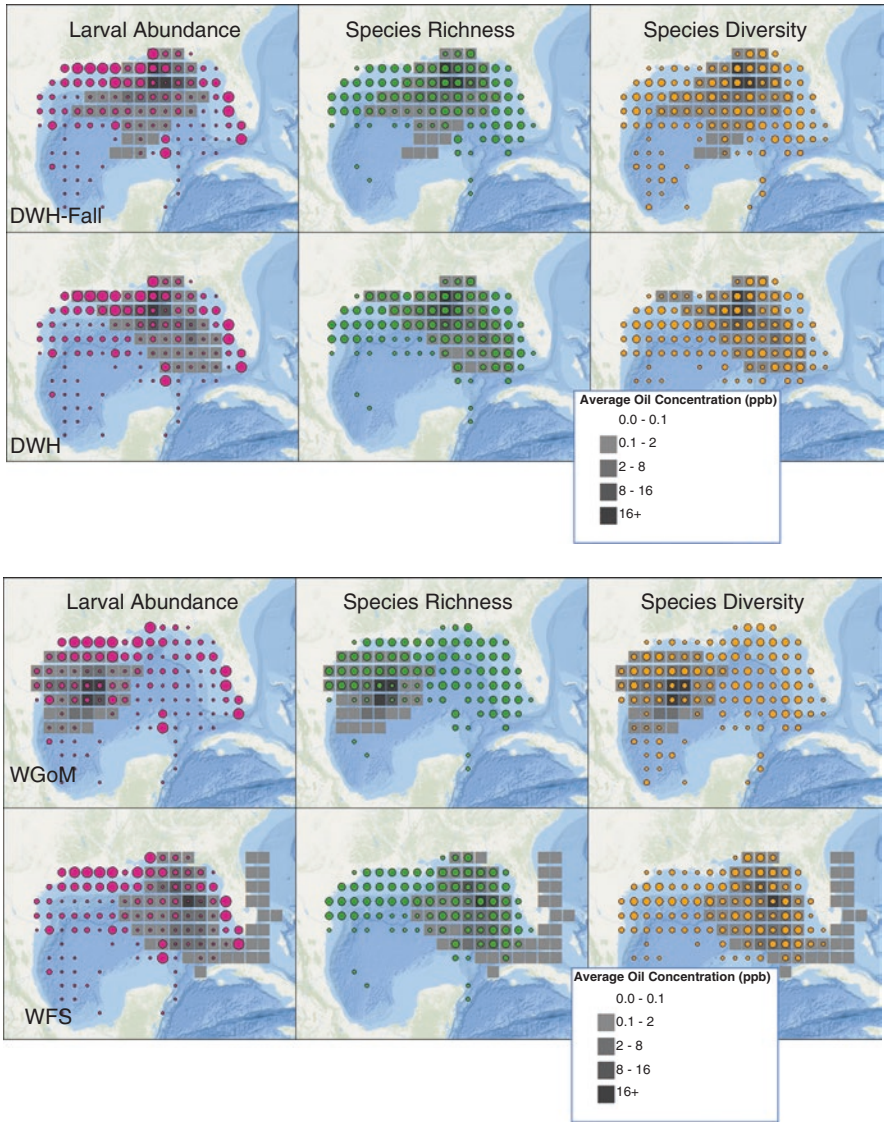

Fig. 26.2 (**upper**) Indexed values for the sensitivity attributes of larval abundance, estimated species richness, and Shannon diversity index (left to right) spatially mapped against two simulated blowouts (top to bottom), DWH-Fall = the *Deepwater Horizon* spill but starting in the Fall (September vs. April) and DWH = the *Deepwater Horizon* scenario. (**lower**) Indexed values for the sensitivity attributes of larval abundance, estimated species richness, and Shannon diversity index (left to right) spatially mapped against two simulated blowouts (top to bottom), WGoM Western Gulf of Mexico, WFS West Florida Slope

26.4 Description of Ecological and Economic Datasets

Southeast Area Monitoring and Assessment Program (SEAMAP) Ichthyoplankton counts and taxonomy were used to create a 1° latitude × 1° longitude grid of estimated abundance by species for the GoM. Samples included came from seasonal surveys from 2000 to 2015 collected via bongo nets. Standardized abundance was calculated for each sample by the estimated number of organisms under a 10 m^2 surface area. These standardized abundances were then calculated across all years and all samples within each 1° × 1° grid and divided by the total number of samples within that block. More information regarding the sampling techniques, species selection, and standardized abundance calculations from raw counts can be found in Chancellor (2015). A total of 58 species of larval fishes were included (Table 26.1).

Coastal Reef Fish and Coastal Migratory Pelagics Annual landings (pounds), reported to the Southeast Coastal Fisheries Logbook Program, and estimates of annual revenues for individual coastal species were assigned to each 1° × 1° grid rectangle. Estimated revenue per grid rectangle is a function of annual trip-level landings and ex-vessel prices aggregated and provided by National Marine Fisheries Service (NMFS)/Southeast Fisheries Science Center (SEFSC) (Overstreet & Liese 2018). Ex-vessel prices represent the unit price paid at the time of landing by fish dealers to fishers for harvested but unprocessed catch. Grids with less than three vessels reporting trip records were omitted to prevent identifying confidential proprietary information. Fifty-nine species were included in the coastal reef fisheries data (Table 26.2).

Highly Migratory Species (HMS) Landings for eight HMS (Table 26.2) were provided by NMFS/SEFSC for each 1° × 1° grid rectangle and were estimated by applying the proportion of numbers of individual species caught in each grid rectangle, as reported to the Atlantic Highly Migratory Species Fisheries Logbook Program, to total trip-level catch (pounds gutted weight). The resulting pounds for each HMS were aggregated for each grid cell annually from 2013 to 2016. Revenue for the HMS pounds was estimated for all species using the average price from NMFS' commercial landings in the GoM for available years 2013–2016 (Personal communication from the National Marine Fisheries Service, Fisheries Statistics Division. [September 2018]). For blue shark and porbeagle shark, the average price per pound for "general sharks" was used, as no specific information was available for them.

Shrimp Revenue estimates for the three dominant species of shrimp (white, brown, pink) were provided by NMFS/SEFSC for each 1° × 1° grid rectangle and were estimated from aggregated landings reported to the Gulf of Mexico Shrimp Permit Cellular Electronic Logbook program during years 2011–2016 and from price per pound reported by port agents and trip tickets (Table 26.2). All three data groupings used to estimate revenues adhere to confidentiality standards and are not adjusted for inflation.

Table 26.1 Scientific and common names of larval species used in developing environmental sensitivity indices herein. Data were collected on SEAMAP larval fish sampling cruises (Chancellor 2015)

Scientific name	Common name	Scientific name	Common name
Acanthocybium solandri	Wahoo	*Margrethia obtusirostra*	Bighead portholefish
Aplatophis chauliodus	Tusky eel	*Micropogonias undulatus*	Croaker, Atlantic
Bairdiella chrysoura	Silver perch	*Mugil cephalus*	Mullet, striped
Benthosema suborbitale	Lanternfish, smallfin	*Mugil curema*	Mullet, silver
Bonapartia pedaliota	Longray fangjaw	*Myrophis punctatus*	Speckled worm eel
Bregmaceros cantori	Striped codlet	*Nesiarchus nasutus*	Black gemfish
Carapus bermudensis	Atlantic pearlfish	*Notolychnus valdiviae*	Lanternfish, topside
Ceratoscopelus warmingii	Lanternfish, Warming's	*Oligoplites saurus*	Leather jack
Chlorophthalmus agassizi	Shortnose greeneye	*Ophichthus gomesii*	Shrimp eel
Chloroscombrus chrysurus	Atlantic bumper	*Ophichthus rex*	King snake eel
Cynoscion arenarius	Sea trout, white	*Opisthonema oglinum*	Herring, Atlantic thread
Cynoscion nebulosus	Sea trout, spotted	*Peprilus burti*	Butterfish, gulf
Decapterus punctatus	Scads, round	*Peprilus paru*	Harvestfish
Diogenichthys atlanticus	Lanternfish, longfin	*Pollichthys mauli*	Lightfish, stareye
Diplospinus multistriatus	Striped escolar	*Pomatomus saltatrix*	Bluefish
Engyophrys senta	Founder, spiny	*Pristipomoides aquilonaris*	Wenchman
Etrumeus teres	Herring, round	*Rachycentron canadum*	Cobia
Euthynnus alletteratus	Tuna, little (tunny)	*Rhomboplites aurorubens*	Snapper, vermilion
Gempylus serpens	Snake mackerel	*Sardinella aurita*	Sardine, Spanish
Harengula jaguana	Herring, scaled	*Sciaenops ocellatus*	Drum, red
Hygophum reinhardtii	Lanternfish, Reinhardt's	*Scomber colias*	Mackerel, Atlantic chub
Katsuwonus pelamis	Tuna, skipjack	*Scomberomorus cavalla*	Mackerel, king
Lagodon rhomboides	Pinfish	*Scomberomorus maculatus*	Mackerel, Spanish
Larimus fasciatus	Drum, banded	*Selar crumenophthalmus*	Scads, bigeye
Leiostomus xanthurus	Spot	*Serraniculus pumilio*	Pygmy sea bass
Lobotes surinamensis	Atlantic tripletail	*Stellifer lanceolatus*	Drum, star
Lutjanus campechanus	Snapper, red	*Thunnus thynnus*	Tuna, bluefin
Lutjanus griseus	Snapper, mangrove	*Trachurus lathami*	Scads, rough
Luvarus imperialis	Louvar	*Xiphias gladius*	Swordfish

Table 26.2 Common and scientific names of species and families of fish and shrimp used in developing coastal reef fish, coastal migratory pelagics, and shrimp and highly migratory species fisheries' landings and revenue data

Coastal species		Highly migratory species		Shrimp species	
Scientific name	Common name	Scientific name	Common name	Scientific name	Common name
Acanthocybium solandri	Wahoo	*Isurus oxyrinchus*	Shark, mako	*Farfantepenaeus aztecus*	Shrimp, brown
Apsilus dentatus	Snapper, black	*Katsuwonus pelamis*	Tuna, skipjack	*Litopenaeus setiferus*	Shrimp, white
Archosargus probatocephalus	Sheepshead, Atlantic	*Lamna nasus*	Shark, porbeagle	*Penaeus duorarum*	Shrimp, pink
Balistes capriscus	Triggerfish, gray	*Prionace glauca*	Shark, blue		
Balistes vetula	Triggerfish, queen	*Thunnus alalunga*	Tuna, albacore		
Calamus bajonado	Porgy, jolthead	*Thunnus albacares*	Tuna, yellowfin		
Calamus leucosteus	Porgy, whitebone	*Thunnus obesus*	Tuna, bigeye		
Calamus nodosus	Porgy, knobbed	*Thunnus thynnus*	Tuna, bluefin		
Canthidermis sufflamen	Triggerfish, ocean	*Xiphias gladius*	Swordfish		
Carangidae	Jacks				
Caulolatilus microps	Tilefish, blueline				
Centropristis striata	Sea bass, Atlantic, black				
Coryphaena	Dolphinfish				
Ephippididae	Spadefish				
Epinephelus adscensionis	Hind, rock				
Epinephelus cruentatus	Graysby				
Epinephelus drummondhayi	Hind, speckled				
Epinephelus flavolimbatus	Grouper, yellowedge				
Epinephelus guttatus	Hind, red				
Epinephelus morio	Grouper, red				
Epinephelus mystacinus	Grouper, misty				
Epinephelus nigritus	Grouper, Warsaw				

(continued)

Table 26.2 (continued)

Coastal species		Highly migratory species		Shrimp species	
Scientific name	Common name	Scientific name	Common name	Scientific name	Common name
Epinephelus niveatus	Grouper, snowy				
Etelis oculatus	Snapper, queen				
Euthynnus alletteratus	Tuna, little (tunny)				
Haemulidae	Grunts				
Haemulon album	Margate				
Haemulon plumieri	Grunt, white				
Lachnolaimus maximus	Hogfish				
Lopholatilus chamaeleonticeps	Tilefish				
Lutjanidae	Snappers				
Lutjanus analis	Snapper, mutton				
Lutjanus apodus	Snapper, schoolmaster				
Lutjanus buccanella	Snapper, blackfin				
Lutjanus campechanus	Snapper, red				
Lutjanus cyanopterus	Snapper, cubera				
Lutjanus griseus	Snapper, mangrove				
Lutjanus jocu	Snapper, dog				
Lutjanus synagris	Snapper, lane				
Lutjanus vivanus	Snapper, silk				
Malacanthus plumieri	Tilefish, sand				
Mycteroperca bonaci	Grouper, black				
Mycteroperca microlepis	Grouper, gag				
Mycteroperca phenax	Scamp				
Mycteroperca venenosa	Grouper, yellowfin				
Ocyurus chrysurus	Snapper, yellowtail				
Pagrus pagrus	Porgy, red				

(continued)

Table 26.2 (continued)

Coastal species		Highly migratory species		Shrimp species	
Scientific name	Common name	Scientific name	Common name	Scientific name	Common name
Pomatomus saltatrix	Bluefish				
Pristipomoides aquilonaris	Wenchman				
Rachycentron canadum	Cobia				
Rhomboplites aurorubens	Snapper, vermilion				
Scomberomorus cavalla	Mackerel, king				
Scomberomorus maculatus	Mackerel, Spanish				
Seriola dumerili	Amberjack, greater				
Seriola fasciata	Amberjack, lesser				
Seriola rivoliana	Jack, Almaco				
Seriola zonata	Banded rudderfish				
Serranidae	Groupers				
Sparidae	Scups or porgies				

26.5 Calculation of Sensitivity Attributes

Six sensitivity attributes were created forming our trial ESIs. These were the following:

Biological All SEAMAP samples were assigned to the same 1° grid rectangle block system as for fishery landings. The following three attributes were calculated for SEAMAP larval samples within each grid rectangle:

1. *Species richness of larval fish species* – Larval species richness was estimated using the *specpool* function from the *vegan* package in *R*. This function computes the asymptotes of the rarefaction curves to estimate the total species richness per grid rectangle and allows comparisons among grid rectangles with different sampling frequencies (Gotelli and Cowell 2001; Cowell et al. 2004). Grid rectangles with less than five samples were excluded from this calculation.

We used the first-order jackknife method to estimate the number of missing species, $\hat{f}_0$, (Oksanen 2018):

$$\hat{f}_0 = f_1 \frac{N}{N-1} \tag{26.1}$$

where f_1 is the number of species found in only one site and N is the total number of sites. The jackknife estimator operates under the assumption that we miss about as many species as we only see once (Smith and van Belle 1984). The estimated species richness , Sp, is the sum of the species observed, So, plus the estimated number of missing species, $\hat{f}_0$:

$$\mathrm{Sp} = \mathrm{So} + \hat{f}_0 \tag{26.2}$$

2. *Shannon-Wiener diversity of larval fish species* – The Shannon-Wiener diversity index (Hill 1973) was calculated for each grid rectangle using the *diversity* function in the *vegan* package. The Shannon-Wiener diversity calculation used in this chapter is (Oksanen 2018):

$$H = -\sum_{i=1}^{S} p_i \ln p_i \tag{26.3}$$

where p_i is the proportion of species i and S is the number of species such that the $\sum p_i = 1$.

3. *Overall abundance of larval fish species* – Larval abundance was calculated for each grid rectangle by summing the total abundance for all species within the block and dividing by the number of samples.

$$Abundance = \left(\sum_{i=1}^{m} x_i\right) / n \tag{26.4}$$

where x_i is the standardized abundance for each species, i within the grid rectangle, m is the number of species, and n is the number of samples within the grid rectangle.

Economic Data:

4. *Revenue value of coastal species* – Coastal species revenue (CRev) was calculated as the sum of revenue from all coastal species within each grid rectangle.
5. *Revenue value of HMS* – HMS revenue (HMRev) was calculated as the sum of revenue from all HMS within each grid rectangle.
6. *Revenue value of shrimp species* – Shrimp revenue (SRev) was calculated as the sum of revenue from all shrimp species within each grid rectangle.

26.6 Creation of the ESIs

Each attribute was normalized to a relative (0–1) by finding the proportion of the total within each grid rectangle.

$$vI_j = v_j / (\sum_{j=1}^{n} v_j) \tag{26.5}$$

where v_j is the value of the attribute v for grid rectangle, j and n is the total number of grid rectangles, and vI_j is the indexed value.

The cumulative sensitivity equation was modeled as a multi-attribute linear utility function combining the sensitivity attributes such that the cumulative sensitivity (CS) at grid rectangle j is:

$$CS_j = \sum_{i=1}^{N} k_i * (vI_{ij}) \tag{26.6}$$

where N is the number of included sensitivity attributes, k_i is the coefficient assigned to the ith attribute, and VI_{ij} is the indexed score of the ith sensitivity attribute at grid rectangle j.

The CS variable is then mapped onto the 1° × 1° grid resulting in a spatial distribution of the environmental sensitivity index. The sensitivity of the coefficients (k) was analyzed by creating the CS variable map under three different methods for weighting k: all coefficients having equal weights ($k = 1$), economic sensitivity coefficients weighted more heavily ($k_1 = 1.3$, $k_2 = 0.7$), and environmental sensitivity coefficients weighted more heavily ($k_1 = 0.7$, $k_2 = 1.3$).

26.7 Comparison with Modeled Oil Well Blowouts

To demonstrate the utility of the proposed ESIs, four oil well blowouts were modeled using the open-source Connectivity Modeling System (CMS) adapted with an oil module (Paris et al. 2012, 2013; Berenshtein et al. 2020a). Origin locations for the scenarios were chosen at locations with similar depths to the DWH blowout and to represent locations where drilling is currently occurring or proposed. For each scenario, oil droplets were released during 87 days (similar to DWH) and tracked for a total of 90 days. In each scenario, oil droplets were released at a depth of 1222 m in accordance to the conditions of the DWH oil well blowout. Total petroleum hydrocarbon (TPH) concentrations (ppb) are obtained by normalizing the total oil mass to the mass of water in 0.02° grid boxes in the upper 20 m, and the daily averages are further determined from the 2 hourly output products.

The simulated oil well blowouts scenarios are:

1. *Deepwater Horizon* control (DWH) – Located in the central GoM with a DWH origin point
   Origin: 28.736 N, 88.365 W Start Date: April 20, 2010

2. *Deepwater Horizon* September (DWH Sept) – Located in the central GoM with a DWH origin point and a September start date
   Origin: 28.736 N, 88.365 W Start Date: September 1, 2010
3. Western GoM – Located in the western GoM where drilling is currently active.
   Origin: 27.000 N, 85.168 W Start Date: April 20, 2010
4. West Florida Slope (WFS) – Located in the eastern GoM on the continental slope where drilling has been prohibited at least until 2022.
   Origin: 26.600 N, 93.190 W Start Date: April 20, 2010

We use the ESIs summed over all grid rectangles to compare and rank the sensitivity to these four blowout scenarios.

TPH concentrations per day were obtained by normalizing the total oil mass to the mass of water in 0.02° grid boxes in the upper 20 m. The average oil concentration (in ppb) for each 1° × 1° grid was further calculated by the summation of the simulated oil concentration per grid per day and then finding the average oil concentration over all 90 days. This was calculated for each oil well blowout scenario:

$$OC_{sj} = (\sum_{i=1}^{90}(\sum_{k=1}^{n} o_{ki}))/90 \tag{26.7}$$

where OC_{sj} is the oil concentration for scenario s at 1° × 1° grid rectangle j, o_{ki} is the kth oil concentration in grid rectangle j during day i, and n is the total number of oil concentration measurements within block j during day i. The six ecological and economic attributes are mapped with the average oil concentration for each scenario (Figs. 26.1 and 26.2).

The distribution of values of OC_{sj} (Fig. 26.3, left) shows a highly skewed distribution with a few, 1° × 1° grid rectangles near the well blowout origins having very high oil concentrations (Figs. 26.1 and 26.2). Because these oil concentrations are averaged over 90 days, there were likely areas and days where episodic higher oil exposures within blocks occurred. The OC_{sj} values were transformed into a piecewise root function where any oil concentration between 0 and 1 average ppb was assigned a value of 1 and OC_{sj} values greater than one were transformed by the square root function:

$$OI_{sj} = \begin{cases} 1 & when\ OI_{sj} > 0\ and < 1 \\ OC_{sj}^{\left(\frac{1}{2}\right)} & when\ OI_{sj} \geq 1 \end{cases} \tag{26.8}$$

This transformation emphasizes the importance of moderate oil concentrations that may affect larval fish and contamination levels that would result in fishery closures (Berenshtein et al. 2020b) while reducing the multiplication factor of the most heavily oiled areas to a maximum of 5.47. The distributions of the original OC_{sj} and OI_{sj} values are plotted in Fig. 26.3.

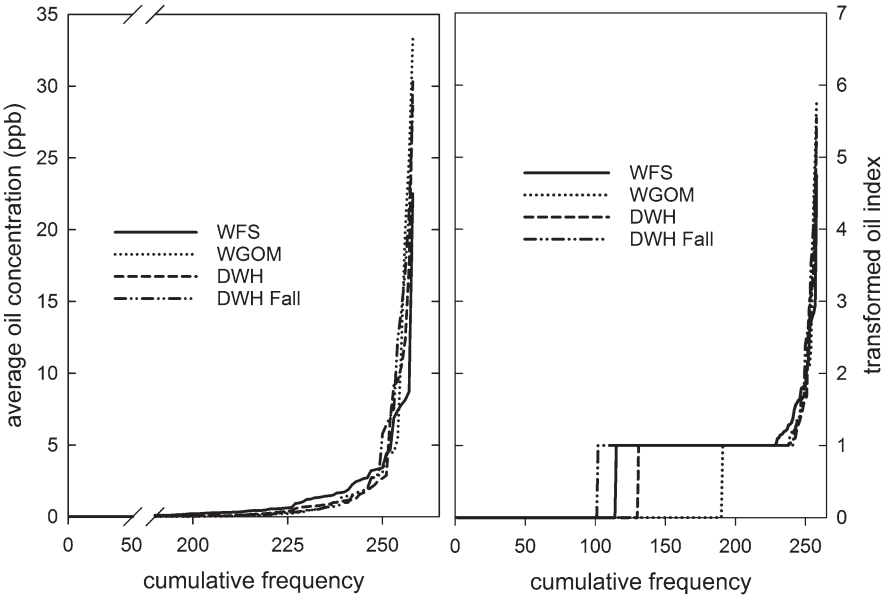

Fig. 26.3 Sorted distribution by 1° grid rectangle of the average oil concentration (OC) distribution for all four scenarios (left) and transformed oil concentration index (OI) for all scenarios (right). The OI is a square root transformation of the OC with values between 0 and 1 rounded to 1

The overall sensitivity for each oil well blowout was then calculated as:

$$ES_k = \sum_{i=1}^{n} (CS_{ij} * (OI_{ijk})) \tag{26.9}$$

where ES_k is the overall environmental sensitivity of oil well blowout k, CS_{ij} is the cumulative sensitivity at point (i j), OI_{ij} is the oil index score at point (i, j) for spill k, and n is the number of 1° × 1° grid rectangles.

26.8 Results

Overall sensitivity was calculated for each oil scenario and attribute pair for a total of 24 measures (Fig. 26.4; Table 26.4). Coastal species' revenue had relatively similar sensitivity scores for all scenarios except for the Western GoM blowout where the corresponding score was lower than for any other oil scenario – attribute pair.

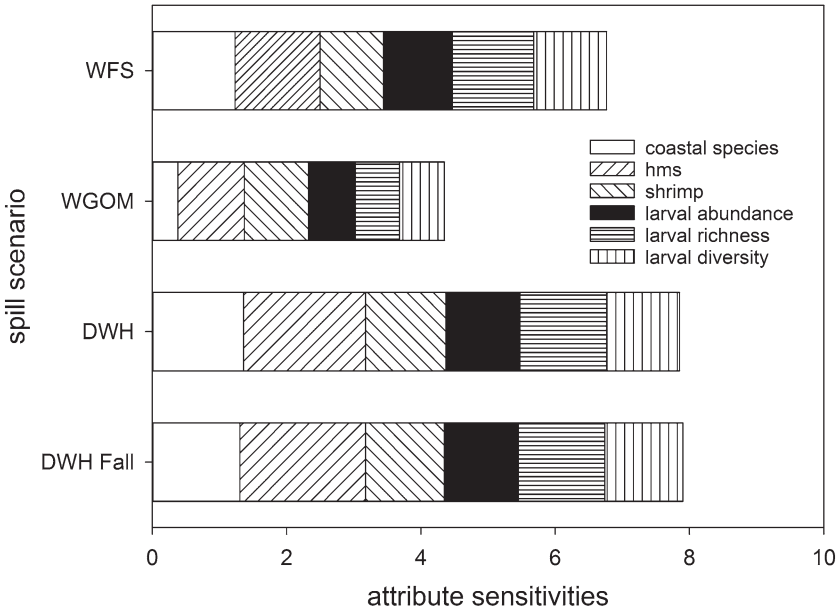

Fig. 26.4 Summed relative attribute sensitivities for ecological (larval abundance, richness, diversity) and economic impacts (on fisheries for coastal species, highly migratory species, and shrimps) of four simulated deepwater oil blowouts in the Gulf of Mexico. Weighting is equal for all attributes

Both of the *Deepwater Horizon* simulations were especially problematic for highly migratory species as most of the reported fishing activity took place within this region. Shrimp fisheries were impacted almost evenly for all four scenarios. For all six attributes, the Western GoM spill had the lowest overall sensitivity score. DWH and DWH Sept had similar impact scores for all scenarios. For this study, the larval sensitivity and economic resource attributes were aggregated over all seasons. However, larvae demonstrate significant seasonality with some species occurring during the spring (swordfish, bluefin tuna, round herring), summer (cobia, Spanish mackerel, king mackerel, spotted sea trout, little tunny), or fall (scaled herring, vermilion snapper, red drum, Chancellor 2015, Table 26.3). In real-world spills such as the DWH oil well blowout, season will thus be a major factor in determining fish species sensitivity and impacts.

The summation of the sensitivity indices for all six attributes (ES_k) was initially calculated with equally weighting coefficients for each term: $k = 1$ (Table 26.4). Under this first weighting scheme model, DWH and DWH Sept had the highest overall sensitivity followed by the WFS and then Western GoM.

The impacts of differential weighting of the relative importance of ecological and economic measures were simulated by varying the coefficients, k_i, for each of the six attributes. For the second weighting scheme model, k for larval measures

Table 26.3 Proportions of total catch for selected species from SEAMAP larval surveys, by month (Chancellor 2015)

	Month											
Species	1	2	3	4	5	6	7	8	9	10	11	12
Swordfish	0.31	0.00	0.00	0.33	0.15	0.11	0.00	0.04	0.05	0.00	0.00	0.00
Herring, round	0.10	0.10	0.62	0.03	0.01	0.00	0.00	0.00	0.00	0.00	0.04	0.09
Lanternfish, smallfin	0.15	0.18	0.12	0.16	0.16	0.03	0.01	0.03	0.02	0.01	0.02	0.11
Tuna, bluefin	0.00	0.00	0.00	0.22	0.78	0.00	0.00	0.00	0.00	0.00	0.00	0.00
Sea trout, white	0.01	0.09	0.43	0.02	0.00	0.04	0.24	0.03	0.07	0.05	0.02	0.01
Lanternfish, longfin	0.09	0.11	0.11	0.18	0.23	0.03	0.01	0.05	0.02	0.02	0.03	0.12
Lanternfish, Warming's	0.07	0.08	0.08	0.24	0.24	0.04	0.01	0.04	0.03	0.04	0.05	0.09
Tuna, skipjack	0.00	0.02	0.04	0.22	0.35	0.10	0.01	0.14	0.08	0.03	0.01	0.00
Wahoo	0.00	0.00	0.00	0.18	0.28	0.09	0.10	0.22	0.13	0.00	0.00	0.00
Cobia	0.00	0.00	0.00	0.28	0.09	0.16	0.26	0.07	0.06	0.00	0.00	0.08
Sea trout, spotted	0.00	0.00	0.03	0.00	0.01	0.11	0.65	0.07	0.09	0.04	0.00	0.00
Tuna, little (tunny)	0.00	0.00	0.00	0.06	0.03	0.17	0.31	0.31	0.11	0.00	0.00	0.00
Mackerel, Spanish	0.00	0.00	0.00	0.00	0.01	0.29	0.38	0.17	0.15	0.00	0.00	0.00
Snapper, red	0.00	0.00	0.00	0.00	0.01	0.27	0.35	0.15	0.16	0.05	0.01	0.00
Mackerel, king	0.00	0.00	0.00	0.00	0.01	0.22	0.18	0.28	0.25	0.05	0.00	0.00
Sardine, Spanish	0.00	0.02	0.00	0.11	0.04	0.14	0.06	0.14	0.27	0.22	0.01	0.00
Herring, Atlantic thread	0.02	0.00	0.01	0.00	0.00	0.11	0.36	0.23	0.17	0.01	0.05	0.03
Herring, scaled	0.00	0.00	0.00	0.00	0.01	0.40	0.16	0.15	0.04	0.00	0.23	0.00
Snapper, vermilion	0.00	0.00	0.00	0.02	0.02	0.10	0.13	0.21	0.31	0.17	0.03	0.00
Drum, red	0.00	0.00	0.00	0.00	0.00	0.00	0.01	0.01	0.44	0.52	0.00	0.00

Catches from all samples were aggregated by month and divided by the total number of samples collected during that month. Proportions were calculated as the proportion of standardized abundance each month aggregating to the total. Shading indicates months of higher proportion of total spawning activity

was increased by 30% (×1.3), and *k* for the economic measures was reduced by 30% (×0.7). This change maintained the same relative ranking of overall sensitivity as the equally weighted method. For the third weighting scheme model, *k* for the larval measures was reduced by 30% (0.7), and *k* for the economic measures was increased by 30% (1.3). This change also maintained the relative rankings of the spills.

Table 26.4 Relative cumulative sensitivity of each of four deepwater oil spill scenarios with respect to three economic environmental sensitivity indices and three environmental sensitivity indices

ESI attribute	Spill scenario			
	DWH Sept	DWH	WGoM	WFS
Coastal species revenue	1.31	1.36	0.38	1.23
HMS revenue	1.87	1.82	0.99	1.27
Shrimp revenue	1.17	1.20	0.95	0.95
Larval abundance	0.96	0.98	0.57	0.94
Larval species richness	1.29	1.29	0.66	1.21
Larval Shannon diversity	1.01	1.00	0.56	1.00
Weighting Scheme				
Larval k = 1, economic k = 1	1.27	1.27	0.68	1.10
Larval k = 1.3, economic k = 0.7	1.21	1.22	0.66	1.08
Larval k = 0.7, economic k = 1.3	1.28	1.28	0.77	1.07

The bottom three rows test the overall result as functions of different weighting coefficients (*k*) for economic and environmental attributes. Relative impact by scenario for each individual attribute (top six rows) and combined for all six attributes for three *k* weighting schemes (bottom three rows)

26.9 Discussion

Quantitative approaches to ESI formulation using multi-attribute utility models and their application to simulated oil spills demonstrate the potential to (1) quantify sensitivities of spatially explicit offshore areas to local oil spills across many metrics without having to subjectively concatenate maps and to (2) compare potential sensitivities of different oil spill scenarios ranging widely over the GoM. The latter is particularly important as a potential tool for identifying specific locations (at varying spatial scales) that may be too environmentally or economically sensitive to allow oil development. In this sense, such a planning tool could conceivably be brought into the oil facility siting process.

While we demonstrate the MAUM method for assessing oil spill sensitivity across six metrics, there are many more data sets that can be incorporated into such an analysis. These include abundance and distribution data for marine mammals and sea turtles (Frasier 2020), seabirds, deepwater corals, noncommercial fishes (including mesopelagic communities; Sutton et al. 2020), and areas where primary production is high. Potential additional economic attributes include the spatial distributions of recreational fishing, commercial and cruise ship activity, locations of renewable energy infrastructure, and military preparedness, as well as other human-centric uses and invaluable archeological sites including shipwrecks in the Gulf (e.g., lost ships of Cortez).

The weighting coefficients in this chapter are varied to show the sensitivity of the overall estimated impact of an oil well blowout to the individual attributes. In future

applications, these coefficients can be varied to (1) add or subtract weight from an attribute due to oil well blow out characteristics (e.g., increasing the weight of k for spills where dispersants are used to account for organisms that are potentially harmed by dispersants) or (2) to add or subtract weight from an attribute where one is deemed "more important" than another (e.g., prioritizing endangered organisms, fisheries with higher revenue values, etc.).

The ESIs described in this chapter also have applications for the development of quantitative models for optimizing the conflicting objectives of maximizing energy production while minimizing potential impacts on species and other economic uses. There is a rich body of literature using linear programming models, GAMS, and other optimization tools for such analyses (e.g., Sanchirico and Wilen 2005; Kobayashi and Polovina 2005). Drilling plans in the GoM have multiple potentially conflicting objectives, including:

1. Maximizing oil production P_j
2. Minimizing the costs of exploration (costs associated with new wells) $k_1 C_j$
3. Minimizing the biological resources at risk in the case of an oil well blowout ES_j
4. Minimizing impacts on human use activities at risk in the case of an oil well blowout HU_j

Murawski et al. (2001) illustrated a similar optimization methodology for minimizing impacts on spatially disaggregated fishery catches while also maximizing the protection of species rarity (e.g., determining the boundaries of marine protected areas). A similar optimization approach could be applied to oil production planning for offshore areas. For example, one might consider the objective function:

$$\max a1 * \sum_j D_j * \left(P_j - \left(k_1 C_j\right)\right) + a2 \sum_j \left(D_j - 1\right) * \mathrm{ES}_j + a3 \sum_j \left(D_j - 1\right) * \mathrm{HU}_j \qquad (26.10)$$

where D_j is an element of the design vector with values of 0 and 1 indicating if site j is included in the selected drilling plan, P_j is the potential(or actual) oil/gas production potential at spatial block j, C_j is a variable with values of 0 and 1 indicating if a site is currently being drilled, k_1 is the cost of exploration and drilling at a new site, ES_j is the sum of the biological resource ESI values, HU_j is the sum of the human use ESIs at site j, and a1, a2, and a3 are weighted coefficients. Oil production for unexplored blocks, although uncertain, can be quantified for the purposes of such modeling in a number of potential ways: (1) using the average water depth of the block with the regression model fitted to existing block productivity to forecast production potential, (2) using geostatistical methods and existing well production data to forecast production of unexplored blocks, (3) using exploration data (e.g., seismic) compiled by the oil companies to predict resource potential (Murawski et al. 2020, Fig. 2.6), or (4) compiling spatial data from within known geological plays (BOEM 2018; Locker and Hine 2020).

The goal of such modeling is to understand the potential trade-offs of environmental protection vs. potential foregone economic opportunities or negative impacts

of various spatial regulatory schemes. Presumably, the models could be elaborated by incorporating a number of other considerations such as trans-boundary impacts (across national boundaries) as a penalty function (actions to be avoided). As well, if accident potentials vary spatially, such data could be incorporated. A key feature to be considered in such analyses is the spatial block size being analyzed. In our example (Figs. 26.1 and 26.2), we used a 1° × 1° block size which is a reasonable trade-off of spatial granularity for the purposes of illustration but is far larger than typical lease blocks offered in the US GoM. Certainly more precise block-by-block analyses could be undertaken, subject to the availability of the required data sets at this resolution. The other consideration in spatial scaling of such optimization methods is the likely spatial extent of deep blowouts. For spills similar in volume and distribution to DWH, about 12 1° × 1° blocks were significantly impacted, but this varied by season and spill location (Figs. 26.1 and 26.2).

While spatial optimization methods cannot be the only decision support tool for informing drilling plans, the applications are useful as input into the process of determining oil and gas development planning with a focus on protecting valuable economic and ecological resources. Using such tools can help visualize and quantify the inherent trade-offs that must be considered in balancing energy production with resource protection.

Acknowledgments This research was made possible by a grant from the Gulf of Mexico Research Initiative, CIMAGE II/III. Data for this chapter were collected under the Southeast Area Monitoring and Assessment Program (SEAMAP) or provided by National Marine Fisheries Service (NMFS). The authors would like to thank Allison Shideler for providing HMS landings data and Jo Williams and James Primrose for providing shrimp landings and revenue estimates. The scientific results and conclusions, as well as any views or opinions expressed herein, are those of the authors and do not necessarily reflect those of NOAA or the Department of Commerce.

References

Adler E, Inbar M (2007) Shoreline sensitivity to oil spills, the Mediterranean coast of Israel. Assessment analysis. Ocean Coast Manag 50:24–34

Alves TM, Kokinou E, Zodiatis G (2014) A three-step model to assess shoreline and offshore susceptibility to oil spills: the South Aegean (Crete) as an analogue for confined marine basins. Mar Pollut Bull 86:443–457

Antonio F, Mendes R, Thomaz S (2011) Identifying and modeling patterns of tetrapod vertebrate mortality rates in the Gulf of Mexico oil spill. Aquat Toxicol 105:177–179

Berenshtein I, Perlin N, Ainsworth CH, Ortega-Ortiz JG, Vaz AC, Paris CB (2020a) Comparison of the spatial extent, impacts to shorelines, and ecosystem and 4-dimensional characteristics of simulated oil spills (Chap. 20). In: Murawski SA, Ainsworth C, Gilbert S, Hollander D, Paris CB, Schlüter M, Wetzel D (eds) Scenarios and responses to future deep oil spills – fighting the next war. Springer, Cham

Berenshtein I, Perlin N, Murawski SA, Graber H, Samantha Joye S, Paris CB (2020b) Evaluating the effectiveness of fishery closures for deep oil spills using a 4-dimensional model (Chap. 23). In: Murawski SA, Ainsworth C, Gilbert S, Hollander D, Paris CB, Schlüter M, Wetzel D (eds) Scenarios and responses to future deep oil spills – fighting the next war. Springer, Cham

BOEM Offshore Statistics by Water Depth (2018) Available online: https://www.data.boem.gov/Leasing/OffshoreStatsbyWD/Default.aspx

Carls MG, Rice SD, Hose JE (1999) Sensitivity of fish embryos to weathered crude oil: Part I. Low-level exposure during incubation causes malformations, genetic damage, and mortality in larval pacific herring (*Clupea pallasii*). Environ Toxicol Chem 18:481–493

Carmichael RH, Graham WM, Aven A, Worthy G, Howden S (2012) Were multiple stressors a "perfect storm" for northern Gulf of Mexico bottlenose dolphins (*Tursiops truncatus*) in 2011? PLoS One 7:e41155

Carmona S, Gherardi D, Tessler M (2004) Environment sensitivity mapping and vulnerability modeling for oil spill response along the São Paulo State coastline. J Coast Res 39:1455–1458

Castañedo S, Pombo C, Fernandez F, Medina R, Puente A, Juanes J (2008) Oil spill vulnerability atlas for the Cantabrian Coast Bay of Biscay, Spain. Int Oil Spill Conf Proc:137–144. https://doi.org/10.7901/2169-3358-2008-1-137

Chancellor E (2015) Vulnerability of larval fish populations to oil well blowouts in the northern Gulf of Mexico. (Unpublished master's thesis), College of Marine Science, University of South Florida, Saint Petersburg, FL

Cowell RK, Mao XC, Chang J (2004) Interpolating, extrapolating, and comparing incidence-based species accumulation curves. Ecology 85:2717–2727

DOI Secretary Zinke Announces Plan for Unleashing America's Offshore Oil and Gas Potential (2018) Available online: https://www.doi.gov/pressreleases/secretary-zinke-announces-plan-unleashing-americas-offshore-oil-and-gas-potential. Accessed on Oct 2018

Energy Information Administration (EIA) (2018) Energy Information Administration Gulf of Mexico fact sheet. Available online: https://www.eia.gov/special/gulf_of_mexico/. Accessed on Oct 2018

Etnoyer PJ, Wickes LN, Silva M, Dubick JD, Balthis L, Salgado E, MacDonald IR (2016) Decline in condition of gorgonian octocorals on mesophotic reefs in the northern Gulf of Mexico: before and after the Deepwater Horizon oil spill. Coral Reefs 35:77–90

Fattal P, Maanan M, Tillier I, Rollo N, Robin M, Pottier P (2010) Coastal vulnerability to oil spill pollution: the case of Noirmoutier Island (France). J Coast Res 25(5):879–887

Feeny D, Furlong W, Torrance G, Goldsmith C, Zhu Z, DePauw S, Denton M, Boyle M (2002) Multiattribute and single-attribute utility functions for the health utilities index Mark 3 System. Med Care 40:113–128. http://www.jstor.org/stable/3767552

Frasier K (2020) Evaluating impacts of deep oil spills on oceanic marine mammals (Chap. 25). In: Murawski SA, Ainsworth C, Gilbert S, Hollander D, Paris CB, Schlüter M, Wetzel D (eds) Scenarios and responses to future deep oil spills – fighting the next war. Springer, Cham

Gotelli NJ, Cowell RK (2001) Quantifying biodiversity: procedures and pitfalls in the measurement and comparison of species richness. Ecol Lett 4:379–391

Haney JC, Geiger HJ, Short JW (2014) Bird mortality from the Deepwater Horizon oil spill. II. Carcass sampling and exposure probability in the coastal Gulf of Mexico. Mar Ecol Prog Ser 513:239–252

Hicken CE, Linbo TL, Baldwin DH, Willis ML, Myers MS, Holland L, Larsen M, Stekoll MS, Rice SD, Collier TK, Scholz NL, Incardona JP (2011) Sublethal exposure to crude oil during embryonic development alters cardiac morphology and reduces aerobic capacity in adult fish. Proc Natl Acad Sci U S A 108(17):7086–7090

Hill MO (1973) Diversity and evenness: a unifying notation and its consequences. Ecology 54:427–473

Huber GP (1974) Multi-attribute utility models: a review of field and field-like studies. Manag Sci 20:1393–1402

Incardona JP, Collier TK, Scholz NL (2004) Defects in cardiac function precede morphological abnormalities in fish embryos exposed to polycyclic aromatic hydrocarbons. Toxicol Appl Pharmacol 196:191–205

Incardona JP, Swarts TL, Edmunds RC, Linbo TL, Aquilina-Beck A, Sloan CA, Gardner LD, Block BA, Scholz NL (2013) Exxon Valdez to *Deepwater Horizon*: comparable toxicity of both crude oils to fish early life stages. Aquat Toxicol 142–143:303–316

Jensen JR, Ramsey EW, Holmes JM, Michel JE, Savitsky B, Davis BA (1990) Environmental sensitivity index (ESI) mapping for oil spills using remote sensing and geographic information system technology. Int J Geogr Inf Syst 4:181–201

Jensen JR, Halls JN, Michel J, Carolina S (1998) A systems approach to environmental sensitivity index (ESI) mapping for oil spill contingency planning and response. Photogramm Eng Remote Sens 64:1003–1014

Kankara RS, Arockiaraj S, Prabhu K (2016) Environmental sensitivity mapping and risk assessment for oil spill along the Chennai Coast in India. Mar Pollut Bull 106:95–103

Kassomenos PA (2004) Risk analysis for environmental hazards: the case of oil spills, in Crete. Global Nest 6:39–51

Kazanis E, Maclay D, Shepard N (2015) Estimated oil and gas reserves Gulf of Mexico OCS region December 31, 2013; Bureau of Ocean Energy Management (BOEM) report; BOEM: New Orleans, LA, USA

Knudsen RR, Druyor RD (2009) USCG Sector St Petersburg – digital area contingency plan for oil spill response. C. f. S. analysis. St Petersburg, Florida, Florida Fish and Wildlife Conservation Commission – Fish and Wildlife Research Institute

Kobayashi DR, Polovina JJ (2005) Evaluation of time-area closures to reduce incidental sea turtle take in the Hawaii-based longline fishery: Generalized Additive Model (GAM) development and retrospective examination. NOAA Technical Memorandum NMFS-PIFSC-4, 39 pp

Lan D, Liang B, Bao C, Ma M, Xu Y, Yu C (2015) Marine oil spill risk mapping for accidental pollution and its application in a coastal city. Mar Pollut Bull 96:220–225

Lee M, Jung J-Y (2015) Pollution risk assessment of oil spill accidents in Garorim Bay of Korea. Mar Pollut Bull 100:297–303

Locker S, Hine AC (2020) An overview of the geologic origins of hydrocarbons and production trends in the Gulf of Mexico (Chap. 4). In: Murawski SA, Ainsworth C, Gilbert S, Hollander D, Paris CB, Schlüter M, Wetzel D (eds) Scenarios and responses to future deep oil spills – fighting the next war. Springer, Cham

Maitieg A, Lynch K, Johnson M (2018) Coastal resources spatial planning and potential oil risk analysis: case study of Misratah's coastal resources, Libya. In: 19th International conference on geography and environmental studies. https://www.researchgate.net/publication/323445887_Coastal_Resources_Spatial_Planning_and_Potential_Oil_Risk_Analysis_Case_Study_of_Misratah%27s_Coastal_Resources_Libya

McCrea-Strub A, Kleisner K, Sumaila UR, Swartz W, Watson R, Zeller D, Pauly D (2011) Potential impact of the Deepwater Horizon oil spill on commercial fisheries in the Gulf of Mexico. Fisheries (Bethesda) 36:332–336

Murawski S, Fogarty M, Rago P, Brodziak J (2001) Quantitative methods for MPA design, with application to the NE USA. Marine protected areas: design and implementation for conservation and fisheries restoration. Woods Hole Oceanographic Institution, 27–29 August 2001

Murawski SA, Hollander DJ, Gilbert S, Gracia A (2020) Deep-water oil and gas production in the Gulf of Mexico, and related global trends (Chap. 2). In: Murawski SA, Ainsworth C, Gilbert S, Hollander D, Paris CB, Schlüter M, Wetzel D (eds) Scenarios and responses to future deep oil spills – fighting the next war. Springer, Cham

Nelson JR, Grubesic TH (2018) The implications of oil exploration off the Gulf Coast of Florida. J Mar Sci Eng 6. https://doi.org/10.3390/jmse6020030

Nelson J, Grubesic T, Sim L, Rose K, Graham J (2015) Approach for assessing coastal vulnerability to oil spills for prevention and readiness using GIS and the Blowout and Spill Occurrence Model. Ocean Coast Manag 112:1–11

Niedoroda A, Davis S, Bowen M, Nestler E, Rowe J, Balouskus R, Schroeder M, Gallaway B, Fechhelm R (2014) A method for the evaluation of the relative environmental sensitivity and marine productivity of the outer continental shelf. Prepared by URS Group, Inc., Normandeau Associates, Inc., RPS ASA, and LGL Ecological Research Associates, Inc. for

the U.S. Department of the Interior, Bureau of Ocean Energy Management. Herndon, VA OCS Study BOEM 616, 80 pp. + appendices

NOAA Office of Response and Restoration (2018) Environmental Sensitivity Index (ESI) maps https://response.restoration.noaa.gov/resources/environmental-sensitivity-index-esi-maps

Oksanen J (2018) Vegan: ecological diversity. https://CRAN.R-project.org/package=vegan

Olita A, Cucco A, Simeone S, Ribotti A, Fazioli L, Sorgente B, Sorgente R (2012) Oil spill hazard and risk assessment for the shorelines of a Mediterranean coastal archipelago. Ocean Coast Manag 57:44–52

Overstreet E, Liese C (2018) Economics of the Gulf of Mexico reef fish fishery-2015. NOAA technical memorandum NMFS-SEFSC-724. 78 p.

Paris CB, Hénaff ML, Aman ZM, Subramaniam A, Helgers J, Wang DP, Kourafalou VH, Srinivasan A (2012) Evolution of the Macondo well blowout: simulating the effects of the circulation and synthetic dispersants on the subsea oil transport. Environ Sci Technol 46:13293–13302

Paris CB, Helgers J, Van Sebille E, Srinivasan A (2013) Connectivity Modeling System (CMS): a multi-scale tool for the tracking of biotic and abiotic variability in the ocean. Environ Model Softw 42:47–54

Perlin N, Berenshtein I, Vaz A, Faillettaz R, Schwing P, Romero I, Schlüter M, Liese A, Viamonte J, Noirungsee N, Gros J, Paris C (2020) Far-field modeling of deep-sea blowout: sensitivity studies of initial conditions, biodegradation, sedimentation and SSDI on surface slicks and oil plume concentrations. In: Murawski SA, Ainsworth C, Gilbert S, Hollander D, Paris CB, Schlüter M, Wetzel D (eds) Deep oil spills: facts, fate and effects. Springer, Cham

Petersen J, Michel J, Zengel S, White M, Lord C, Plank C (2002) Environmental sensitivity index guidelines. Version 3.0. NOAA Technical Memorandum NOS OR&R, 11

Pulster EL, Gracia A, Snyder SM, Romero IC, Carr B, Toro-Farmer G, Murawski SA (2020) Polycyclic aromatic hydrocarbon baselines in Gulf of Mexico fishes (Chap. 15). In: Murawski SA, Ainsworth C, Gilbert S, Hollander D, Paris CB, Schlüter M, Wetzel D (eds) Scenarios and responses to future deep oil spills – fighting the next war. Springer, Cham

Romero AF, Abessa D, Fontes R, Silva G (2013) Integrated assessment for establishing an oil environmental vulnerability map: case study for the Santos Basin region, Brazil. Mar Pollut Bull 74:156–164

Sanchirico JN, Wilen JE (2005) Optimal spatial management of renewable resources: matching policy scope to ecosystem scale. J Environ Econ Manag 50:123–146

Santos CF, Carvalho R, Andrade F (2013) Quantitative assessment of the differential coastal vulnerability associated to oil spills. J Coast Conserv 17:25–36

Schwacke LH, Smith CR, Townsend FI, Wells RS, Hart LB, Balmer BC, Collier TK, De Guise S, Fry MM, Guillette LJ Jr (2013) Health of common bottlenose dolphins (*Tursiops truncatus*) in Barataria Bay, Louisiana, following the *Deepwater Horizon* oil spill. Environ Sci Technol 48:93–103

Sissine F (2007) Energy Independence and security act of 2007: a summary of major provisions. Washington, DC, Congressional Research Service (Library of Congress)

Smith EP, van Belle G (1984) Nonparametric estimation of species richness. Biometrics 40:119–129

Sutton T, Cook A, Moore J, Frank T, Judkins H, Vecchione M, Nizinski M, Youngbluth M. (2017) Inventory of Gulf oceanic fauna data including species, weight, and measurements. Meg Skansi cruises from Jan. 25–Sept. 30, 2011 in the northern Gulf of Mexico. [data set]. Gulf of Mexico Research Initiative Information and Data Cooperative (GRIIDC), Harte Research Institute, Texas A&M University – Corpus Christi. https://doi.org/10.7266/N7VX0DK2

Sutton T, Frank T, Judkins H, Romero IC (2020) As Gulf oil extraction goes deeper, who is at risk? Community structure, distribution, and connectivity of the deep-pelagic fauna (Chap. 24). In: Murawski SA, Ainsworth C, Gilbert S, Hollander D, Paris CB, Schlüter M, Wetzel D (eds) Scenarios and responses to future deep oil spills – fighting the next war. Springer, Cham

Szlafsztein C, Sterr H (2007) A GIS-based vulnerability assessment of coastal natural hazards, state of Brazil. J Coast Conserv 11:53e66

Tran T, Yazdanparast A, Suess EA (2014) Effect of oil spill on birds: a graphical assay of the *Deepwater Horizon* oil spill's impact on birds. Comput Stat 29:133–140. https://link.springer.com/content/pdf/10.1007%2Fs00180-013-0472-z.pdf

U.S. Bureau of Ocean Energy Management (BOEM) (2018) 2019–2024 National Outer Continental Shelf Oil and Gas Leasing Draft Proposed Program. Available at: https://www.boem.gov/NP-Draft-Proposed-Program-2019-2024, 380 pp

Part V
Preparing for and Responding to the Next Deepwater Spill

Photo Credit: C-IMAGE Consortium

Chapter 27
Preparing for the Inevitable: Ecological and Indigenous Community Impacts of Oil Spill-Related Mortality in the United States' Arctic Marine Ecosystem

Paul M. Suprenand, Carie Hoover, Cameron H. Ainsworth, Lindsey N. Dornberger, and Chris J. Johnson

Abstract While hydrocarbon exploration and extraction in the Arctic ebb and flow, reduced sea ice has opened new travel routes across the Arctic. The opening of the Northwest Passage has allowed larger ships (including oil tankers) and higher traffic into remote regions. More ice loss is expected in the future. With this comes the potential for hydrocarbon spills. To quantify the ecosystem impacts of a spill in the Alaska North Slope region, an Ecospace model using the Ecopath with Ecosim software was developed. We highlight the impacts of four potential hydrocarbon contamination scenarios: a subsurface crude oil pipeline release, a surface platform oil spill, a surface cruise ship diesel spill, and a surface tanker oil spill. Hydrocarbon contamination was modeled using SIMAP (Spill Impact Model Analysis Package), which was developed from the oil fate sub-model in the Natural Resource Damage Assessment Model for the US Department of the Interior and under the Comprehensive Environmental Response, Compensation and Liability Act of 1980 (CERCLA). Spatial-temporal SIMAP results were coupled to the Ecospace model. We show that in all four hydrocarbon contamination scenarios, there are spatial changes in harvested species resulting in long-term declines in harvest levels for the

P. M. Suprenand (✉)
Mote Marine Laboratory, Sarasota, FL, USA

University of Northern British Columbia, Prince George, BC, Canada
e-mail: psuprenand@saintstephens.org

C. Hoover
Centre for Earth Observation Science, University of Manitoba, Winnipeg, MB, Canada
e-mail: carie@cariehoover.com

C. H. Ainsworth · L. N. Dornberger
University of South, College of Marine Science, St. Petersburg, FL, USA
e-mail: ainsworth@usf.edu

C. J. Johnson
University of Northern British Columbia, Prince George, BC, Canada
e-mail: chris.johnson@unbc.ca

S. A. Murawski et al. (eds.), *Scenarios and Responses to Future Deep Oil Spills*,
https://doi.org/10.1007/978-3-030-12963-7_27

communities within the model area (Nuiqsut, Kaktovik, and Barrow Alaska), depending on the severity of the scenario. Responses to hydrocarbon events are likely to be slow in the Arctic, limited by the ice-free season. We highlight this area for scenario testing as ecological impacts are also an issue of food security to the local communities and human health issue.

Keywords Oil spill · Alaska · Arctic · Indigenous · First nations · Beaufort sea · Inuit

27.1 Introduction

Hydrocarbon development has and continues to remain a polarizing issue in Arctic regions. Despite contamination from drilling and potential spills, it offers economic benefits to isolated communities. Hydrocarbon contaminants impact marine animal growth, reproductive success, respiration rates, feeding rates, ability to avoid predation, blood chemistry, acclimatization, and health (Englehardt et al. 1977; Babcock 1985; O'Clair and Rice 1985; AMAP 2010; McIntosh et al. 2010). Hydrocarbon exposure may also result in animal death. Hydrocarbons include oil and diesel fuel, as well as their chemical constituents, polycyclic aromatic hydrocarbons (PAHs). The PAHs are the soluble components of weathered oil or diesel that include a suite of toxins including benzene and naphthalene (Laender et al. 2011; Collier et al. 2013). Hydrocarbon exposure pathways include inhalation, ingestion, and absorption (NRC 2003). In general, hydrocarbon contamination impacts may be more severe to Arctic animals than animals acclimatized to warm climates (Korn et al. 1979; Yunker and Macdonald 1995), and PAHs may be more abundant in high latitudes (Maher 1992; Perkins et al. 2005; Rice et al. 2013).

In studies testing the toxicity of hydrocarbons in relation to temperature, species-specific responses vary (AMAP 2010). In cold-water environments, marine phytoplankton can have a low tolerance to hydrocarbon exposure (Østgaard et al. 1984). Hydrocarbons are believed to limit light transmission and photosynthesis (González et al. 2009; AMAP 2010; Brussaard et al. 2015) and change phytoplankton community assemblages (González et al. 2013). Lipophilic compounds may accumulate in and damage cellular membranes (Sikkema et al. 1995). Impacts such as these have also been observed in benthic plants (e.g., macroalgae;(Stepaniyan 2008)). Ultraviolet B (UVB) may enhance hydrocarbon toxicity (Almeda et al. 2016). Marine zooplankton mortality generally increases with increasing hydrocarbon concentrations, PAH-associated heavy metals may bioaccumulate, and egg production or hatching rates are reduced (AMAP 2010; Almeda et al. 2013, 2014). Benthic invertebrates, from bivalves to echinoderms, demonstrate similar impacts when exposed to hydrocarbons (Stickle et al. 1984, 1985; Mageau et al. 1987; Karinen et al. 1990; Geraudie et al. 2014; Dornberger et al. 2016). Fish, having been more extensively studied, show hydrocarbon toxicity impacts across all life stages. Fish exposed to hydrocarbons may experience inhibited spawning, altered gonadal

development, and growth, as well as heart arrhythmia and increases in toxicopathic liver lesions (Heintz et al. 2000; Incardona et al. 2009; Collier et al. 2014). Although less work has been done to understand the impacts of hydrocarbons on marine mammals and birds, studies indicate effects ranging from the loss in their ability to insulate themselves from the cold climate to death via ingested toxins (Englehardt et al. 1977; Øritsland et al. 1981; Stehn and Platte 2000).

In the coming decades, oil production, oceanic shipping, and ecotourism are predicted to increase (BREA 2013; ANDR 2015; Dennis and Mooney 2016). An increase in these types of activities also increases the potential for hydrocarbon contamination in the Beaufort Sea (BREA 2013). From 1996 to 2008, the US Department of Environmental Conservation reports thousands of hydrocarbon spills, equating to 2.7 million gallons of hazardous/toxic substances and 396,000 gallons of crude oil being released from the North Slope oil fields alone, with the frequency of spills increasing (NAEC 2015). Of the thousands of oil spills, many hundreds took place in the Beaufort Sea marine ecosystem (Robertson et al. 2013). On the Canadian side of the Beaufort Sea, hundreds of hydrocarbon reserves have been identified (Osadetz et al. 2005), and drilling programs have been developed (IORVL 2012) or are currently underway (BREA 2013). Programs that cross both the US and Canadian areas of the Beaufort Sea include the Izok Corridor Project (http://www.mmg.com/en/Our-Operations/Development-projects/Izok-Corridor.aspx), which plans to use large shipping vessels to transport materials, as well as the emergence of tourism operators that use large cruise ships (i.e., the Crystal Serenity) to transport passengers. In both cases, these marine vessels store tens of thousands of barrel fuel. The danger of a spill from a vessel was highlighted by the M/V Selendang Ayu, which experienced engine failure, ran aground, broke apart, and spilled over a million liters of heavy bunker C fuel oil into Alaskan waters in 2004. While shipping vessels may present a low probability of producing a hydrocarbon contamination event (i.e., oil or diesel spill), cruise ships have a high probability (NRC 2014). These types of potential hydrocarbon contaminations are considered worst-case scenarios (NRC 2014).

In addition to hydrocarbon contamination events in the Beaufort Sea, the geographical and seasonal inaccessibility of the high latitudes could make hydrocarbon spill response efforts essentially ineffective. “The U.S. is not adequately prepared to respond to a large spill in broken ice conditions in the Arctic and sub-Arctic region,” stated Dr. Amy Merten, co-director of the Office of Response and Restoration’s Coastal Response Research Center (NOAA online news feature, 2017; https://oceanservice.noaa.gov/news/features/jun09/arctic.html). Although hydrocarbon contamination response research was started in the 1970s (Lewis 1976), more collaborative work has taken place in recent years (Hansen and Lewandowski 2011; Mullin 2012). Hydrocarbon contaminant response efforts may require ice breakers to reach impacted areas or under sea-ice controls to keep the spill from spreading. In worst-case scenarios (NRC 2014), toxic exposures would persist longer in Arctic ecosystems (MacGregor and McLean 1977; Venosa and Holder 2007; Baussant et al. 2009). This is due to the seasonal low temperatures and high sea-ice extent during the fall to winter transition, which could hinder

open-ocean response efforts and thereby lead to acute and chronic toxic hydrocarbon exposures to marine animals.

If hydrocarbon contamination occurs in the Beaufort Sea marine ecosystem, what are the impacts to Arctic animals and the indigenous communities that rely on them for subsistence? The Beaufort Sea marine ecosystem includes the Iñupiat subsistence use areas of northern Alaska and the Inuvialuit Settlement Region (ISR) of the Inuit in northern Canada (Canada 1984). Collectively, the Beaufort Sea is home to nine Arctic indigenous communities. The US indigenous communities live in Barrow, Nuiqsut, and Kaktovik, and the Canadian indigenous communities live in Aklavik, Inuvik, Tuktoyaktuk, Paulatuk, Ulukhaktok, and Sachs Harbour. These communities heavily rely on the harvesting (catch) of marine animals for traditional foods, which have an important cultural value, provide essential nutrition, and contribute to reoccurring food security (NDH 2013; Hoover et al. 2016, 2017). Thus, the condition of the Beaufort Sea marine ecosystem influences the health of harvested animals, thus the health of each indigenous community.

The condition of the Beaufort Sea also impacts animal distribution, therefore food availability to indigenous communities. Beluga and bowhead whales are caught throughout the Beaufort Sea marine ecosystem, although sea-ice extent influences their seasonal distributions and migrations, therefore availabilities to each indigenous community (Fraker 1980; Harwood and Smith 2002). Walrus and seals also have seasonal distributions that are influenced by sea-ice extent and migration. For example, walrus can be found around the Alaskan North Slope at certain times of the year (BOWFEST 2009), and spotted seals travel to the Beaufort Sea during the summer and fall (Porsild 1945; Shaughnessy and Fay 1977). Fish, such as salmon and Arctic char, can be anadromous, or they can be year-round ocean residents, such as Arctic and polar cods, whose life cycles are intimately tied to the seasonal sea-ice extent. Thus, annual cycles of marine-based nutrients have influenced indigenous community diets and traditions for generations (Codon et al. 1995; Berkes and Jolly 2001). For example, bowhead whale catch by indigenous communities has occurred along coastal migration pathways for thousands of years (Braham et al. 1980; Marquette and Bockstoce 1980; Stoker and Krupnik 1993).

Beaufort Sea marine animals and communities are not just influenced by seasonal environmental changes but also the growing concern of climate change. Climate change may also impact the annual cycles of food availability or access with changes in sea surface temperature or sea-ice extent. In general, the Arctic Ocean's sea-ice extent has been reduced by more than 50% since the 1970s (Manabe and Stouffer 1995; Stirling 1997, 2002; Derocher et al. 2004; Stirling and Smith 2004; NOAA 2015), and the loss of this important cryosphere habitat has affected important marine habitats and biodiversity ranging from microbes to polar bears (Horner and Murphy 1985; Francis et al. 1998; Benson and Trites 2002; Gradinger 2002; Higdon and Ferguson 2009). The loss of sea-ice is most pronounced near coastal shelves, which largely affect the sea-ice-pelagic-benthic connections and trophodynamics from the benthos to higher trophic organisms (Bradstreet and Cross 1982; Grebmeier and Barry 1991; Grebmeier et al. 1995). The coastal areas and shelves are important parts of each community's subsistence use area (Braund 2010).

With so many environmental factors impacting the Beaufort Sea marine ecosystem's food web (Suprenand and Hoover unpublished), whole-ecosystem management methods are most appropriate for providing local as well as regional insights into ecosystem functions and management approaches. In lieu of the growing potential for hydrocarbon contamination events, a proactive, whole-ecosystem management approach is vital to protect Beaufort Sea animals and indigenous communities. An ecosystem-based management approach allows for multiple indigenous communities, species, and environmental drivers to the considered simultaneously.

To provide a timely, whole-ecosystem approach to understand environmental and hydrocarbon impacts in the Beaufort Sea marine ecosystem, we developed a spatial-temporal, whole-ecosystem model from 1970 to 2014. We coupled it to four hypothetical oil spill trajectory models and employed a series of species-specific and ecotoxicological functional responses in order to develop methods of identifying impacts to subsistence-caught species and Iñupiat communities. Our model also includes the spatial-temporal integration of environmental variables and subsistence catch rates from each of the nine Beaufort Sea indigenous communities that influence local and regional trophodynamics.

The four US oil spill scenarios are (1) a nearshore pipeline spilling Alaskan North Slope (ANS) crude oil into Prudhoe Bay, (2) a nearshore pipeline spilling ANS crude from a platform, (3) a coastal cruise ship spilling diesel off of the ANS, and (4) a shipping tanker spill of medium crude oil near the US-Canadian maritime border. Scenario 1 represents the failure of two segments of the North Slope pipeline system (5000 bbls per segment; (ADNR 2009)); scenario 2 a Shell Oil 2011 oil spill well blowout (Shell 2010); scenario 3 the Crystal Serenity tourist cruise ship grounded, using diesel instead of heavy fuel oil, and 100% leakage; and scenario 4 a crude oil spill from the tanker specified for the Izok Mine Corridor Project. Spill specifics per scenario also coincide with spatial-temporal probabilities of the hydrocarbon contamination, as the oil dispersion depends on environmental factors such as oceanic currents and wind. Our approach is intended to provide natural resource management strategies that are focused on animal conservation and mitigating indigenous community impacts along Alaska's North Slope Borough.

27.2 Material and Methods

27.2.1 Model Area and Indigenous Communities

The present Ecopath with Ecosim (EwE) and Ecospace models consider the entire Beaufort Sea marine ecosystem area ranging from 67.5 to 75° N and −112.5 to −158° W or approximately 476,000 km^{-2} that include estuarine, coastal, and oceanic habitats ranging from 0 to 3000 m of water depth. The Beaufort Sea marine ecosystem also encompasses Iñupiat subsistence use areas of northern Alaska (United States), the Inuvialuit Settlement Region (ISR) of the Inuit in northern

Canada (Canada 1984), and the southern Beaufort Sea (SB) management unit for polar bears established by the International Union for the Conservation of Nature and Natural Resources (IUCN) Polar Bear Specialist Group (IUCN 2010). The model area represents a little over three percent of the Arctic Ocean's area, yet it is an important habitat for migratory bowhead and beluga whales (Fraker 1980; Harwood et al. 2002; DFO 2013), a distinct population of polar bears (Amstrup et al. 2007), and nine indigenous (Iñupiat and Inuvialuit) communities that rely on subsistence catch of marine animals in coastal waters ranging from Alaska to the Northwest Territories. For the present study, the spatial extent of the subsistence use areas for Barrow, Nuiqsut, and Kaktovik are determined by the combined subsistence catch effort maps reported in Braund (1993, 2010).

27.2.2 Ecopath with Ecosim and Ecospace Models

Our Ecopath model considers 36 functional groups, which includes single species and aggregated groups of species. These functional groups range from top predators (marine mammals) to primary producers and detritus, and implicitly cover all species within the food web. There are eight marine mammal groups, one bird, nine fish groups, six benthic, six zooplankton, and six producer/ detritus groups. These are referred to as the functional groups of: (1) polar bears, (2) beluga whales, (3) gray whales, (4) bowhead whales, (5) walrus, (6) ringed seals, (7) bearded seals, (8) spotted seals, (9) birds, (10) char and Dolly Varden, (11) ciscoes and whitefish, (12) salmonids, (13) herring and smelt, (14) Arctic and polar cods, (15) capelin, (16) flounder and benthic cods, (17) small benthic marine fish, (18) other fish, (19) arthropods, (20) bivalves, (21) echinoderms, (22) mollusks, (23) worms, (24) other benthos, (25) jellies, (26) macro-zooplankton, (27) medium copepods, (28) large copepods, (29) other meso-zooplankton, (30) micro-zooplankton, (31) producers >5 μm, (32) producer <5 μm, (33) ice algae, (34) benthic plants, (35) pelagic detritus, and (36) benthic detritus.

In general, an Ecopath model represents an instantaneous "snap-shot" of material fluxes in the ecosystem according to the constraints of mass balance and the conservation of energy (Christensen and Walters 2004). The Ecopath portion of the Beaufort Sea model required biomass (tonnes (t)· km^{-2}) for each functional group, as well as their respective ratios of production per unit biomass (production ratio, yr^{-1}) and consumption per unit biomass (consumption ratio, yr^{-1}) according to Hoover et al. (2016), and a life table based on natural mortality (Barlow and Boveng 1991). For this Beaufort Sea model, biomass is calculated using information provided from stock assessments, fishery independent monitoring samples, subsistence catch reports, and other published literatures. Production of a functional group is determined for all components of the food web and linked through diet proportions (Eq. 27.1), where the production P of the functional group *i* is represented as:

$$Pi = \sum B_j * \mathrm{M2}_{ij} + Y_i + E_i + \mathrm{BA}_i + P_i * \left(1 - \mathrm{EE}_i\right) \tag{27.1}$$

Pi was dependent upon the biomass B_j of each predator group *j*, with predation mortality on group *i* from group *j* as $M2_{ij}$. Here Y_i represents the subsistence community catch, the net migration rate E_i is the emigration-immigration, biomass accumulation is BA_i, and the ecotrophic efficiency EE_i represents the proportion of production accounted for within the system (consumed by predators, exported from the system, fishing or migration) (Christensen et al. 2005).

The Ecospace model map is comprised of a grid of pixels, or cells, and each cell represents an individual Ecosim simulation and habitat type. All functional groups in the model are assigned a set of habitat preferences according to functional group-specific depth ranges. Each map cell, with the exception of land cells, thus predicts biomass (population) densities of multiple species and age classes, predator-prey interactions, and fishing mortalities based on trophodynamics, which affects adjacent cells and spatial distributions according to Eq. 27.2. Eight habitat types are created to describe the depth ranges that are 0–10 m, 10–20 m, 20–50 m, 50–100 m, 100–200 m, 200–300 m, 300–1000 m, and >1000 m. Depth ranges are assigned to each Ecospace pixel using Grid Extract from the National Centers for Environmental Information, National Oceanic and Atmospheric Administration (http://maps.ngdc.noaa.gov/viewers/wcs-client/) at the 0.1 by 0.1 decimal degree resolution. This is the resolution of the Ecospace model and all additional map layers (discussed below) that impact functional group foraging arenas:

$$\frac{dB_{i,x,y}}{dt} = \mathrm{GE}_i \sum_{\text{prey}} Q\left(B_{i,x,y}, B_{\text{prey},x,y}\right) - F_{i,x,y}B_{i,x,y} - M_{0i}B_{i,x,y} - \sum_{\text{pred}} Q\left(B_{\text{pred},x,y}B_{i,x,y}\right) + I_{i,x,y} - m_{i,x,y}B_{i,x,y} \tag{27.2}$$

where Eq. 27.2 describes the biomass movement according to the Ecosim equations, with the addition of *x* and *y* coordinates referring to individual Ecospace cells, as well as movement into and out of those cells. The first term ($\mathrm{GE}_i \sum_{\text{prey}} Q\left(B_{i,x,y}, B_{\text{prey},x,y}\right)$) describes the consumption gain, the second term ($F_{i,x,y}B_{i,x,y}$) the loss due to fishing, the third term ($M_{0i}B_{i,x,y}$) the loss due to other mortality, the fourth term ($\sum_{\text{pred}} Q\left(B_{\text{pred},x,y}B_{i,x,y}\right)$) the loss due to predation, and the fifth and sixth terms biomass gain due to immigration ($I_{i,x,y}$) and loss due to emigration ($m_{i,x,y}B_{i,x,y}$).

Additional map layers include spatial-temporal sea-ice extent, sea surface temperature, and chlorophyll *a* for every month from January 1970 to December 2014. Sea-ice extent and sea surface temperature data come from the British Atmospheric Data Centre (2010), and are converted into mean monthly Ecospace maps to match the 0.1 by 0.1 decimal degree resolution. Similarly, remotely sensed chlorophyll *a* data from 2003 to 2014 come from the Giovanni online data system (Giovanni MODIS-Aqua data) and are also converted into mean monthly Ecospace maps with the same resolution. Monthly mean maps are necessary in dynamic Ecospace simulations, because they update environmental variable values in each Ecospace cell and for each time step (month) throughout the 45-year simulation according the methods of Steenbeek (2012), as well as allows for the all environmental variables

to synergistically influence spatial-temporal functional group distributions through a series of functional responses.

A functional response describes the nature of the relationship a functional group has with an environmental variable. For example, whales migrate to the Beaufort Sea marine ecosystem when sea-ice extent decreases (Hornby et al. 2016) and sea surface temperature increases, giving them greater access to prey. In total, we created functional group responses for depth ranges, sea-ice extent, sea surface temperature, and chlorophyll *a*, which are linked to Ecospace map layers and the affected functional group(s). The validation, sensitivity analyses, and other tests of model robustness are discussed in Suprenand and Hoover (unpublished). Furthermore, annual subsistence catch rates and efforts are defined in Suprenand and Hoover (unpublished), which describes the 117 fisheries we created, one for each community and functional group they catch (e.g., Barrow polar bears, Barrow beluga whales, etc.).

27.2.3 SIMAP (Spill Impact Model Analysis Package) Modeling

We used the model algorithms in SIMAP (Spill Impact Model Analysis Package) (French 2003, 2004) that have been developed over the past three decades to simulate fate and effects of hydrocarbon contamination events under a variety of environmental conditions. SIMAP originated from the oil fates sub-model in the Natural Resource Damage Assessment Model for Coastal and Marine Environments (NRDAM/CME) for the US Department of the Interior for use in "type A" Natural Resource Damage Assessment (NRDA) regulations under the Comprehensive Environmental Response, Compensation and Liability Act of 1980 (CERCLA). The model has been validated with more than 20 case histories, including the Exxon Valdez and other large spills (French et al. 1997; French 2003, 2004; French and Rowe 2004) as well as test spills designed to verify the model (French et al. 1997).

For our purposes the SIMAP oil fate model estimates distributions and mean concentrations of hydrocarbons in the water column, surface, and sediments for each Ecospace cell over a period of 390 days. This time duration was the longest possible run time that the SIMAP model is capable of, given the specifics of our hydrocarbon contamination scenarios. The SIMAP model also included georeferenced data for wind, current, coastlines, bathymetry, shorelines, ecological habitats, temporally varying land-fast ice coverage, temperature, and salinity to drive the movement and fate of a hydrocarbon contamination in the Beaufort Sea marine ecosystem. The properties and composition of the oil and diesel are inputs based on bulk and hydrocarbon chemistry measurements of representative oil samples (Table 27.1).

After 390 days we assume that the hydrocarbons are no longer present in the ecosystem, and are removed from the Beaufort Sea marine ecosystem simulations. This conservative approach is taken so that the potential recovery time of impacted functional groups (and guilds, also discussed below) can be observed once all

Table 27.1 Oil properties of the crude oil simulated in modeling from Environment Canada (http://www.etc-cte.ec.gc.ca/databases/oilproperties/)

Oil name/source	Oil type	API gravity	Viscosity (cP at 25 °C)	Interface tension (dyne/cm)	Emulsion maximum water content (%)
Alaska North Slope crude (2002)	Medium crude	30.9	23.3 at 0 11.5 at 15	27.3	72.9
Diesel Fuel Oil (2002)	Diesel	38.8	2.760 at 25 2.760 at 15	27.5	0

hydrocarbon-related impacts are removed from trophodynamics and related effects to community catch. Furthermore, SIMAP modeling is limited to simulating hydrocarbon contamination events starting in 2008 and up to present day. As our model is calibrated and validated from 1970 to 2014, we selected a time period after 2008, at least 2 years before 2014, and during a high ice-free summer for SIMAP model simulations. Thus, all contamination scenarios start in 2011.

27.2.4 Integrating Impacts of Hydrocarbon Exposure

We use the SIMAP hydrocarbon contamination model output to provide spatial-temporal estimates of Beaufort Sea hydrocarbon concentrations (oil or diesel, g/m^2) in the water column and on the surface as well as in the sediments in four hydrocarbon contamination scenarios (HCES): (1) a nearshore pipeline spilling Alaskan North Slope (ANS) crude oil into Prudhoe Bay, (2) a nearshore pipeline spilling ANS crude from a platform, (3) a coastal cruise ship spilling diesel off of the ANS, and (4) a shipping tanker spill of medium crude oil near the US-Canadian maritime border (Table 27.2). Lastly, we integrate these concentrations into the Ecospace model using spatial-temporal concentration maps for sediment and water column concentrations for each time step that match the 0.1 by 0.1 decimal degree resolution. Concentrations for each time step are calculated based on the uptake and depuration rates of the bioavailable oil (discussed below).

27.3 Functional Responses

We develop ecotoxicological functional responses to hydrocarbon exposure from SIMAP model results for marine mammals, birds, fish, invertebrates, zooplankton, and primary producers. Eco-toxicological forcing functions represent direct mortality via toxicity and indirect mortality through mechanical impacts and sublethal effects to reduce functional group productivity. The hydrocarbon concentration is used as the independent predictor variable in a dose-response model, predicting declines in

Table 27.2 SIMAP model parameters for three-dimensional hydrocarbon contamination scenarios

	• Scenario 1	• Scenario 2	• Scenario 3	• Scenario 4
Location (lat/long)	70.33° N/−148.35° W	70.50° N/−148.35° W	71.37° N/−148.07° W	70.68° N/−143.65° W
Location	Prudhoe Bay	Alaska Shelf near Prudhoe Bay	Alaska Shelf near Point Barrow	Alaska Shelf near Kaktovik
Event description	Pipeline oil release	Platform oil spill	Cruise ship diesel spill	Tanker oil spill
Depth of release	Subsurface	Surface	Surface	Surface
Max. water depth	1 m	6.5 m	182 m	360 m
Oil name	Alaska North Slope crude	Alaska North Slope crude	Diesel	Alaska North Slope crude
Oil type	Medium crude	Medium crude	Diesel fuel	Medium crude
Spill rate	1000 bbls/day	16,000 bbls/day	Pulse	Pulse
Spill duration	10 days	30 days	7 days	7 days
Total oil spilled	10,000 bbls	480,000 bbls	13,523 bbls	533,000 bbls
Start date	Start: ice-free season August 1, 2011	Start: ice-free season September 1, 2011	Start: ice-free season August 24, 2011	Start: ice-free season October 1, 2011
Model run	390 days	390 days	390 days	390 days

functional group productivity. The dose-response model was first described by Dorberger et al. (2016) and has been used in similar ecosystem models (Ainsworth et al. 2018). Dornberger et al. (2016) suggested the most parsimonious and best fit model for hydrocarbon-related impacts to group productivity is a "hockey stick" response, which implies that there is an oil concentration threshold, below which there is no effect. Our forcing function for productivity is derived from this hockey stick response and applied to create productivity scalars between 0 and 1 (Eq. 27.3):

$$P^{*} = \begin{cases} 1 & \text{if } [\text{Oil}] < [\text{Oil}]_{\text{thresh}} \\ Z / \left(Z + m * \varphi * \log\left[\text{Oil} / \text{Oil}_{\text{thresh}} \right] \right) & \text{otherwise} \end{cases} \tag{27.3}$$

P^{*} represents productivity scalar under oil exposure, Z is baseline total mortality from Ecopath, $[\text{Oil}]_{\text{thresh}}$ *is* the threshold below which there is no mortality from oil, m is a coefficient describing the slope of the response, and φ represents sensitivity of the group to nearshore oil contamination. φ values are based initially on expert consensus from NCEAS meeting participants (Ainsworth unpublished data) and were determined based on feeding habits and/or how intimately groups associate with the substrate or intertidal area.

Nearshore oil sensitivity for forcing functions were scaled to be between 0.5 and 1.5 for the creation of a productivity scalar, so that the average sensitivity had a value of 1.0. Lower than average sensitivities (value <1.0) resulted in a smaller productivity change from oil, while higher than average sensitivities (value >1.0) increased the magnitude of the productivity decline. These sensitivities are then applied to the slope of the productivity response to estimate the total productivity scalar across oil concentrations, which are incorporated into the Ecospace model as forcing functions. Hydrocarbon contamination values are provided by SIMAP model simulations, and $\text{Oil}_{\text{thresh}} = 0.907$ ppm and $m = 0.2885$ yr^{-1} are used to be consistent with Ainsworth et al. (2018), based on an early iteration of the calculations in Dornberger et al. (2016). For primary producers, a productivity scalar of 0.5 was used for all groups whenever oil was present. This was determined based on reduced light transmissions and photosynthesis when oil is present (González et al. 2009; AMAP 2010; Brussaard et al. 2015). Monthly Ecospace map values thus represent input into the pool of bioavailable oil (oil), which depurated according to $\text{oil}_{t+1} = \text{oil}_{t} \bullet e^{-\theta}$. Monthly bioavailable oil is calculated by using the daily SIMAP hydrogen concentration per cell, uptake rates of 10%, and depuration rates of 2.4%. This is close to values subsequently calculated in exposure experiments (Miller et al. 2017).

27.3.1 Identifying Ecological Impacts to Animals and Indigenous Communities

To identify ecological impacts in each of the hydrocarbon contamination events, we examine changes in Ecospace populations, distributions, catch per community, and nutrient content per catch per community, according to functional group guilds

(groups of functional groups) found within the subsistence use areas of Barrow, Nuiqsut, and Kaktovik. The functional group guilds are (1) polar bears, (2) whales, (3) pinnipeds, (4) birds, and (5) fish. Impacts are determined by comparing hydrocarbon contamination scenarios to the reference scenario. Ecological impacts are expressed as the percent change of the total population (biomass), percent change of distributions (biomass) per Ecospace pixel, percent change in spatial-temporal, and total subsistence catch, as well as the percent change in nutrient content per community. Ecological impacts are examined as annual means occurring over the duration of the hydrocarbon contamination events (12-month period), running means from hydrocarbon contamination event to model simulation end (41-month period), as well as means in the final year of our Ecospace simulations (2014; 12-month period). Nutrient values (kilocalories (kcal g^{-1}), protein (g g^{-1}), lipid (g g^{-1}), and carbohydrate (g g^{-1})) per gram per functional group caught and used in guild-related calculations. Lastly, we calculate the change factor, referred to in this study as the multiplier of change, for each community's nutrients derived from subsistence catch.

27.4 Results

27.4.1 SIMAP (Spill Impact Model Analysis Package) Modeling

The SIMAP modeling results in each scenario reveal widespread hydrocarbon contamination along Alaska's North Slope, particularly in subsistence use areas (Fig. 27.1). Overall, SIMAP modeling shows that the highest concentrations of hydrocarbons are found in nearshore areas in each scenario, which likely impacts polar bear, pinniped, and bird populations more than other marine animals because of their associations with land-sea foraging and haul-out and nesting areas, respectively.

27.4.2 Identifying Ecological Impacts to Animals and Indigenous Communities

27.4.2.1 Biomass

Across all hydrocarbon contamination scenarios, the polar bear, pinniped, bird, and fish populations are negatively impacted, particularly in scenarios 2 and 4. In general, whale populations are mostly unaltered. However, their populations are mostly impacted in areas immediately surrounding the hydrocarbon contamination source and not throughout the marine ecosystem. Temporary impacts to beluga whales can be observed in scenarios 1 and 2. In the first year of the hydrocarbon contamination events, and looking at acute regional and negative impacts to guild populations, polar bears are mostly impacted in scenarios 2 through 4, whales in scenarios 1 and 2,

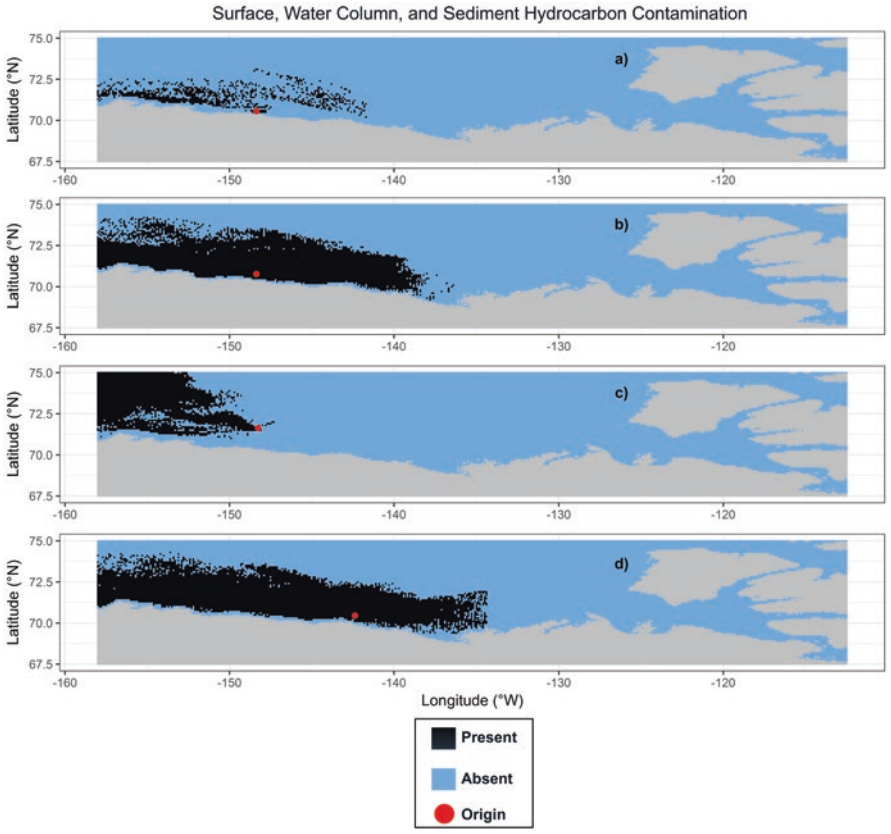

Fig. 27.1 Hydrocarbon contamination footprints for (**a**) scenario 1 pipeline leak, (**b**) scenario 2 platform leak, (**c**) scenario 3 cruise ship spill, and (**d**) scenario 4 tanker spill. Black dots represent oil/diesel, blue dots represent unaffected waters, and red dots are spill origin

pinnipeds in scenarios 2 through 4, birds in scenario 2 and 4, and fish in all scenarios. Chronic regional impacts that continue to impact population dynamics for at least 2 years following the complete removal of any hydrocarbon contamination are observed in polar bears, pinnipeds, birds, and fish in scenarios 2 and 4. In the continuum of negative impacts resulting from hydrocarbon contamination in the Beaufort Sea, we consider scenarios 1 and 3 to lightly impact guild populations, whereas scenarios 2 and 4 heavily impact guild populations. These impacts are most notable in the Nuiqsut and Kaktovik subsistence use areas of Alaska, less so near Barrow.

27.4.2.2 Subsistence Catch

In terms of subsistence use area impacts per scenario, we also find there is little effect to community subsistence catch of marine animals in scenarios 1 and 3 (less than +1% across all guilds) but significant effects to subsistence catch in scenarios

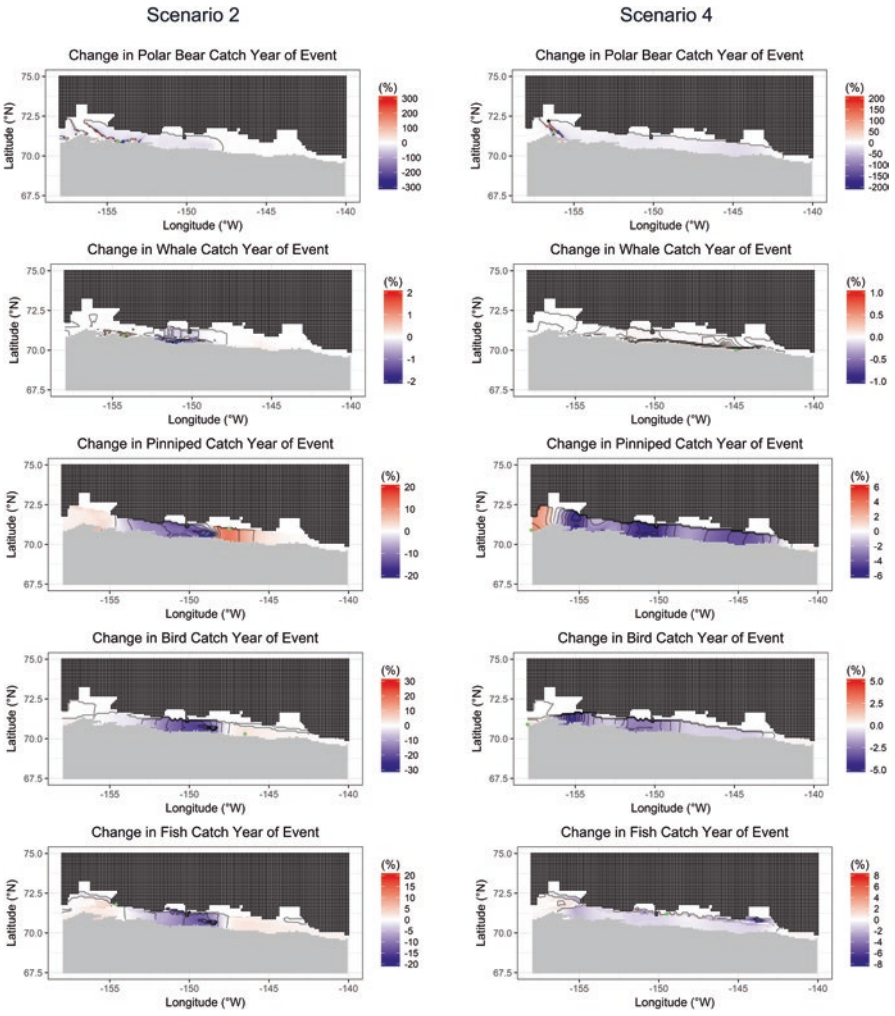

Fig. 27.2 Spatial-temporal annual catch means per guild for scenarios 2 and 4. Blue dots represent spatial catch minimum, and green dots represent spatial catch maximum. Black cross-hatching indicates open-ocean area outside of the US subsistence community use areas

2 and 4 (Fig. 27.2). Overall, effects to subsistence catch in scenarios 2 and 4 are observed immediately following hydrocarbon contamination events, and these effects continue for at least 2 years following the removal of hydrocarbon-related consequences to marine animals. As with guild population impacts, subsistence catch of whales is generally not affected in any scenario. The opposite is true for all other animal guilds.

Subsistence catch of polar bears is affected in scenarios 2 and 4 and is most markedly affected in the Nuiqsut and Kaktovik subsistence use areas. However, there are excessive increases and decreases (±300%) of Barrow's subsistence catch of

polar bears in areas surrounding Barrow Canyon, due to their ability of polar bears to move to other areas within the model. Pinniped subsistence catch effects from hydrocarbon contamination are more dynamic in scenarios 2 and 4. In scenario 2, the pinniped subsistence catch is significantly reduced in Nuiqsut and increased in limited areas for the communities of Barrow and Kaktovik as pinniped populations cluster into smaller areas (Fig. 27.2). In scenario 4, the pinniped subsistence catch is significantly reduced throughout all subsistence use areas, with a small increase in clustering west of Barrow. The spatial affects to subsistence catch of birds and fish are similar to those observed with pinnipeds.

When total catch is examined in scenarios 2 and 4, we find that each indigenous community is affected differently (example scenario 2; Fig. 27.3), and those effects alter community-specific nutrients provided by subsistence catch (example scenario 2; Fig. 27.4). For example, in scenario 2 Kaktovik catches more pinnipeds for the duration of the simulation. Concurrently, Kaktovik catches less of all other guilds until their subsistence catch of polar bears recovers 22-months after the start of the hydrocarbon contamination event (within 1% of the reference model's catch). Consequently, the community obtains smaller amounts of proteins and fewer calories. In scenario 4, Kaktovik catches fewer polar bears and pinnipeds until recovery, which occurs

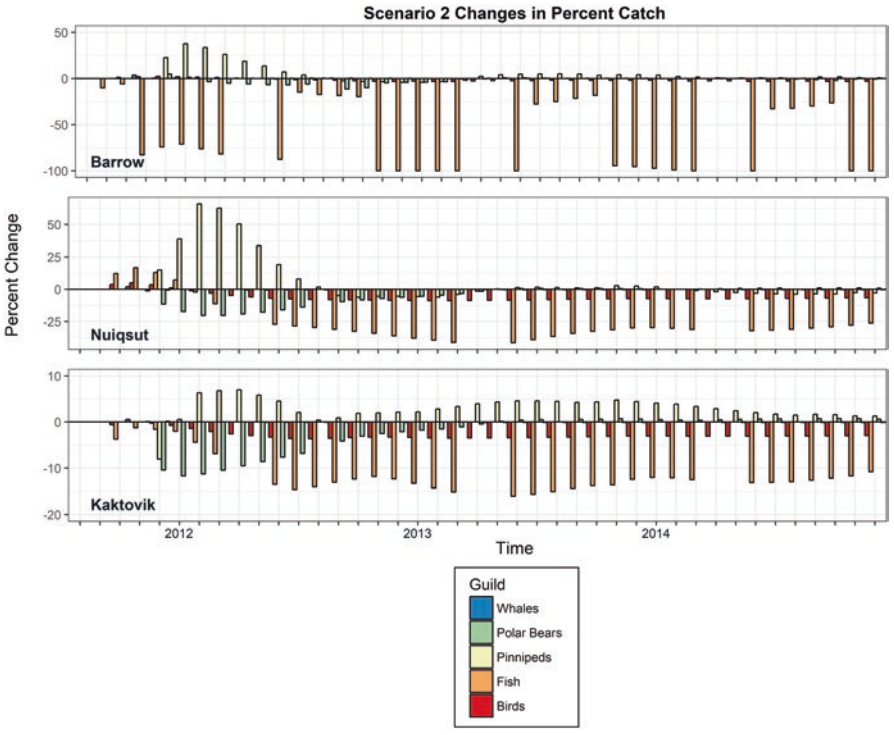

Fig. 27.3 Total community catch per guild and community, scenario 2 (hypotherical oil spill occuring September 1, 2011)

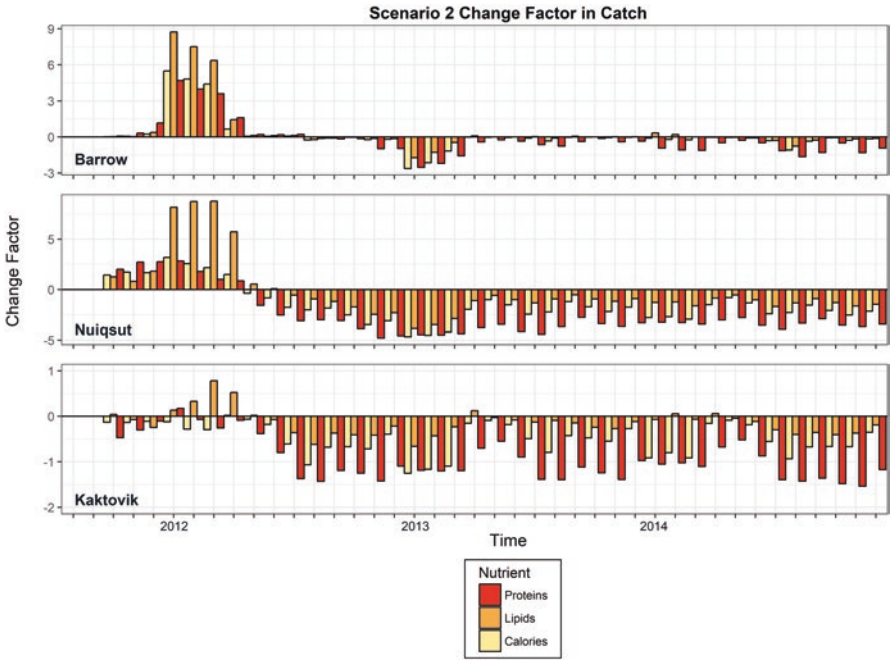

Fig. 27.4 Nutrient (proteins, lipids, and calories) change – factor per community, scenario 2 (hypotherical oil spill occuring September 1, 2011)

26-months after the start of the hydrocarbon contamination event. Katkovik's available nutrients are largely reduced throughout scenario 4. Across all scenarios, and indigenous communities, there is (1) a decrease in polar bear catch with recovery occurring approximately 2 years after the start of the hydrocarbon contamination event, (2) an overall increased reliance on pinniped catch, (3) a decrease in bird catch, and (4) a decrease in fish catch, at least until December 2014.

27.5 Discussion

In complex marine ecosystems such as the Beaufort Sea, management approaches to control anthropogenic influences may include the use of quotas on marine animal catch (Braund 1992), community conservation plans for community-driven ecological stewardship of their subsistence use areas (Aklavik 2008), as well as model-derived spill fate probabilities to decide oil and gas lease options for oceanic hydrocarbon exploration and extraction (MMS 2003). What is missing in these important management approaches are concerted efforts to understand how they are interrelated and how they might influence animal distributions. It is also necessary to understand how animal distributions are influenced by environmental and

anthropogenic drivers. Our present study is aimed at examining these synergisms. Moreover, our model is the first to provide a progressive approach aimed at revealing the complexity and response of Beaufort Sea's marine ecosystem when it is stressed by potential hydrocarbon contamination impacts that influence marine animal distributions and the Iñupiat communities that rely on the animals for traditional foods and their cultural identity. Using this multidisciplinary data integration approach, the present study is aimed at protecting an Arctic marine ecosystem already undergoing large reductions in sea-ice extent, increases hydrocarbon extraction activities, and increases in shipping and tourism. Our approach is intended to provide natural resource management strategies that are focused on animal conservation along Alaska's North Slope Borough.

The scenarios with the largest hydrocarbon contamination volumes (scenarios 2 and 4) demonstrate the most significant changes to marine animal distributions. Unfortunately, these two scenarios represent common Beaufort Sea hydrocarbon extraction and shipping activities. As a whole, shipping is projected to increase as the annual Arctic sea-ice extent continues to diminish (Comiso 2006). This increases the likelihood of a hydrocarbon contamination event. The marine animal guilds most impacted by the large-scale hydrocarbon contamination scenarios, and those also heavily relied upon by the indigenous communities, are polar bears, pinnipeds, birds, and fish. Thus, hydrocarbon contamination impacts the upper food web. For example, polar bear population decreases due to hydrocarbon contamination are further impacted by pinniped population decreases, which are in turn impacted by fish population decreases and increasing community catch of pinnipeds. And, some animal guilds, such as fish, do not recover pre-contamination distributions in the 3 years following the onset of a hydrocarbon contamination event. Likewise, the timeline for recovery of species is unknown and therefore not captured in this model timeframe. Hydrocarbon contamination impacts to marine animals vary, but the resident killer whale population (AB pod) in the Prince William Sound exposed to hydrocarbons in the 1989 Exxon Valdez oil spill lost 33% of their members, and another transient population (AT1 pod) lost 41% of their members in 1 years' time (e.g., (Fraker 2013)). Almost four decades later, neither killer whale pod has fully recovered.

As indicated in hydrocarbon contamination scenarios 2 and 4, significant changes to marine animal distributions also change the availability of food for indigenous communities. This potential indigenous community food insecurity from hydrocarbon contamination results in a net loss of animals caught within subsistence use areas. Community responses to this loss may include an increased reliance on certain food sources, such as the increased subsistence catch of pinnipeds observed in the present study. This increased reliance on pinnipeds for food further impacts the distributions of other subsistence-caught animals, such as polar bears or fish, both of which indigenous communities also rely on. This change in subsistence catch for each community ultimately leads to a sustained loss of essential proteins, lipids, and calories from traditional foods.

Changes in scenarios 2 and 4 subsistence catch reveal significant and sustained alterations to the animal-based nutrients available to all Iñupiat communities. With the concentration of animal distributions in subsistence use areas, communities

initially have an increase of available nutrients. This increase remains for approximately 6 months after the onset of a hydrocarbon contamination event, after which communities have a sustained loss in available proteins, lipids, and calories. This loss is most pronounced in the proteins provided by subsistence catch. As the subsistence-caught animals are the most important source of proteins for indigenous communities and contribute to overall food security (Wesche and Chan 2010; Huet et al. 2012), the sustained loss of protein in hydrocarbon contamination events strongly suggests food insecurity. In addition to the negative impact on food security, replacement of harvested foods with store-bought foods is expensive, has no cultural relevance, and often provides less nutrition (Pearce et al. 2010; CCA 2014). These compounding financial and cultural impacts are important to consider in the context of remote Arctic Inupiat communities.

Food security is one of the long-standing concerns for Arctic indigenous communities, which includes the concerns of availability and pollution of their traditional foods (ICC 2012). The longest running Arctic marine mammal program, the Beaufort Sea Beluga Monitoring Program in the Mackenzie River delta of the ISR, has over 40 years of science, and hunter observations for the Alaska Canada shared stock of belugas (Loseto et al.: in press). While potential impacts on beluga populations may be captured here, such extensive programs do not exist to quantify the impacts for other species because of a lack of data. Our present approach to simulating hydrocarbon contamination-related impacts to community food security is also too conservative. This is because hydrocarbon contaminations as large as scenarios 2 or 4 would likely persist in the Beaufort Sea's marine ecosystem for decades. Thus, our removal of hydrocarbons in Ecospace simulations after 1 year underestimates the chronic impacts to marine animals and indigenous community health that may occur for decades. This is because Arctic animals and people may act as sources and sinks of bioaccumulated toxins (ICC 2012). Finally, the consumption of animals harvested during a spill event can pose a threat to human health if precautions are not taken and needs to be considered.

> The UN's Office of the High Commissioner for Human Rights (OHCHR) has recognized the importance of food security for indigenous peoples – not just from a caloric perspective but also from the broader socio-cultural perspective. In its paper on The Right to Adequate Food, the significance of food and its accessibility is acknowledged as being "inextricably grounded in …socio-cultural traditions and [the] special relationship to ancestral territories and resources (Guatemala 2002). Food and its procurement and consumption are often an important part of their culture, as well as of social, economic and political organization. For Iñupiat, this linkage between food and culture is inextricable." – The Right to Adequate Food, UNHCHR, Fact Sheet No. 34, and Food security across the Arctic (UN 2010)

Although our model provides novel approaches and insights into ecosystem-wide impacts of hydrocarbon contamination, similar ecological models have been previously developed to capture changes in trophodynamics before and after the 1989 Exxon Valdez oil spill in Prince William Sound (Okey and Pauly 1998). More recently, models have been developed to look back at the impacts of the 2010 *Deepwater Horizon* oil spill in the Gulf of Mexico (Rohal et al. unpublished). What is distinctly unique in our current Ecospace model is the ability to couple SIMAP

modeling to dynamic spatial-temporal changes in all environmental variables influencing Beaufort Sea ecology for each hydrocarbon contamination scenario and time step. For example, previous Ecospace models required a static map of each environmental variable, such as sea-ice extent, which would drive trophodynamic changes in the summer months the same as in the winter months. As the Arctic marine ecosystem is characterized its changing seasonal sea-ice extent, our Ecospace model is able to capture monthly, seasonal, annual, and decadal influences of important (and rapidly changing) environmental drivers, which define suitable foraging areas (e.g., polar bears and seals), habitable areas (whales and ice algae), as well as seasonal primary productivity. In contrast, the static map approach in ecological modeling limits insights into seasonal and annual changes in Arctic ecology. Thus, we conclude that our novel multidisciplinary data integration approach combines many important elements of current Arctic ecological management approaches and provides more realistic responses of the Beaufort Sea marine ecosystem; this is already undergoing large reductions in sea-ice extent, increases hydrocarbon extraction activities, and increases in shipping and tourism.

Acknowledgments We could like to thank Mote Marine Laboratory and their scientists, Drs. Michael Crosby and Dana Wetzel for their support and guidance in this work, Fulbright Canada for awarding P. Suprenand the Fulbright Postdoctoral Scholar Award in Northern Issues (2016–2017), Ocean Conservancy for a research grant and guidance from the organization's employees, Andrew Hartig and Sarah Bobbe, the Bureau of Ocean Energy Management for sharing Beaufort Sea marine animal population data (Interagency Agreement M07PG13152, BOEMRE 2010-048, and the University of Alaska, Fairbanks agreements M10AC200004, M12AC00011), and the University of Northern British Columbia, in particular Dr. Gary Wilson, as each person and organization had a special contribution that made this research possible. C. Hoover would like to thank ArcticNet and Fisheries and Oceans Canada. C. Ainsworth and L. Dornberger were able to participate thanks to a grant from the Gulf of Mexico Research Initiative to the Center for Integrated Modeling and Analysis of Gulf Ecosystems (C-IMAGE) (GRI2011-I-072).

References

ADNR (2009) Beaufort Sea areawide oil and gas lease sales, final finding of the Director. Alaska Department of Natural Resources, Division of Oil & Gas

Ainsworth CH, Paris C, Perlin N, Dornberger LN, Patterson WF III, Chancellor E, Murawski S, Hollander D, Daly K, Romero IC, Coleman F, Perryman H (2018) Impacts of the Deepwater Horizon oil spill evaluated using an end-to-end ecosystem model. PLoS One 25:e0190840

Aklavik Co (2008) Aklavik Inuvialuit community conservation plan (Akaqvikmiut Nunamikini Nunutailivikautinich), The Community of Aklavik, the Wildlife Management Advisory Council (NWT) and the Joint Secretariat

Almeda R, Wambaugh Z, Wang Z, Hyatt C, Liu Z, Buskey EJ (2013) Interactions between zooplankton and crude oil: toxic effects and bioaccumulation of polycyclic aromatic hydrocarbons. PLoS One 8:e67212

Almeda R, Baca S, Hyatt C, Buskey EJ (2014) Ingestion and sublethal effects of physically and chemically dispersed crude oil on marine planktonic copepods. Ecotoxicology 23:988–1003

Almeda R, Harvey TE, Connelly TL, Baca S, Buskey EJ (2016) Influence of UVB radiation on the lethal and sublethal toxicity of dispersed crude oil to planktonic copepod nauplii. Chemosphere 152:446–458

AMAP (2010) Assessment (2007) Oil and gas activities in the Arctic - effects and potential effects, Depression of feeding and growth rates of the seastar *Evasterias troschelii* during long-term exposure to the water-soluble fraction of crude oil, Oslo, Norway

Amstrup SC, Marcot BG, Douglas DC (2007) Forecasting the range-wide status of polar bears at selected times in the 21st century Administrative Report. US Geological Survey, p 1–126

ANDR (2015) Chapter one: executive summary and director's final finding and signature

Babcock MM (ed) (1985) Morphology of olfactory epithelium of pink salmon, *Oncorhynchus gorbuscha*, and changes following exposure to benzene: a scanning electron microscopy study, Wiley , Chichester, England

Barlow J, Boveng P (1991) Modeling age-specific mortality for marine mammal populations. Mar Mamm Sci 7:50–65

Baussant T, Bechmann RK, Taban IC, Larsen BK, Tandberg AH, Bjornstad A, Torgrimsen S, Naevdal A, Oysaed KB, Jonsson G, Sanni S (2009) Enzymatic and cellular responses in relation to body burden of PAHs in bivalve molluscs: a case study with chronic levels of North Sea and Barents Sea dispersed oil. Mar Pollut Bull 58:1796–1807

Benson AJ, Trites AW (2002) Ecological effects of regime shifts in the Bering Sea and eastern North Pacific Ocean. Fish Fish 3:95–113

Berkes F, Jolly D (2001) Adapting to climate change: social-ecological resilience in a Canadian western Arctic community. Conserv Ecol 5:18

BOWFEST (2009) Bowhead whale feeding ecology study (BOWFEST) in the western Beaufort Sea: 2009 Annual report, National Marine Mammal Laboratory, Alaska Fisheries Science Center, National Marine Fisheries Service, National Oceanic and Atmospheric Administration

Bradstreet MSW, Cross WE (1982) Trophic relationships at high Arctic ice edges. Arctic 35:1–12

Braham HW, Fraker MA, Krogman BD (1980) Spring migration of the western Arctic population of bowhead whales. Mar Fish Rev 42:36–46

Braund SR (1992) Traditional Alaska Eskimo whaling and the bowhead quota. Arctic Res 6:37–42

Braund SR (1993) North Slope subsistence study Barrow, 1987, 1988 and 1989, U. S. Department of the Interior, Minerals Management Service

Braund SR (2010) Subsistence mapping of Nuiqsut, Kaktovik, and Barrow, United States Department of the Interior

BREA (2013) Updated oil and gas exploration & development activity forecast, Canadian Beaufort Sea 2013–2028. LTLC Consulting in association with Salmo Consulting Inc., Lin Callow

Brussaard CPD, Peperzak L, Beggah S, Wick LY, Wuerz B, Weber J, Arey JS, van der Burg B, Jonas A, Huisman J, van der Meer JR (2015) Immediate ecotoxicological effects of short-lived oil spills on marine biota. Nat Commun 7:11206

Canada I-INA (1984) The Western Arctic Claim, the inuvialuit final agreement. Indian Affairs and Northern Development:115, Ottawa

CCA (2014) Aboriginal food security in Northern Canada: an assessment on the state of knowledge. Council of Canadian Academies, Ottawa

Centre BAD (2010) HadISST 1.1 - Global sea-ice coverage and SST (1870-present)

Christensen V, Walters CJ (2004) Ecopath and Ecosim: methods, capabilities and limitations. Ecol Model 172:109–139

Christensen V, Walters C, Pauly D (2005) Ecopath with Ecosim: a user's guide Version 5. Fisheries Centre: University of British Columbia

Codon RG, Collings P, Wenzel G (1995) The best part of life: subsistence hunting, ethnicity, and economic adaptation among young adult Inuit males. Arctic 48:31–46

Collier TK, Anulacion BF, Arkoosh MR, Dietrich JP, Incardona J, Johnson LL, Ylitalo GM, Myers MS (2013) Effects of fish on polycyclic aromatic hydrocarbons (PAHs) and naphthenic acid exposures. Org Chem Toxicol Fish 3:195–255

Collier TK, Arkoosh MR, Johnson L, Yitalo GM (2014) Effects on fish of polycyclic aromatic hydrocarbons (PAHs) and naphthenic acid exposures. In: Fish physiology organic chemical toxicology of fishes, vol 33, pp 195–255

Comiso JC (2006) Abrupt decline in the Arctic winter sea ice cover. Geophys Res Lett 33:L18504

Dennis B, Mooney C (2016) A luxury cruise ship sets sail for the Arctic, thanks to climate change Washington Post
Derocher AE, Lunn NJ, Stirling I (2004) Polar bears in a warming climate. Integr Comp Biol 44:163–176
DFO (2013) Tarium Niryutait: marine protected area management plan, Fisheries and Oceans Canada & Fisheries Joint Management Committee, Winnipeg, MB, Fisheries and Oceans Canada
Dornberger L, Ainsworth C, Gosnell S, Coleman F (2016) Developing a polycyclic aromatic hydrocarbon exposure dose-response model for fish health and growth. Mar Pollut Bull 109:259–266
Englehardt FR, Geraci JR, Smith TJ (1977) Uptake and clearance of petroleum hydrocarbons in the ringed seal, *Phoca hispida*. J Fish Res Board Can 34:1143–1147
Fraker MA (1980) Status and harvest of the Mackenzie stock of white whales (*Delphinapterus leucas*). Report of the International Whaling Commission. 30:451–458
Fraker MA (2013) Killer whale (*Orcinus orca*) deaths in Prince William Sound, Alaska, 1985-1990. Human and Ecological Risk 19:28–52
Francis RC, Hare SR, Hollowed AB, Wooster WS (1998) Effects of interdecadal climate variability on the oceanic ecosystems of the NE Pacific. Fish Oceanogr 7:1–21
French DP, Rines H, Masciangioli P (1997) Validation of an orimulsion spill fates model using observations from field test spills. Proceedings of the Twentieth Arctic and Marine Oilspill Program (AMOP) Technical Seminar, Emergencies Science Division, Environment Canada, p 933–961
French DP (2003) Development and application of damage assessment modeling: example assessment for the North Cape oil spill. Mar Pollut Bull 47:341–359
French DP (2004) Oil spill impact modeling: development and validation. Environ Toxicol Chem 23:2441–2456
French DP, Rowe JJ (2004) Evaluation of bird impacts in historical oil spill cases using the SIMAP oil spill model 27th Arctic and Marine Oil Spill Program (AMOP) Technical Seminar, Emergencies Science Division, Environment Canada, Ottawa, ON, p 421–452
Geraudie P, Bakkemo R, Ravuri CS, Helgason LB, Jørgensen E, Camus L (2014) Sublethal effects of marine diesel on Arctic scallop fitness, Akvaplan-niva AS Rapport 6108, Tromsø
González J, Figueiras FG, Aranguren-Gassis M, Crespo BG, Fernández E, Morán XAG, Nieto-Cid M (2009) Effect of a simulated oil spill on natural assemblages of marine phytoplankton enclosed in microcosms. Estuar Coast Shelf Sci 83:265–276
González J, Fernandez E, Figueiras FG, Varela M (2013) Subtle effects of the water accommodated fraction of oil spills on natural phytoplankton assemblages enclosed in mesocosms. Estuar Coast Shelf Sci 124:13–23
Gradinger RR (2002) Sea ice, a unique realm for microorganisms. In: Bitten G (ed) Encyclopedia of environmental microbiology. Wiley, pp 2833–2844
Grebmeier JM, Barry JP (1991) The influence of oceanographic processes on pelagic-benthic coupling in polar regions: A benthic perspective. J Mar Syst 2:495–518
Grebmeier JM, Smith WO Jr, Conover RJ (1995) Biological processes on Arctic continental shelves: ice-ocean-biotic interactions. In: Smith WO Jr, Grebmeier JM (eds) Arctic Oceanography: marginal ice zones and continental shelves. American Geophysical Union, Washington, pp 231–261
Guatemala DoA- (2002) Indigenous peoples' global consultation on the right to food: a global consultation
Hansen K, Lewandowski M (2011) Using demonstrations to advance approaches to response for oil in ice environments Arctic Technology Conference, OTC Paper 909318
Harwood LA, Norton P, Day B, Hall PA (2002) The harvest of beluga whales in Canada's western Arctic: hunter-based monitoring of the size and composition of the catch. Arctic 55
Harwood LA, Smith TG (2002) Whales of the Inuvialuit Settlement region in Canada's Western Arctic: an overview and outlook. Arctic 55

Heintz RA, Rice SD, Wertheimer AC, Bradshaw RF, Thrower FP, Joyce JE, Short JW (2000) Delayed effects on growth and marine survival of pink salmon *Oncorhynchus gorbuscha* after exposure to crude oil during embryonic development. Mar Ecol Prog Ser 208:205–216

Higdon JW, Ferguson SH (2009) Loss of Arctic sea ice causing punctuated change in sightings of killer whales (*Orcinus orca*) over the past century. Ecol Appl 19:1365–1375

Hoover C, Ostertag S, Hornby C, Parker C, Hansen-Craik K, Loseto L, Pearce T (2016) The continued importance of hunting for future Inuit food security. Solutions 7:40–51

Hoover C, Parker C, Hornby C, Ostertag S, Hansen- Craik K, Pearce T, Loseto LL (2017) Cultural relevance in Arctic food security initiatives. In: Duncan J, Bailey M (eds) Sustainable food futures: multidisciplinary solutions, pp 17–33

Hornby CA, Hoover C, Iacozza J, Barber DG, Loseto LL (2016) Spring conditions and habitat use of beluga whales (*Delphinapterus leucas*) during arrival to the Mackenzie River Estuary. Polar Biol:1–16

Horner R, Murphy D (1985) Species composition and abundance of zooplankton in the nearshore Beaufort Sea in winter-spring. Arctic 38

Huet C, Rosol R, Egeland GM (2012) The prevalence of food insecurity is high and the diet quality poor in Inuit communities. J Nutr 142:541–547

ICC (2012) Food security across the Arctic, Canada

Incardona JP, Carls MG, Day HL, Bolton JL, Collier TK, Scholz NL (2009) Cardiac arrhythmia Is the primary response of embryonic Pacific Herring (*Clupea pallasii*) exposed to crude oil during weathering. Environ Sci Technol 43:201–207

IORVL (2012) Beaufort Sea exploration joint venture, preliminary information package, Calgary/Alberta

IUCN (2010) Polar bears. Gland, Switzerland/Cambridge, UK

Karinen JF, Rice SD, Babcock MM (1990) Reproductive success in Dungeness crab (*Cancer magister*) during long-term exposures to oil-contaminated sediments, U.S. Dep. Commer., NOAA, Arctic Environmental Assessment Center, 222 W. 8th Ave., No. 56, Anchorage, AK 99513

Korn S, Moles DA, Rice SD (1979) Effects of temperature on the median tolerance limit of pink salmon and shrimp exposed to toluene, naphthalene, and Cook Inlet crude oil. Bull Environ Contam Toxicol 21:521–525

Laender FD, Hammer J, Hendricks AJ, Soetaert K, Janssen CR (2011) Combining monitoring data and modeling identifies PAHs as emerging contaminants in the Arctic. Environ Sci Technol 45:9024–9029

Lewis EL (1976) Oil on the sea ice. Institute of Ocean Science, Patricia Bay/Victoria

MacGregor C, McLean AY (1977) Fate of crude oil spilled in a simulated Arctic environment International Oil Spill Conference. American Petroleum Institute, Washington, D.C., pp 461–463

Mageau C, Engelhardt FR, Gilfillan ES, Boehm PD (1987) Effects of short-term exposure to dispersed oil in Arctic invertebrates. Arctic 40:162–171

Maher WA (1992) Preparation and characterization of water-soluble fractions of crude and refined oils for use in toxicity studies. Bull Environ Contam Toxicol 29:268–272

Manabe S, Stouffer RJ (1995) Simulation of abrupt climate change induced by freshwater input to the North Atlantic Ocean. Nature 378:165–167

Marquette WM, Bockstoce JR (1980) Historical shore-based catch of bowhead whales in the Bering, Chukchi, and Beaufort Seas. Mar Fish Rev 42:5–19

McIntosh S, King T, Wu D, Hodson PV (2010) Toxicity of dispersed weathered crude oil to early life stages of Atlantic herring (*Clupea harengus*). Environ Toxicol Chem 29:1160–1167

Miller C, Medvecky RL, Sherwood TA, Wetzel DL (2017) Uptake, depuration and residence time of polycyclic aromatic hydrocarbons in red drum (*Sciaenops ocellatus*) exposed to south Louisiana crude oil. Poster presented at the Gulf of Mexico Oil Spill & Ecosystem Science Conference, New Orelans, LA

MMS (2003) Beaufort Sea planning area oil and gas lease sales 186, 195, 202: final environmental impact statement

Mullin J (2012) The oil and gas industry's commitment to responsible arctic operations: an innovative arctic oil spill response technology - joint industry program Proceedings Offshore Technology Conference

NAEC (2015) Oil and gas industry toxic spills 1996–2008

NDH (2013) Nutrition fact sheet series, Inuit traditional foods, Nunavut Department of Health, Munaqhiliqiyitkut, Minstère da la Santé

NOAA (2015) Happening now: Arctic sea ice sets record low, National Oceanic and Atmospheric Administration

NRC (2003) Cumulative environmental effects of oil and gas activities on Alaska's North Slope, Committee on Cumulative Environmental Effects of Oil and Gas Activities on Alaska's North Slope, Board of Environmental Studies and Toxicology, Polar Research Board, Division of Earth and Life Studies, National Research Council (NRC)

NRC (2014) Responding to oil spills in the Arctic marine environment, Committee on Responding to Oil Spills in the U.S. Arctic Marine Environment, Ocean Studies Board Division of Earth and Life Sciences, Polar Research Board Division of Earth and Life Sciences, Marine Board Transportation Research Board, National Research Council of the National Academies

O'Clair CE, Rice SD (1985) Depression of feeding and growth rates of the seastar *Evasterias troschelii* during long-term exposure to the water-soluble fraction of crude oil. Mar Biol 84:331–340

Okey TA, Pauly D (1998) Trophic mass-balance model of Alaska's Prince William Sound ecosystem for the post-spill period 1994-1996. Fish Cent Res Rep 6:1–143

Øritsland NA, Engelhardt FR, Juck FA, Hurst RA, Watts PD (1981) Effects of crude oil on polar bears. Northern Affairs Program, Department of Indian Affairs and Northern Development, Ottawa

Osadetz KG, Dixon J, Dietrich J, Snowdon LR, Dallimore SR, Majorowicz JA (2005) A review of Mackenzie Delta-Beaufort Sea Petroleum Province Conventional and non-conventional (gas hydrate) petroleum reserves and undiscovered resources: a contribution to the resource assessment of the proposed Mackenzie Delta-Beaufort Sea marine protected areas, Geological Survey of Canada, Open File 4828

Østgaard K, Hegseth EN, Jensen A (1984) Species-dependent sensitivity of marine planktonic algae to Ekofisk crude oil under different light conditions. Bot Mar 27:309–318

Pearce T, Smit B, Duerden F, Ford JD, Goose A, Kataoyak F (2010) Inuit vulnerability and adaptive capacity to climate change in Ulukhaktok, Northwest Territories, Canada. Polar Rec 46:157–177

Perkins RA, Rhoton S, Behr-Andres C (2005) Comparative marine toxicity testing: cold-water species and standard warm-water test species exposed to crude oil and dispersant. Cold Reg Sci Technol 42:226–236

Porsild AE (1945) Mammals of the Mackenzie Delta. Can Field Nat 59:4–22

Rice SD, Campbell LK, Pearson L, Higman B (2013) Oil spill occurrence rates for Alaska North Slope crude & refined oil spills, Report to Bureau of Ocean and Energy Management, OCS Study BOEM 2013–205

Robertson TL, Campbell LK, Pearson L, Higman B (2013) Oil spill occurrence rates for Alaska North Slope crude & refined oil spills

Shaughnessy PD, Fay FH (1977) A review of the taxonomy and nomenclature of North Pacific harbour seals. J Zool 182:385–419

Shell (2010) Beaufort Sea regional exploration oil discharge prevention and contingency plan. Shell Offshore Inc., Anchorage

Sikkema J, de Bont JA, Poolman B (1995) Mechanisms of membrane toxicity of hydrocarbons. Microbiol Rev 59:201–222

Steenbeek JG (2012) Bridging the gap between modelling tools using Geographic Information Systems. University of British Columbia

Stehn R, Platte R (2000) Exposure of birds to assumed oil spills at the Liberty Project, United States Fish & Wildlife Service, Migratory Bird Management, Unpublished Report Prepared for the Minerals Management Service

Stepaniyan OV (2008) Effects of crude oil on major functional characteristics of macroalgae of the Barents Sea. Ecology 34:131–134
Stickle WB, Rice SD, Moles A (1984) Bioenergetics and survival of the marine snail *Thais lima* during long-term oil exposure. Mar Biol 80:281–289
Stickle WB, Rice SD, Villars C, Metcalf W (1985) Bioenergetics and survival of the marine mussel, *Mytilus edulis* L., during long-term exposure to the water-soluble fraction of Cook Inlet crude oil. In: Vernberg F, Thurberg FP, Calabrese A, Vernberg WB (eds) Marine pollution and physiology: recent advances. University of South Carolina Press, Columbia, pp 427–446
Stirling I (1997) The importance of polynyas, ice edges, and leads to marine mammals and birds. J Mar Syst 10:9–21
Stirling I (2002) Polar bears and seals in the eastern Beaufort Sea and Amundsen Gulf: a synthesis of population trends and ecological relationships over three decades. Arctic 55
Stirling I, Smith TG (2004) Implications of warm temperatures and an unusual rain event for the survival of ringed seals on the coast of southeastern Baffin Island. Arctic 57
Stoker SW, Krupnik II (1993) Subsistence whaling. In: Bruns JJ, Montague JJ, Cowles CJ (eds) The bowhead whale. Society of Marine Mammalogy., Spec. Publ. No. 2, pp 579–629
UN (2010) The right to adequate food, UN Office of the High Commissioner for Human Rights (OHCHR)
Venosa AD, Holder EL (2007) Biodegradability of dispersed crude oil at two different temperatures. Mar Pollut Bull 54:545–553
Wesche SD, Chan HM (2010) Adapting to the impacts of climate change on food security amoung Inuit in the western Canadian Arctic. EcoHealth 7:361–373
Yunker MD, Macdonald RW (1995) Composition and origins of polycyclic aromatic hydrocarbons in the Mackenzie River and on the Beaufort Sea Shelf. Arctic 48:118–129

Chapter 28
Summary of Contemporary Research on the Use of Chemical Dispersants for Deep-Sea Oil Spills

Steven A. Murawski, Michael Schlüter, Claire B. Paris, and Zachary M. Aman

Abstract Mitigation options for deep-sea oil spills are indeed few. In the open ocean, far from land, booming, burning, and mechanical pickup of oil at the sea surface may be of limited value due to wave and wind conditions. The use of chemicals to disperse oil into smaller droplets is predicated on the assumptions that smaller droplets are more easily dissolved into surrounding waters and that smaller droplets are degraded by bacterial action more rapidly than are larger droplets. During the *Deepwater Horizon* accident, a novel use of dispersants injected directly into the subsurface source of the blowout was undertaken to treat the oil prior to surfacing. The presence of subsurface "plumes" of small droplets and dissolved oil observed during DWH raised the issue of active measures to sequester oil in the subsurface vs. allowing it to surface. Reducing the concentration of volatile organic compounds surfacing near workers was also a stated objective of subsurface dispersant injection (SSDI) application. Aquatic toxicity testing has evolved significantly from a sole focus on short-term mortality to evaluate a variety of sublethal physiological, genotoxic, and immunogenic impacts affecting animal health and fitness of exposed populations. In this chapter we consider a number of pressing – and heretofore unresolved – issues surrounding the use of dispersants as an oil spill mitigation tool. Further, we advocate continued, targeted research to help resolve ongoing controversies regarding dispersant use.

S. A. Murawski (✉)
University of South Florida, College of Marine Science, St. Petersburg, FL, USA
e-mail: smurawski@usf.edu

M. Schlüter
Hamburg University of Technology, Hamburg, Germany
e-mail: michael.schlueter@tuhh.de

C. B. Paris
University of Miami, Rosenstiel School of Marine & Atmospheric Science, Miami, FL, USA
e-mail: cparis@rsmas.miami.edu

Z. M. Aman
University of Western Australia (M050), Crawley, WA, Australia
e-mail: zachary.aman@uwa.edu.au

S. A. Murawski et al. (eds.), *Scenarios and Responses to Future Deep Oil Spills*,
https://doi.org/10.1007/978-3-030-12963-7_28

Keywords Oil dispersants · Oil droplets · Oil toxicity · Trade-off analyses · Subsurface dispersant injection (SSDI) · Deep-sea blowout

28.1 Introduction

In its 2005 report titled "Oil Spill Dispersants: Efficacy and Effects," the National Research Council (NRC 2005) noted in its preface "The use of chemical dispersants as an oil spill countermeasure in the United States has long been controversial." That report was published 5 years before the *Deepwater Horizon* (DWH) disaster, where nearly 7 million l (1.8 million gallons) of dispersants were used. About 1 million gallons were applied at the sea surface. An additional 0.8 million gallons were applied at the top of the broken blowout preventer (BOP) in a process termed subsurface dispersant injection (SSDI), despite the fact that there were no pre-spill data with which to judge the efficacy or impacts of SSDI (Coastal Response Research Center 2010). The DWH event resulted in the second-largest quantity of dispersants ever used to mitigate a marine oil spill. During the 1979–1980 Ixtoc 1 blowout in the Campeche region of Mexico, about 9000 t (~2.6 million gallons, assuming specific gravity of dispersants is ~0.9) of various dispersants were applied at the sea surface (Jernelöv and Lindén 1981; Linton and Koons 1983). Despite the experiences during, and research conducted after both Ixtoc 1 and DWH, there remain fundamental questions regarding the efficacy and effects of dispersant use. It is fair to say that of the many controversial and unresolved scientific issues regarding deep oil spills and responses to them, dispersant use may be the most controversial, and it continues to bedevil the industry, the government regulators, the environmental nongovernmental organization (e-NGO) community, and especially the public. There remains deep distrust by the public regarding the motives for justifying dispersant use, their potentially deleterious effects on the environment and people, and the decision-making process for authorizing dispersant use in the case of oil spills. While many questions about dispersant use still remain (NRC 1989, 2005; Malone et al. 2018, 2020; NASEM 2019), particularly related to dispersant use for subsurface blowouts, some of the most pressing questions include:

- How toxic are commonly used dispersants for field-relevant species?
- Are dispersants + oil more toxic than oil alone or dispersants alone?
- How effective is SSDI in creating subsurface plumes of small droplets vs. plume effects due to natural processes?
- Do dispersants increase or decrease biodegradation?
- Does SSDI reduce the presence of volatile organic compounds (VOCs) at the sea surface, thus potentially reducing inhalation exposure to humans and wildlife?
- What are the trade-offs of sequestering oil in the deep sea by the use of SSDI (subject to the efficacy question) vs. allowing more oil to surface and potentially come ashore?

In this chapter we provide a brief review of the current state of understanding regarding dispersant use and especially focus on the six questions posed above to provide context for important research recommendations moving forward (Murawski 2020).

28.2 Dispersants: A Brief Precis

Although accidental and wartime releases of oil and related hydrocarbons into the marine environment have occurred for the last hundred or more years, it was not until the *Torrey Canyon* accident in 1967 that large quantities of degreasing chemicals (Smith 1968) were used to break up crude oil to presumably allow faster oil dispersal and degradation. The first chemicals to be applied as dispersing agents were commercially available paintbrush cleaners (Linton and Koons 1983) which proved to be highly lethal to marine life (Smith 1968). In the mid-1960s to the 1970s, the second- and third-generation dispersing agents were developed that reduced the use of hydrocarbon-based solvents and thus lowered toxicity to marine life (Farn 1976). Since the 1980s, dispersants have been used in a relatively small number of marine oil spill cases (~20), generally confined to offshore or open coastal regions. Dispersants are not allowed to be used in the United States in fresh waters and, during the DWH accident, were restricted to use beyond 3 miles from the coast. During the *Exxon Valdez* oil spill, a single test application from an aircraft was made before abandoning the plan to apply dispersants in that nearshore coastal area with many sensitive ecological sites.

While there are several dozen formulations of chemical dispersants, the most common are Corexit® (several versions distinguished by numerical code), as well as Dasic Slickgone NS®, and Finasol OSR 52®, among numerous others. Their chemical formulations are protected intellectual property but may be generally characterized as strong – typically ionic – surfactants (i.e., surface-active agents). Similar to household detergents, these surfactants function to reduce the interfacial tension between oil and water thereby promoting, across a breadth of agitation conditions, the formation of smaller oil droplets. The solvents used to deliver these surfactants will readily dissolve in either the aqueous or hydrocarbon phases, making it difficult to track post-release solvent concentration. Corexit® 9500A is comprised of cetyltrimethylammonium bromide, l-α-phosphatidylcholine, sodium dodecyl sulfate, Tween 20, and dioctyl sodium sulfosuccinate, or DOSS. DOSS is readily tracked and conserved in the environment and has been used to understand the distribution of dispersant-treated oil in the environment (Kujawinski et al. 2011; White et al. 2014). The long-term persistence of elevated DOSS concentrations on beaches and in the deep sea demonstrates that at least some of the components of dispersants are persistent in the environment.

Various dispersant brands and formulations have been subjected to a variety of short-term comparative toxicity studies using model invertebrate and fish species (e.g., Hemmer et al. 2011). In tests with the mysid shrimp, *Americamysis bahia*, and

the inland silversides fish, *Menidia beryllina*, and based on lethal concentrations resulting in 50% mortalities (LC_{50}), most dispersants would be classed under EPA criteria as being slightly to moderately toxic (Hemmer et al. 2011). A wider variety of species have been tested in the laboratory emphasizing the toxicity of the dispersants, crude oils, and the chemically dispersed crude oils (see the recent meta-analysis in NASEM 2019). Generally the second- and third-generation dispersants have been found to be less toxic than crude oil or chemically dispersed oil, although the ordering of toxicity between crude oil and chemically dispersed oil is idiosyncratic of experimental conditions and protocols and species being tested (NASEM 2019).

The application of SSDI was unique to the DWH spill, and many subsequent studies have been directed to understanding the efficacy of that modality in sequestering oil in the deep sea by reducing droplet sizes to diameters small enough to appear near-neutrally buoyant. Similarly, lighter molecular weight hydrocarbons (e.g., methane and BTEX compounds) are highly water-soluble, and most dissolved into the seawater before surfacing. Open questions exist regarding the role that dispersants played both in the creation of deep plumes and reduction in surfacing VOCs. Below we consider each of the six questions posed above in more detail.

28.3 How Toxic Are Dispersants for Species in the Wild?

Numerous studies have sought to understand the toxicity of dispersants themselves and have addressed the question regarding whether oil combined with dispersants (e.g., chemically dispersed oil) is more or less toxic to various biota (see Bejarano et al. 2013, 2014, 2016; Barron et al. 2020; Mitchelmore et al. 2020; NASEM 2019). Beyond testing of the *relative* toxicity of various dispersant formulations with and without oil, understanding the presence of various species associated with a particular spill is critical in making decisions regarding the use of dispersants as a response option. For example, with respect to DWH, a number of species are highly sensitive to dispersants and dispersant-oil mixtures including shallow and cold-water corals that occur in the vicinity of the site (Goodbody-Gringley et al. 2013; DeLeo et al. 2016; Frometa et al. 2017). Likewise, mesopelagic species are distributed at depths where deep oil plumes existed during DWH, and contamination levels, in some cases, exceeded those of shallower water species (Romero et al. 2018). Toxicity testing has generally involved model species because they tend to be easily maintained in a laboratory setting and are hearty. However, results from model species may be biased when extrapolated to field-relevant species, which may be more sensitive. Thus, testing is evolving toward using species representative of ecosystems wherein dispersants will actually be used. However, most of these studies have been done *post hoc* of significant spills rather than being conducted in anticipation that an accident in a particular region may occur (e.g., *Exxon Valdez*, *Cosco Busan*, DWH accidents). With respect to ultra-deep spills, understanding the trade-offs of using SSDI involves evaluating the sensitivity of deepwater vs. pelagic and coastal

species (Barron et al. 2020; Mitchelmore et al. 2020). In most cases neither the baseline studies of the biodiversity and abundance nor contaminant concentrations of cryptic deepwater species have been adequately evaluated to logically inform such trade-off analyses.

28.4 Is There Toxic Synergy Between Dispersants and Oil?

A large number of laboratory-based studies have tested the toxicity of dispersants alone, crude and refined oils alone, and chemically dispersed oils (Bejarano et al. 2013, 2014, 2016; Mitchelmore et al. 2020; NASEM 2019, include syntheses of these data). Conclusions regarding the relative toxicity of oil vs. chemically dispersed oil are mixed, with some studies indicating crude>dispersed and vice versa (e.g., Vosyliene et al. 2005). In evaluating the state of the science, the NASEM (2019) discussed the many variations in species, experimental protocols, and toxic agents being assessed. A meta-analysis of recent studies indicate that chemically dispersed oil is no more toxic than untreated oil at concentrations ≤100 mg oil L^{-1} (NASEM 2019). However, a number of factors confound a simple answer to this question, including: (1) the choice of what oil components are being used to define toxicity (e.g., total petroleum hydrocarbons (TPHs), total or subsets of polycyclic aromatic hydrocarbons (TPAHs)) and how they are weighted (e.g., by the relative toxicity of each component of the oil (toxic units)), (2) the choice of methods to manufacture and maintain dispersed oil treatments (e.g., variable dilution vs. variable loading protocols), (3) whether or not the oil concentrations are monitored during and post experiments to determine if target concentrations are maintained, (5) test duration (e.g., acute short-term, chronic, or hybrid exposure trials), and (6) the toxic end points for the experiment (lethal vs. sublethal effects).

With respect to oil components being tested, there is considerable variation among laboratory-based studies (NASEM 2019) with TPH and TPAH being the most prevalent, but other oil components such as individual parental PAHs (e.g., naphthalene, phenanthrene, etc.) are the subject of numerous investigations. The latter approach makes interpretation of laboratory to field results difficult since animals exposed to real spills rarely encounter single compounds. Thus, many studies report TPH as a result of testing whole crude oils. The issue with this approach is obviously that different crude oils are made up of differing admixtures of components and especially toxic and carcinogenic PAHs (e.g., NASEM 2019). Comparing TPH and even TPAHs among studies is thus conditioned on oil type, and interpretation is made more difficult by the weathering state of the crude oils used, as they rapidly loose more volatile components and lighter weight aromatics.

Lower molecular weight PAHs (e.g., two-benzene ringed) tend to be less toxic and carcinogenic than heavier compounds (three and greater benzene rings). To account for differences in toxicity by compound, the so-called “toxic unit” scaling (Di Toro and McGrath 2000; Redman and Parkerton 2015) provides a weighting scheme to estimate a single quantity scaling a particular oil type and weathering state.

Laboratory exposure studies require a target contaminant exposure concentration applied over a specific exposure period. Maintaining target concentrations is difficult because of evaporation of water and hydrocarbons from the test container, as well as weathering of the oil components. There are two methods generally used to prepare solutions for testing and maintenance of the concentrations over the test period. The *variable dilution* method utilizes a one-time manufacture of a relatively highly concentrated solution of a water-accommodated fraction (WAF), generally using an impeller to mix the solution. The WAF solution is then diluted to the target concentration for the experiment. This method, however, has several drawbacks (NASEM 2019). Because the WAF is comprised of both dissolved hydrocarbons and microdroplets, it is difficult to maintain the total concentration of hydrocarbons in the test media due to differential dissolution and dilution of the microdroplets. One way to account for this factor is to filter out the microdroplets (which likely have lower toxicity to biota than dissolved hydrocarbons), but few studies do this, and extrapolation to the field becomes more difficult since real oil spills are comprised of both microdroplets and dissolved hydrocarbons.

An alternative method for manufacturing WAFs for exposure testing is to produce a series of test media at varying concentrations (*variable loading*) and estimate a dose-response curve based on a particular toxic end point (e.g., LC_{50} mortality of the test subject) as a function of the various loading levels. The NASEM (2019) conducted an analysis of variable loading-based experiments demonstrating still variable results regarding the relative toxicity of dispersed vs. crude oils.

The issue of test duration is also critical to understanding toxicity of oil and dispersant+oil, especially in relation to end points that do not result in short-term mortality (Mitchelmore et al. 2020; Grosell et al. 2019; Portnoy et al. 2020). Clearly, concentrations of hydrocarbons resulting in significant mortality to various life stages over a short test duration (e.g., 96 h) establish thresholds for significant individual and population-level effects (e.g., *Deepwater Horizon* Natural Resource Damage Assessment Trustees 2016). These may occur at PAH exposure levels (noting the caveats above) of ~1–10 ppm, depending on the species, life stage, exposure duration, and other factors. However, lower contaminant concentrations applied over a longer period may result in a lower threshold for significant mortality arising from exposures. An important trend in oil spill toxicity studies following DWH has been the rise in projects assessing sublethal effects and their consequences for population outcomes. While short-term mortality is a consequential outcome of exposure, so too can be sublethal exposures that compromise various internal processes within organisms. Thus, there have been a number of recent studies emphasizing physiological, immunogenic, and genomic end points of oil and dispersant exposures (Whitehead et al. 2011; Incardona et al. 2013; Grosell et al. 2019) as they relate to the overall fitness of exposed individuals and populations. All of these sublethal end points may be consequential for populations since these metrics are variously associated with nutritional state, ability to fight disease and injury, and reproduction (Mitchelmore et al. 2020; Grosell et al. 2019; Portnoy et al. 2020).

28.5 Do Dispersants Increase or Decrease Biodegradation?

The dissolution and biodegradation of the live oil as it rises in the water column lead to hydrocarbon partitioning between organic and aqueous phases and dominate the weathering process. The use of chemicals to disperse oil into smaller droplets is predicated on the assumptions that smaller droplets are more easily dissolved into surrounding waters and that smaller droplets are degraded by bacterial action more rapidly than are larger droplets. However, chemical dispersants may not have the expected effect on biodegradation. Of the surfactants of Corexit 9500, only Tween 20 assists the growth, while the other ingredients slow growth (Bookstaver et al. 2015). The impact of chemical dispersants on biodegradation is still debated (Kleindienst et al. 2015a, b). Bio-surfactants are seen as better since they are less toxic, and better at enhancing biodegradation yet a more expensive option (Cai et al. 2016).

28.6 On the Efficacy of SSDI

After the DWH incident, a number of research organizations have sought to better understand the efficacy of SSDI with respect to small oil droplet formation and mitigation of VOCs at the sea surface. Funding for these studies has included the oil and gas industries, through the American Petroleum Institute (API; Nedwed 2017) and SINTEF (Daling et al. 2017), and independent research sponsored by the Gulf of Mexico Research Initiative (Gros et al. 2017; Pesch et al. 2018; Malone et al. 2018, 2020) among other organizations.

The rise rate of droplets is dependent both on droplet size and its degree of gas saturation (Pesch et al. 2018). Droplet diameters of ~70 microns and smaller are functionally neutrally buoyant and thus, given natural turbulence, will appear to be sequestered in the deep sea should a blowout occur there (Paris et al. 2012). Research conducted to date indicates that in the presence of dispersants, the surface tension declines twofold or greater with dispersant/oil volume ratios of 0.01:0.04. All empirical evidence shows that droplet sizes are reduced in the presence of dispersants, both at sea-level pressures and in deeper waters (Li et al. 2008; Brandvik et al. 2013). The critical question, however, is not *if* small droplets can be created by SSDI during ultra-deep spills but the extent to which small droplets would occur in the *absence* of SSDI because of the dynamics of subsurface blowouts (Fig. 28.1). Putting it another way, what are the relative contributions of SSDI and natural processes to the formation of deep subsurface oil plumes as observed during DWH (Diercks et al. 2010)? Having an adequate answer to this fundamental question has enormous theoretical and practical value since, if SSDI can create submerged plumes that would otherwise not form or only partially form, then SSDI as a response measure for the next ultra-deep spill becomes an important consideration,

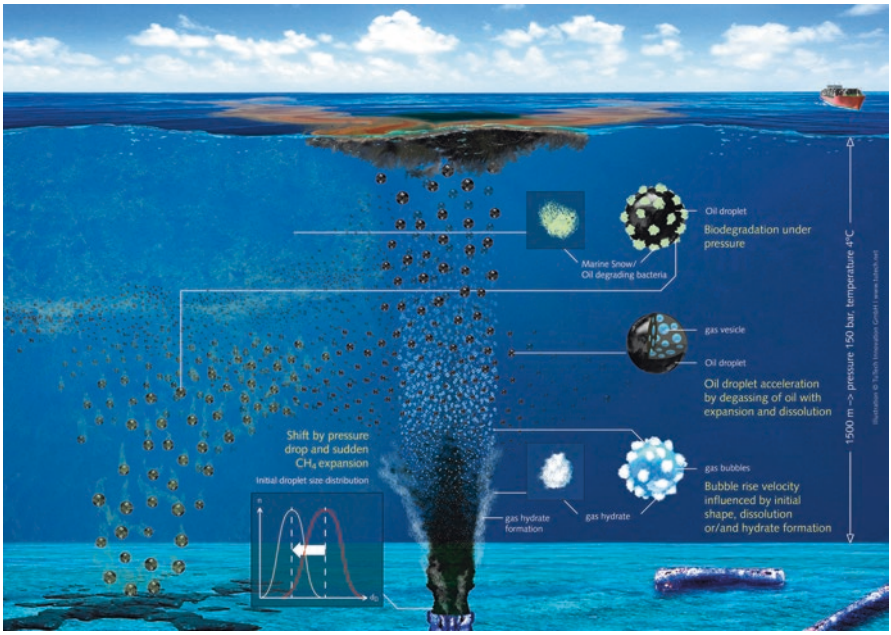

Fig. 28.1 Fundamental processes associated with a deep oil/gas well blowout (e.g., >1500 m) to be considered in the evaluation of response measures and especially the application of subsurface dispersant injection (SSDI)

notwithstanding the trade-offs of toxicity in the deep plume layers vs. at the sea surface (e.g., French-McCay et al. 2018).

Evidence for the formation of small droplets in the presence of dispersants comes in the form of experiments (at small scales), field observations conducted during and after DWH (Li et al. 2008; Brandvik et al. 2013), and modeling studies. A number of laboratory studies have conducted or summarized (Socolofsky et al. 2015; NASEM 2019) experimental approaches to estimate oil droplet sizes from scaled-up lab experiments, test tanks, and, in one case, a field-scale experiment (DeepSpill; Johansen and Rye 2003). These experiments have been undertaken in six main facilities: the SINTEF tower facilities in Trondheim, Norway; the OHMSETT tanks in New Jersey; the Southwest Research Institute high-pressure facility in San Antonio, Texas; the high-pressure test facility at the Hamburg University of Technology Germany (Pesch et al. 2018; Malone et al. 2018, 2020); and in stirred tank studies at the University of Western Australia (Aman et al. 2015) and the University of Hawaii (Masutani and Adams 2000; NASEM 2019). Extrapolating the behavior of a real-world blowout in the ultra-deep from these experiments is complicated by a number of factors. The experiments are limited in scale to nozzle diameters far smaller than the ~0.5 m diameter pipe at the top of the DWH blowout preventer (BOP). As nozzle diameter affects maximum droplet diameter, scaling of the experimental results requires the use of scaling metrics (e.g., Reynolds-Weber scaling)

or alternative metrics such as turbulent kinetic energy (TKE) and energy turbulence dissipation rate (TDR). Importantly, for the jet injection experiments, nozzle diameters ranged from 1.5 mm (SINTEF and Hamburg) to 25–50 mm (OHMSETT) and 120 mm in DeepSpill. Because of their small scale, the results of the jet experiments require substantial – that is, multiple orders of magnitude – scaling-up and *extrapolation* to emulate the DWH and similar conditions. Likewise, the plurality of previous experiments used ambient sea-level pressures rather than the 15 MPa ambient pressure extant at DWH (and higher for deeper simulated blowouts). Finally, a number of the protocols have used "dead" vs. "live" (e.g., methane saturated) crude oil for droplet size experiments. Obviously, real-world blowouts create a chaotic multiphase (oil, gas, water) flow that is also influenced by the exit pipe diameter and including any jagged edges and restrictions (e.g., pipe bends, partially closed shear rams, etc.) and sudden pressure drops associated with oil from the formation exiting into the ocean, all that might be part of the casualty (Boufadel et al. 2018). Experiments to date with "live" oil have emphasized the criticality of gas inclusion to the dynamics of oil and gas droplets and gas bubbles, which in turn interact in multiphase flow (Malone et al. 2018, 2020).

A variety of models have been used to predict droplet size and fate with and without the use of dispersants (e.g., the SINTEF, ASA, and CMS modeling systems). Depending on the selection of subsets of experiments conducted, the impact of SSDI on small droplet formation is based on models (e.g., ASA, SINTEF, and CMS modeling systems described by the Socolofsky et al. 2015 model intercomparisons). Contingent on the subset of experimental data chosen for incorporation in the models, the fraction of oil droplets accumulating in deep plumes as a result of the application of SSDI ranges from about 20% (CMS) to essentially all of the oil mass (ASA). Thus, understanding how well experiments replicate realistic chemical and physical characteristics of the blowout, as well as oil and gas behavior under extreme pressure, is critical for validating model performance under such uncertainty.

One of the important revelations from the DWH accident was the discovery of deep subsurface oil plumes emanating from the broken well and extending horizontally for up to 13 km (primarily southeast of the broken well) during May 9–16 (Diercks et al. 2010) and further extending to up to 35 km from the well during June 19–28 (Camilli et al. 2010). The timing of these discoveries is important because while small quantities of SSDI were injected starting in on April 30 (2200 gallons), it was not until May 20 (after such injections were fully authorized by the EPA) that significant quantities of SSDI were used (Fig. 28.2).

Diercks et al. (2010) observed relatively high oil concentrations (maximum 189 μg L^{-1} of PAHs) in the subsurface plume between May 9 and 16, 2010. The use of SSDI was initiated on April 30, was shut down between May 5 and 9, resumed for 2 days, and again shut down between May 12 and 14 (Fig. 28.2). On May 5, BP's sampling (BP 2016) detected PAH concentrations >800 μg L^{-1} below 1200 m, two orders of magnitude higher than PAH levels detected at the surface (BP 2016). About 44.1 thousand gallons of dispersants were used in SSDI during the time period before and when Diercks et al. (2010) and BP initiated sampling (Fig. 28.2). If we assume a

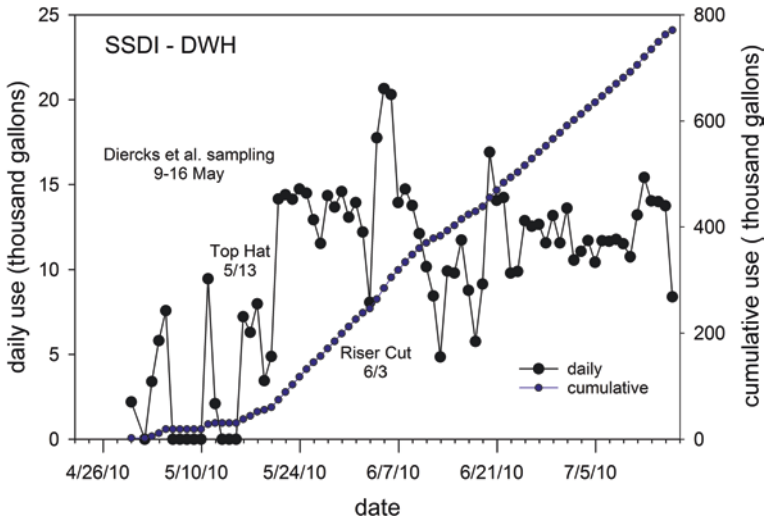

Fig. 28.2 Daily and cumulative use of subsurface-applied dispersant injection (SSDI, thousands of gallons) at the DWH wellhead. (Data available from BP Gulf Science Data 2016)

flow rate of 60,000 barrels per day (BPD) prior to the riser cut (McNutt et al. 2011; Spaulding et al. 2017), this results in an estimated 42.84 million gallons of oil spilled during this period and gives a dispersant-oil percentage of 0.1029% as of the last day of the Diercks et al. (2010) expedition, equivalent to a dispersant/oil ratio of 1:972. This is about 1/4 of the ratio of 0.4% equivalent to the 1:250 target dispersant to oil application rate, which is likely below the effective threshold, since the lower slick was up to 35 km long by the time higher dispersant usage was authorized (Fig. 28.2). Obviously, then, the subsurface plume sampled by Diercks et al. (2010) and BP Data1, BGS (2016) was created by processes other than SSDI.

What physical mechanisms might create small droplets and dissolved hydrocarbons in the absence of dispersants? Experiments with live oil "jets" at pressures equivalent to the DWH spill site (15 MPa or 150 bar) reveal a series of phenomena consistent with the video observations at the wellhead (Pesch et al. 2018; Malone et al. 2018, 2020; Youtube.com 2018). Rising oil droplets saturated with gas expand upon exit from the jet nozzle (Malone et al. 2018, 2020). During this sudden, explosive exit, methane exits the rising oil droplets as the droplets expand due to the sudden change in pressure (e.g., Boyles law). Under these conditions, droplets can fracture due to this sudden pressure drop, resulting in the formation of oil/gas/water emulsions consistent with the light-brown fluids escaping the broken DWH wellhead (YouTube 2018) and the high-pressure nozzle experiments (Malone et al. 2018, 2020; Pesch et al. 2018). The light-brown emulsion consistently seen in actual and experimental (miniature) blowouts is comprised of microdroplets of oil, gas, and water. The appearance of this emulsion has been termed the "Cappuccino Effect"; the microdroplets were difficult to measure with experimental camera equipment (Aman et al. 2015; Malone et al. 2018) and generally smaller than ~70 μm necessary to remain suspended in the subsurface

or rising so slowly that biodegradation occurs before surfacing. Not all escaping oil forms such emulsions, and thus there is likely a wide spread in oil droplet size distributions blowing out from the broken well.

One of the most critical and enlightening sets of experiments involved using "live" oil under high pressure and simulating a pressure drop (Malone et al. 2020) as was the case for DWH (Werely 2011; Aliseda et al. 2010; McNutt et al. 2011). Simulating a pressure drop of 10 MPa resulted in a bimodal distribution of oil droplets (Malone et al. 2020). In this case the smaller mode consisted of small droplet sizes most of which would appear as neutrally buoyant, while the larger mode was of a size likely to rise to the sea surface. These experiments were conducted without SSDI. Under the actual DWH conditions (8.6 MPa pressure drop), it is reasonable to expect a large proportion of the oil droplets escaping the well would be comprised of the smaller mode.

Is there any empirical evidence of a pressure drop sufficient to create explosive outgassing of the escaping oil from a deep blowout? As calculated from field measurements (Aliseda et al. 2010) and simulated in laboratory experiments conducted by Pesch et al. (2018), there was a pressure drop (approximate 86 bar = 1250 psi) between the failed blind shear ram (BSR) of the BOP and the contact point between the BOP exit and the ambient ocean. The physical constraint of a pressure drop within this confined volume – that is, the top half of the BOP stack – means that a significant portion of the natural reservoir pressure was expended *immediately* upstream of the near-field plume. As the riser was later sheared at the top of the BOP, fluids then exiting from the top of the BOP stack (Fig. 28.3) would have had

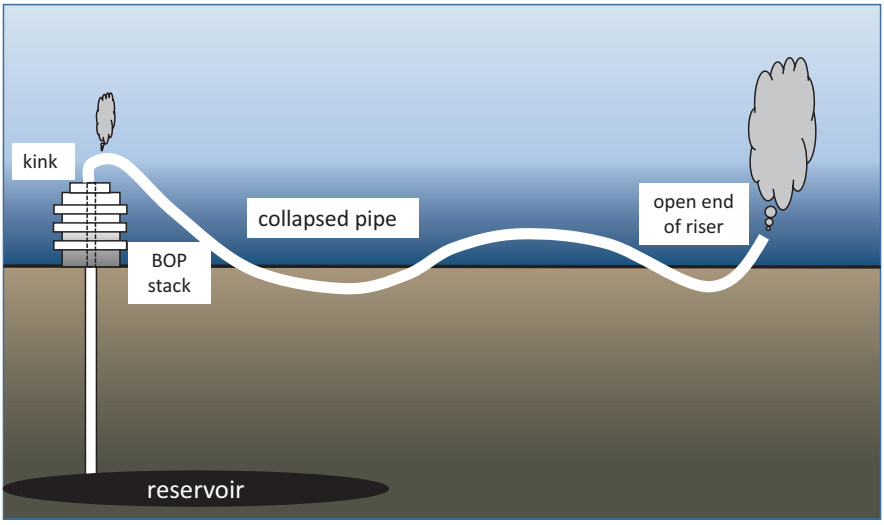

Fig. 28.3 Diagram of the fallen riser pipe and blowout preventer (BOP) from DWH prior to severing the riser at the LMRP (lower marine riser package). Prior to severing, the majority of oil flow was from the riser pipe end, with much smaller quantities from the riser kink jets. (Figure redrawn from Wereley 2011 and McNutt et al. 2011)

insufficient residence time to dissipate turbulence induced from this orifice-type pressure drop; this complex and important physical reality has only been considered in a minority of experimental and modeling approaches to date.

It has been conjectured by some that small holes at the "riser kink" (Fig. 28.3) and along the riser of 50–100 cm^2 surface area accounted for the small diameter of droplets observed in the intrusions preceding the significant use of SSDI (Diercks et al. 2010) under the theory that smaller diameter holes create smaller droplets. However, during the period prior to severing the riser pipe, the vast majority of the flow was *actually* through the broken end of the riser (Fig. 28.3), which had a cross-sectional area of 214 in^2 or 1381 cm^2 (Aliseda et al. 2010) from a mean pipe radius of 8.25 inches or 21 cm (or about 14–28 times the cross-sectional area of the kink). The flow from the end of the riser was estimated to account for 74% of total DWH flow during this period (Wereley 2011, and repeated in Spaulding et al. 2017). The combination of the wide riser pipe cross-sectional area and the high volume flow through it, without the addition of SSDI, is likely insufficient to produce sufficient numbers of oil particles sufficiently small to generate the observed intrusion plume. A more likely scenario is that the 86 bar pressure drop at the BOP, in combination with the turbulent dynamics of the multiphase flow, as simulated in the high-pressure autoclave (Aman et al. 2015) and pressure-drop experiments (Malone et al. 2020), was responsible for contributing to the formation of these small droplet diameters as observed in subsurface plumes prior to the application of SSDI.

Is there a correlation between the quantity of SSDI applied and the resulting relative volume of oil in deep intrusions vs. that rising to the surface? The main argument for the use of SSDI is that by applying it in large quantities (up to 1% of oil volume), more oil would be sequestered in deep plumes thereby reducing oil volume at the surface and thus decreasing the quantity of oil requiring surface-deployed mitigation measures. The relationship between application volume and the proportion of oil sequestered in the deep can take three forms. Disregarding the nonsensical SSDI relationship in which more oil comes to the surface with increasing SSDI volume, if there is no significant impact of the SSDI on surfacing oil, then the relationship would be horizontal. If, however, increasing SSDI (in volume or percentage as a function of oil volume flow) results in a greater proportion of the volume being sequestered (the underlying assumption of the use of SSDI), then, all things being equal, there should be a negative relationship between SSDI volume and the ratio of surface to deep oil concentration. This model assumes there are no multiday lags or cumulative effects that would result if there is little cross-current flow at depth and no significant oil degradation due to bacterial consumption, resulting in accumulation of oil in the deep sea near the wellhead. If the cumulative effects are large (e.g., little cross-current flow and little bacterial action on the oil) then, in fact, the relationship between SSDI use and the ratio of oil at the surface vs. oil at depth would be even *steeper* (more negative) than the no-lag relationship. A first-order test of the efficacy of SSDI in significantly sequestering oil is given by the ratio of surfacing to deep oil concentration as a function of daily SSDI use, with the null hypothesis that there was no effect and the alternative hypothesis that there was an effect (significant negative slope). Paris et al. (2018) tested these relationships using

nearly 2500 daily measurements of oil concentrations (PAHs) in the water column from the BP Gulf Science Data (Data1, BGS 2016; Data2, BGS 2016). They found no significant correlations between daily dispersant use and the ratio of PAHs in deep intrusion layers, further supporting the hypothesis that deep plumes were, at least partially, formed by small oil droplets created by the combination of a severe and turbulent pressure drop immediately upstream of the jet formation, followed by rapid outgassing of live oil at the wellhead.

Studies and data summarized above, involving theory, laboratory, and field-based experiments, thus support the hypothesis that SSDI, while a factor in reducing droplet size when being applied, was not the exclusive or perhaps even the dominant reason for the creation and maintenance of deep oil droplet plumes resulting from the DWH accident. Thus, the relative contributions of SSDI and natural processes to deep plume formation remain a seminal and unresolved question.

28.7 VOCs and Dispersant Use

The issue of VOCs and their abatement from deep oil spills is important for three compelling reasons. First, as was the case for both DWH and Ixtoc 1, crews of workers were stationed above the uncontrolled well blowouts in order to both undertake oil recovery and mitigation activities (mechanical recovery and controlled burns) and aboard ships drilling relief wells to kill the blowout. Surfacing oil around them presents both a fire hazard and emits potentially toxic fumes from VOCs. Second, if VOCs surface, they present an inhalation risk to marine mammals, birds, and other wildlife. Third, depending on weather, wind, and transport, VOCs may present an inhalation risk to affected civilian populations ashore and particularly on the coast. Several authors have addressed the issue of VOCs from the well and how dispersants may affect VOC concentrations in the atmosphere above the well blowout. Sampling from aircraft above the DWH when it was active, DeGouw et al. (2011) and Ryerson et al. (2012) were able to determine both the atmospheric concentrations of various volatile compounds and, using subsurface data collected from the wellhead, estimate losses of various BTEX and other compounds during their ascent to the sea surface and eventually to the atmosphere. Their data show substantial reductions of most (and in some cases virtually all) water-soluble, volatile compounds for a single day (June 10, 2010). As with the droplet size discussion, the question then remains – is the reduction of VOCs between the wellhead and the sea surface due to the application of dispersants, to natural processes, or to some combination of both? Since compounds such as methane and benzene are highly water-soluble, it stands to reason that the ascent of over 1500 m (one mile) would result in substantial reduction in their concentration. Using this logic, then, a well blowout at 3000 m would likely contain even fewer of these compounds, although the loss function by depth has not been estimated. The rate of VOC loss to water solubility is likely, again, a function of oil droplet size and the interfacial tension between oil and water. The latter is also likely affected by oil type.

Using data from VOC meters aboard ships in the vicinity of the surfacing oil around DWH, Nedwed (2017) was unable to establish statistical correlation between daily volume of dispersants used and atmospheric VOC concentrations near the rising plume. However, this was not a controlled study as VOC meters were used intermittently, ships changed locations, and wind and ocean current flow conditions changed over the course of the spill event. Using near-field droplet formation models and results of some of the droplet size experiments described above, Gros et al. (2017) estimated that 27% of the mass of hydrocarbons (oil and molar equivalents in gas) were dissolved prior to surfacing and that by reducing droplet and gas bubble sizes by factors of about three, the addition of dispersants increased the dissolution of VOCs by over 25% from the no-treatment case. Crowley et al. (2018) used a different subsurface droplet model (OILMAPDEEP) also concluding that VOCs were dramatically reduced with dispersant use. These are significant results and support the case for SSDI but are also dependent on the assumption that the addition of SSDI was the dominant factor in the formation of subsurface plumes of dissolved hydrocarbons and small oil droplets (see above).

28.8 Trade-Offs in Oil Distribution from a Subsurface Blowout

To disperse or not to disperse? During an actual oil spill response scenario, many factors bear on the choice of response methodologies, in combination, or as standalone measures (Aurand et al. 2000). Structured decision-making is used in these cases, as a strategy to weigh the potential risks to people and wildlife, as well as operational contingencies and efficacy of various methodologies applied to the particular scenario being assessed. Known by various acronyms such as NEBA (Net Environmental Benefit Analysis; DeMicco et al. 2011), ERA (Ecological Risk Assessment), CERA (Comparative Ecological Risk Assessment), CRA (Comparative Risk Assessment), and SIMA (Spill Impact Assessment), the goals of these evaluations are to essentially weigh the "best worst choice" with respect to mitigation techniques. While these tools vary in scope, degree of quantitative rigor, and flexibility (Crowley et al. 2018; Bock et al. 2018; French-McCay et al. 2018), they share several common attributes centered around an operational model of how the oil spill scenario interacts with components of the ecosystem and how the use of response measures compares in terms of efficacy and impacts (Aurand et al. 2000).

In considering the choice of response measures with respect to an ultra-deep spill, the most common justification for dispersant use – keeping oil from interacting with highly sensitive coastal habitats – must be weighed against the consequences of measures that would sequester oil and related compounds in mid-depths and accumulate toxicity within the planktonic food chain or on the bottom in the deep sea (assuming dispersants are effective in doing so). For spill locations such as

the deepest parts of the Gulf of Mexico, relatively small quantities of oil may reach the coast even without the use of dispersants because of the intensive weathering of surfacing oil far from shore (Berenshtein et al. 2020). In such a case, the trade-off analysis must balance the sensitivity, diversity, and productivity of deepwater resources (e.g., cold-water corals, mesopelagic fishes) against the risk to surface dwelling biota (e.g., Bock et al. 2018) and critical food plankton throughout the water column undergoing ontogenetic and diel migrations. In particular, deep-dwelling biota may be longer-lived, less productive, more diverse, and more sensitive at early life stages than biota occupying comparable shallower waters. Likewise, because of diel vertical migrations of both mesopelagic prey (e.g., Romero et al. 2018) and their predators (tunas, swordfish (*Xiphias gladius*), etc.; Orbesen et al. 2017), oil components sequestered in the deep sea may impact surface dwelling epipelagic fishes and other species they in turn interact with. Little is currently known concerning critical life history parameters for deepwater ecological resources as input for trade-off analyses. Many questions thus persist regarding the efficacy of dispersants and the toxicity of dispersed vs. crude oil. Trade-offs must therefore be viewed critically and as a framework rather than a definitive statement of how dispersants should be used in response to future ultra-deep blowouts.

28.9 Summary

The discussions above highlight both critical questions that apply specifically to dispersant use in the case of ultra-deep oil well blowouts and the state of scientific knowledge regarding those seminal questions. Much has been learned in the 9 plus years since DWH about toxicity, fate, and efficacy of dispersants. In particular, novel sampling methods (both in the ocean and in the atmosphere) have been combined with sophisticated hydrodynamic models to assess dispersant effectiveness. More sophisticated sublethal metrics of oil and dispersant toxicity have been put into operational use. More realistic experiments involving the unique physical and chemical characteristics of an actual deepwater blowout have been undertaken. The next major oil spill will be informed with an arsenal of techniques to assist responders in evaluating which response measures are likely to be most successful while minimizing downside risks. There remain, however, a number of important and unresolved questions. The final chapter of this book, (Murawski 2020) considers a series of recommendations for additional high-priority experiments, data collection activities, and related monitoring studies to help narrow the uncertainty in understanding the efficacy and effects of dispersant application in the case of the next ultra-deep oil spill.

Acknowledgments This research was made possible by a grant from the Gulf of Mexico Research Initiative/C-IMAGE I, II and III.

References

Aliseda A, Bommer P, Espina P, Flores O, Lasheras JC, Lehr B, Leifer I, Possolo A, Riley J, Savas O, Shaffer F, Wereley S, Yapa P (2010) Deepwater Horizon release estimate of rate by PIV. Report to the Flow Rate Technical Group. Available at: https://www.doi.gov/sites/doi.gov/files/migrated/deepwaterhorizon/upload/Deepwater_Horizon_Plume_Team_Final_Report_7-21-2010_comp-corrected2.pdf

Aman Z, Paris CB, May EF, Johns ML, Lindo-Atichati D (2015) High-pressure visual experimental studies of oil-in-water dispersion droplet size: implication for oil transport. Chem Eng Sci 127:392–400

Aurand D, Walko L, Pond (2000) Developing consensus ecological risk assessments: environmental protection in oil spill response planning a guidebook. United States Coast Guard, Washington, D.C, p 148

Barron M, Chiasson S, Bejarano A (2020) Ecotoxicology of deep ocean spills (Chap. 27). In: Murawski SA, Ainsworth C, Gilbert S, Hollander D, Paris CB, Schlüter M, Wetzel D (eds) Deep oil spills: facts, fate and effects. Springer, Cham

Bejarano AC, Levine E, Mearns A (2013) Effectiveness and potential ecological effects of offshore surface dispersant use during the *Deepwater Horizon* oil spill: a retrospective analysis of monitoring data. Environ Monit Assess 185:10281–10,295

Bejarano AC, Clark JR, Coelho JM (2014) Issues and challenges with oil toxicity data and implications for their use in decision making: a quantitative review. Environ Toxicol Chem 33:732–742

Bejarano AC, Farr JK, Jenne P, Chu V, Hielscher A (2016) The Chemical Aquatic Fate and Effects database (CAFE), a tool that supports assessments of chemical spills in aquatic environments. Environ Toxicol Chem 35:1576–1586

Berenshtein I, Perlin N, Ainsworth C, Ortega-Ortiz J, Vaz AC, Paris CB (2020) Comparisons of the spatial extent, impacts to shorelines and ecosystem, and 4-dimensional characteristics of simulated oil Spills (Chap. 20). In: Murawski SA, Ainsworth C, Gilbert S, Hollander D, Paris CB, Schlüter M, Wetzel D (eds) Scenarios and responses to future Deep Oil Spills – fighting the next war. Springer, Cham

Bock M, Robinson H, Wenning R, French-McCay D, Rowe J, Hayward Walker A (2018) Comparative risk assessment of oil spill response options for a deepwater oil well blowout: Part II. Relative risk methodology. Mar Pollut Bull 133:984–1000

Bookstaver M, Bose A, Tripathi A (2015) Interaction of Alcanivorax borkumensis with a surfactant decorated oil-water interface. Langmuir 31:5875–5881

Boufadel MC, Gao F, Zhao L, Özgökmen T, Miller R, King T, Robinson B, Lee K, Leifer I (2018) Was the *Deepwater Horizon* well discharge churn flow? Implications on the estimation of the oil discharge and droplet size distribution. Geophys Res Lett 45. https://doi.org/10.1002/2017GL076606

Brandvik PJ, Johansen Ø, Leirvik F, Farooq U, Daling PS (2013) Droplet breakup in subsurface oil releases—Part 1: experimental study of droplet breakup and effectiveness of dispersant injection. Mar Pollut Bull 73:319–326. https://doi.org/10.1016/j.marpolbul.2013.05.020

Cai Z, Gong Y, Liu W, Fu J, O'Reilly SE, Hao X, Zhao D (2016) A surface tension based method for measuring oil dispersant concentration in seawater. Mar Pollut Bull 109:49–54

Camilli R, Reddy CM, Yoerger DR, Van Mooy BAS, Jakuba MV, Kinsey JC, McIntyre CP, Sylva SP, Maloney JV (2010) Tracking hydrocarbon plume transport and bio-degradation at *Deepwater Horizon*. Science 330:201–204. https://doi.org/10.1126/science.1195223

Coastal Response Research Center (2010) *Deepwater Horizon* dispersant use meeting report, May 26–27, 2010, revision 3. University of New Hampshire, available at: https://crrc.unh.edu/sites/crrc.unh.edu/files/dwh_dispersants_meeting_final_report.pdf

Crowley D, French-McCay D, Santos L, Chowdhury B, Markussen R (2018) Modeling atmospheric volatile organic compound concentrations resulting from a deepwater oil well blowout – mitigation by subsea dispersant injection. Mar Pollut Bull 136:152–163

Daling PS, Brakstad OG, Brandvik PJ, Davies E, Grøsvik BE, Meier S, Nepstad R, Nordtug T, Vikebø F (2017) SubSea Dispersant Injection (SSDI) – a "state of the art" and the need for further documentations. Norwegian Institute of Marine Research report 2017:00007 A. https://brage.bibsys.no/xmlui/bitstream/handle/11250/2476897/2017_00007A_Subsea_dispersion-pre-project-FINAL.pdf?sequence=1

Data1, BGS (2016) Chemical analysis of oil samples from the Gulf of Mexico and adjoining states from May 2010 to March 2014. Filename: WaterChemistry_W-01v02-01_xTab. https://data.gulfresearchinitiative.org/data/BP.x750.000:0005

Data2, BGS (2016) Subsea dispersant application records collected during the Deepwater Horizon (DWH) accident near the Mississippi Canyon block 252 wellhead from April 30 to July 22, 2010 Filename: DispersantApplication_OTH-02v01-01. https://data.gulfresearchinitiative.org/data/BP.x750.000:0018#

Deepwater Horizon Natural Resource Damage Assessment Trustees (2016) *Deepwater Horizon* oil spill: final programmatic damage assessment and restoration plan and final programmatic environmental impact statement. Retrieved from http://www.gulfspillrestoration.noaa.gov/restoration-planning/gulf-plan

DeGouw JA, Middlebrook AM, Warneke C, Ahmadov R, Atlas EL, Bahreini R, Blake DR, Brock CA, Brioude J, Fahey DW, Fehsenfeld FC, Holloway JS, Le Henaff M, Lueb RA, McKeen SA, Meagher JF, Murphy MD, Paris CB, Parrish DD, Perring AE, Pollack IB, Ravishankara AR, Robinson AL, Ryerson TB, Schwarz JP, Spackman JR, Srinivasan A, Watts LA (2011) Organic aerosol formation downwind from the *Deepwater Horizon* oil spill. Science 331:1295

DeLeo DM, Ruiz-Ramos DV, Baums LB, Cordes EE (2016) Response of deep-water corals to oil and chemical dispersant exposure. Deep Sea Res II Top Stud Oceanogr 129:137–147

DeMicco E, Schuler PA, Omer T, Baca B (2011) Net Environmental Benefit Analysis (NEBA) of dispersed oil on near shore tropical ecosystems: tropics–the 25th year research visit. In: International Oil Spill Conference Proceedings (IOSC), American Petroleum Institute. abs282

Di Toro DM, McGrath JA (2000) Technical basis for narcotic chemicals and polycyclic aromatic hydrocarbon criteria. II. Mixtures and sediments. Environ Toxicol Chem 19:1971–1982

Diercks A-R, Highsmith RC, Asper VL, Joung D, Zhou Z, Guo L, Shiller AM, Joye SB, Teske AP, Guinasso N, Wade TL, Lohrenz SE (2010) Characterization of subsurface polycyclic aromatic hydrocarbons at the *Deepwater Horizon* site. Geophys Res Lett 37:L20602. https://doi.org/10.1029/2010GL045046

Farn RJ (1976) Sinking and dispersing oil (Chap. 8). In: Wardley-Smith J (ed) The control of oil pollution. Graham and Trotman, London

French-McCay D, Crowley D, Rowe JJ, Bock M, Robinson H, Wenning R, Hayward Walker Joeckel AJ, Nedwed TJ, Parkerton TF (2018) Comparative risk assessment of spill response options for a deepwater oil well blowout: Part 1. Oil spill modeling. Mar Pollut Bull 133:1001–1015

Frometa J, DeLorenzo ME, Pisarski EC, Etnoyer PJ (2017) Toxicity of oil and dispersant on the deep water gorgonian octocoral *Swiftia exserta*, with implications for the effects of the *Deepwater Horizon* oil spill. Mar Pollut Bull 122:91–99

Goodbody-Gringley G, Wetzel DL, Gillon D, Pulster E, Miller A, Ritchie KB (2013) Toxicity of Deepwater Horizon source oil and the chemical dispersant, Corexit® 9500, to coral larvae. PLoS One 8(1):e45574. https://doi.org/10.1371/journal.pone.0045574

Gros J, Socolofsky SA, Dissanayake AL, Jun I, Zhao L, Boufadel MC, Reddy CM, Areya JS (2017) Petroleum dynamics in the sea and influence of subsea dispersant injection during *Deepwater Horizon*. Proc Natl Acad Sci 114:10065–10,070

Grosell M, Griffitt RJ, Sherwood TA, Wetzel D (2019) Digging deeper than LC/EC50: non-traditional endpoints and non-model species in oil spill toxicology (Chap. 29). In: Murawski SA, Ainsworth C, Gilbert S, Hollander D, Paris CB, Schlüter M, Wetzel D (eds) Deep oil spills: facts, fate and effects. Springer, Cham

Hemmer MJ, Barron MG, Greene R (2011) Comparative toxicity of eight oil dispersants, Louisiana sweet crude oil (LSC) and chemically dispersed LSC to two aquatic test species. Environ Toxicol Chem 30:2244–2252

Incardona JP, Swarts TL, Edmunds RC, Linbo TL, Aquilina-Beck A, Sloan CA, Gardner LD, Block BA, Scholz NL (2013) *Exxon Valdez* to *Deepwater Horizon*: comparable toxicity of both crude oils to fish early life stages. Aquat Toxicol 142:303–316

Jernelöv A, Lindén O (1981) Ixtoc 1: a case study of the world's largest oil spill. Ambio 10:299–306

Johansen Ø, Rye H (2003) Deepspill—field study of a simulated oil and gas blowout in deep water. Spill Sci Technol Bull 8:433–443

Kleindienst SK, Paul JH, Joye SB (2015a) Assessing the impacts of chemical dispersants on microbial community composition and activity. Nat Rev Microbiol 13:388–396. https://doi.org/10.1038/nrmicro3452

Kleindienst S, Seidel M, Ziervogel M, Grim K, Mailkin S, Harrison S, Loftis KM, Perkins MJ, Field JA, Sogin M, Dittmar T, Passow U, Medeiros PM, Joye SB (2015b) Chemical dispersants can suppress the activity of natural oil-degrading microorganisms. Proc Natl Acad Sci USA 48:14900–14,905

Kujawinski EB, Kido Soule MC, Valentine DL, Boysen AK, Longnecker K, Redmond MC (2011) Fate of dispersants associated with the *Deepwater Horizon* Oil Spill. Environ Sci Technol 45:1298–1306

Li Z, Lee K, King T, Boufadel M (2008) Oil droplet size distribution as a function of energy dissipation rate in an experimental wave tank. In: Proceedings of the international oil spill conference, pp 621–626

Linton T, Koons CB (1983) Oil dispersant field evaluation Ixtoc 1 Blowout, Bay of Campeche, Mexico. Oil Petrochem Pollut 1:183–188

Malone K, Pesch S, Schlüter M, Krause D (2018) Oil droplet size distributions in deep-sea blowouts: Influence of pressure and dissolved gases. Environ Sci Technol 52:6326–6333. https://doi.org/10.1021/acs.est.8b00587

Malone K, Aman ZM, Pesch S, Schlüter M, Krause D (2020) Jet formation at the spill site and resulting droplet size distributions (Chap. 4). In: Murawski SA, Ainsworth C, Gilbert S, Hollander D, Paris CB, Schlüter M, Wetzel D (eds) Deep oil spills: facts, fate and effects. Springer, Cham

Masutani SM, Adams EE (2000) Experimental study of multi- phase plumes with application to deep ocean oil spills. TA&R Proj. 377, Bureau of Ocean Energy Management, Regulation and Enforcement, Washington, DC. Available at http://www.boemre.gov/tarprojects/377.htm

McNutt MK, Camilli R, Crone TJ, Guthrie GD, Hsieh PA, Ryerson TB, Savas O, Shaffer F (2011) Review of flow rate estimates of the *Deepwater Horizon* oil spill. Proc Natl Acad Sci 109. www.pnas.org/cgi/doi/10.1073/pnas.1112139108

Mitchelmore C, Bejarano A, Wetzel D (2020) A synthesis of *Deepwater Horizon* oil and dispersant aquatic standard laboratory acute and chronic toxicity studies (Chap. 28). In: Murawski SA, Ainsworth C, Gilbert S, Hollander D, Paris CB, Schlüter M, Wetzel D (eds) Deep oil spills: facts, fate and effects. Springer, Cham

Murawski SA (2020) Perspectives on research, technology, policy and human resources for improved management of ultra-deep oil and gas resources and responses to oil spills (Chap. 29). In: Murawski SA, Ainsworth C, Gilbert S, Hollander D, Paris CB, Schlüter M, Wetzel D (eds) Scenarios and responses to future deep oil spills – fighting the next war. Springer, Cham

National Academies of Sciences, Engineering and Medicine (NASEM) (2019) Report of the committee on evaluation of the use of chemical dispersants in oil spill response. National Academies Press, Washington, DC

National Research Council (NRC) (1989) Using oil spill dispersants on the sea. The National Academies Press, Washington, DC, 352 pp

National Research Council (NRC) (2005) Oil spill dispersants: efficacy and effects. The National Academies Press, Washington, DC, 377 pp

Nedwed T (2017) Overview of the American Petroleum Institute (API) joint industry task force subsea dispersant injection project. Int Oil Spill Conf Proc 2017:678–703

Orbesen ES, Snodgrass D, Shideler GS, Brown CA, Walter JF (2017) Diurnal patterns in Gulf of Mexico epipelagic predator interactions with pelagic longline gear: implications for target species catch rates and bycatch mitigation. Bull Mar Sci 93. https://doi.org/10.5343/bms.2016.1008

Paris CB, Le Hénaff M, Aman ZM, Subramanian A, Helgers J, Wang D-P, Kourafalou VH, Srinivasan A (2012) Evolution of the Macondo well blowout: simulating the effects of the circulation and synthetic dispersants on the subsea oil transport. Environ Sci Technol 46:13293–13302

Paris CB, Berenshtein I, Trillo ML, Faillettaz R, Olascoaga MJ, Aman ZM, Schlüter M, Joye SB (2018) BP Gulf Science Data reveals ineffectual sub-sea dispersant injection for the Macondo blowout. Front Mar Sci 5(389). https://doi.org/10.3389/fmars.2018.00389

Pesch S, Jaeger P, Jaggi A, Malone K, Hoffmann M, Krause D, Oldenburg T, Schlüter M (2018) Rise velocity of live-oil droplets in deep-sea oil spills. Environ Eng Sci 35(4):289–299. https://doi.org/10.1089/ees.2017.0319

Portnoy D, Fields A, Greer J, Schlenk S (2020) Genetics and oil: transcriptomics, epigenetics and genomics as tools to understand animal responses to exposure across different time scales (Chap. 30). In: Murawski SA, Ainsworth C, Gilbert S, Hollander D, Paris CB, Schlüter M, Wetzel D (eds) Deep oil spills: facts, fate and effects. Springer, Cham

Redman AD, Parkerton TF (2015) Guidance for improving comparability and relevance of oil toxicity tests. Mar Pollut Bull 98:156–170

Romero IC, Sutton T, Carr B, Quintana-Rizzo E, Ross SW, Hollander DJ, Torres JJ (2018) Decadal assessment of polycyclic aromatic hydrocarbons in mesopelagic fishes from the Gulf of Mexico reveals exposure to oil-derived sources. Environ Sci Technol (online). https://doi.org/10.1021/acs.est.8b02243

Ryerson TB, Camilli R, Kessler JD, Kujawinski EB, Reddy CM, Valentine DL, Atlas E, Blake DR, de Gouw MS, Parrish DD, Peischla J, Seewald JS, Warneke C (2012) Chemical data quantify Deepwater Horizon hydrocarbon flow rate and environmental distribution. Proc Natl Acad Sci USA 109:20246–20253

Smith JE (1968) *Torrey Canyon* pollution and marine life. Cambridge University Press, New York

Socolofsky SA, Adams EE, Boufadel MC, Aman ZM, Johansen Ø, Konkel WJ, Lindo D, Madsen MN, North EW, Paris CB, Rasmussen D, Reed M, Rønningen P, Sim LH, Uhrenholdt T, Anderson KG, Cooper C, Nedwed TJ (2015) Intercomparison of oil spill prediction models for accidental blowout scenarios with and without subsea chemical dispersant injection. Mar Pollut Bull 96:110–126

Spaulding M, Lib Z, Mendelsohn D, Crowley D, French-McCay D, Bird A (2017) Application of an integrated blowout model system, OILMAP DEEP, to the *Deepwater Horizon* (DWH) spill. Mar Pollut Bull 120:37–50

Vosyliene MZ, Kazlauskiene N, Joksas K (2005) Toxic effects of crude oil combined with oil cleaner simple green on yolk-sac larvae and adult rainbow trout *Oncorhynchus mykiss*. Environ Sci Pollut Res Int 12:136–139

Werely S (2011) Gulf oil spill Particle Image Velocimetry (PIV) In: McNutt M, Camilli R, Guthrie G, et al (eds) Plume Calculation Team, PIV Report. Assessment of flow rate estimates for the Deepwater Horizon/Macondo Well oil spill. Flow Rate Technical Group report to the National Incident Command, Interagency Solutions Group, March 10, 2011: https://engineering.purdue.edu/~wereley/oilspill/Deepwater_Horizon_June_V.pdf

White HK, Lyons SL, Harrison SJ, Findley DM, Liu Y, Kujawinski EB (2014) Long-term persistence of dispersants following the *Deepwater Horizon* oil spill. Environ Sci Technol Lett 1:295–299

Whitehead A, Dubansky B, Bodinier C, Garcia TI, Miles S, Pilley C, Raghunathan V, Roach JL, Walker N, Walter RB, Rice CD, Galvez F (2011) Genomic and physiological footprint of the *Deepwater Horizon* oil spill on resident marsh fishes. Proc Natl Acad Sci USA 109:20298–20302

Youtube.com (2018) BP's riser Gulf oil spill plume disaster, the other *Deepwater Horizon* gusher. https://www.youtube.com/watch?v=d0dnrOdmvco

Chapter 29
Perspectives on Research, Technology, Policy, and Human Resources for Improved Management of Ultra-Deep Oil and Gas Resources and Responses to Oil Spills

Steven A. Murawski

Abstract This chapter considers a series of research, technology, policy, and human resource-relevant recommendations aimed at identifying ultra-deep wellsite locations that may be problematic for risk of an oil spill, as well as enhancing prevention, preparedness, response, and subsequent injury assessment associated with ultra-deep oil spills. While various groups have offered research and process improvement recommendations, numbering in the high hundreds, this chapter focuses on 20 key research gaps and 4 policy changes that would improve outcomes for ultra-deep oil spill prevention and response. Recommended policy changes include (1) inclusion of site-specific risk assessments as an element of lease sale identification and approval, (2) collection of environmental baselines (both broad-scale and installation-specific) and ongoing monitoring of oil contaminants, (3) improved transparency and data sharing for oil facility management and accidental releases, and (4) more formal international engagement in siting, oil spill preparedness, response, and impact assessment.

Keywords Science priorities oil spills · Ultra-deep oil spills · Oil spill response · Deep-sea oil policy · Law of the Sea · Oil spill baselines

29.1 Introduction

As prescribed in the Oil Pollution Act of 1990 (OPA-90), the principal science advisor to the US Coast Guard during marine oil spills is the National Oceanic and Atmospheric Administration (NOAA). Although most of NOAA's responsibilities

S. A. Murawski (✉)
University of South Florida, College of Marine Science, St. Petersburg, FL, USA
e-mail: smurawski@usf.edu

S. A. Murawski et al. (eds.), *Scenarios and Responses to Future Deep Oil Spills*,
https://doi.org/10.1007/978-3-030-12963-7_29

for oil spill technical assistance funnel through its Office of Response and Restoration (OR&R, part of the National Ocean Service), because of the immense size and multidimensionality of the *Deepwater Horizon* (DWH) spill, it rapidly expanded into an "all hands on deck" situation, not only for the NOAA but also for the various bureaus of the Department of the Interior (e.g., Minerals Management Service [MMS] which would later become the Bureau of Offshore Energy Management [BOEM] and the Bureau of Safety and Environmental Enforcement [BSEE], US Fish and Wildlife Service, National Park Service, US Geological Survey) as well as the Environmental Protection Agency (EPA), the Food and Drug Administration (FDA), the National Aeronautics and Space Administration (NASA), the Department of Energy (DOE), the White House Office of Science and Technology Policy (OSTP), the US Army Corps of Engineers (COE), and others.

With all the considerable agency and industry expertise in oil spill preparedness, how presumptuous is it of me (a fisheries biologist) to offer science recommendations for improved management of marine oil and gas including oil spill response? During the initial phases of the *Deepwater Horizon* (DWH) accident, I was employed in Federal government service as the Chief Scientist of the National Marine Fisheries Service (a bureau of NOAA). My duties during the spill expanded to include being one of the principal science advisors to the Administrator of the NOAA (Lubchenco et al. 2012; McNutt et al. 2012) for the incident. As part of the spill advisory team, we organized and provided a daily science briefing to the Administrator and other senior NOAA staff, gathering and updating information relating to the many science-informed aspects of the spill including modeling of surface trajectories for first responders, weather forecasts, Loop Current dynamics, seafood safety and fishery closure recommendations, wildlife resources at risk, deployment of physical (ships and planes) and personnel assets, and many other issues. As well, I chaired the "Joint Analysis Group," a committee of Federal agency, and later academic scientists charged with analyzing DWH environmental data tracking subsurface oil plumes, oxygen depletion, and related real-time environmental parameters (JAG 2011). During this period, I briefed members of the Administration, Congress, and the media and coordinated with academic and state agency scientists throughout the Gulf of Mexico (GoM) region in an effort to help unify a balkanized (federal, state, academic, private industry) science response to the myriad issues experienced during the spill. After the DWH Macondo well was capped, I retired from Federal service after 35 years, assuming a faculty position at the University of South Florida (USF), one of the salient academic institutions involved in independent science regarding the spill. While not initially involved in post-spill science at the USF, I subsequently helped craft a proposal to the Gulf of Mexico Research Initiative (GoMRI) which led to the creation of the Center for Integrated Modeling and Analysis of Gulf Ecosystems (C-IMAGE) as a funded GoMRI consortium. Beginning in 2011, I served as director of C-IMAGE, overseeing a group of 18 national and international institutions and involving over 140 scientists, technicians, and students (http://www.marine.usf.edu/c-image/). In addition to serving as both a Federal and academic manager of science programs related to the DWH and other

oil spills, I testified to the National Commission on the BP *Deepwater Horizon* Oil Spill and Offshore Drilling (2011) and served on the National Academies Panel on Evaluation of the Use of Chemical Dispersants in Oil Spill Response (NASEM 2019). Thus, I have some diverse perspectives on research gaps and priorities moving forward.

Far more comprehensive and compelling than my own experiences and opinions, however, a number of relevant institutions and panels have offered science priorities and after-action assessments, especially including member agencies of the Federal Interagency Coordinating Committee on Oil Pollution Research (ICCOPR 2015), as well as the National Commission on the BP *Deepwater Horizon* Oil Spill and Offshore Drilling (2011), the Offshore Energy Safety Advisory Committee which was formed as a FACA by the DOI Secretary to provide recommendations, the National Incident Commander's Report (2010), and the National Academy of Engineering-National Research Council's report on DWH (NAE-NRC 2012), among others (e.g., Varanasi 2013). Assessments from significant spills predating DWH have also recommended specific research and process improvements to address these issues (e.g., NRC 2003, 2005; Peterson et al. 2003; AMSA 2010; Soto et al. 2014). It is from these various perspectives that I distill and discuss priorities for research, technology, policy, and human resource development related to future deep oil spill prevention, response, and assessment.

29.2 Research, Technology, Policy, and Human Resource Priorities

While a large number of studies have recommended additional research and technological improvements relevant to deep (≥300 m) and ultra-deep water (≥1500 m deep) oil exploration and development, the most comprehensive assessment of these priorities is that produced by ICCOPR and published in 2015 (ICCOPR 2015). Their assessment process, involving its 15 member Federal agencies and hundreds of subject-area experts, sorted research and technology priorities into 4 main classes (prevention, preparedness, response, and injury assessment and restoration; Fig. 29.1) and 25 subject areas (SAs) within them (ICCOPR 2015). The comprehensive process undertaken by ICCOPR identified a total of 900 research gaps and 570 specific research needs to fill them. Importantly, not all of these gaps and needs were specific to ultra-deep water oil drilling and included a variety of subjects including potential spills from vessel accidents and pipeline ruptures, Arctic oil and gas vulnerabilities, and other subject areas peripheral or ancillary to the ultra-deep situation. Of the 570 identified research needs, 150 of them were identified as priorities, with the following breakdown by class: 33 in prevention, 12 in preparedness, 72 in response, and 33 in injury assessment/restoration. My assessment of the identified 150 priorities is that about 70 of them are specifically or tangentially related to ultra-deep exploration and development.

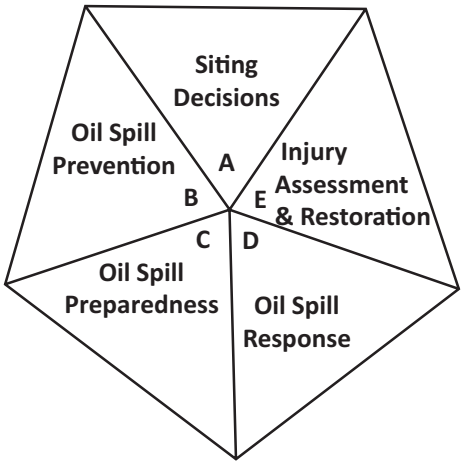

Fig. 29.1 Priorities for ultra-deep oil spill well siting decisions (A), oil spill prevention (B), preparedness (C), response (D), and injury assessment (E). Graphic is based on ICCOPR (2015) supplemented with an additional classification (facility siting decision-making)

Below I distill a number of, what I consider to be, high-priority recommendations (Table 29.1) for actions and crosswalk them with the five categories outlined in Fig. 29.1. I further comment on policy and human resource needs to better address management imperatives, potentially leading to less risk-prone ultra-deep exploration and production and more efficient and effective responses should future deepwater blowouts occur.

29.2.1 Oil and Gas Facility Siting in Ultra-Deep Waters

The siting of oil and gas exploration and production facilities is a vital factor in determining the risks of deepwater accidents, many aspects of the effectiveness of oil spill response activities, and the short- and long-term impacts from them. In the USA, the siting process includes complex interaction between government regulators (at both political and administrative levels), the oil and gas industry, and the independent scientific and nongovernmental organization (NGO) communities who can comment upon pending lease sales. Under the Outer Continental Shelf Lands Act of 1953, the process is initiated by the Department of the Interior, e.g., which announces pending lease sales upon which the industry can bid (e.g., BOEM 2017a, 2018). The lease sale process determines which specific blocks can be bid upon and which are reserved from sale because of compelling safety, economic, ecological, or other factors. In the eastern GoM, a moratorium on lease sales exists until 2022, because of a variety of political and other consequential factors (Murawski et al. 2020). Clearly, site-specific risks and ecological sensitivity should be two important factors determining which lease blocks are offered in such sales, as well as determining where recoverable oil and gas reserves exist.

Risks of a catastrophic accident such as DWH (with its tremendous spatial and temporal scales) are difficult to quantify given their relative infrequency (Ji et al. 2017),

Table 29.1 Some scientific research and technological development priorities relevant to the various requirement categories (Fig. 29.1) related to oil spills in ultra-deep waters

Science/technology priority	Deep water oil and gas requirement categories				
	A	B	C	D	E
Baselines for oil contamination (sediments, water, biota, people); broadscale and installation-specific	Medium	N/A	Medium	Medium	Exceptional
Deepwater biodiversity and productivity (microbes, benthos, fishes, mammals)	Exceptional	N/A	High	High	Exceptional
Offshore habitat sensitivity indices	Exceptional	N/A	High	Exceptional	High
Spatial connectivity of ecological resources (horizontal and vertical)	High	N/A	Medium	High	Exceptional
Background variability of ecosystems and species to disentangle oil stressors from natural variation	High	N/A	Low	Low	Exceptional
Chronic vs. acute toxicity studies and protocols specifically for deep biota	Low	N/A	N/A	High	Exceptional
Relationship between SSDI and fate of oil constituents including VOCs	N/A	N/A	Low	Exceptional	Medium
Assess historical recovery rates of various resources exposed to previous spills and mitigation techniques	High	N/A	N/A	High	Exceptional
Evaluate recovery rates of various biota in laboratory and mesocosm experiments	Low	N/A	Low	Medium	Exceptional
Relationships between SSDI and surface applications of dispersants	N/A	N/A	High	Exceptional	Medium
Field-based SSDI experiments	N/A	N/A	High	Exceptional	High
“Spill of opportunity” SSDI measurements (droplet sizes)	N/A	N/A	High	Exceptional	Medium
Lab-based high-pressure/low-temperature experiments with and w/o dispersants	N/A	Low	High	Exceptional	Medium
Modeling factors controlling MOSSFA intensity/distribution	Low	Medium	Medium	High	High
Deep oil reservoir characteristics (oil type, depth, temperature, pressure, GOR, rock and sediment strata, etc.)	Exceptional	Exceptional	Exceptional	Exceptional	Medium
Enhanced subsurface situational awareness capability	Medium	Exceptional	High	Exceptional	High
Improved water column oceanography (surface, pelagic, ultra-deep current flow rates, ambient conditions)	Exceptional	Exceptional	Exceptional	Exceptional	High
Improved 4-D oil spill transport and weathering models	High	High	Medium	Exceptional	High
Risk-based siting models	Exceptional	High	High	High	Medium
Social and economic dependency and spill impacts on communities	High	N/A	Low	High	Exceptional

A, siting decisions; B, spill prevention; C, spill preparedness; D, spill response; E, injury assessment and ecosystem restoration). Five relative priority determinations are provided: N/A (not applicable), low, medium, high, and exceptionally important priority

constantly changing circumstances in the industry (Murawski et al. 2020), and the multiplicity of technical, human, and environmental factors contributing to the overall risk profile. Traditional risk assessment methodologies (e.g., Ji et al. 2017) utilize the historical frequency of accidents either directly or as a function of the quantity of resource produced. Thus, for example, the calculated risks of at least one platform-based spill ≥10,000 barrels in the Central and Eastern Planning Areas of the GoM were estimated at between 83% and 95% during 2017–2066 (Ji et al. 2017). However, because the industry is changing so quickly – extending into deeper parts of the Gulf – previous hazard statistics that are aggregated at high levels may not be particularly informative. Currently the maximum lease depth of existing wells is 2960 m (Murawski et al. 2020). Alternative approaches that take into account hazard statistics incorporating various operating characteristics of the industry (e.g., Shultz 1999; Iledare et al. 1997; Jablonowski 2007; Muehelenbachs et al. 2013) provide more detail on factors positively and negatively associated with a variety of platform-related incidents. For example, Muehelenbachs et al. (2013) found a positive statistical relationship between increasing water depths and accident probability (Fig. 29.2), even when controlling for wellsite complexity, quantity of oil and gas produced, and age of the platform. They found that the risk of a serious accident (in a number of categories) increased 8.5% for every 30 m of water depth below the platform. The importance of a mechanistic understanding of risk factors also applies to changes in operating practices and administrative oversight, which may have *reduced* the likelihood of future accidents, all things being equal. In addition to relatively unknown frontier aspects of the ultra-deep, a number of critical factors contributing to the risk of an uncontrolled blowout at extreme depths include (1) high reservoir pressures and temperatures of oil and gas saturation of oil contained under

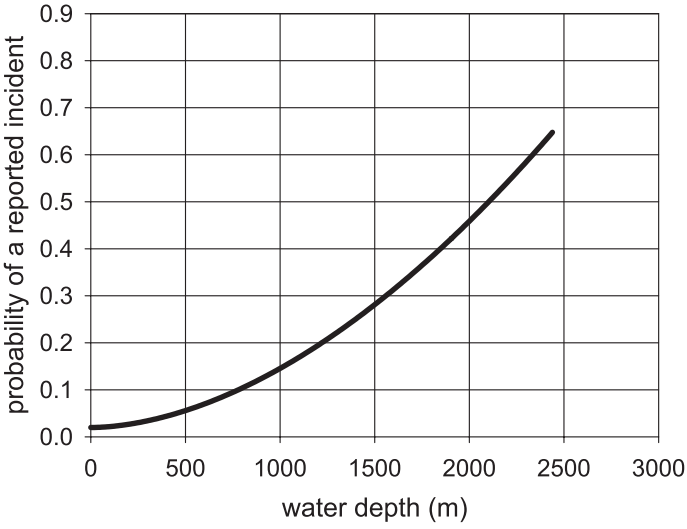

Fig. 29.2 Probability of reported oil platform accident as a function of water depth (m). (The figure is minimally modified from Muehlenbachs et al. (2013), with permission from Elsevier)

extreme pressures, which add risk of an uncontrolled well blowout should the BOP fail or there is loss of static containment; (2) rock and sediment strata that may be heavily fissured, unstable, or brittle, resulting in difficulty securing a casing or resulting in other situations that would allow oil and gas to penetrate rock strata upward to the water interface (such as the Chevron subsurface leak off Brazil in 2011); and (3) up to 3000 m of water between the sea surface and the blowout preventer (BOP) and the oceanographic factors impinging on such a long pipe string.

In some locations, such as in the Eastern GoM, surface currents can flow at rates exceeding 0.8 ms^{-1} putting enormous pressures on the risers. Thus, monitoring and predicting currents, eddies, and other water column attributes, and extreme weather is critical for allowing sufficient time to safely secure risers connecting ships to bottom apparatuses should conditions warrant. In addition to these issues, there are other environmental factors including the presence of unique, sensitive, or rare species in the ultra-deep that may be intolerant of oil and gas exploration or other risks that deem a particular block or area to be withdrawn from lease consideration. These environmental factors include the presence of unique benthic fauna such as chemosynthetic and deep coral communities that may be disrupted or destroyed (Demopoulos et al. 2015). Likewise, while mesopelagic and bathypelagic fish populations may not be as productive as their shallow water counterparts, a large fraction of the 1500+ fish species known from the GoM (McEachran 2009) exist only in the bathypelagic realm. The region is so undersampled that recent deep trawling expeditions found 460 species with 50 being new range records for the Gulf and numerous previously undescribed species (Fisher et al. 2016; Sutton et al. 2020). The deep GoM region is among the most diverse bathypelagic realms in the world. As Fisher et al. (2016) also describe, oil-weathering rates in the deep sea are much lower than for (warmer) surface waters, thus potentially resulting extended toxic exposures to this diverse community of species, should a deep-sea blowout occur. Because all of the gas and much of the benzene-toluene-ethylbenzene-xylene (BTEX) compounds in oil released in ultra-deep blowouts will be dissolved in the deep subsurface, bathypelagic species can be exposed to higher toxic concentrations than surface-dwelling fishes. This will potentially be exacerbated by the use of subsurface dispersant injection (SSDI), depending on its efficacy, in the event that it is used for future ultra-deep blowouts (French-McCay et al. 2018). Previous trade-off analyses have assumed it preferable to trap dispersed oil droplets in the deep sea vs. having oil surface, based in part on the assumption of greater ecological sensitivity in surface waters and along potentially impacted coasts (French-McCay et al. 2018). However, even the incomplete information available for deep-sea biota (Fisher et al. 2016; Sutton et al. 2020) reveals a highly diverse and potentially sensitive community of species in deep waters. Additionally, through diel vertical migrations, this community has connectivity with epipelagic resources including economic resources such as tunas, swordfish, and marlins (as predators; Fisher et al. 2016). Clearly, additional research to document the biodiversity, population status, and baseline oil contamination and to understand the potential toxicity of subsurface oil and gas to these communities is required to make an informed trade-off analysis involving SSDI or other response measures.

Risk assessments can be based purely on statistical approaches (Ji et al. 2017) taking into account previous accident frequency and spill volumes, or they can be more mechanistic, considering the specific environmental challenges faced when drilling and producing from a defined play or site (e.g., Muehlenbachs et al. 2013; Mark-Moser et al. 2015). In the past, Environmental Impact Assessments (EISs) and the lease block sales that they support have been defined for very large regions or planning areas (BOEM 2017a, b, 2018). Such a wholesale approach does not allow differentiation of the mechanistic risks that may be associated with different sites. Thus, one recommendation I propose is to conduct more intensive site-specific EIS and risk assessment evaluations when such factors may be important in classifying at-risk blocks (Table 29.1, column A).

While environmental/habitat sensitivity indices (E/HSIs) are used in current planning documents (e.g., BOEM 2018, page 7–40, Table 7.8), they also are primarily summarized at a coarse level of spatial resolution (e.g., for entire planning areas and comparisons among them; BOEM 2018). Since deepwater biota are distinctive from those located on continental shelves and at coastal margins, oil spills in those areas will encounter different biota, and thus resources at risk will be different (BOEM 2017a, 2018). For example, the blocks surrounding the Flower Gardens National Marine Sanctuary may be particularly sensitive and deserving of exclusion from drilling even though they are not within the sanctuary boundaries.

Given the considerations outlined above, there is, therefore, ample justification for the research priorities appropriate to siting of deepwater exploration and production facilities highlighted in Table 29.1 (Column A). Of the 20 research priorities listed, the most pressing for facility siting include studies of deepwater biodiversity, development of Environmental or Habitat Sensitivity Indices (E/HSIs) for the deep regions, deep oil reservoir characterization, and improved water column oceanography (including predictions), leading to location-specific risk-based decision-making.

29.2.2 Oil Spill Prevention

The concept of risk-based decision-making is likewise the centerpiece of recommendations from the NAE-NRC (2012) study, which concluded that a "goal-oriented risk management system" be implemented for marine oil and gas exploration and production to enhance oil spill prevention. Important attributes of such a system would include unifying risk management systems among operators, drilling contractors, and service companies, providing more detailed project-specific information to be shared by key personnel and more clearly articulating program changes among stakeholders (i.e., enhancing communication among them). Additionally, from engineering and process management perspectives, cogent recommendations for change have likewise been offered considering all aspects of technical, operational, and oversight of drilling operations (e.g., National Incident Commander's Report 2010; Australian Maritime Safety Authority 2010; National Commission on the BP

Deepwater Horizon Oil Spill and Offshore Drilling 2011; NAE-NRC 2012; ICCOPR 2015; Boebert and Blossom 2016). In response, the BSEE has issued revised blowout preventer regulations and strengthened oversight of offshore drilling regulations, all of which should result in reduced probabilities of accidents. These regulations, however, remain controversial within the industry and political spheres. Given the large number of previous evaluations of the systems failures leading to the DWH accident and my own lack of expertise in drilling and oil production management, I instead offer science and research priorities primarily related to increasing understanding the environment in which drilling operations are being conducted (Table 29.1; Colum B). The main priorities recommended include better understanding of the geological setting of the oil and gas reservoir underlying ultra-deep drilling operations, improving water column oceanographic monitoring and more sophisticated modeling to better understand specific hazards to operations. This includes technological developments to collect and process real-time data and to transmit it to operators and regulators for potential hazard detection, warnings, and mitigation, including improved 4-D models of water column physics. All of these research priorities, if acted upon, would help prevent ultra-deep accidents.

29.2.3 Oil Spill Preparedness

Similar to spill prevention, being prepared for accidents in the ultra-deep involves understanding hazards that are potential antecedents to deep blowouts. Preparations of the response community are a critical human resource requirement for successful responses, and this aspect is discussed in detail below (human resources). In particular, relatively high priorities for spill preparedness include improved understanding of environmental factors contributing to catastrophic spills and factors that determine oil and gas fate (distribution, concentrations, weathering, etc.) and understanding how effective various mitigation measures can be (e.g., surface-applied dispersants and SSDI, booming, controlled burns, sinking agents, etc.). Further, there still remains the contentious issue of whether the use of SSDI is protective of the health of response workers (McGowan et al. 2017). This is a critical issue for response planning and several research recommendations are relevant (Table 29.1, Column C). Perhaps one of the most important issues determining the timeliness and effectiveness of response efforts is training for response, using realistic scenarios, based on previous experiences, and for spills that may occur in frontier regions of technology, geography, and operations. As we saw with DWH, while the response system was prepared for large-scale tanker accidents, the scenario of an ultra-deep blowout of extreme volume and duration was a "war" no one anticipated fighting. As well, large-scale spills in novel settings may involve nontraditional communities of responders, new technologies and disciplines, and unprecedented oversight by the government (NIC 2010) including the development of ad hoc advisory and decision-making arrangements.

The oil spill response community must anticipate and prepare for such eventualities and reach out beyond the norms for low-level spills and put mechanisms into place that use the nontraditional cadre of responders that have unique expertise in science and communication (e.g., academicians and the media). Using these communities may help to avoid some of the pitfalls extant in the DWH response (NIC 2010; National Commission on the BP Deepwater Horizon Oil Spill and Offshore Drilling 2011). Training exercises should be as realistic as possible and anticipatory of the unique conditions the "next war" may entail (e.g., depths approaching 3000 m or even deeper, different types of oil, etc.) including both tabletop and actual response simulations.

29.2.4 Oil Spill Response

Crafting and executing an effective repertoire of response measures require closing the gaps in uncertainty regarding the utility, efficacy, and potential impacts of various mitigation approaches. For example, despite considerable research on the topic, there remains considerable dispute regarding the relative contributions of the physics of deep blowouts vs. the contributions of SSDI in forming microdroplets that remain essentially suspended in deep water (Paris et al. 2018; Malone et al. 2018, 2020; NASEM 2019). Three major research modalities can help close this critical information gap (Table 29.1, Column D), including additional laboratory-based research (Pesch et al. 2018, 2020; Malone et al. 2018, 2020), collection of relevant data from appropriate "spills of opportunity," and field-scale experimentation (Johanssen and Rye 2003). While much can be learned from laboratory studies since important variables can be isolated and controlled for, the challenge for small-scale experiments (and field-based trials as well) is the scaling-up of results and conclusions where spill volumes, jet diameters, and other pertinent conditions may be an order of magnitude or smaller in experimental facilities as opposed to actual blowouts. Spills of opportunity and field-based experimentation present key research opportunities since scaling may not be as critical. Spills of opportunity obviate the need for scaling, but there are a number of technical, safety, and administrative constraints in such approaches. These include mustering trained personnel, equipment, and the challenges of logistics during an active spill. Furthermore, if, for example, the variable of interest is oil droplet diameter from free-flowing blowouts with and without the addition of SSDI, authorities may consider such science priorities as secondary to closing the well and may thus not allow such science to proceed (as was the case initially in DWH). Field-scale experimentation such as the "DeepSpill" experiments in 2000 (Johanssen and Rye 2003) provided considerable useful information a decade later during the response to DWH. While controlled releases of moderate volumes of crude oil and gas into the environment to monitor, track, and estimate oil and gas fate are controversial, the potential payoffs in helping to resolve controversy regarding the efficacy of SSDI make such experiments high priorities for consideration by environmental managers. A combination of

laboratory and field-based experimentation combined with appropriate simulation models would provide a powerful approach to predict the effects of SSDI in many alternative deepwater blowout scenarios (Table 29.1, Column D). Such experiments would have a global impact.

To fully understand the fate of oil and gas with respect to response measures, one important consideration in the use of dispersants is the utility of surface-applied dispersants if SSDI has previously been applied during the same spill. The current generation of dispersants works best in breaking large droplets of fresh crude into smaller ones, but are relatively ineffective when applied to "mousse" oil/mineral aggregates and other weathered by-products. Such an examination is a priority in order to minimize the application of dispersants that may be ineffective under such circumstances. Also, more robust modeling of the spatial dynamics of the fate of oil, gas, BTEX compounds, and other components for ultra-deep blowouts will allow for greater understanding of how oil and gas will affect sensitive habitats and species.

29.2.5 Injury Assessment and Ecosystem/Community Restoration (NRDA)

The Natural Resource Damage Assessment (NRDA), recovery of affected resources and lost use thereof by the public are major components prescribed by OPA-90. Science and research associated with the NRDA and related recovery processes are crucial to understanding factors resulting in resource injury and for identifying specific actions that lead to ecological and economic recovery. In the wake of large-scale spills such as *Exxon Valdez* and DWH, there have been consistent conclusions that adequate pre-spill baseline contamination and ecosystem monitoring studies would have made the NRDA process much more focused on the incremental impacts of the spill rather than being focused on deconvolving a particular spill from background contamination from various anthropogenic inputs and natural factors. In fact, rare is the ecological field-based oil spill study that has *not* bemoaned the lack of such pre-spill data (e.g., Varanasi 2013). While adequate baselines for contaminants and the underlying variability of ecological communities are extremely useful in assessing injury from a specific incident, so too can such background data exonerate operators if post-spill monitoring data show no measurable effect. Thus, it is in the best interests of the industry to advocate for the collection of adequate baseline information. In heavily utilized ocean basins, such as the GoM, hydrocarbon components and especially toxic polycyclic aromatic hydrocarbons (PAHs) result from a wide variety of sources including natural seeps, atmospheric deposition, coastal runoff, and oil spills from surface transport (ships), pipeline leaks, ship collisions, and platform accidents (NRC 2003). Additionally, water that is produced with oil, gas, and gas condensates is generally treated at offshore platforms and either disposed of overboard or reinjected into sub-bottom strata (generally only at very shallow wells). The importance of careful accounting for all sources of oil

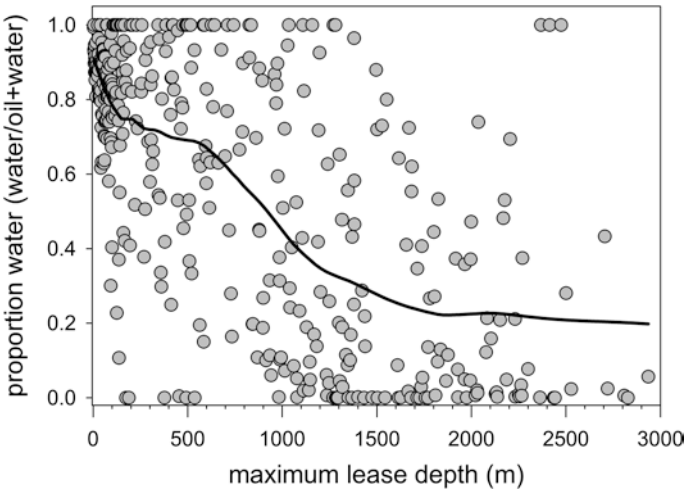

Fig. 29.3 Proportion of produced water (total water ÷ total water + oil) from Gulf of Mexico oil and gas leases in 2017, by maximum lease depth (m). (Data are derived from the Bureau of Ocean Energy Management (BOEM): https://www.data.boem.gov/. Line is a loess smooth with ø = 0.3 of the data). Data do not account for the ages of leases

contamination is illustrated by the example of produced waters (Sauer et al. 1997; Zhao et al. 2008). Permitting under the Clean Water Act (EPA 2017) stipulates that produced water that is reintroduced into the environment can contain no more than 29 ug/l (ppm) of crude oil and grease as a monthly average and only one exceedance of 42 ppm per month (EPA 2017). The total quantity of water produced by wells in the US GoM in 2017 was 500.7 million barrels (Fig. 29.3), incidentally about 77% of total crude oil production in the same year (Murawski et al. 2020). Importantly, while oil production increases exponentially with water depth (Murawski et al. 2020), the quantity of produced water as a function of crude oil volume declines substantially as water depths exceed 1500 m (Fig. 29.3). In fact, while 53% of crude oil production in the northern GoM in 2017 was from ultra-deep wells, only about 14% of produced water came from the ultra-deep. Assuming that the average contamination of total petroleum hydrocarbons (TPH) in treated produced waters was 29 ppm (near a 1993 estimate of 23.5 ppm; EPA 2017), then the total quantity of oil introduced into the GoM from treated produced waters was about 14,500 barrels.

Baseline oil contamination budgets for water, sediments, and biota can be obtained for broadscale regions (samples obtained from general surveys) or with installation-specific monitoring programs. It is ironic that the industry is required to monitor and report its produced water effluents, but not required to produce similar data from the sediments and water surrounding such facilities or the biota in their vicinity. Having detailed installation-specific baseline data in addition to broadscale monitoring data would allow much more precise assessments of the near- and far-field impacts of future spills and would substantially reduce the current ambiguities as to the sources of contaminants in the aftermath of a spill. Both types of baseline data form the bases

for oil spill injury assessments and recovery recommendations, and the collection of such data constitutes one of the policy recommendations below.

Beyond environmental baselines, injury assessment and restoration require additional studies of contaminant effects and especially the impacts of chronic low-level exposures in addition to acute, high-concentration effects. Apart from NRDA considerations, there are a number of critical scientific priorities to better address impacts of oil spills on, for example, human health, worker safety and economic losses, additional research on community dependencies on natural resources (e.g., oil and gas, fisheries, etc.), and baseline human health metrics for oil and gas workers, responders, and communities at risk are vital for injury assessment (NASEM 2019).

29.2.6 Recommendations for Policy Improvements

The 20 priority recommendations considered above and outlined in Table 29.1 primarily involve scientific and technological improvements aimed at optimizing the cycle of marine oil and gas development and the effectiveness of responses to accidental releases in the ultra-deep. Decisions to actually implement these and other recommendations (e.g., those of ICCOPR 2015) require both resources and, in some cases, changes in existing laws, policies, and administrative guidance. Many of the recommendations will require additional, significant financial resources as well as a commitment by industry and governments to process improvements. Below I outline four policy enhancements supported by the science and technology recommendations articulated above and in Table 29.1. The policy recommendations listed below, however, should not be considered as a complete list of policy changes required necessary to achieve the goals of a less risk-prone, more transparent, and more responsive system for ultra-deep oil and gas management and accident response capacity. I propose the following changes to existing policies:

1. *Conduct site-specific risk assessments as an element of lease sale identification and approval.*

As noted above, while risk assessments included in programmatic EISs include the frequencies of previous accidents, ultra-deep drilling involves unquantified and unprecedented risks due to extreme environmental conditions. Likewise, there may be highly sensitive, cryptic species and communities in the ultra-deep that present unacceptable risks in some specific locations. Site-specific risk assessments can take such factors into account before lease sales are offered for such areas, if sufficient pre-lease data and baselines are available.

2. *Collect broadscale and installation-specific baseline and ongoing monitoring of oil contaminants.*

The collection and monitoring of environmental baselines, via both broadscale surveys and installation-specific monitoring, should be a requirement of permits to

explore and produce oil and gas. As a permit condition, operators could be required to provide periodic monitoring data to EPA or other appropriate authorities, under the supervision of federal agencies – much like they are currently required to do for produced waters. There are ample precedents for such user-financed monitoring programs as a condition for access to public resources. Under Federal Clean Water Act permitting, for example, monitoring of wastewater treatment facilities is required of operators discharging into public waterways. The format, frequency, and QA/QC for such monitoring are overseen by the EPA. Likewise, in Federal fisheries management, routine operator-financed bycatch monitoring is employed in Alaska and elsewhere as a monitoring tool to assure compliance with regulations and to contribute to stock assessment (Alaska Fisheries Science Center and Alaska Regional Office 2018). If clean water compliance and fisheries management require user-financed monitoring of operations, there is no excuse for an activity potentially much more damaging to the environment not having a commensurate level of routine sampling done under appropriate agency supervision. The costs for facility-based monitoring should be borne by the permittee as a permit condition. Collection and analysis of broadscale baselines are likely more the province of the Federal agencies and state trustees and could be financed through appropriations or other novel funding vehicles, the results of which should be incorporated in programmatic environmental impact statements (EISs).

3. *Improve transparency and data sharing.*

While much of the data from oil and gas production and leasing activities are available to the public, other information critical to understanding the risks, impacts, and implications of oil and gas activities remains elusive. For example, the EPA collects and monitors produced water compliance data, but those data are not readily available for public inspection. Because oil and gas production occurs on public lands, such data on where, how much, and to what an effect those activities are having is an underlying principal of natural resource management of common property resources. Federal agencies, industry, and academic researchers must be dedicated to open and timely data sharing and transparency as a standard operating principle. Such data should include routine monitoring results and, in the case of large-scale spills requiring NRDA intervention (such as DWH) response, NRDA-collected and restoration data. Additionally, these data should be located in discoverable, user-friendly archives such as the NOAA DIVER database (https://www.diver.orr.noaa.gov/) allowing information sharing at all levels.

4. *Improve international engagement in siting, preparation, response and impact assessment. Ratify the Law of the Sea Treaty.*

As the DWH and other spill simulations outlined in Berenshtein et al. (2020) and evaluated by Chancellor et al. (2020) indicate, large-scale oil spills in locations such as the GoM are not limited to the exclusive economic zones (EEZs) of the country of origin but can extend throughout waters of Mexico, Cuba, and the USA and beyond the GoM. While formal international cooperation on oil spill response planning and preparation currently exists (e.g., formal plans between the USA and Mexico and impending joint plans between Cuba and the USA), there is also ample reason to

consider joint coordination of both siting priorities (so as to protect sensitive areas) and injury assessment activities. This may include the development of new mechanisms under which to conduct such activities. Doing so will increase trust, result in more uniform arrangements between governments and multinational corporations, and potentially lead to better and less risk-prone decision-making. Additionally, as Admiral Thad Allen highlighted in his DWH after-action assessment (NIC 2010), ratifying the Law of the Sea Treaty by the USA would be an important step in improving oil and gas safety and spill response. Our simulations of potential GoM oil spills have documented that deepwater spills within the Gulf will affect resources in the three GoM countries and the Bahamas, at a minimum. As Admiral Allen pointed out (NIC 2010): "Given the continued need to recover hydrocarbons from the Gulf for the foreseeable future and the prospect of further oil exploration in the Arctic, the United States must move forward to ratify the Law of the Sea Treaty which provides a governance framework for international spill response. There are a host of reasons why this Nation should not delay in meeting our international responsibility and ratify this treaty. The potential and the need to plan for international responses to oil spills is just one more compelling reason to do this." The fact that all three GoM countries are more aggressively pursuing marine hydrocarbon development means that there is a compelling reason to cooperate further to assure this development is done under consistent safety, environmental and human health standards.

29.2.7 Human Resource Development

A number of system-level assessments of DWH and other large spills have highlighted human error, lack of training, and lack of coordination as contributing factors to those large-scale spills and the extent of their impacts. Clearly, the human factor is absolutely critical not only in preventing spills in the first place but in terms of coordinated, effective, and efficient responses. Greater emphasis on coordination among the industry-government-academic nexus and realistic emergency spill response training would go far in reducing the chances of another ultra-deep spill and improve responses should they occur. The Canadian example of certifying HQP (highly qualified personnel) that the Coast Guard and DFO Canada use is a concrete example of expertise entrainment. Cross-training, internships, intergovernmental personnel act (IPA) exchanges, and common educational programming all can improve communication and reduce artificial barriers to improved operations.

29.3 Summary

In the aftermath of large-scale oil spills, there are invariably calls for additional regulatory oversight, enhanced research, development of new prevention and response technologies, and systems management approaches to reduce the probability of similar accidents occurring in the future. With frontier oil and gas development

extending through the ultra-deep, oil spills therein have revealed startling gaps in our knowledge of the deep-sea environment and how oil spills will behave. Other frontier areas such as the Arctic and in developing nations' EEZs are equally deficient in relevant environmental information for informed decision-making. Importantly, the research, policy, and human resource development recommendations contained herein, if fully implemented, should reduce the probability of uncontrolled blowouts in the deep sea and other frontier areas of oil and gas exploration and production, improve the effectiveness of response measures, and reduce injuries to sensitive natural resources and people.

Acknowledgments The priority recommendations contained herein were culled from the literally hundreds similar recommendations offered by the Federal agencies, industry groups, NGOs, and academic researchers and in various after-action reports stemming from oil spills. In particular, these perspectives benefitted from discussions with oil spill experts including David Westerholm and Lisa DiPinto at NOAA and Robyn Conmy at EPA. Likewise, discussions with many colleagues in the industry were helpful in winnowing the list to include the most feasible options. Last, my colleagues at C-IMAGE were instrumental in articulating many of the research priorities. That being said, the responsibility for including specific recommendations as part of this chapter lies only with me.

References

Alaska Fisheries Science Center and Alaska Regional Office (2018) North Pacific Observer Program 2017 Annual Report. AFSC Processed Rep. 2018–02, 136 pp. Alaska Fisheries Science Center, NOAA, National Marine Fisheries Service, 7600 Sand Point Way NE, Seattle WA 98115. Available at http://www.afsc.noaa.gov/Publications/ProcRpt/PR2018-02.pdf

Australian Maritime Safety Authority (AMSA) (2010) Response to the Montara wellhead platform incident. Report of the incident analysis team. March 2010. Available online from: https://www.amsa.gov.au/marine-environment/incidents-and-exercises/response-montara-wellhead-platform-incident

Berenshtein I, Perlin N, Ainsworth C, Ortega-Ortiz J, Vaz AC, Paris CB (2020) Comparison of the spatial extent, impacts to shorelines and ecosystem, and 4-dimensional characteristics of simulated oil Spills (Chap. 20). In: Murawski SA, Ainsworth C, Gilbert S, Hollander D, Paris CB, Schlüter M, Wetzel D (eds) Scenarios and responses to future Deep Oil Spills – fighting the next war. Springer, Cham

Boebert E, Blossom JM (2016) *Deepwater Horizon*: a systems analysis of the Macondo disaster. Harvard University Press. 290 pp

Chancellor E, Murawski SA, Paris CB, Perruso L, Perlin N (2020) Comparative environmental sensitivity of offshore Gulf of Mexico waters potentially impacted by ultra-deep oil well blowouts (Chap. 26). In: Murawski SA, Ainsworth C, Gilbert S, Hollander D, Paris CB, Schlüter M, Wetzel D (eds) Scenarios and responses to future Deep Oil Spills – fighting the next war. Springer, Cham

Demopoulos AWJ, Bourque JR, Cordes E, Stamler KM (2015) Impacts of the *Deepwater Horizon* oil spill on deep-sea coral-associated sediment communities. Mar Ecol Prog Ser 561:51–68. https://doi.org/10.3354/meps11905

Fisher CR, Montagna PA, Sutton TT (2016) How did the *Deepwater Horizon* oil spill impact deep-sea ecosystems? Oceanography 29:182–195. https://doi.org/10.5670/oceanog.2016.82

French-McCay D, Crowley D, Rowe JJ, Bock M, Robinson H, Wenning R, Hayward Walker A, Joeckel J, Nedwed TJ, Parkerton TF (2018) Comparative risk assessment of spill response

options for a deepwater oil well blowout: part 1. Oil spill modeling. Mar Pollut Bull 133:1001–1015

Iledare OO, Pulsipher AG, Dismukes DE, Mesyanzhinovet D (1997) Oil spills, workplace safety and firm size: evidence from the U.S. Gulf of Mexico OCS. Energy J 18:73–89

Interagency Coordinating Committee on Oil Pollution Research (ICCOPR) (2015) Oil pollution research and technology plan: Fiscal years 2015–2021. 270 pp. https://www.bsee.gov/sites/bsee_prod.opengov.ibmcloud.com/files/bsee-interim-document/statistics/2015-iccopr-research-and-technology-plan.pdf

Jablonowski CJ (2007) Employing detection controlled models in health and environmental risk assessment: a case in offshore oil drilling. Hum Ecol Risk Assess 13:986–1013

Ji Z-G, Johnson WR, DuFore CM (2017) Oil-spill risk analysis Gulf of Mexico Outer Continental Shelf (OCS) lease sales, Eastern Planning Area, Central Planning Area, and Western Planning Area, 2017–2022, and Gulf-wide OCS program, 2017–2086. OCS Report BOEM 2017–010. 57 pp.

Johansen Ø, Rye H (2003) DeepSpill—Field study of a simulated oil and gas blowout in deep water. Spill Sci Technol Bull 8:433–443

Joint Analysis Group, *Deepwater Horizon* Oil Spill (JAG) (2011) Review of R/V *Brooks McCall* data to examine subsurface oil. NOAA Technical Report NOS OR&R 24, Silver Spring, MD 69 pp.

Lubchenco J, McNutt MK, Dreyfus G, Murawski SA, Kennedy DM, Anastas PT, Chu S, Hunter T (2012) Science in support of the *Deepwater Horizon* response. Proc Natl Acad Sci U S A 109:20212–20221

Malone K, Pesch S, Schlüter M, Krause D (2018) Oil droplet size distributions in deep-sea blowouts: influence of pressure and dissolved gases. Environ Sci Technol 52:6326–6333. https://doi.org/10.1021/acs.est.8b00587

Malone K, Aman ZM, Pesch S, Schlüter M, Krause D (2020) Jet formation at the spill site and resulting droplet size distributions (Chap. 4). In: Murawski SA, Ainsworth C, Gilbert S, Hollander D, Paris CB, Schlüter M, Wetzel D (eds) Deep Oil Spills: facts, fate and effects. Springer International, Cham

Mark-Moser M, Disenhof C, Rose K (2015) Gulf of Mexico geology and petroleum system: overview and literature review in support of risk and resource assessments. NETL-TRS-4-2015; EPAct Technical Report Series; U.S. Department of Energy, National Energy Technology Laboratory: Morgantown, WV; p 28

McEachran JD (2009) Fishes (Vertebrata: Pisces) of the Gulf of Mexico. In: Felder DL, Camp DK (eds) Gulf of Mexico–origins, waters, and biota, vol 1.: Biodiversity. Texas A&M University Press, College Station, pp 1223–1316

McGowan CJ, Kwok RK, Engel LS, Stenzel MR, Stewart PA, Sandler DP (2017) Respiratory, dermal, and eye irritation symptoms associated with Corexit™ EC9527A/EC9500A following the *Deepwater Horizon* oil spill: findings from the GuLF STUDY. Environ Health Perspect 097015:1–7. https://ehp.niehs.nih.gov/doi/pdf/10.1289/EHP1677

McNutt MK, Chu S, Lubchenco J, Hunter T, Dreyfus G, Murawski SA, Kennedy DM (2012) Applications of science and engineering to quantify and control the *Deepwater Horizon* oil spill. Proc Natl Acad Sci U S A 109:20222–20228. https://doi.org/10.1073/pnas.1214389109

Muehlenbachs L, Cohen MA, Gerarden T (2013) The impact of water depth on safety and environmental performance in offshore oil and gas production. Energy Policy 55:699–705. https://doi.org/10.1016/j.enpol.2012.12.074

Murawski SA, Hollander DJ, Gilbert S, Gracia A (2020) Deep-water oil and gas production in the Gulf of Mexico, and related global trends (Chap. 2). In: Murawski SA, Ainsworth C, Gilbert S, Hollander D, Paris CB, Schlüter M, Wetzel D (eds) Scenarios and responses to future Deep Oil Spills – fighting the next war. Springer, Cham

National Academies of Sciences, Engineering and Medicine (NASEM) (2019) Report of the committee on evaluation of the use of chemical dispersants in Oil Spill response. National Academies Press, Washington DC. xxx pp

National Academy of Engineering and National Research Council (NAE-NRC) (2012) Macondo Well *Deepwater Horizon* Blowout: lessons for improving offshore drilling safety. The National Academies Press, Washington, DC. https://doi.org/10.17226/13273

National Commission on the BP Deepwater Horizon Oil Spill and Offshore Drilling (2011) Deep water: the Gulf oil disaster and the future of offshore drilling. Report to the President. 398 pp. https://www.gpo.gov/fdsys/pkg/GPO-OILCOMMISSION/pdf/GPO-OILCOMMISSION.pdf

National Incident Command (NIC) (2010) National incident commander's report: MC252 Deepwater Horizon. National incident command, Deepwater Horizon response. https://www.hsdl.org/?abstract&did=767583

National Research Council (NRC) (2003) Oil in the sea III: fates and effects. The National Academies Press, Washington, DC

National Research Council (NRC) (2005) Oil spill dispersants: efficacy and effects. The National Academies Press, Washington, DC, p 377

Paris CB, Trillo ML, Olascoaga MJ, Aman ZM, Schlüter M, Joye SB, Berenshtein I (2018) BP Gulf science data reveals ineffectual sub-sea dispersant injection for the Macondo blowout. Front Mar Sci (in press)

Pesch S, Jaeger P, Jaggi A, Malone K, Hoffmann M, Krause D, Oldenburg T, Schlüter M (2018) Rise velocity of live-oil droplets in deep-sea oil spills. Environ Eng Sci. 35(4):289–299 https://doi.org/10.1089/ees.2017.0319

Pesch S, Schlüter M, Aman Z, Malone K, Krause D, Paris CB (2020) Behavior of rising droplets and bubbles – impact on the physics of deep-sea blowouts and oil fate (Chap. 5). In: Murawski SA, Ainsworth C, Gilbert S, Hollander D, Paris CB, Schlüter M, Wetzel D (eds) Deep Oil Spills: facts, fate and effects. Springer International, Cham

Peterson CH, Rice SD, Short JW, Esler D, Bodkin JL, Ballachey BE, Irons DB (2003) Long-term ecosystem response to the *Exxon Valdez* oil spill. Science 302:2082–2086

U.S. Bureau of Ocean Energy Management (BOEM) (2018) 2019–2024 National outer continental shelf oil and gas leasing draft proposed program. Available at: https://www.boem.gov/NP-Draft-Proposed-Program-2019-2024 380 pp

Sauer TC, Costa HJ, Brown JS, Ward TJ (1997) Toxicity identification evaluations of produced water effluents. Environ Toxicol Chem 16:2020–2028

Shultz J (1999) The risk of accidents and spills at offshore production platforms: a statistical analysis of risk factors and the development of predictive models. Doctoral Dissertation. Department of Engineering and Public Policy, Carnegie Mellon University, Pittsburgh

Soto LA, Botello AV, Licea-Durán S, Lizárraga-Partida M, Yáñez-Arancibia Y (2014) The environmental legacy of the Ixtoc 1 oil spill in Campeche sound, southwestern Gulf of Mexico. Front Mar Sci 1:1–9

Sutton TT, Frank T, Judkins H, Romero IC (2020) As Gulf oil extraction goes deeper, who is at risk? Community structure, distribution, and connectivity of the deep-pelagic fauna (Chap. 24). In: Murawski SA, Ainsworth C, Gilbert S, Hollander D, Paris CB, Schlüter M, Wetzel D (eds) Scenarios and responses to future Deep Oil Spills – fighting the next war. Springer, Cham

U.S. Bureau of Ocean Energy Management (BOEM) (2017a) Gulf of Mexico OCS Lease Sale. Final Supplemental Environmental Impact Statement 2018. Volume I: Chapters 1–8 and keyword Index. https://www.boem.gov/BOEM-EIS-2017-074-v1/ 412 pp. 4–123 etc.

U.S. Bureau of Ocean Energy Management (BOEM) (2017b) Assessment of technically and economically recoverable hydrocarbon resources of the Gulf of Mexico Outer Continental Shelf as of January 1, 2014. OCS Report BOEM 2017–005. 44 pp. https://www.boem.gov/BOEM-2017-005/

U.S. Environmental Protection Agency (EPA) (2017) Final National Pollutant Discharge Elimination System (NPDES) General Permit No. GEG460000 for Offshore Oil and Gas Activities in the Eastern Gulf of Mexico. Region 4 Permit

Varanasi U (2013) Making science useful in complex political and legal arenas: a case for front-loading science in anticipation of environmental changes to support natural resource laws and policies. Wash J Environ Law Policy 2013:238–265

Zhao L, Chen Z, Lee K (2008) A risk assessment model for produced water discharge from offshore petroleum platforms – development and validation. Mar Pollut Bull 56:1890–1897

Correction to: Linking Abiotic Variables with Macrofaunal and Meiofaunal Abundance and Community Structure Patterns on the Gulf of Mexico Continental Slope

Paul A. Montagna, Jeffrey G. Baguley, Michael G. Reuscher, Gilbert T. Rowe, and Terry L. Wade

Correction to:
Chapter 7 in: S. A. Murawski et al. (eds.),
***Scenarios and Responses to Future Deep Oil Spills*,**
https://doi.org/10.1007/978-3-030-12963-7_7

The book was inadvertently published without including the name of Michael G. Reuscher as a co-author of Chapter 7. This has now been updated and the correct order of authors is as follows:

Paul A. Montagna, Jeffrey G. Baguley, Michael G. Reuscher, Gilbert T. Rowe, and Terry L. Wade

The updated online version of this chapter can be found at
https://doi.org/10.1007/978-3-030-12963-7_7

S. A. Murawski et al. (eds.), *Scenarios and Responses to Future Deep Oil Spills*,
https://doi.org/10.1007/978-3-030-12963-7_30

Index

S. A. Murawski et al. (eds.), *Scenarios and Responses to Future Deep Oil Spills*,
https://doi.org/10.1007/978-3-030-12963-7